UNIVERSITY OF SOUTHAMPTON

ON THE ROLE OF LONGITUDINAL STRING VIBRATIONS IN THE GENERATION OF VIOLIN SOUND

by

Nigel Harris BE (Civil)

Institute of Sound and Vibration Research
Faculty of Engineering and Applied Science

Thesis submitted for the degree of
Doctor of Philosophy

March, 2003

ABSTRACT

FACULTY OF ENGINEERING AND APPLIED SCIENCE
INSTITUTE OF SOUND AND VIBRATION RESEARCH

Doctor of Philosophy

ON THE ROLE OF LONGITUDINAL STRING VIBRATIONS IN THE GENERATION OF VIOLIN SOUND

by Nigel Harris

The 'primary' source of longitudinal string vibration (LSV) is the non-linear stretching of the transversely vibrating string. 'Secondary' LSV is generated by the dynamic activity of the body. The effect of a periodic variation of string tension on violin dynamics and sound is examined.

A qualitative structural analysis of the static forces on the body from string tension suggests that the difference between back and belly arching shape affects the magnitude and direction of the deformation of the body. The static deformation of the violin body caused by an increase in string tension is measured and shown to approach that of a "Nullstrahler" or simple source radiator. Parameters are developed that largely define the arching shape of the plates and the relationship between the front and back plate shapes. Five violins are made exhibiting controlled differences only in these parameters.

Using a shaker to excite the open G string at resonance, a series of dynamic tests are done to investigate the effect of different bridge and string termination mobilities on the transverse string vibration (TSV) displacement, and the LSV developed in the string. The effect of arching shape on the TSV, LSV and the radiated sound are investigated. Complementary evidence is gained from reciprocal excitation of the violin by a reverberant room sound field.

Above 1500Hz, the radiated sound pressure is dependent on the choice of the geometric parameters that relate the front and back plate shapes to each other. The spectrum of the radiated sound pressure is more closely related to the LSV spectrum than the spectrum of the TSV displacement. Below 1500Hz the radiated sound pressure varies as the inverse of the height of the belly cross arches in the end bouts. Some of the TSV energy entering the violin is transformed into secondary LSV energy. This combines with the primary bellying LSV. The modal responses to the LSV force in the string apparently contribute significantly to the radiated sound.

The violin shows a different spectrum of radiated sound pressure per unit transverse force on the bridge from the string than published spectra of radiated sound pressure per unit of external force applied to the bridge. The admittances of a violin bridge to forces applied directly by a vibrating string are estimated at 196Hz intervals. The admittance to transverse force from the string is estimated to have a quite different spectrum from that found by others who applied an external force to the bridge of a violin with damped strings. The estimated bridge pseudo-admittance to LSV force is found to be significantly higher than the admittance to transverse force. The powers exchanged between the string and the bridge via both LSV and TSV are estimated and compared with the radiated sound power.

ACKNOWLEDGEMENTS

I undertook this project to bring scientific veracity and written expression to the insights gained in half a lifetime of making, playing and listening to the violin. I would like to acknowledge gratefully the contribution of:

my supervisor, Prof. F. J. Fahy, for taking a chance on me when I walked into his office in 1996, and giving me the opportunity to undertake this project; for his enthusiasm, profound knowledge of acoustics and valuable guidance throughout the project;

the members of my review board, Prof. T. Leighton, and Dr. M. Wright, for their perceptive criticisms and constructive suggestions;

my friend, Prof. Nicholas Wiseman, for his encouragement to undertake this project and advice and help with computer problems;

my violinmaking partner, Roger Sheldon, for his assistance with some experimental work, being a sounding board in many discussions, and showing no sign of impatience with the time it has taken and the consequent loss of earnings;

my wife Margaret for her love, unflagging encouragement, and generously foregoing the company of her husband in evenings and weekends for several years.

This work is dedicated to the memory of

Giles Alexander Harris, 1971 –1997.

Nigel Harris, 23 St. Paul's Place, Canonbury, London. January 2003.

LIST OF CONTENTS

LIST OF SYMBOLS AND ABBREVIATIONS

List of symbols

a	amplitude of transverse displacement of a string
α	acceleration of a point
f	frequency
f_1	frequency of first harmonic
f_n	frequency of the nth harmonic
f_R	ring frequency
c	phase speed
E	modulus of elasticity, Young's modulus
ρ	density of material
T	static tension in string
L	string length
a_x	cross sectional area
k_{st}	spring stiffness of string
k_{tt}	sensitivity of string anchor transducers
k_{tp}	sensitivity of tailpiece transducers
M_m	modal mass
m	mass per unit length, of string
P	total vertical load on bridge from strings
P_{spec}	spectrum of time-average power
R_e	real part
I_m	imaginary part
C	amount of vertical load on bridge, which is carried on the cross arch
L	amount of vertical load on bridge, which is carried on the long arch
T_{LSV}	amplitude of string tension under LSV
TF	transfer function
TF_{an}	analyser output voltage for a transfer function (volts/volt)
S_{tt}	auto spectrum of string tension vibration
Π	time average power transferred at a point
F	force

v	velocity
$\bar{v}_m$	space average velocity in the magnet gap
ω	angular frequency
T_{tt}	peak value of force in a spectrum
I	moment of inertia
K	flexural stiffness of a strip or plate
δ	deflection
Δ_{st}	static deflection of a beam under its own weight
k_{tt}	tailpiece transducer sensitivity
Y	mobility
Y	complex admittance
$\|Y\|$	magnitude of the admittance

List of abbreviations

EBX	end bouts cross arch
CBX	centre bouts cross arch
BEAR	Balance end arch ratio. The end arch ratio of a plate such that there will be no force moving the end bouts up or down (zero deviation).
EAR	End arch ratio.
LSV	String tension vibration, the periodic variation in the static tension of a string. String bellying LSV, and bridge rock LSV, refer to the cause of the LSV.
C/L ratio	Ratio of long arch to cross arch support of the bridge.
V156	Violin 156, normal EAR and medium deviation.
V157HD	Violin 157, normal EAR high deviation.
V157LE	Violin 157 fitted with wrong belly to give low EAR and normal deviation.
V158HD	Violin 158, normal EAR and high deviation.
V158HE	Violin 158 fitted with wrong belly to give high EAR and normal deviation.

RMS	Root mean square value of spectrum.
EMF	Electromotive force, voltage.
Q	Quality factor of a resonance peak.

Chapter 1

INTRODUCTION

1.1 Historical development

The violin first appeared about 1525, and apart from gaining its fourth string by 1550, has remained essentially unchanged; although changes have been made to the way in which it is set up for playing, in order to adapt it to modern conditions. The lack of an apparent evolutionary period can be explained by the fact that it was the amalgamation of the best features of three of the instruments in use at the time. The characteristic hourglass outline and the arched front and back came from the lira da braccio.

Within the confines of what constitutes a violin, there is scope for individual makers to bring their own ideas to the shaping of the parts, the graduation of the thickness, and to the varnishing. Most successful in these matters were the Italians Andrea Amati, Nicolo Amati, Antonio Stradivari, Giuseppe Guarneri Del Gesu, and the Tyrolian, Jacob Stainer. These makers, whose work was done between 1580 and 1740, were the trendsetters, each having made a considerable break from the style of their training to establish the highest reputation for the sound of their instruments. The vast majority of violinmakers, then and now, are simply content to copy the models of these masters. The old master patterns may easily be identified by the characteristic shape shown in the outline, and in the shape of the arching of the plates. A violin maker who wished to emulate the sound of a particular master's instruments would reproduce, by faithful copying, the outline and plate arching characteristic of the works of that master. This is done in the belief that these features are responsible for the sound quality of the instrument. The writer has been unable to find any published scientific material that might explain the connection between these features and the tone quality of the instrument.

The developmental process employed by the old masters must have been one of make it, play it, think about it, and then try a change to see what happens. Indeed the instruments left by these makers do show a more or less continuous process of experimentation. The great difficulty with this

process is that the tonal differences involved in the many very small changes being tried, are themselves very small, and it requires a very experienced and trained ear to audit them. Furthermore the changes tried, or experiments run, must carefully be thought out and form part of an overall conception, perhaps led by a hypothesis or a guessed insight. The necessary personal attributes for this work are given to few rare individuals in the history of the craft.

1.2 Future development

Many believe that the violin is now fully evolved to perfection and cannot be improved further. Certainly there has not been any change to the instrument since the early part of the 19th century. Others would say that today we are not able to make violins that are as good as those made by the great makers of the past. We live in an age where the scientific method is applied to problem solving. In 1819 Felix Savart confidently wrote "It is to be presumed that we have arrived at a time when the efforts of scientists and those of artists are going to unite to bring to perfection an art which has for so long been limited to blind routine" (Savart, 1819). The problem has proved surprisingly intractable and despite hopes being raised several times, blind routine has still not been replaced.

What contribution can the scientist make to the violin? To be of use to the violinmaker, science based studies must ultimately address the following matters.

- The relationship of the shape and thickness of the principal parts of the violin to its tonal quality.
- A specification of the physical and mechanical properties required of the surface coating.
- An objective means of assessing the sound of a violin.
- A method of accelerating the time it takes for a violin to reach tonal maturity.

To make progress in these areas it is necessary that we must first achieve a comprehensive picture of how a violin works. This project attempts to add to this picture.

1.3 The author's background

The author offers the following biographical sketch, to indicate what disciplines are being brought to the subject.

"I was born in New Zealand, and as a child learned to play the violin. After completing a degree in civil engineering at the University of Canterbury, I practised as a structural engineer. During the 1970s, I began to take a close interest in the published research material on violin acoustics. It became apparent to me that, the obvious fact that the front and back plates of violins were of a different shape had not been explained in any of the literature. Indeed contemporary violinmakers only made these differences because they appeared in the classical examples that they used as models to copy. I then produced a simple structural analysis of the static deformation of a violin body under the tension of the strings, and this led me to realise that the resulting deformations of the body were likely to be very dependent on the shape differences between the front and back. To find the degree to which the tone of the violin depended on these differences, I began making violins with controlled variations in plate shapes, and listening carefully to the resulting tone. This led in time to my learning Italian and going to Italy, mainly to study the Italian varnishing tradition, and finally to my becoming a full time violinmaker in 1981. Subsequently, in 1984, I moved to England and continued to experiment in a systematic way. I eventually felt the need to support my research with scientific measurement, and so I approached ISVR and was accepted as a part time postgraduate research student.

This work results then from a strongly interdisciplinary study. In order gain the insight presented in this thesis I have drawn on knowledge acquired as a violin player, a violin maker, a structural engineer and a scientific researcher."

1.4 Scope of the research

The principal focus of attention in this project is the contribution made by longitudinal string vibration to the radiated sound of a violin. The abbreviation LSV is used henceforth to denote 'longitudinal string

vibration', meaning a periodic change in the tension of the string, or the group of four strings.

The presentation begins with a qualitative static analysis of the forces and deformations of the violin body under string tension. The analysis is extended to suggest that classic violin arching shapes might enhance those body deformations that would be most likely to radiate sound. The initial static analysis is supplemented by measurement of the deformation caused by static string tension on a violin. The generation of LSV by 'string-bellying' is demonstrated both theoretically and experimentally. The modal vibration of the body also generates LSV. One of the many modal motions that generate LSV is 'bridge-rock' and this is demonstrated both theoretically and experimentally. The possibility that the arching shape would affect the radiated sound of a violin had been investigated systematically by making a number of violins (about 220) with small differences in the arching of the plates. This was done in the course of the writer's work as a violinmaker and was outside the supervised PhD programme. However since the conclusions reached by this make and play testing are relevant to the project, they are presented. From this and the qualitative theoretical static analysis, dimensional parameters that control the shape of the plates were identified as being likely to have an effect on the effectiveness with which the LSV forces can drive the violin to radiate sound.

Five violins were specially made to exhibit variations in the dimensional parameters 'EAR' and 'deviation' (later defined). These parameters largely control the arching shapes of the back and belly. Tests were also done on strings and bridges mounted on artificial supports providing differing mobilities. A number of special purpose measurement instruments were made. Using each violin the G string was driven to a standard first harmonic transverse displacement and the LSV force generated at the tailgut and the radiated sound were measured. The results were examined to see if there was a link between the radiated sound and the arching parameters and a link between the radiated sound and the magnitude of the LSV developed.

The admittance of the violin bridge to internal forces caused by a vibrating string is estimated and compared to the admittance found by others to an externally applied force. The power flow from the string to the violin through the bridge and the saddle is estimated and this is compared with the sound power radiated by the violin.

Chapter 2

BACKGROUND

2.1 Previous work

2.1.1 Introduction

Felix Savart was perhaps the first acoustics researcher to write about the violin, and laid down his understanding of the primary action that drives it [Savart, 1819]. This has remained to this day the widely accepted explanation of how a violin is driven, and is fully described by Lothar Cremer in his book, "The Physics of the Violin" [Cremer, 1983]. The bow sets up transverse vibrations in the string, which are in turn imparted to the bridge. The bridge sits on the violin and is supported on its bass side by the bass bar and on its treble side by the close proximity of the sound post. The sound post extends to the back plate and provides a rather more rigid support than the bass bar. The impulse from the transverse vibration of the string causes the bridge to move largely in its own plane in a manner that can best be understood as a rotation about a point.

This point is not fixed, due to the frequency dependent variation of the impedance of the body under the bridge feet. However, throughout much of the range it is located between the bridge feet, rather closer to the more rigid sound post side. This movement of the bridge lifts the bass bar and with it a large part of the front, and to a lesser extent, depresses the sound post and with it part of the back; and then reverses the action. The alternate moving apart and together of the plates initiates a limited breathing action in the body. Cremer presents a theoretical evaluation of the magnitude of these forces and the expected bridge rotation.

These actions are centred at the bridge area, which is at a point remote from the widened plate areas (called the "end bouts"). It has been assumed that body resonance must play a significant role in enabling the small forces generated in the bridge area to move the end bout plate areas. These areas are reported to move rather more than the bridge area in the range up to 3000Hz [Moral and Jansson, 1982].

2.1.2 The vibration of the strings

The vibrations of the strings have been closely examined. Helmholtz made the notable discovery of the stick-slip action of the bow on the string and the resulting travelling kink and saw tooth waveform. Further notable contributions were made by Raman. The body of knowledge related to the string is comprehensively presented by Cremer. Of particular relevance to this thesis is that longitudinal resonances in the string have been demonstrated [Lee and Rafferty, 1983]. The possibility that longitudinal vibrations would be set up in a vibrating string as the result of its length changing throughout the cycle has been mentioned by several writers. Most have expected the resulting tension vibration to be an octave above the transverse vibration although Woodhouse has suggested they are mistaken [Woodhouse, 1977]. While the possibility that longitudinal string vibration might contribute to the radiated sound has been recognised, there is no published work on the subject.

2.1.3 The vibration of the bridge

The translation, twisting and bending motions of the bridge were experimentally measured [Minaert and Vlam, 1937]. The motions of the top of the bridge were also investigated dynamically by Boutillon and Weinreich and the mobilities were found to be of the same order (Boutillon and Weinreich, 1999).

The violin bridge has been shown to have resonance frequencies at 3000Hz, which involved a top half rotation, and 6000Hz, which involves vertical bounce (Reinicke, 1973). The ability of the bridge to transfer force to a rigid base was shown to increase significantly at the 3000Hz resonance but not noticeably so at the 6000Hz resonance. In 1998, experiments were reported that showed that the bridge on a real violin behaves as a rigid lever at all frequencies within the range 0 to 5 kHz, there being no resonance within it [Runnemalm, Molin and Jansson, 1998]. There must of course be elastic deformation in the bridge but this research reported that the resonance shown in a bridge mounted on a rigid base did not occur when it was mounted on a real violin.

2.1.4 Experiments in total loudness

Spectra of the total loudness of the violin were examined by sounding all the notes on the violin. In 1937, Saunders used hand bowed excitation [Saunders, 1937]. He concluded that the perfect violin should be even on all notes, although none of the violins he tested came near this.

Similar spectra were produced by Raman, Meinel, Rohloff and Pasqualini, but these all used mechanical bowing [Raman, 1920: Meinel, 1937: Rohloff, 1940: Pasqualini, 1938-39]. Meinel compared many violins with a Strad. and concluded, unlike Saunders, that the total sound should be low between 1000 and 2000Hz to avoid a nasal tone, strong from 2000Hz to 3000Hz to get brightness, and strong at low frequencies to get carrying power. How such detailed conclusions were reached from the total loudness without spectral analysis is not clear. Total sound measurement and no easy means of spectrally analysing the result limited progress. Later, sine wave excitation by driving the bridge electromechanically eliminated the need to spectrally analyse the result.

2.1.5 The radiated sound spectrum

By using swept sine wave electromagnetic excitation of the bridge, radiated sound spectra can be produced. By this means Saunders produced radiation response curves for a number of Stradivari violins, and instruments by contemporary makers [Saunders, 1946]. Despite attempts to identify characteristic differences that would distinguish those of Stradivari from those of the other makers, no consistent differences were found.

Dunnwald produced radiated sound spectra and by comparing the result for Italian violins with others, he suggested that certain features of the shape of the response curve could be objective indicators of tonal quality [Dunnwald, 1985].

Langhoff measured the radiated sound spectrum of a number of violins and devised a 3D system for their presentation [Langhoff, 1994]. Attempt was made to relate the 3D presentation to the tonal quality of the instruments.

Using the principal of acoustic reciprocity, Arnold and Weinreich placed the violin in a sound field measured the resulting string vibrations and sound

pressure inside the body [Arnold and Weinreich, 1982]. From the data collected, they were able to produce spectra of resonance in the lower frequency range.

Considerable similarity of shape exists between the spectrum of bridge admittance produced by Jansson and the radiated sound spectrum produced by Dunnwald [Dunnwald, 1982: Jansson, 1997]. Both experiments were done by the excitation of the bridge by electromagnetic drivers. This similarity was also demonstrated by Cremer who reproduced curves (after Beldie) of bridge admittance and sound pressure level in a reverberant room. In terms of received wisdom about how the violin works these experiments could be said to show that violin radiation varies as the bridge admittance, and therefore depends on body resonance.

2.1.6 The bridge admittance

The spectrum of variation of bridge admittance with frequency has been investigated. The bridge has been driven with electromagnetic drivers and its movement recorded. The admittance of the body and the position of its resonances were inferred from these data. Moral and Jansson swept the bridge with a sine wave excitation and measured the bridge admittance. The modal shapes corresponding to the main resonances were found by interferometry [Morral and Jansson, 1982: also Jansson, 1994: Saldner, Molin and Jansson, 1996]. The bridge admittance has also been inferred by exciting the violin by impacting the bridge with a pendulum.

Dunnwald compared the admittance spectra of ten Italian master violins, ten fine modern violins, and ten cheap factory violins [Dunnwald 1985]. The main difference lay in the range above 2kHz. The fine modern violins responded more strongly in this area than the old Italians and the factory violins were weaker in this area than the old Italians. Generally, the spectra of bridge admittance are more variable than the spectra of total loudness. This is simply the result of the averaging effect of many harmonics being included in the total loudness spectra.

Boutillon and Weinreich, proposed a new method for measuring the admittance of the bridge, but perhaps more significantly showed that the bridge has admittances of comparable order in the three coordinate

directions [Boutillon and Weinreich, 1999]. They also showed that a force applied in one of the coordinate directions produced movement in the other two directions. In this thesis, close attention is given to those components of string vibration that would excite vertical and out of plane bridge movement. Boutillon and Weinreich's work is highly relevant to this.

Although the admittance of the bridge to an external force has been well studied there does not appear to have been any work done on the admittance of the bridge to transverse force from a vibrating string.

2.1.7 The shape of body modes

The shape of some individual single frequency modes has been investigated. As early as 1931, Backhaus showed that at about 685Hz a good violin radiates as a monopolar or simple source radiator, called in German a "Nullstrahler" [Backhaus 1931]. Below that frequency, the modal shapes form bipolar radiators. As the frequency rises above 700Hz there is an increasing tendency for the surface to break up into smaller radiating areas. Backhaus concluded that the ability to form a Nullstrahler at 685Hz was a characteristic of good Italian violins. Schelleng drew attention to the need for some explanation for Backhaus's observation that good violins radiated as a Nullstrahler at about 650 to 700Hz [Schelleng, 1968]. The problem was that there is no natural body resonance at that frequency. It lies between strong resonances at 500 and 750Hz. This interesting point is addressed in the work of this thesis.

A comprehensive modal analysis of the violin was done by Marshall [Marshall, 1985]. The mathematical process of modal analysis was believed to have eliminated the effect of modal overlap. Modal overlap causes the operating shape at any frequency to have substantial contributions from more than one mode. Of particular relevance to this thesis is that he identified a Nullstrahler (breathing in the whole body) at 690Hz and additionally breathing in the lower bouts only, at 478Hz and in the upper bouts only, at 930Hz. Jansson tested 25 violins of soloist quality and found that a common factor was a dominant C3 mode. He described this as a major parameter of high quality violins. The C3 mode is the same mode referred to by the Americans as the B1 mode. It is the monopole or Nullstrahler mode. This mode dominated the violin's response in the range

500-600Hz. The position of this resonance was found to be a matter of the stiffness of the back and the magnitude was found to relate to the position of the sound post [Jansson, Niewczyk and Fryden, 1996].

The modal shapes of the many modes that make up the spectrum have been investigated [Marshall, 1985: Jansson, Molin and Saldner, 1994]. The resonances have been categorised as wood or body resonances, air resonances, and bridge resonances, and all have been fairly exhaustively examined [Hutchins 1990, 1998: Shaw, 1990].

It is recognised that of the many modes identified (something like 35 in the range up to 1300Hz), only a few of them may be significant sound radiators. Arnold and Weinreich have suggested that, at any forcing or driven frequency, a violin moves in a combination of four basic normal modes [Arnold and Weinreich, 1982]. These are a breathing motion when the violin expands and contracts and so inhales and exhales, a bending motion, a Helmholtz motion when the air vibrates in and out of the sound holes, and an internal air sloshing motion. In this thesis, the causes of the breathing and bending components are studied in some detail.

Violins with and without sound posts have been studied by exciting the violin both directly at the bridge and reciprocally in a sound field [Saldner, Molin and Jansson, 1995]. The modal shapes were examined by holography. This showed that at some frequencies several modes contribute substantially to the response.

2.1.8 The air modes

Jansson examined the air modes within the body cavity of a violin and on a body immobilised by encasing it in plaster [Jansson, 1973]. In addition to the well-known Helmholtz mode that radiates through the sound hole, there are a number of other modes. At least one of these is coupled to the top plate vibrations.

By changing the body holes on a violin, the effect on the radiated sound spectrum of varying the air modes was examined [Hutchins, 1990].

2.1.9 The relative position of the principal modes

After trying radiated sound spectra, Saunders returned again to the loudness curves and pointed out that the relative position of the air mode and the principal wood modes may be a simple and important determinant of violin tonal quality [Saunders, 1953]. He was again guided by his conviction that a uniform loudness spectrum was desirable.

This idea was taken up by Hutchins, who measured the response curves for many violins and discussed tonal preferences with the owners. From this she concluded that the frequency gap between the principal air mode A1 and the principal body mode B1 determined what sort of player would like the violin. Soloists seemed to prefer a 65 to 80Hz gap and chamber music players preferred a gap some 20Hz smaller. The gap could be widened by the maker tuning the free top plate to a higher resonant frequency.

2.1.10 Damping and varnish

The damping effect of varnish was investigated by Meinel and shown to give a modest reduction in the amplitude of his loudness curve [Meinel, 1957]. His experiments on strips of varnished wood showed that hard varnishes had a greater damping effect at higher frequencies.

Conversely, Schelleng found the damping effect of varnish to be independent of frequency [Schelleng 1968]. He claimed that the varnish reduced the tonal volume of a violin by 2 to 5 dB across the whole frequency spectrum. He also found that a detached belly could be damped three times as much as a detached back.

The effect of varnish on the long and cross grain stiffness and damping has been studied, and the resulting effect on the modal shape found [Schleske, 1998]. The effects varied considerably with the varnish and in general reduced modal displacements by 2.6db. No measurement of the effect on radiated sound was reported.

The damping effect on the radiating modes has given rise to a consensus among many scientists that varnish is necessary for the preservation of the instrument but the less applied the better. The conviction held by many makers that the varnish is responsible for the supremacy of certain Old

Italian violins is dismissed as unlikely by most scientists [Gough, 2000]. The effect of varnish on the radiated sound of a bowed violin does not appear to have been measured.

2.1.11 Desirable tonal qualities

The harmonic content of played notes on the violin has been analysed to investigate the subjective effect of spectrum shape. Rohlhoff suggested that good Italian violins produce a tone that is strong in the 6th and 11th harmonics [Rohlhoff, 1950].

It has been mentioned that Meinel reported what to do to avoid a nasal tone. Emil Leipp says a nasal sound is a quality of good Italian instruments [Leipp, 1969]. This conflict is typical of the subjective nature of what constitutes good sound.

2.1.12 Acoustic properties of the components

The violin is assembled from parts and it is not unreasonable to assume that if the two principal parts, the back and the front, are closely investigated it may be possible to write a prescription for them, such that when assembled they would produce a good violin. Accordingly, the resonances of the detached plates have received much attention. This has been related to achieving control by adjusting the thickness of the plates.

In the 1830s, Savart examined the detached plates of a number of Guarneris and Stradivaris, and using the method of Chladni, mapped the modal shapes and recorded their frequencies. This is the only recorded information on detached plates that we can be reasonably sure would make a fine violin. The value of these violins today makes it unlikely that the opportunity will occur again.

Beldie, in 1969, mapped all the free plate modes of the back and belly, both with and without the bass bar and using various holding and tapping places [Beldie, 1976].

Hutchins et. al. from the 1950s have concentrated on establishing recommended eigenmode shapes and frequencies for detached backs and fronts such that when assembled into an instrument the tonal result will

be good and predictable [Hutchins, 1962]. This does involve "make and play " testing with its inevitable subjective judgements.

Hutchins' recommendations have been refined over the years, and involve the placing of three of the natural plate modes at predetermined frequencies [Hutchins, 1998]. Hutchins also used hologram interferometry to map the free plate modes and developed a system for altering wood thicknesses to achieve ideals of modal shape. How these ideals were established was not made clear.

2.1.13 The arching of the front and back

Nearly all the violins made by the old masters show a pronounced difference between the arching shape of the front and back plates [Sacconi, 1972]. It has been suggested by some that there should not be any such difference, and that where there is, it is the result of long-term creep in the wood [Leipp, 1969]. Most violinmakers find this explanation unconvincing and so they reproduce the arching shapes of classical examples. There does not appear to be any published work that suggests why this difference should exist.

Cremer modelled the arched plates as a stiff hat with a flexible brim. The mass of the stiff hat and the flexibility of the brim were seen as the significant variables that determined the plates performance. He was not alone in having this concept. It has been suggested by a number of people that the reason a violin gets better with age is that the glue on the purfling weakens, and the "hat" becomes more flexible in its brim.

Some work has been done to see if high arched violins show different bridge admittance spectra to moderately arched violins [Jansson, Benedykt and Niewczyk, 1997]. It was tentatively concluded that the 500-600Hz peak (Nullstrahler) was more easily achieved in violins of moderate arch height.

2.1.14 The function of the sound post

The acute sensitivity of violin sound to the placing of the sound post is well known to makers and players alike. Work has been done in this field, which has shown that the violin's modal shapes and their resonance frequencies are very insensitive to the position of the sound post, and even insensitive to the difference between a violin with a sound post or without a

soundpost. [Schelleng, 1971: Bissinger, 1995, 1998: Saldner Molin and Jansson, 1995]. This has left the acute sensitivity of a violin's tone to the position of the sound post without explanation.

A concise summary of existing wisdom is provided by Colin Gough [Gough, 2000].

2.2 Comments and observations on received wisdom

The violin is seen then as being excited by the transverse vibrations of the string, and this excitation engages a host of natural resonances in the body. The art of violinmaking is the art of placing these resonant peaks at appropriate points in the frequency spectrum. If this is the art of violin making, expressed in terms of received scientific wisdom, then immediately we have a problem. There is no common factor in the location of resonant modes in the frequency spectrum, which is exclusive to violins of fine tone. If the object of this placement is to ensure that they fuse together to form a continuous even response, then it should be noted that the resonant response spectra of great classical violins come nowhere near achieving this. If the object of the placement is to establish formants, it should be noted that the radiated sound spectra of fine violins do not show sufficient consistency for an ideal formant to be found. Early experimentation was done with a bowed excitation. This was replaced with direct bridge excitation. With the availability of fast Fourier analysis, there would seem to be no reason not to return to bowed excitation.

The literature often confuses the difference between a modal shape and an operating shape. The shapes determined by experimental method can rarely be identified as arising from an individual resonance. At low frequencies, some widely separated modes could perhaps be excited in isolation. Studies of violin modes are usually based on the modes established in a violin that is excited by some means other than string swinging. It is suggested in this thesis that these modes may not be representative of the modes excited in the bowed violin.

The placing of the resonant peaks is to be controlled simply by the graduation of the thickness of the front and back plates. The effect on the sound caused by the shape of the arching of the plates is not understood

rationally and so traditional classical models are followed. Believing that plate arching played no significant part in the driving of a violin, Savart designed a simplified violin that had completely flat plates like a guitar. It did not catch on.

No case has been made that the position of the body resonances is a determinant of tonal merit. That is not to say that it is without effect on the sound. The amount of wood left in the plates clearly affects the mass and stiffness of the excited modes. However, having suitable mass and stiffness available does not mean the violin will adopt the best operating shapes and optimise the sound quality.

Hutchins claims that there is some tonal benefit in controlling the plate thicknesses to place the eigenfrequencies of some of the principal modes in certain relationships. Good violins have been made in compliance with these recommendations, and in contravention of them. There is no reason to believe that these criteria bestow any benefit. To correctly place these eigenmodes, it may be necessary to place certain limitations on the arching shape that can be used, and would therefore act as a control on the shape of the plate as well as its thickness. If so, then it would be up to the violinmaker to find these restrictions. In practice, violinmakers would only use the eigenmodes as a control on plate thickness, not shape. She writes, "in an analytical sense the eigenmodes and eigenfrequencies of the parts, fully define those parts". In principle, one cannot disagree with that, but to really fully define those parts may require the defining of so many eigenmodes that it becomes impractical to describe it in that way alone. If one were to define the arching shape and two of the principal eigenfrequencies, the definition becomes much sharper and the violinmaker would know how to go about making it. The mass and stiffness are not defined by the eigenfrequencies, but it could be assumed that the use of what is traditionally recognised as good wood would ensure that appropriate values are obtained.

Most violinmakers of today are all well aware of the plate tuning recommendations made to them by scientists who believe that correctly placed resonant peaks are the main determinant of good tone. Most violinmakers who have tried this have found it to be irrelevant and

disregard it. The wide variation in the plate thicknesses found in classical violins would indicate that there is a considerable variation in the eigenfrequencies between these violins.

There is no published work that seeks to identify the relative importance of stiffness, mass, and resonance frequency as determinants of tonal consistency in violin plates. All three of these are, or have been, used by violinmakers. The writer uses the plate flexural stiffness for this purpose and is not aware of there being any other makers who do (see Appendix E). The writer has satisfied himself that a much greater degree of consistency between violins can be achieved by working to fixed relationships of plate stiffness rather than plate resonance frequencies.

Hutchins suggestion that the frequency gap between the A0 mode (the Helmholtz air mode) and the B1 mode (the first body mode) may be important is a restatement of what violinmakers have always known. The resonance frequency of the A0 mode is proportional to the square root of the ratio of the area of the sound holes to the volume of the body. The sound hole area and the body volume vary little between violins and the square root further reduces the variation in the A0 modal frequency. The gap between the A0 mode and the B1 mode is largely a matter of the position of the B1 mode. The B1 modal frequency is sensitive to the thickness of the wood. It should be noted that the flexural stiffness of the plate is also sensitive to the thickness of the wood. Therefore, in adjusting the wood thickness one is altering the plate flexural stiffness and the frequency gap between the A0 and B1 mode. Should one work to criteria of resonance, or perhaps flexural stiffness? Violinmakers have always known that the more wood one leaves in the body the more it will appeal to the heavier player. Hutchins found that the greater the frequency gap between the A0 and B1 mode the more the violin will appeal to stronger players.

It is the writer's belief that the variation in radiated sound between old violins, new violins and factory violins as shown by Dunnwald, may reflect certain 20th century tendencies in lutherie. Factories over-thin violin plates to get a bland inoffensive but weak sound, while makers of fine violins have reacted against this tendency by leaning the other way and, more often than not, leaving too much wood in the plates. Had the three groups of

violins all contained violins of the same weight, the spectra produced might have looked much the same.

The failure of existing theories to explain such basic things as the sensitivity of the sound post, and why the plates of a violin are arched upwards, does suggest that these basics need to be re-examined.

One would expect that if the sound radiation of a violin were highly dependent upon structural resonance then the sound would alter audibly if the plates were damped. In fact, the violin is surprisingly insensitive to damping. It is possible to touch firmly with the fingers almost anywhere on the vibrating plate surface without making much audible difference to the radiated sound. One would also expect the tone quality and volume of sound to vary from one note to another on the violin as various resonances are excited. There is indeed considerable variation note to note, but these are nowhere near as great as would be consistent with typical modal quality factors.

There is a belief widely held among experts and connoisseurs of old violins that the superior sound of Cremonese violins is due to the varnish [Hill, 1901]. The research done to date does not account for this. Those with confidence in science would say that the superiority of Cremonese violins is unlikely to be due to the varnish. Those who sympathise with the prevailing opinions of violin experts would say that the contribution of varnish to violin tone is not fully understood scientifically. For example, the writer has found that it makes a clearly audible difference to the sound whether the varnish penetrates into the wood slightly, or if it is not allowed to penetrate at all. There is no obvious reason why this should be so since it cannot be explained by changes in damping or in the mass/stiffness relationship. In this thesis some evidence is presented that would suggest that the radiated sound spectrum of a violin could be considerably changed in shape by varnishing.

There is no tonal quality that has been universally agreed to be superior. While the German, Meinel, has advised us how to ensure that the tone is not nasal, the Frenchman, Liepp, is telling us that the Italian tone is always nasal. It seems that the Italian sound is all things to all men. The German who likes a hard sound, the Frenchman who likes a nasal sound

or the Englishman who likes a mellow sound all find the old Italian violin to be the embodiment of these preferences. It is notable that pianos, organs and singers all follow these national tonal preferences, which arguably stem from the quality of the spoken language, which for most of us is our earliest musical experience. It would appear that if the tone has it all, the listener could take from it what they will.

Tests have been done on many occasions over at least 200 years, where several violins of contrasting age and value are played solo to a discerning audience. They were asked to rank them in some way. These tests invariably produce results that show no strong consensus and often put a cheap violin ahead of a fine Stradivarius. Players continue to make great sacrifices to buy antique violins made by makers of high reputation. Either the players are wrong in thinking that some violins are better than others, or the testing system of playing violins solo to an audience is unable to highlight the significant difference. Since the science of violin acoustics has been unable to account for significant differences in violin tone quality and rather idealised tests made with audiences have not established a clear superiority for any violins, some scientists have concluded that there is no difference. This viewpoint was argued by Beament [Beament, 1997]. To uphold this view requires more confidence in science than the collected consensus of players and listeners accumulated over several centuries. MacIntyre and Woodhouse have suggested that the evidence for the superiority of some violins is probably present in all the data that has been collected but that it lies camouflaged. The human ear and brain can recognise auditory patterns that are undetectable when seen visually as scientific data [MacIntyre and Woodhouse, 1978].

The writer believes that there is such a thing as a superior violin, and that they are sufficiently rare and sufficiently better as to create the high prices they bring. The main distinguishing attribute they have is their ability to produce a quality of tone that can be heard when played with a considerable number of competing musicians. The violin concerto is the classic situation. This is not likely to be a matter of being simply louder. There has been very little done scientifically to identify if there is a band in the quality of the tone produced, which helps this communication with the audience. It could be argued that if there were such a band it would show

up in the swept sine wave radiated sound spectra (with external excitation of the bridge) as a formant.

2.3 The Starting Point for this project

The sound radiation from a violin arises through the excitation of vibrational modes. Each mode may be excited at resonance by a string harmonic, or may be forced at a frequency above or below resonance. When operated below its resonance frequency, a mode does not normally contribute significantly to the radiated sound. The modes excited at any one frequency will depend also on the disposition of the forces applied to the body. It could be argued that the shape of the violin body has evolved to provide an optimum palette of modes for excitation. It would follow then that any change to the shape of the body would result in a change in radiated sound because of a change in the modal shapes and frequencies. The writer will endeavour to show that certain back and belly shape characteristics are capable of determining the driving forces on the plates. Alteration of these shape characteristics favour co-operation between string and body modes and hence have an important influence on radiated sound level and quality. They may also influence playability. It is suggested that any such influence is through the effect on the driving force on the plates rather than the change in the geometry per se.

To date, consideration of the driving forces on the body of a violin stops at some estimate of the transverse forces on the bridge from the vibrating string. In this thesis the driving forces at the three entry ports to the body are considered, and going beyond the ports into the body itself, a static analysis is made of the internally developed forces within the body. In addition to the forces arising from the transverse vibration of the strings, consideration is given to the forces arising from the longitudinal vibration of the strings.

It is obvious that the magnitude of the static force on the box is very large compared with the small bridge rocking forces generated by the transverse vibration of the strings. Since longitudinal string vibration is to be abbreviated to LSV, it seems logical to call transverse string vibration TSV, henceforth. Most violinmakers are aware that the body does deform under

the action of the static forces. This is most easily observed when the strings are brought up to full tension. Violin plates, which previously conformed to the shape of a template, show significant movement when the strings are tightened. If there were any variation in the static forces on the body, there would be a consequential change to the shape of the body. Such variations could come from periodic vibrations in the string tension (LSV).

Most of the previous work done on the violin has been based upon measurement of the response of a violin when excited externally, by electromagnetic or impact excitation of the bridge. The work of this project suggested that the contribution of some of the LSV could be lost if the bridge was excited externally, so a repeatable means of string swinging excitation of the violin was developed. Violins with various arching shapes both with and without varnish were tested.

Chapter 3

LONGITUDINAL STRING FORCE AND BODY MOTION

3.1 Introduction

The body of the violin has an input from the vibrating string through three ports. These are the bridge, the saddle (the ebony insert over which the tailgut passes), the stopped end of the string (or if the string is open, the nut at the end of the finger board). More energy probably enters the body through the bridge than the other input ports, but in this chapter qualitative consideration is given to the input at all three ports. The bridge input is widely understood to arise from the transverse force at the top of the bridge (TSV force), but this thesis investigates the role of longitudinal string vibration (LSV). In this chapter, the forces applied to the ports from string vibration are assessed and a qualitative static analysis of the body deformations caused by a static application of these forces is presented.

When the strings on a violin are brought up to tension, forces are applied to the body, which must cause it to deform. Any action that causes a fluctuation in the tension of the strings must also cause a fluctuation of the body shape. We begin by looking at ways in which the string tension might fluctuate.

3.2 Origin of longitudinal string vibrations

LSV can arise from the stretching of the string as it swings, and from the relative movements of the bridge, the nut and the saddle. The resulting LSV vibrations may be reinforced by the natural longitudinal resonances of the string, and resonances of the tailpiece.

3.2.1 String-bellying longitudinal string vibrations

Consider a string stretched between rigid a support, which has been set in transverse resonant vibration in a single mode. Each time the string swings away from the straight-line position, it must stretch, and on its return, it will shorten again. For every cycle of transverse vibration, there must be two such lengthening and shortenings, with two consequential fluctuations in string tension. Thus, every transverse vibration of the string would appear to induce an LSV in the string of double the frequency. This will be

referred to as the 'string-bellying longitudinal string vibration' or 'bellying LSV'. The magnitude of this vibration increases non-linearly with the amplitude of transverse vibration.

The amount by which the string stretches can be calculated for each string mode as follows.

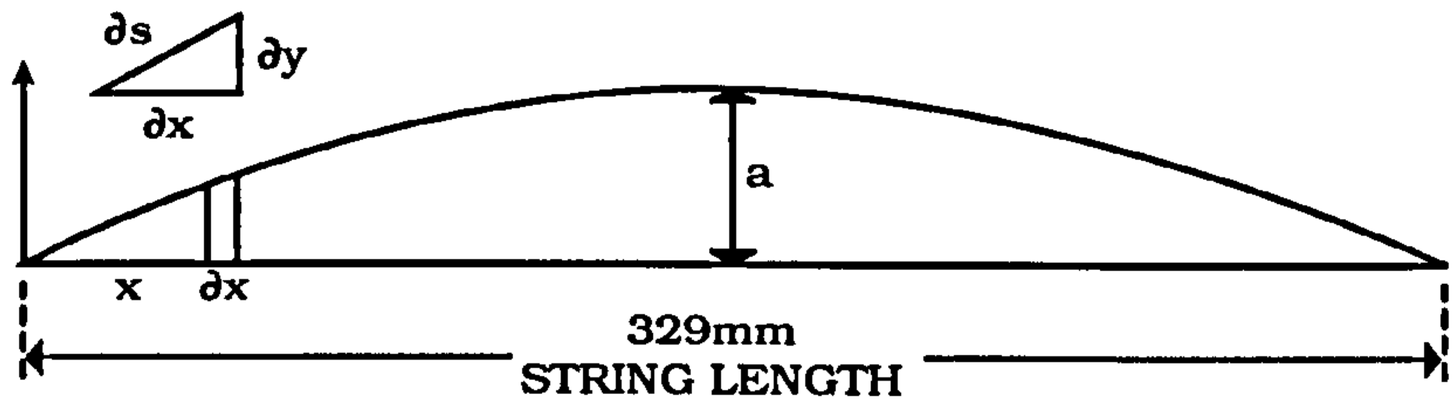

The deformed shape of the string is taken as being a sine curve. This assumption is only valid if the increase in string tension as the string stretches is ignored. If that effect is included the calculation becomes more complex and it is found that a number of higher harmonics are introduced. Since the predominant effect of string bellying is to introduce a string tension vibration of twice the frequency the complication of the higher order harmonics has been omitted.

$$\delta s^2 = \delta y^2 + \delta x^2$$

$$\left(\frac{\delta s}{\delta x}\right)^2 = 1 + \left(\frac{\delta y}{\delta x}\right)^2$$

$$\frac{\delta s}{\delta x} \approx 1 + \frac{1}{2}\left(\frac{\delta y}{\delta x}\right)^2, \text{ when } \left(\frac{\delta y}{\delta x}\right) \text{ is very small.}$$

$$ds = \left[1 + \frac{1}{2}\left(\frac{dy}{dx}\right)^2\right]dx$$

$$\text{and} \quad s = \int_0^L \left(1 + \left(\frac{dy}{dx}\right)^2\right)^{1/2} dx$$

$$= \int_0^L \left(1 + \frac{1}{2}\left(\frac{dy}{dx}\right)^2\right) dx t \quad y = a_n \sin\frac{n\pi x}{L}.\cos n\omega_1 t$$

Let $y = a_n Sin\left(\frac{n\pi x}{L}\right) Cos n\omega_1 t$ where ω_1 is the natural frequency of the fundamantal mode.

$$\left(\frac{dy}{dx}\right)^2 = \left(\frac{na_n\pi}{\mathrm{L}}\right)^2 Sin^2\left(\frac{n\pi x}{\mathrm{L}}\right)Cos^2(n\omega_1 t)$$

$$\text{Therefore } s = \int_0^{\mathrm{L}} dx + \frac{1}{2}\left(\frac{n\pi a_n}{\mathrm{L}}\right)^2 Cos^2(n\omega_1 t)\int_0^{\mathrm{L}} Sin^2\left(\frac{n\pi x}{\mathrm{L}}\right)dx$$

$$= \mathrm{L} + \frac{n^2\pi^2 a_n^2}{4\mathrm{L}}Cos^2(n\omega_1 t)$$

$$\text{and } \Delta\mathrm{L} = s - \mathrm{L} = \frac{n^2\pi^2 a_n^2}{4\mathrm{L}}Cos^2(n\omega_1 t)$$

$$\text{But } Cos^2 2\phi = 2Cos^2\phi - 1, \text{ so } Cos^2\phi = \frac{1}{2}(1 + Cos2\phi)$$

$$\text{Therefore } \Delta\mathrm{L} = \frac{n^2\pi^2 a_n^2}{8\mathrm{L}}(1 + Cos2n\omega_1 t) \text{ of which the time varying part is,}$$

$$\Delta\mathrm{L}(t) = \frac{n^2\pi^2 a_n^2}{8\mathrm{L}}Cos2n\omega_1 t$$

Let us assume that the string extends from a fixed tailpiece, over a bridge to the playing length and then to a fixed point at the other end of the playing length. Then the total length from the tailpiece to the other end will be able to stretch.

$$\text{Then, } \Delta\mathrm{T} = k_{st}\frac{\Delta\mathrm{L}}{(\mathrm{L} + \mathrm{L}_1)} \text{ where } k_{st} \text{ is the spring stiffness of the string, } (\mathrm{L} + \mathrm{L}_1)$$

is the length of the string from the nut to the tailpiece, and L_1 is the length from the bridge to the tailpiece.

Thus the amplitude of the LSV force in the string is given by,

$$\mathrm{F}_{\text{bellying LSV}} = k_{st}\frac{n^2\pi^2 a_n^2}{8\mathrm{L}(\mathrm{L} + \mathrm{L}_1)} \text{ at twice the frequency of the n}^{\text{th}} \text{ harmonic.....(3.1)}$$

If the string is assumed to be vibrating simultaneously in an arbitary number of modes, each at its natural frequency ω_n,

$$\left(\frac{dy}{dx}\right)^2 = \left(\frac{\pi}{\mathrm{L}}\right)^2\left[\Sigma_n na_n \cos\frac{n\pi x}{L}\sin(\omega_n t + \phi_n) \times \Sigma_m a_m \cos\left(\frac{m\pi x}{\mathrm{L}}\right)\sin(\omega_m t + \phi_m)\right]$$

$$\text{so} \quad \mathrm{s} = \mathrm{L} + \frac{1}{2}\left(\frac{\pi}{\mathrm{L}}\right)^2\int_0^{\mathrm{L}}\left[\Sigma_n\Sigma_m nma_n a_m \cos\left(\frac{n\pi x}{\mathrm{L}}\right)\cos\left(\frac{m\pi x}{\mathrm{L}}\right)\sin(\omega_n t + \phi_n)\sin(\omega_m t + \phi_m)\right]dx$$

The cross terms within the integral disappear because of orthogonality. This equation can be simplfied to give the string extension,

$$\Delta\mathrm{L} = \frac{\pi^2}{8\mathrm{L}}\Sigma_n n^2 a_n^2[1 - \cos 2(\omega_n t + \phi_n)]$$

$$\text{So, } \Delta\mathrm{T} = \frac{k_{st}\pi^2}{8\mathrm{L}(\mathrm{L} + \mathrm{L}_1)}\Sigma_n n^2 a_n^2[1 - \cos 2(\omega_n t + \phi_n)]$$

Taking the time-varying part only gives,

$$\Delta\mathrm{T}(\mathrm{t}) = -\frac{k_{st}\pi^2}{8\mathrm{L}(\mathrm{L} + \mathrm{L}_1)}\Sigma_n n^2 a_n^2 Cos(2\omega_n t + \phi_n), \text{ which is the sum of the time dependent}$$

tensions in each mode.....(3.1a)

The analysis given above assumes that the string tension is the same on both sides of the bridge. This would certainly be true as we consider this as a static model. It was shown dynamically by Boutillon and Weinreich that the bridge does move considerably normal to its plane [Boutillon and Weinreich, 1999]. It would of course only require microns of movement of the tip of the bridge to justify the assumption. If the bridge were to make this accommodation it would require bending of the bridge, as has been shown to happen by Minaert and Vlam, or a bridge tilt which seems very possible if the belly wood between the sound post and the bridge foot should flex [Minaert and Vlam, 1937].

The bellying LSV force can be evaluated as a function of amplitudes of string displacement and for vibration at various harmonics. Fig. 3.1 shows the result for an open third string (Thomastic Dominant mittel gauge).

Example: For a first harmonic vibration of third string measuring 6mm (peak to peak): a_n=3mm. Vibrating string length L=328mm. Extra string length involved in stretching L_1=55mm. k_{st}= 2213N (from Appendix B) for a third string.

$$F_{bellying} = 2213 \times 1000 \frac{1^2 \pi^2 3^2}{8 \times 328 \times 383} = 196.1 mN$$

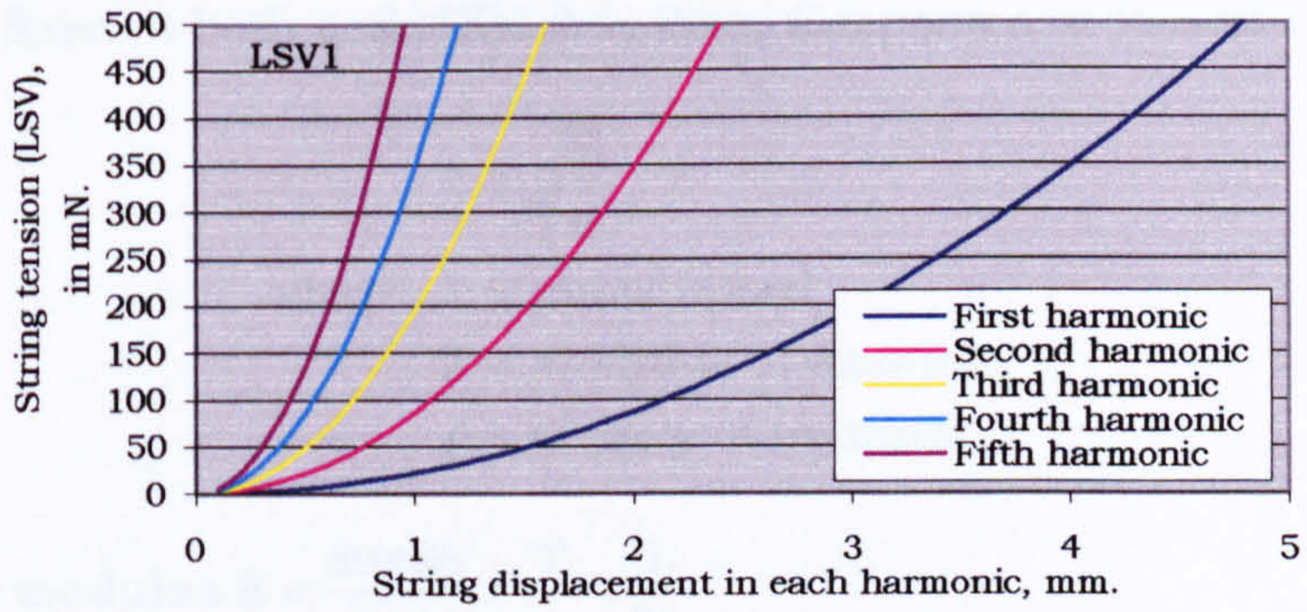

Fig. 3.1. Theoretical string tension caused by bellying, shown for a "Dominant" D string.

String-bellying LSV is the only significant cause of LSV that is directly due to string vibration, in the sense that it arises in the string itself.

3.2.2 Longitudinal resonances in a string

In longitudinal vibration, the straight tensioned string behaves like a bar, and therefore would have resonance frequencies corresponding to each harmonic of longitudinal vibration. In assessing these resonance frequencies one is at once confronted with a very complex mathematical model. The end restraint conditions must have certain mechanical impedances that certainly are not known to us. Then there is the factor of the change in direction of the string as it crosses the bridge. This may cause some of the longitudinal wave to be reflected at the bridge while permitting the remainder to continue.

We might consider the simple case of a bent string of length L with rigid end fixings and ignore the effect of the bend and any inertial forces arising from out of plane bridge deformation.

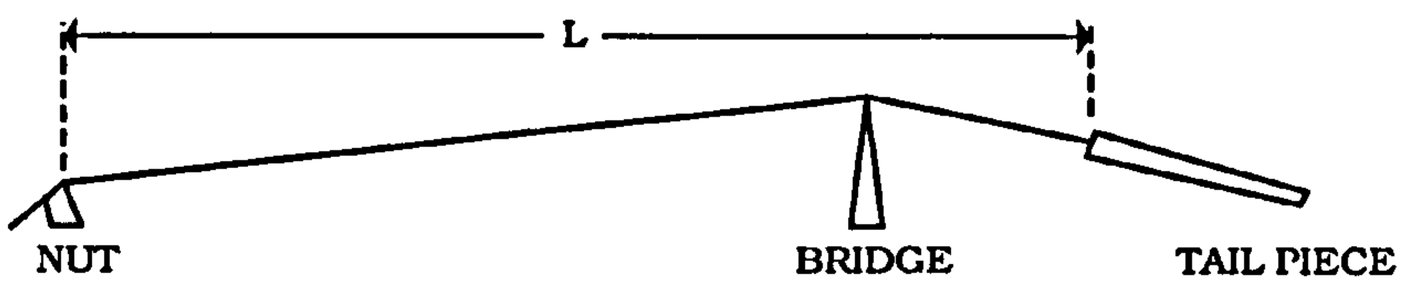

From Kinsler, Frey, Coppens and Sanders, for longitudinal vibrations in a bar rigidly fixed at both ends [Kinsler, Frey, Coppens and Saunders, 1982].

$$c = \sqrt{\frac{E}{\rho}}$$

where c = phase speed
E = modulus of elasticity
ρ = density of material

$$\text{The elastic modulus } E = \frac{\text{stress}}{\text{strain}} = \frac{T}{a_x} \times \frac{L}{\delta L}$$

where T = string tension
L = string length
a_x = cross sectional area

A small change in string tension δT is related to a small change of length δL by $\delta T = k_{st} \times \frac{\delta L}{L}$

where k_{st} = the spring constant (the force required to stretch a 1m long string by 1m.)

Therefore $E = \frac{k_{st}}{a_x}$

and hence $c = \sqrt{\frac{k_{st}}{a_x \rho}}$

but $a_x \rho = m$ (mass per unit length)

Therefore $c = \sqrt{\frac{k_{st}}{m}}$

and the resonance frequency of a string of length L fixed at both ends is given by $f = \frac{nc}{2L}$

or $f = \frac{n}{2L}\sqrt{\frac{k_{st}}{m}}$ ----------(3.2)

Using the values of string spring constant and mass per unit length, determined as described in Appendix B, we find the resonance frequencies (in Hz) to be as follows:

1st string,	5209	10418					
2nd string,	1976	3952	5928	7904	9880		
3rd string,	1821	3642	5463	7284	9105		
4th string,	1313	2626	3939	5252	6565	7878	9191

It must be stressed that these figures have a very tenuous connection to the reality of a real violin, but do perhaps at least indicate the order of magnitude of the longitudinal resonance frequencies and their density. We are interested in violin behaviour in the range 150 to 10,000Hz and it is quite clear that there are a considerable number of possible longitudinal resonance frequencies within that range. It is not known to what extent these resonances would modify the LSV on a violin.

It is well known that longitudinal resonance frequencies can be excited by bowing at an acute angle to the string, as is frequently done by beginners. The writer found that bowing at an angle to the string did not excite the longitudinal and transverse resonances at the same time. Attempts to find a bowing angle that might do so resulted in an oscillation from transverse

to longitudinal. A bow apparently can only execute one stick slip frequency at a time. Lee and Rafferty experienced the same difficulty with the bowed excitation but they were able to excite both vibrations simultaneously by plucking the string [Lee and Rafferty, 1983]. They measured the longitudinal resonance frequencies of the third string at 2700Hz, and the fourth string at 1350Hz. They also showed that the Q of these resonances was higher than that of the TSV. The type of string used was not specified in the report.

There would appear to be no reason why longitudinal resonances should not be excited when the LSV resonance frequency of a string coincides with a particular LSV excitation. In the experimental work of this project, no evidence was found that would point to the excitation of longitudinal string resonance. This may be a consequence of having sampled the spectrum at intervals of 6Hz, which may be wide in comparison with the high Q resonance peaks found by Lee and Rafferty.

3.2.3 Bellying LSV force compared with TSV force

The bellying LSV and TSV forces are both related to the amplitude of the transverse displacement of the string. It is therefore possible to find the relative magnitudes of their components acting in the plane of the bridge.

The LSV force in the string from bellying has been shown to be given by:

$$\text{Bellying LSV force} = k_{st}\frac{\left(\frac{n}{2}\right)^2 \pi^2 a_{n/2}^2}{8L(L+L_1)} \text{ at the frequency of harmonic n.}$$

The static vertical force on the bridge from a string tension T is 0.37T (see section 3.3.1). Therefore, the vertical vibrational force on bridge from bellying LSV is given by;

$$F_{\text{bellying LSV}} = k_{st}\frac{0.046\left(\frac{n}{2}\right)^2 \pi^2 a_{n/2}^2}{L(L+L_1)} \text{ at the frequency of harmonic n.}$$

The force on the bridge from the transverse vibration of the string should now be found. Imagine a sinusoidally curved string of mean tension T, and modal displacement amplitude a_n. The displacement y at any point

distance x from the end is given by:

$$y = a_n \sin n\pi \frac{x}{L}$$

$$\text{The slope} \quad \frac{dy}{dx} = a_n \frac{\pi}{L} n \times \cos \frac{\pi x}{L}$$

$$\text{At } x = 0, \text{ the slope } = a_n . \frac{\pi}{L} \cdot n = \frac{\text{transverse force}}{\text{string tension}} = \frac{F_{TSV}}{T}$$

Therefore the horizontal force on the bridge from the transverse vibration of the string is;

$$F_{TSV} = T \frac{a_n n\pi}{L}$$

$$\text{and} \quad \frac{F_{\text{Bellying LSV}}}{F_{TSV}} = \frac{k_{st}}{87T} \frac{n\pi}{(L+L_1)} \frac{(a_{n/2})^2}{a_n} \text{----------(3.3)}$$

At the odd numbered harmonics, there can be no contribution from $a_{n/2}$, so the ratio is zero. The ratio of vertical bellying LSV force on the bridge to TSV force on the bridge is clearly non-linear. The contribution of the bellying LSV force to the transverse force on the bridge is negligible compared with that due to the mean string tension.

By taking equation 3.3 and leaving out the constants we can write that, $\frac{F_{\text{Bellying LSV}}}{F_{TSV}} \propto n \frac{(a_{n/2})^2}{a_n}$. In the case of the bowed string the value of a_n declines as the inverse of n (saw tooth wave). Therefore for the bowed string all the even numbered harmonics have a ratio $\frac{F_{\text{Bellying LSV}}}{F_{TSV}}$, which is a constant. At all the odd numbered harmonics, the ratio is zero.

As an example, the ratio of vertical bellying LSV force to TSV force on the bridge can be evaluated for the second harmonic of a bowed open G string. If the string is strongly bowed, the transverse displacement in the first harmonic might realistically be .0015m. If the assumption is made that a_n declines as the inverse of n, then second harmonic displacement is 0.00075m. So

k_{st} =2804, T=40N, $(L+L_1)$=0.383m, n=2, and a_n=0.00075m, $a_{n/2}$=0.0015.

This gives the ratio $\frac{\text{LSV}_{\text{bellying}} \text{ force}}{F_{TSV}} =$ 0.043.

Later in the thesis, the ratio of the LSV force in the string to the TSV force on the bridge is LSV force is frequently quoted. The ratio of the LSV force in the string to the transverse TSV force on the bridge for the bowed G string is found by; $\frac{\text{LSV}_{\text{bellying}}\ \text{force}}{\text{TSV force}} = \frac{0.043}{0.37} = 0.116.$

It is shown later that the bowed string does not simply produce a bellying LSV of double the frequency, but rather a mix of the same frequency and double the frequency.

It would appear from these figures that the contribution to the force on the bridge from bellying LSV is smaller than that of the TSV. The relative contribution could be investigated more meaningfully by comparing the associated power exchanged. This is discussed in Chapter 12. It is also shown experimentally that the LSV force in string is somewhat higher than that found by the theoretical analysis of string vibration given above. This is in part due to LSV being developed as part of the modal response of the structure. One such response is 'bridge-rock LSV'.

3.2.4 Bridge rocking longitudinal string vibrations

There are four strings on a violin. The first and second strings divert to the right (the violin upright and viewed towards the belly) as they pass over the bridge and the third and fourth strings divert to the left as they pass over the bridge. All the strings have different tension in them and different spring stiffnesses. It will be helpful in understanding what is to follow if one imagines all the strings being replaced with one single string, which combines the tensions of each of the four strings, and runs on a line that follows the centroid of the group of four strings. Since the 1st and 2nd strings have a combined tension which is greater than the combined tensions of the 3rd and 4th strings, the replacement single string will run a little to the right of the centre of the bridge. This one string will be called the 'combined string'.

Fig. 3.2 shows a cross section through the belly of the violin immediately behind the bridge. The four strings and their replacement 'combined string' are shown on the bridge. The movement of the bridge relative to the violin is a rotation about a point. The centre of rotation of the bridge is

shown located on the surface of the belly between the centreline and the sound post. (In fact, the movement of the bridge is rather more complex

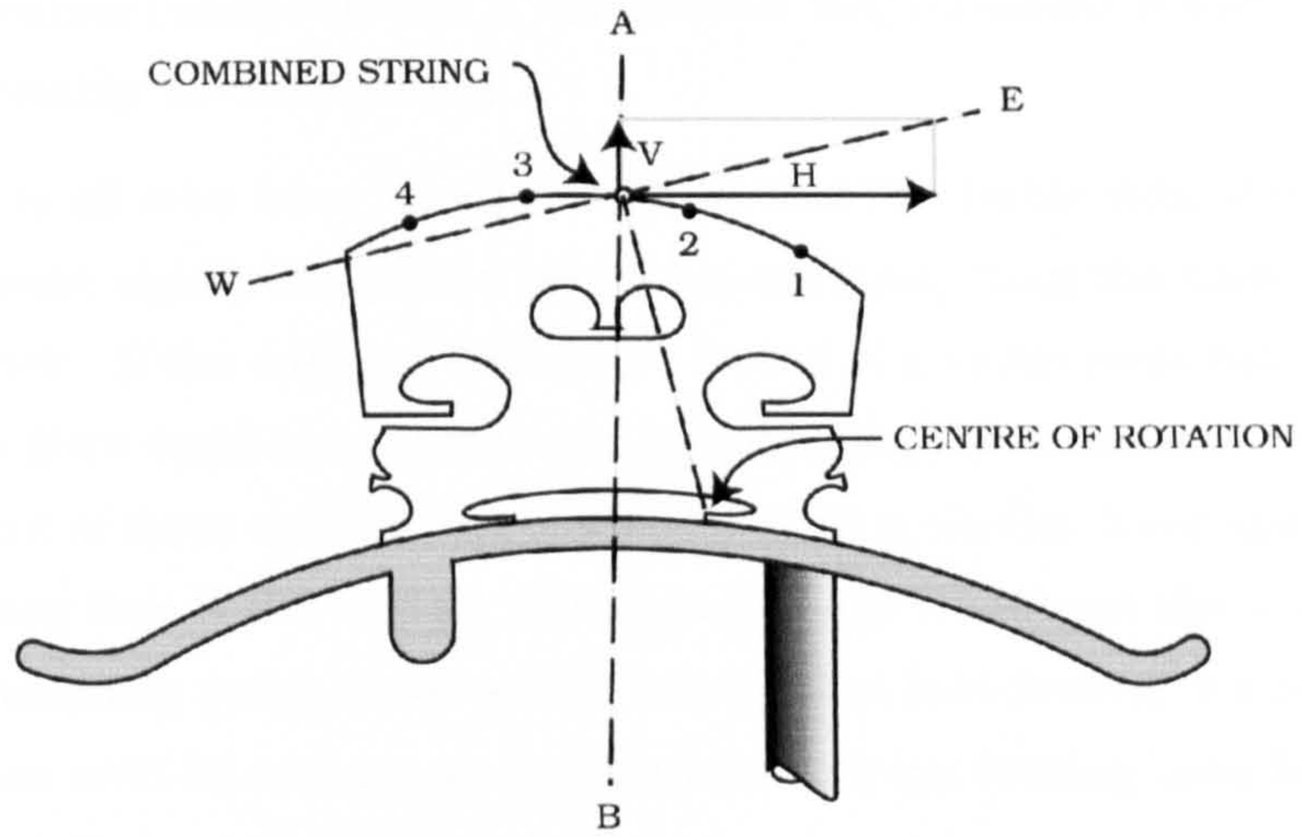

Fig. 3.2. Bridge rocking analysed.

than a rotation about a point; this matter is examined in greater depth in Chapter 12.) The line of action of the combined string is shown as AB, B being located close to the centre of the violin and at the underside of the front plate. When the bridge rotates about its centre of rotation, the combined string will move in an arc whose tangent EW runs at right angles to a line extending from the combined string position to the centre of rotation.

This displacement may be split into two components; a component which runs in the line AB, which shall be called the V component because it is close to vertical, and an H or horizontal component which runs at right angles to the V component. As the bridge rocks, the V component periodically stretches and shortens the combined string and therefore creates in the combined string a vibration of string tension. The frequency of this tension vibration is the same as that of the rotation of the bridge. This vibration will be referred to frequently as the 'bridge-rocking longitudinal string vibration' or 'bridge-rock LSV'.

The H component of the combined string motion does require the string to stretch. Each time the combined string moves sideways away from its neutral position it must be stretched and allowed to shorten on its return. For every cycle of bridge rotation there must be two cycles of tension rise and fall in the combined string, so the frequency of the consequent

combined string tension fluctuation must be an octave above the frequency of rotation. By inspection of the geometry, the magnitude of the combined string vibration caused by the H component displacement is very small and may reasonably be disregarded.

It is clear to all who have handled a violin that the treble side of the bridge is much more rigidly supported by the sound post, than the bass side is by the bass bar. If the edges of the centre bouts of a violin were held from moving, a force applied at the sound post foot would cause little movement at the point of force application compared with a similar force applied at the bass bar foot of the bridge. A rocking bridge would act like a cam and would alternately push down on the sound post foot (taking the centre bouts down with it) and up on the combined string (taking bass bar up with it) and then reverse the action.

The effect of the cam action in prising the violin and strings apart will be to do work on both. There will therefore be an energy input into the violin at the bridge foot and into the strings at the bridge top. (This is true for the application of static forces being considered here. In the dynamic situation energy can only enter the string and body if there is a loss by damping, which will be shown to be so.) The rotation of the bridge alternately raises the tension in the strings and bends the violin in its length, and then reduces the string tension and allows the violin to straighten in its length. It is similar to an archer drawing an arrow, the arrow being like the bridge. Modal analysis of the violin has identified many bending modes in the body [Marshall, 1985].

Bridge-rock LSV is obviously not developed by the string motion itself, but is the result of violin bridge movement that alters the string length. The energy input from TSV is stored in the body through twist of the bridge platform and through LSV by putting tension in the string and bending the body in its length. Bridge-rock LSV uses some of the energy that goes into the violin as TSV energy. Bridge-rock LSV is a conversion of part of the TSV energy. Why should we make this distinction between energy entering the violin from TSV and that from LSV? It will be suggested that the body may be moved by the LSV forces in a different way from the TSV force; and that these movements give rise to sound radiation.

We can assess the relative magnitude of the TSV force on the bridge and the bridge-rock LSV force on the bridge. The transverse force on the bridge from the transverse vibration of the string is given by; TSV force $= T\frac{n\pi}{L}a_n$, where T is the string tension, and a_n is the amplitude of the transverse displacement of the string in the nth harmonic. Now consider a bridge rocking about a treble foot that is held from movement by the sound post. The transverse force on the bridge (TSV force) will cause the top of the bridge to move with a velocity $v = Y \times$ (TSV force) where Y is the bridge admittance in the bowing direction in the plane of the bridge.

The corresponding displacement amplitude is given by

$$x = \frac{v}{\omega} = Y.T\frac{n\pi}{L}.a_n\frac{1}{2\pi f_1 n} = \frac{YTa_n}{2Lf_1}$$

Since the horizontal distance from the G string notch to the sound post foot of the bridge is approximately the same as the vertical distance from the G string notch to the sound post foot, the vertical displacement amplitude of the bridge at the G string notch is approximately equal to x also.

If the G string notch rises vertically by x, but is permitted to also move in the direction of the string by a small amount to equalise the string tension each side of the bridge the increase in string length is given by,

$$\Delta L = 2x\mathrm{Sin}\,\theta$$

where θ is the angle of rise in the string from the nut to the bridge, which is assumed to be equal to the angle of rise in the string from the tailpiece to the bridge. The corresponding rise in string tension each side of the bridge is given by; $\Delta T = k_{st}\frac{\Delta L}{(L+L_1)}$, where L is the length of the string from the nut to the bridge and L_1 is the string length from the tailpiece to the bridge.

By substitution $$\Delta T = 2k_{st}\mathrm{Sin}\theta.\frac{YTa_n}{2Lf_1(L+L_1)}.$$

$$F_{\text{vertical bridge rock}} = 4k_{st}\mathrm{Sin}^2\theta.\frac{YTa_n}{2Lf_1(L+L_1)}.$$

The ratio of the vertical component of the bridge-rock LSV force on the

bridge to the transverse force on the bridge is;

$$\frac{F_{\text{vertical bridgerock}}}{\text{TSV force}} = 4k_{st}\text{Sin}^2\theta.\frac{YTa_n}{2Lf_1(L+L_1)}.\frac{L}{Tn\pi a_n}.$$

$$\frac{F_{\text{vertical bridgerock}}}{\text{TSV force}} = 2k_{st}\text{Sin}^2\theta.\frac{Y}{n\pi f_1(L+L_1)}.$$

This can be evaluated for a typical bow excited first harmonic vibration of the open G string. Much published data suggests that at a body resonance the bridge admittance in the lower frequency modes might be about 0.1 s/kg. A rise of the G string notch by 1unit lifts the G string by 1 unit, the D string by 2/3 units, A string by 1/3 units, and does not lift the E string at all. The effective spring stiffness of the group of four strings can be taken as that of the G string, plus 2/3 of the D string stiffness, plus 1/3 of the A string stiffness. From Appendix B, the effective combined string spring stiffness is $K_{st} = 2804+(0.67\times2213)+(0.33\times1711)= 4849N$

$\theta = 11.5^0$, Y=0.1 s/kg, L=0.328m, L_1=.055m,

For the open G string;

$$\frac{F_{\text{vertical bridgerock}}}{\text{TSV force}} = \frac{2\times4849\times0.1\times\text{Sin}^2 11.5^0}{196(0.328+.055)n\pi}$$

$$\frac{F_{\text{vertical bridgerock}}}{\text{TSV force}} = 0.164/n.$$

To find the ratio of the LSV force within the string to the TSV force acting on the bridge we divide the above ratio by $2\text{Sin}\theta$.

$$\frac{\text{LSV}_{\text{bridge-rock}}\ \text{force}}{\text{TSV force}} = .413/n.$$

The above calculation assumes that the violin is rigid throughout the cycles of bridge rotation. Clearly there would be some bending in the length of the instrument and this would reduce the amount of string stretch required to accommodate the bridge movement. Also the ratio is inversely dependent on the harmonic number so the relative force from bridge-rock LSV would decline with rising harmonic number. The above calculation tells us that it is likely to be significant in the lower harmonics.

3.2.5 Primary and secondary LSV

The primary cause of forces and motions in the bowed violin is the interaction of the bow and the string and all the motions of the strings and

body could be seen as effects. In this model, the forces in the strings and those acting on the body would be regarded as internal forces and not as primary driving forces; as effects rather than causes. This is a valid way of looking at the violin.

Alternatively, we could see the vibrating length of the string as the driver of the violin and could analyse the forces and motions applied to the body at the bridge and the ends of the string. One might conclude from this that the most important force applied by the vibrating string to the body is a transverse force at the bridge, and so set out to investigate how the violin responds to that driving force. In this model, the forces imposed on the body by the string are seen as primary driving forces and all forces and motions that occur beyond the ends of the vibrating length of the string are seen as responses or secondary forces.

It is apparent that we can choose an interface within the whole system of the bowed violin and say that the forces or motions crossing that interface are driving forces and put energy into the other part of the system. It is convenient to call the forces crossing the interface to drive the system 'primary forces'. The system responds to these primary forces by undergoing motions, which will induce internal forces. These 'secondary' or response forces and motions will involve the structures both sides of the chosen interface.

In this study, the chosen interface is the tail gut, the underside of the bridge feet and the nut at the entry to the peg box. This interface divides the body into two substructures, the driving substructure (bridge string and tailpiece) and the body. The forces arising within the driving substructure will be called primary forces. The application of these forces across the interface will excite a response in the violin as a whole. This response will excite forces in both the driving and the driven substructures. These response forces will be called secondary forces.

Consider the driving structure on a rigid base. The TSV force on the bridge will apply equal and opposite vertical forces at the bridge feet. A TSV force will also be applied at the nut. Bellying LSV will apply a force at both feet of the bridge and a tension at the nut and tail gut. Dynamically, there could be resonances within the driving substructure, which alter the relative values of the forces applied to the blocked base of the driving substructure. These resonances could come from the strings, the tailpiece

and the bridge. The forces applied to the blocked base by the driving substructure are called 'primary' driving forces.

If we now release the bass bar foot of the bridge from the blocked base, the TSV force at the bridge can rotate the bridge about the sound post foot and bridge-rock LSV can be generated. The rotating bridge has a cam action and widens the gap between the blocked sound post foot and the strings. This results in bridge-rock LSV. Bridge-rock LSV is, by the definitions given in this discussion, not primary LSV but happens as part of the violin's response to the driving force. It is therefore secondary LSV.

Bridge-rock LSV is potentially capable of driving the violin. Part of the 'primary' driving by TSV force has been transformed into 'secondary' driving by LSV force.

The position of the interface between the driving substructure and the remainder of the violin is an arbitrary matter and there can be no right or wrong choice. The choice is made to best clarify the concepts being investigated. In our case, the concept is LSV and the writer has chosen an interface that enables bridge-rock LSV to be seen as a response that is capable also of being a driver. The experimental work that is presented later will show that the amount of LSV force in the string is greater than that due to primary LSV alone. The question of whether secondary LSV can drive the violin will be shown to be an important issue in the role of LSV in the generation of violin sound.

In order to explain these principles it has been necessary to talk about the violin in a cause and effect way. The bowed violin assumes a steady state that involves a combination of steady vibrational modes. These modes involve periodic variation in string tension and LSV force. That LSV force cannot be separated into primary and secondary parts. The dynamic interaction between the driving substructure and the body is examined both experimentally and theoretically in Chapter 10.

3.2.6 The deformations of the bridge

As the bridge rises, it will stretch the combined string on both sides of the bridge (ie, the playing length and the short length that goes to the tailpiece). The playing length of the string will stretch more, so that as the bridge rises it will not rise perfectly vertically but the top of the bridge will

move slightly. This will actually cause the bridge to bend backwards rather than just lean, because the feet of the bridge are wide enough to be effectively fixed to the belly (the vertical reaction must lie within the middle third of the base so no part of the contact area goes into tension). The reverse will happen when the bridge drops. It could be predicted that the top of the bridge will bend backwards and forwards normal to its own plane. Furthermore, the belly between the bridge foot and the sound post would bend as the load on the sound post is increased and this would rotate the bridge foot normally to its plane and put a bending moment in the bridge. Consider what happens if the combined string is replaced with its four constituent strings. When the bridge rises, the tension in the first string is increased because its diversion from the centre line of the violin is increased and we have shown that this would cause a backward bending of the bridge. The same would apply to a lesser extent to the second string. The third and fourth strings would have their diversion from the centre line of the violin reduced and so would undergo a reduction in tension and the bridge would bend forward. The bridge would be caused to twist, and when the translation of the bridge reverses, the twist will go in the opposite direction. Note that the frequency of this twisting action is that of the TSV, like the corresponding bridge-rock LSV vibration.

In 1937, Minnaert and Vlam published what has been regarded as the definitive work on the measured movements of the violin bridge [Minnaert and Vlam, 1937]. They reported a strong rotational movement in the plane of the bridge, a flexure of the vertical axis at the same frequency as the fundamental, and a twisting action of the same frequency. The relative strengths of the translational, flexing and twisting vibrations varied with frequency. They did not advance any theory to account for their observed bridge movements but the preceding analysis is entirely consistent with their findings.

In a static situation, the tension in the string will be the same each side of the bridge. In a dynamic situation, the bridge may be required to move laterally to maintain equal tensions each side of the bridge. There may be enough inertial resistance offered by the bridge to this motion to induce small inequalities of tension each side of the bridge and this will show up as LSV. Is this primary or secondary LSV? Since it arises within the

driving substructure, it is primary LSV. Any small effect it may have would be to moderate the relative magnitude of the LSV forces going into the body at the saddle and the nut. It should be noted that on a real violin the platform of wood on which the bridge sits must undergo a considerable amount of flexure. Flexural motions that would move tilt the bridge normal to its plane would also moderate the LSV, but since this flexure is on the driven side of the interface, the LSV induced by it is by our definition secondary.

3.3 Deformation of a violin body under string tension

If the forces and displacements set up in a violin caused by the static tension in the strings were understood, it would give a helpful start to understanding how a violin might move under string tension vibrations. Of course, as the frequency rises inertial effects become increasingly significant, and the simple static approach becomes less relevant. It will, however, be shown that this approach provides strong clues as to how the violin might radiate sound and good reason for some of the important design features of the violin.

The static analysis of a complex shell structure like a violin is perhaps most accurately undertaken by finite element analysis. However the simple method given here has the virtue of providing a much clearer appreciation of how the violin supports the strings, than getting an answer from the rather 'black box' finite element method. In particular, the interaction of the opposing effects of the long and cross arch support systems is brought out.

3.3.1 The violin as a plane frame

The literature contains several attempts to represent the violin as a two-dimensional plane frame [Leipp, 1969], but these have been, at the best, unhelpful. It is for this reason that the rationale behind the developing of the structural model that is used will be set out in some detail.

Fig. 3.3 shows a block of wood about 50mm square in section and about 500mm long. On it is mounted a bridge BD and ABC is a tensioned string. The forces applied to the block by the string are shown below: (a) shows a

bending affect and (b) shows a compression down the length of the block. This is not a very helpful breakdown. Because the compression is applied eccentrically to the centroid of the block, it also induces bending in the block. Consider now fig. 3.4. If we drill a hole in both ends of the block of wood and insert a dowel, and keeping the string on exactly the same line fix

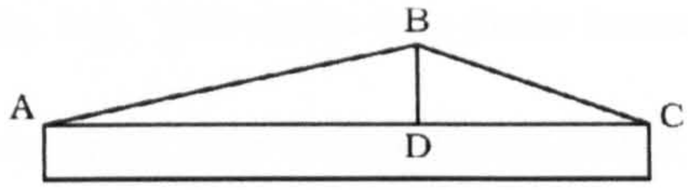

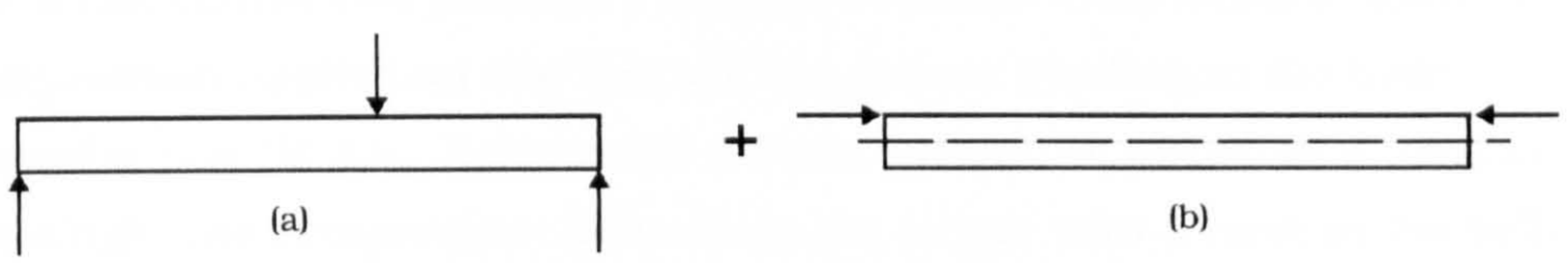

Fig. 3.3. Wrongly separating bending from direct compression.

it to the dowels at A' and C', then as shown in (b), we are now applying the compression down the centroidal axis where it will not induce bending. 3.4(a) then, fully describes the bending induced in the block, which is greater than that shown in 3.3(a) because it includes the bending shown in 3.3(b).

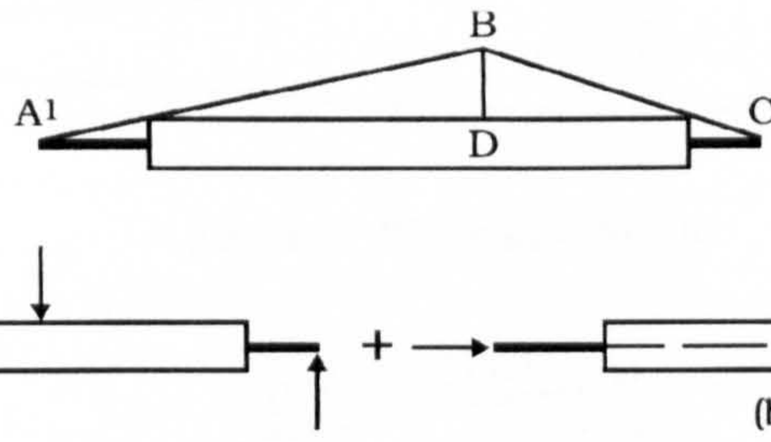

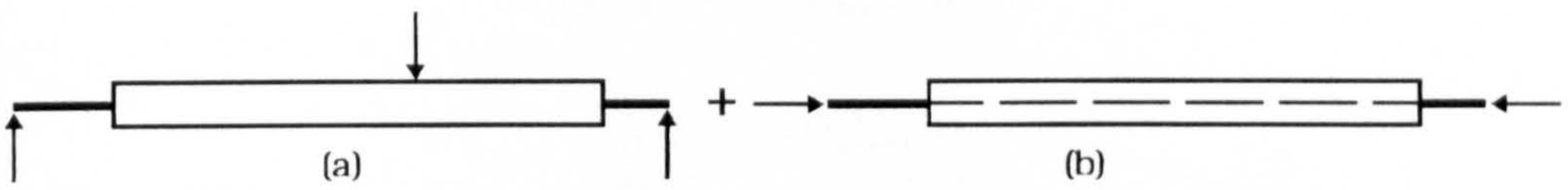

Fig. 3.4. Correctly separating bending from direct compression.

Consider now fig. 3.5. Replacing our block with a violin and adding the appropriate dowels we can present the problem as a box with a compression down the length of its centroidal axis, combined with a transverse force applied at the bridge line causing the instrument to bend.

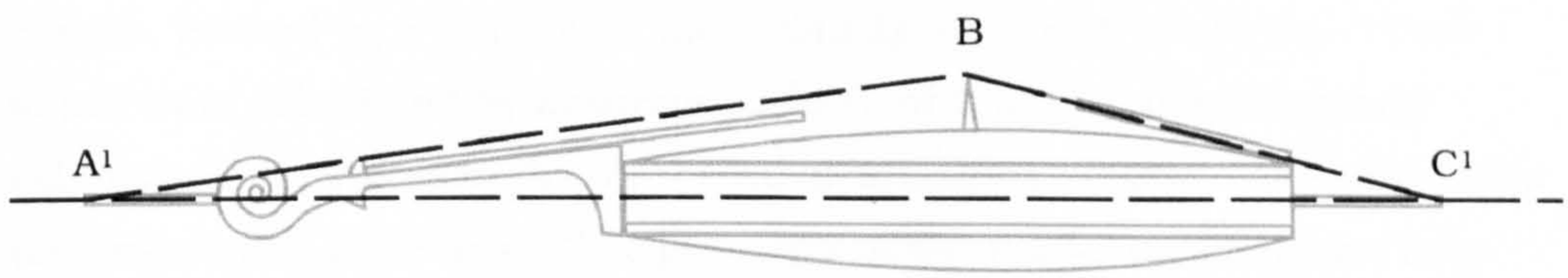

Fig. 3.5. Towards a separation of bending and compression in a violin.

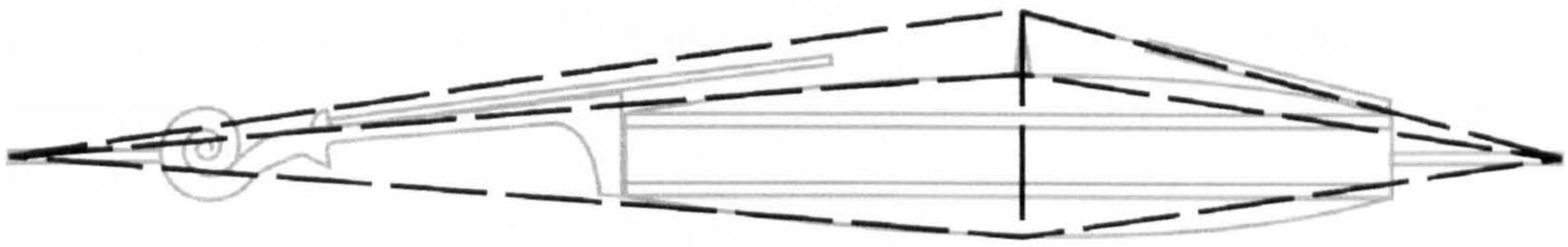

Fig. 3.6. The violin as a plane frame.

(The position of the centroidal axis varies throughout the length of the body but a calculation can produce a realistic estimate of its location such that a compression applied on this line will not induce bending in the body.) Consider now fig 3.6. Remove the dowels, put in the sound post, replace the single line compression force down the length with a force in the belly acting towards the bridge and a force in the back acting towards the bottom of the sound post. We have now reduced the structure of the violin to that shown in fig. 3.7. ABC represents the string, ADC represents the upper and lower belly, AEC represents the upper and lower back, BD

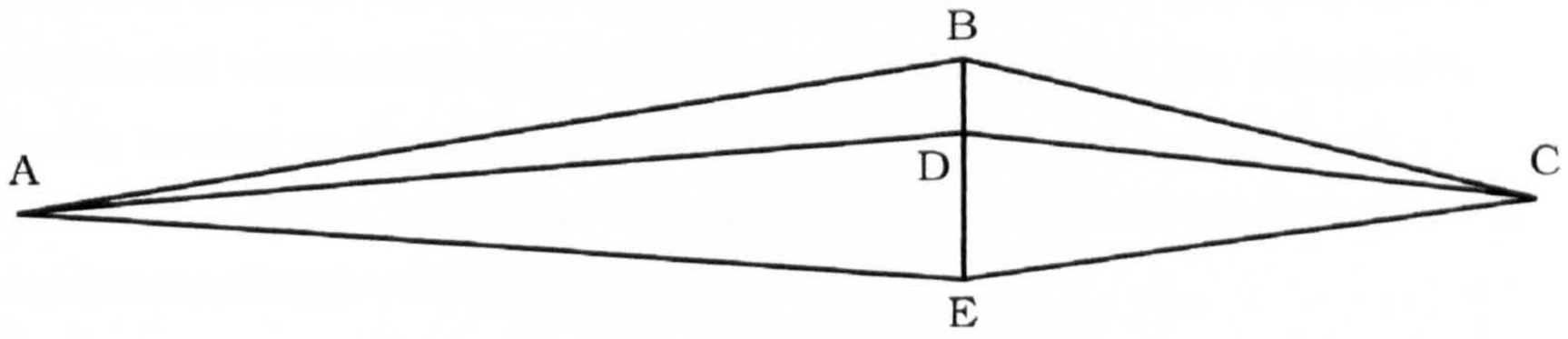

Fig. 3.7. The plane frame.

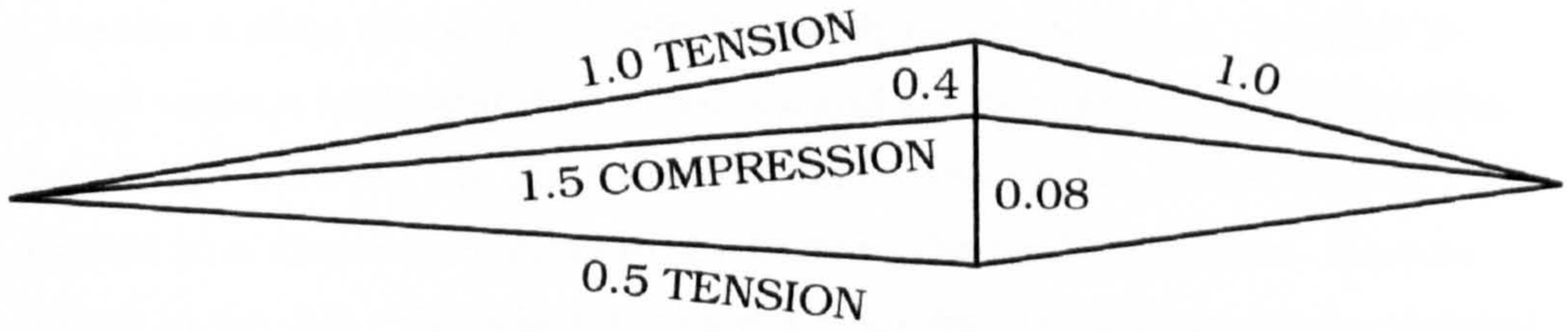

Fig. 3.8. The force vectors in a violin.

the bridge and DE the sound post. In fig. 3.8 the forces set up in the system, caused by a tension in the string AB of 1 unit, is shown. These forces were calculated by assuming a force of 1 unit in the string and calculating the forces in the all the other members by static analysis. This analysis is not given here. The geometry of the model is not shown here but it assumes the dimensions of a fairly standard "Strad" model violin. Although the forces shown have been accurately calculated for the model shown in fig 3.7 it is accepted that the model itself greatly simplifies what

is undoubtedly a very complex structure. The analysis does show an approximation of the relative magnitude of the forces in the main components of the violin and shows that the sound post functions as an essential member in the supporting truss that carries the string force.

This analysis shows that:

1. The strings push down on the bridge with a force of about 37% of the tension in the strings.

2. The sound post carries only about 1/5 of the bridge force the remaining 4/5 being carried by the compressive force in the belly, which tends to make the plate buckle upwards.

3. The load in the sound post is resisted by a tension in the back of the instrument, which is only about 1/3 as great as the compression in the belly.

The above analysis and its conclusions apply to each of the four strings, but only concern the overall stability of the instrument. There would be additional internal forces caused by the sound post and the strings not being located on the centreline of the body. These forces have been considered by the writer but to present them here would not contribute to understanding the essential issues.

3.3.2 The forces in the front and back plates

Consider a plate like a violin belly but with no sound holes. Imagine it placed upon a table and supported around all its edges on small marbles (no friction between the plate and the table) and on top of it a load is applied in a direction normal to the belly in the bridge position. This is shown in fig. 3.9. The edges of the plate are free to move in any horizontal direction but not in a vertical direction. Predictably, the load would cause the crown of the plate to sag, and some horizontal movement of the plate edges. If we now apply a horizontal force at both ends of the plate, equal but opposite in direction, the sag in the crown can be reversed to some extent. The force P at the crown can be carried either on the "long arch" ABC, or on the "cross arch" DBE. In fact what happens is that the long and cross arches both share in the support, the proportion being carried by each depending on the relative stiffness of the two systems. Let us call the load carried on the cross arch system, C, and that on the long arch L.

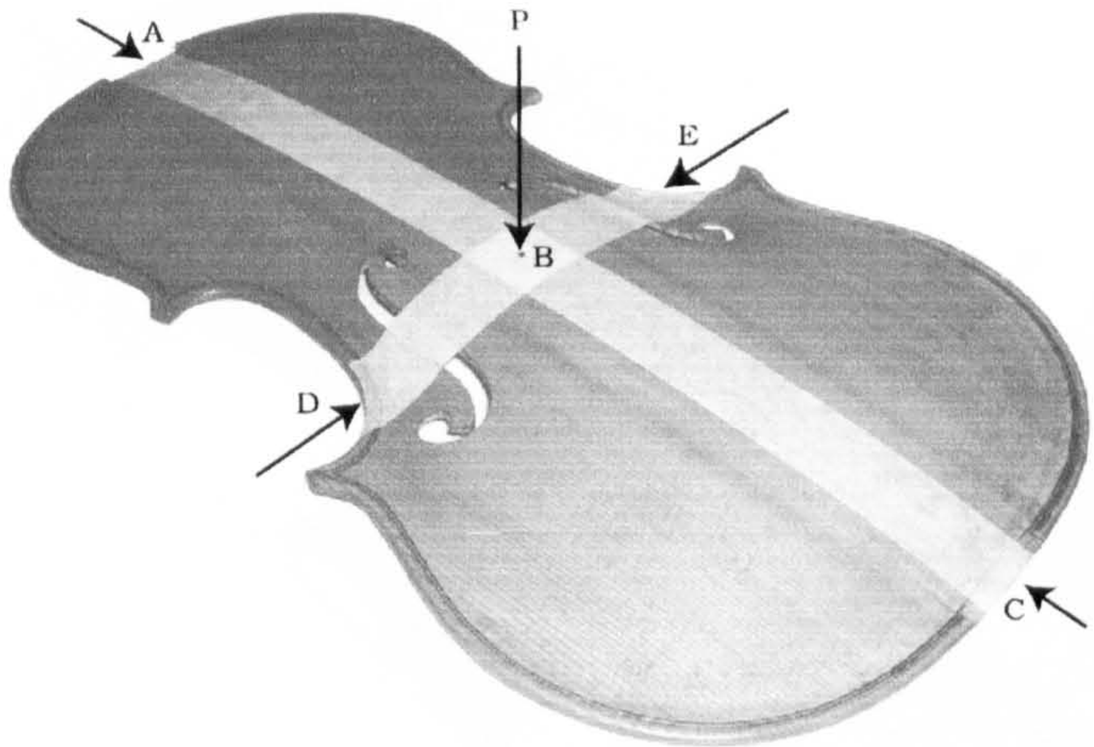

Fig. 3.9. The bridge load splitting into the long arch and the cross arch.

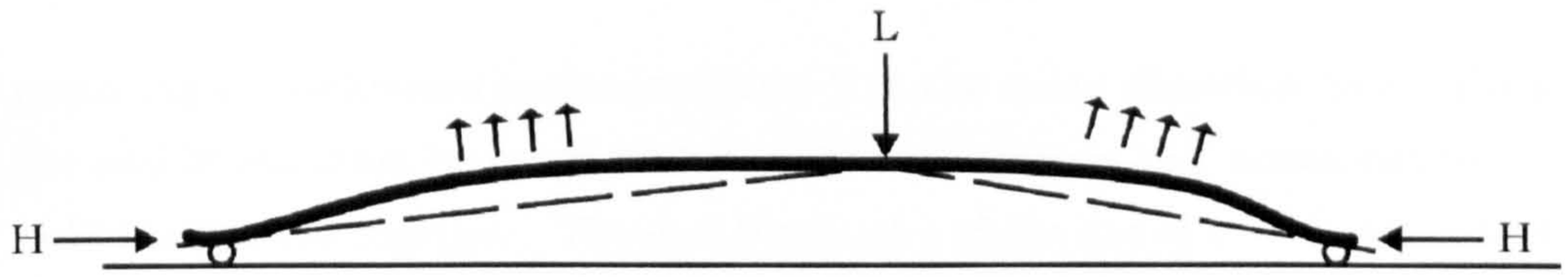

Fig. 3.10. The forces and movements in the long arch.

Such that P = C+L. Considering first the long arch support system. Fig. 3.10 shows a long section through the plate carrying a load L at the bridge resisted by a horizontal reaction at the ends. A line of action of the thrust at the ends is shown going in a straight line to the bridge. This line of thrust is eccentric to the line of the wood and this eccentricity will induce in the wood an upward buckling. Clearly then, the result of carrying a load on the long arch alone is to cause the crown of the end bouts cross arches to rise, and the plate edges in the end bouts, to pull in. Consider now the cross arch support system.

Fig. 3.11 shows a violin belly with a cut made across the plate at the end bouts cross arches. The load C at the bridge is carried on the centre bouts cross arch to the two side arches. The sound holes intervene in the most direct path to the side arch but the forces can spread out and get around the sound hole. To support the abutments of the side arches will require a horizontal force, which can be split into two components H and X. Force H can be provided by the end thrusts at the neck and saddle, but not without

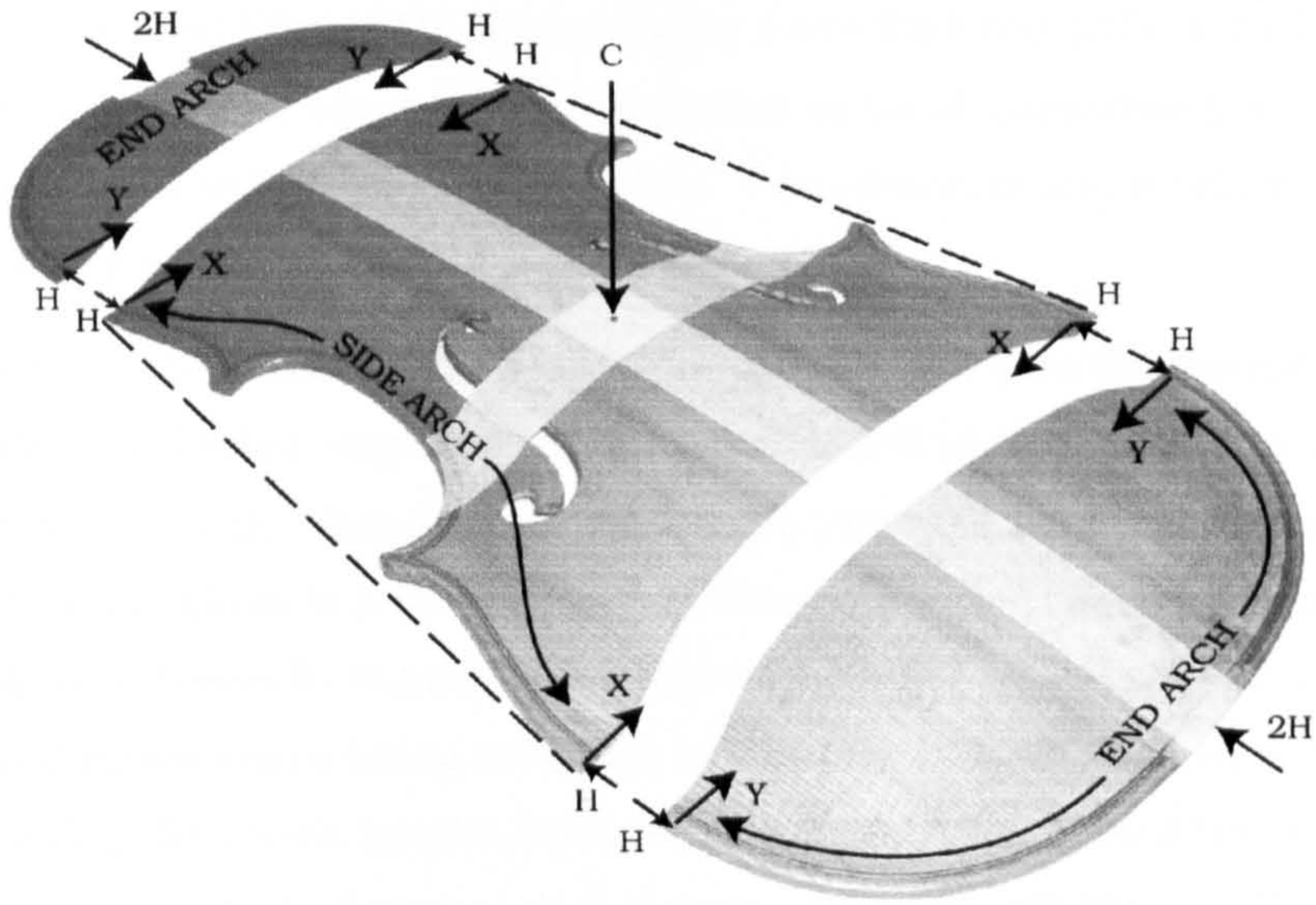

Fig. 3.11 The forces in the cross arch support of the bridge.

requiring an additional horizontal force Y in the same direction as X. Thus the end bouts must be cross-tied to provide the forces X+Y necessary to hold the system together. The end bouts of a violin are of course cross tied by the end bouts cross arches, and the force X+Y tending to spread the end bouts must pull the crown of the end bouts cross arches down.

Where does this lead to? There are two support systems for the bridge load, both acting in parallel. The bridge load P will split between the two systems in proportion to their relative stiffness. The component going into the long arch system is L and that into the cross arch system is C. Component L lifts the end bouts cross arch (EBX arch), and component C lowers the EBX arch. Does it go up or does it go down? That depends on the height of the EBX arch. If the EBX arches were very low compared to the centre bouts cross arch (CBX arch), they would approach the line of thrust of the long arch in fig. 3.10, and the upwards buckling tendency in the long arch would be very weak. Although the downwards buckling tendency caused by the spreading of the EBX arches in fig. 3.11 would also be weakened, it would not be weakened to the same extent since the EBX arch would have to go completely flat to reduce the downwards buckling tendency to zero. It can be seen then, for the plate in our example, that if the ratio of the EBX arch height to the CBX arch height is low the EBX arch will drop and the end bouts will widen. If this ratio is high the EBX arch will rise and the end bouts will narrow. It follows then that there

must be a ratio of EBX/CBX arch height, such that the EBX arch height remains unmoved. This ratio will be shown to be of considerable importance and will often be referred to. For convenience, it will be called the 'balanced end arch ratio' or simply the BEAR.

Now consider the back plate. If one ignores the fact that the sound post is off centre, in all other respects the plate is loaded in the same way as the belly, except that the direction of the load is reversed and the reaction at the ends of the plate is a tension rather than a compression. It can then be seen that it behaves in exactly the same way as the belly but with all the forces and movements being reversed in direction. Note then that if the ratio of EBX/CBX arch height is higher than the BEAR, the EBX arch height will drop, and of course, if it is lower than the BEAR, it will rise. This is the exact opposite to what happens in the belly.

3.3.3 Shaping the plates to increase the static deformation

There now exists the possibility of controlling the direction of movement of the plates by adjustment their arching shapes. If a plate can be designed that can deform in one direction, or in the opposite direction or not at all, one could consider how best to maximise the static deformation of the body.

To maximise the radiated sound it is necessary to maximise plate movements. The type of plate movement to be encouraged is that which results from the TSV force acting on the bridge, the lifting of the bass bar on one side of the body and the depressing of the sound post on the other. When a transverse vibration lifts the bridge on the left side (as viewed normal to the belly) it has been shown that the back and the belly move further apart and the violin breathes in. The lifting of the bridge also increases the tension in the string. It is necessary then to design a belly and a back that move apart when the string tension is increased. The belly EBX arch will lift if it is built higher than the BEAR and the back EBX arch will lift if it is built lower than the BEAR. So if this were done, the violin would breathe in and out, in phase with the bridge rocking induced breathing, using energy available from string tension vibrations. While we are considering the body deformations under string tension it clear that in

addition to the breathing action, the body will bend in its length as the back is stretched and the belly is shortened.

The forces causing these plate movements are generated in the end bouts where the plate surface areas are broad, and in that sense, they could be said to be on target. It is hard to see the upper and lower back of a violin being effectively driven by the sound post, or even the upper and lower belly being strongly driven by the flexible ends of the bass bar. From the earliest times, violins have been made with the arching shaped in this way. This could not have happened if the experiments with small changes in arching shape had not been rewarded with perceptible tonal results. The belly tends to rise more steeply into the long arch at the ends than the back, and has a longer flat area in between. The back long arch is somewhat more pointed. For convenience the amount by which the EBX arches are built either above or below the BEAR will be referred to as "the deviation", because it creates a deviation in the line of the long arch. In the discourse that follows, reasons are advanced to support the contention that the BEAR, and to a lesser extent the deviation, affect the sound of the violin and need to be carefully controlled in violin making to ensure tonal consistency between violins.

3.3.4 Synchronising plate edge movements

The plates discussed above were assumed to have edges that were free to move in a horizontal plane. In a real violin the edges are glued to the sides, but this need not be a restraint to the free movement of the plate edges provided the back and the belly both tend to move the plate edges in the same direction and by the same amount. Under these conditions, the sides would simply move sideways normal to their surface and offer no resistance to the plate. If a violin were built with arching showing a large deviation in the back and a small deviation in the belly, in other words the arching is low in the ends compared to the centre, the back will be strongly driven, the belly weakly driven and the back will tend to induce larger edge movements than the belly. Under these circumstances, work will be done in inducing non-radiating rib twisting movements, and there will not be a harmonious edge movement. One might call this a "back driven" arching. Similar lack of harmony in plate edge movement would occur if the belly had a large deviation and the back had a small deviation, a "belly driven"

arching. The use of inappropriate deviations could also cause unwanted movement of the neck as a cantilever.

Careful choice of deviations could enable the two plates to work in harmony with the ribs and with each other. In the centre bouts, such harmony seems less possible. The side arches in the back are in tension to resist the pull from the CBX arch, while the side arches in the belly are in compression to support the load of the bridge from the CBX arch. This conflict is resolved by the presence of the sound holes, enabling the centre bouts sides to move with the back. The bridge load being spread along the belly by the bass bar can find its way to the plate edges beyond the sound holes.

The above argument leads to the expectation that the choice of the correct BEAR and the correct deviation from it, may be important determinants of relative plate forces and movements and therefore of the modes excited and their shapes.

3.3.5 The EAR of a violin

Ideally, when building a violin one should begin by knowing what the BEAR should be, and then making the belly higher than that and the back lower than that, by the deviation. There would be different figures for the upper and lower bouts. In assessing the built violin it would be possible to measure the cross arch heights and assuming the deviation is the same for the back and belly calculate the BEAR. What we actually are calculating is an "end arch ratio", but there is no way of knowing if it is the "balanced end arch ratio". This "end arch ratio" will be much referred to in this thesis and will be abbreviated to the EAR of a violin. It is a property of the geometry of a violin (while the BEAR is a property of a detached plate). The EAR, or end arch ratio, is defined as the average of the ratio of the rise of the EBX arch to that of the CBX arch, for the back and the belly. It will be different for the upper and lower bouts. The amount, by which the belly is higher than this and the back lower, is called the Deviation. It will be different for the upper and lower bouts. Using this newly introduced terminology, we can see that a violin of high EAR would tend to be belly driven, and a violin of low EAR would tend to be back driven.

Fig. 3.12 shows a side view of 3 violins by noted classical makers. The Stainer violin has a higher arch height than the other violins, which is characteristic of the work of this maker. It will be shown in Chapter 4 that when the arching height is increased the BEAR is higher. By comparison with the other violins shown it is possible to see that the EAR has been made higher in the Stainer. The Stainer also has a large deviation. This is also a feature of many of Stainer's violins. The Stradivari shows a lower EAR as is required by a violin with a lower arch height. The deviation of this violin is still high. The Guarneri has an arching height about the same

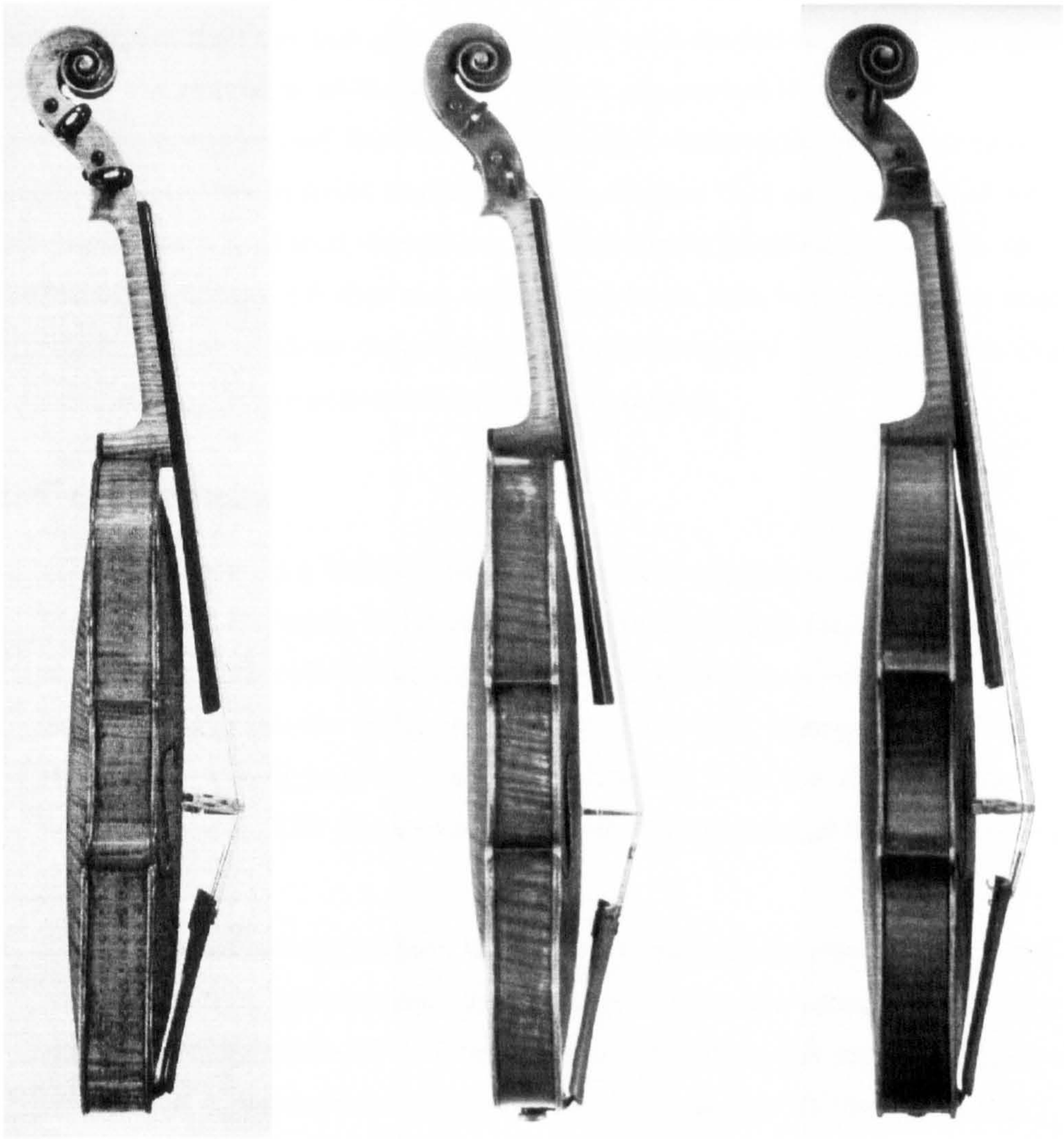

Jacob Stainer, 1672. Ashmoleum Museum. | **Stradivari, 1702. ex David Oistrakh.** | **Guarneri Del Gesu, 1742. ex Paganini.**

Fig. 3.12. Side view of three classical violins, showing the back and belly long arch. The variation in deviation can be seen.

as that of the Strad., and so has a similar EAR. The deviation is lower than that of the Strad., particularly so in the upper bouts. The tonal effect of all these design features can be predicted in the light of information presented later in this thesis.

3.3.6 The relevance of the EAR and deviation parameters

In the broadest sense, the above discussion leads to the possibility that the geometry of violin plates may affect the sound radiated by the violin. From an experimental point of view, it is impractical to test every possible nuance of variation in violin plate geometry. The qualitative analysis given above does suggest that the two parameters, EAR and deviation, might have an effect on the response of the violin. This is supported by both the qualitative analysis and the fact that classical violin models consistently exhibit differences in front and back plate shapes that can be defined by the parameters EAR and deviation. Furthermore, anecdotal evidence is presented in Chapter 5 that the author has been able to optimise the tone of violins by use of these descriptors of violin geometry. This suggests that they must have some relevance to violin dynamics.

3.4 Conclusions

- When a string on a violin is set in transverse vibration (TSV), a longitudinal vibration (LSV) of twice the frequency is induced in the string. This we call 'bellying LSV'. Bellying LSV is an extra form of input energy into the violin in addition to the TSV energy input. The magnitude of bellying LSV varies non-linearly with the TSV, and the ratio LSV force/TSV force increases with the transverse displacement of the string.

- The TSV of the string causes the bridge to rock in its own plane. This rocking motion induces periodically a tension in the strings (LSV). We call this 'bridge-rock LSV'. The bridge-rock LSV is not an extra input of energy but a conversion of some of the TSV energy. Bridge-rock LSV will be of the same frequency as that of the bridge motion.

- Violin strings have a considerable number of longitudinal resonance frequencies. Theoretically, these could appear in the LSV spectrum.

- The strings, tailpiece and bridge have arbitrarily been defined as a 'driving' substructure of the violin. Forces and motions that originate in this substructure are seen as driving the body as a whole. The driving energy comes from the TSV force on the bridge and the bellying LSV force. The LSV that originates in the driving substructure is called 'primary LSV'.
- LSV will also arise as a consequence of body motions and this LSV has been called 'secondary LSV'. Bridge-rock LSV is an example of secondary LSV and is capable of driving the violin using energy transformed, or redistributed, from TSV.
- When the static tension in the strings is increased, the violin bends in its length.
- In addition to bending, the body shape will alter. The increased bridge load can be resolved into two components, one carried on the 'long arch', and the other on the various arches comprising the 'cross arch support system'. The forces in the belly long arch will act to lift the belly EBX arch. The forces in the belly cross arch will act to lower the belly EBX arch. The direction of these predicted movements are reversed for the back.
- The net movement of the EBX arch depends on the height of the EBX arch compared to that of the CBX arch. In the belly, if the ratio of the height of the EBX/CBX is high, the arch will rise. If it is low, the arch will drop. In the back, the reverse is the case.
- The EAR, or end arch ratio, of a violin is defined as the average of, the ratio of the rise of the EBX arch to that of the CBX arch, for the back and the belly. Violins have two EAR, one for the upper bouts and one for the lower bouts. The deviation is the amount by which the belly is higher than this, and the back is lower than this. Thus, the belly EBX arch height is the belly CBX arch height multiplied by the EAR, plus the deviation. The back EBX arch height is the back CBX arch height multiplied by the EAR, minus the deviation.
- There may be a value of EAR that will optimise the radiated sound of the violin.

Much of the above is based on an unconfirmed qualitative static analysis, but it is presented at this stage to give the reader some understanding of the purpose of the experimental work that is presented.

Chapter 4

MEASUREMENT OF THE DEFORMATION OF THE BODY BY STATIC STRING TENSION

4.1 Introduction

In order to check the theoretical predictions about the deformation of a violin body by static string force, the deformation of a violin was actually measured. This work was carried out at the National Physical Laboratory, Twickenham, London, with the assistance of NPL technical staff. The machine used was a co-ordinate measuring machine, Zeiss UPMC 550. The violin used for this purpose was the medium EAR violin 156 and was unvarnished.

4.2 Method of measurement

The points where measurement was required were marked on the surface of the violin. The position in space of all these points was measured first with all the strings on at normal tension, and again with the string tension released.

A reference origin for all the measurements had to be selected. The theoretical considerations that have been presented leads one to expect that with increasing string tension the violin will bend in its length, and certain distortions will take place within the arch of the front and back plates. It was decided to define a reference plane.

To do this polished steel balls were attached with sealing wax to the belly at each of four points. These points were located on the surface of the belly, close to the edge at the widest point of the lower and upper bouts. These points would not necessarily lie in a common plane but the machine's computer established a best-fit plane. Within this datum plane, a Y axis was established for body length measurements and a Z axis for body width measurements. Normal to the plane, an X axis was established for plate rise and fall measurements. When the violin deforms the balls will all move differently but the computer would redefine a new best-fit plane.

The deformation of each point is given in relation to the best-fit plane through the steel balls. The location of the balls was chosen to coincide with points that are not likely to move much themselves. If the violin bends it is likely that the ends would come up and the middle go down, leaving the ball locations unmoved. If the end bout plate areas should move apart it is likely that the plate edges, where the balls are, would not move much (except within the datum plane rather than normal to it). The position chosen for the steel balls would also provide a datum for discovering any change in the end bouts cross arch heights.

The machine probed each point with a pressure of 0.05N, and any deformations resulting from this were common to the readings both with and without string tension. Once the machine has been shown the location of the points it will robotically return to take fully automated readings. For each of the two set-ups the machine took three series of readings and processed the average and standard deviation. The machine was started and left running after working hours had finished.

The violin was held in the testing apparatus for a week to fully stabilise the moisture content of the wood to the unvarying 45% relative humidity of the room. After the string tension had been altered the clamps were released to permit the violin to move to a new shape without any restraint. The measurements were made to a precission of 0.0001mm. The standard deviation for these measurements does justify them being quoted to

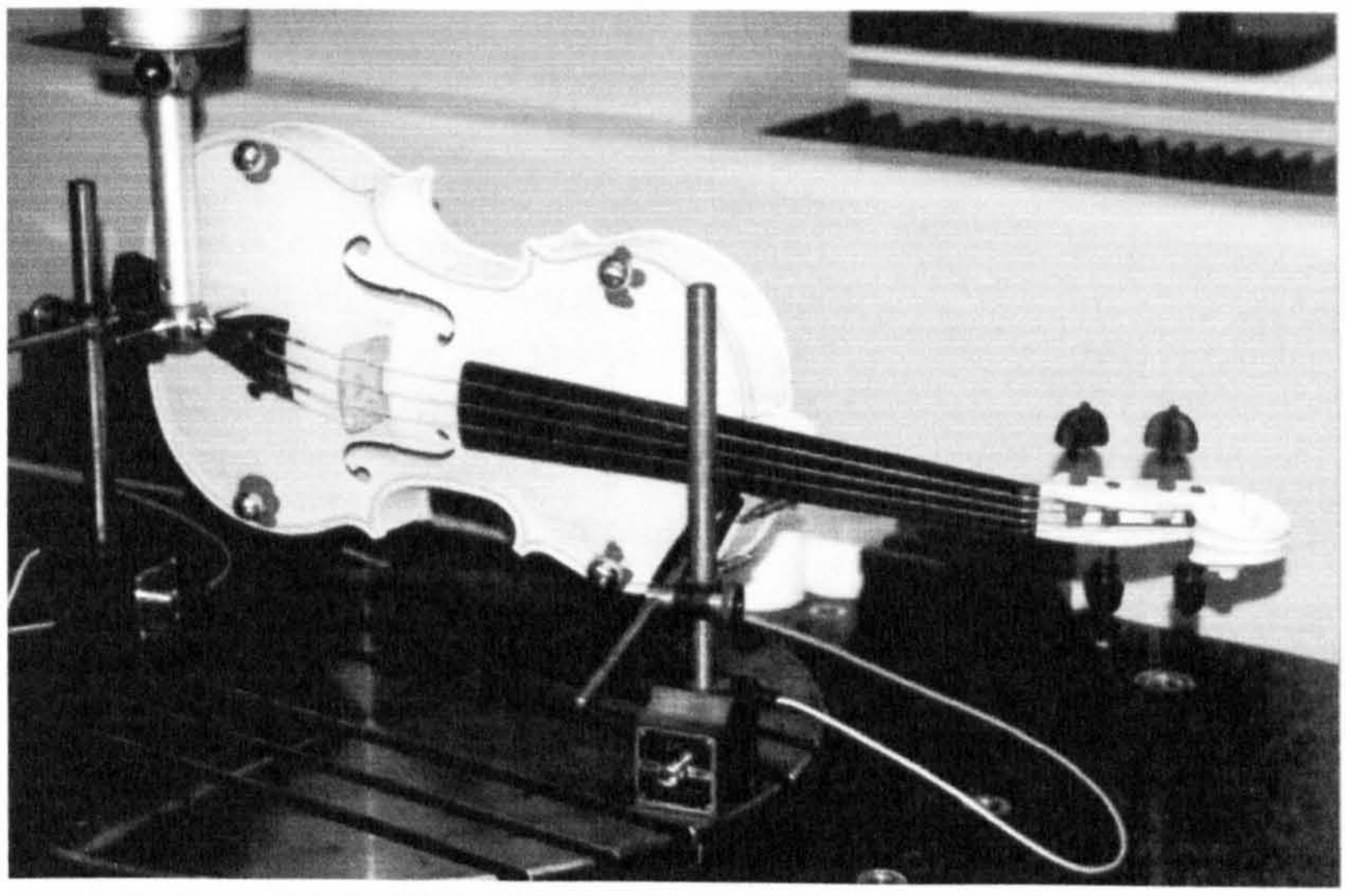

Fig. 4.1. Violin mounted in the co-ordinate measuring machine

0.001mm. Fig. 4.1 shows the violin being held for measurement with the steel balls

attached. The probe is located near the tailpiece and extends horizontally towards the violin from the vertical shaft. The violin was unvarnished.

4.3 The measured deformation

Fig. 4.2 shows a view from the outside looking at the back and belly. Positive measurements denote a movement away from the surface pictured

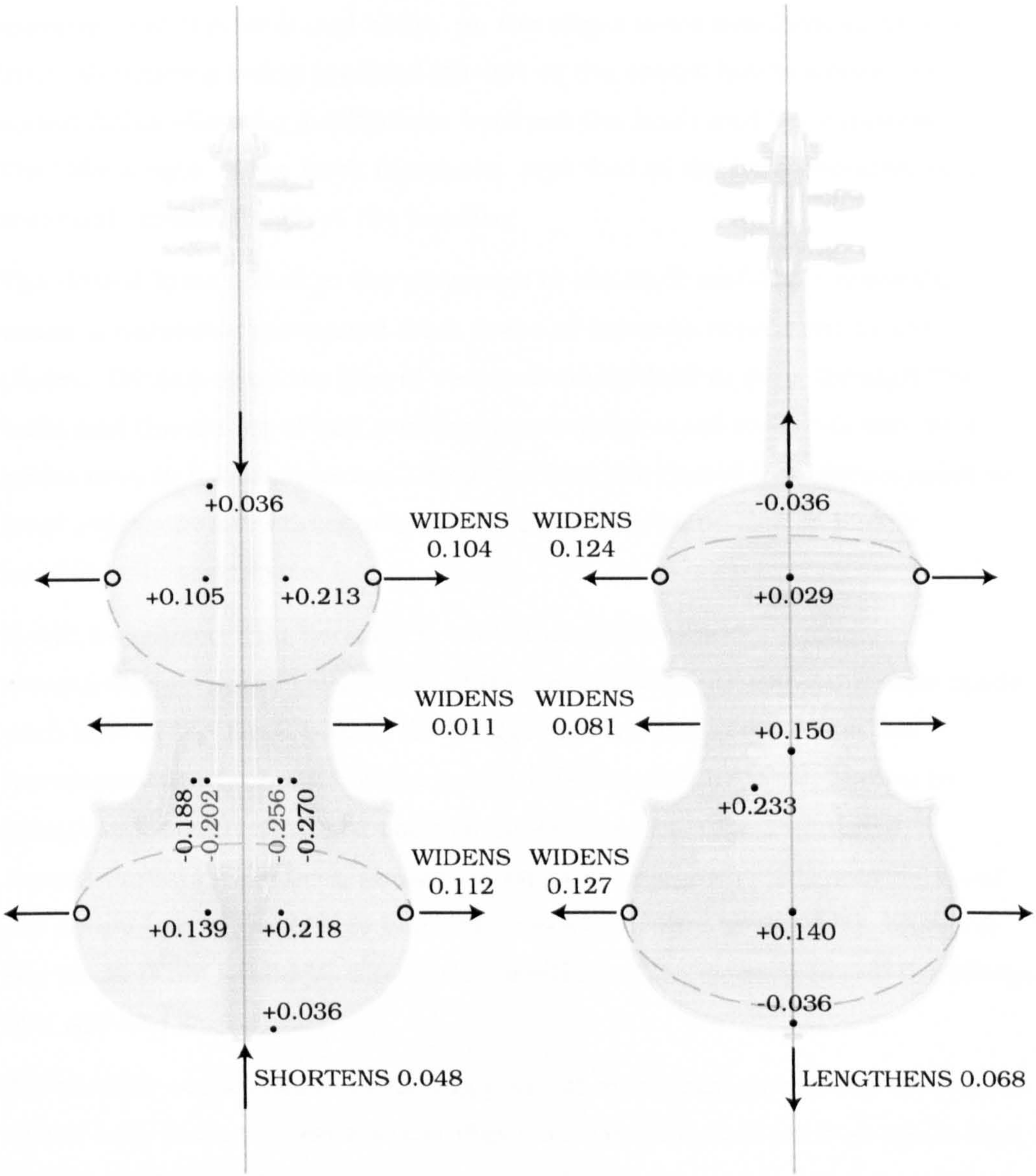

Fig. 4.2. Static deformation caused by raising string tension from zero to normal playing tension, in mm.

towards the reader. Negative measurements denote the opposite. It should first be noticed that the violin bends in its length, both the back and the belly centre bouts moving in the same direction. The length of the back increases and the belly shortens. The end bouts cross arches of both the back and the belly lift, as predicted by the qualitative analysis. It was not possible from the qualitative analysis to make any prediction as to what outline changes may take place. The measurements show that the violin widens in the upper bouts, the centre bouts and the lower bouts of both the back and the front, and that there is fairly close agreement between the movement of the back and belly. ie, the edges move synchronously with little rib twisting being involved (except at the centre bouts where the sound holes allow for a difference between the back and belly movements). That the length of the back increases, and that of the belly reduces, is the inevitable consequence of the bending.

The dotted lines added to the diagrams of the back and front separate areas of outwards movement from areas of inwards movement in the plates. By definition the line of zero movement had to pass through the balls and the choice of ball position was only guessed to be relevent to a nodal line, in dynamic terms. None the less the dotted line shown must at least represent something reasonably close to a nodal line in a slow bending vibration cycle.

It will be noticed that because it was impossible to make a single measurement on the centre line of the belly, two measurements were made each side of the fingerboard, the bridge and the tailpiece. From the measurements each side of the bridge it is possible by interpolation to calculate measurements at each of the bridge feet. The calculated measurements have been shown in red in the diagram. The movement of the treble foot of the bridge is a little more than that of the sound post on the back. This would be due to the bending of the wood between the bridge foot and the sound post.

A fortunate consequence of having pairs of measurements down the length of the belly is that it reveals that there is a considerable twist at the bridge, and a smaller twist in the opposite direction in the end bouts cross arches. Clearly what is happening is that the bass bar is resisting bending of the

violin in its length. Since the stiffness of the bass bar influences the twisting at the bridge, it seems likely that the amount of bridge-rock LSV may be directly dependent on the stiffness of the bass bar. This is investigated in Chapter 12.

4.4 Discussion of results

The fact that substantial areas of the back and belly move apart from each other was predicted by the qualitative analysis, but it was a surprise to find that the sides of the body also move apart from each other over nearly all the periphery. This may have particular significance in the case of a cello, its sides being proportionately much deeper than those of the violin and viola. The deformation of the body was not measured at enough pionts to be able to conclude that its internal volume increases and "breathes in", but this does seem to be possible. In a violin the rise in string tension which would produce the deformations measured here would be associated with a rotation of the bridge causing an additional lift at the bass bar foot of the bridge and an additional depression at the sound post foot. This would extend further the area of outward movement of the belly, to the point where all but a small area around the soundpost foot of the bridge would be involved in the outwards, or breathing, action. This form of operating shape must correspond with the Nullstrahler action first reported by Backhaus, but as Weinreich pointed out this can not radiate well below the frequency of the Helmholtz resonance because air will be sucked in and out of the sound hole. [Backhaus, 1931, Weinreich G].

Deformation under static forces can not be assumed to be a predictor of dynamic behaviour. But it would have validity at very low frequency. It has been demonstrated by others that the violin forms breathing modes but the driving mechanism for this was assumed to be that of the rocking bridge lifting the bass bar and depressing the sound post [Marshall, 1985]. It has been shown here that a periodic variation in string tension, without any bridge rocking can also induce breathing. Since one of the principal causes of periodic variation in string tension is the rocking of the bridge, both these breathing-inducing actions will apply simultaneously.

The fact that the end bouts cross arches simultaneously rise in arch height and widen in arch width is notable. This can only happen if the wood is stretched normal to its grain and/or the reverse curve in the arch straightens. In order to encourage these deformations it would be logical to build the arch in a shape that deviates away as much as possible from a direct line of thrust from the centre to the edge, so that the forces in the arch can pull it straight. Violin arches are built this way.

4.5 Conclusions

- Static tension causes bending in the length, an increase in the rise of all four end bouts cross arches and apart from an inwards movement of the belly edge in the area near the neck and tail saddle, it is probable that all other parts of the periphery of the belly and the back move outwards.
- These movements can be combined with the static displacements caused by a bridge rotation. Then the the violin body enlarges by outward movement in every part, except a small area at the ends of the belly and an area of the belly centred on the sound post.

Chapter 5

MAKE AND PLAY TESTING PROGRAMME.

After the author had developed the ideas presented in Chapter 3 they were tested first by applying the principles to the making of violins. This chapter presents the methods of applying the principles to violin making and the tonal results achieved. This work was done before the supervised PhD programme and is not claimed to exhibit the standards of rigour and objectivity normal to PhD research. It has been included to demonstrate the method of application of the principles and an indication of the sort of tonal effect that results from variation in the EAR and deviation.

5.1 Introduction

The violin appeared in about 1550 and from that date exhibited plate shapes with differences between the front and back that are apparently capable of encouraging breathing modes. The apparent lack of any developmental move towards this can be explained by the violin being an amalgamation of several other instruments in use at the time. The evolution of differences in plate shape between the back and front may have taken place in the precursors to the violin such as the lira da bracio. Varying the plate shapes must have an audible tonal effect or this evolution would not have happened. Since the birth of the violin, many makers have experimented with the effect of varying the shape of the front and back plates. However, the differences referred to above have survived.

The writer has tested the effect of these plate shape differences by building instruments with careful control of the EAR and deviation to find if they affect the sound in a consistent way and to see if it was possible optimise tone by controlling their value. There now follows a description of the methods used. Much of this concerns practical methods and matters of experimental control. About 200 instruments have been made and played and the relevant constructional details have been kept in a record book. These details include all the arching shape details, the EAR, the deviation, the plate thicknesses, the resonance frequency of the free plates in the ring mode and X mode, and the weight of the plates. Additionally, notes were

made about the playing and tonal characteristics of the instrument. It is accepted that some of the evidence is anecdotal, but it is considered relevant to the question of the influence of EAR on the sound of a violin.

5.2 Practical matters

When making a violin plate, the optimum EAR and the deviation must first be known. First, it must be decided where in the length of the body are the centres of the end bouts. (i.e., the points at which the EBX arch heights are measured) Consider a plate of fairly standard violin proportions, such as is shown in fig. 5.1. One could, by inspection, pick a sort of acoustic centre of the upper and lower bouts. In 1976 when the writer began this study, a point was chosen 20% of the distance from the top edge for the upper bouts, and the lower bouts 79% from the top edge. This has been used since then. The actual position is not critical but it is sensible to choose a point where it would be appropriate to place an arching template during the shaping process.

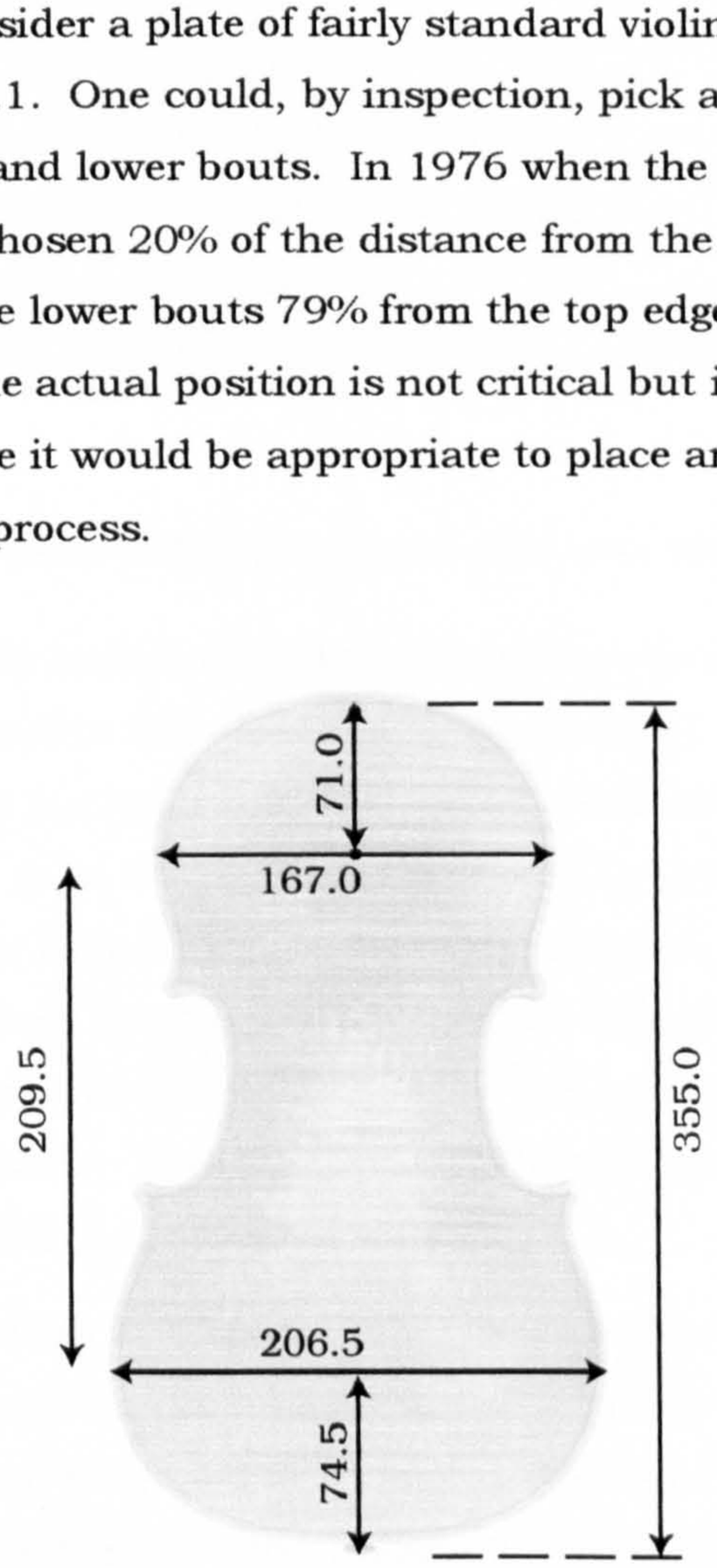

Fig. 5.1. Dimensions of violin analysed.

If one could chose a value for the EAR such that it equalled the BEAR (the balanced end arch ratio), the deviation would then induce the same forces in the front and back plates and presumably give compatible edge

movements. It must not be forgotten that the BEAR is the ratio of the height of the EBX arch to the height of the CBX arch, such that the buckling force in the end bouts from the long arch is balanced by the opposite pull of the EBX arch. The BEAR must then depend on the ratio of the force in the long arch, to the force in the cross arch support system, (ie) the C/L ratio. If the plate shown in fig 5.1 were simplified to make the end bouts the same width, and a load were placed at the central bridge

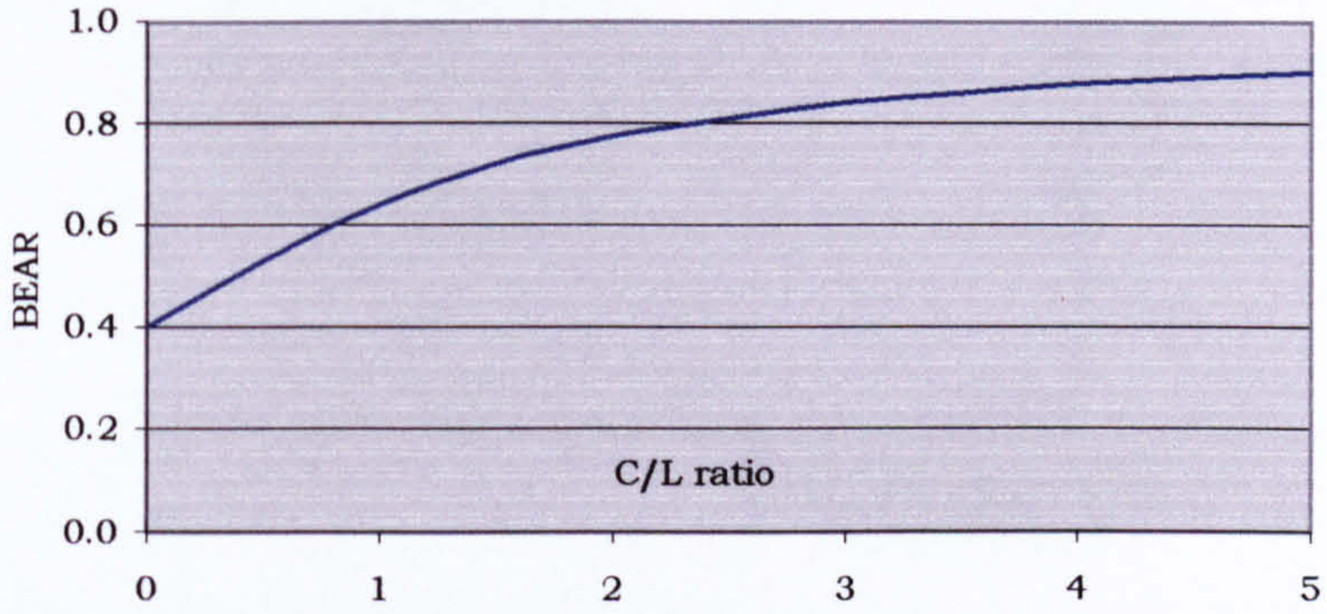

Fig. 5.2. Relationship between the balanced end arch ratio, BEAR, and the C/L ratio.

position, it is possible to derive a relationship between the BEAR and the C/L ratio. Fig. 5.2 shows this relationship graphically. It can be seen that when the C/L is zero (i.e. C is zero), the BEAR would be 0.4, which means the long arch would go in a straight line to the ends because there would be no EBX arch force to counter. At the other extreme, as the C/L gets high the EBX arch force becomes so big that the long arch must depart a long way from the straight line to balance it. This shows how the BEAR varies with the C/L ratio. Now how is the C/L ratio (and hence the BEAR) affected by the general shape of the violin?

Fig. 5.3 shows a number of springs (each representing an arch), interconnected in a network representing a violin plate. The bridge load P is split into two components C and L. L goes through a spring representing the long arch. C goes first through a spring representing the CBX arch, then splits into two springs representing the side arches, then through the end arch springs. The side and end arch springs are cross-tied through the EBX arch spring. The C/L ratio and hence the BEAR, depends on the relative stiffness of all the springs in each system. A reasonable assessment of the relative stiffness of the various arches in the violin can

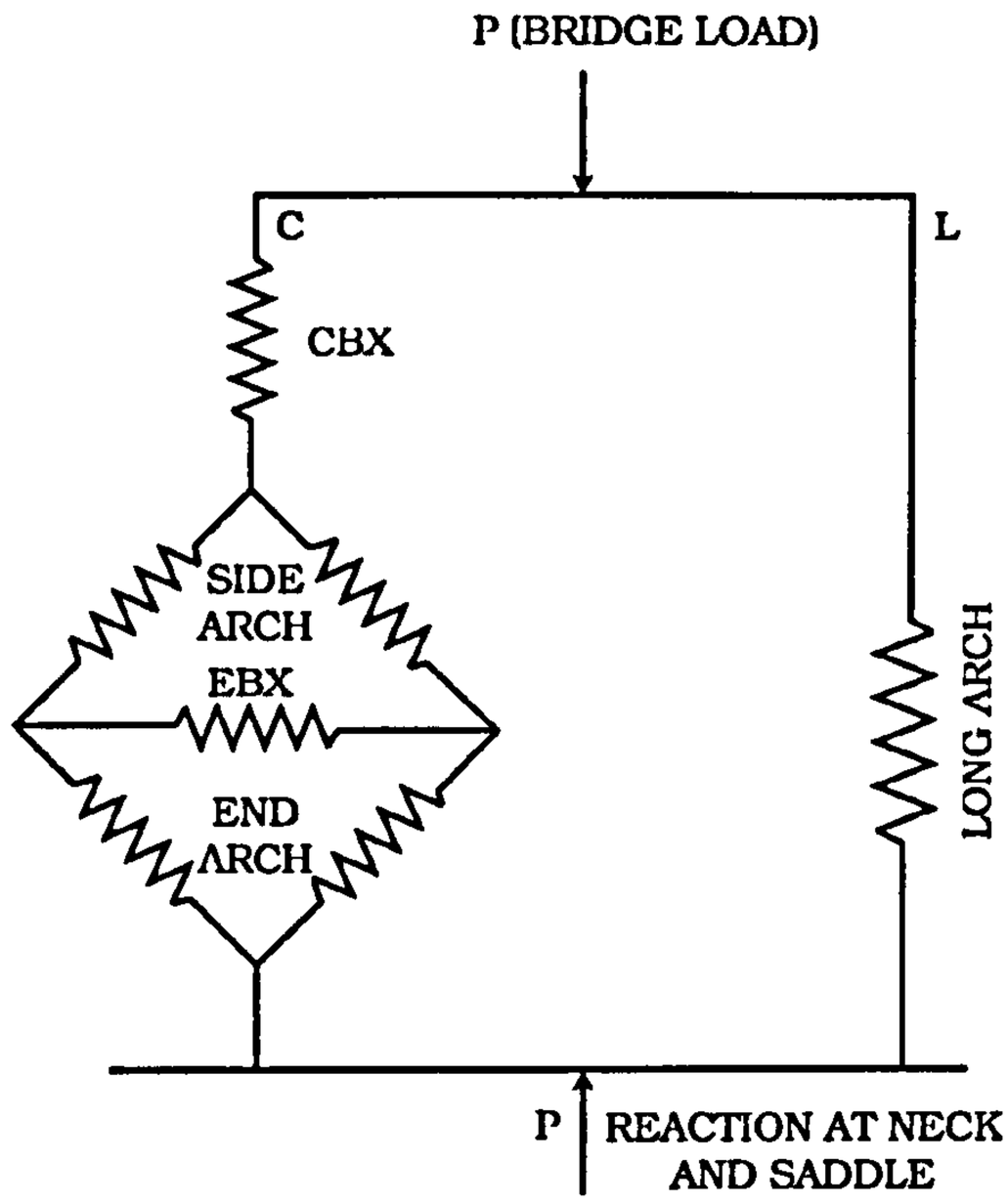

Fig. 5.3. The long and cross arch support systems, representing the arches as springs.

be made. Since arch stiffness is generally closely related to the dimensions of the arch, it is possible to build up, by calculation, a picture of how the BEAR varies with changes in the outline shape and the arching height.

The results of these calculations have two uses. They can be used to estimate how much to alter the EAR by when a change in the geometry of the instrument is being made. They can also be used to make an intelligent

	Effect on the BEAR of a 5% increase	Effect on the BEAR of a 5% decrease
Width of centre	0.992	1.008
Width of end bouts	0.986	1.014
End arch rise	1.014	0.986
Side arch length	0.967	1.034
Side arch rise	0.992	1.008
Arching height	0.980	1.020
Deviation of the CBX arch	0.996	1.004
Combining the CBX deviation and the arching height.	0.976	1.024

decision about whether a change is likely to be beneficial. Supposing in the violin shown in fig. 5.1, it was decided to widen the centre by 5% and lower the arching by 5%, the change in BEAR could be found.

The change to BEAR caused by widening the centre 5%, is given by the chart as 0.992.

But widening the centre reduces the side arch rise.

The change in side arch rise = $109 \times 0.05/2 = 2.725$mm.

The change in side arch rise as a percentage = $2.725 \times 100/38.8 = 7\%$

Therefore the change in BEAR= $1 + 0.008 \times 7/5$ (1.008 from the chart)

= 1.0112

Change in BEAR caused by lowering the arching, including the change in the CBX arch deviation, (from the chart) = 1.024

The total change to the BEAR is therefor: $0.992 \times 1.0112 \times 1.024 = 1.027$

It has been shown how the BEAR varies with the C/L ratio, and with the geometry of the instrument, but not how to find a value for it. Any thought of finding a value for the EAR by calculation is out of the question since the mathematical model would be too idealised to get an answer of the accuracy required. To calculate the figures shown in the table above did require calculating the BEAR for each geometric change, but while the relative values are useful, the actual value is not good enough. What sort of accuracy is required? The results of the tests made showed that if the optimum EAR was say 0.61, then any variation beyond the range ± 0.008 (i.e., ± 1.3%) has an audible effect on the sound. The deviation, on the other hand, is not at all critical. The deviation is the amount by which the belly is built above the EAR and the back below the EAR. The best way to find the optimum EAR is to make and test violins until finally an EAR is found which suits the maker's tonal objectives.

5.3 Tonal evaluation in relation to the EAR

As instruments of varying EAR were made and the tone carefully audited, it soon became clear that being able to make instruments in a way that ensured that the EAR was the same every time was essential in achieving a

consistently good tone. Tonal criteria were found by which to judge if the violin has been built with the optimum EAR.

1. The EAR of the lower bouts strongly (and almost exclusively) affects the sound of the 4th string. There is however some influence on the 3rd string.

2. The EAR of the upper bouts most strongly affects the 2nd string, again with some influence on both the 3rd string and the 1st string.

3. If the EAR is too low, the sound is woolly, fuzzy, and muffled. A player would say that it is not open. The term "open" is an expression much used by players and is readily understood by all who play, even a little. A further consequence of the EAR being too low is that the tone is impure and identifiably hollow in quality. (It sounds as though the sound is emanating from the inside of a large tank.)

4. If the EAR is too high, the sound is thinner, edgy, cold, astringent and perceptibly nasal.

5. As the EAR is raised from a low starting point, the characteristics in (3) above gradually fade away until a point is reached where, quite sharply, the characteristics in (4) above appear. The change from, low EAR, to medium EAR, and to high EAR tonal characteristics, are quite sharp.

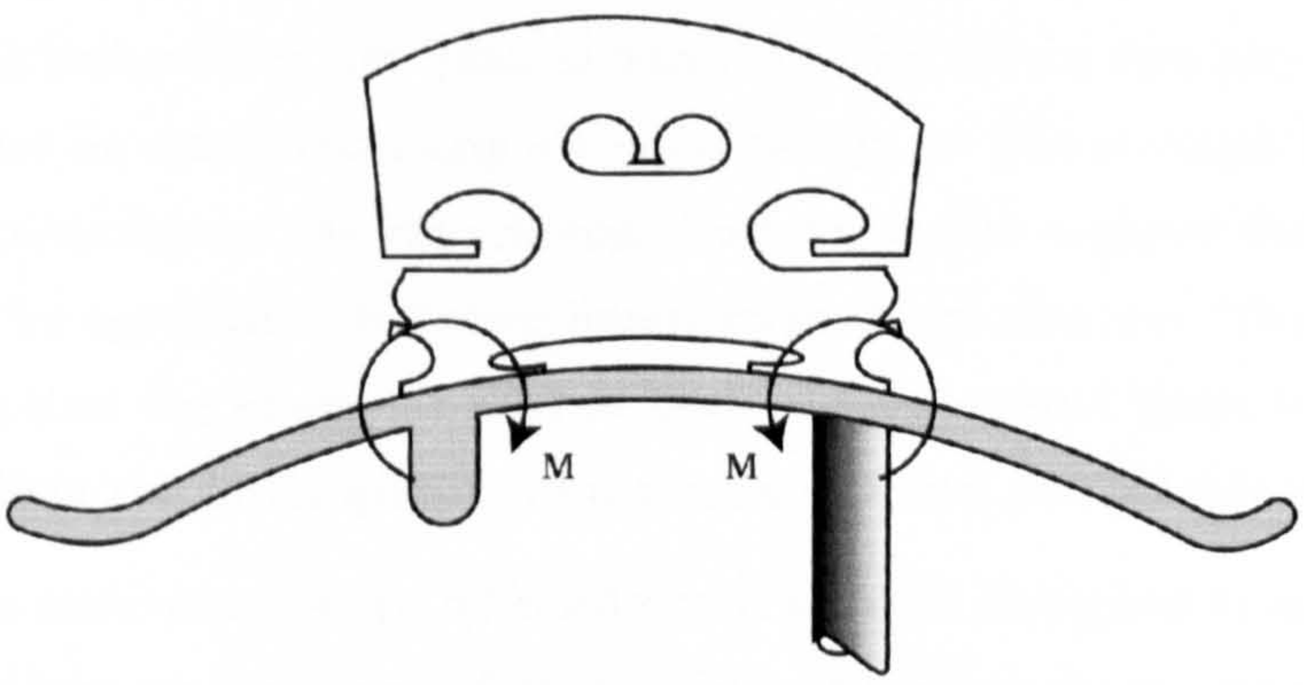

Fig. 5.4. Effect of a narrow bridge on a violin.

To assist in judging the tonal results additional tests can be made. In fig. 5.4 the centre bouts cross arch of a belly is shown. It shows that if an unusually narrow bridge is put on; an eccentricity is created between the

sound post and the bridge foot, and the bass bar and the bridge foot. These eccentricities induce bending moments in the belly, which tend to lower the arch height. This makes the arch behave as though it is more flexible than it really is, thus lowering the C/L ratio by transferring bridge load from the cross arch to the long arch system.

An alternative way of achieving the same effect is to move the sound post out closer to the side of the instrument thus creating a similar eccentricity. Now that the instrument has had its C/L lowered, it would require a lower EAR. If the EAR was previously right or too high, the tone will now be made worse and will have the characteristics of EAR too high. If the EAR was previously too low, the tone will have been improved. The converse of this is that if the sound post is put nearer to the centre of the instrument the arch becomes stiffer, attracts load on to the cross arch system, and raises the C/L ratio. This means that the instrument needs a higher EAR. If the EAR was previously right or too low, the sound will get worse. If the EAR was previously too high, the tone will now improve. There is sufficient information here to determine if the EAR of an instrument is either too high or too low, in each of the upper and the lower bouts. It is widely known that the width of the bridge and distance of the soundpost from the centre of the instrument affects the tone. By understanding the means by which it affects the tone, we can use it as an aid in finding a suitable EAR.

Who is to say what is wrong and what is right, tonally? This is the maker's choice. The writer does not wish to assert in this thesis that any particular tone is better or worse than any other (although he has strongly held personal opinions), as the experience of others would suggest that there is unlikely to be agreement between listeners in these matters. The writer does assert that the choice of EAR in both the upper and lower bouts does certainly affect the tonal quality in a consistent and predictable way.

The writer's instruments are all made with an EAR designed to produce a tone that is just on the verge of moving into the tonal characteristics in (4) above. At this point, the tone is open, clear, pure, and untainted. The strings feel firm under the bow, and the instrument has a feeling of power. This is, of course, the writer's subjective opinion and is included to illustrate the tonal aspects that can be influenced by the choice of EAR.

Violin tonal quality is very sensitive to the EAR. It is therefore necessary to exercise very refined control of the arching of the instrument to achieve the same tonal result every time. These refinements involve taking into account the effect of the wood thickness and the effect of the arching shape on the EAR. A presentation of how this was done is given in Appendix F.

5.4 The effect of varnish

The writer has experimented extensively with varnishes. It is not intended to include the results of these experiments in this thesis. There is one observation that does have relevance to the propositions advanced in the thesis. On several occasions, the writer had cause to entirely remove the varnish from a violin. This was done on two violins made by the writer and two old violins of different makers. The varnish was removed by solvents. In each case, the varnish was removed while the violin was set up for playing. The varnish was removed in stages as follows. The sides, the back, the belly not including the area between the sound holes or under the finger board and tail piece, and finally the area between the sound holes including around the bridge. After the last stage the violin strings, tailpiece and fingerboard were removed and the area under the tailpiece and fingerboard was stripped. Between all stages, the violin was played by the writer and any effect on the sound noted.

The conclusion reached in every case was that there was no significant effect on the sound until the area between the sound holes and around the bridge was stripped. The effect on the sound was quite definite when this area was stripped. It is accepted that this evidence may be subjective but it was thought to be of sufficient interest to be worth including.

5.5 Evaluation of the results

It was suggested that the traditional shape of the violin could only have evolved if variations in the EAR affected the sound. The writer has satisfied himself that the sound of a violin varies considerably with the EAR. It shows little sensitivity to the deviation. The writer found that there is an optimum value for the EAR, which gave the best tonal attributes. No claim is made that the subjective judgement involved would produce the same

choice of EAR regardless of who was auditing the tonal result. It is claimed though that it is unlikely that anyone would like the tonal result produced by violins of extreme values of EAR. It follows that consistency of tonal quality can be assisted by building violins to a repeatable value of EAR. This has been confirmed by the writer. The tone of a low EAR violin becomes metallic and hollow in quality. The tone of a high EAR violin becomes thin and edgy.

5.6 Conclusions

- The tone of a violin has been perceived by the author to be very sensitive to the EAR but less sensitive to the deviation.
- The EAR of the lower bouts of a violin affects the tone on the fourth string with some influence on the third string.
- The EAR of the upper bouts of a violin affects the tone on the second string with some influence on the first and third strings.
- The feeling that a good violin is firm in the string implies that the transverse vibration of the string is influenced by the vibration of the body that it is on.
- The tonal effect of applying varnish may be limited to the area between the sound holes.

Chapter 6

EXPERIMENTAL PRELIMINARIES

6.1 The experimental programme

The experimental programme had several objectives.

1. To demonstrate experimentally the different causes of LSV and investigate their relative contributions.
2. To investigate the influence of EAR and deviation on the spectrum of transverse vibration of the string, the LSV, and the radiated sound.
3. To investigate the relative importance of TSV and LSV in driving the violin.
4. To see if there is evidence of LSV influencing the modal responses.

In the course of the work, some interesting experimental results were found concerning the effect of varnish on violin behaviour. These results raise issues that require further research, but it was thought that they were of sufficient interest to be included as an appendix to the thesis.

The remainder of this chapter deals with the design of the basic apparatus used, the calibration of the test equipment and the finding of suitable instruments for testing.

6.2 Properties of the violins and strings

6.2.1 The violins

Violins used for testing had to incorporate the differences in arching that were to be examined, while being as similar as possible in all other respects. Violin tone varies with the nature of the wood used (no two pieces being completely identical), the shape of the arching, the graduation of the thickness of the plates, the sealers and varnishes used, the dimensions of the bridge and adjustment of the soundpost. It also varies with its age, and the temperature and humidity of the room in which it has recently been. It is common experience among violinists that the sound of a violin varies considerably with the way it has been played, which leaves a

semi permanent change in the sound. Although this has not been explained scientifically, and therefore may not be accepted by some, there is justification for being cautious and excluding this as a factor in comparing violins. The solution to these problems was to make new violins for testing.

Three violins were made from wood cut from adjacent positions in the same board. That the wood was substantially the same was confirmed during the graduation of the plate thickness, when the same thickness gave close to the same free plate modal frequencies in the three main modes. The violin arching shapes were of the same basic shape except as necessary to achieve the different EAR and deviations. Some of the tests were carried out before varnishing and some after. The same bridge was used on all the violins and the writer, working to the same criteria, did the adjustment of the soundposts.

The three violins are numbered as follows. The EAR plus or minus the deviation is shown. The deviation is also shown as a percentage of the EAR. If the centre bouts arch height is H, the belly end bouts arch height is H × (EAR+deviation), and the back end bouts arch height is H × (EAR – deviation).

V158LD	Normal EAR	Low deviation.	
Upper bouts.	0.604 plus or minus 0.051		8.4%
Lower bouts.	0.622 plus or minus 0.065		9.7%

V156	Normal EAR	Average deviation.	
Upper bouts	0.605 plus or minus 0.080		13.2%
Lower bouts	0.621 plus or minus 0.089		14.3%

V157HD	Normal EAR	High deviation.	
Upper bouts	0.606 plus or minus 0.108		17.3%
Lower bouts	0.622 plus or minus 0.131		21.0%

The term "normal EAR", means the violin is made with an EAR that the writer has determined gives the tone that he most likes, and always uses. It should be noted that the deviation of the high deviation violin is about double that of the low.

By temporarily interchanging the fronts of V157 and V158, two more violins were made, which with V156 again, gave the following. The % variation in EAR is shown taking the normal EAR as being 100%.

V157LE	Low EAR	Average deviation.	
Upper bouts	0.576 plus or minus 0.078		95%
Lower bouts	0.587 plus or minus 0.095		

V156	Normal EAR	Average deviation.	
Upper bouts	0.605 plus or minus 0.080		100%
Lower bouts	0.621 plus or minus 0.089		

V158HE	High EAR	Average deviation.	
Upper bouts	0.633 plus or minus 0.805		105.3%
Lower bouts	0.657 plus or minus 0.096		

It should be noted that the variation in the EAR is comparatively small and in fact, many violins are made, and have been made, with an EAR much lower than the low EAR violin tested, and much greater than the high EAR violin tested.

Since violins of low or high EAR would be tonally unacceptable to the writer, it was important that they could be remade easily into good violins. The instruments were always kept together in the same room and were played only by the writer. One of the violins was used in a manner later described as a "detached body". This was V156.

6.2.2 The strings

The strings used in all the research were a plain steel E string and the other strings were "Thomastic Dominant mittle gauge". It is perhaps the most commonly used violin string today. For various reasons, it was necessary to know the spring stiffness of the strings. The spring stiffness is defined in this thesis as the force required to stretch a 1m long string by 1m (it is therefore independent of the string length in the same way as other properties such as Young's modulus and the density). It has the units N/(m/m), or simply N. The method used for finding this is described in Appendix B. The accuracy shown represents a 95% chance that the error would be less than the tolerance quoted. The strings were also weighed to find their mass per unit length.

The properties found are as follows:

1st string, stiffness k_{st} 6688 N +or- 15.5%,	0.00041 g/mm +or- 5%.
2nd string, stiffness k_{st} 1711 N +or- 32%,	0.00075 g/mm +or- 5%.
3rd string, stiffness k_{st} 2213 N +or- 12%,	0.00114 g/mm +or- 5%.
4th string, stiffness k_{st} 2804 N +or- 19%,	0.00279 g/mm +or- 5%.

6.3 Apparatus

The equipment and measuring devices that were made are described below. The calibration of these devices and the derivation of the conversion factors used in the processing of the results are given.

6.3.1 Test bed

Nearly all of the tests conducted were carried out on a rig built on a heavy steel and timber laminated base, designed to minimise the possibility of vibration transmission. The violin scroll and peg box was securely glued and screwed to the base, and the other attachments were clamped on as and where required. A rigid welded steel anchor was made up to form a fixing point for the end of the string opposite the peg box, and attached with G cramps to the bed, where required. See fig. 6.1.

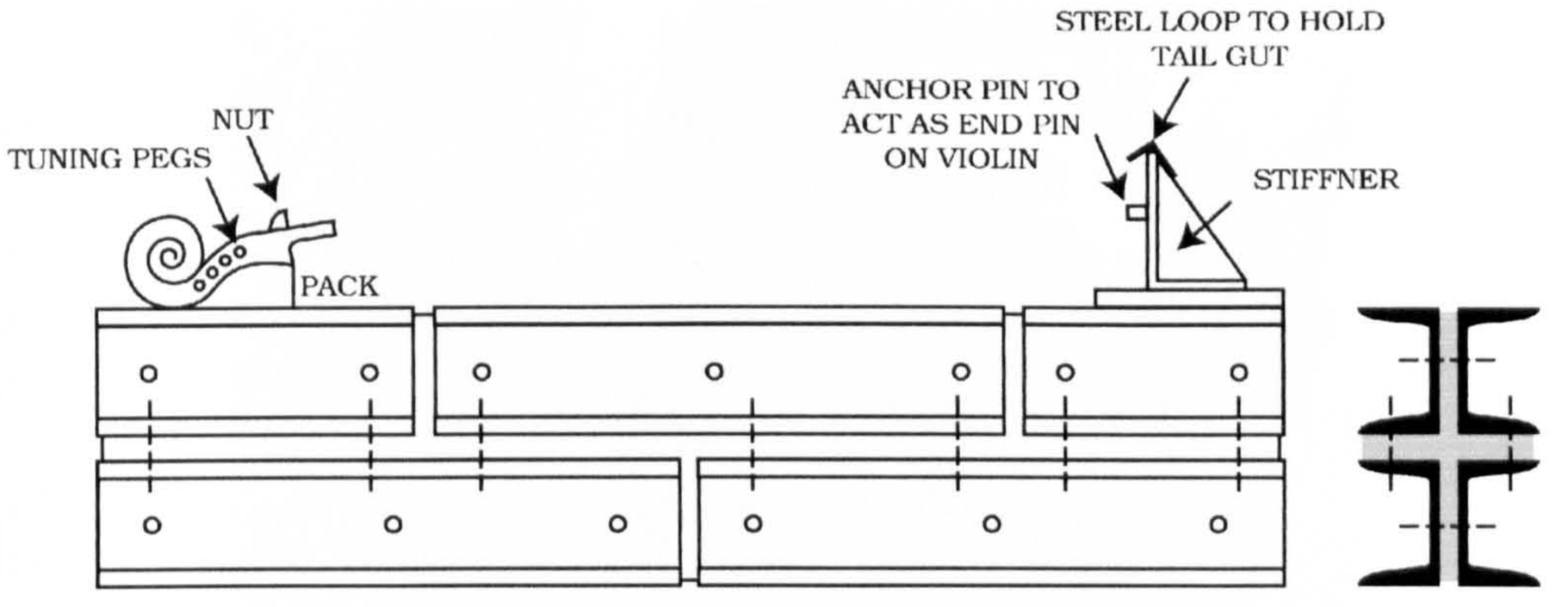

Fig. 6.1. Non conductive base.

6.3.2 Driving the string

In some of the experimental work, the string was driven by a shaker. To do this a fine wire stinger was attached to the shaker and, bent to form a notch over the string at the other end. This is shown diagrammatically in fig. 6.2. The stinger was bent so that when lowered on to the string until it was straight it applied a small downward pressure on the string to ensure a firm fit. The position of the stinger on the string was 3mm from the end in the experiments presented in Chapters 7,8 and 9. The experiments in the higher harmonics presented from Chapter 10 onwards were all done with stinger contacting the string 8mm from the end. The string was driven at the end remote from the bridge. This was a precaution to eliminate the possibility of the shaker drive having some influence over the bridge motion other than via the string vibration. See fig. 6.3. Hacklinger has also suggested that a force could be applied to the bridge by using a shaker to

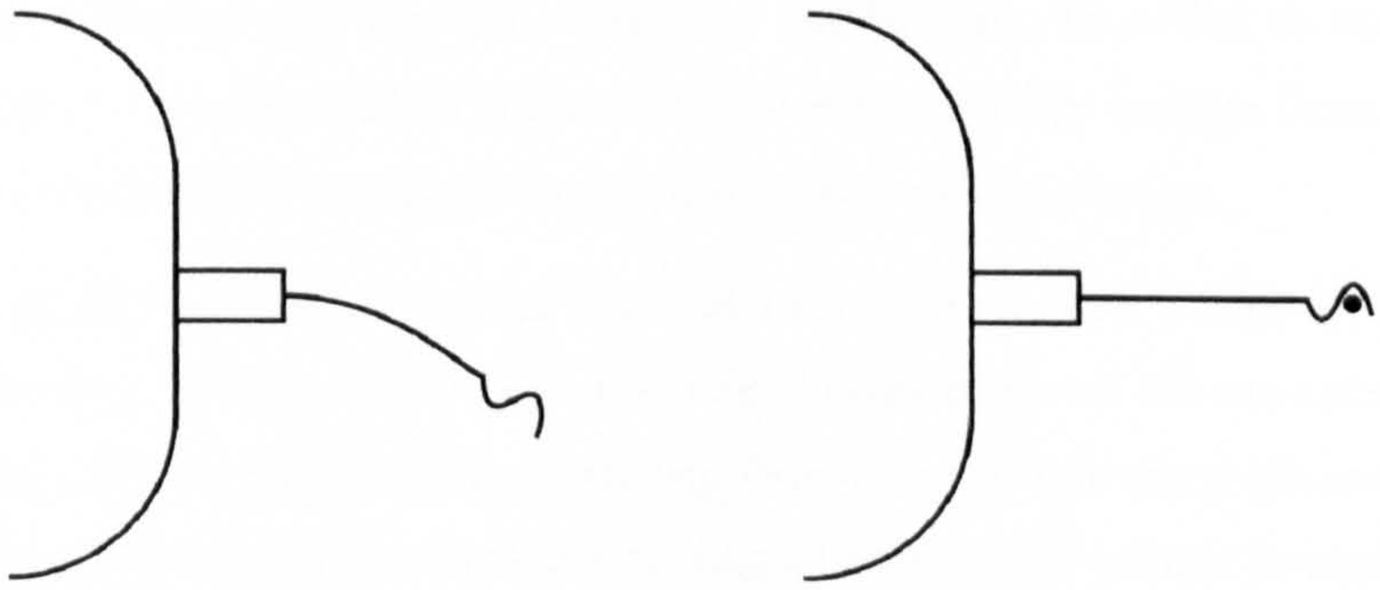

Fig. 6.2. Stinger for driving the string, shown on and off the string.

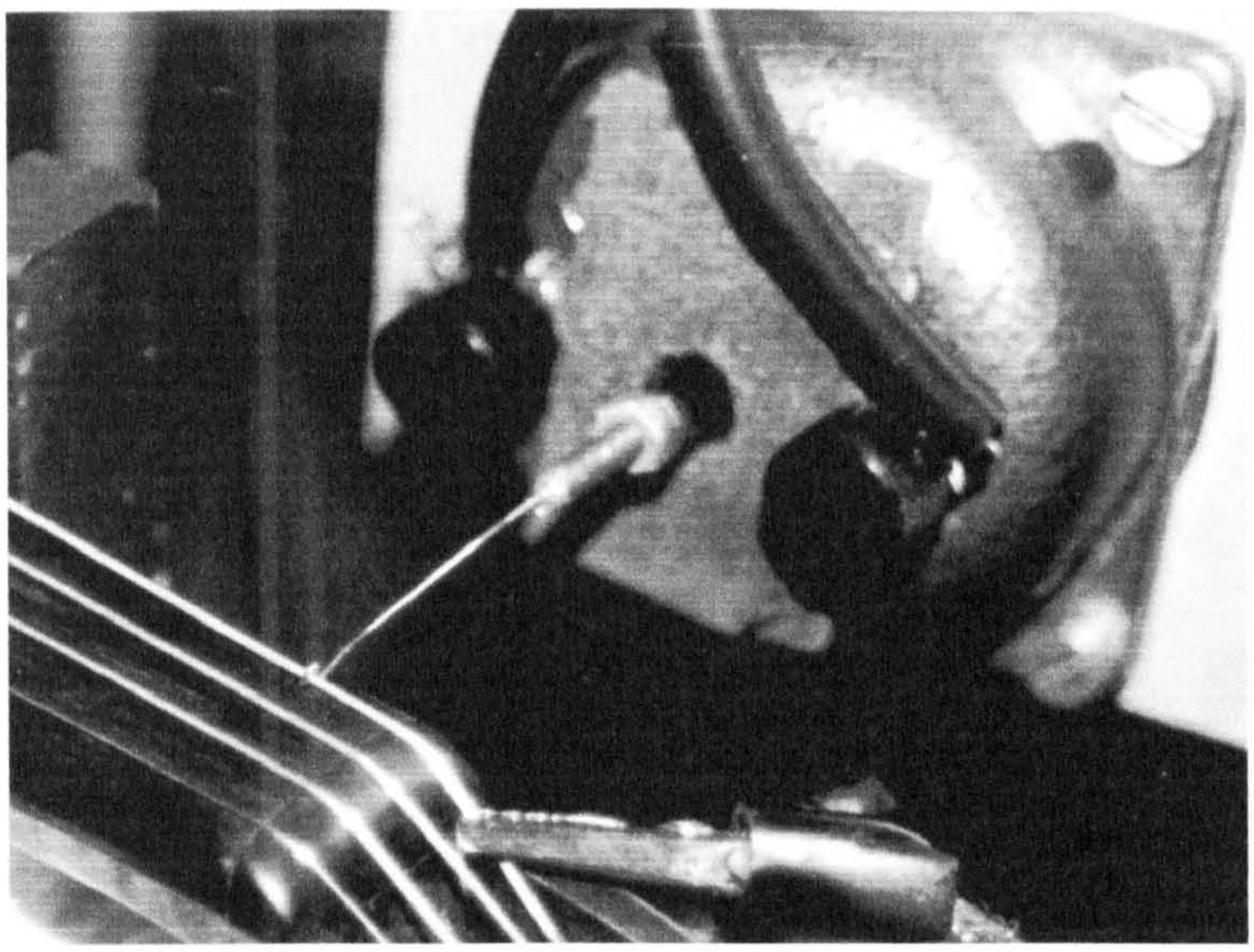

Fig. 6.3. Shaker driving a string.

drive the string, but he had the string damped [Hacklinger, 1978].

A detailed discussion of the repeatability of driving the string with a shaker is given in section 10.2.1.

6.3.3 Spectral analysis

A real time fast Fourier analyser type DI-2200 serial number 951215 was used to record and spectrally analyse the detected signals.

6.3.4 Measurement of the transverse displacement of the string

The force exerted on the bridge by the vibration of the string could have been measured directly by small transducers located at the string notches. However in this work there was a need to distinguish between the TSV force on the bridge and the LSV force on the bridge. In order to make this distinction it was decided to infer the TSV force on the bridge from measurements of the transverse displacement of the string.

The strings are built of a Perlon (German for Nylon) core wrapped in a spiral of metal, and are therefore electrical conductors. To measure the transverse velocity of the string, strong ferrite magnets were placed to create a magnetic field around the string at any point where it was required to detect the motion of the string. The movement of the string induced an EMF in the string, which was picked up by clipping on wires, outside the

playing length of the string. The peak-to-peak transverse displacement at the centre of the string length was measured with a simple scale (to a precision better than ± 0.3mm).

$$\text{EMF at analyser} \propto \frac{\text{lines cut}}{\text{time}}$$
$$\propto \frac{\text{displacement}}{\text{time}}$$
$$\propto \text{displacement}.f$$
$$\text{and therefore the displacement} \propto \frac{\text{EMF}}{f}$$

For some of the experiments the magnets were positioned in several locations in the length of the string so that all the harmonics could be

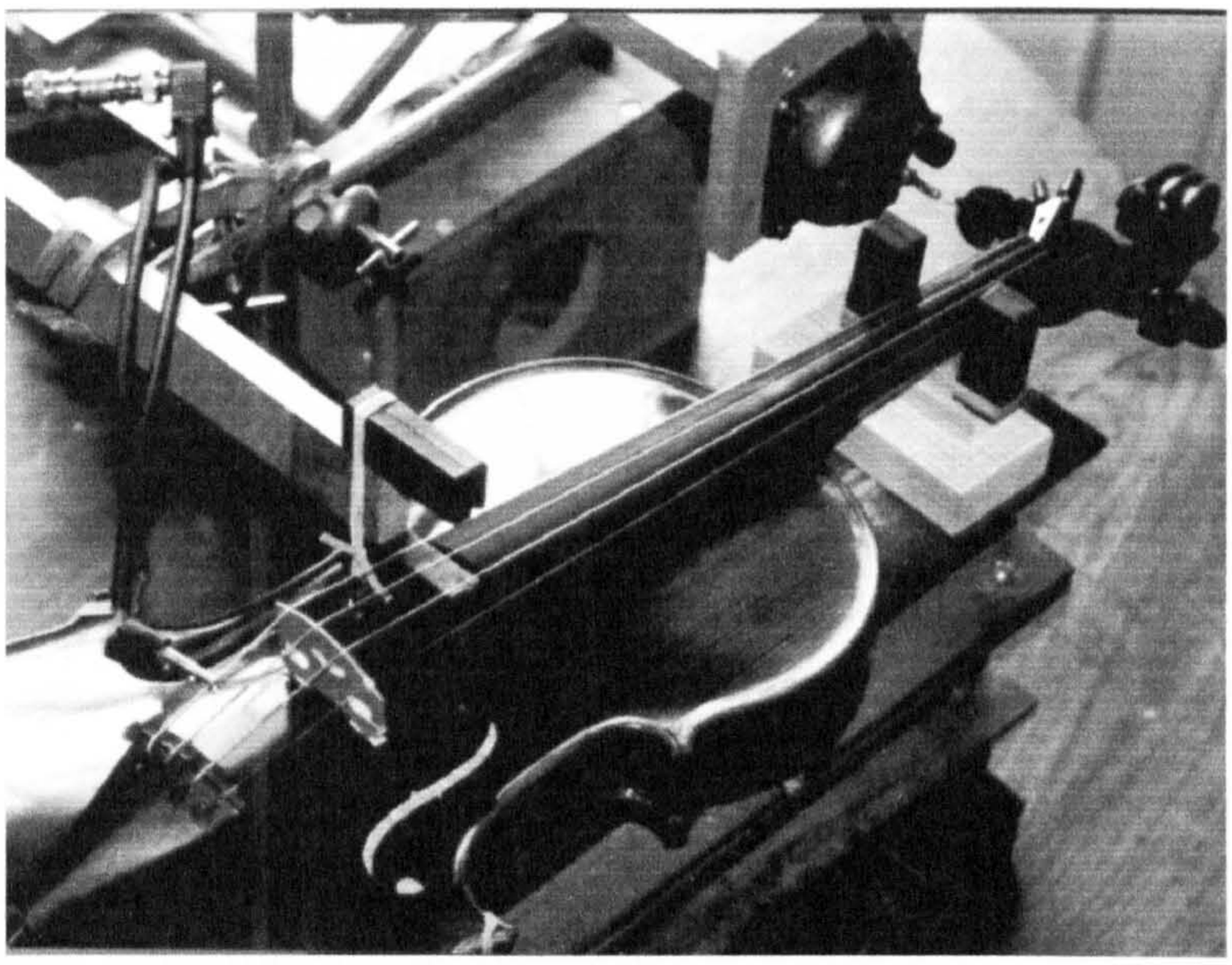

Fig. 6.4. Magnet locations for measuring the amplitude of transverse displacement, or of vertical displacement, of the 4th string.

detected. The magnets were positioned 50 mm from the bridge end of the string. The set of magnets near the bridge was oriented to create a field that would pick up horizontal motion. By setting magnets at the other end of the string oriented to detect vertical movement, it was found that the vertical component of movement was very small. The set up is shown in fig. 6.4.

It was not possible to locate the magnet so that it would record all the harmonics in equal proportion to their amplitudes. Therefore, the recorded signal was divided by $\mathrm{Sin}\left(\frac{n\pi x_0}{L}\right)$, where L is the string length and x_0 is the distance from the end to the magnet position, and n is the harmonic number. This factor tends to zero every 1280Hz and gives an unrealistically high correction at harmonics close to these frequencies. The fact that the magnet had an appreciable width would round off the correction at these points. A sensible allowance was made for this.

Additionally a correction was made for the sinc effect due to the magnet being relatively wide in relation to the wavelengths of the higher harmonics. The recorded signal was divided by $\frac{L}{n\pi a}\mathrm{Sin}\left(\frac{n\pi a}{L}\right)$, where 2a is the effective width of the magnetic field, which was taken as 12mm.

These factors are derived as follows. The average string velocity at over a magnet width of 2a, centred at x_0 from the end of a string vibrating at frequency ω, whose displacement amplitude is given by $y = A\sin\frac{n\pi x}{L}$ is,

$$\bar{v}_s = \frac{j\omega A}{2a}\int_{x_0-a}^{x_0+a}\mathrm{Sin}\left(\frac{n\pi x}{L}\right)dx$$

$$= j\omega A\frac{L}{n\pi a}\mathrm{Sin}\left(\frac{n\pi a}{L}\right)\times\mathrm{Sin}\left(\frac{n\pi x_m}{L}\right)$$

The factored analyser voltages were then all divided by the frequency. This gives a figure proportional to the displacement amplitude. Then the displacement amplitude at the centre of the string length in the first harmonic was compared to the measured string displacement amplitude and all the analyser voltages were scaled accordingly. The error involved in measuring the centre amplitude with a scale is not significant in relation to the dynamic range of the spectrum, which was displayed on a log scale through several orders of magnitude.

6.3.5 Measuring LSV.

Several devices were used for measuring LSV force.

The force gauge A standard force gauge, B&K 803120, type 8200, was used with a charge amplifier with a gain of .01 V/pC and an amplification of 30dB i.e. 31.7. The force gauge produced 3.9 pC/N.

Analyser output = LSV force $\times 3.9 \times .01 \times 31.6$

LSV force = Analyser output (Volts) $\times 0.8088$, Newtons.

String anchor transducers In order to measure the LSV force on a violin set up in playing condition with four strings on it, a standard violin tailpiece was fitted with a small piezoelectric transducer at each string anchor. The transducers were described as type PZT-3A, B/N 00992, and measured 10mm by 5mm by 2mm. To make a smooth path for the nylon chord that passes around the transducers, they were ground with a water stone to have a D end as shown fig. 6.5.

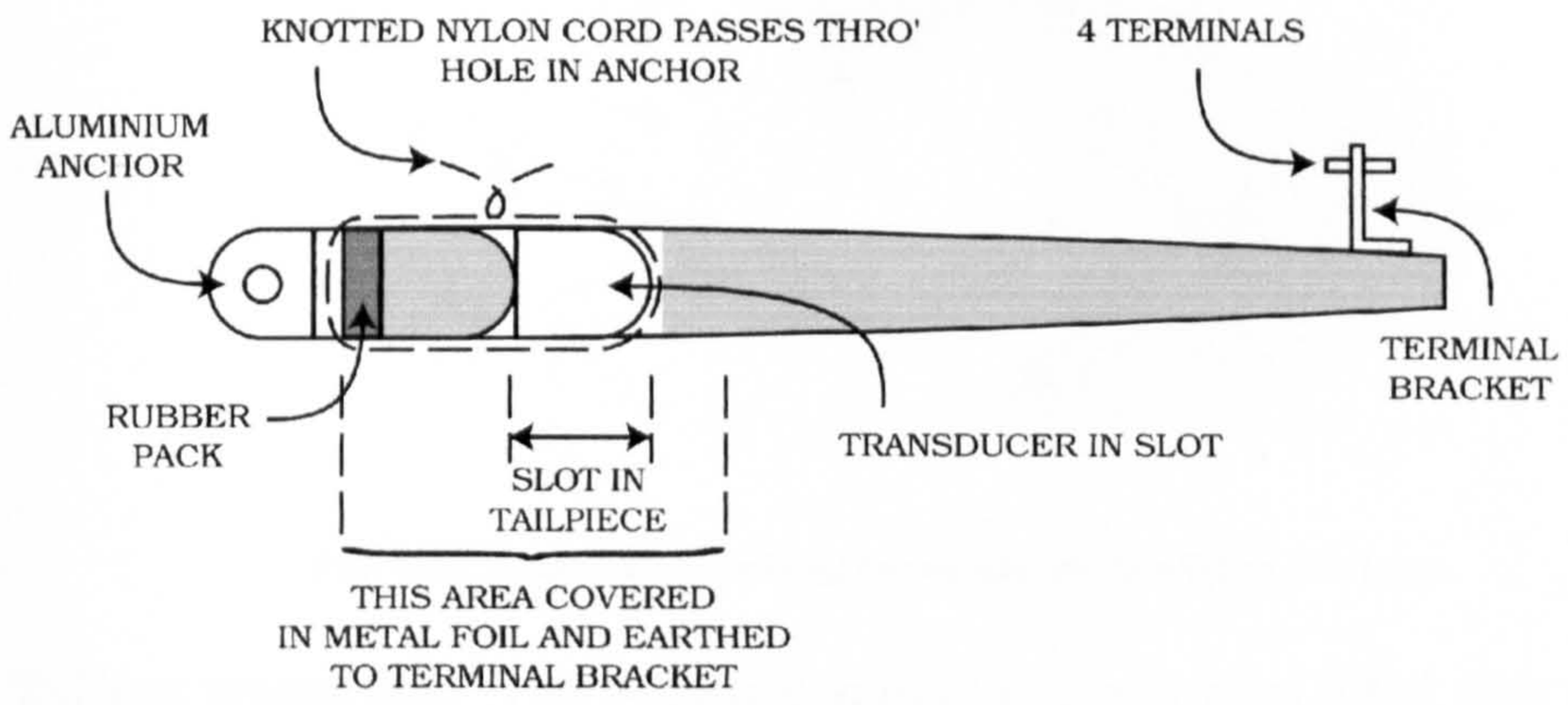

Fig. 6.5. Long section of tailpiece, showing tranducers at string anchors.

Several versions of the tailpiece where made and tested and several methods were used for its calibration. The details of the calibration of these transducers are given in Appendix C. The calibration figures are shown as positive if a tension increase gave a positive charge. The calibrations are:

1st string, transducer sensitivity k_{tt}, +36 pC/N +or- 77%.

2nd string, transducer sensitivity k_{tt}, -20 pC/N +or- 77%

3rd string, transducer sensitivity k_{tt}, +45 pC/N +or- 86%

4th string, transducer sensitivity k_{tt}, -50 pC/N +or- 62%

This tailpiece was used with a charge amplifier that produced 0.01V/N and

amplified by 20dB.

Analyser output = LSV force $\times k_{tt} \times 0.01 \times 10$

LSV force = Analyser voltage $\times 10/k_{tt}$

Fig. 6.6 shows the finished tailpiece. The metal foil wrapping was found to be necessary in order to avoid interference from the ambient electrical field in the room.

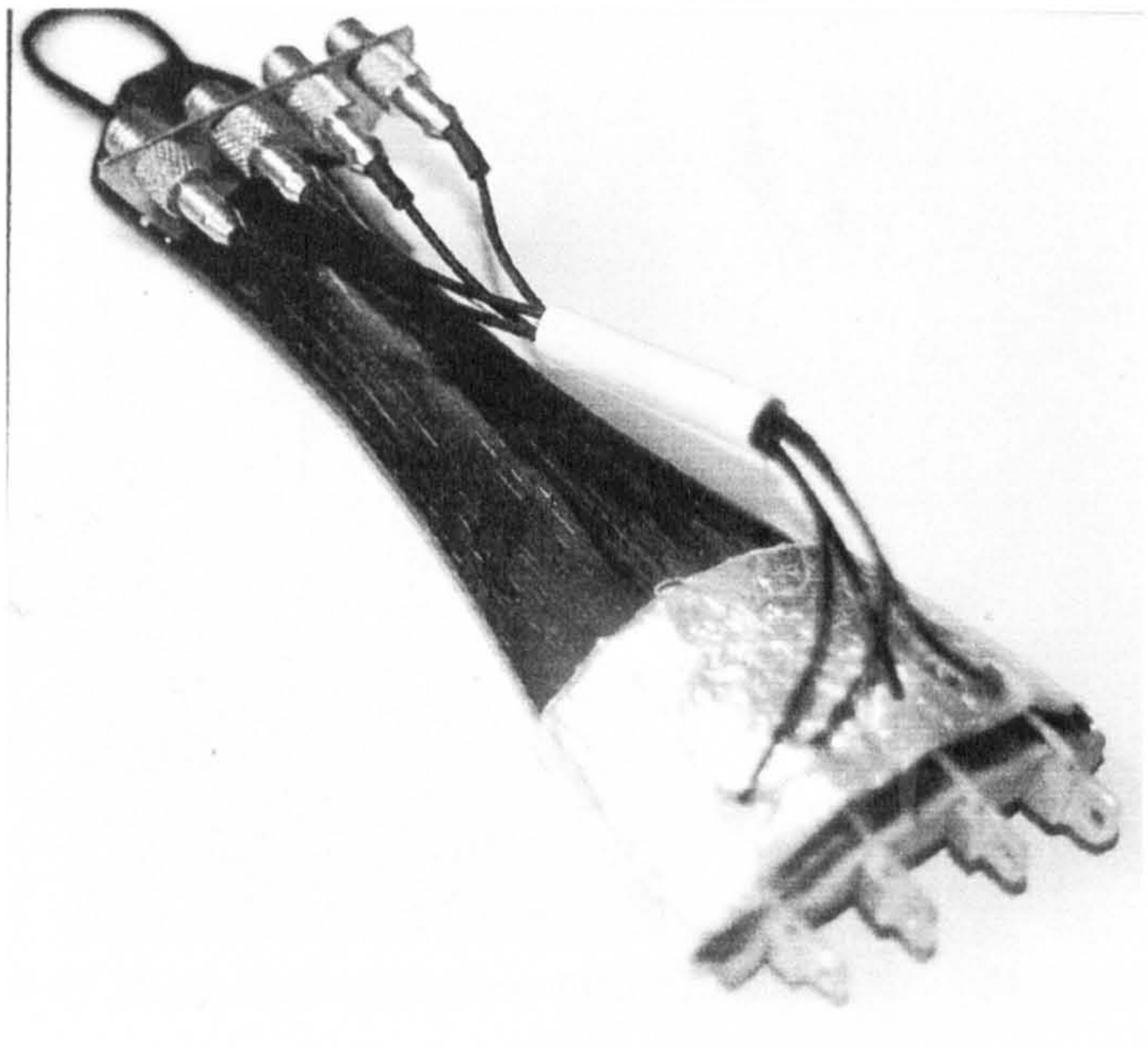

Fig. 6.6. Tailpiece showing transducers at string anchors.

Tailgut transducer Two standard violin tailpieces were fitted with a transducer under the anchor point for the tail gut, in such a way that it would be subject to the tension force in the tail gut. This is shown diagrammatically in fig. 6.7, and in the photo in fig. 6.8. The area surrounding the transducer was covered with metal foil shielding. Two versions of this were used, and the details of the calibration of each one is given in Appendix D.

The calibrations are: Mark 1, +43.1 ρC/N +or- 52%

Mark 2, +23.3 ρC/N +or- 20%

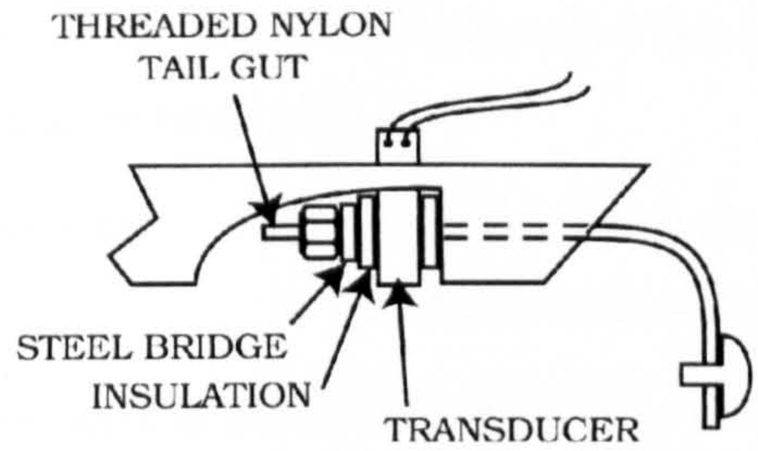

Fig. 6.7. Diagram of transducer at the tail gut anchor.

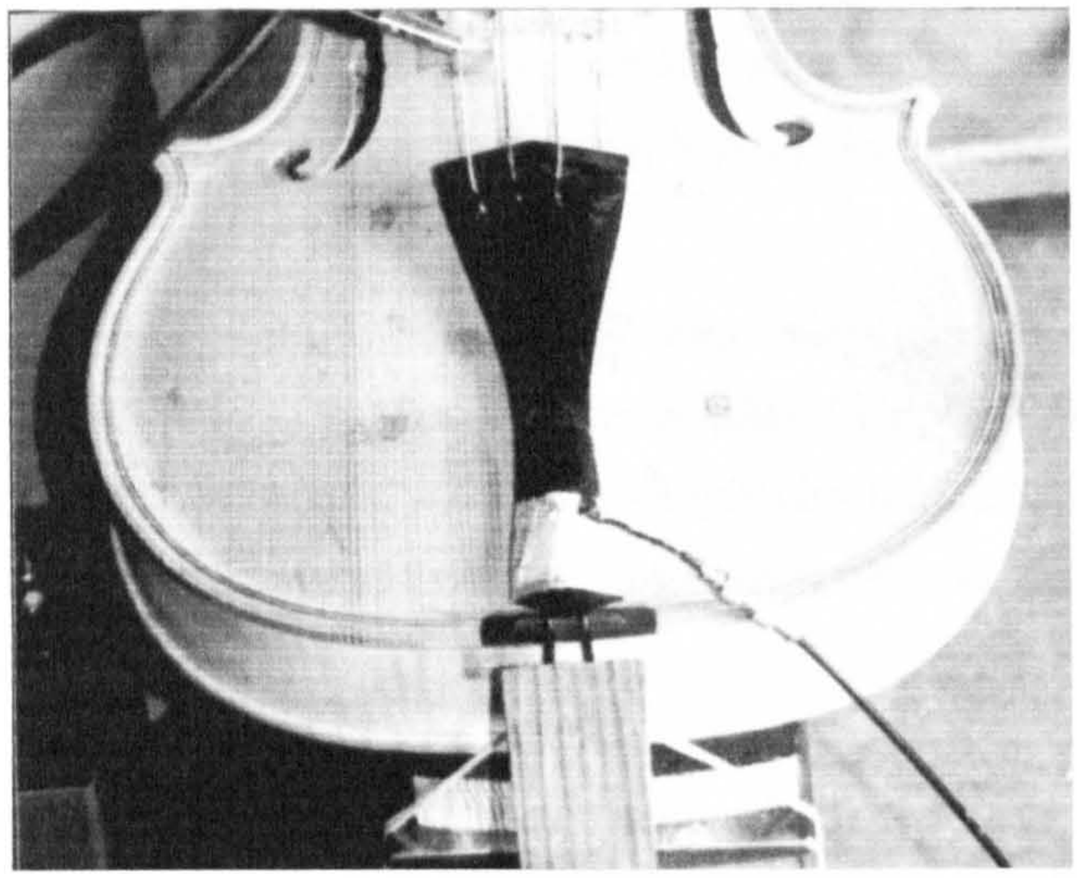

Fig. 6.8. Photo of the tailpiece with the transducer at the tail gut.

Mark 1 was used with a charge amplifier that produced 10 mV/pC, and amplified by 20db. The analyser voltages were converted to LSV as follows:

$$\text{LSV force} = \text{Analyser voltage}/(43.1 \times .01 \times 10)$$

$$= \text{Analyser voltage} \times 2.32 \text{ Newtons}$$

Mark 2 was used with a charge amplifier that produced 100 mV/pC.

$$\text{LSV force} = \text{Analyser voltage}/(23.3 \times 0.1)$$

$$= \text{Analyser voltage} \times 0.429 \text{ Newtons}$$

6.3.6 Measurement of movement

The movement of the violin surface was calculated from the measured acceleration at the point. The accelerometer used was an Endevco Mod. 25B S/N BL 43. The calibration of the accelerometer is given by the manufacturer at 4.912 mV/EU. This was used with a signal conditioner in

which the sensitivity was set to the calibration of the accelerometer. The output scaling was set at 500mV/EU

The acceleration is given by: $\alpha = 2 \times 9.81 \times$ Analyser volts, m s^{-2}

$\alpha = 19.62 \times$ Analyser volts, m s^{-2}

To convert the accelerations to displacements they were divided by $(2\pi f)^2$, to give a displacement in metres.

The polarity of the accelerometer had to be determined. This was done by holding the accelerometer in the hand, and bringing the hand swiftly downwards. The acceleration was seen on the screen of the oscilloscope, and the direction of movement, which gave a positive voltage output, was noted.

Vertical movement at the top of the bridge was calculated from the velocity at the point. The velocity was recorded by a laser Doppler velocimeter, LDV. The LDV, ISVR No. 1585787 has a sensitivity of 6.24V/ms^{-1}. This was used without further amplification. To convert the velocity to displacement it was divided by $(2\pi f)$.

6.3.7 Measurement of radiated sound pressure level

The radiated sound pressure level was measured by a microphone, B&K ½ inch free field, type 4191, SN 1838444. The signal was amplified. Generally, the results are comparative only and no attempt was made to calibrate the measurement system. The microphone was suspended on a 2m long string from a beam. It was made to swing through a wide arc during recording. The data was acquired by the analyser during 15 averages. The mean square pressure in a reverberant space excited by a pure tone exhibits large spatial variation because of the interference effect caused by reflections from the enclosure boundaries. Spatially averaging of the sound field by traversing the microphone is routinely employed in standardised methods for estimating the spatial average mean square reverberant sound pressure that is proportional to the sound power radiated by the source. In the absence of a mechanised device, swinging was employed as a practical means of achieving a spatial average. The distance from the violin to the microphone was set at about 2 metres, but this would vary during the swing motion. Since the microphone was

positioned within the reverberant field, its distance from the violin was not critical.

The recorded radiated sound of the violin included the sound radiated by the shaker that was used to drive the string. Therefore, it was necessary separately to record the noise coming from the shaker. It was difficult to measure this sound because when the stinger was removed from the string the unloaded shaker increased its amplitude and emitted more sound. However each time the sound radiated by the violin and shaker was measured the stinger was removed from the string while still running and the sound emitted by the shaker alone was measured. When analysed, the sound of the shaker alone was much stronger in the first few harmonics and weaker in the upper harmonics compared with that of the violin plus shaker. After some consideration, it was decided that ¼ of the recorded shaker rms sound pressure be subtracted from the recorded sound of the violin and shaker together. If as much as ½ was subtracted, parts of the resulting spectrum became negative (not at the harmonic peak frequencies but in the noise areas between the harmonic peaks). By subtracting ¼ of the shaker sound more plausible results were achieved. This reduced the first four harmonics of each string by respectively about 20%, 2%, 6%, and 4%. Clearly, the greatest possibility for inaccuracy is in the first harmonic. The error in the upper harmonics is not of significance. The results of all these experiments are comparative and any error involved being common to all results would not affect the validity of the comparison. Effort was made to reduce the sound radiated by the shaker with some success.

Chapter 7

STRING-BELLYING LONGITUDINAL STRING VIBRATIONS

7.1 Introduction

In Chapter 3 we drew a distinction between the driving substructure and the rest of the violin. Bellying LSV is the principal source of LSV within the driving substructure. It is possible separately to generate and examine string-bellying LSV. This was done on a blocked base. To reduce the amount of LSV arising from tailpiece resonance, the tailpiece was replaced by a force gauge. A third string of normal playing length and tension was passed over the centre of a bridge and anchored to the force gauge. The bridge was of the size of a normal violin bridge, but had no piercing in it to make it rigid in its own plane. See fig 7.1.

7.2 With a single frequency input

7.2.1 Method

First, a single frequency excitation was applied and a steady vibration established. This was done by driving the string at its resonance frequency by a shaker located about 3mm from the end of the string remote from the bridge. To detect most of the lower harmonics present, the magnet was placed at 1/5 of the string length from the bridge. The traces show that the first harmonic is much stronger than the upper harmonics. See fig.

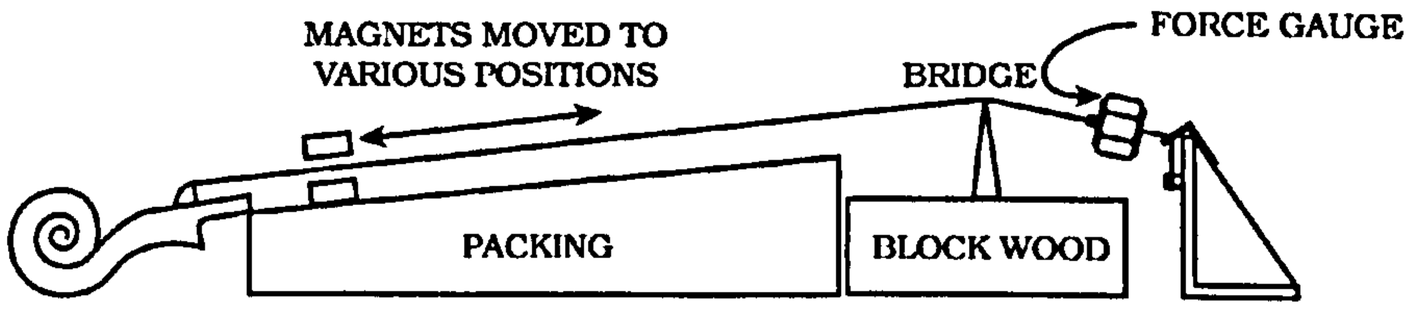

Fig. 7.1. Apparatus for generating and measuring string bellying LSV.

7.2. The EMF generated by the string motion was related to the amplitude of transverse displacement of the string by measuring the peak-to-peak transverse displacement at midlength of the string with a scale.

The computer used by the writer at the time of processing the experimental results presented in this chapter was severely limited in hard disc space. To limit the amount of graph drawing data that was stored in the computer the analyser was set to sample the spectrum at 20Hz intervals. The peaks that were picked up were depressed and broadened by the averaging process adopted by the analyser. However, since the excitation was sustainable over time it was possible to zoom in and increase the number of lines to achieve a more precise figure. The peak values found this way were noted and the graph drawing data held in the computer was scaled up to these values. The resulting peaks shown in the graphs are correct for peak heights but are somewhat exaggerated in width.

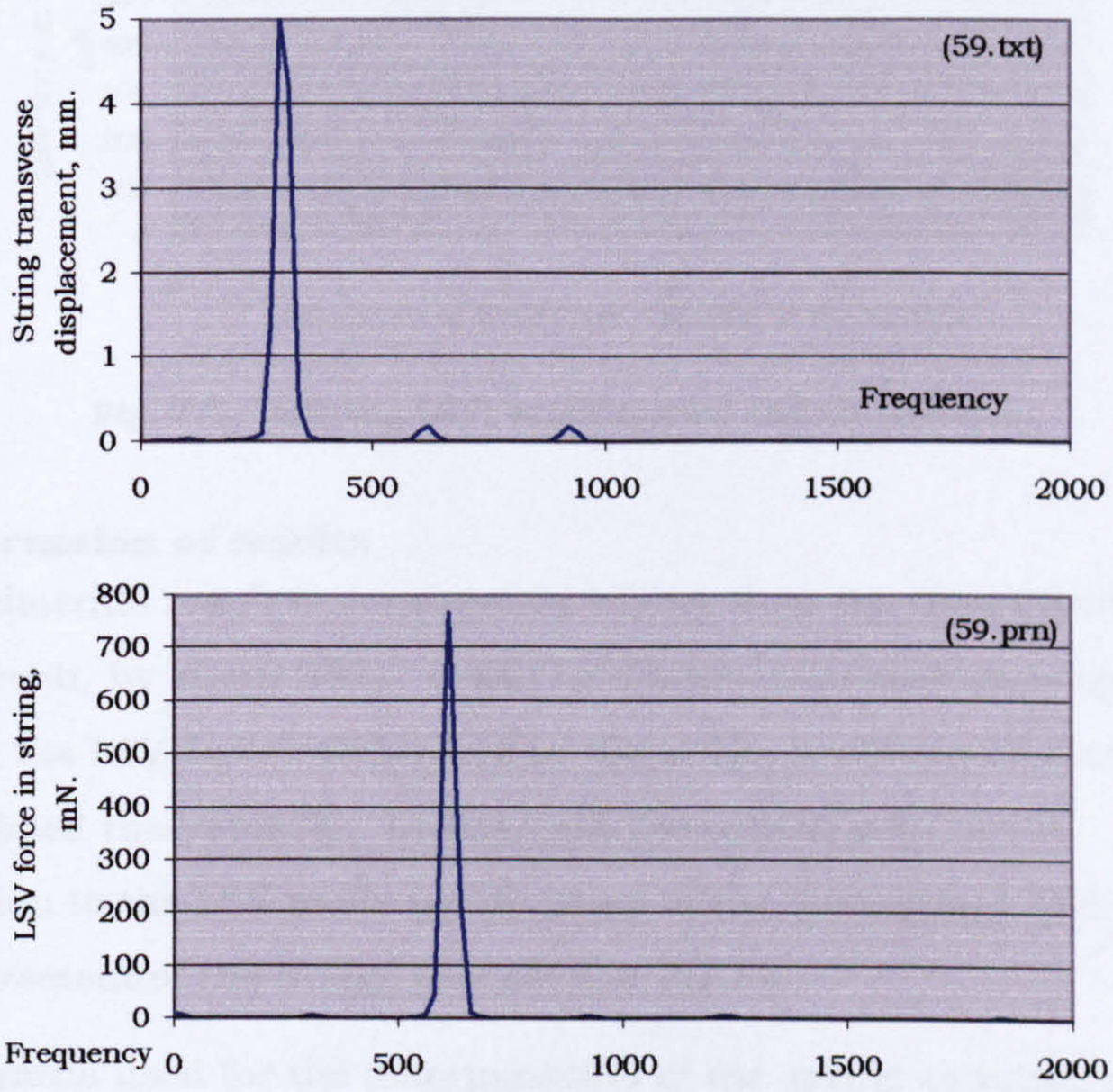

Fig. 7.2. String displacement and LSV, shaker driven string, high amplitude.

7.2.2 Results

The graphs should be read as representing a single frequency excitation. The pair of spectra shown in fig. 7.2 shows first the string transverse displacement followed by the corresponding LSV force. These results show that by driving the string with a shaker it is possible to set up a predominantly first harmonic transverse vibration in the string. They also show that the resulting LSV is an equally dominant doubling of the frequency. Fig. 7.2 shows the result for the maximum amplitude of transverse displacement tested. Four other amplitudes were also tested and the results of all five tests are shown in fig. 7.3.

Fig. 7.3 shows the string amplitudes and LSVs, plotted on the theoretically derived graph, previously shown in fig.3.1.

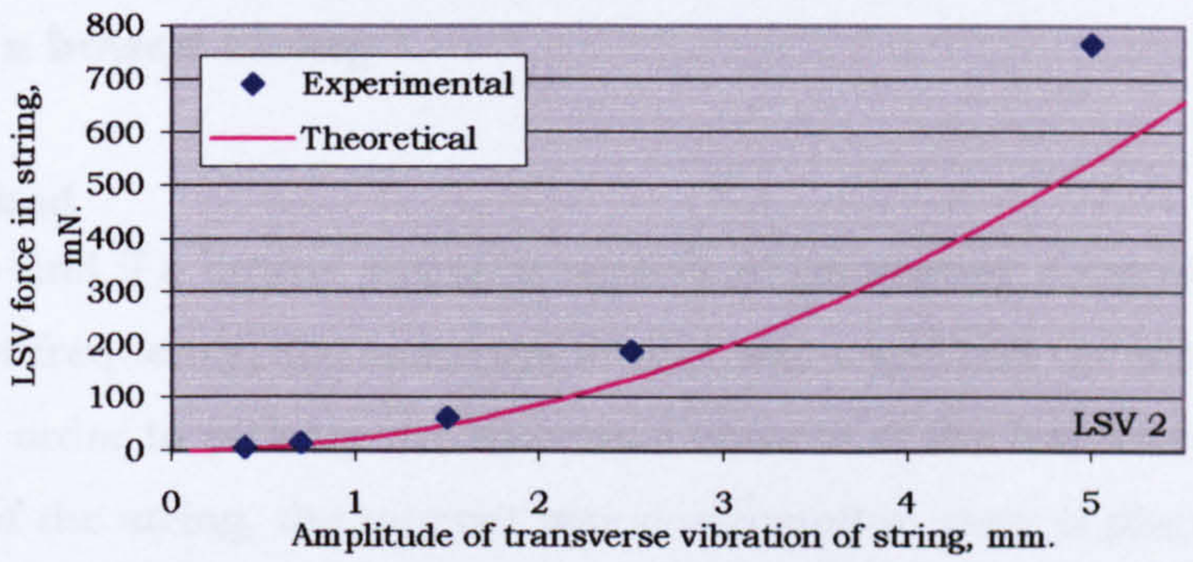

Fig. 7.3. Bellying LSV, experimental and theoretical.

7.2.3 Discussion of results

The experimental result is consistently higher than the theoretically derived result, by about 35%. It will be shown in subsequent experimental work that the LSV force established in the string is always greater than that predicted theoretically. In this case the reason may be the contribution to the LSV made by vibration of the force gauge and by out of plane movement of the bridge (see section 3.2.5).

The apparatus used for the determination of the spring constant of the strings, which is shown in Appendix B, is similar to that used in this experiment. In the determination of the spring constant, the bridge was placed symmetrically in the centre of the string length, with the intention

of discouraging the bridge from vibrating normal to its plane. By inspecting the coherence of the transfer function, it was concluded that the resulting spectra of LSV force were free of the effects of parasitic vibration up to about 600Hz. The LSV force in all four strings rose from about 700Hz to a strong peak at 980Hz, the height of which was 10 to 62 times the base level LSV force amplitude. The frequency of this vibration was constant and therefore independent of the string characteristics. Attempts to ascertain the cause failed. Evidence is presented at several points in the thesis that there is a considerable amount of resonance within the driving substructure that increases the measured LSV in proportion to that predicted theoretically. LSV generated within the driving substructure is 'primary LSV' and is capable of driving the violin.

7.3 With a bowed string

7.3.1 Method

In order to find if a bowed string is capable of generating a similar doubling of frequency, the same apparatus was used and the string was bowed. In order to pick up the harmonic content of the transverse vibration of the string, the magnet was positioned in several places.

At mid length, to pick up the 1st, 3rd, 5th, 7th, and 9th harmonics.

At the ¼ point, to pick up the 2nd, 6th, 10th harmonics.

At the 3/8 point, to pick up the 4th harmonic.

There had to be three independent data sets, one for each magnet location. The mid length peak to peak amplitude of string vibration was estimated at 3.5 mm by using a simple scale. It is interesting to note that it would be close to impossible to bow a string to such a high transverse displacement if it were on a real violin. The analyser was set to trigger a bowed stroke at 50% and the output was the average of 12 strokes. This was found reasonably reproducible. It was possible to discard any data sets where the bowing was at a level that did not match the others by inspection of the string tension trace on the analyser, which was independent of the magnet position. Any small differences were adjusted by scaling the data in the computer to make the three LSV traces converge. The voltages recorded by

the analyser representing the LSV, were checked for precision by zoom, which proved more difficult because of the unsustainable signal. Here again it was found that the recorded traces were an underestimate. The recorded figures were scaled up to reach the figure found by zoom.

7.3.2 Experimental result

The spectra shown in fig. 7.4 are for a strong bow stroke close to the bridge. The correct maximum value at any harmonic is the greatest of those shown in the graph. For the reason stated in section 7.2.1, while the peak heights are correct the peak widths are exaggerated. The harmonic content of this stroke (shown in fig. 7.4) is fairly typical of published bow strokes near to the bridge and shows the classic 1/n dependence of a saw tooth wave [Pickering, 1991]. The resulting bellying LSV is shown in fig. 7.5.

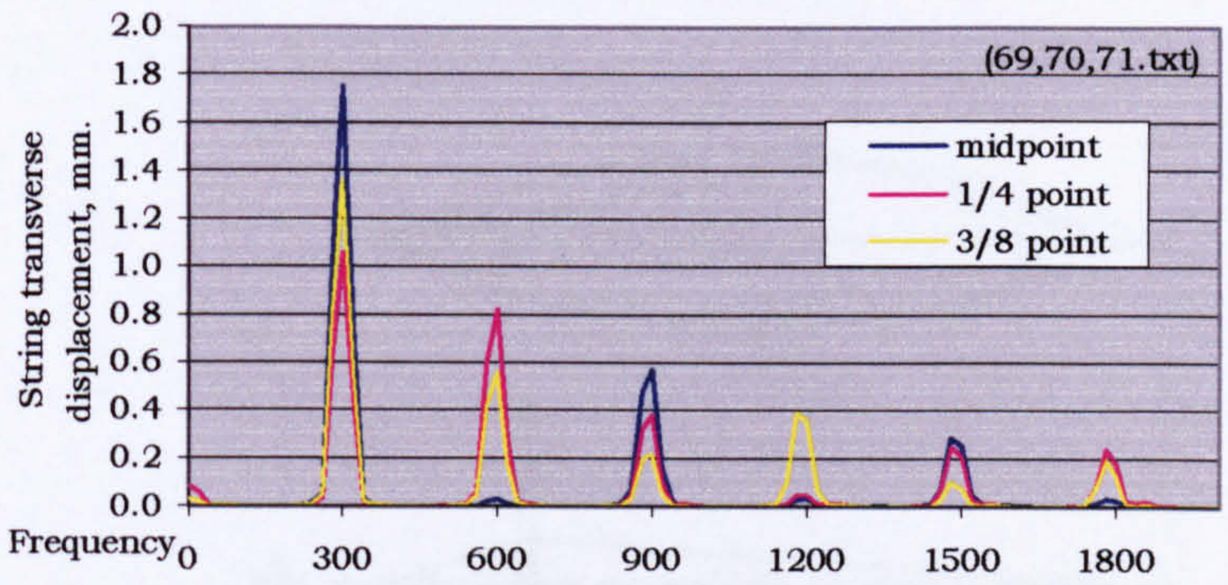

Fig. 7.4. RMS displacement, bowed string.

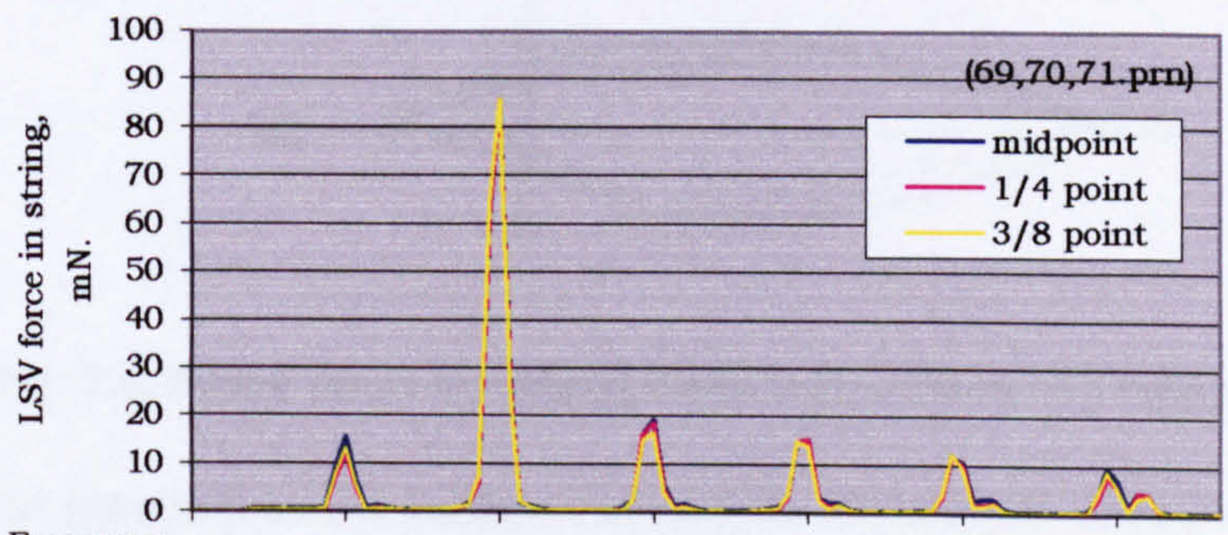

Fig. 7.5. Bellying LSV, bowed string.

A number of similar traces were produced, with bowings of various strengths and position, and these showed relatively little variation from the above graph. The significant feature is the marked weakness in the 1st harmonic and a marked strengthening of the 2nd harmonic.

7.3.3 Theoretical prediction

It is possible to make a theoretical prediction of the bellying LSV generated by a bowed string. Woodhouse has suggested that the bowed string would not give an LSV of double the frequency [Woodhouse, 1977]. If it were possible to bow the string at the normal point of bow contact, in such a way that there was no permanent transverse displacement of the neutral position of the string, the familiar Helmholtz motion would be set up. There is a kink in the string with straight lines between, which cycles from end to end within the curved envelope. This is shown in the top diagram of fig. 7.6.

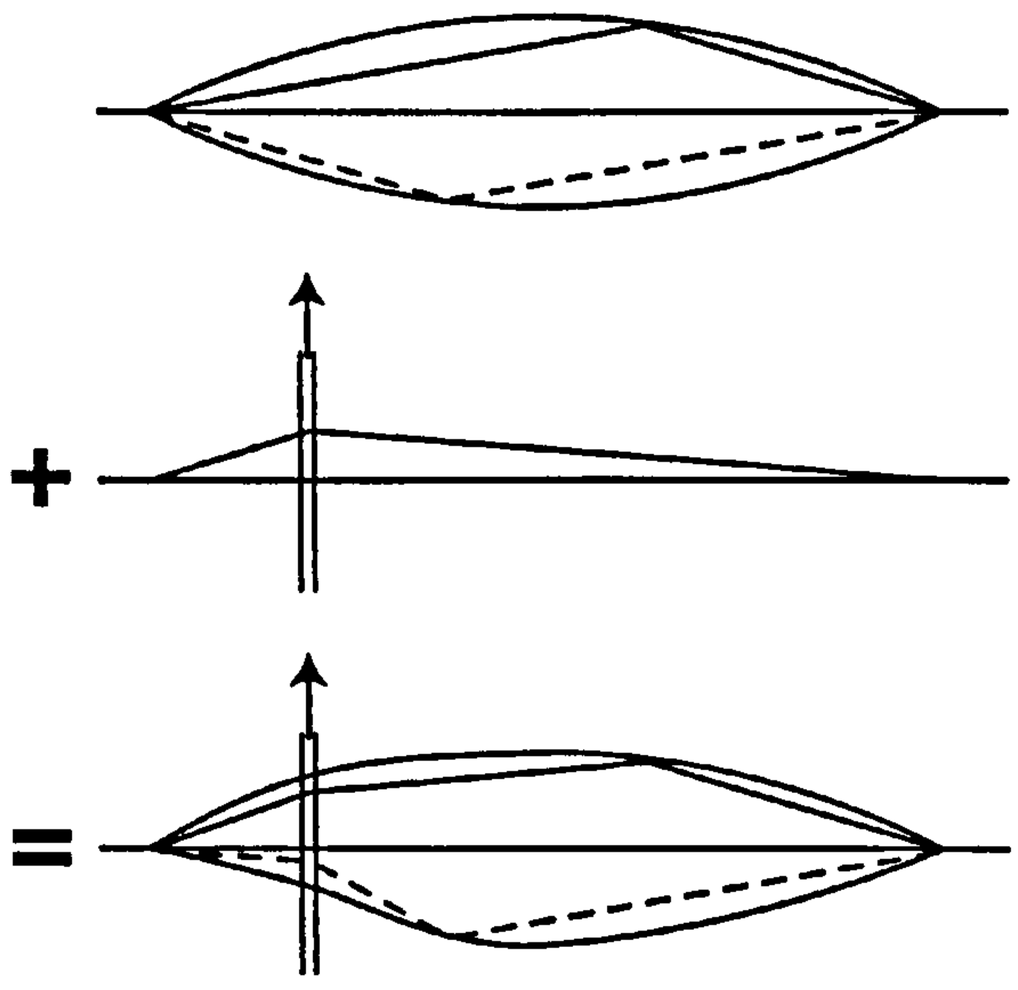

Fig. 7.6. String shape combining Helmholtz motion and bellying.

This can be resolved into a number of simple sinusoidal harmonics. Consider any one harmonic. In that harmonic, the string would have its shortest length when it passes through the straight-line position. Either side of this, the length and tension increases. This is a symmetrical

displacement and clearly produces an LSV of double the transverse frequency in that harmonic. In practise, it is not possible to set up a vibration that is fully symmetrical about the straight-line position of the string because the bow must introduce a permanent transverse deformation [Woodhouse, 1977]. This shifts the line of symmetry to the bent shape shown in the second diagram of fig. 7.6. The combined string shape and envelope of motion is shown in the bottom diagram. The string length will still vary equally both sides of the bent line of symmetry.

The string transverse displacement can be expressed as the sum of a static and a dynamic function of the distance along the string as follows;

$$y = \mathrm{A}(x) + \Sigma_n \left[a_n Sin \frac{n\pi x}{\mathrm{L}} . Cos\, n\omega_1 t \right]$$

The slope $\frac{\delta y}{\delta x} = \mathrm{A}'(x) + \frac{\pi}{\mathrm{L}} \Sigma_n \left[a_n Cos \frac{n\pi x}{\mathrm{L}} Cos\, n\omega_1 t \right]$

The change in string length is given by

$$\delta s = \int_0^{\mathrm{L}} \left[1 + \frac{1}{2} \left(\frac{\delta y}{\delta x} \right)^2 \right] dx$$

The n^{th} term of the expansion $\left(\frac{\delta y}{\delta x} \right)^2$ can be written,

$$\left(\frac{\delta y}{\delta x} \right)^2 = \left[\mathrm{A}'(x) + \frac{\pi}{\mathrm{L}} \Sigma_n a_n Cos \frac{n\pi x}{\mathrm{L}} Cos\, n\omega_1 t \right] \left[\mathrm{A}'(x) + \frac{\pi}{\mathrm{L}} \Sigma_m a_m Cos \frac{m\pi x}{\mathrm{L}} Cos m\omega_1 t \right]$$

$$= [\mathrm{A}'(x)]^2 + \mathrm{A}'(x) \frac{\pi}{\mathrm{L}} \left[\Sigma_n a_n Cos \frac{n\pi x}{\mathrm{L}} Cos\, n\omega_1 t + \Sigma_m a_m Cos \frac{m\pi x}{\mathrm{L}} Cos\, m\omega_1 t \right] +$$

$$\left(\frac{\pi}{\mathrm{L}} \right)^2 \{ \Sigma_n \ldots\ldots \times \Sigma_m \ldots\ldots \}$$

The first term is independent of time and derives from the static deformation. The second and third terms are dynamic, the second being linear and the third being non-linear. Without any knowledge of the bowing force, we cannot proceed further with the theoretical evaluation of δs or of the LSV. Because of orthogonality, after integration the third term only contains terms of the form $\left(\frac{\pi}{\mathrm{L}} \right)^2 \left\{ \Sigma_n a_n^2 Cos^2 \frac{n\pi x}{\mathrm{L}} Cos^2\, n\omega_1 t \right\}$. The second term would give an LSV of the same frequency as the transverse

wave, and the third term an LSV of double the frequency of the transverse wave. Theoretically then, the bowed string will not produce an LSV of entirely doubled frequency. The experimental result shown in fig. 7.5 was for a strong bow stroke fairly close to the bridge. It is interesting to note that since A appears in the linear term the position of the bow must affect the ratio of linear to nonlinear LSV. Bowing closer to the bridge will raise the ratio of second harmonic to first harmonic in the LSV of the bowed string. The writer found some evidence of this during the experimental work.

The experiment conducted above was not on a real violin with four strings fitted. There is some indication from experimental work presented later (Section 13.6.3) that the amount of string bellying LSV in a actual violin does not vary much at each harmonic. If there was a complete doubling of frequency, the bellying LSV would only exist at the even numbered harmonics.

If the whole of the first harmonic TSV transverse displacement of 1.75mm were to cause a second harmonic LSV, then the resulting LSV force would be 66.6 mN. The experimental result of 85.7 mN, is some 28% higher than the theoretical figure. While this discrepancy is a little less than that of the shaker driven string, it cannot be assumed that all the first harmonic TSV produces second harmonic LSV. There is again evidence of the effect of resonances within the driving substructure having reinforced the LSV vibration.

7.4 Conclusions

- The bowed string generates bellying LSV.
- The LSV developed is largely of double the frequency of the first harmonic of the transverse vibration but there is some LSV of the same frequency as the first harmonic of the transverse vibration.
- The magnitude of the LSV developed has a non-linear relationship to the TSV, and broadly follows the relationship predicted theoretically in Chapter 3.

- The the LSV arising from bellying has been reinforced by resonances within the driving substructure. This has contributed to the 'primary LSV'.

Chapter 8

BRIDGE-ROCK LONGITUDINAL STRING VIBRATIONS

8.1 Experimental method

In an attempt to model the generation of LSV from the rise and fall of the bridge, it was again necessary to create an idealised set up. Using the stringing geometry of a real violin, the body was replaced by the rubber-mounted bridge used in the determination of the spring constant. This bridge support is described in Appendix B. It contrives to enable the bridge to move vertically at the bass foot, to move vertically very much less at the treble foot and to be restrained from any horizontal movement at the base. The bridge is restrained at the base from tilt normal to its plane by the 'belly' on which it is mounted, as is the bridge on a violin. The tailpiece that was used was the one fitted with transducers at the string anchors and so it was possible to measure the LSV at each string. The bridge was driven horizontally by a wire stinger attached to a shaker. The shaker was driven with broadband random noise. The bridge base was restrained from horizontal movement and the dissimilar elasticity of the rubber base mountings caused the bridge to rotate about a point located somewhere between the bridge feet somewhat nearer the first string side. The set up is shown in fig. 8.1. An LDV recorded the magnitude of the velocity of the vertical motion of the bridge at a point immediately adjacent to the string groove. The transverse vibration of the strings was damped with foam plastic. Various levels of damping were tried with little difference in the result. The final recorded traces were done with a light level of damping, to suppress any string bellying.

With one string on the bridge at a time, mounted at the centre of the bridge, the following transfer function was recorded:

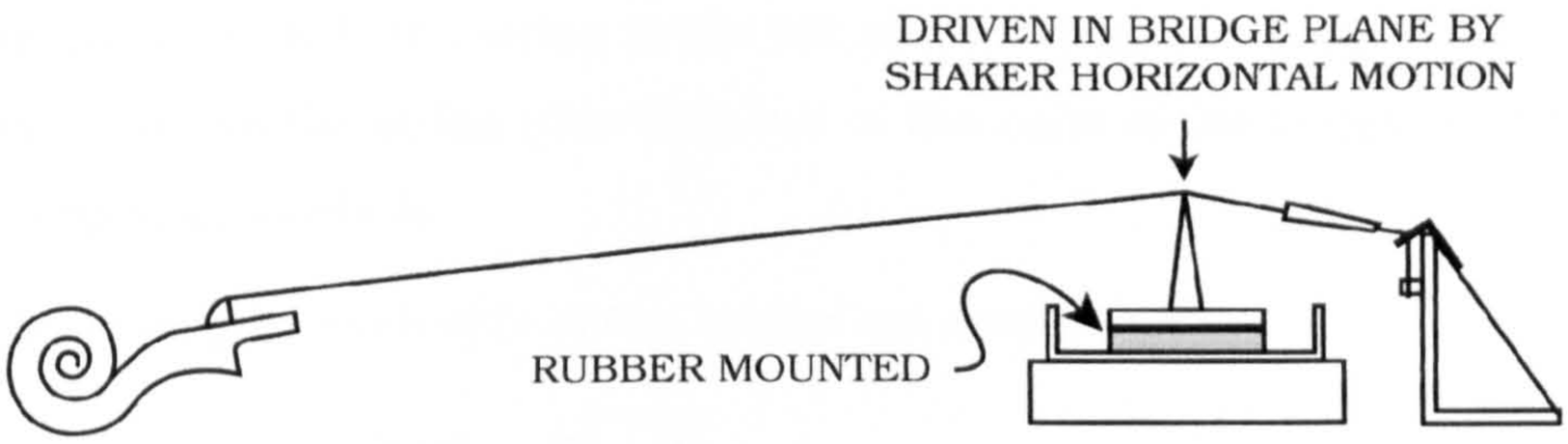

Fig. 8.1. Apparatus for generating and measuring bridge-rock LSV.

$$TF_{an} = \frac{\text{Tail force transducer output}}{\text{LDV output}}$$

$$= \frac{T_{LSV} k_{tt} \times 10 \times 10}{v \times 6240} \quad mV/mV$$

where k_{tt} =Tail transducer sensitivity in pC/N

but $v = 2\pi f R$ where R= bridge rise displacement, m.

$$\therefore \quad TF_{an} = \frac{T_{LSV} k_{tt} \times 100}{6240 \times 2\pi f R}$$

$$\frac{T_{LSV}}{R} = TF_{an} . \frac{6240 \times 2\pi f}{100 k_{tt}}$$

$$= .392 \times \frac{TF_{an} \times f}{k_{tt}} \quad N/mm$$

for 1st string $\frac{T_{LSV}}{R} = .0118\ TF_{an}.f$ N/mm

2nd string $\frac{T_{LSV}}{R} = .0199\ TF_{an}.f$ N/mm

3rd string $\frac{T_{LSV}}{R} = .0086\ TF_{an}.f$ N/mm

4th string $\frac{T_{LSV}}{R} = .0086\ TF_{an}.f$ N/mm

8.2 Theoretical result

The experimental result is shown with the theoretical result on the same graphs, (figs 8.2 to 8.5 inclusive). The theoretical result is the LSV force induced by unit bridge rise due purely to the stretching of the string.

Referring to fig. 8.1, the string to the left of the bridge is L long and slopes upwards H and the string plus tailpiece to the right of the bridge is *l* long and slopes upwards *h*.

The base lengths each side of the bridge are respectively,

$\sqrt{L^2 - H^2}$ and $\sqrt{l^2 - h^2}$

If the bridge rises by 1 unit, and the other terminations do not move, the

new length of string $= \sqrt{(L^2 - H^2) + (H+1)^2} + \sqrt{(l^2 - h^2) + (h+1)^2}$

Change in string length$= \left[\sqrt{L^2 + 2H + 1} - L\right] + \left[\sqrt{l^2 + 2h + 1} - l\right]$

Using actual figures gives a change in length due to 1mm bridge rise of,

$= \left[\sqrt{330^2 + (2 \times 47.25) + 1} - 330\right] + \left[\sqrt{175^2 + (2 \times 41.25) + 1} - 175\right]$

=0.383 mm.

$$\text{Strain} = \frac{\text{Change in length}}{\text{Original length}} = \frac{0.383}{385}$$

where, 385=string length not including tailpiece.

Force in string due to stretching $= k_{st} \times \frac{0.383}{385}$ N.

For 1st string, force=6.648 N/mm of bridge rise.

For 2nd string, force=1.700 N/mm

For 3rd string, force=2.199 N/mm

For 4th string, force=2.787 N/mm

8.3 Results

The graphs show for each string, the tension force in the string for 1mm rise in the bridge.

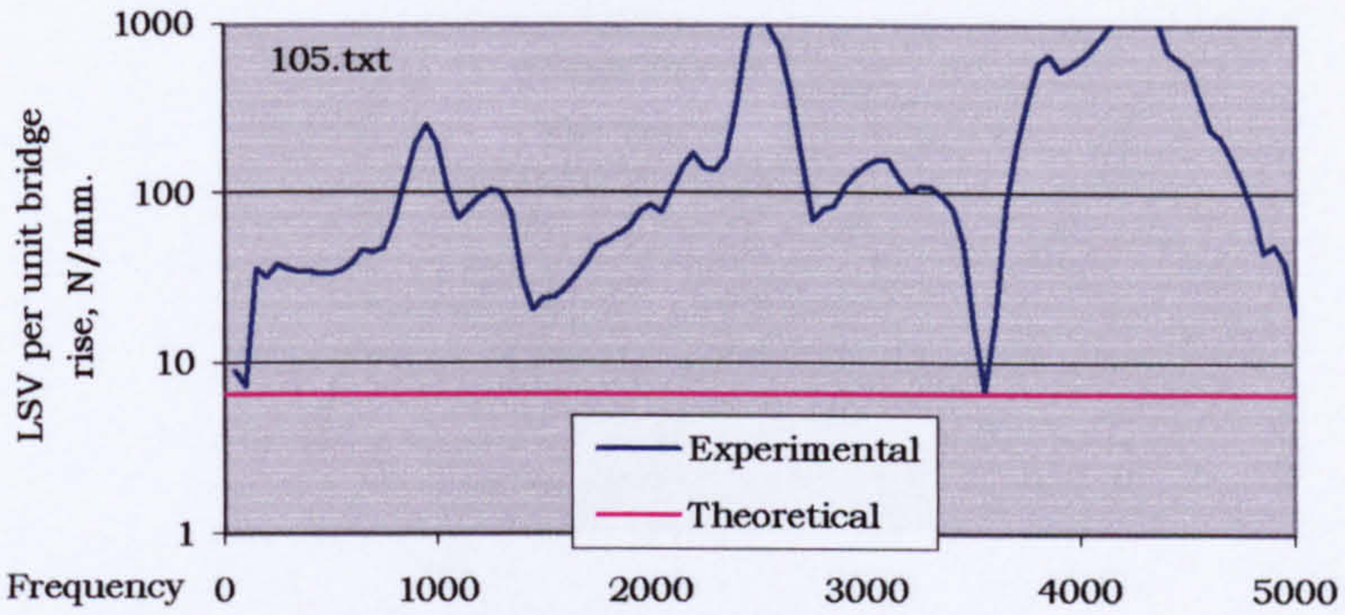

Fig. 8.2. 1st string. LSV force/unit bridge rise.
Bridge-rocked by shaker driving with broadband noise.

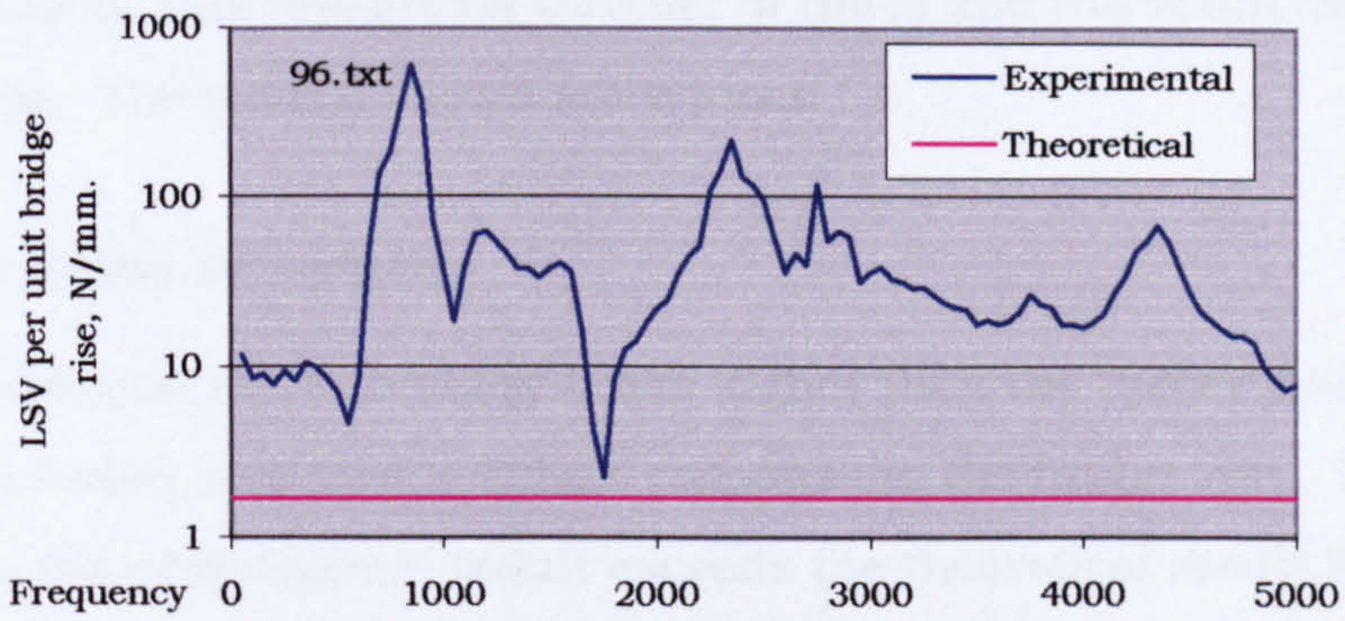

Fig. 8.3. 2nd string. LSV force/unit bridge rise.
Bridge-rocked by shaker driving with broadband noise.

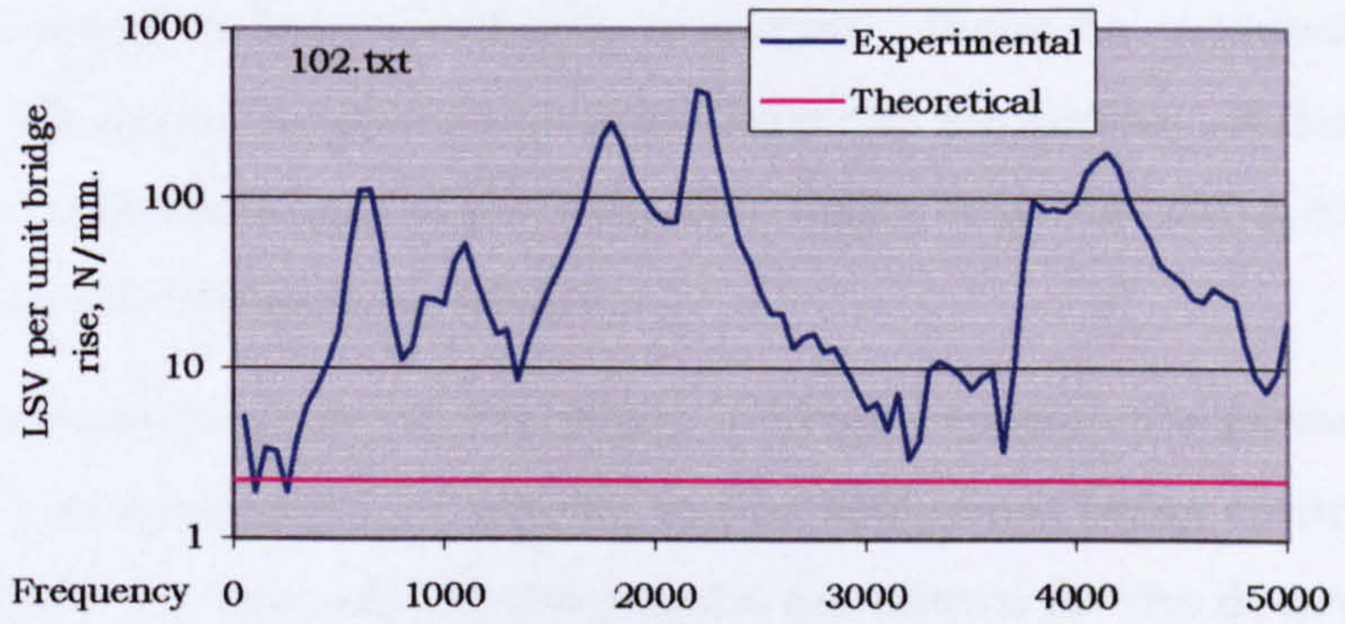

Fig. 8.4. 3rd string. LSV force/unit bridge rise.
Bridge-rocked by shaker driving with broadband noise.

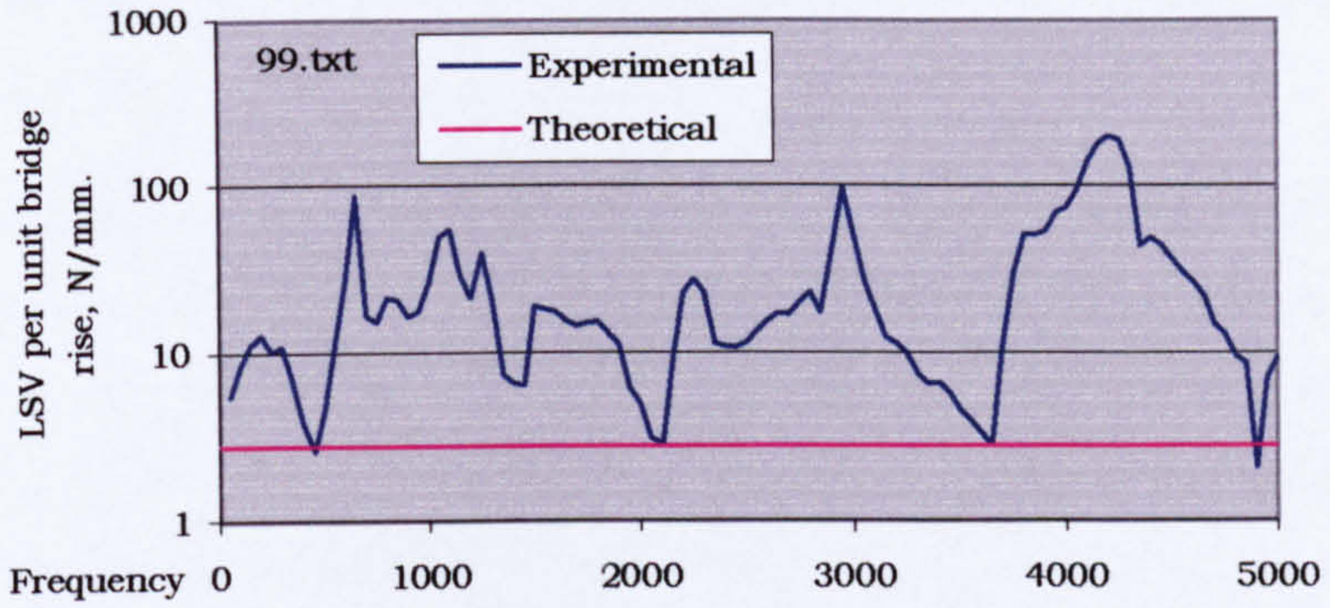

Fig. 8.5. 4th string. LSV force/unit bridge rise.
Bridge-rocked by shaker driving with broadband noise.

The experiment was repeated a number of times and the result varied with each repeat. The results shown are typical.

8.4 Discussion of results

The experimental result is many times higher than the theoretical prediction based on a purely elastic response to the bridge rise. The average of the experimental result exceeds the theoretical result for the E,A,D and G strings by 21, 29, 25 and 10 times respectively. The experimental result only approaches the theoretical figure at the troughs. It is possible that LSV has been generated by the resonances of the combined string, tailpiece and tailgut system. It can be expected that considerable dynamic effects will arise from the asymmetry of the bridge position, the introduction of the tailpiece, using only one string at a time, and driving the bridge by a shaker.

There was some evidence in the string bellying experiments presented in Chapter 7 of secondary LSV caused by the bridge not being centred on the string length. In Appendix B, the graphs are shown for the determination of the spring stiffness of the strings. To avoid inducing LSV by bridge movement normal to its plane, the set-up was made symmetrical. There was no tailpiece either so the capacity for added resonance was reduced. The resulting curves for LSV force per unit bridge rise showed no resonance at all in the range up to 600 to 700Hz, but there was a peak at 980Hz, which was from 10 to 62 times higher than the base LSV force. It

is apparent from this that the asymmetry of the bridge position introduces secondary LSV.

There has clearly been an additional and very substantial increase in the LSV caused by introducing the tailpiece into the experimental set-up. There was only one string on the bridge and tailpiece in each test, and this may have left the tailpiece much less restrained against translational and torsional movement than that of a tailpiece with four strings on it. At each of the three string anchors that did not have a string attached, there was a loosely held transducer and an aluminium eye. These were free to vibrate. These random vibrations would have a non-linear relationship to the bridge rise, but a linear relationship is assumed in the graphs presented. The output of transducers at these unattached anchors was measured and found to be of the same order as the anchor that was holding the string. Reciprocally, the output from the transducer that was holding the string may well have picked up the vibration of the unattached anchors at the other string positions. For these reasons the experimental result would almost certainly not be representative of real violin behaviour. The experiments presented in Chapters 6 and 7 and in Appendices A and B, all show that resonances within the driving substructure are capable considerably reinforcing the primary LSV generated by string bellying and the secondary LSV generated as a response to the modal action of the body.

Boutillon and Weinreich point out that the admittance of the bridge on a violin is of a similar order in the three coordinate directions x, y and z, and so any slight tendency of the bridge driver to have a component normal to the plane of the bridge would excite dynamics normal to the bridge [Boutillon and Weinreich, 1999].

Results are presented later of experiments done with four strings on the tailpiece and with the string driving the bridge rather than the bridge being driven by a shaker, and the results are presented in Chapter 9.

8.5 Conclusions

- LSV was developed in the string by rocking the bridge.
- The bridge–rock LSV was submerged in a large amount of secondary LSV arising from the system dynamics.

Chapter 9

LSV IN THE LOWER HARMONICS

Having looked at bridge-rock LSV and bellying LSV separately, it is now necessary to compare the relative magnitudes and therefore the importance of the two causes of LSV.

9.1 Single string

9.1.1 Experimental method

We begin with the simple case of only one string on the bridge. If this string were mounted on a violin, it would become part of the structure of the instrument and would be subject to the influence of the body dynamics. Input from the body could enter the string at the nut and saddle. This would make it difficult to say that the LSV is due to bridge-rock and/or bellying. If an elastic bridge support such as mounting it on rubber were used, it would not be representative of a real violin unless the actual bridge foot mobilities were reproduced. The method followed was to mount the bridge on a violin, but the string ends at the nut and tailgut were taken to supports that were independent of the violin body. This gave

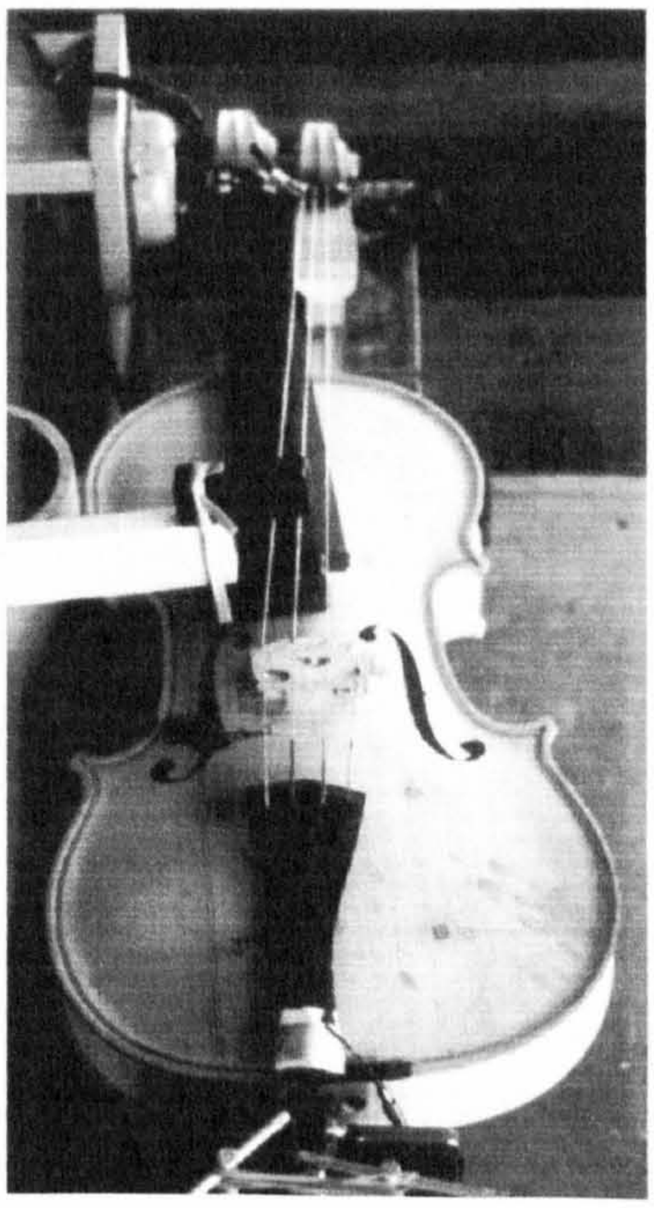

Fig. 9.1. Use of the "detached body".

the bridge the correct mobility, permitted bridge-rock interaction with the body at the bridge but eliminated the complication of interaction with the body at the string ends. The violin used in this way is referred to as a "detached body". The body chosen for this had been made with the normal EAR used on all the violins made in our workshop. The body was mounted on a sponge rubber block under the button at the top end of the back and the other at the bottom end of the back near the endpin. There were rigid supports under the sponge rubber blocks. The static force of the strings on the bridge was transmitted through the body to the blocks. The load of the body on the blocks would have compressed the rubber and made the support more rigid. The violin was thus able bend in its length in response to this static force. The strings and bridge were placed to comply with normal violin geometry. See fig. 9.1. The violin mounted in this way would still be able to respond to LSV forces applied at the bridge but the need for a reaction applied at the mountings must have had a modifying effect on the body dynamics.

9.1.2 With a single frequency input

The single frequency input has the virtue that any higher harmonics that appear must be due to bellying LSV. With only a third string on, the string was driven by a shaker at the end remote from the bridge and at differing amplitudes. As before the zoom was used to improve the accuracy of the recorded peaks.

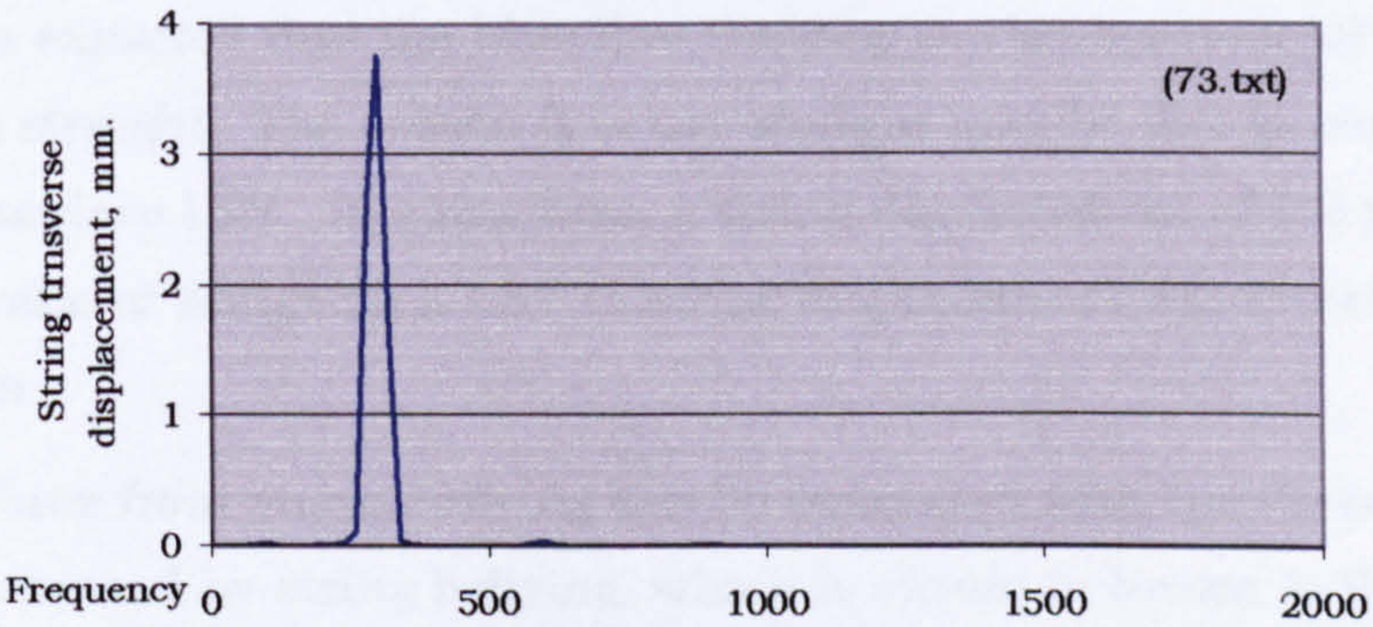

Fig. 9.2. Shaker driven 3rd string. Harmonic content of transverse displacement at a displacement of 3.75mm. Note, band width is shown much wider than actual.

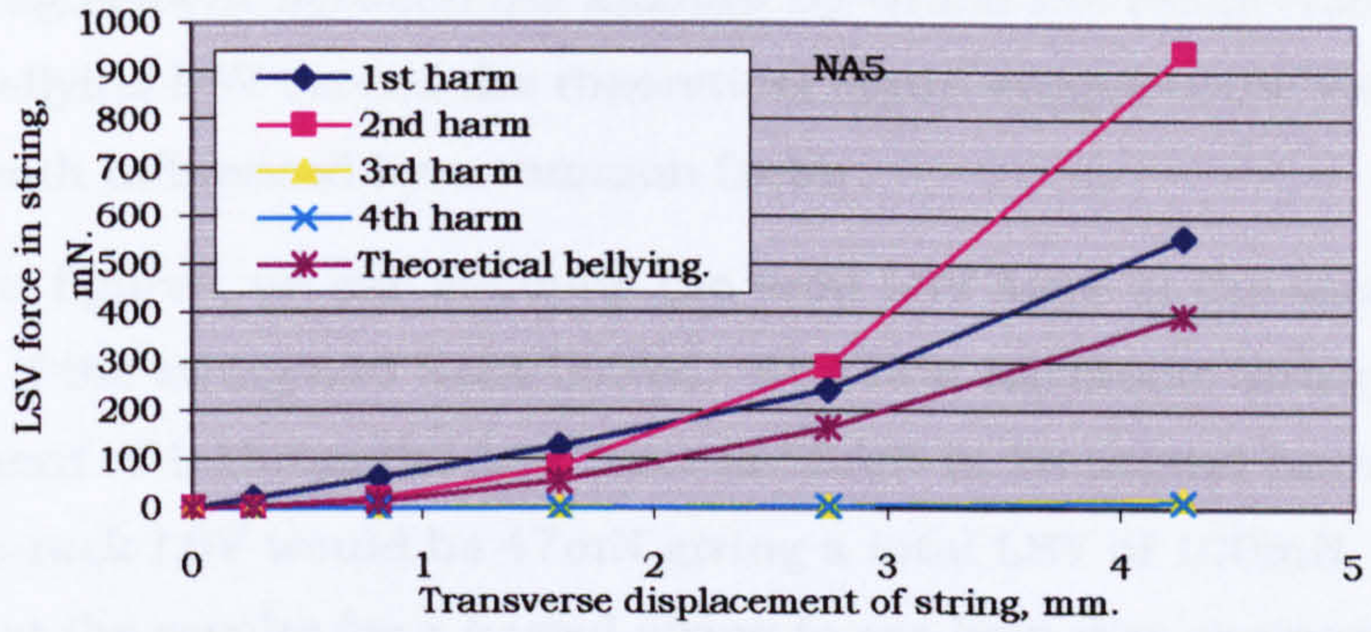

Fig. 9.3. LSV, detached body, single 3rd string , shaker driven.

Again, this spectrum (fig 9.2, the width of the signal peak is incorrectly shown, see section 7.2 for reason) shows that the shaker can produce close to a sinusoidal input. The string was driven to various displacements and the resulting LSV was noted. From this data, fig. 9.3 was produced.

At the lowest amplitude, the correspondingly low LSV shows negligible second harmonic, but as the amplitude rises there is an increasing proportion of second harmonic in the mix. The only possible reason for there being first harmonic present is bridge-rock LSV, and the only possible reason for the second harmonic being present is bellying LSV. Fig. 9.3 therefore presents bridge-rock LSV in blue and bellying LSV in red. The third and fourth harmonics are probably the result of their small presence in the shaker drive.

Since bridge-rock LSV has a linear relationship to the string displacement, it could be expected that the blue line showing the bridge-rock LSV force should be straight. The reason it is not straight may be due to some non-linear secondary LSV. In going from a string displacement of 0.8 mm to 4.25 the ratio of bridge-rock LSV to string displacement has increased by 1.63 times.

The LSV force from string bellying can be compared with the theoretical LSV force caused by string bellying, which is shown in brown in fig. 9.3. Here again the LSV not only exceeds the theoretical figure considerably but does so nonlinearly in that the divergence increases with rising string displacement. In going from a string displacement of 0.8mm to 4.25 mm, the ratio of experimental LSV to theoretical LSV has increased 1.65 times.

The close agreement between the amount by which the bridge-rock LSV and the bellying LSV exceed the theoretical figure supports the view that they are both influenced by a common factor.

From these figures, we can estimate the total LSV force at the second harmonic if the string had been bowed. At a first harmonic string displacement of 1.15mm the LSV force is 53mN in be second harmonic and the bridge-rock LSV would be 47mN giving a total LSV of 100mN. We will now look at the results for a bowed string to see how they compare.

9.1.3 With a bowed input

Using the same apparatus, the string was then bowed at five different levels. The relative amplitude of the transverse displacement of the string was spectrally analysed and is shown in fig. 9.4. The relative harmonic content of the transverse amplitude did not vary significantly with the bowing level.

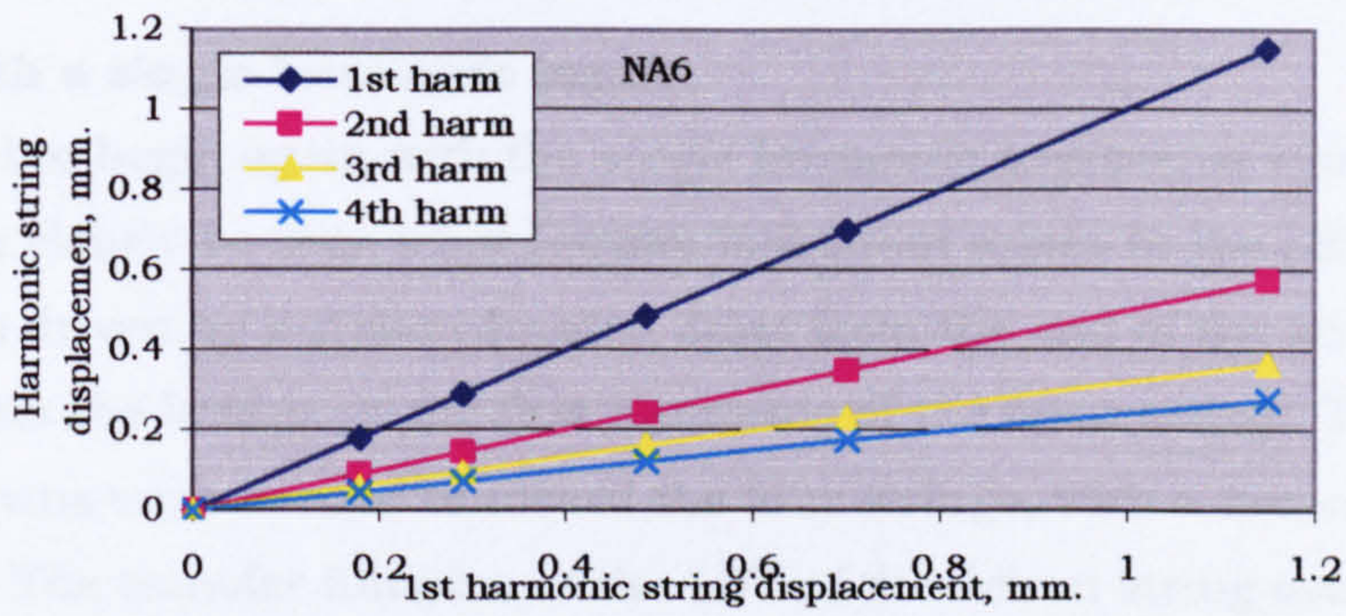

Fig. 9.4 Transverse string displacement in each harmonic, single 3rd string, bowed.

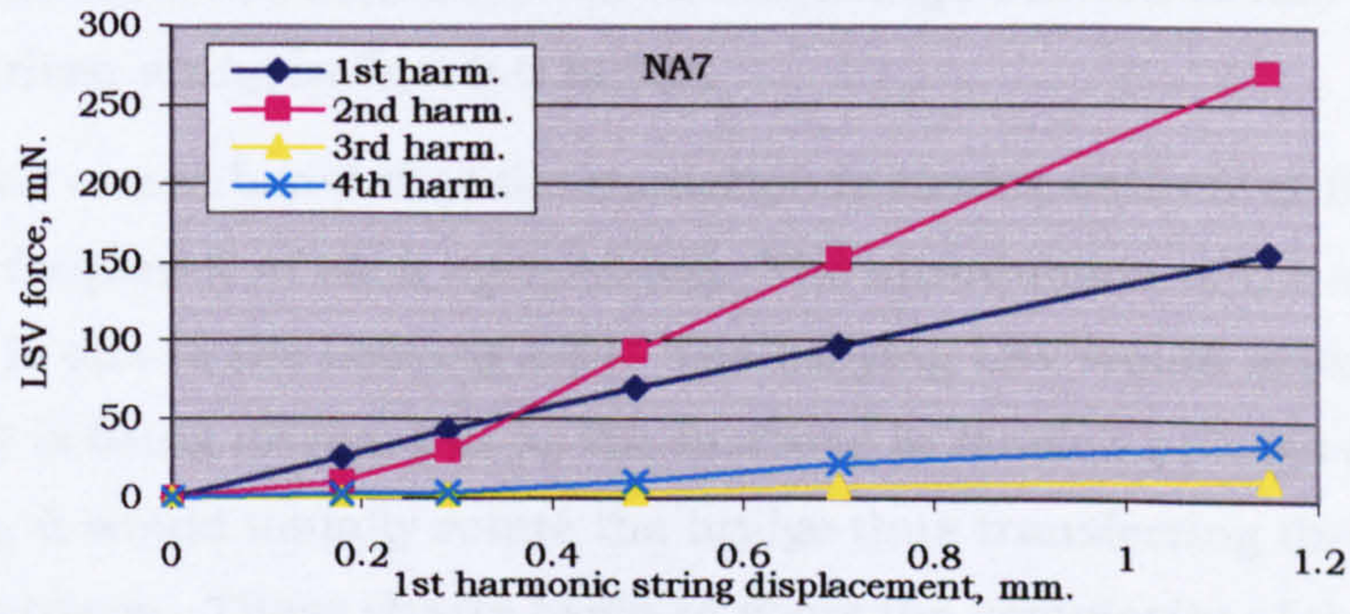

Fig. 9.5 LSV force, detached body, single 3rd string, bowed.

The harmonic content of the resulting LSV (shown in fig. 9.5) shows a movement towards a progressive strengthening of the second and fourth harmonics. It cannot be said that the entire second harmonic is due to bellying LSV because some of it must be due to second harmonic bridge-rock LSV. In section 9.1.1 we calculated from the experimental results that the LSV in bowed string at the second harmonic frequency would be 100mN. In fact, the experimentally found result shown in fig. 9.5 is an LSV force of 271mN. This was contributed to approximately equally by bellying LSV and by bridge-rock LSV. Experimental results for shaker driven string and the bowed string were related to each other on an equal basis a number of times in the course of this research and in all cases, the bowed string produced higher LSV.

9.2 With four strings on

To get closer to a real violin we now look at four strings over the bridge.

9.2.1 With a single harmonic input

It is useful to begin again with the single harmonic transverse vibration, so that it can clearly be seen what harmonic content arises in the LSV. The string was driven by a shaker located 3mm from the end of the string remote from the bridge, at the first harmonic of the open string. Three separate runs were needed to record the four strings, with a two-channel analyser. The transfer function of the LSV of the driven string over that of each of the other three strings was recorded. The results were slightly scaled to normalise on a standard LSV for the driven string. From these transfer functions the actual LSV in all the strings was found and is shown for each driven string in figs. 9.6 to 9.9.

It should be remembered that the excitation is almost entirely of first harmonic frequency of each open string. The introduction of the second harmonic is due to the bellying LSV. The bellying LSV would arise in the string that is being driven, but as the increase in tension presses down on the bridge, it would usually rotate the bridge thus transferring the LSV to the other strings. These charts begin to show the complexity of the violin. One could have expected to get the greatest strengthening of the second harmonic in the string that was being driven. While this did happen in the

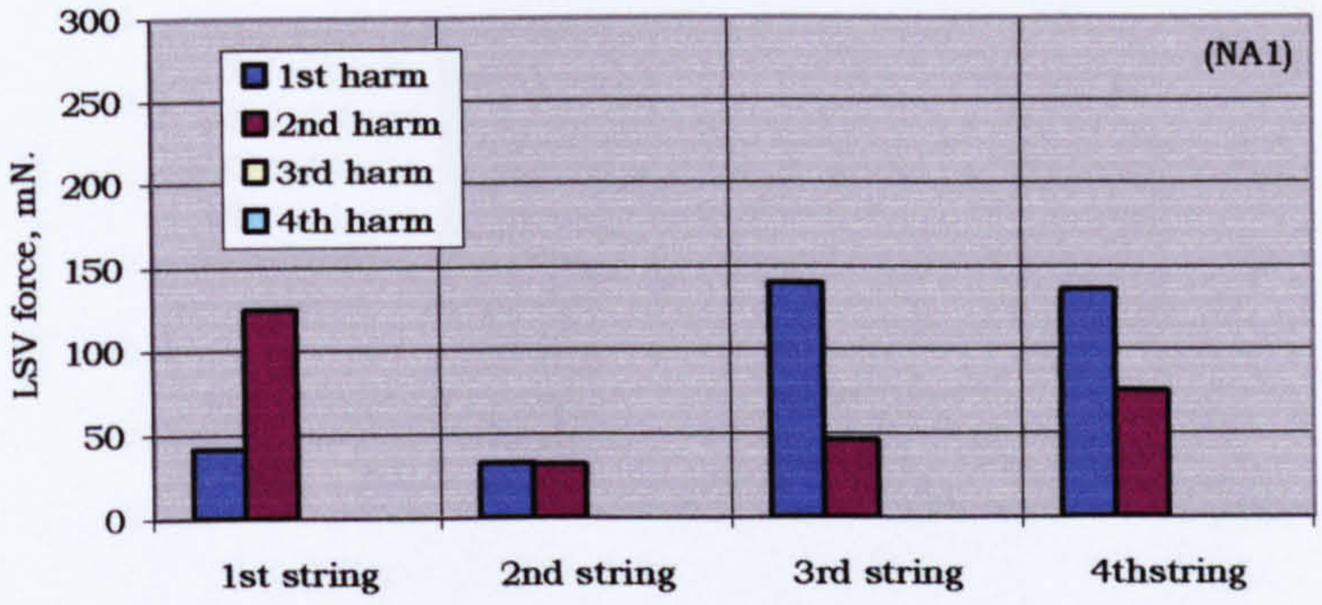

Fig. 9.6. LSV, detached body, single frequency shaker driven 1st string.

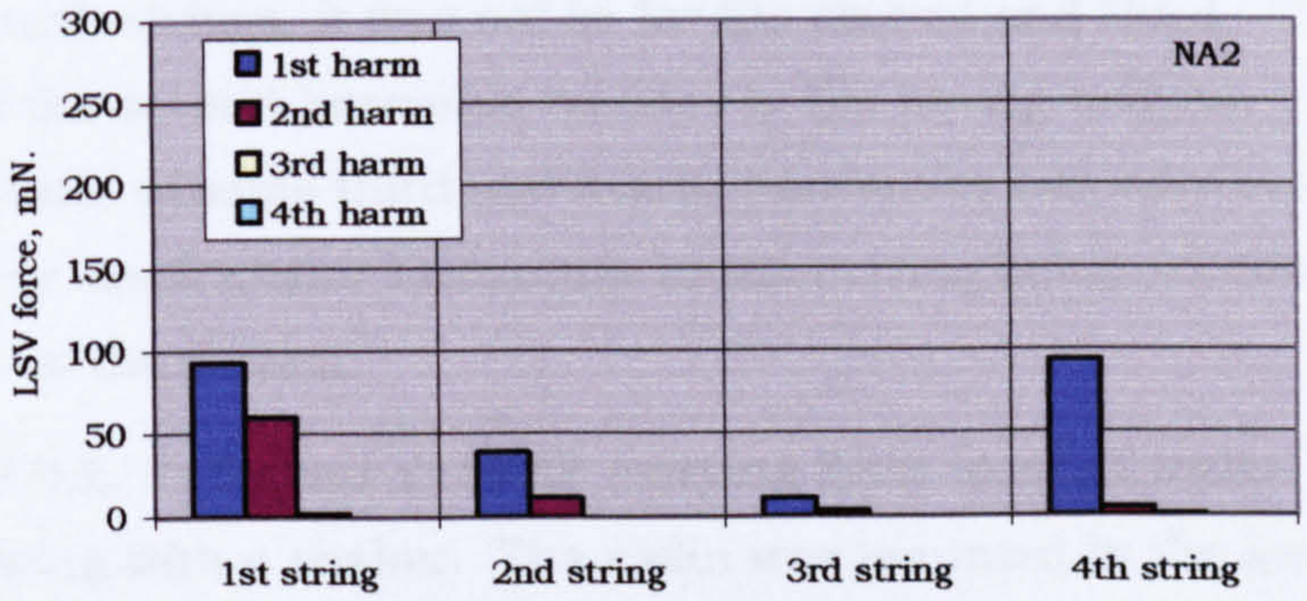

Fig. 9.7. LSV, detached body, single frequency shaker driven 2nd string.

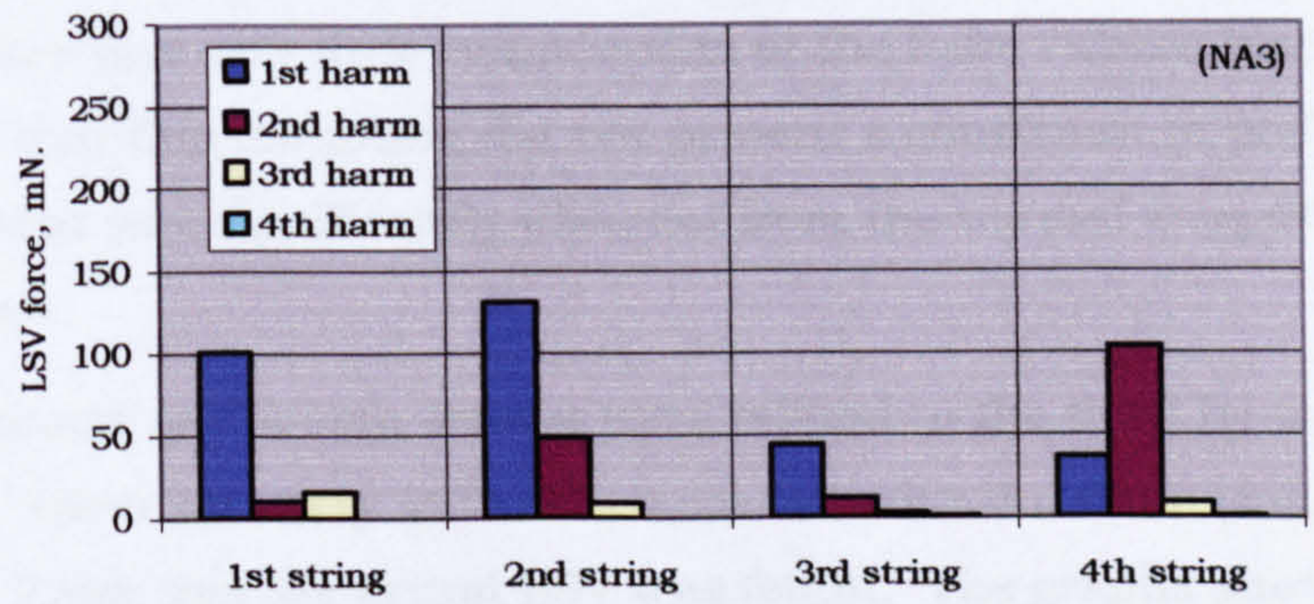

Fig. 9.8. LSV, detached body, single frequency shaker driven 3rd string.

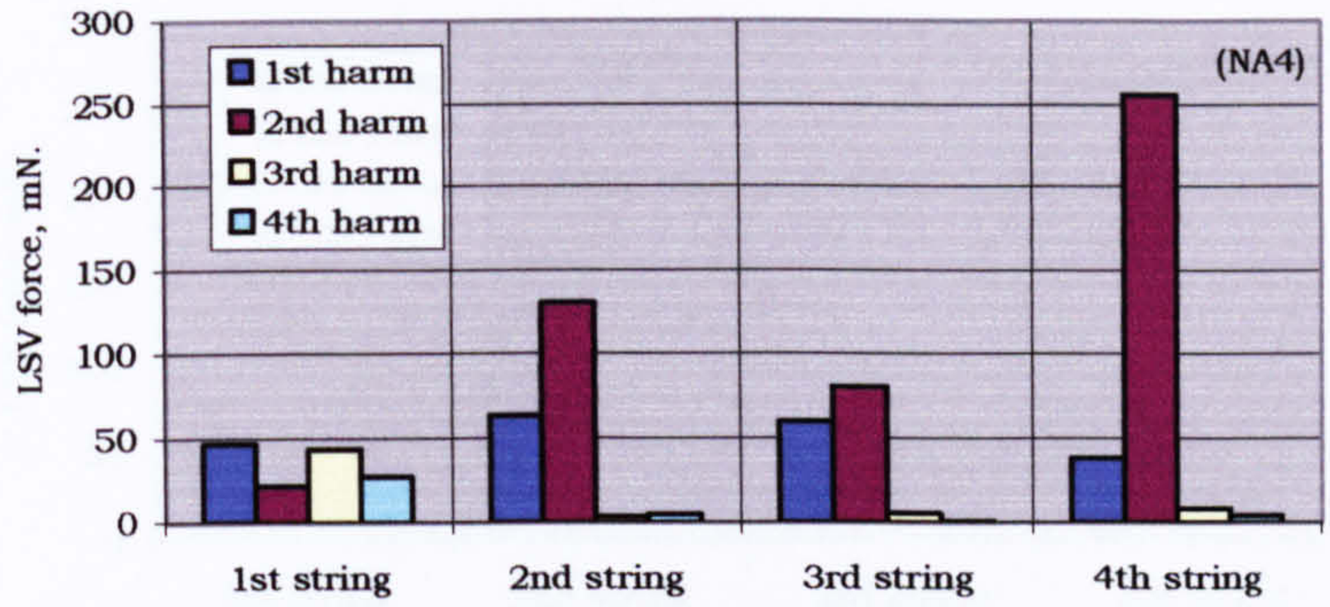

Fig. 9.9. LSV, detached body, single frequency shaker driven 4th string.

first and fourth strings, it was not so for the second and third. The strong presence of the second harmonic testifies to the strong bellying LSV effect. The appearance of some third and fourth harmonics can only have come from the very small higher harmonics in the driving being reinforced by resonances in the system.

Violins V157LE, V156 and V158HE (varying EAR) were all tested by driving the third string with a shaker. The violin was mounted in the same way as the detached body with a sponge rubber block under the button at the top end of the back and the other at the bottom end of the back near the endpin. The body was very lightly held down onto these blocks with rubber bands. There was very little compression of the foam rubber blocks and it is believed that this mounting did not present a constraint to body dynamics that was significantly different from the normal support provided by a violinist.

The first second and fourth strings were related to the third by transfer functions. There was very little difference between the three violins in their response. From this the actual LSV was found. The graphs shown in fig. 9.10 are typical of all three. It will be seen also that they were not very different from the detached body third string shown in fig. 9.8. This a little surprising and perhaps arises from the fact that the excitation was by shaker and not by the bow. It could of course mean that there is no link between the LSV developed in a violin (at least in the lower harmonics) and the EAR.

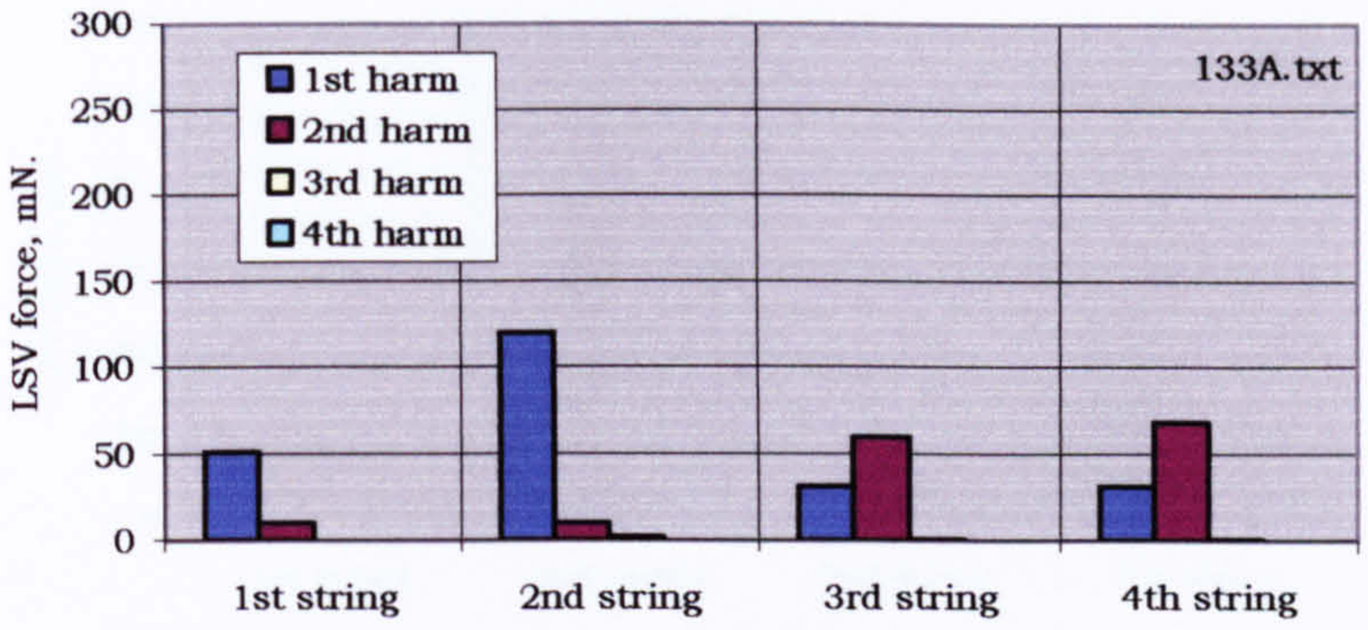

Fig. 9.10. LSV, V156, single frequency shaker driven 3rd string.

9.2.2 With a bowed input

The bowing is the average of 12 strokes recorded with the analyser triggered at 50%. An experienced violinist did them and by constantly watching the transverse displacement amplitude, a good degree of reproducibility was achieved. Any slight variation in bowing strength was compensated for by normalising on the LSV of the bowed string. The bow stroke was a strong one. The detached body was used first. The LSV for each string is shown in figs.9.11 to 9.14. Again, this shows a similar picture to the single harmonic input but it does reflect the more harmonically rich input from the bow. There is also a reduction in the relative strength of the second harmonic of the bowed string due to the string transverse displacement amplitude being less for the bowed string than for the shaker driven string.

Figs. 9.15 to 9.18 shows the result for the same experiment on V156. There are differences between the results from the detached body and the real

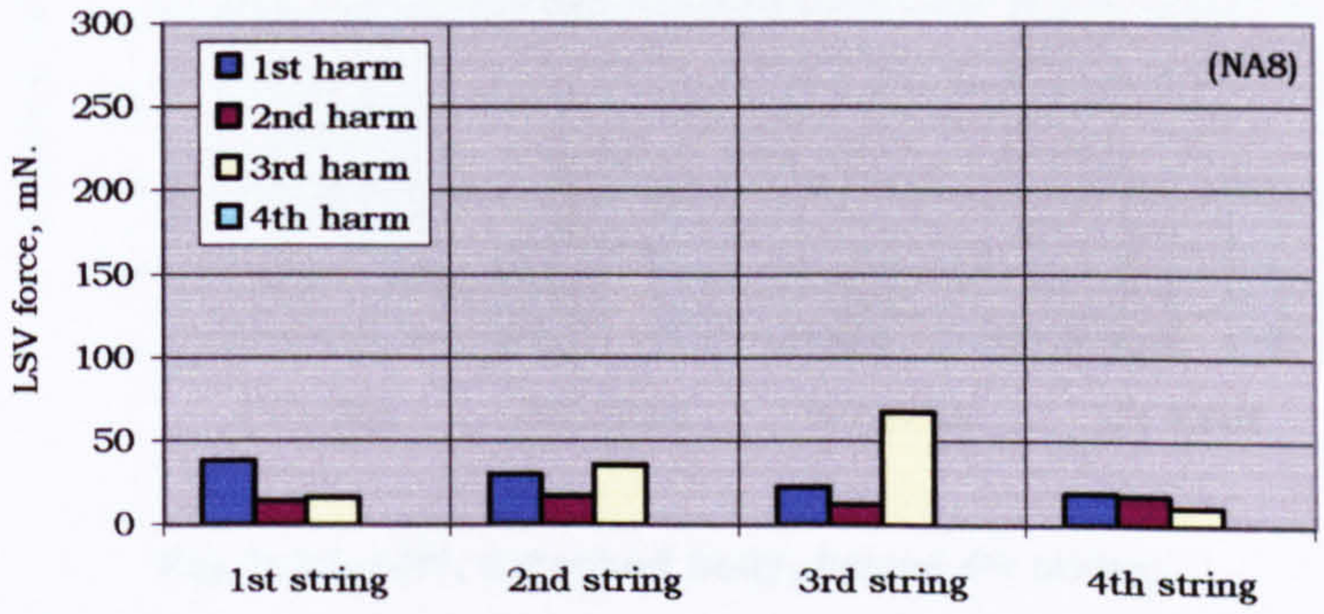

Fig. 9.11. LSV, detached body, bowed 1st string.

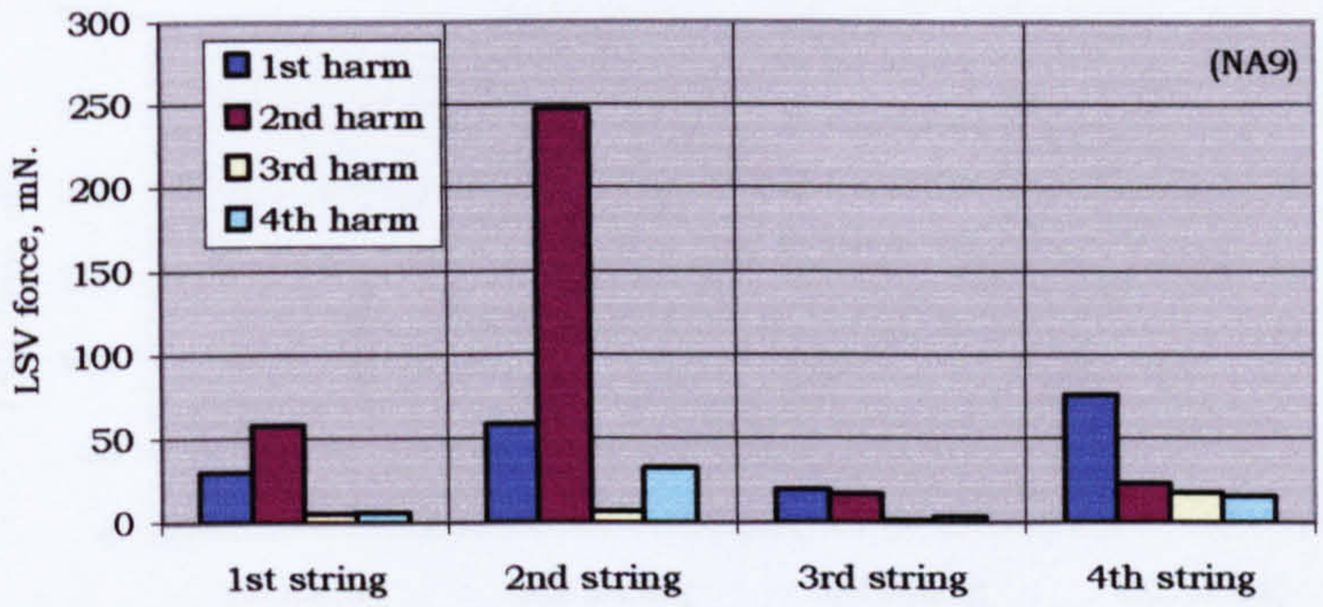

Fig. 9.12. LSV, detached body, bowed 2nd string.

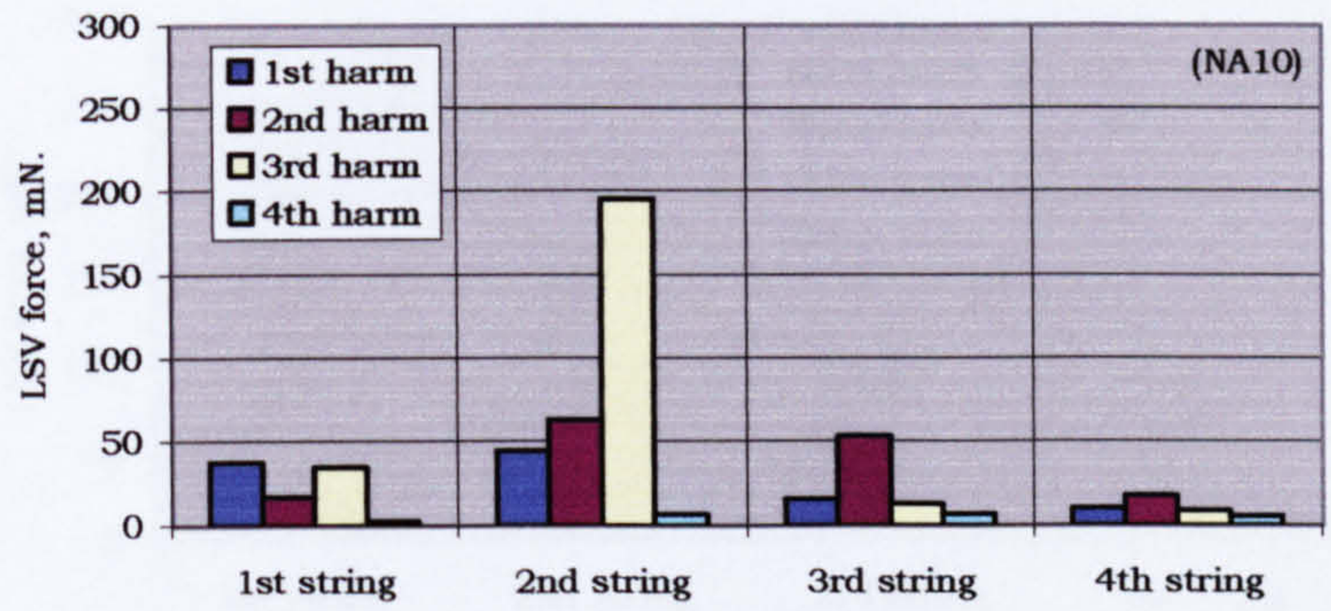

Fig. 9.13. LSV, detached body, bowed 3rd string.

violin. It would appear that the LSV in the string being bowed is similar for both violins. The difference arises in the non-bowed strings but it is difficult to make a valid general comment. This does point to the possibility that there would be a clearer difference in the amount of bridge rocking.

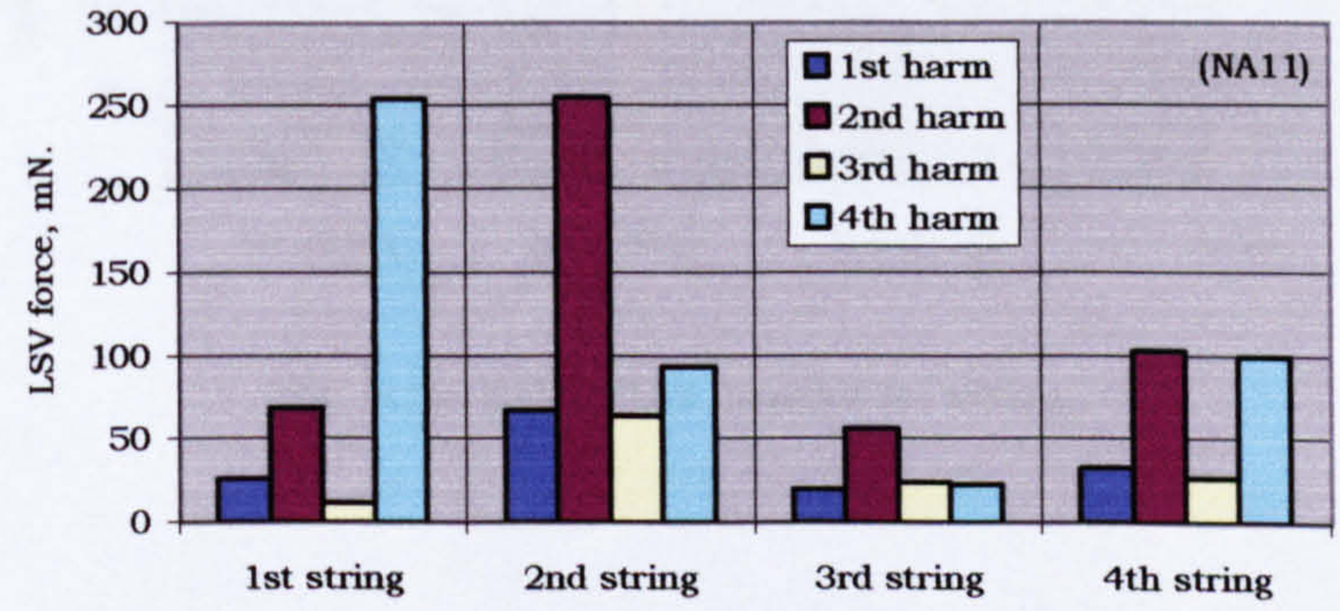

Fig. 9.14. LSV, detached body, bowed 4th string.

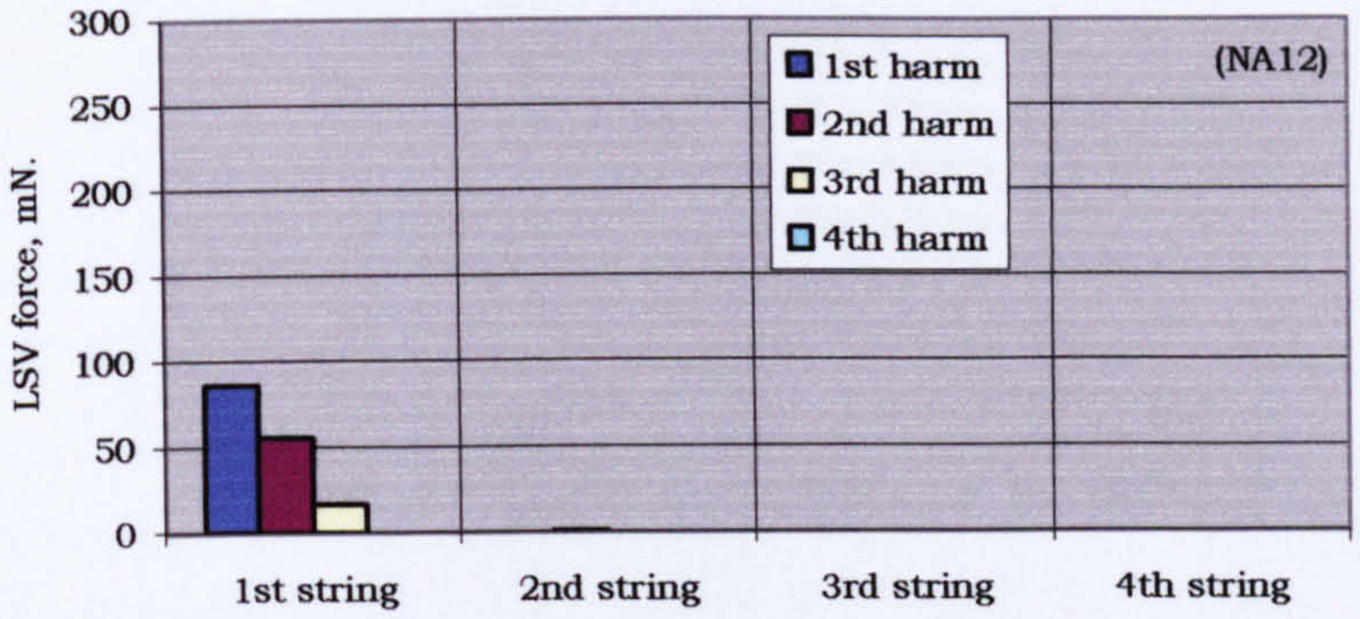

Fig. 9.15. LSV, V156, bowed 1st string.

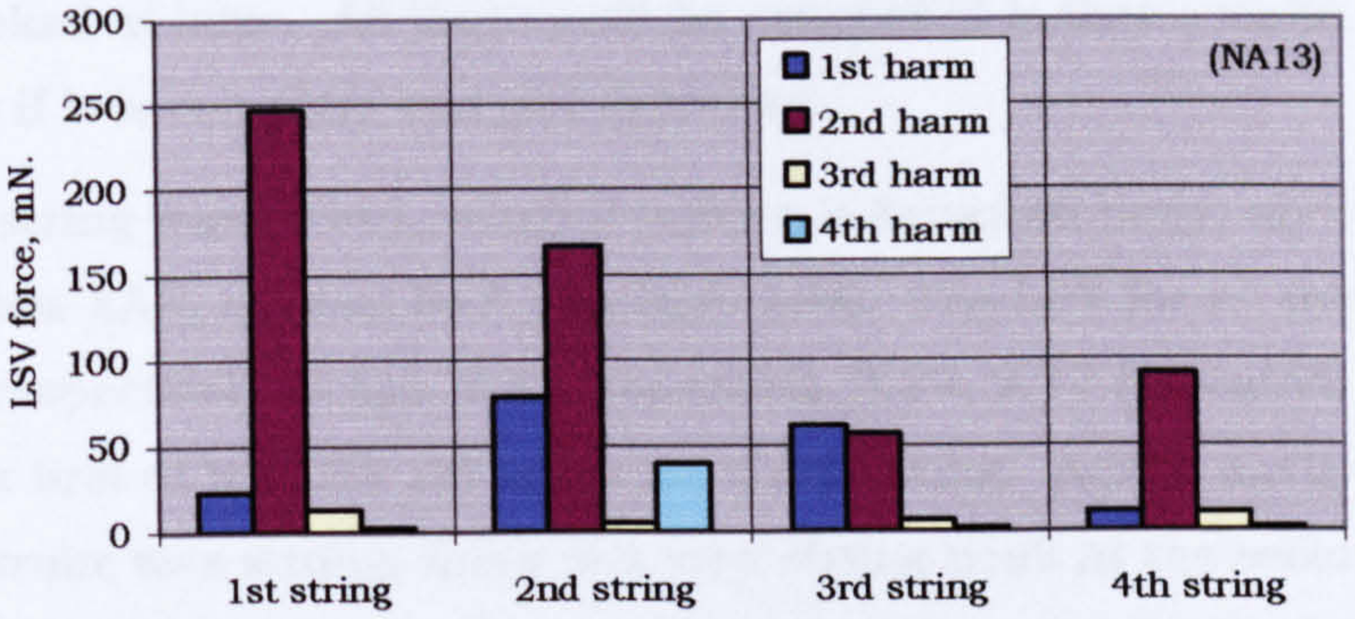

Fig. 9.16. LSV, V156, bowed 2nd string.

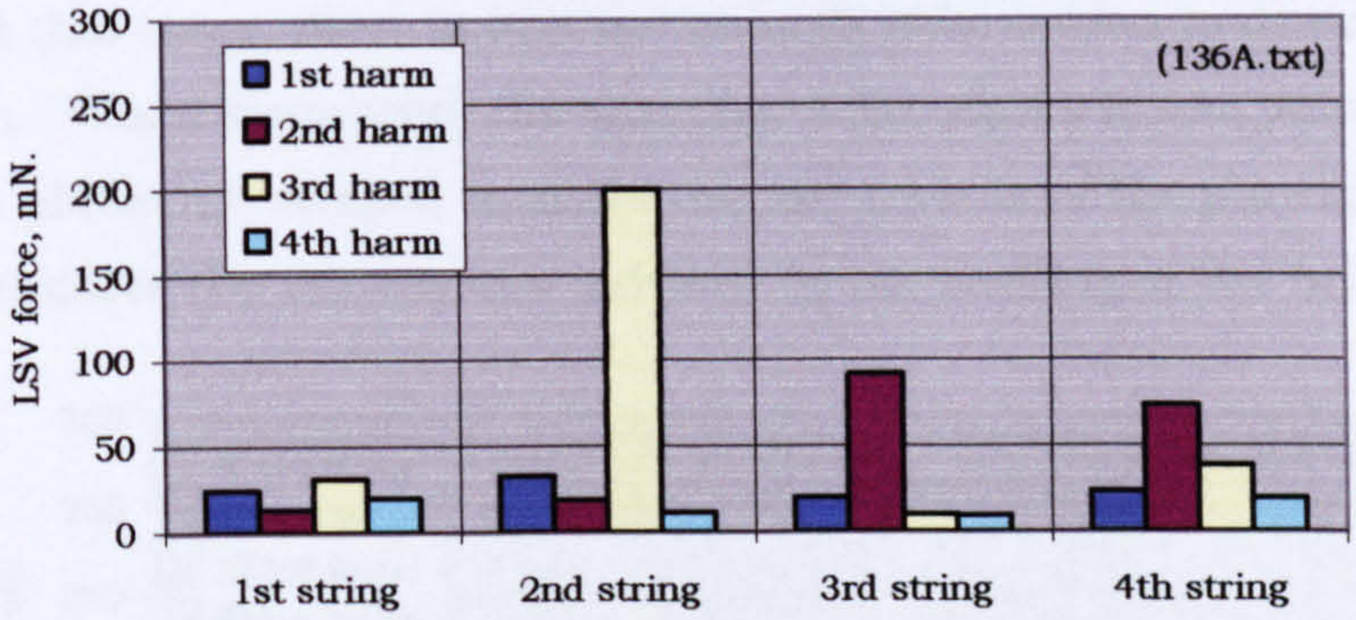

Fig. 9.17. LSV, V156, bowed 3rd string.

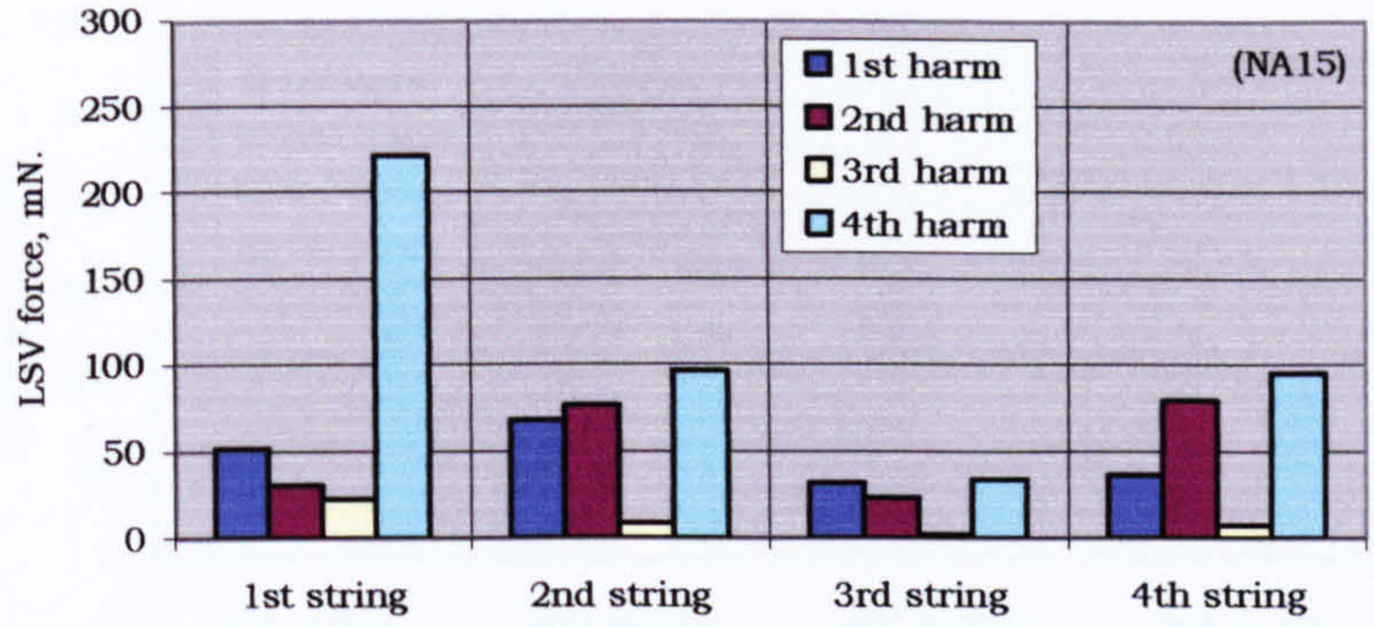

Fig. 9.18. LSV, V156, bowed 4th string.

That is looked at later. All that could be concluded is that a violin behaves differently if it is complete and not detached.

The third string was bowed, when it was on a detached body, and on violins of low EAR, normal EAR and high EAR. The LSV for all the strings is shown respectively in figs. 9.13 (repeated), 9.19, 9.17 (repeated) and 9.20. Look first at the LSV set up in the third string. Again, partly because the bow stroke was strong, there is a very strong peak at the second harmonic, caused by the dominance of the bellying LSV. While this peaks at 219mN on V158HE, and 143mN on V157LE, it is only 90 on V156, and 53mN on the detached body. One could speculate on the explanation for this but at this stage, there is just not enough information to draw any conclusion. When discussing the shaping of the plates it was pointed out that violin plates are shaped to make the movements of the plates, induced by LSV, reinforce the movements induced by the rocking of the bridge.

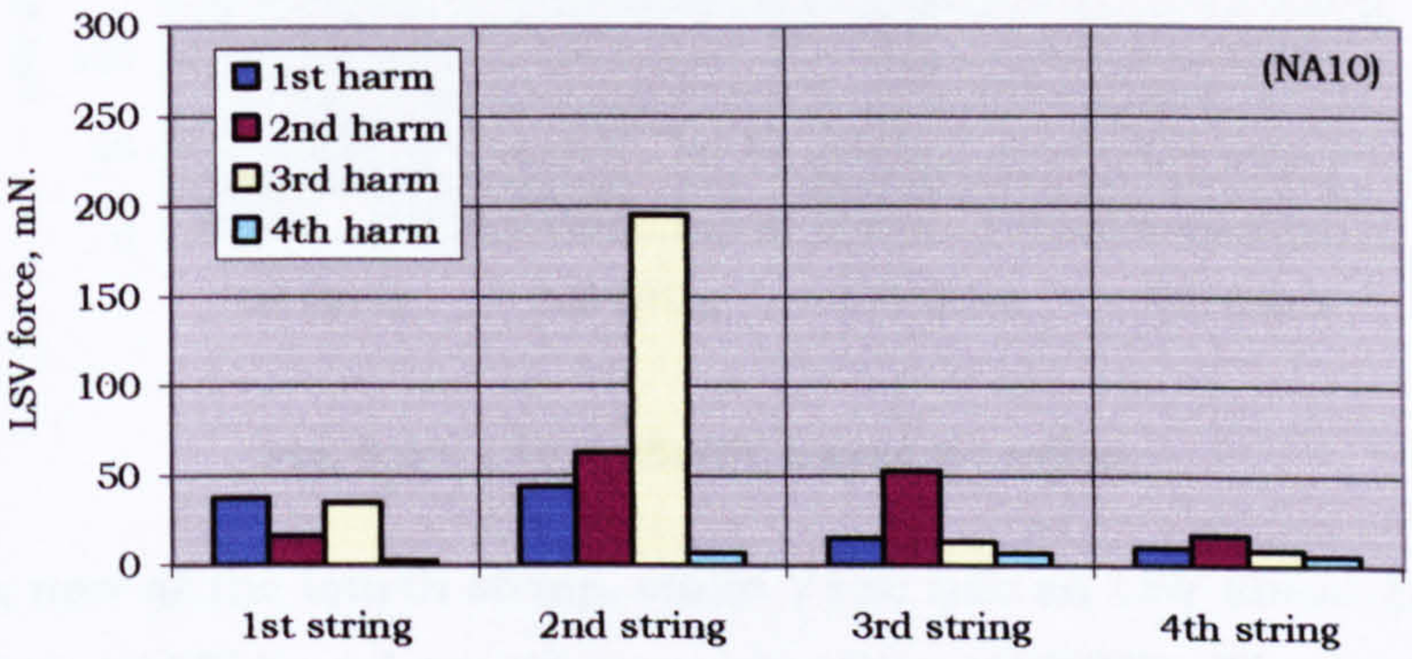

Fig. 9.13. (repeated) LSV, detached body, bowed 3rd string.

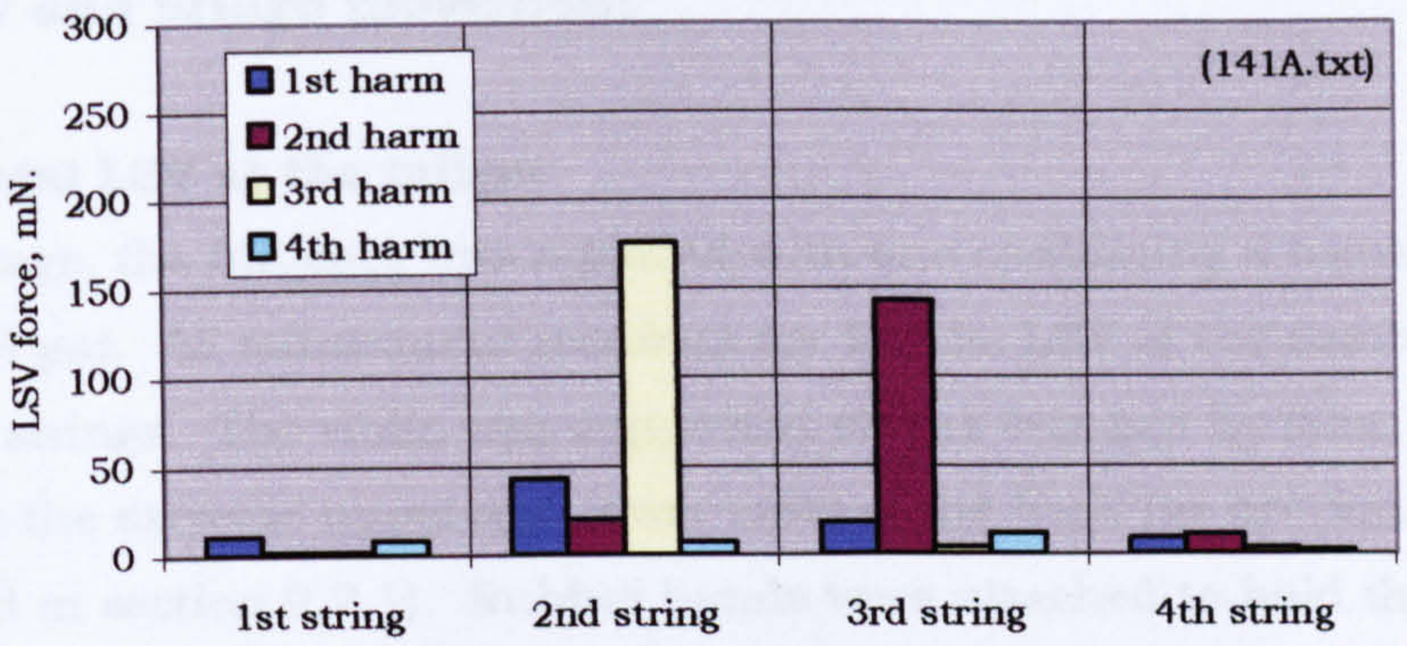

Fig. 9.19. LSV, V157LE, bowed 3rd string.

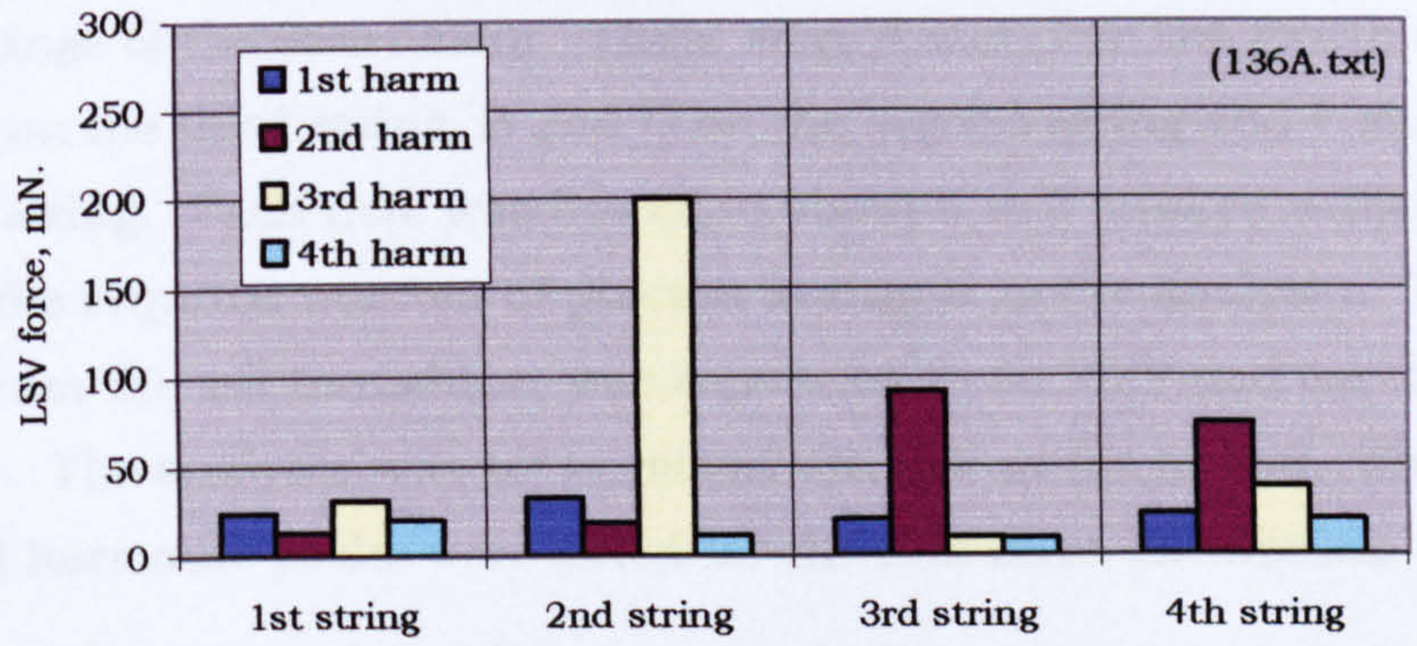

Fig. 9.17. (repeated) LSV, V156, bowed 3rd string.

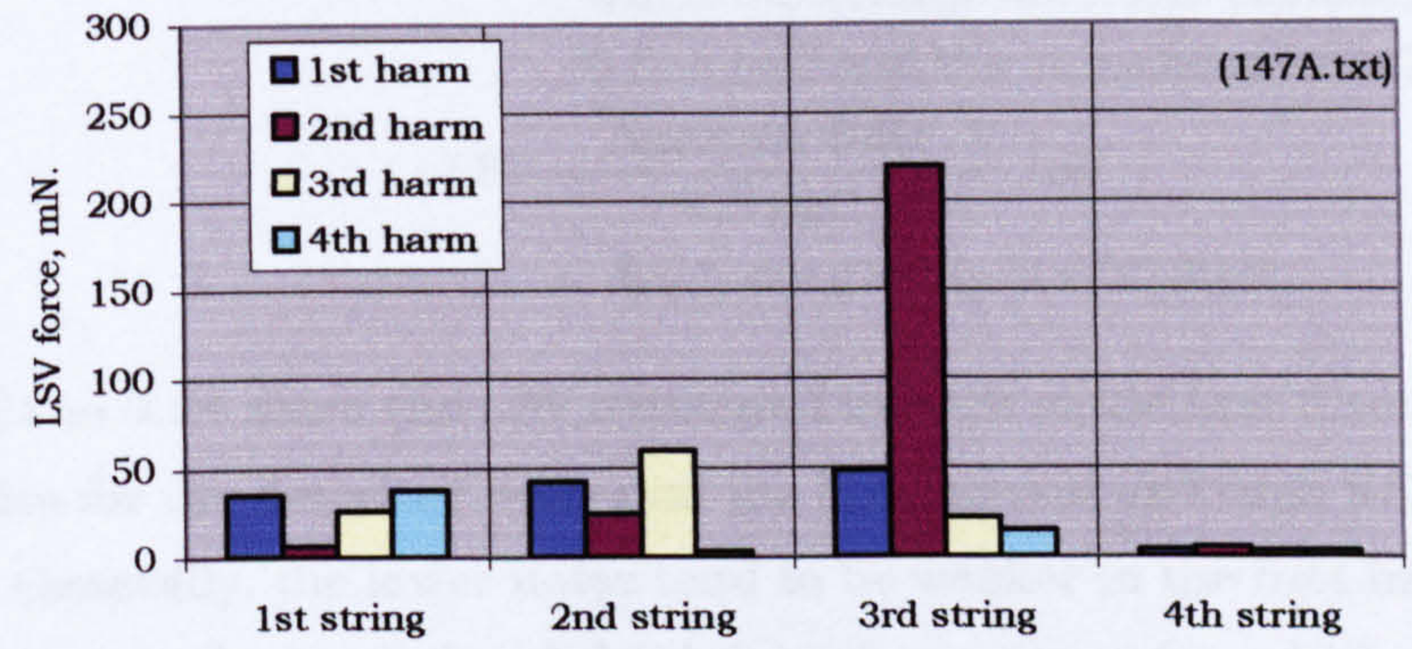

Fig. 9.20. LSV, V158HE, bowed 3rd string.

If we look now at the fourth string, violin V156 has an LSV about five times greater than V157LE and ten times greater than V158HE. The other noticeable difference is the low LSV carried by the first string of V157LE. It would seem logical to look next at the rocking of the bridge.

9.3 LSV and bridge movement

9.3.1 Total LSV at the tailgut

At this stage, the tailpiece was replaced with one containing a transducer at the tail gut. All subsequent readings are for the LSV of the combined group of strings. The violin was supported on the test bed by foam rubber blocks at the extreme upper and lower ends of the back (as previously described in section 9.2.1). Rubber bands were attached to hold the violin down on to the blocks. The violin was bowed while in this position. This was not necessary in the case of the detached body, which was held down by the string pressure. Seven notes were selected to cover the low and middle range of the instrument. These were A and C on the fourth string, E and G on the third string, B and D on the second string and F sharp on the first string. Each note was bowed to about 6 to 8 strokes sufficient to achieve the required number of process averages on the analyser. The output from the tail transducer was converted to an EMF and fed to the analyser. The analyser was set to record the LSV at the tailgut. The recorded harmonic peaks were noted for the first three harmonics.

The LSV was processed as follows.

$$\text{String tension vibration, LSV} = \frac{\text{EMF analyser}}{\text{transducer sensitivity} \times .01 \times 10}$$

where the charge amplifier calibration is 0.01 v/pC and the amplification is 20dB.

$$\text{LSV} = \frac{\text{Analyser EMF, V}}{4.31\,\text{pC/N}}.\text{inN}$$

$$= \text{Analyser EMF in V} \times 0.232\,\text{N}.$$

Figs. 9.21 to 9.24 show the LSV developed in each of the first three harmonics for the detached body and the low, normal and high EAR violins. Generally, the lower notes tend to be weaker in the first harmonic and stronger in the second and third than the upper notes, which are dominated by the first harmonic. The only other point is that V156 maintains a higher average LSV than the others, and the detached body the lowest. There are not any major differences.

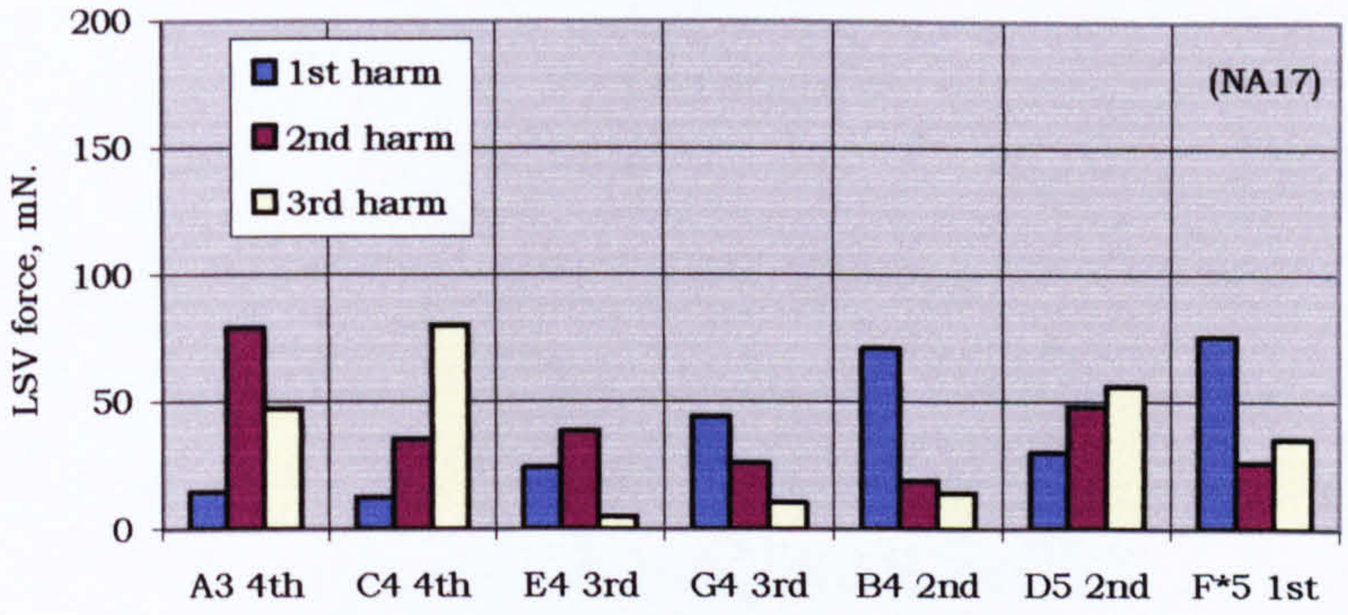

Fig. 9.21. LSV at tailgut, detached body, bowed string.

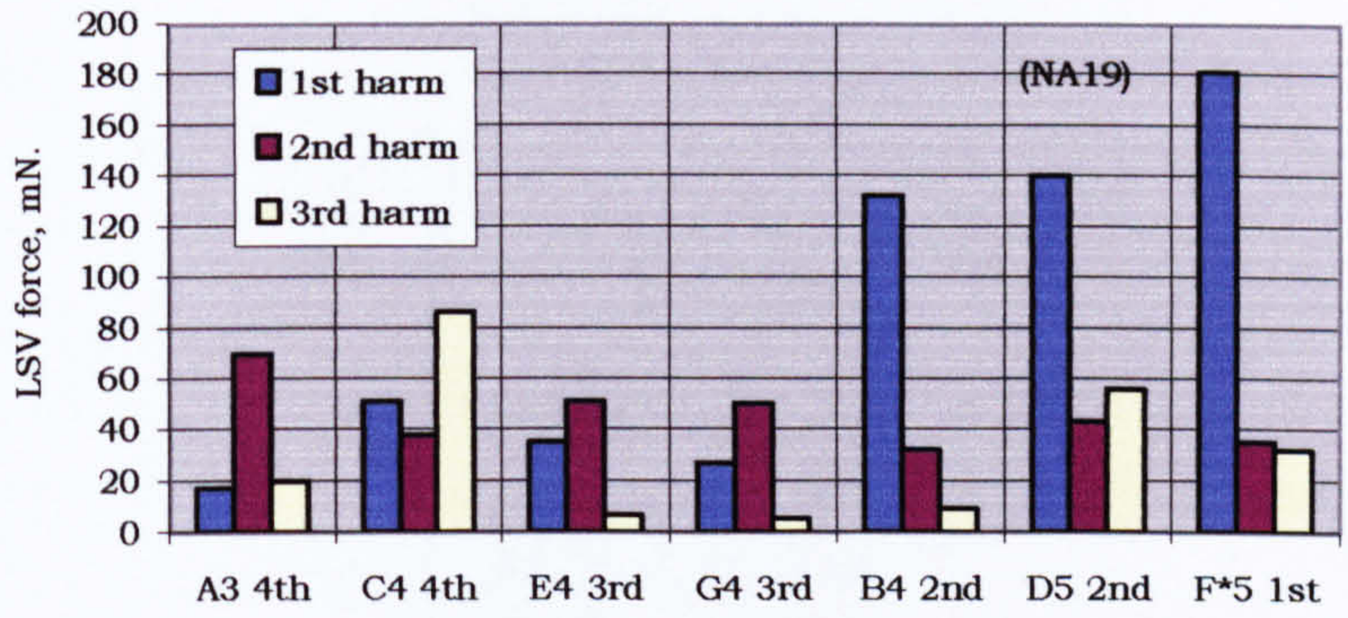

Fig. 9.22. LSV at tailgut, V157LE, bowed string.

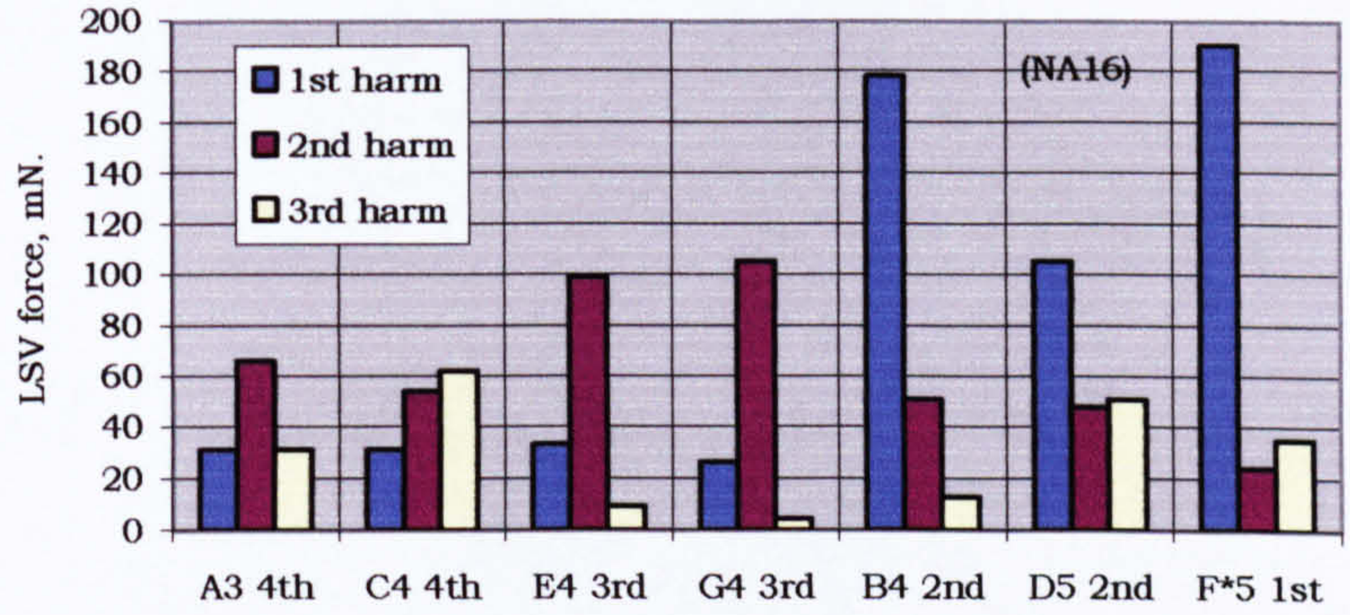

Fig. 9.23. LSV at tailgut, V156, bowed string.

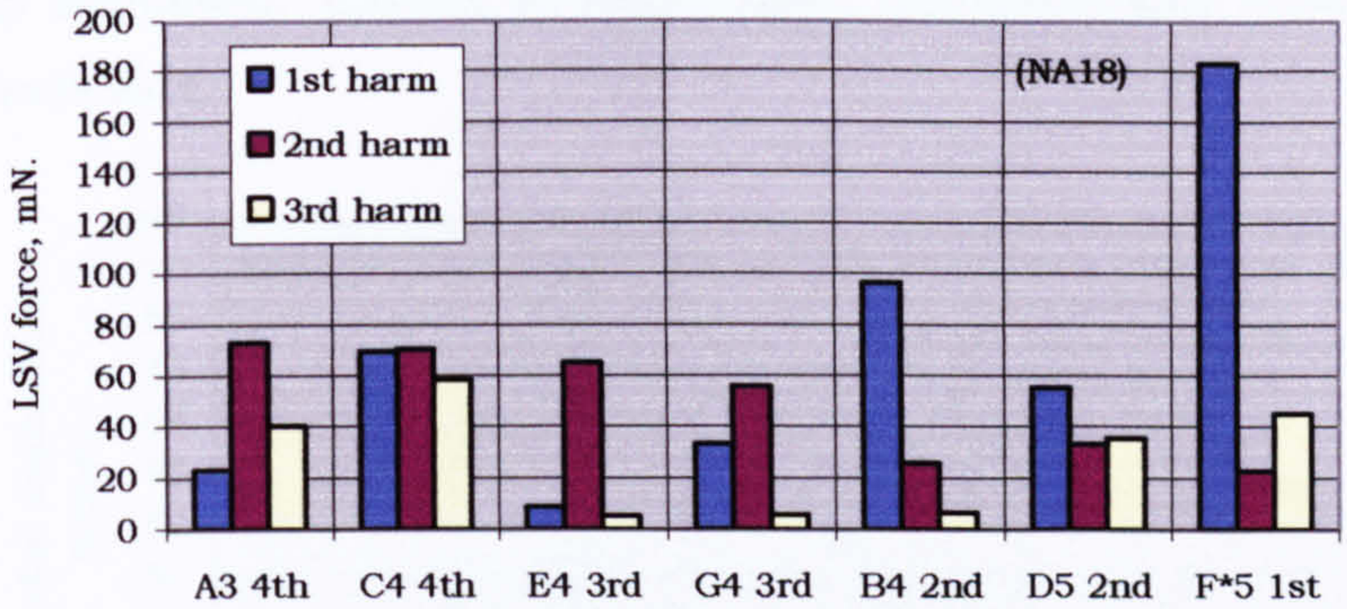

Fig. 9.24. LSV at tailgut, V158HE, bowed string.

9.3.2 Bridge movement

The above experiment was repeated, this time recording the vertical velocity of each side of the top of the bridge in turn by using the LDV. The magnitude and phase of this movement was related to that of the LSV and was recorded as a transfer function LDV/LSV. The LSV was recorded on the second channel. The transfer function was processed as follows, to give the amplitude of the bridge movement.

$$TF_{an} = \frac{\text{LDV output}}{(\text{Transducer output}) \times (\text{Amplification})}$$

where TF_{an} = Analyser recorded transfer function

LDV output = $v \times 6.24$ Volts

and $v = a\,\pi\,f$ where a = bridge displacement.

Therefore the LDV output = $2a\,\pi\,f \times 6.24$ Volts.

$$\text{Therefore } TF_{an} = \frac{2a\,\pi\,f \times 6.24}{LSV \times 43.1 \times .01 \times 10}$$

$$a = TF_{an} \times LSV \times \frac{1}{f} \times \frac{43.1 \times .01 \times 10 \times 10^{6}}{2\pi \times 6.24} \text{ in microns.}$$

Figs 9.25 to 9.28 show the displacement amplitude for each side of the bridge, and for each note, on each instrument.

There are differences here. V158HE shows a generally lower level of bridge movement than the others do. V156 shows a more uniform and marginally stronger bridge movement than the others do. Most interestingly the movement of the treble and bass sides of the bridge are not as different as

is generally supposed. Indeed, in some cases, the treble side moves more than the bass side.

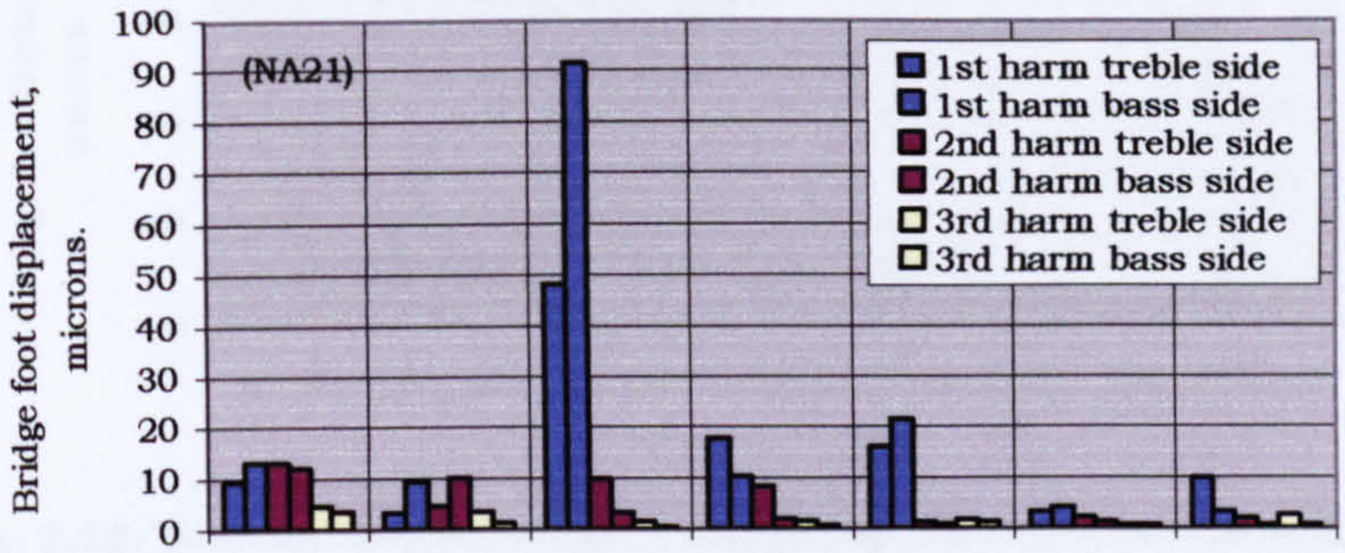

Fig. 9.25. Vertical displacement at bridge top, detached body, bowed string.

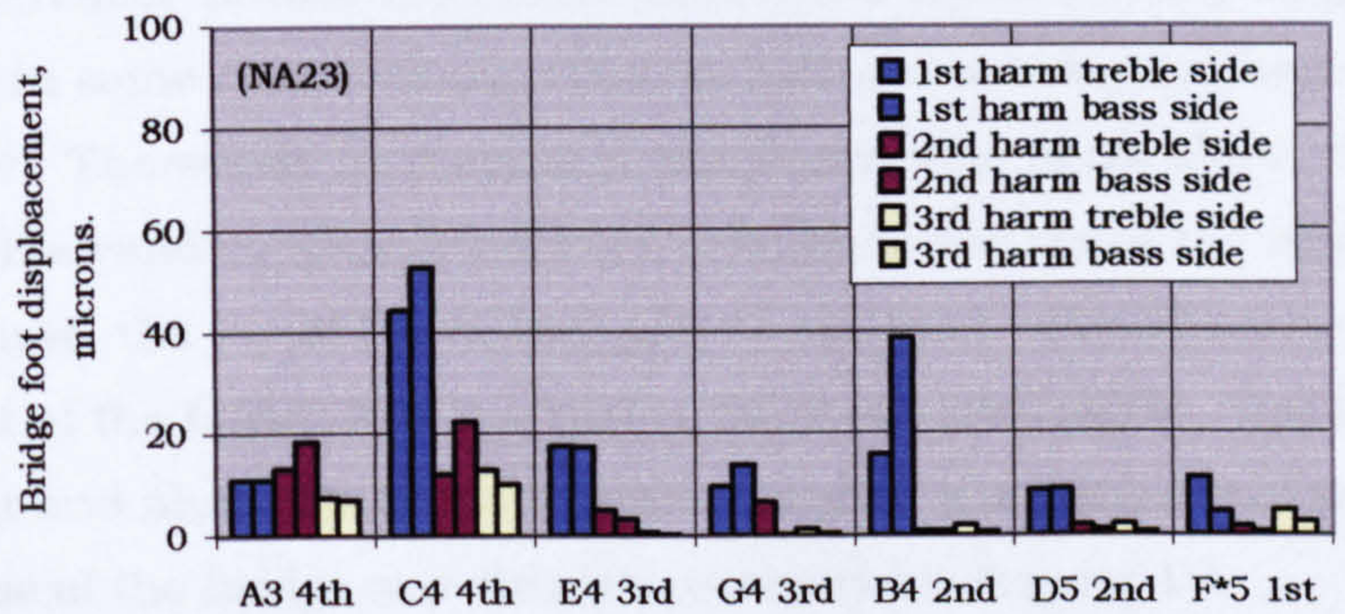

Fig. 9.26. Vertical displacement at bridge top, V157LE, bowed string.

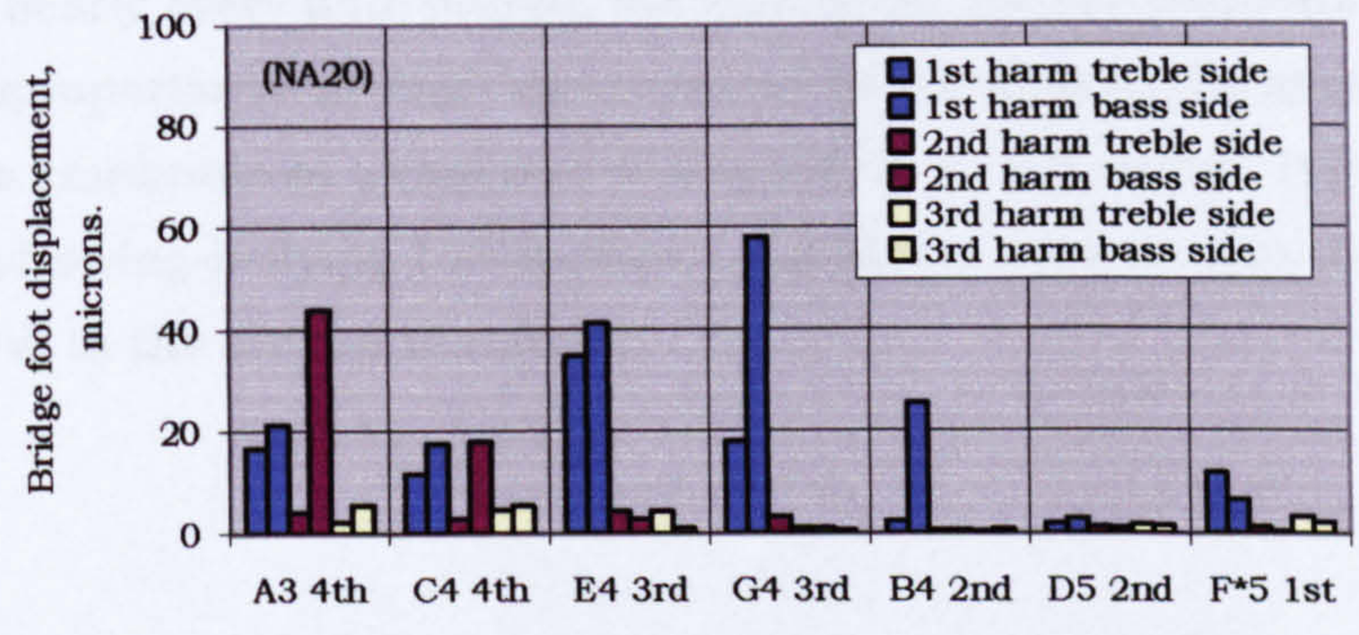

Fig. 9.27. Vertical displacement at bridge top, V156, bowed string.

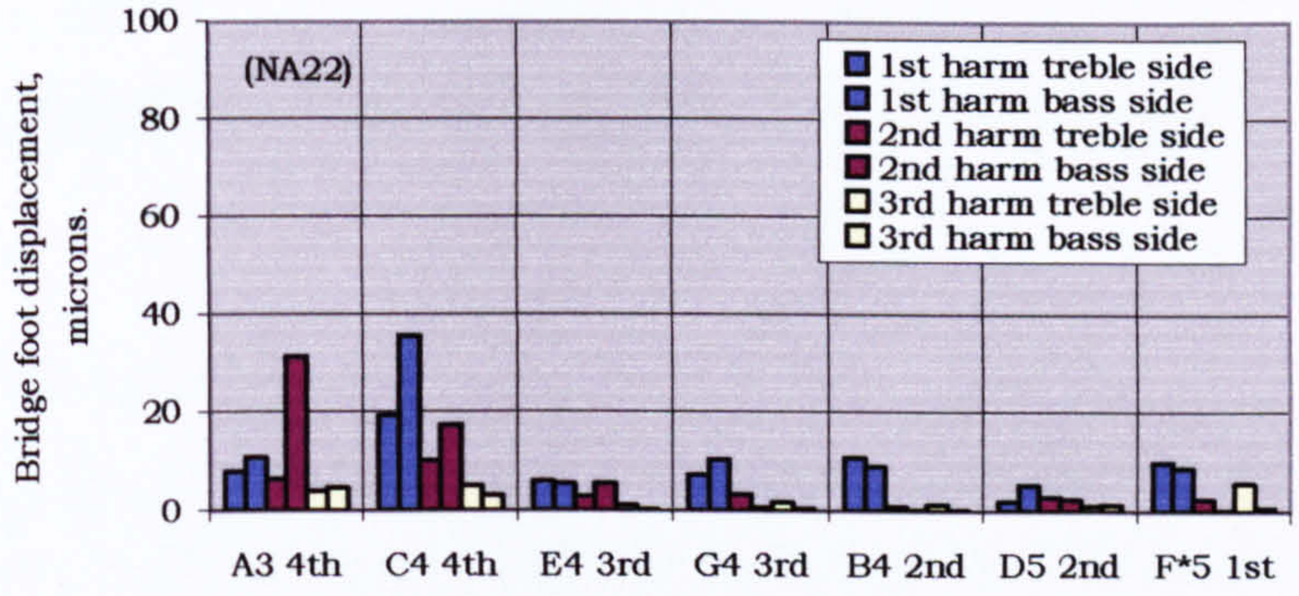

Fig. 9.28. Vertical displacement at bridge top, V158HE, bowed string.

The recorded phase of the bridge movements also showed that the movement of each side of the bridge was not separated by a neat 180 deg. phase difference. Indeed the phase differences showed a very large range of variation, in some cases coming close to both sides being in phase with each other. The widely held concept that the bridge rocks about the sound post is still a valid concept for motion relative to the top of the sound post but of course, the top of the sound post is not fixed. The absolute movement of the bridge feet is a rather more complex affair. The bridge movement and phase for a much larger range of harmonics was measured at the base of the bridge and this is presented in Chapter 12.

9.4 Conclusion

- In nearly every note played, the LSV of the second harmonic was disproportionately high compared to its strength in the spectrum of the amplitude of transverse displacement of the string. It is clear that string-bellying LSV makes a significant contribution to the total LSV, in the second harmonic.

Chapter 10

EXPERIMENTS USING SHAKER EXCITATION

10.1 Introduction

In the experiments described in Chapter 9, the LSV force was measured separately for each string at the string anchors. The qualitative analysis presented in Chapter 3 suggested that the total LSV force of the four strings combined was the significant factor in the driving of the violin. In this Chapter, the experiments concern the total LSV force in the group of four strings, as measured at the tail gut.

In Chapter 9, the results were presented of experiments designed to investigate the relative contributions of string bellying and bridge-rock to the total LSV in the lower harmonics. The results failed to produce any consistent evidence that might point to differences in the LSV in violins of different EAR.

Violin tone is harmonically very rich and the timbre and carrying power is thought to be dependent on the upper harmonics. In this chapter, the results of experiments concerning the LSV developed over an extended frequency range are presented. All the experiments reported henceforth cover a frequency range extending from zero to 10kHz.

10.2 Excitation over an extended range

In Chapters 11 to 13 of this thesis, the results of tests are presented which were made to investigate any differences that may exist in the effect of different shapes of arching on the generation of LSV and radiated sound. These tests required a sustained excitation, so that several spectra could be recorded. String-bellying LSV originates from the string motion and acts on the violin at three ports. The spatial disposition of the input forces from the driving substructure to the body may have a significant effect in determining the relative degrees to which modes are excited. Therefore, it is necessary to involve the swinging of the string in the excitation of the violin.

Considerable effort was put into an unsuccessful attempt to find the operating shape of the violin while the open G string was hand bowed, by using a small volume velocity transducer. This experience showed that for most experiments it was not practical to hand bow the string because of the difficulty of repeating accurately, and sustaining, the excitation. Bowing machines have been made in some research establishments but they are not simple pieces of equipment, and the excitation is still very dependent on the bow pressure and velocity, and the position of the bow on the string.

10.2.1 Driving by shaker

Excitation by driving the string with a shaker has the main disadvantage of not producing a typical bowed spectrum, in that it is weak in harmonic content. On the other hand, it is sustainable and repeatable.

By adjusting the driving frequency to be slightly off the resonance frequency of the string, it is possible to introduce a rich harmonic content into the transverse vibration of the string. Unfortunately, driving off resonance was not found to give easily repeatable results. It was found that a certain amount of harmonic content was introduced by driving at resonance and this was found to be a repeatable condition.

Following the presentation of an earlier version of this thesis it was suggested that all the results obtained by shaker excitation of the open G string at resonance are unreliable because of the extreme sensitivity of the response to combinations of the driving frequency and driving force. It was suggested that it is possible in the testing of only one violin to produce all the differences seen between the various test violins. This sensitivity was clearly recognised at an early stage in the project and the assistance of Dr. D J Thompson *(Dynamics Group, ISVR, University of Southampton)* was sought for a theoretical explanation, since he had developed models and computational analyses of point-excited string vibration. His study did indeed reveal that if the driving frequency should drift either side of the string resonance frequency there is a rapid increase in the dynamic stiffness of the string. Thus the force required to drive the string at a frequency slightly above or below the resonance frequency would greatly increase, resulting in a larger kink being formed in the string at the driving

point. This kink could generate harmonics in the string by non-linear stretching action. At resonance the kink is small enough to be a negligible source of harmonics. *(A personal communication from Dr. Thompson)* A study was made to identify the cause of the higher harmonics in the TSV spectrum of the driven string. Three potential causes were examined: the shaker, the kink in the string and the non-linear stretching of the string.

The source of the harmonic content set up in the string vibration when it is driven by a shaker could come in part from the harmonic impurity inherent in the displacement of the shaker. This was measured and it was found that the relative content of the higher harmonics in the shaker displacement compared to the fundamental was very much less than that set up in the string (when the string was driven to a 3.25mm displacement amplitude). The resonant response of the higher modes to unit displacement excitation should not differ significantly from that of the fundamental except in regard to shaker position. The harmonic content in the TSV from this cause would predictably be sensitive to the position in the length of the string of the point of application of the driver. It was found experimentally that the harmonic content was not perceptibly sensitive to the position of the point of the driver, which is consistent with the shaker not directly being the source of the higher harmonics. It was concluded that the shaker drive was not the source of the higher harmonic content in the vibrating string. If there had been non-linearity in the shaker driving of the string it would be dependent on the magnitude of the shaker coil excursion rather than the magnitude of the driving force. Since the string was driven at a point 8 mm from the end, the excursion of the coil would be small (about 0.17mm). Furthermore, since the fundamental mode displacement was held the same in all the tests the excursion of the coil would have been close to the same in all cases. It was concluded that the contribution to the harmonic content from the shaker was probably small, but whatever it was it would not vary with each excitation.

Dr. Thompson's analysis showed that provided the string is driven at resonance, the force applied to the string is very small, the resulting kink in the string is small and any harmonic content in the string resulting from stretching by the kink would also be very small. The kink in the string from the shaker does not propagate along the string and so no harmonics

are introduced by this means (unlike the bowed string). Fig. 10.0 shows how the increase in string length varies with the excitation frequency when the string is driven to a constant harmonic displacement of 6.5mm peak to peak over a range of frequency *(provided by Dr. Thompson)*.

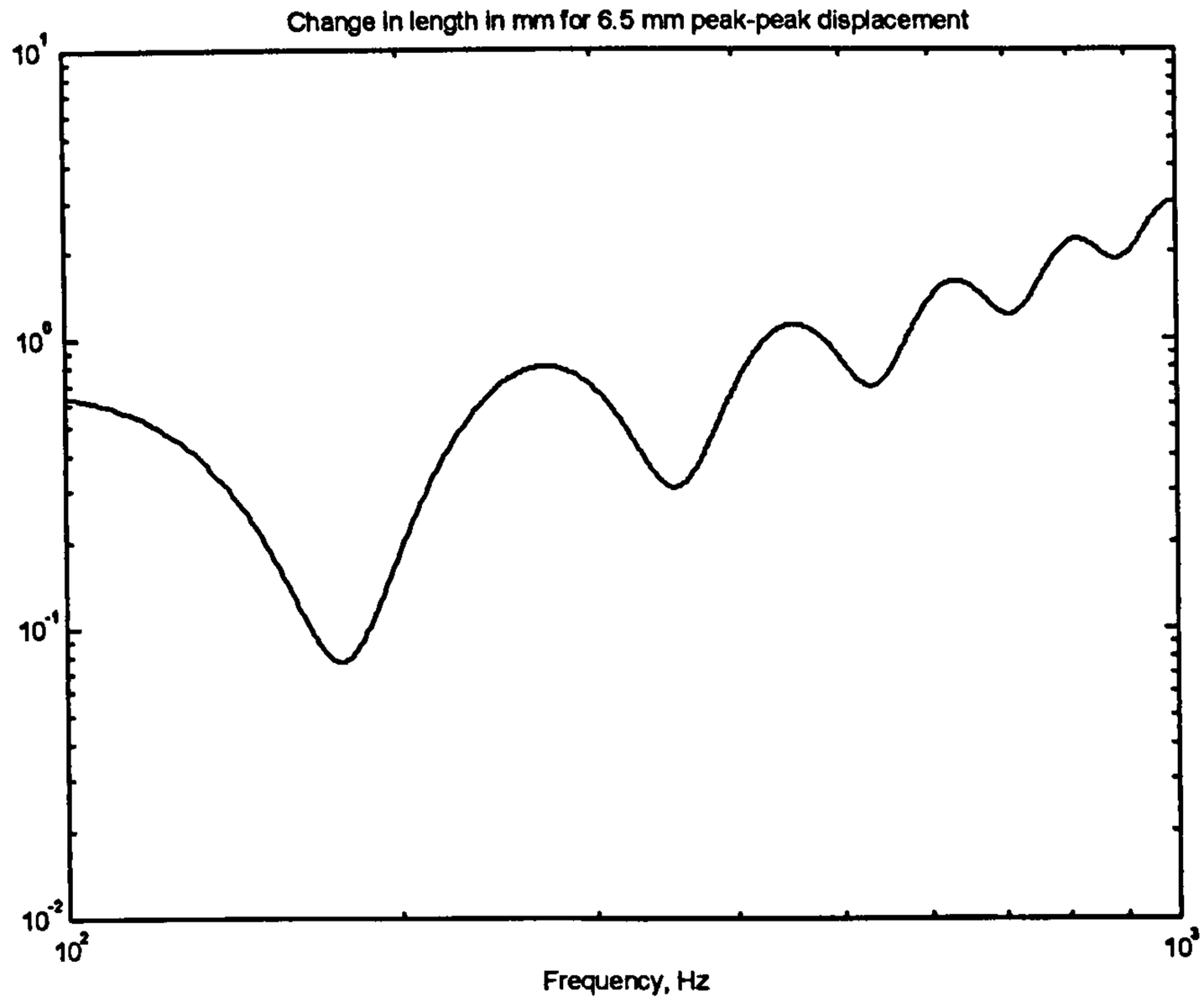

Fig. 10.0. Change in length of a G string when driven to a constant transverse displacement of 6.5mm peak to peak, by a transverse force applied by a shaker at a point 8mm from the end of the string. The change is lowest at the string harmonic frequencies and rises each side of them.

We are only concerned with the first harmonic shown in fig. 10.0 at 196Hz. At the trough there is a narrow frequency band where apparently the frequency can drift slightly with little effect on the string length, and hence the harmonic content. However, experimentally the sensitivity was found to be greater than this graph would suggest. This is an indication of the complex behaviour of this non-linear system.

Simple sinusoidal transverse vibration of a string can only be realised if the static string tension does not vary throughout the cycle. This ideal is approached only at very small transverse displacement amplitudes. In our experimental work, the string was always driven to a transverse displacement amplitude of 6.5 mm (peak-to-peak) measured at the centre

of the string length. At a displacement this large, the variation in string tension throughout the cycle will produce odd harmonics of the TSV. The experimental results show that the shaker established in the string a broad spectrum of harmonics in the transverse displacement of the string. These spectra generally showed an overall declination with rising harmonic number, and showed greater strength in the higher harmonics if the string was on a real violin rather than less dynamically active rigs. The means by which these broad spectra of harmonics are generated is far from clear. It is widely accepted in the literature that the non-linearity in the string tension caused by relatively large transverse displacements must generate higher harmonics but a full study of these effects does not appear to have been made.

Dr Thompson has shown that a tensioned string held between immovable supports and driven in a pure first harmonic excitation will, through non-linearity, generate a third harmonic but this will be in the first harmonic mode shape and is therefore non-resonant. A limitation was placed on this theoretical investigation by having to make simplifying assumptions to find the roots of an intractable differential equation so it was not possible to confirm that higher odd numbered harmonics are generated in the same way. However, a physical approach to the problem can be helpful. A single frequency wave in a string would show a sinusoidal variation of the string displacement with time. In the case of a non-linear relationship between the string tension and the string transverse displacement the sinusoidal variation would become squashed, by the flattening of the top of the peaks. This tendency would be slight but the ultimate extension of this tendency would be to approach a square wave. This tendency towards a squaring of the wave would add the odd numbered harmonics to the first harmonic. Dr Thompson's analysis also showed that a second harmonic LSV acting on a bridge with a TSV motion in the first harmonic would produce a component of force on the bridge at the third harmonic. This has been confirmed experimentally and theoretically by others [Legge and Fletcher, 1984].

Bridge flexibility in the string direction can, in principle, enable the LSV at the even numbered harmonics to induce TSV in the string via parametric excitation. One view that recurs in the literature is that support mobility has a significant effect on the formation of the TSV in the string from non-

linear variation of string tension. The effects of alterations in support mobility on both the TSV and the LSV are examined experimentally later in this chapter. It is not possible to provide a rigorous theoretical basis for the establishment of the TSV spectra in the shaker driven string, but the experimental evidence that it does happen is presented.

It is believed that the main source of the harmonics in the string vibration is the non-linear stretching of the string coupled with the motion of the bridge and terminations. Vibrations that arise this way are independent of the position of application of the driver.

Given the sensitivity of the excitation to the setting of the controls of frequency and shaker current it is conceded that a failure to apply appropriate measures to monitor and control string resonance could allow unpredictable amounts harmonic content to be introduced by the string kink (the second cause mentioned above). This would make the excitation variable and would seriously compromise any conclusions drawn from the experimental results.

As a result of this clear indication of the need to exercise extreme care in checking that steady state conditions were maintained, a constant watch was kept on the shaker current (or input force), string amplitude and the envelope of the TSV harmonic spectrum. All tests and observations were subject to repetition in order to ascertain that resonance could be achieved and maintained using the above-stated monitoring measures. It was found that by fixing the shaker current and varying the frequency, there were up to three resonance conditions that produced maxima in the first harmonic displacement. These corresponded to a node in the string in front of the bridge by about 3mm, behind the bridge by about the same amount and at (or at least very close to) the bridge. Of the three conditions it was decided to use the one where the node was at the bridge (or very close to it). This was determined by lifting the stinger from the string and plucking the string and then setting the shaker frequency to match that of the plucked string. The final fine-tuning was made by adjusting the driving current and frequency to give the required first harmonic string displacement with the minimum driving current (force). This also gave the lowest response in the upper harmonics of the TSV. If during the time required to record the

experimental data there was any straying from the initial setting, as could be most sensitively observed by loss of string displacement in the first harmonic, the measurements were discarded and the setting readjusted for a new beginning. At all times that the shaker was driving the violin while measurements were being made there were two people involved. The writer constantly monitored the string first harmonic displacement and the TSV displacement response spectrum as shown on the screen of the analyser in order to ensure that there was no straying from the original settings. The writer's violin-making partner Roger Sheldon, who has a degree in physics, controlled the instrumentation to enable the recording of the various data. These included the TSV (as indicated by the string velocity in the magnet gap), the LSV force, radiated sound, the acceleration at each bridge foot in turn and the acceleration at the saddle.

Tests were done on three groups of violins. The first group consisted of strings mounted on non-violin test rigs designed to investigate the differences in TSV and LSV due to variations in bridge mobility and string termination mobility. These showed appreciable differences in TSV in the higher harmonics (the fundamental having been standardised). This result is consistent with the important role that support mobility plays in the generation of non-linear TSV in the string. The second group consisted of three violins that differed only in the EAR. These showed much closer agreement in the TSV. The last group was three violins that differed only in deviation. These showed only small differences in TSV. It is clear that where there was very little difference in the violins, the TSV induced by the shaker drive was almost the same. This supports the contention that the excitation and the associated response were adequately repeatable (all the TSV spectra in these three groups are shown in Chapters 10 and 11). There is no reason to doubt that the differences in behaviour in the rigs tested in the first group are not due to differences in the excitation.

Certain phenomena were observed in the spectra of the string velocity at the magnet gap as indicated by the current generated in the string. There was always a periodic rise and fall in the spectral peak heights similar to a scalloping effect. It was not appreciated at the time of conducting the experiments that some form of scalloping was to be expected in these spectra as the result of the magnet not being located at the same point in

the wavelength of the all the string modes (see section 10.2.2 for a full discussion of this). The scalloping was thus regarded as some sort of systematic error and an effort was made to minimise it. It was shown in Chapter 6 that a correction should be applied to the string velocity at the magnet, which would apply a counter form of scalloping and even out the spectrum.

It was also noted that there was a dropping out of the lower order even numbered harmonics in two of the nine magnetically transduced velocity spectra (and hence the TSV spectra) shown in the thesis. Where this happened it was found to be consistently repeatable and impossible to eliminate. It was concluded that this phenomenon was not due to a systematic error but was a real behavioural characteristic of the structure when excited by a shaker (a suggested explanation for it is given in Chapt.12).

10.2.2 Derivation of the transverse displacement of the strings.

In section 6.3.4, the method of measuring the transverse velocity of the string was described.

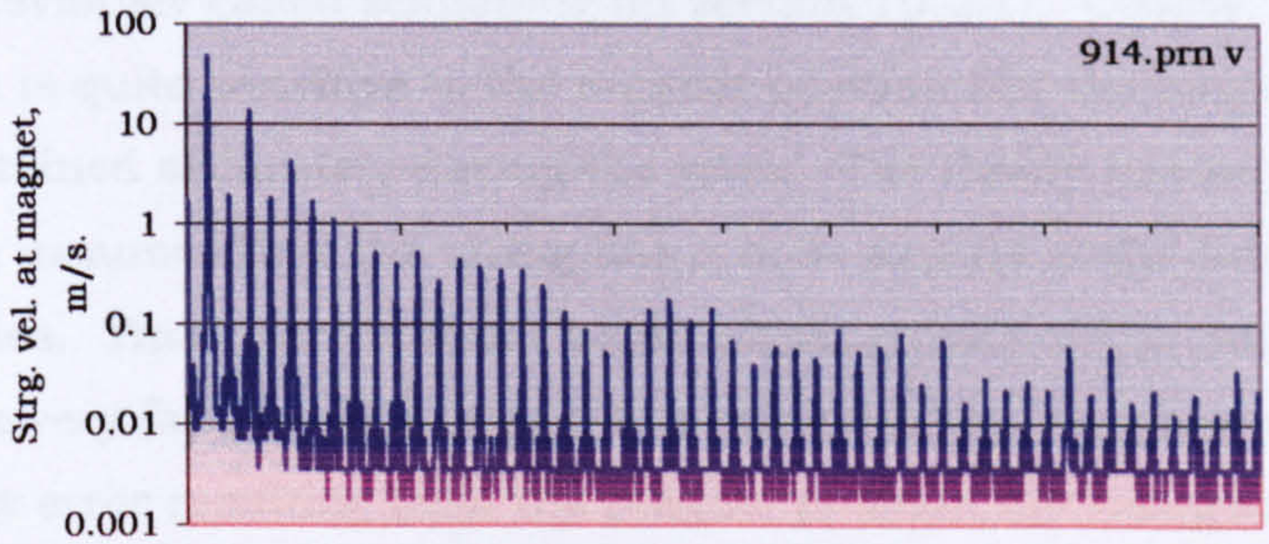

Fig. 10.1 A. Indicated rms string velocity at the point of location of the magnet, shaker driven G string, V157HD varnished.

As an example, fig. 10.1 A shows the rms string velocity at the magnet (averaged over the width of the magnet) for a shaker driven G string on violin V157 varnished. If we ignore the effect of the magnet position relative to the mode shapes, the string transverse displacement is found by dividing the velocities by the angular frequency and scaling the result to give a first harmonic displacement of 3.25mm. The transverse displacement of the string found in this way is shown in fig. 10.1 B.

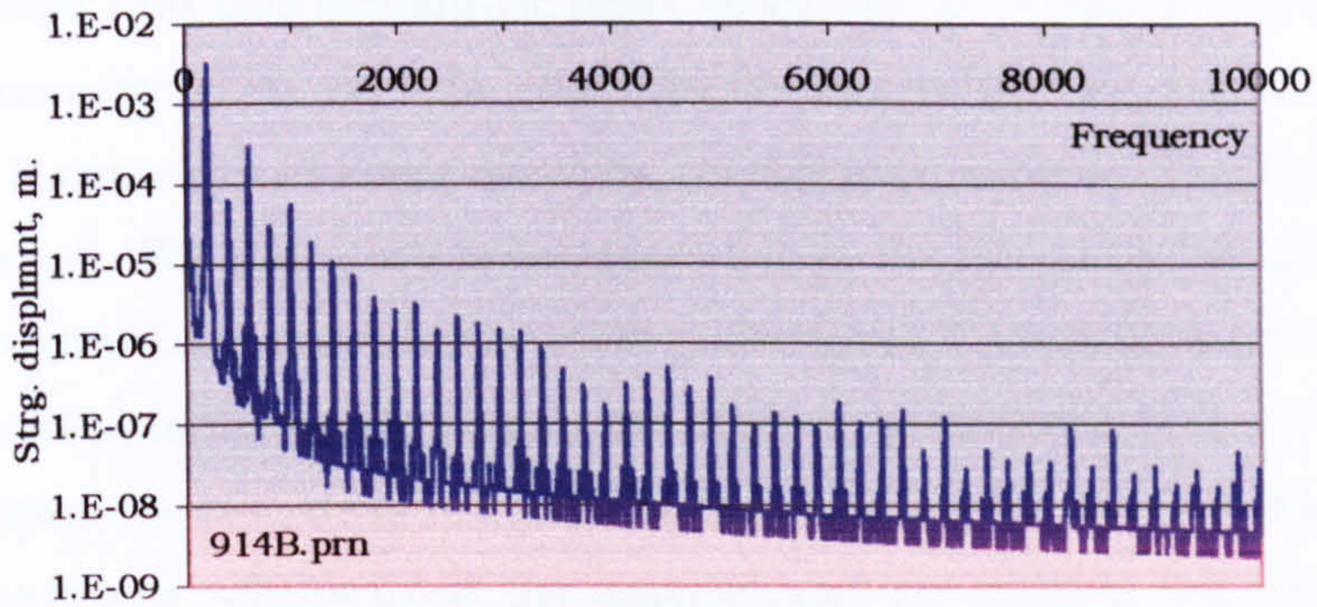

Fig. 10.1 B. Amplitude of transverse displacement, shaker driven G string, V157HD. Calculated with no correction for magnet position or width.

The above assumption is clearly not justified. The relation between the mode displacement amplitude and transverse string velocity at the magnet position varies with the mode order. Accordingly, two corrections were applied, one for the position of the magnet in the length of the string and the other for the width of the magnet in relation to the wavelengths of the modes.

The correction for the position of the magnet in the length of the string has the effect of relatively raising the amplitudes in a periodic way (see fig 10.1C), previously called scalloping (in section 10.2.1). Clearly, this correction is quite sensitive to the magnet position but the magnet position was maintained accurately during the work. The theory behind this correction assumes that the string has a node exactly at the bridge position in all modes. This clearly cannot be so, although one would not expect the node to be very far from the bridge, but this could be a further source of error. Any error resulting from the magnet position not being accurately known in relation to the mode shapes would become progressively greater at the higher harmonics. This correction appears to have introduced a rise in amplitude at frequencies near 2500. This is too low a frequency to be explained by inaccuracy in the magnet position. If the TSV spectra derived from the magnet velocity spectra are to be free of the scalloping effect then there should be reversed scalloping in the measured magnet gap velocity spectra. It was mentioned in section 10.2.1 that scalloping was observed in the magnet gap velocity spectra but this was erroneously thought to be a systematic error at the time, and so an effort was made to eliminate it. It is

now clear that had this scalloping been admitted the applied correction may have countered it. As it is, the applied correction has apparently, in the higher harmonics of some spectra, introduced more scalloping than it has countered. We therefore must accept that the corrected amplitudes become progressively more inaccurate with rising harmonic number. The question arises, is the scalloping in the higher harmonics of the TSV a real physical phenomenon, or is it due to some error in the method used to find the TSV spectrum, which used the magnet and an applied theoretical correction? The fact that the scalloping does not appear in the corresponding LSV spectra does suggest that the real TSV spectra should not show this scalloping either. It is therefore concluded that the scalloping in the higher harmonics of the TSV probably arises as the result of the method of inferring the TSV spectra from the string velocity in the magnet gap. However in the absence of any other rational means of the deriving the TSV spectra from the string velocity spectra the method presented here has been followed in all the TSV spectra presented in Chapters 10 to 13.

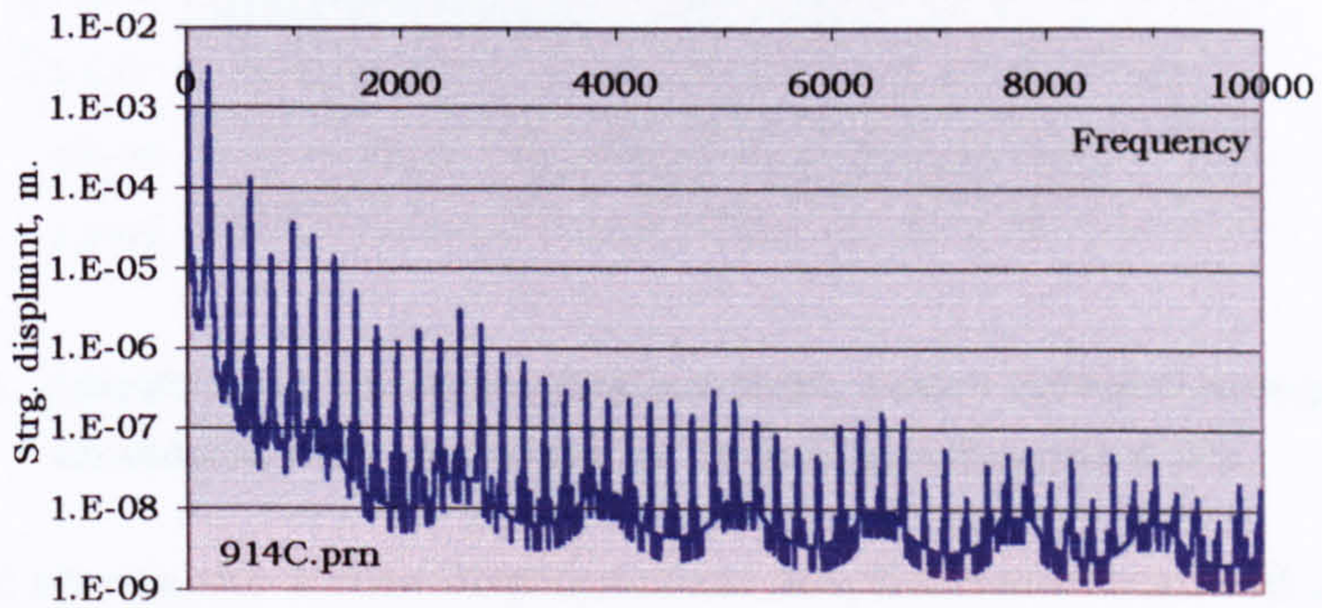

Fig. 10.1 C. Amplitude of transverse displacement, shaker driven G string, V157HD. Calculated with correction for magnet position but not corrected for magnet width.

Fig. 10.1 D shows effect of applying a correction for the width of the magnet in relation to the wavelength only. This has the effect of progressively raising the amplitudes in the higher harmonics. This correction would appear to be justified although the result does give surprisingly high amplitudes at the higher harmonics. Bowed spectra of transverse displacement do not show such a relatively high top end response but the

excitation by shaker causing harmonics from non-linear stretching may do so.

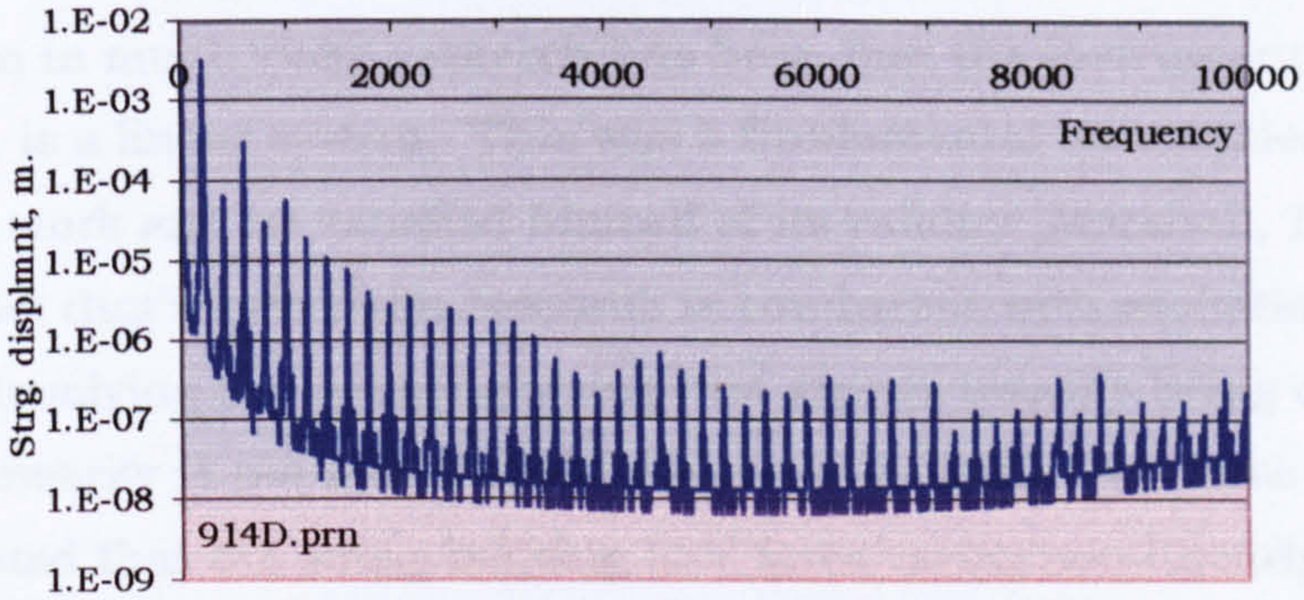

Fig. 10.1 D. Amplitude of transverse displacement, shaker driven G string, V157HD. Calculated with correction for magnet width but not corrected for magnet position.

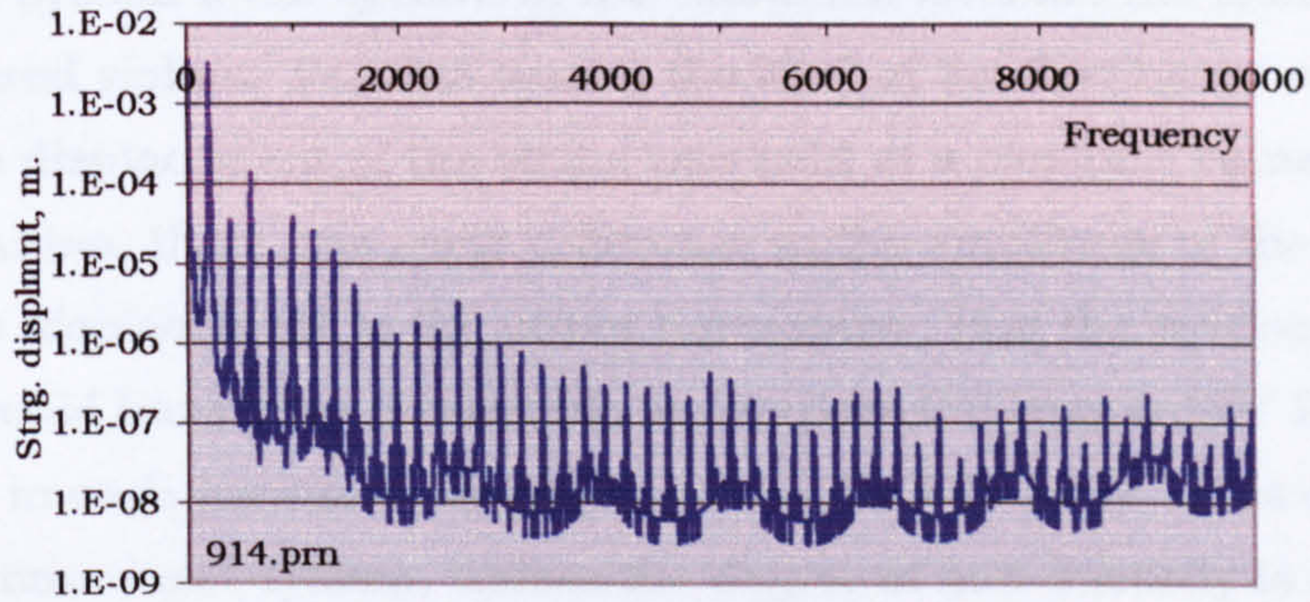

Fig. 10.1 E. Amplitude of transverse displacement, shaker driven G string, V157HD. Calculated with correction for magnet position and width.

Fig. 10.1 E shows the string displacement amplitudes calculated using both corrections. In the example given here, the corrections do appear to have introduced irregularities but also in some cases to reduce them. In some other strings, the corrections appear to have resulted in a reduction of irregularity.

It was decided that since these corrections are theoretically required they should be applied and so this has been done in all the results presented.

10.2.3 Experiments with a non-linear system

Because the harmonic content of a shaker driven string is weak, it was found to be very easy to drive it to a higher amplitude of transverse

displacement than that normally achieved by bowing. This meant that the first harmonic was larger than that of a bowed string, and the higher harmonics were progressively lower than those of a bowed string. A basic assumption in much violin research has been that the instrument, with its strings on, is a linear system. This was a fundamental assumption of Marshall's work and he satisfied himself of its validity [Marshall, 1985]. It is also a fact that much violin research is conducted with excitations other than that involving the swinging string (the strings usually being damped) and non-linearity is not introduced from string bellying. We have demonstrated that the string bellying LSV force varies non-linearly with the TSV force. Since the experiments described in this thesis do involve the swinging string there must be a degree of non-linearity in the dynamic response. Comparisons in behaviour between instruments are valid in a non-linear system if the spectra of the excitation level are the same for all the compared violins. For this reason the level of the first harmonic transverse displacement of the string was held at a constant value. Despite this precaution, there was some difference in the amplitude of the transverse displacement in the upper harmonics. Had the system been linear it would have been reasonable to compare the level of LSV force generated in each harmonic by dividing it by the TSV force. This cannot be done in a non-linear system, unless the degree of non-linearity is small.

The degree of non-linearity can be estimated. Since the main source of non-linearity is string-bellying LSV, some estimate of its relative significance should be helpful. The LSV force generated in the string arises in part from the primary bellying LSV in the string and in part from the secondary LSV arising from the modal activity in the violin. This modal activity is driven by the two primary causes of the string TSV force and string LSV (bellying) force acting on the body. The string LSV (bellying) force has a non-linear relationship to the string TSV force. By finding the ratio of the string LSV (bellying) force to the string TSV force we have an indication of the degree of non-linearity in the total LSV developed in the string.

The ratio of the in-plane forces on the bridge from bellying LSV and TSV can be evaluated using the following formula derived in section 3.2.3;

$$\frac{F_{\text{Bellying LSV}}}{\text{TSV force}} = \frac{k_{st}}{87T}\frac{n\pi}{(L+L_1)}\frac{(a_{n/2})^2}{a_n}$$

where n is the harmonic number of the TSV. This can be evaluated for the transverse string displacements for the driving of violin V157 varnished. This is shown in fig. 10.2.

Because it was impossible to show zero on a logarithmic scale this is shown as 0.00001. It will be noticed that since all the odd numbered harmonics have no bellying LSV the contribution is zero. The ratio of bellying LSV force/TSV force in the second, fourth and sixth harmonics is respectively 0.4, 0.1 and 0.07.

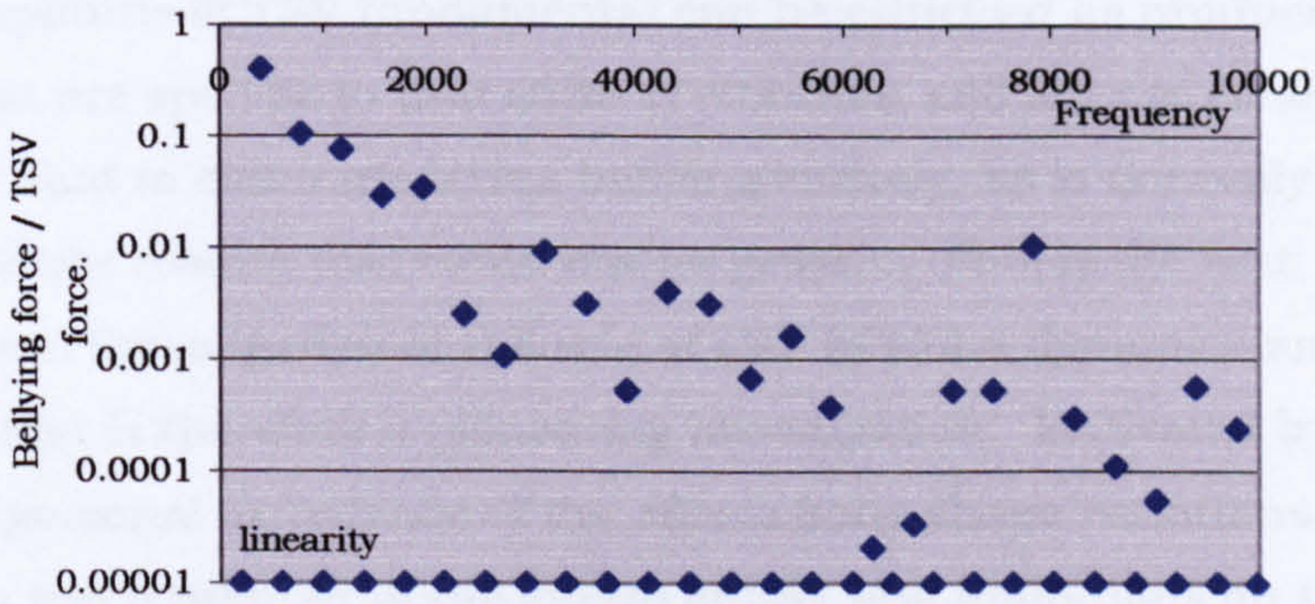

Fig. 10.2. Ratio of estimated bellying LSV force on bridge to TSV force on the bridge. Shown for typical shaker driven string.

In the case of the bowed string, it was shown in section 3.2.3 that the ratio of bellying LSV force to TSV force is 0.043, if all the LSV fully doubles in frequency. The tests on the bowed string in Chapter 7 showed that not all the LSV is double the frequency of the TSV. Therefore, the ratio of 0.043 may be an overestimate. It could argued that the total LSV in the string comprises the primary belling LSV plus the secondary LSV resulting from the modal response of the body caused by the primary bellying LSV and the TSV. In which case the bellying LSV should be weighted to make a greater contribution. So the ratio bellying LSV force/ TSV force would underestimate the degree of non-linearity. However in this case the ratio is still low. This argument would only apply to the LSV in the string; the non-linearity in the body would be represented by the ratio of bellying LSV force to TSV force.

The assumption is made that for the shaker driven string the relative contribution from the non-linear source is small in the higher harmonics. The procedure adopted in the thesis of comparing violin behaviour by comparing ratios of LSV force to TSV force assumes that the LSV varies linearly with TSV. Fig. 10.2 shows that the contribution to the LSV from the non-linear source is theoretically very small above the second harmonic so the LSV as a whole is not significantly non-linear. Had the experiments been done with a bowed excitation the non-linearity would have been greater. It is accepted that the degree of non-linearity is not precisely known.

Since certain components of LSV are inherently non-linear, the selection of a fixed amplitude of TSV fundamental can be criticised as producing results that are specific to that state of vibration and are not generic. It is also a fact that to eliminate string bellying entirely, as is normally done, would produce results that could not be generic. This is the first experimental investigation of the role of LSV in violin dynamics and sound radiation and is therefore a pioneering investigation. Motivated by extensive personal experience of the effects body shape variations it was decided to test a number of the effects of LSV and limitations on time and resources made it impossible investigate these phenomena at differing levels. Although the results are specific to the chosen level of excitation, the work is seminal in raising many questions that offer motivation for further research.

10.3 Transfer of energy from the string to the body by LSV

The vibrations of the violin string have been thoroughly examined by others (Cremer, 1983). In this section, the interaction of the string and body is examined in some detail. The need to do this arises from experimental evidence presented in sections 10.4 and 10.5 that the vibrations of the body on which the string is mounted determine to some extent the spectrum of the transverse displacement of the string.

10.3.1 The variability of the rate of string energy loss

A string held between rigid supports can only lose energy by acoustic and viscous loss to the air and damping caused by the slightly non-elastic or

hysteretic behaviour of the string. When the string is put on a violin, there is an additional loss caused by the transverse movement of the bridge, and other support movements. If one plucks the open string of a violin the displacement of the string dies away within a few seconds. By moving the bridge closer to or further from the sound post by a very small amount, say 0.25mm, the rate of decay of the string vibration can be altered very noticeably. The rate of vibration decay may now vary from extremely fast to surprisingly slow. It is also quite usual to see a plucked string quickly decay in vibration, reaching zero displacement in less than 0.5 seconds, and then revive and decay again at a slower rate (several seconds). Clearly, a small change in the elastic behaviour of the body can make a very significant difference to the rate at which the string loses energy to the body. It is also apparent that there is a transfer of energy from the string to the violin and from the violin back into the string. This may be due to the effect of coupled oscillators but the point of significance is that the rate of energy transfer, and therefore the dynamic coupling, can vary from fast to slow with only a small movement of the sound post.

At a wolf note, the string loses energy at such a fast rate that there is insufficient reflection to sustain a periodic vibration. The string will form a node a little in front of or behind the bridge and accordingly sound a note of higher and lower pitch than that intended, or commonly oscillate from one to the other. It is not known if the loss of energy from the string at a wolf note is due to excess bridge movement alone or if it is contributed to by energy loss through LSV at the ends of the string. The mechanisms of energy transfer are discussed in the following sections.

10.3.2 The loss through in-plane movement of the bridge

At every cycle of string vibration, there is an input of energy from the stick-slip action of the bow and losses to the body by the TSV force on the bridge and the velocity of the string notch in the direction of the force. At any one harmonic the loss into the bridge is dependent on the product of the square of the string force on the bridge (which is proportional to the string displacement), and the real part of the admittance at the bridge.

In the steady state at any one harmonic the energy inflow from the bow into the string must equal (after certain losses) the loss from the string to the

body. If the real part of the bridge admittance at a particular harmonic were high, the energy balance would require that the string displacement amplitude in that harmonic be relatively low resulting in a low transverse force on the bridge to compensate for the high admittance. The strength of any TSV harmonic will depend to some extent on the bridge admittance at that frequency. If the input power from the bow were independent of the amplitude of the TSV harmonic (which it is not) a higher real part of the bridge admittance would be expected to result in a lower TSV amplitude.

There is a large and greatly variable difference in admittance between the transverse movement of the string and that of the bridge. Consequently the loss at the bridge, per cycle, has been reported to be small, the wave amplitude reflection coefficient at the bridge being not less than 0.94. *(This figure was given by Prof. Woodhouse, Cambridge, England, in a personal communication to Prof. Fahy of Southampton, England. He obtained it by calculation from measured input admittances. Prof. Woodhouse added that the figure found, was the result of a very brief investigation.)* This figure is not entirely consistent with the very fast loss from the string in certain conditions (as shown in section 10.3.1). It is possible that under some conditions the reflection coefficient is rather less, but it is also possible that the string loses energy to the body not only by the transverse motion of the bridge but also by motions driven by the LSV force in the string. Generally, in the case of the bowed string, the reflection coefficient must at least be high enough to maintain the periodic vibration of the string.

10.3.3 The loss through yield of the end supports

Cremer suggested that the string could be considered as being fixed at one end and attached to a transversely mounted dashpot representing the bridge, at the other. This idealisation may have overlooked the possibility that the energy loss by movement at both supports in the direction of the string's length could be significant. This could be represented as a dashpot at each end of the string, lying in the line of the string. If LSV were important in actively driving the violin, the string must lose energy by end support movement in line with the string. If the string end supports have a small amount of give in the direction of the string tension, energy will be taken out of the transverse vibration of the string. It is probable that the

main cause of end support give is in the vertical movement of the bridge, which lengthens or reduces the string length.

Lee and Rafferty observed that the time rate of decay in the height of the resonance peaks of a plucked string was noticeably faster for the longitudinal resonance than for the transverse resonance (Lee and Rafferty, 1983). This could indicate that the longitudinal vibration is more closely coupled to the body than the transverse vibration. The admittance of a transversely vibrating infinite string is high in relation to that of the bridge and the coupling between the string and bridge is low. The admittance of a longitudinally vibrating infinite string is one order lower, and the coupling between the longitudinal string vibrations and the body of the violin may be considerably stronger.

The admittance of a transversely vibrating string is given by $Y_{trans} = \frac{1}{\sqrt{mT}}$.

The admittance of a longitudinally vibrating string is given by $Y_{long} = \frac{1}{\sqrt{km}}$.

Each of the four strings will be vibrating with different LSV forces and at different relative phases, but the group of four strings must have a combined net LSV force and phase. Again we can use the concept of a 'combined string' that replaces the four strings with one string located at the centroid of the group and with properties that represent those of the group, the admittance $Y_{Combined\ string}$ is given by;

$$\frac{1}{Y_{combined\ string}} = \Sigma\sqrt{km}\,.$$

The admittance ratio, $\frac{Y_{G\ string\ transverse}}{Y_{Combined\ string}} = \frac{\Sigma\sqrt{km}}{\sqrt{m_G T_G}} = \frac{7.174}{0.334} = 21.47\,.$

Thus, a group of 4 strings in LSV has an admittance 21 times lower than that of single string in transverse vibration. It will be shown in Chapter 12 that the admittance of the bridge to an LSV force applied in the plane of the bridge is higher than it is to transverse force from TSV. These examples have been presented to support the suggestion that the coupling between the LSV and the body may be somewhat stronger than that between the TSV and the body.

10.3.4 Contribution of body resonances to LSV

Because of the admittance mismatch between the string vibrating transversely at resonance and that of the bridge, the vibrations of the body have a relatively small effect on the resonant modes of the string. The TSV force applied to the body results largely from the resonant response of the string. The equivalent resonant response in the string to LSV does not apparently make a significant contribution to the driving of the violin (so far as we have been able to observe). But resonance does play a significant role in determining the magnitude of the LSV force established in the string. If there were a closer coupling between the string and the body in LSV response, than there is to the TSV response, many of the resonant body modes would produce significant strains in the string tension. We would therefore expect that as the modal density increases with rising frequency up to a constant level at 2000Hz, the magnitude of the LSV force would be contributed to increasingly up to 2000Hz and beyond from body resonances. The experimental results presented in Chapters 11 and 12, show a ratio of LSV force to TSV force (transversely on the bridge) of about 0.25. The theoretical analyses of the ratio LSV force/TSV force, shows; LSV force/TSV force from bridge-rock is 0.413/n. When n is odd there is an additional contribution from string bellying in the even numbered harmonics of 0.41 at the 2^{nd}, 0.11 at the 4^{th}, 0.08 at the 6^{th}, 0.03 at the 8^{th} and 10^{th}, and 0.002 at the 12^{th} harmonic. The theoretical prediction and the experimentally measured result do not show great disagreement in the lower harmonics, but there is a much greater disparity at the higher harmonics. Above 2000Hz there would appear to be an increasing contribution from body resonances that alter the string length by means other than by bridge-rock.

10.4 TSV and LSV in the driving substructure with different support mobilities

The literature suggests that support mobility can have a significant effect on the generation of string harmonics from the non-linear stretching of the string. The support mobilities could also be expected to have a significant effect on any energy loss from the string to the body through LSV coupling. The assumption that the TSV established in the string is largely

independent of the support mobilities does not appear to have been examined experimentally.

A series of tests were made with progressive changes to the support mobilities. A string was placed first on a body that provided rigid terminations at the nut and saddle ends. The bridge support was given various degrees of freedom. Finally the effect of permitting mobility at the nut and saddle supports was examined.

10.4.1 TSV and LSV with a rigid bridge

The first of the series of experiments was done with the four strings passing over a bridge supported on a rigid block. The bridge was of normal violin bridge dimensions except that all the normal piercing was omitted to make the bridge rigid in a transverse direction and free to move in a direction normal to its plane. The fixed bridge is described in section 7.1. The geometry of the system was the same as that of a real violin. The strings were attached to a tailpiece and the tail gut was attached to a rigid support. The apparatus was similar to that shown in fig. 7.1 but included a tailpiece in place of the force gauge. This apparatus closely replicates the driving substructure described in Chapter 3.

The frequency range used in this and all the following tests was 0 to 10kHz. The analyser was set to the maximum available resolution of 1600 lines in 10,000Hz, which gave a frequency resolution of 6.25Hz. In the first group the open 4th string was driven (196Hz.). This gave the possibility of showing up to 52 harmonics. The level of excitation was a transverse displacement of 6.5 mm peak to peak, measured at the mid length of the string. All the experimental results reported in this thesis from here on relate to a level of string transverse displacement of 6.5mm peak to peak. (unless otherwise stated)

Fig. 10.3 shows that amplitude of the transverse displacement of the string and fig. 10.4 shows the corresponding LSV force recorded at the tail gut position. In areas of low response, the results fell outside the range of the analyser. It is important to note that by altering the range of the analyser (and applying compression to the strong peaks) it was observed that there was a response at every harmonic number in both the TSV and LSV.

Because the bridge was not able to move in its own plane we see the first, third and fifth harmonics of the LSV are heavily depressed relative to the even harmonics. There is a band from about 4,500Hz to 7,000Hz where the LSV is fairly strong, and again at above 8,500Hz. The source of these bands of stronger response is not known.

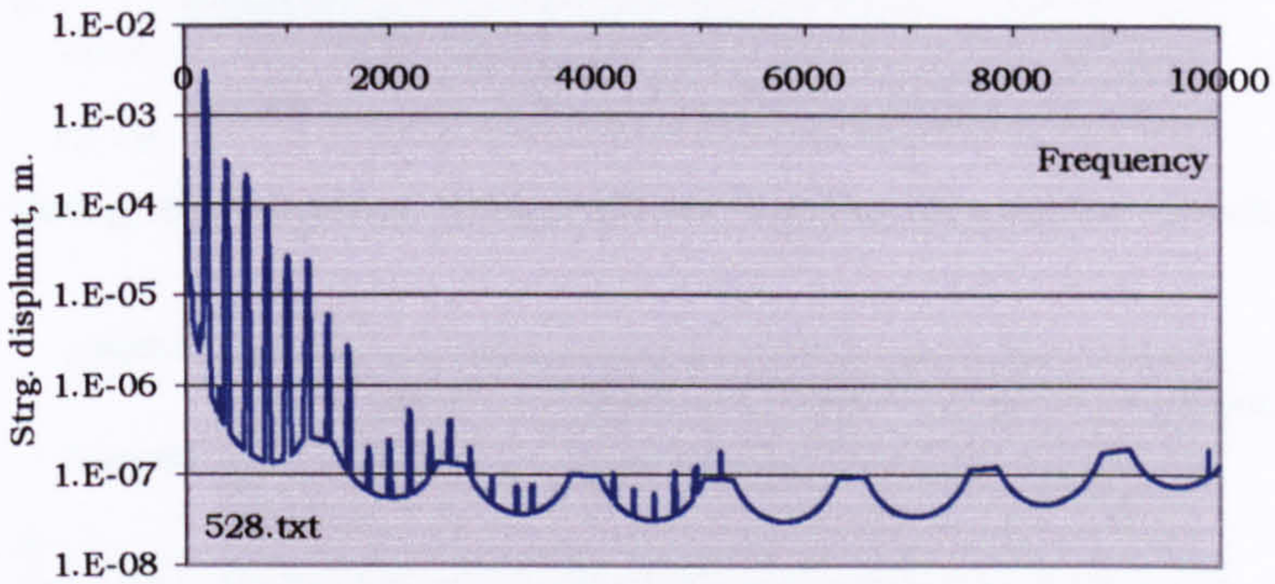

Fig. 10.3 String displacement. Shaker driven G string on a fixed bridge.

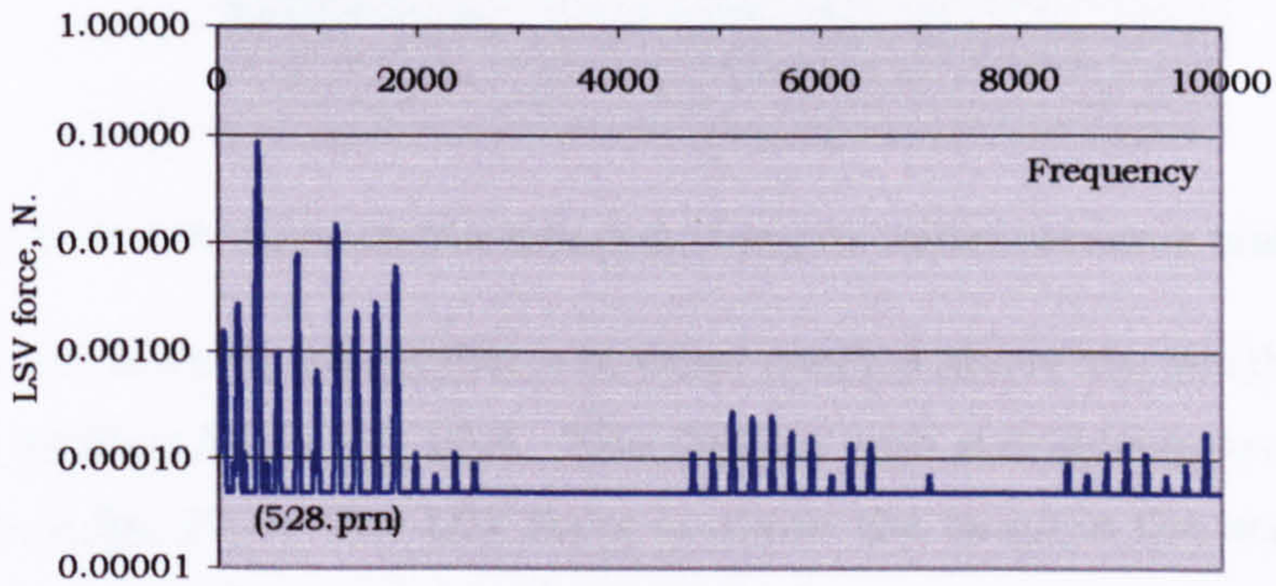

Fig. 10.4. LSV force, shaker driven G string on a fixed bridge.

10.4.2 TSV and LSV with a rubber mounted bridge

The apparatus was changed to replace the bridge with a normal violin bridge and the bridge mounting was changed to the rubber mounting described in section 8.1. The results are shown in figs.10.5 and 10.6. These can be compared with the results for the strings on the rigid bridge. The string displacement in the first harmonic may have been slightly affected by the change in the bridge mounting but the driving force from the shaker was adjusted to make it the same. We can say that the string displacement in the higher harmonics declines in strength relative to the first harmonic with rising harmonic number.

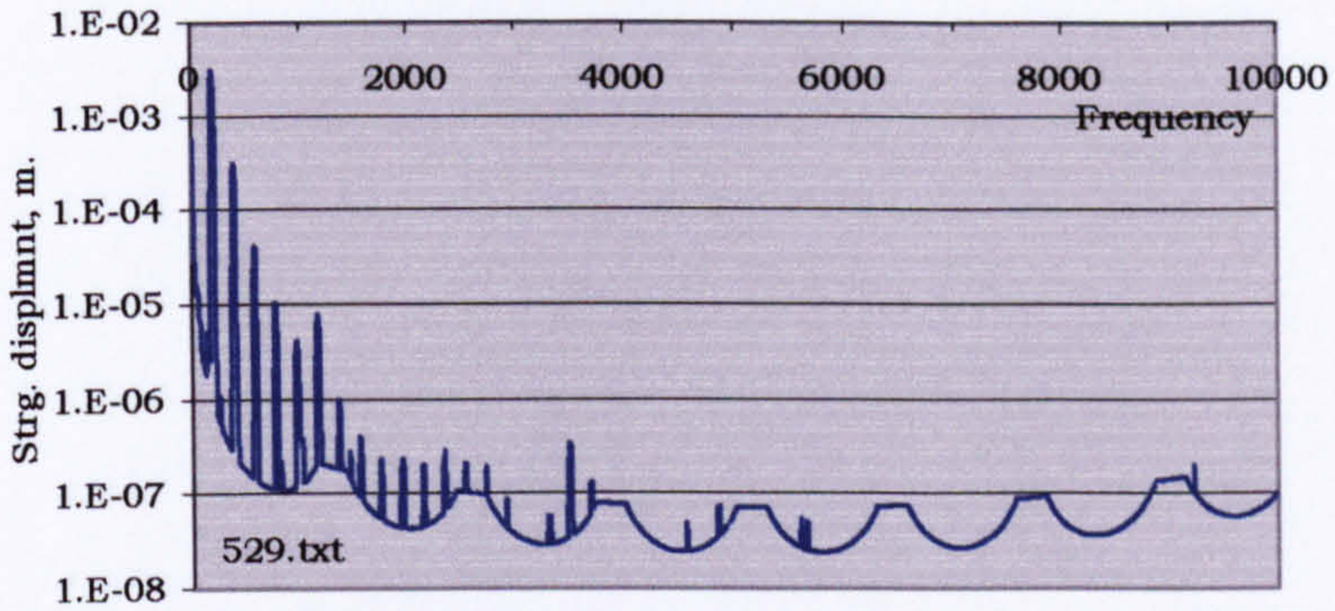

Fig. 10.5 String displacement. Shaker driven G string on a rubber mounted bridge.

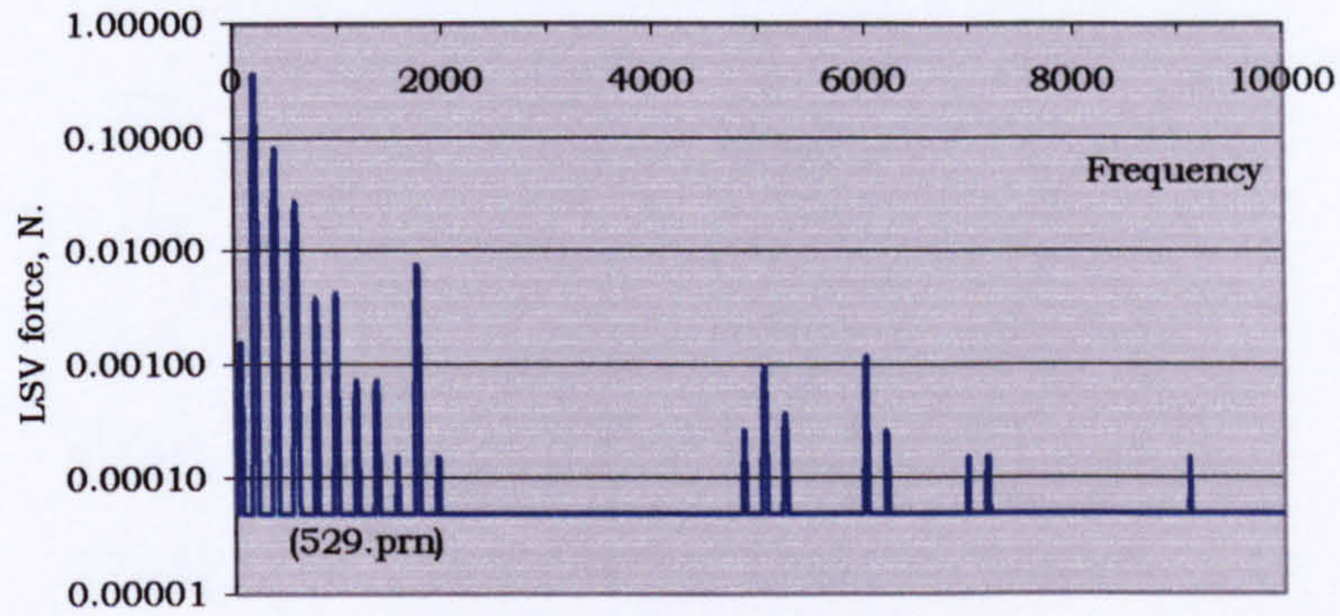

Fig. 10.6. LSV force, shaker driven G string on rubber mounted bridge.

The LSV force harmonics exhibit a sudden decline above the ninth harmonic as they did in fig. 10.4. The decline with rising frequency is more rapid than in fig. 10.4. The LSV force is about the same in the second harmonic but the odd numbered harmonics have strengthened now that bridge-rock is permitted. The bands of strong response in the higher frequencies have become less defined but there are some intermittent strong peaks.

10.4.3 TSV and LSV with the detached body

The apparatus is changed again to replace the rubber bridge mounting with the detached body. This set-up was described in section 9.1. This model most closely replicates the theoretical model of the driving substructure with permitted bridge foot movement to enable the generation of bridge-rock LSV. The generation of string bellying LSV and bridge-rock LSV are demonstrated. Since the string terminals are detached from the body

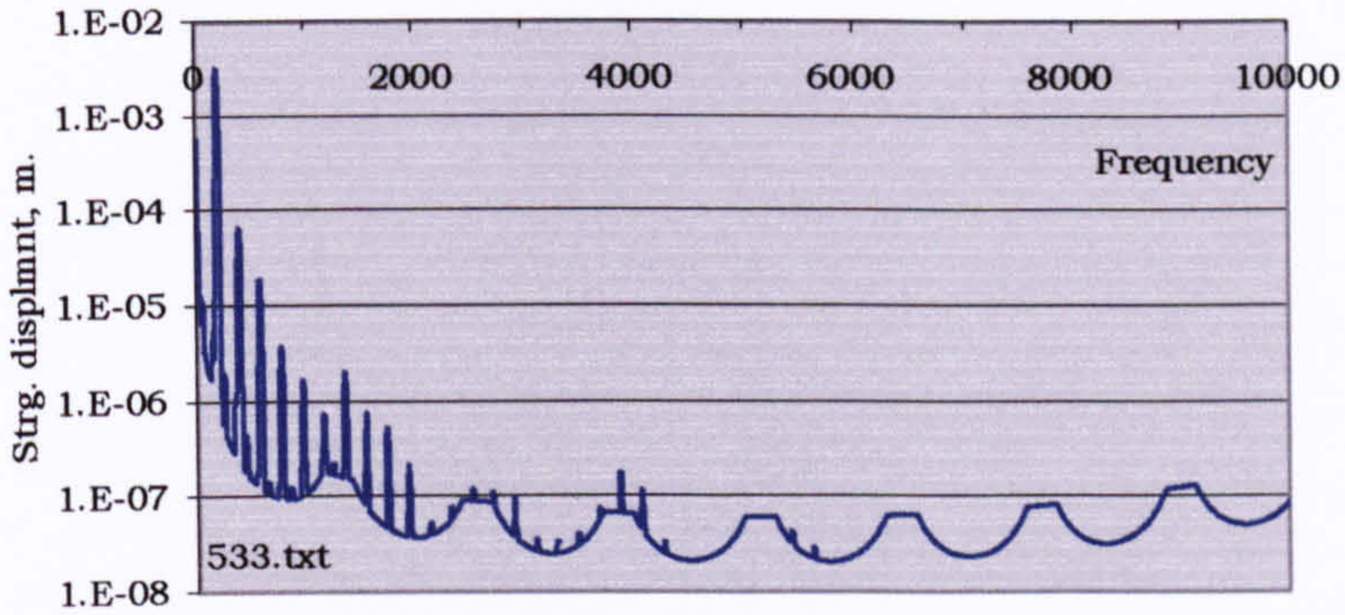

Fig. 10.7 String displacement. Shaker driven G string on a detached body.

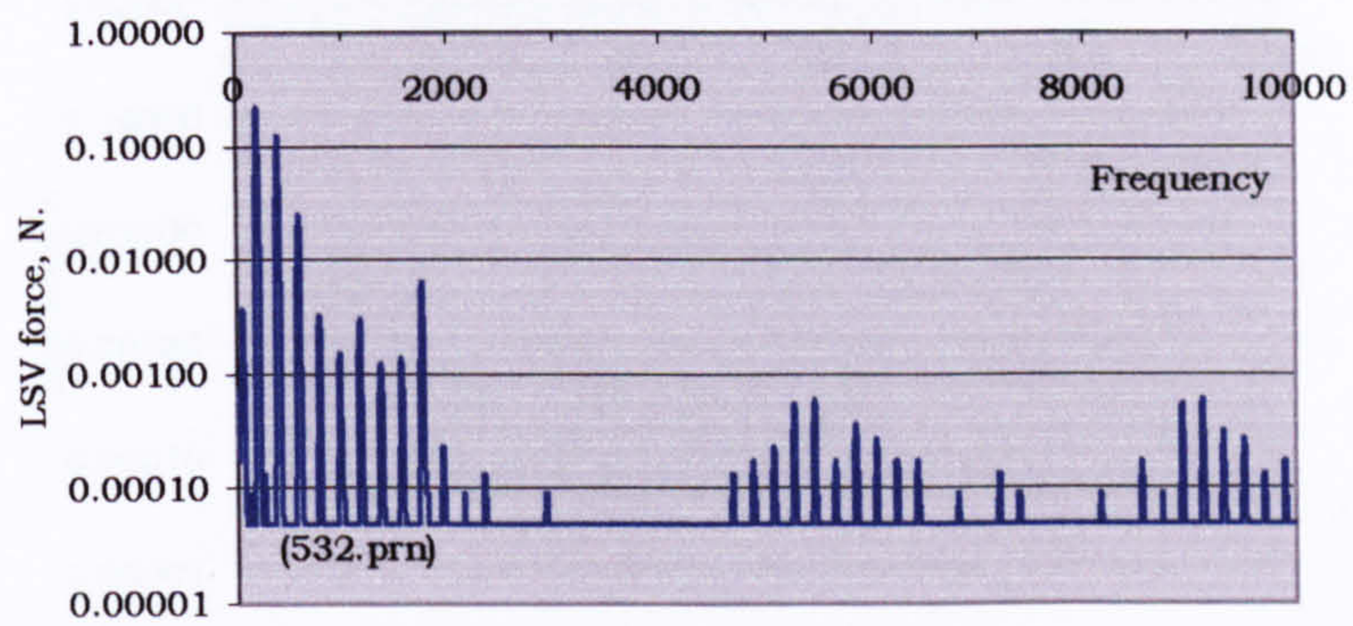

Fig. 10.8. LSV force, shaker driven G string on a detached body.

secondary LSV cannot be attributed to vibration of the body at the string terminations.

Figs. 10.7 and 10.8 show the results. In comparison with the two previous cases there is a further drop in the strength of the upper harmonics of the transverse displacement relative to the first harmonic. The LSV spectrum is not unlike that of the rubber mounted bridge up to the sixth harmonic. The ninth harmonic is also very similar in value. However, the upper harmonic spectrum is more densely filled than in fig 10.6.

10.4.4 TSV and LSV with a real violin

The strings and tailpiece are now transferred to a real violin, V156 normal EAR. The results are shown in figs. 10.9 and 10.10. The string displacement amplitudes return again to levels comparable with the rigid bridge, although there is more variation and the higher harmonic range is more extended. The LSV force amplitude has dropped in the first three harmonics but in the higher harmonics is generally higher and becomes

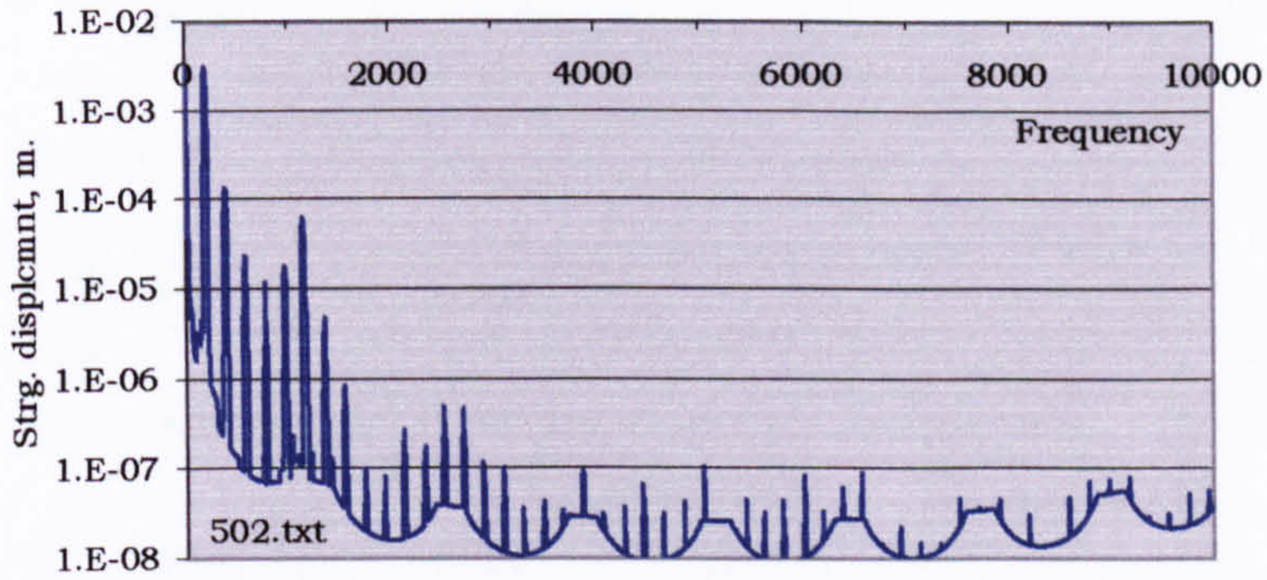

Fig. 10.9 String displacement, shaker driven G string on a real violin (V156).

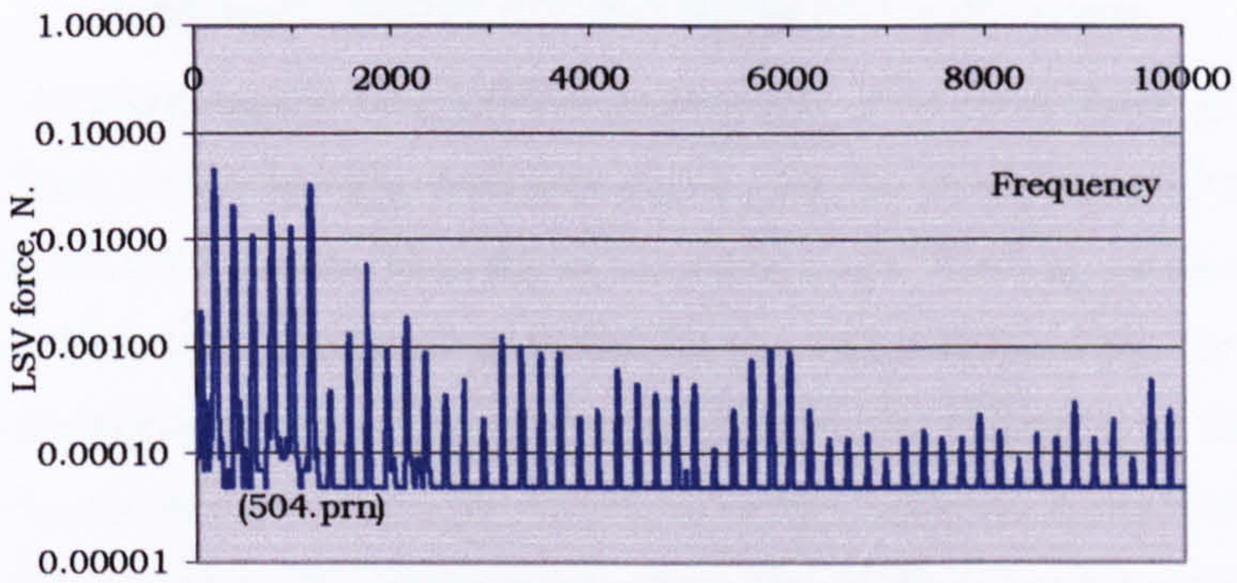

Fig. 10.10. LSV force, shaker driven G string on V156.

more even with rising frequency. The two high frequency bands of strong response that were observed when the bridge was on artificial mounts have now disappeared or become 'absorbed' by the filling in of the weak areas between. The reinforcement of the higher harmonics is probably body driven and the fall in the strength of the lower harmonics may be caused by the flexibility of the string termination associated with resonances of the lower order body modes.

10.4.5 Discussion of results

The relative variation in the strength of the TSV and LSV for the four different test rigs can conveniently be expressed as the ratio of LSV force to the string transverse displacement. Fig. 10.11 shows the ratio of the LSV force to the string transverse displacement. This has been multiplied by the frequency to make the magnitude comparable at all frequencies. That the ninth harmonic is high is common to all the curves and may relate to a resonance within the string-tailpiece coupling.

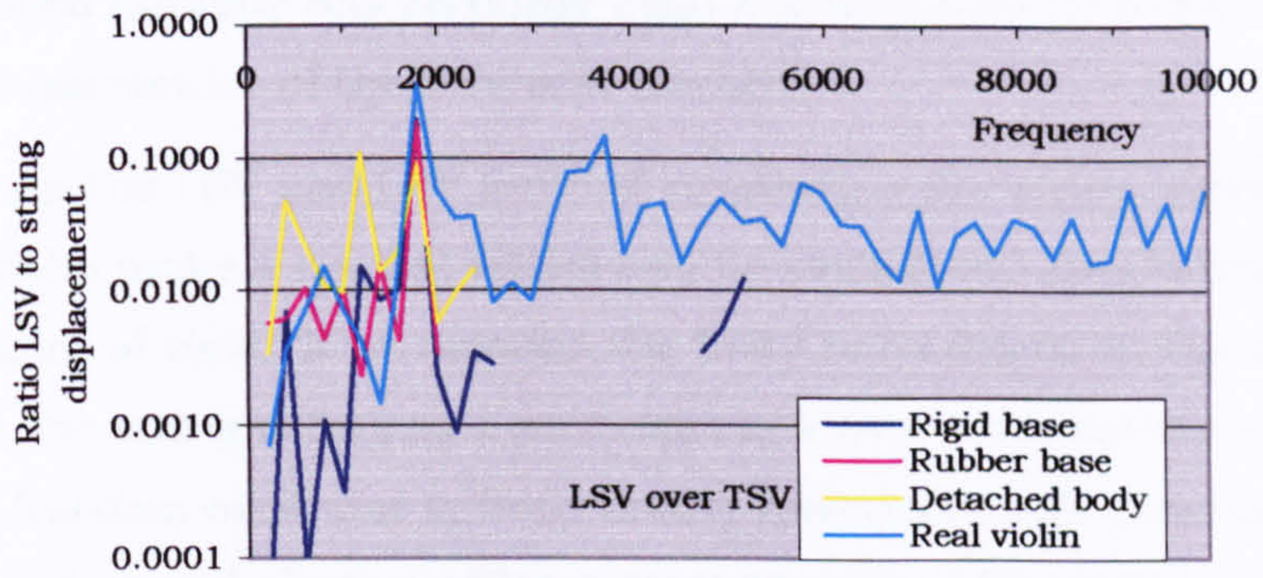

Fig. 10.11. Ratio LSV force to string transverse displacement (muliplied by frequency). Shaker driven G string on various bases.

The effect of increasing the bridge mobility. The first three graph lines show the effect of the bridge mobility alone, as the bridge goes from being immobile in its own plane, to rubber mounted and then mounted on a violin body. There is a progressive rise in the ratio of the LSV force to the TSV string displacement. This is in part due to the filling in of the even numbered harmonics of the LSV force as bridge motion is permitted. But also, by a drop in the TSV displacement in the higher harmonics relative to the fundamental. When the bridge was close to rigid in its own plane it could not drain energy via the TSV force and, however the TSV harmonics were generated, they were largely undamped. The spectrum so established was relatively richer in the higher harmonics than those found for a more mobile bridge. It must be remembered that the first harmonic displacement was set, so any effect that the bridge mobility might have had on this would not be demonstrated. We simply do not have enough information about the dynamics of the test rigs to do any more than speculate on the possible cause of the relative drop in the strength of the higher harmonics of the TSV as the bridge mobility increases. The experimental result must simply stand as an unexplained observation. The rise in ratio of LSV to TSV with increasing bridge mobility does accord with the effect of bridge-rock LSV.

Effect of coupling the string terminations to the violin body.

This may be a demonstration of the suggestion made in section 10.2.1 that the relative strength of the upper harmonic generation in the TSV spectrum (from the non-linear stretching of the string) depends on support mobility.

The increased mobility has certainly been accompanied by a relative rise in the higher harmonics of the TSV and the LSV.

The effect on the TSV and LSV force of connecting the string terminals to a violin body (to make a normal violin) can be considered qualitatively from another point of view. If we assume the body to be driven at the nut and saddle via the string acting as a pure spring a simple model of a single-degree-of-freedom oscillator (a body mode) driven through a spring shows that both below and above oscillator resonance the LSV force is little affected by oscillator response and therefore is much the same as when connected to rigid terminals. However, the spring force drops at oscillator resonance, the degree of drop increasing with decrease of oscillator damping (see first three harmonics in fig. 10.10). On the other hand, if the oscillator is independently driven (by say a TSV force) the LSV will be small off body resonance and rise sharply at resonance. If we see the LSV peaking near well-known low order body resonances on a complete violin compared to a detached body, the body is probably driving the string. If the LSV falls around these frequencies it may well be driving the modes. Comparing figs. 10.8 and 10.10 there seems to be a reduction in the LSV force at the first, second, third and seventh harmonics, suggesting that the body may be being driven through the string. This reasoning would also suggest that the infilling of LSV at the higher harmonics shows that the body is driving the LSV. The LSV thus becomes a by-product of body motion. However all these speculations are only valid if we assume no effect of the change in TSV on the generation of LSV. But since there is a significant change in TSV in going from the detached body to the violin we cannot eliminate this effect.

10.4.6 Confirmation on other strings

In order to check that these tendencies could apply to other strings than the fourth the experiment was repeated on the third string. Figs. 10.12 to 10.14, show the TSV and LSV force for a rigid bridge and a detached body, when the open D string is driven. The fundamental mode amplitude was 4.25mm peak to peak. This shows that the phenomena observed for the G string are not as clearly exhibited when we look at the D string. This may in part be due to our inability to drive the string to such a high transverse

displacement amplitude. Also since the harmonics are further apart than those of the G string some of the lower order body modes may have been missed. The harmonic content of the excitation has changed a little with the changed "body", but the LSV has risen more significantly.

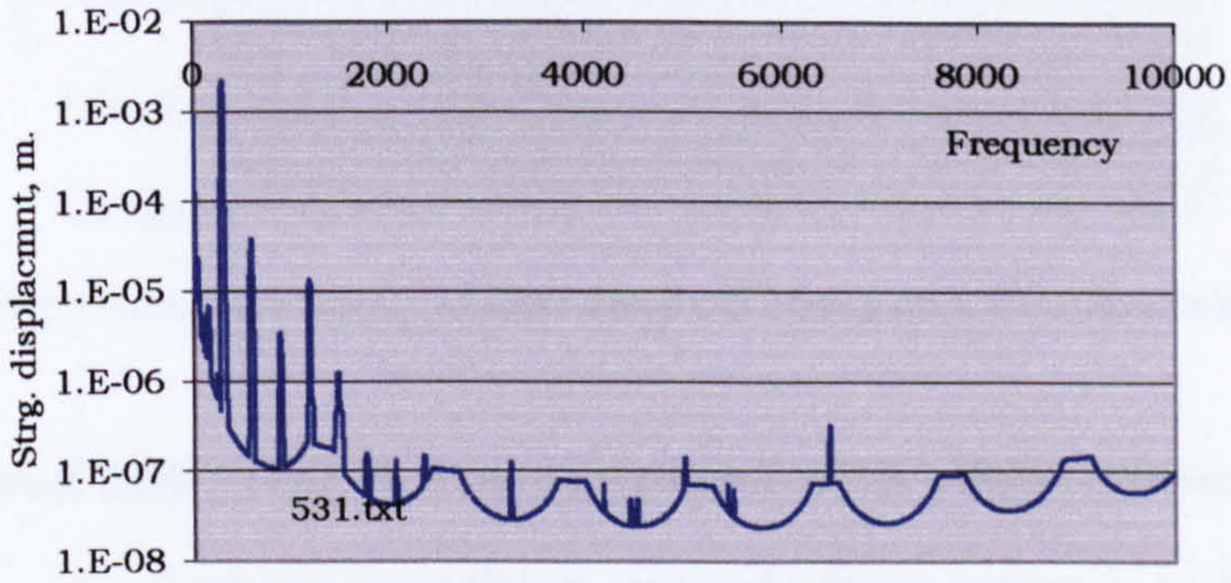

Fig. 10.12. String displacement, shaker driven D string on a fixed bridge.

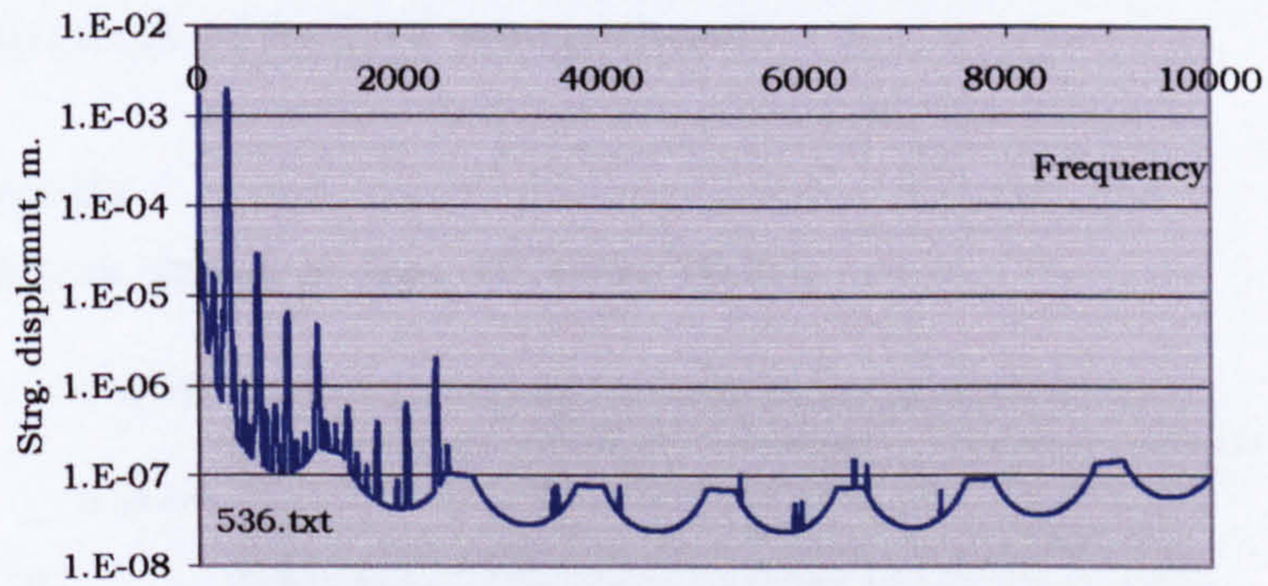

Fig. 10.13. String displacement, shaker driven D string on a detached body.

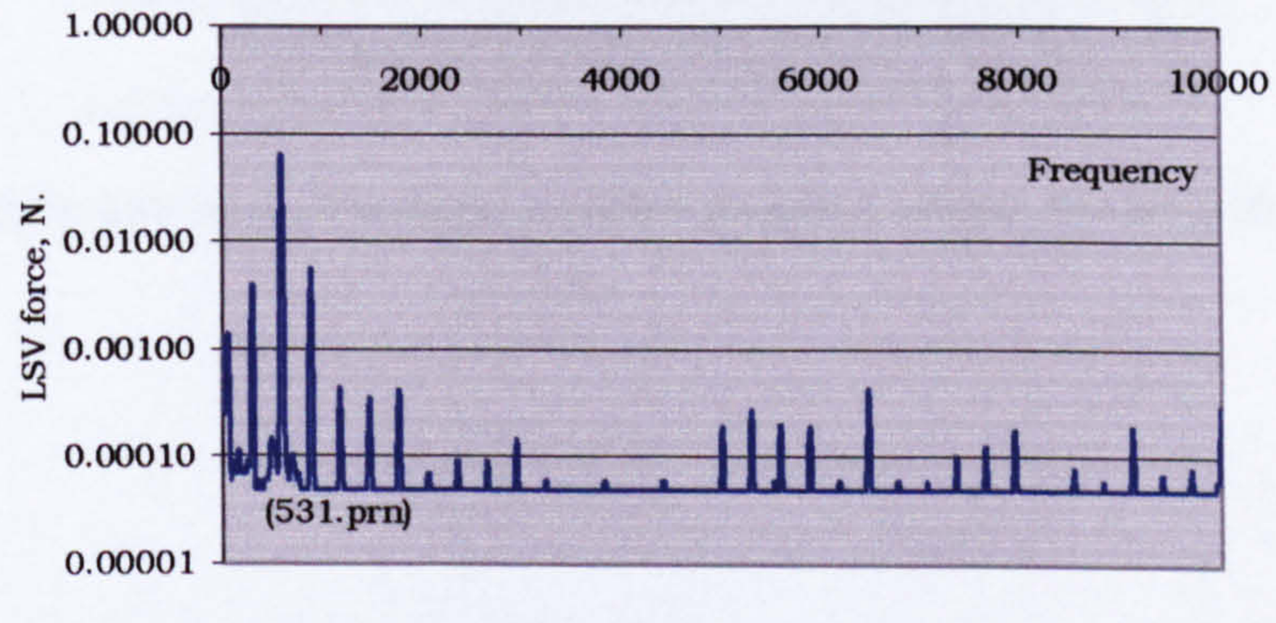

Fig. 10.12. LSV force, shaker driven D string on a fixed bridge.

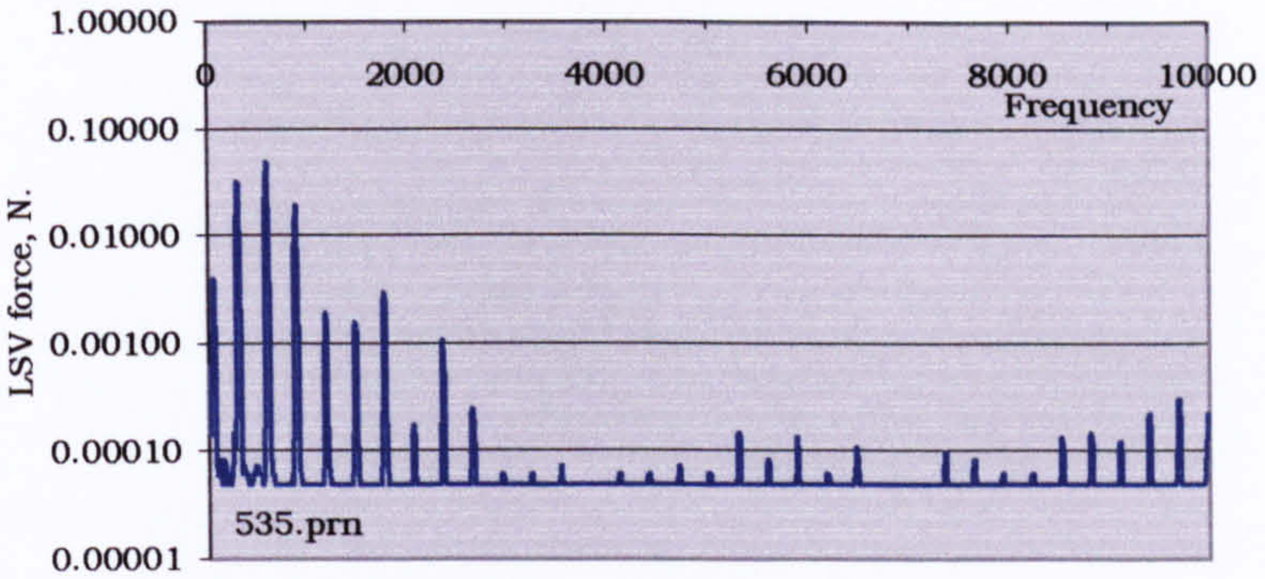

Fig. 10.14. LSV force, shaker driven D string on a detached body.

10.5 Bowed LSV, real violin compared with rubber mount

To find how much richer the LSV content of a bowed system is, the comparison of the rubber mounted bridge and the real violin was repeated but with a bowed excitation. Three notes were bowed on each "instrument" and the spectrum of the LSV was analysed.

10.5.1 Results

The results are shown in figs. 10.15 to 10.20.

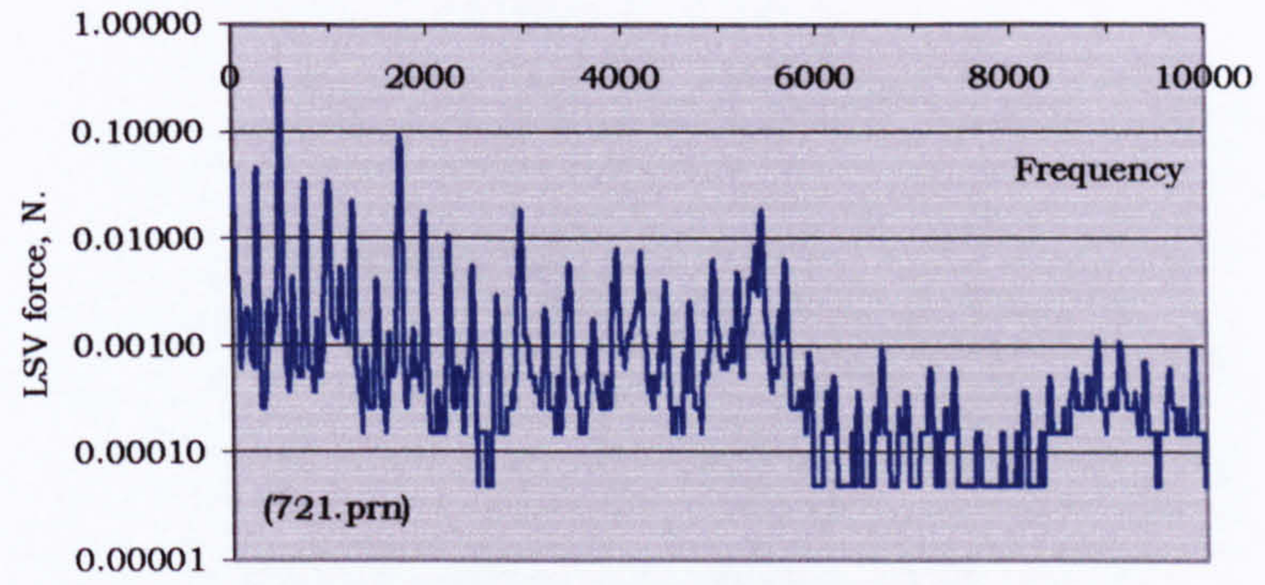

Fig. 10.15. LSV force, 4 strings on rubber mounted bridge, bow B3 (4th string).

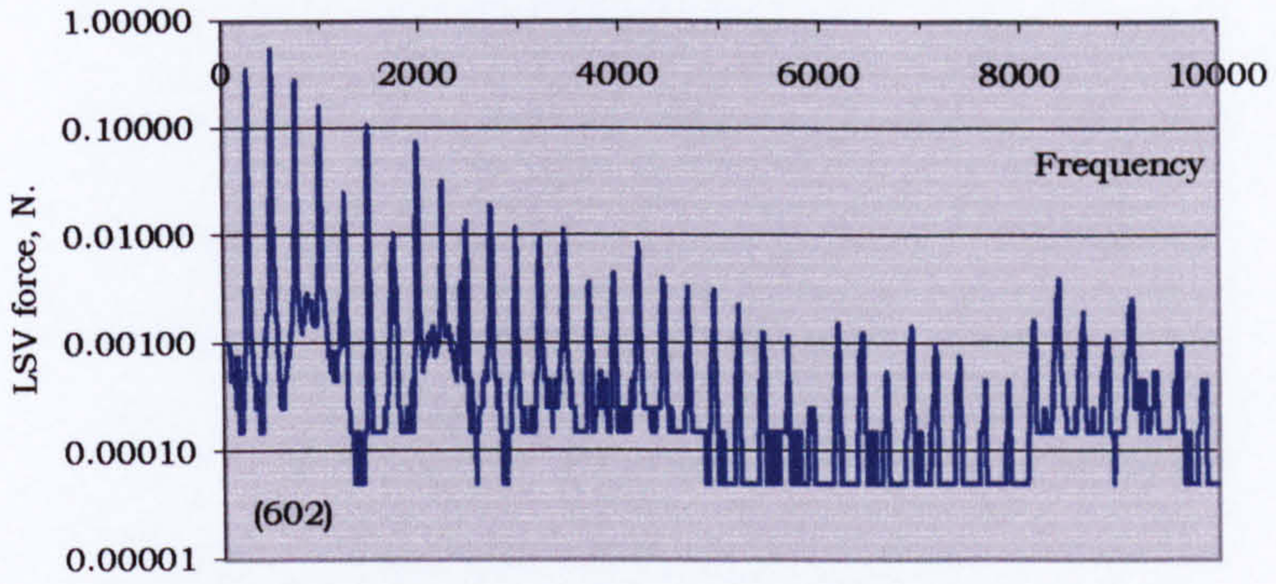

Fig. 10.16. LSV force, V156, bow B3 (4th string).

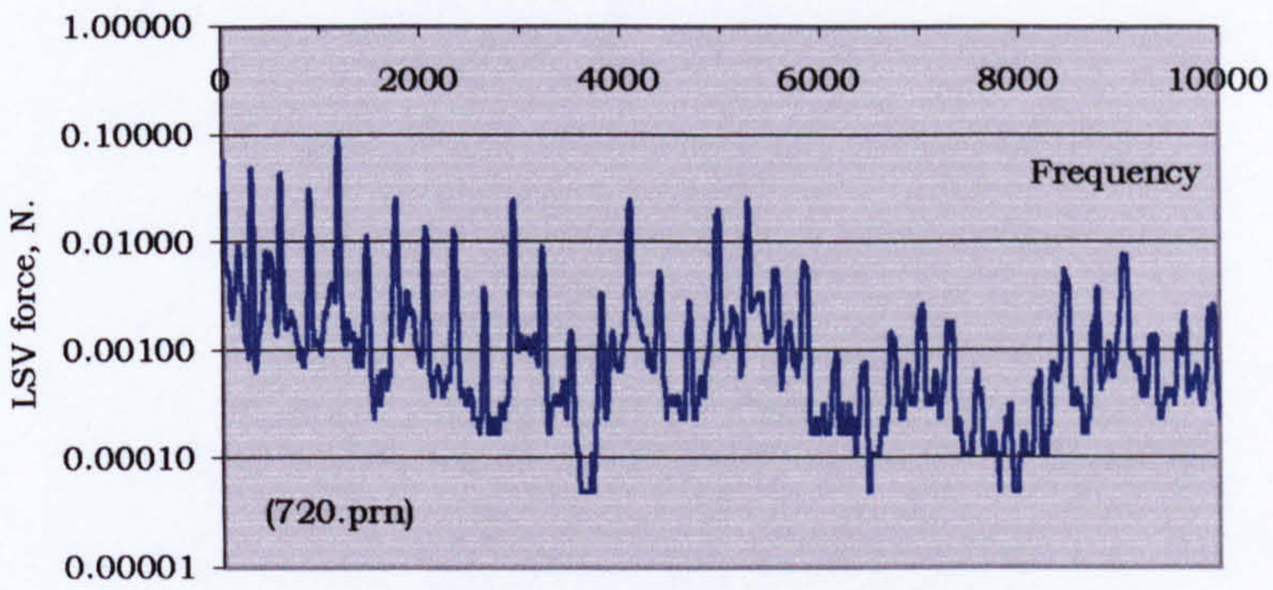

Fig. 10.17. LSV force, 4 strings on rubber mounted bridge, bow D4 (3rd string).

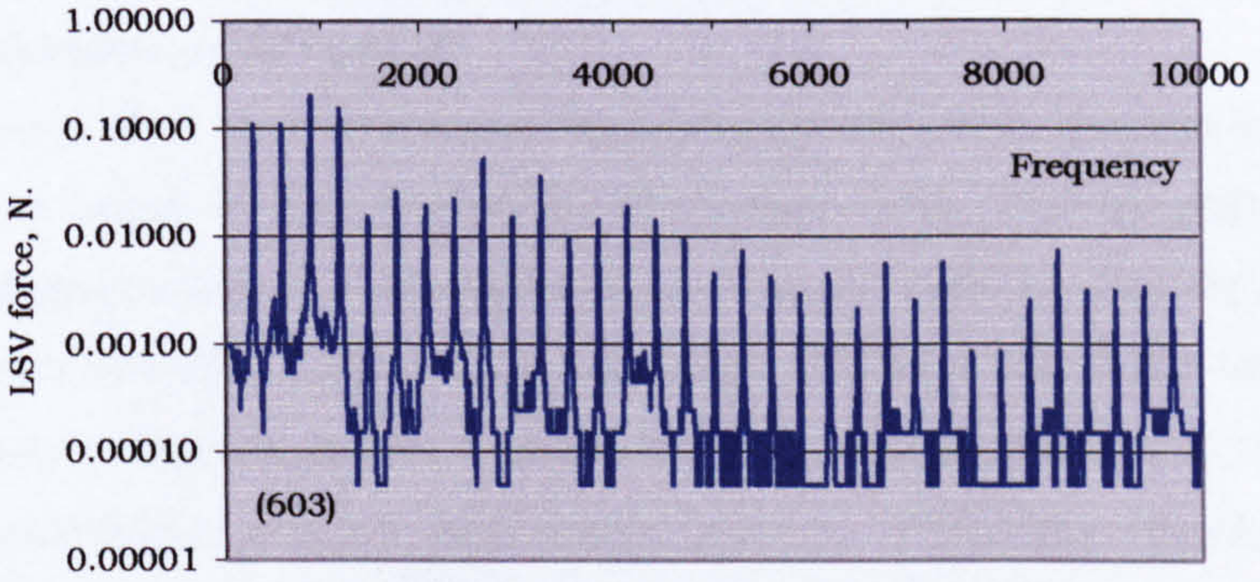

Fig. 10.18. LSV force, V156, bow D4 (3rd string).

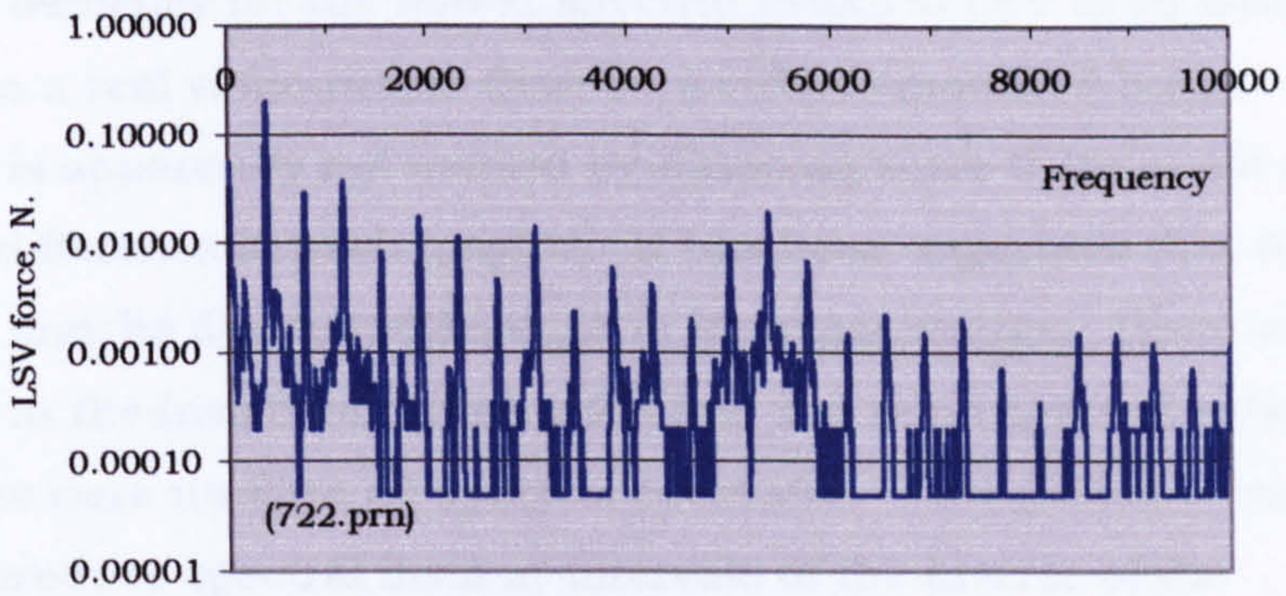

Fig. 10.19. LSV force, 4 Strings on rubber mounted bridge, bow G4 (3rd string).

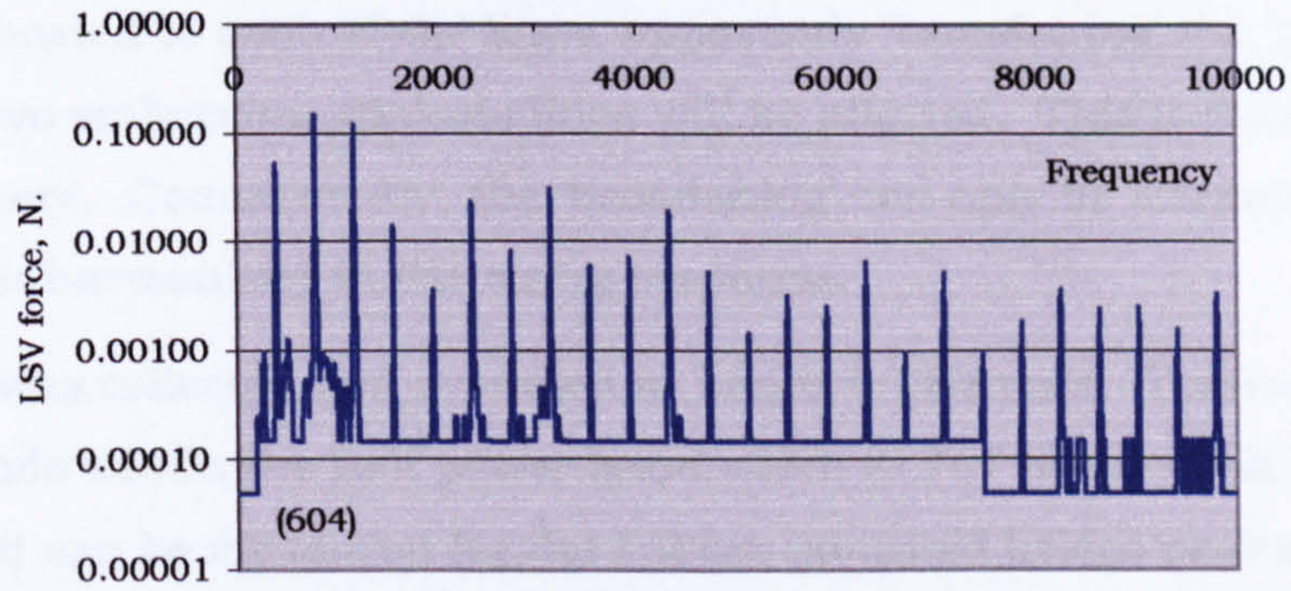

Fig. 10.20. LSV force, V156, bow G4 (3rd string).

10.5.2 Discussion of results

It can be seen that LSV is present in all the possible harmonics in the range, there being 40 harmonics for the lowest note. The magnitude of the upper harmonics is much stronger than those excited by shaker driving. All the notes bowed on the rubber-mounted bridge showed the tendency to respond more strongly in the 5 to 6kHz band, and in the 8.5 to 10kHz band, as was found when it was shaker driven. When the mobility of the end fixing of the string is altered by going to a real violin the response becomes more uniform. The response becomes still more even if the violin is varnished (see Chapter 13). There is no consistent pattern of the LSV force being stronger in the even numbered harmonics. The change in form of the envelope of the LSV force spectrum when changing to a complete violin demonstrates unequivocally that coupling between the string and the end supports substantially affects the generation of LSV.

There is a tendency for the bowed spectral peaks of LSV to be sharper if the string is on a real violin rather than on a rubber-mounted bridge. This difference is apparently not caused by damping since there is not a sufficient difference in peak heights. It has been suggested that the difference may be due to a difference in instrumentation. There was no difference in the instrumentation used and the same spectral estimation parameters were used on all spectral estimates. Pure periodic excitation can only produce spectral lines at intervals of the inverse of the fundamental period. If a line falls between two of the Fourier analysis frequencies (set by the analyser parameters), a proportion of the line energy will be allocated to each of the lines, apparently 'broadening' the 'peak', but only the two embracing analysis lines will be affected. This is clearly not the case here. Consequently, the 'broadening' can only be attributed to a degree of inharmonicity in the string response.

The data was collected and averaged in bands 6.2Hz wide. The number of 6.2Hz bands within the half power band width (0.707 of the peak rms amplitude) can be measured for the rubber mounted bridge peaks and the real violin. By dividing one by the other the ratio of the width to the height of the harmonic peaks can be evaluated. The quality factor of a peak is also calculated in this way but the Q value is normally associated with damping which as previously stated is not believed to be the reason for the difference. To emphasise that we are not dealing with a damping phenomenon the width to height ratio found in this way will be called the 'peak-width ratio'. This was done for the first ten harmonics of each of the three notes. The result was very consistent in every harmonic but the figures following are for the average ratio taken over the first ten harmonics.

The 'peak-width ratio' for the real violin peaks over that for the rubber mounted bridge peaks was for the note of B3, 2.04; for D4, 2.52; and for G4, 2.32.

In the absence of further research we can only speculate as to the cause of the difference in peak-width ratio. Had we measured the peak widths of the TSV spectra there is no doubt that there would have been a similar difference. It is significant that the shaker-driven spectral peaks show no

such apparent widening, which implies that the inharmonicity indicated by the widening is essentially associated with bowed excitation. A possible cause is that the body response through LSV has affected the periodicity of the Helmholtz wave somehow and sharpened the stick–slip mechanism that generated the vibration of the string and 'focused' it. It would appear that this focusing is enhanced by the LSV in the dynamic system of not just the string but also the complete violin.

10.6 Conclusions

- A broad spectrum of LSV force has been observed both with shaker and bowed excitation. The bowed spectrum is much richer in high harmonics relative to the fundamental than the shaker-driven spectrum. This is to be expected since in the latter case the harmonics are fortuitously excited by non-linearity in the stretching of the string, whereas the bow excitation directly induces a harmonically rich response spectrum of both TSV and LSV.
- The spectrum of transverse displacement established in a string by a shaker depends on the dynamic properties of the bridge supports and string terminals.
- The shape of the envelope of the LSV force spectrum is substantially affected by connection to the nut and saddle and is made more even.
- The bowed LSV spectrum shows sharper spectral peaks if the string is mounted on a violin rather than some other sort of flexible mounting. This suggests that the inharmonicity of the string motion is dependent upon communication between the string and the body of the violin, possibly (at least partially) through the agency of LSV. This phenomenon was not seen to any significant degree with the shaker-driven string.
- There was no observable evidence of longitudinal string resonance in the LSV spectra.

Chapter 11

EFFECT OF BODY SHAPE ON TSV AND LSV

11.1 Introduction

In the last chapter, we compared the TSV and LSV developed in strings on artificial supports with strings on a real violin. In this chapter the TSV and LSV generated in violins of differing body shape is examined. The test violins were first assembled as violins of differing EAR. The bellies were then removed and interchanged to make violins of the same EAR but different deviation. These were all tested while still unvarnished. Finally, the three violins of different deviation were varnished and retested.

11.2 Unvarnished violins of differing EAR

11.2.1 Method used

The TSV and LSV developed in three violins of different EAR were compared. Each violin was laid on foam-lined blocks, one at the top of the back near the button and the other at the bottom of the back near the lower edge. The violins were lightly held in position by a rubber band, but very little restraint was needed. The fourth string was driven by a shaker in the manner described in Chapter 10, and the transverse displacement of the string and the LSV were measured. All the violins tested were driven to a mid string length transverse displacement of 6.5mm, peak to peak. The spectra of string transverse displacement are shown if figs. 11.1 to 11.3.

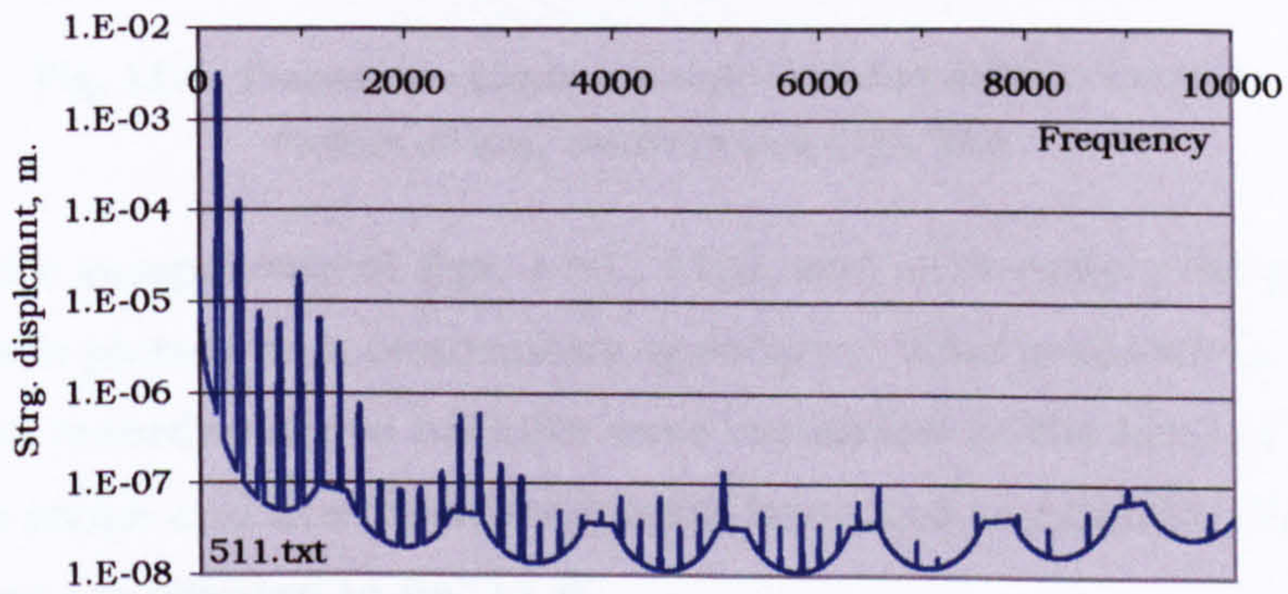

Fig. 11.1 Amplitude of transverse displacement of shaker driven G string, V157LE.

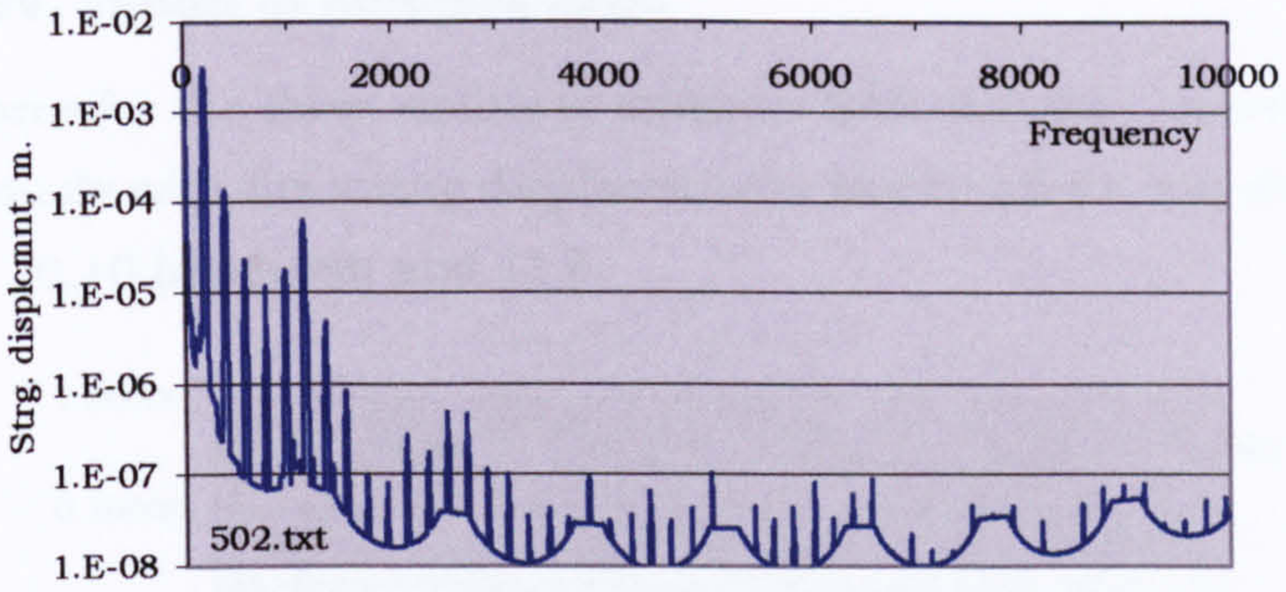

Fig. 11.2 Amplitude of transverse displacement of shaker driven G string, V156.

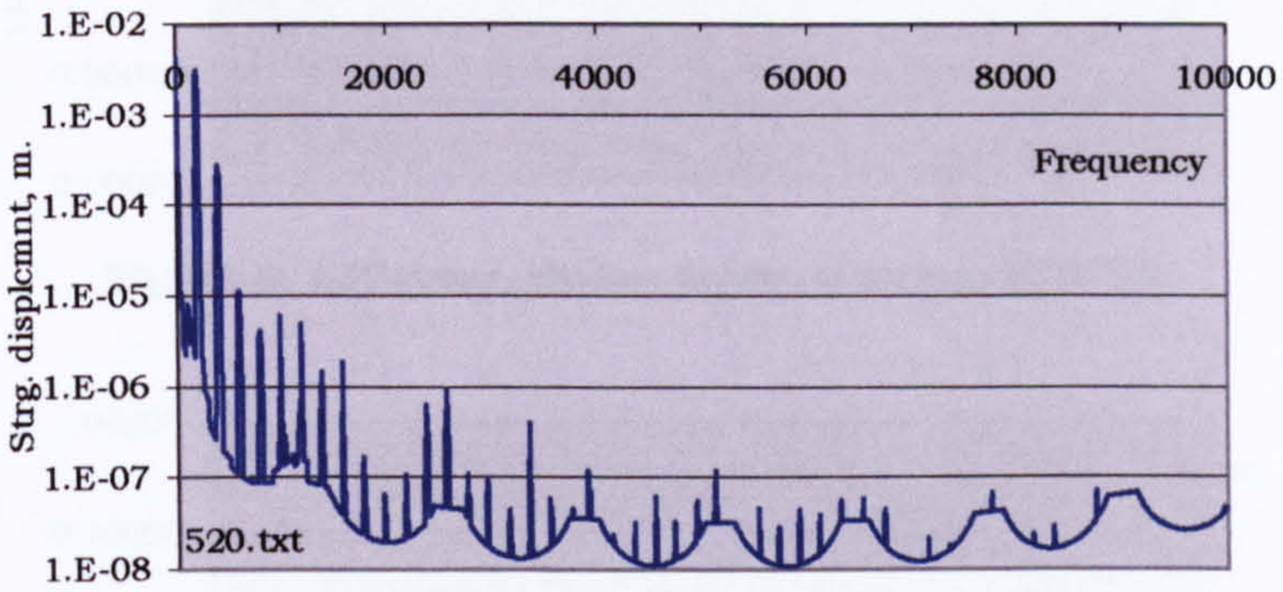

Fig. 11.3 Amplitude of transverse displacement of shaker driven G string, V158HE.

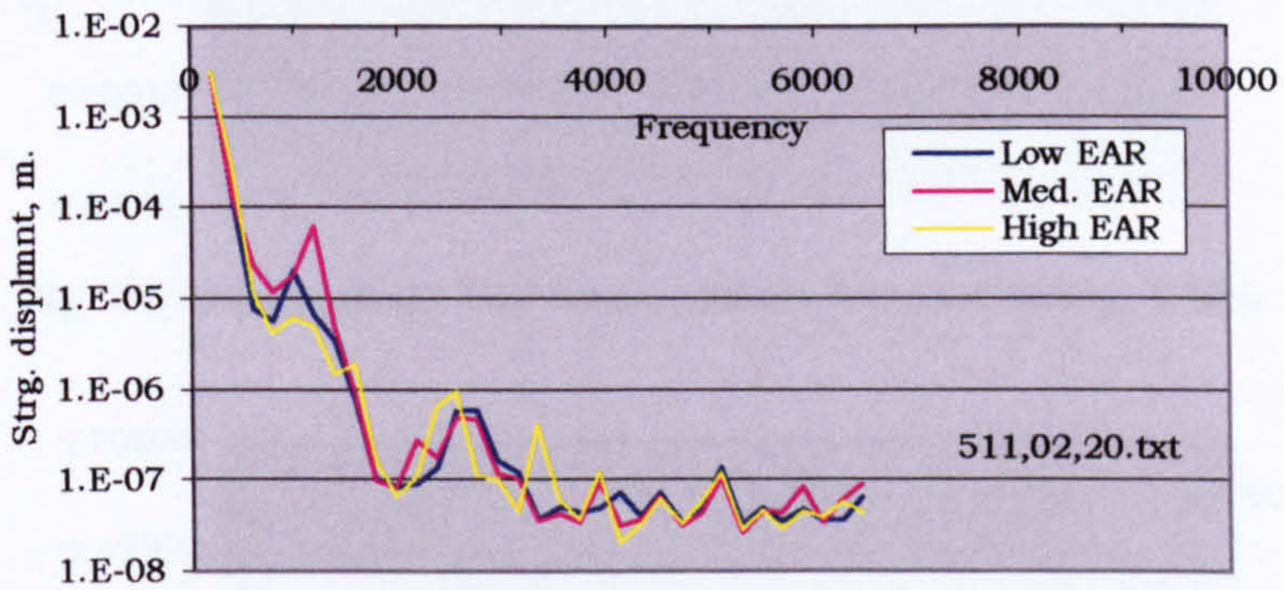

Fig. 11.4 Transverse displacement of shaker driven G string, violins of low, medium and high EAR.

To make the comparison of figs. 11.1, 11.2, and 11.3 easier, the peak heights were plotted as a continuous spectrum. This is shown in fig. 11.4. The results recorded above 6500Hz were measured at the limit of the analyser's range and are therefore intermittent and unreliable. For this reason they are omitted in fig. 11.4.

11.2.2 LSV, violins of different EAR.

The LSV force for the three violins of different EAR that was recorded simultaneously with the string displacements shown above, are shown in figs. 11.5, 10.10 (repeated) and 11.6.

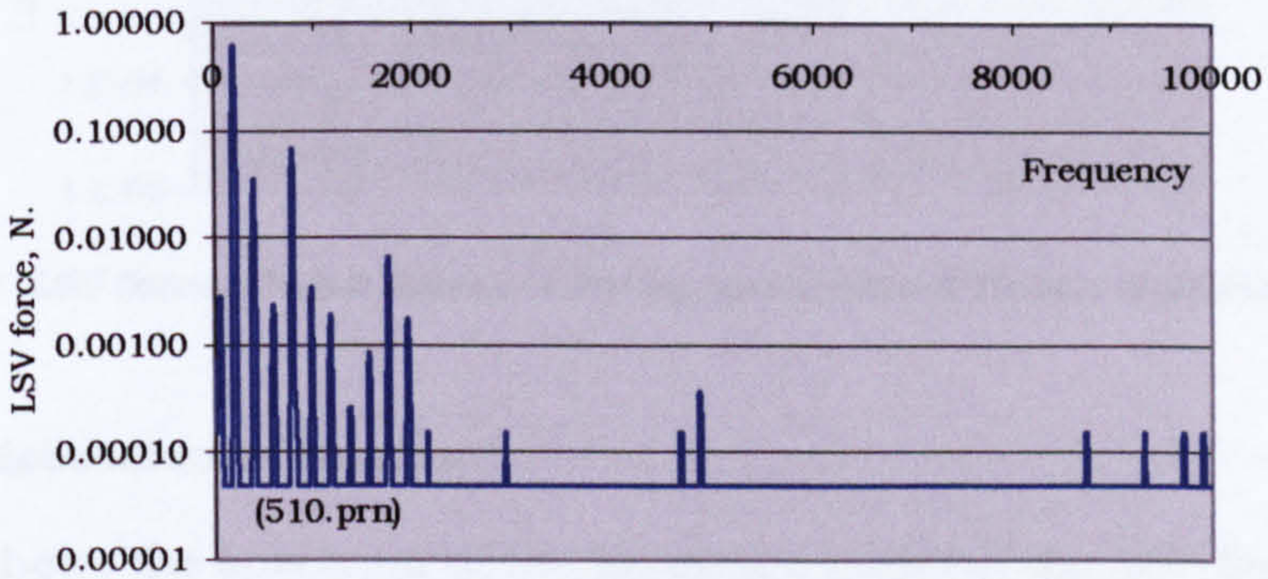

Fig. 11.5 LSV force, shaker driven G string, V157LE.

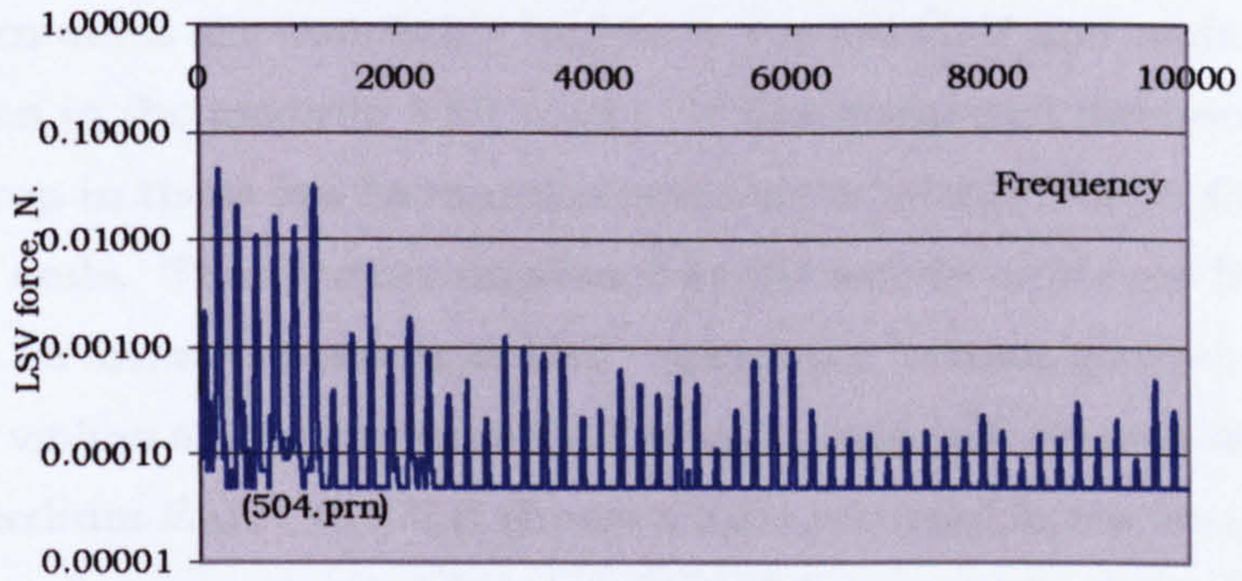

Fig. 10.10 (repeated) LSV force, shaker driven G string, V156.

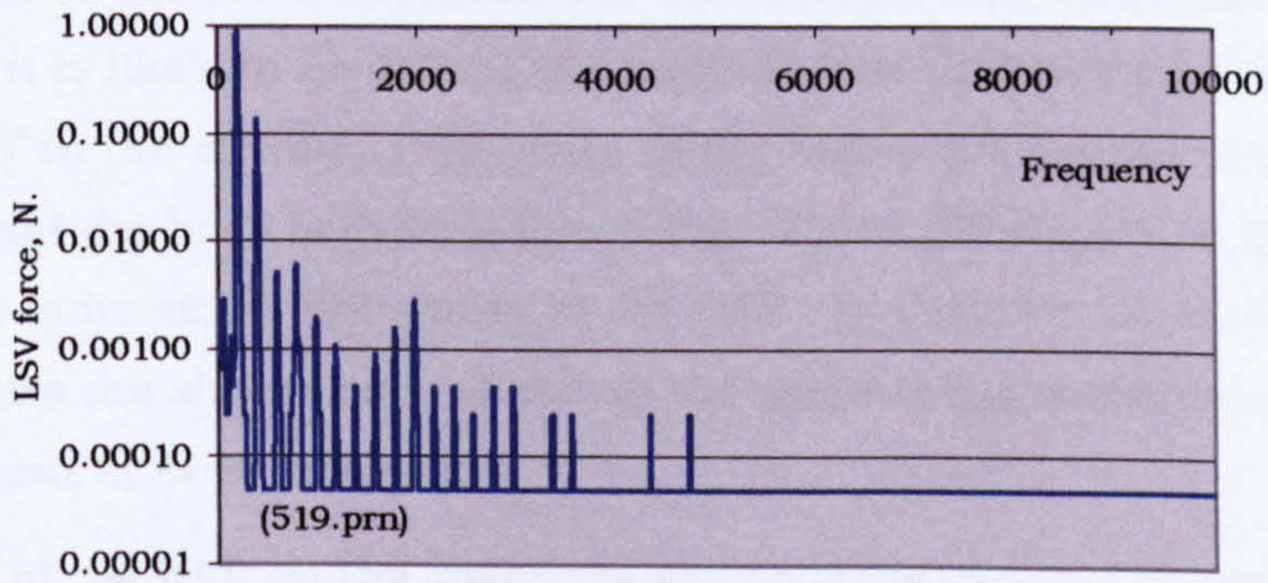

Fig. 11.6 LSV force, shaker driven G string, V158HE

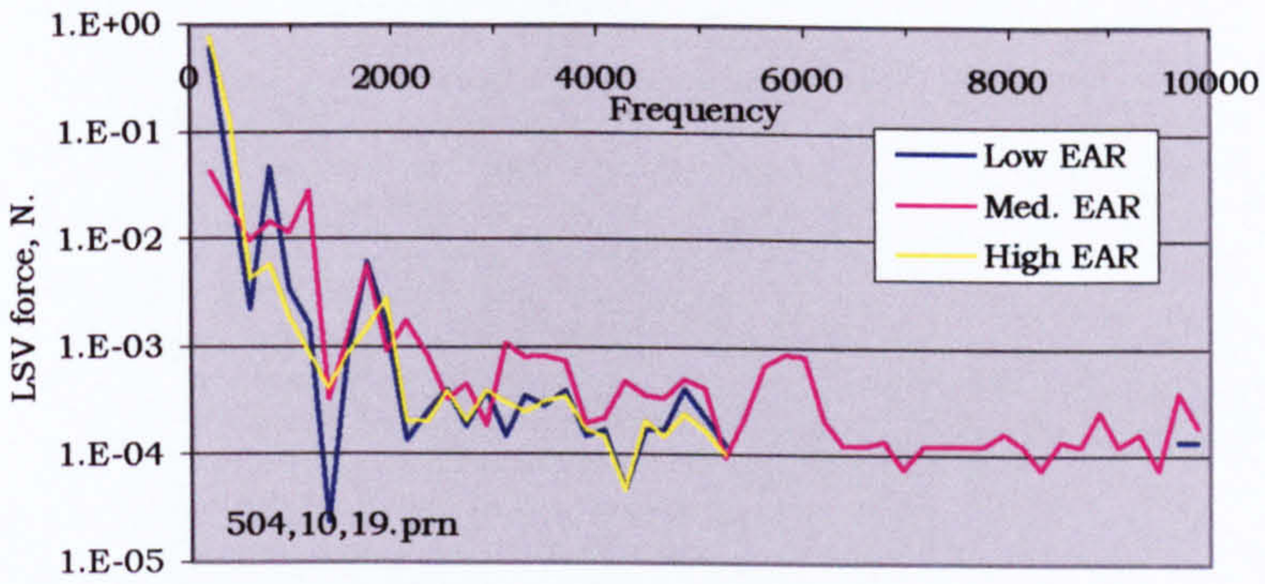

Fig. 11.7 LSV force, shaker driven G string, unvarnished violins of differing EAR.

11.2.3 Discussion of results

Fig 11.7 shows the spectrum of the harmonic peaks of the LSV force. The drop out above 5,200Hz is due to the inability of the analyser to handle a wide dynamic range. Very clear differences are apparent. The first and second harmonics are noticeably higher in the low EAR and high EAR violins, than in the medium EAR violin. It was suggested (section 10.4.5) that the drop in these low harmonics was due to energy loss at the tail gut and string ends. That further implies that the saddle of the medium EAR violin may be more responsive to LSV. Above the bottom quarter of the range, the violins of low and high EAR develop less LSV force than the violin of medium EAR. V157LE shows a little recovery in the top end but falls off even faster at the low frequencies. If the example of the simple oscillator presented in section 10.4.5 is considered, it could argued that the drop in LSV in the lower harmonics in the medium EAR violin shows that LSV force it is likely to be driving the body at those harmonics, and the higher LSV in the medium EAR violin in the higher harmonics could indicate that the body is driving the string. These differences in LSV force arise from quite small differences in the EAR. In Chapter 12, these LSV force spectra are shown normalised on the same string transverse displacement at every harmonic.

The effect of the EAR on the string transverse displacement spectra has been small. Between the third and the eighth harmonics the medium EAR violin is stronger. This is apparently not due to a reduction in the bridge-rock LSV force in this area, so must remain unexplained.

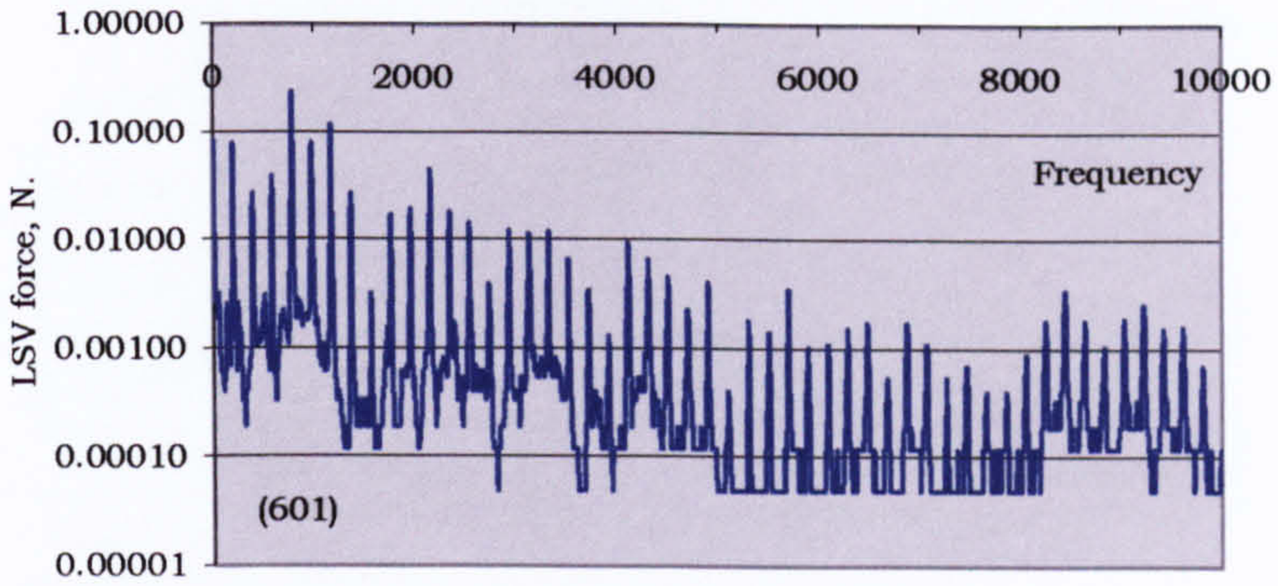

Fig. 11.8 LSV force, V156, bowed G string.

It must be remembered that the LSV force shown in all these examples is that resulting from a shaker driven string. While this is useful for comparative purposes, the level of LSV is well below that which would be produced by a bowed string. To demonstrate this the LSV spectrum for a bowed fourth string of the medium EAR violin is shown in fig. 11.8.

11.2.4 Confirmation with other strings

A similar comparison is made between the same three violins with the D string driven. In this case, it was not possible to drive the string to the standard first harmonic transverse amplitude of 3.25mm. The actual first harmonic amplitudes are stated in the captions. The excitation amplitudes are given in figs. 11.9 to 11.11. The corresponding LSV force spectra are given in figs. 11.12 to 11.14.

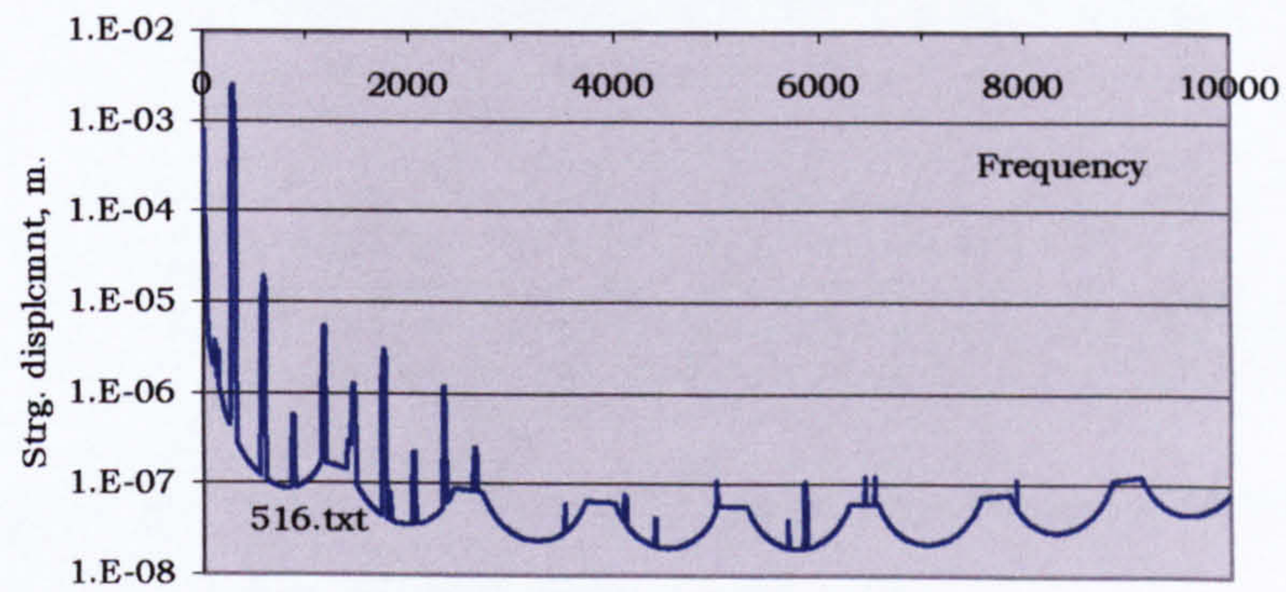

Fig. 11.9. Amplitude of transverse displacement of shaker driven D string (first harmonic 2.5 mm), V157LE.

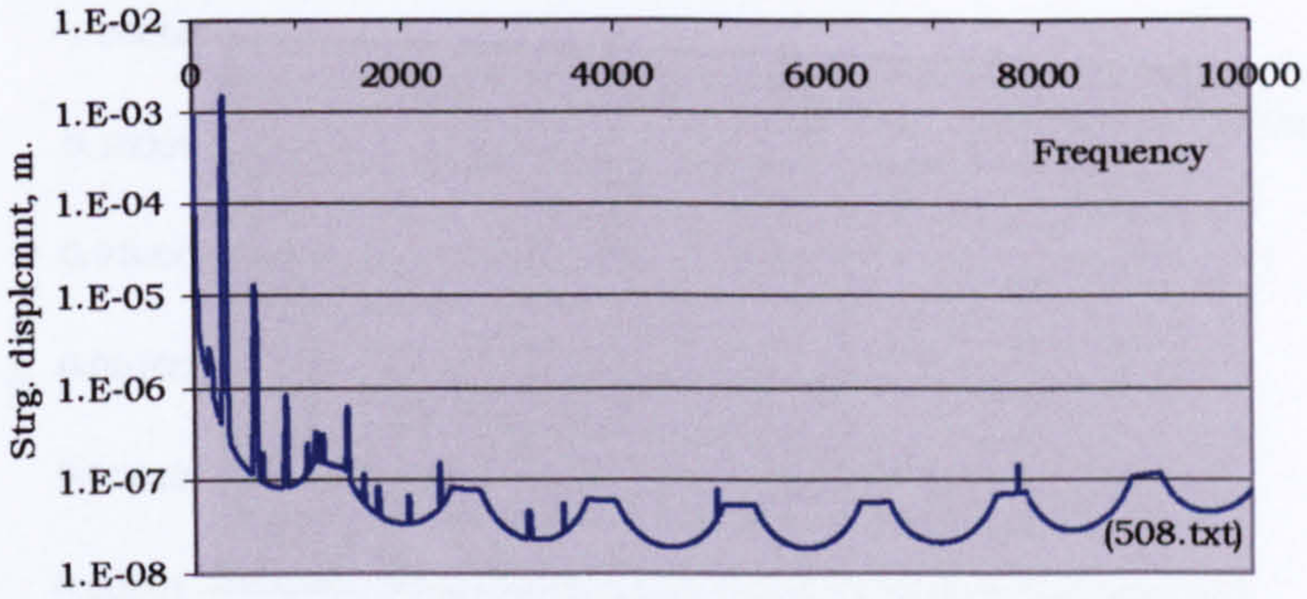

Fig. 11.10. Amplitude of transverse displacement of shaker driven D string (first harmonic 1.5 mm), V156.

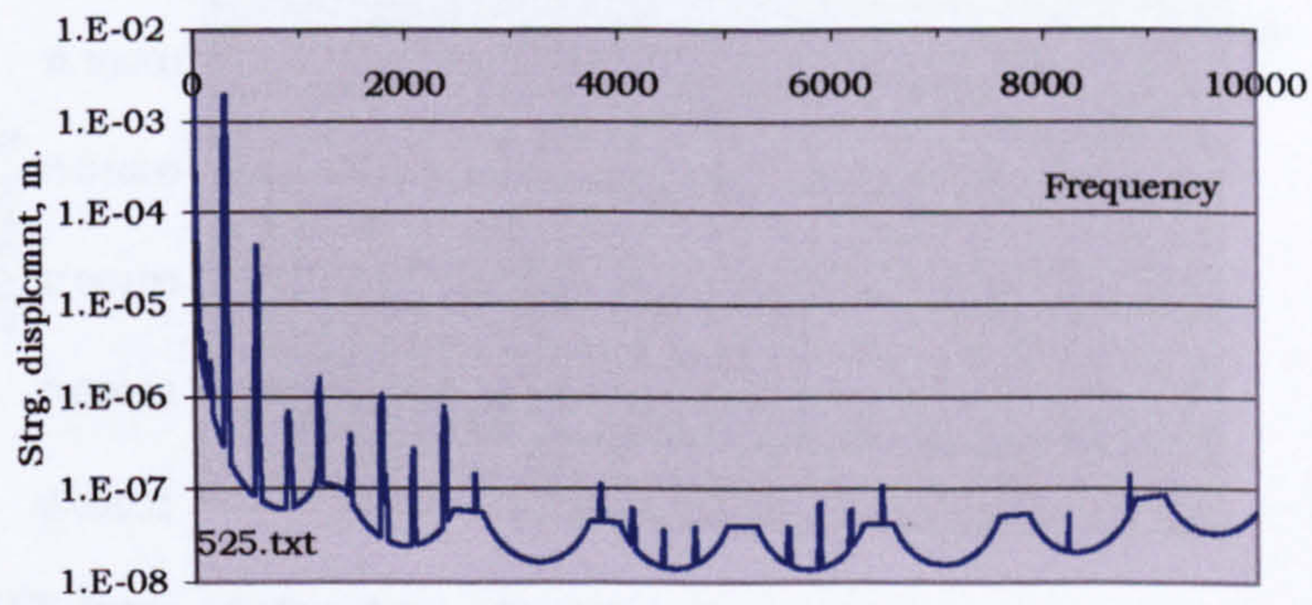

Fig. 11.11. Amplitude of transverse displacement of shaker driven D string (first harmonic 2.5 mm), V158HE.

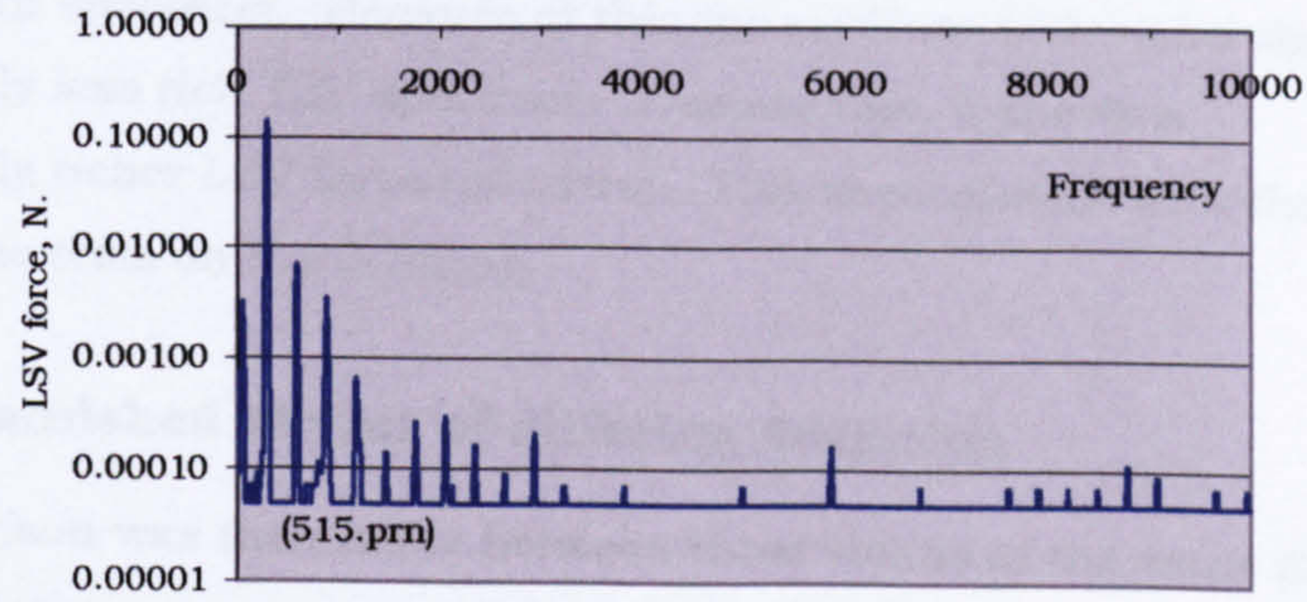

Fig. 11.12. LSV force, shaker driven D string (1st harmonic 2.5mm), V157LE.

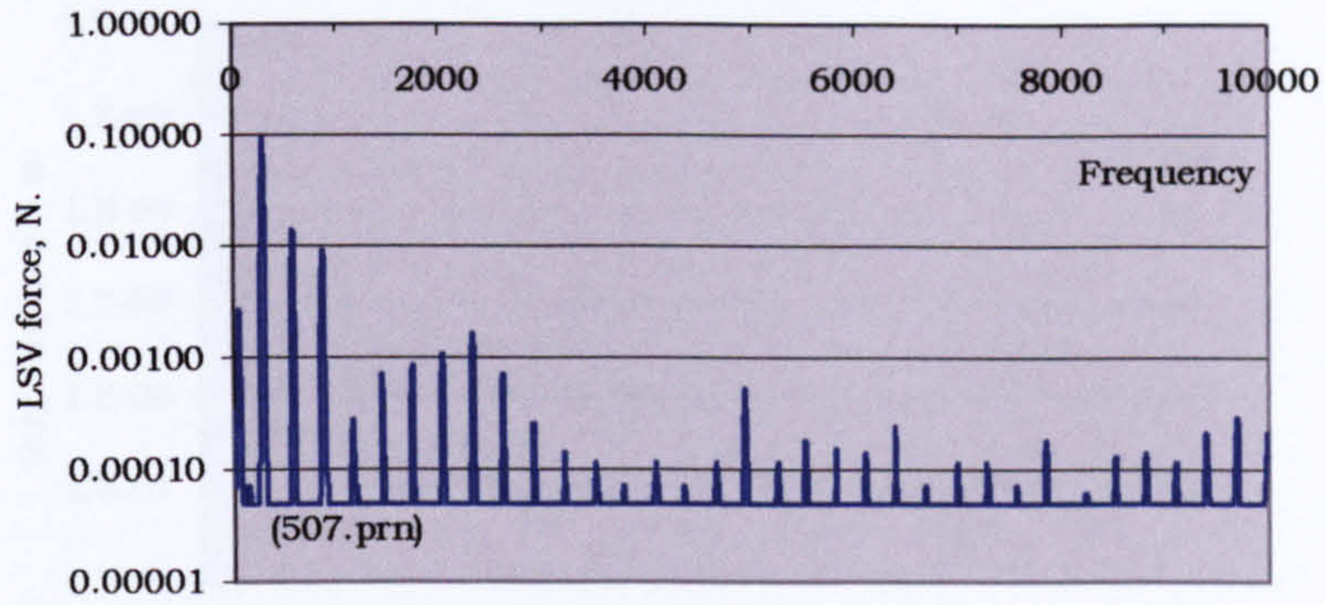

Fig. 11.13. LSV force, shaker driven D string (1st harmonic 1.5mm), V156 med. EAR.

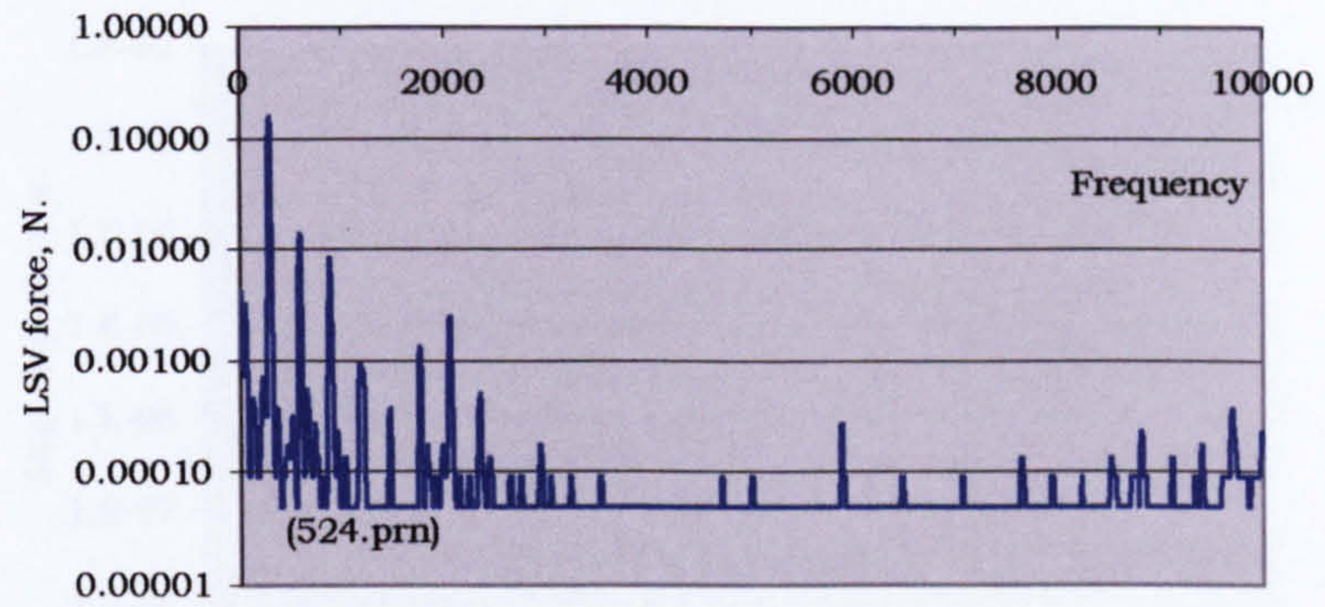

Fig. 11.14. LSV force, shaker driven D string (1st harmonic 2 mm), V158HE high EAR.

The difference in the first harmonic of the transverse displacement has resulted in a difference in the strength of the upper harmonics of the TSV displacement spectrum. Because of this the medium EAR violin shows a harmonically less rich TSV spectrum. Despite this, it shows a harmonically richer LSV force spectrum. This is consistent with the results found for the tests on the G string.

11.3 Unvarnished violins of differing deviation

The comparison was then made between three violins of the same EAR but varying deviation.

11.3.1 Results

The excitation spectra are given in figs. 11.15 to 11.17. The corresponding LSV force spectra are given in figs. 11.18 to 11.20.

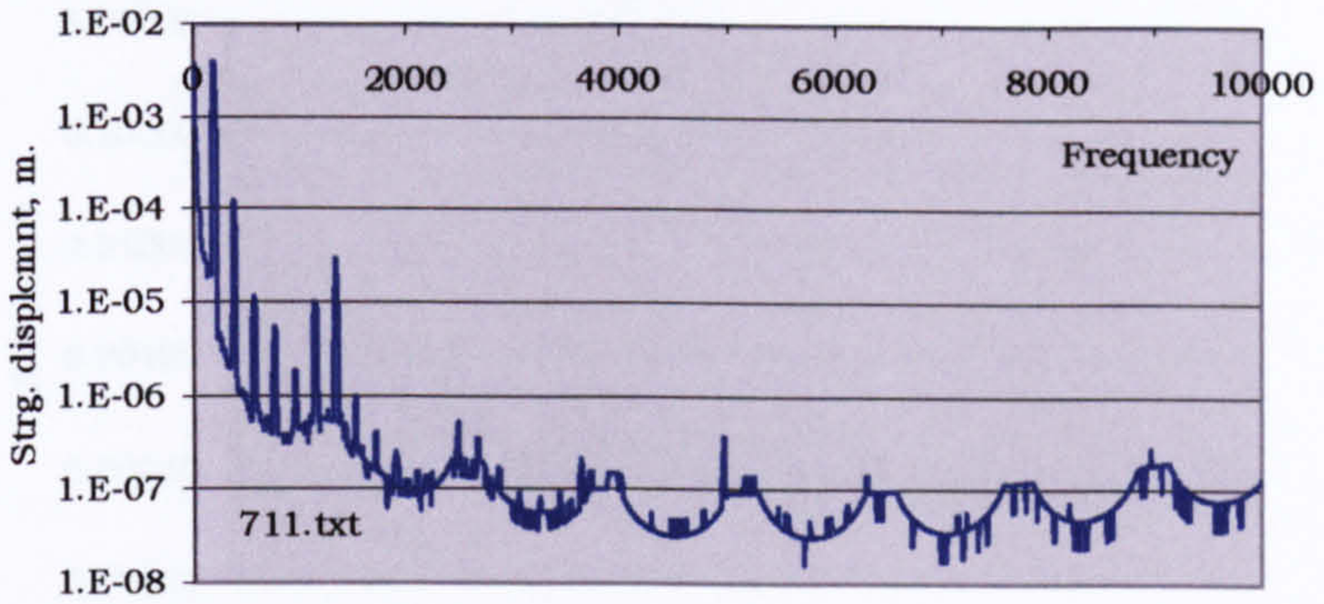

Fig. 11.15. Amplitude of transverse displacement of shaker driven G string, V158LD.

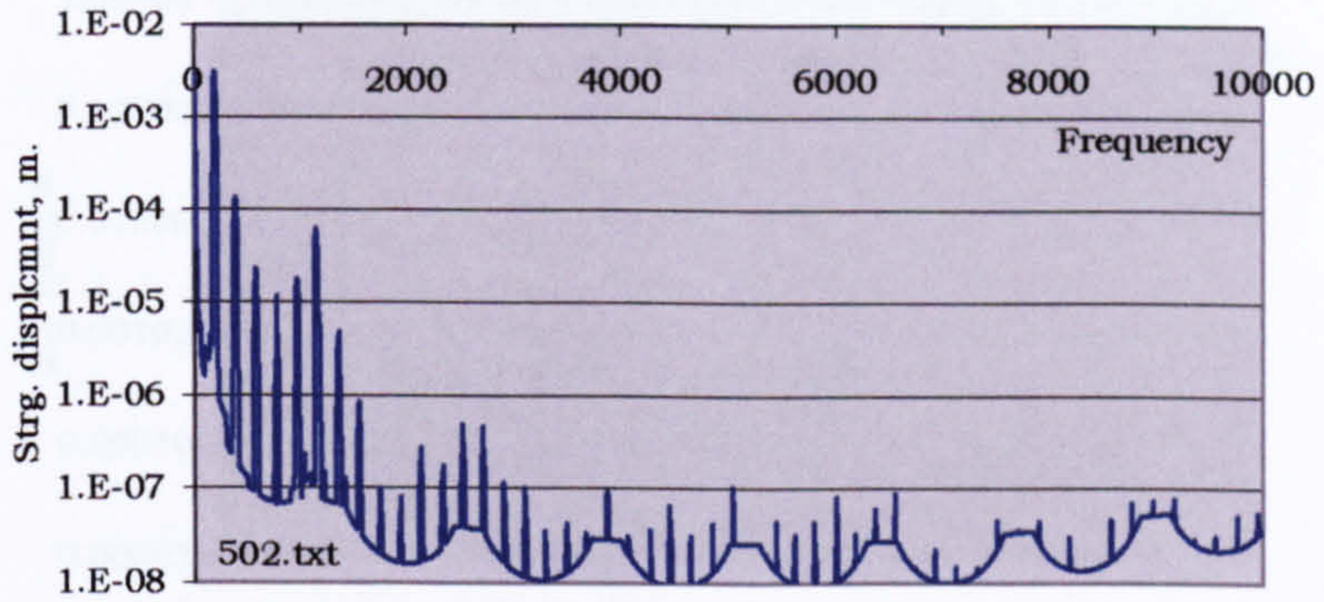

Fig. 11.16. Amplitude of transverse displacement of shaker driven G string, V156.

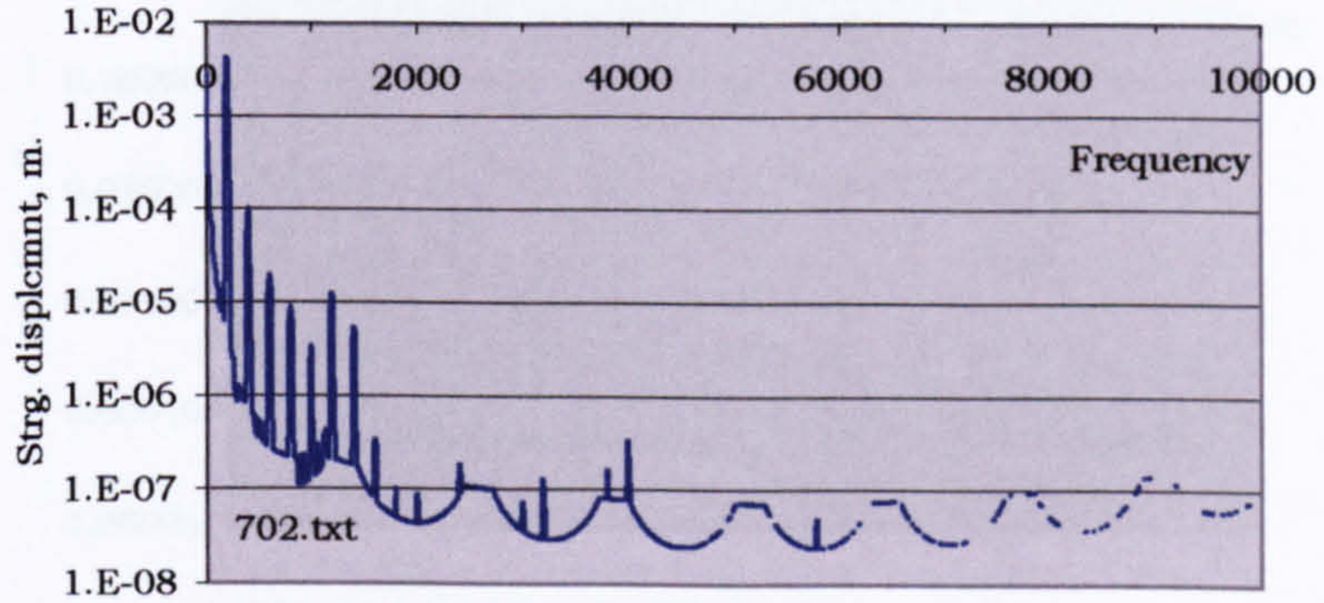

Fig. 11.17. Amplitude of transverse displacement of shaker driven G string, V157HD.

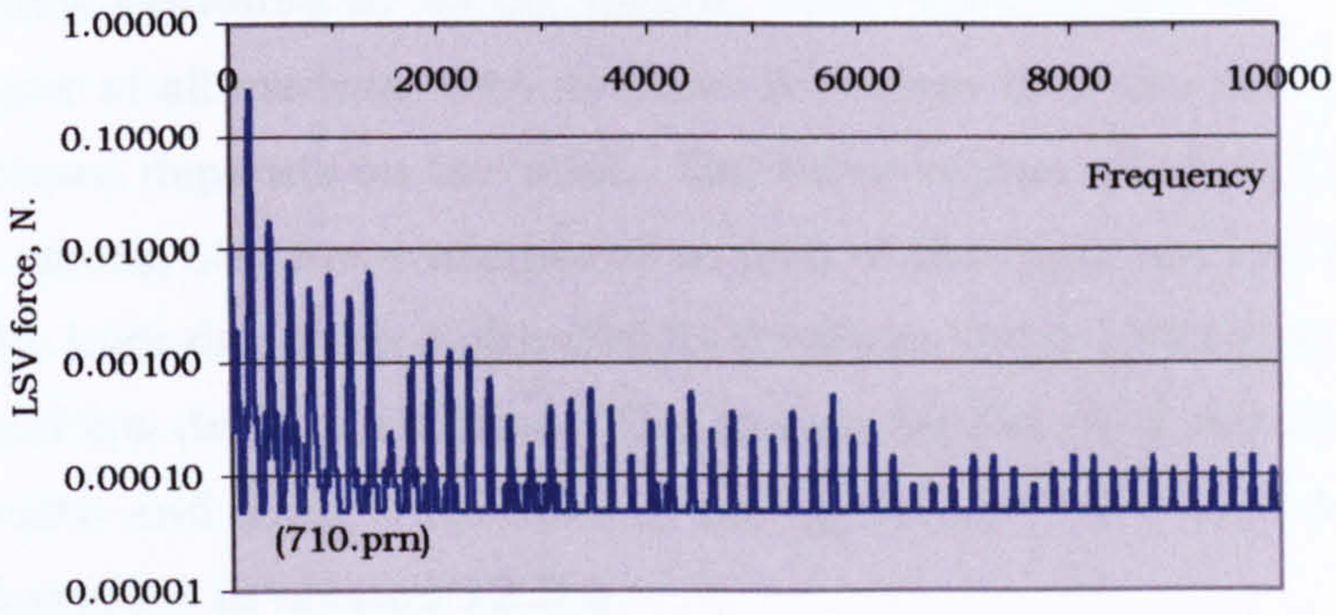

Fig. 11.18. LSV force, shaker driven G string, V157LD.

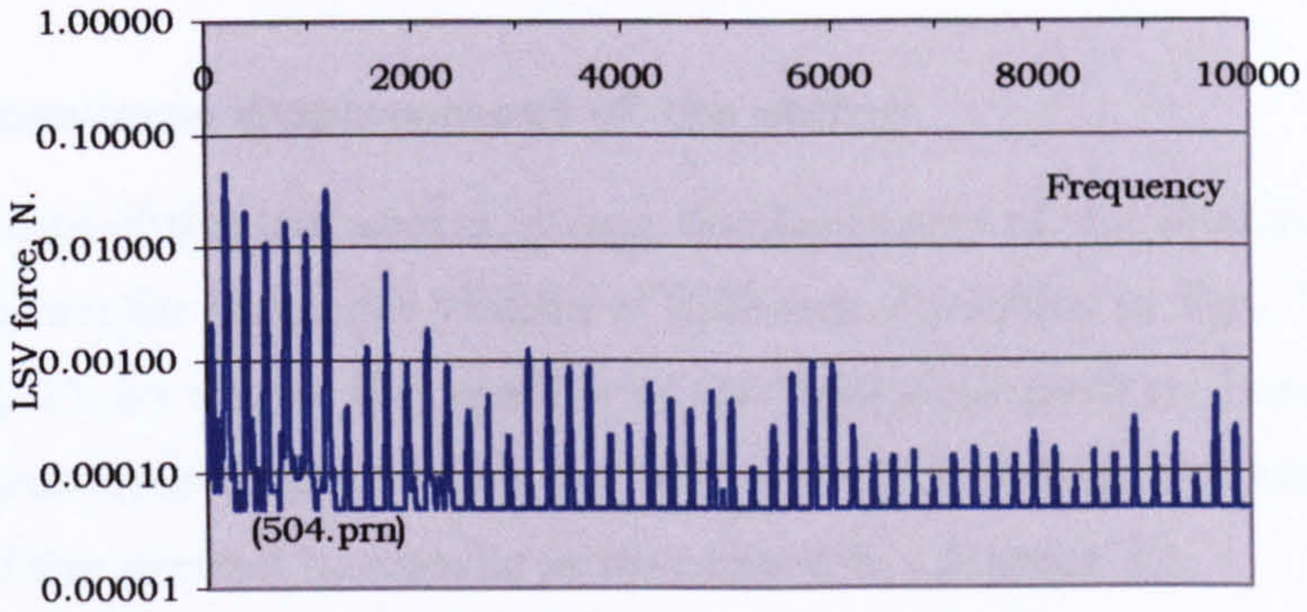

Fig. 11.19. LSV force, shaker driven G string, V156.

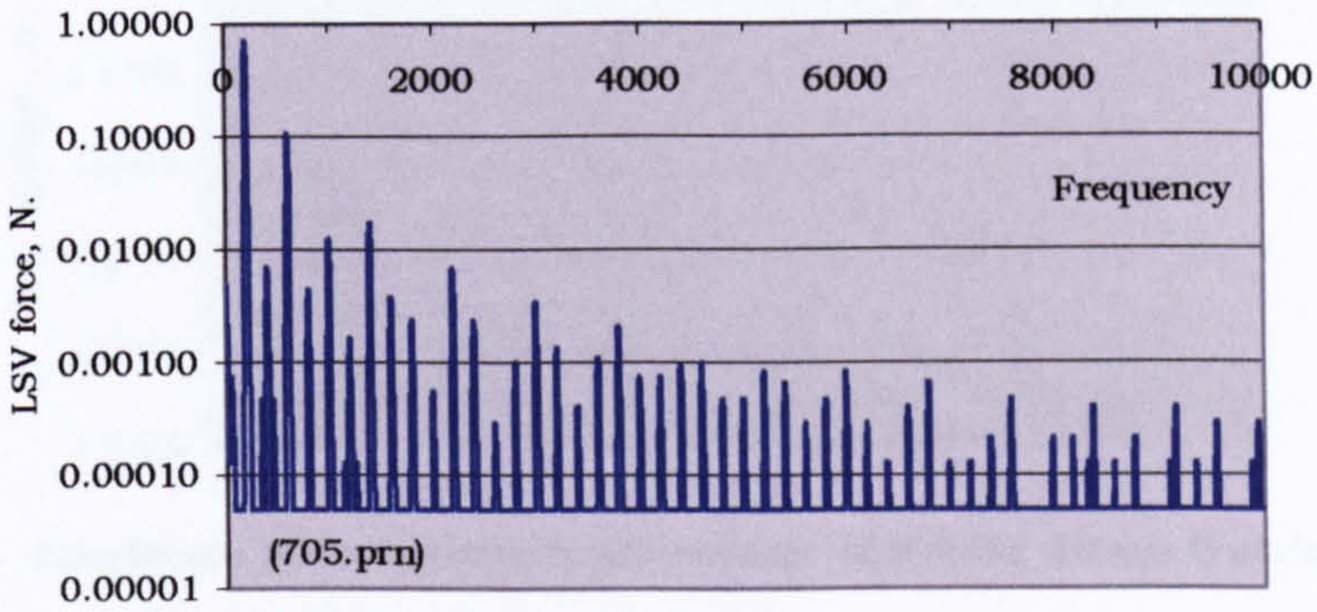

Fig. 11.20. LSV, shaker driven G string, V157 HD.

11.3.2 Discussion of results

There are some differences in the spectra of the transverse string displacement, but these are small and do not show a consistent pattern. The strong response in the third to the seventh harmonics shown by the medium EAR violin (fig. 11.4) and not shown for the low and high EAR

violins, is now exhibited by all the violins, thus confirming it is characteristic of all medium EAR violins. It is clear that the amount of LSV force developed depends on the EAR. The three violins all of medium EAR all show a strong LSV force compared to that of the high and low EAR violins. The high deviation violin clearly develops more LSV force than the medium and low deviation violins. The reason for the drop out of the second, fourth and sixth harmonics in the spectrum of the high deviation violin is discussed in section 12.3.6.

11.4 Varnished violins of differing deviation

11.4.1 Transverse displacement of the string

The amplitude of the transverse string displacement of the shaker driven string is shown for the three violins of different deviation in figs. 11.21 to 11.23. Fig. 11.24 shows the spectra of the harmonic peaks. This shows that the transverse displacement spectra are substantially the same. The drop out of the second harmonic is discussed in Chapter 12.

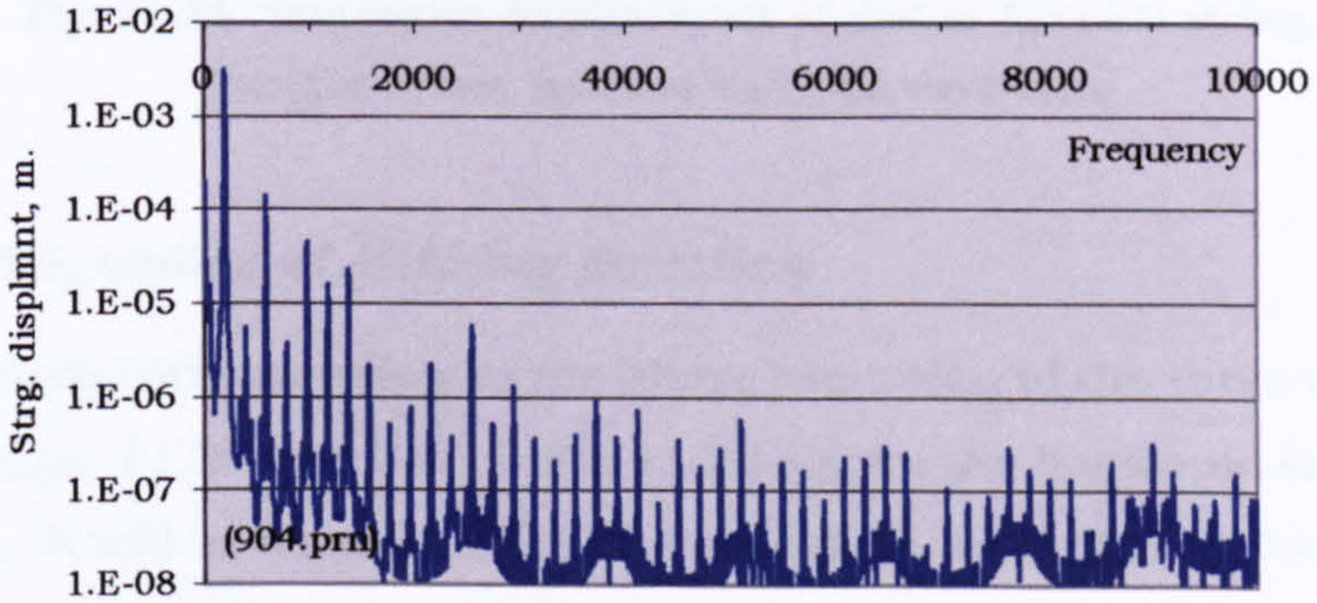

Fig. 11.21. Amplitude of transverse displacement of shaker driven G string, V158LD.

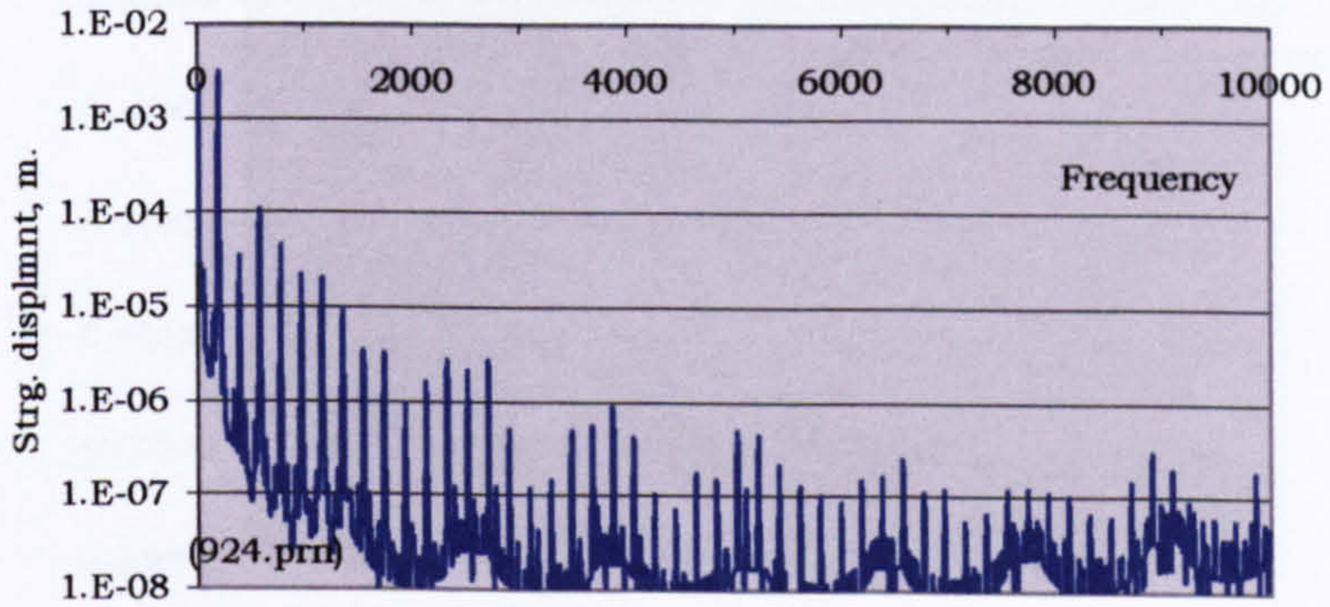

Fig. 11.22. Amplitude of transverse displacement of shaker driven G string, V156MD.

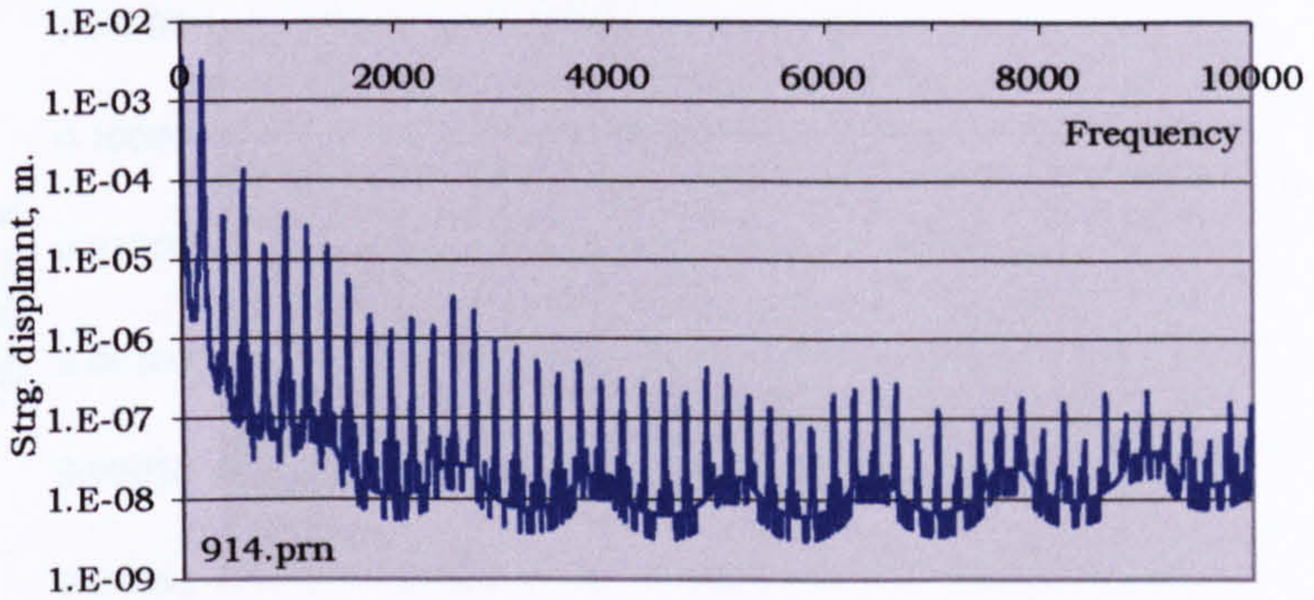

Fig. 11.23. Amplitude of transverse displacement of shaker driven G string, V157HD.

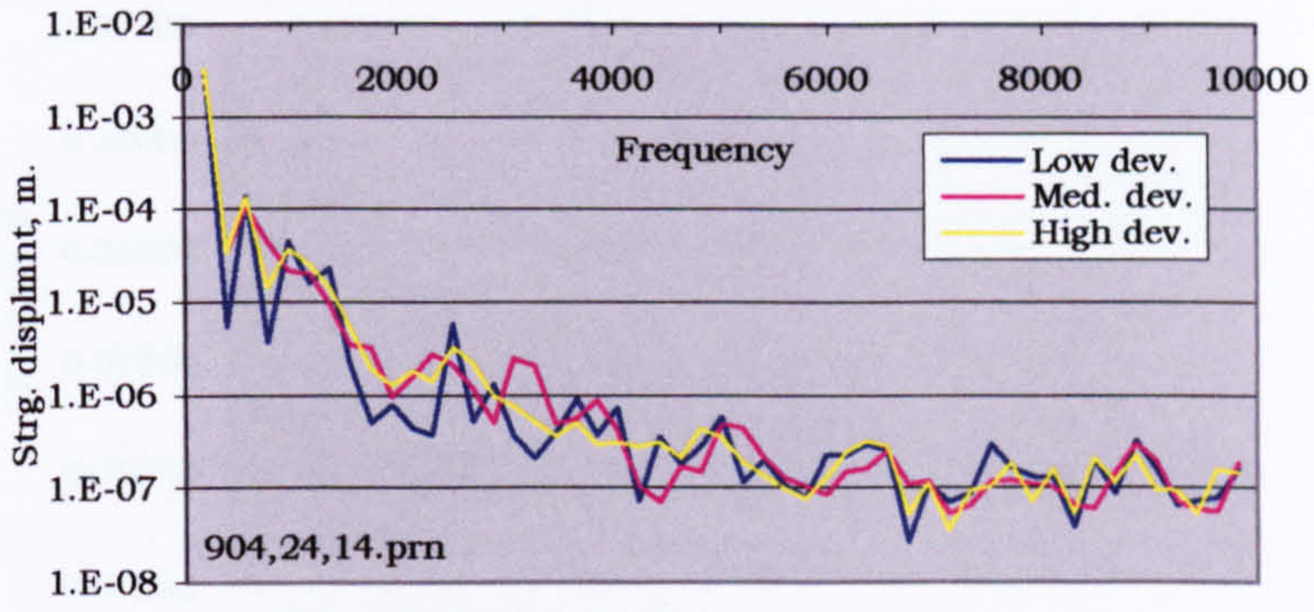

Fig. 11.24 Transverse displacement of shaker driven G string, violins of low, medium and high deviation.

11.4.2 LSV, violins of differing deviation

The LSV force corresponding to the above excitation of the three violins is shown in figs. 11.25 to 11.27. Fig 11.28 shows the harmonic envelope spectrum. It will be seen that the high deviation spectrum is clearly higher than the low deviation spectrum, and that of the medium deviation violin

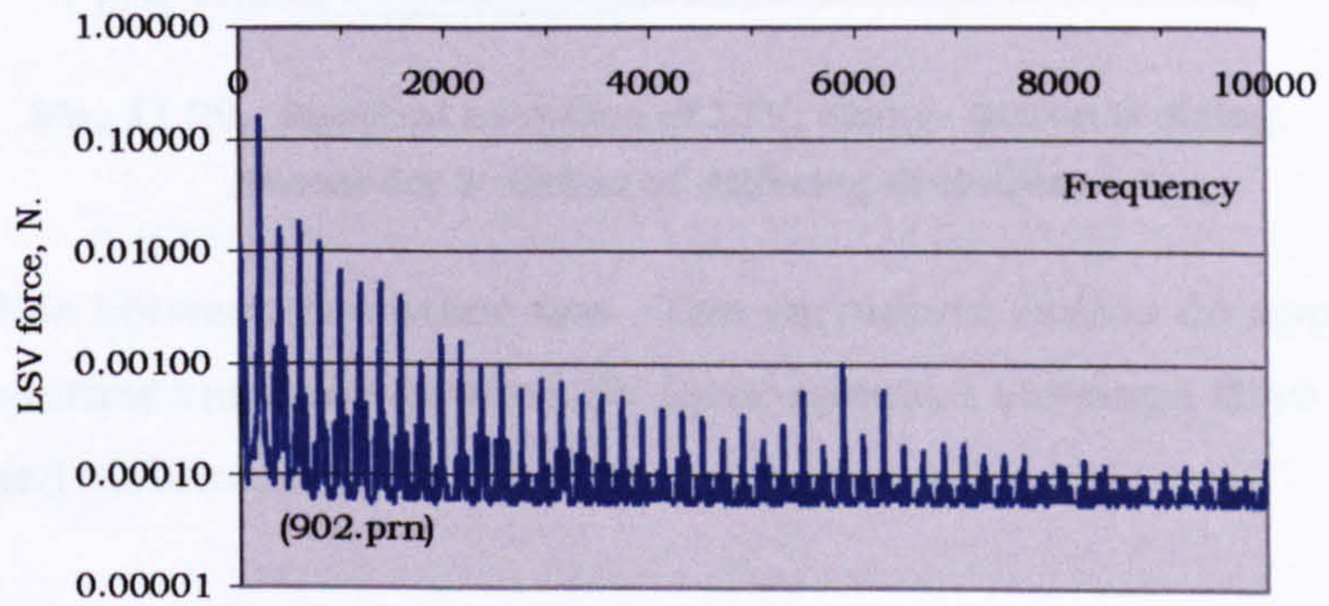

Fig. 11.25. LSV force, shaker driven G string, V158LD.

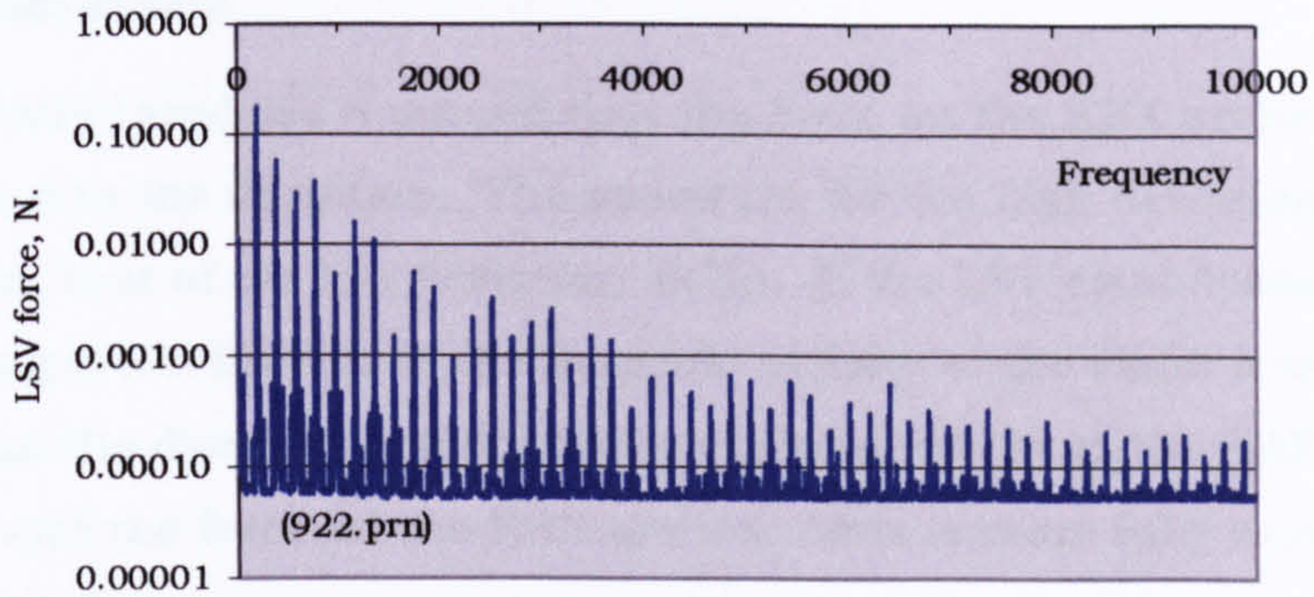

Fig. 11.26. LSV force, shaker driven G string, V156MD.

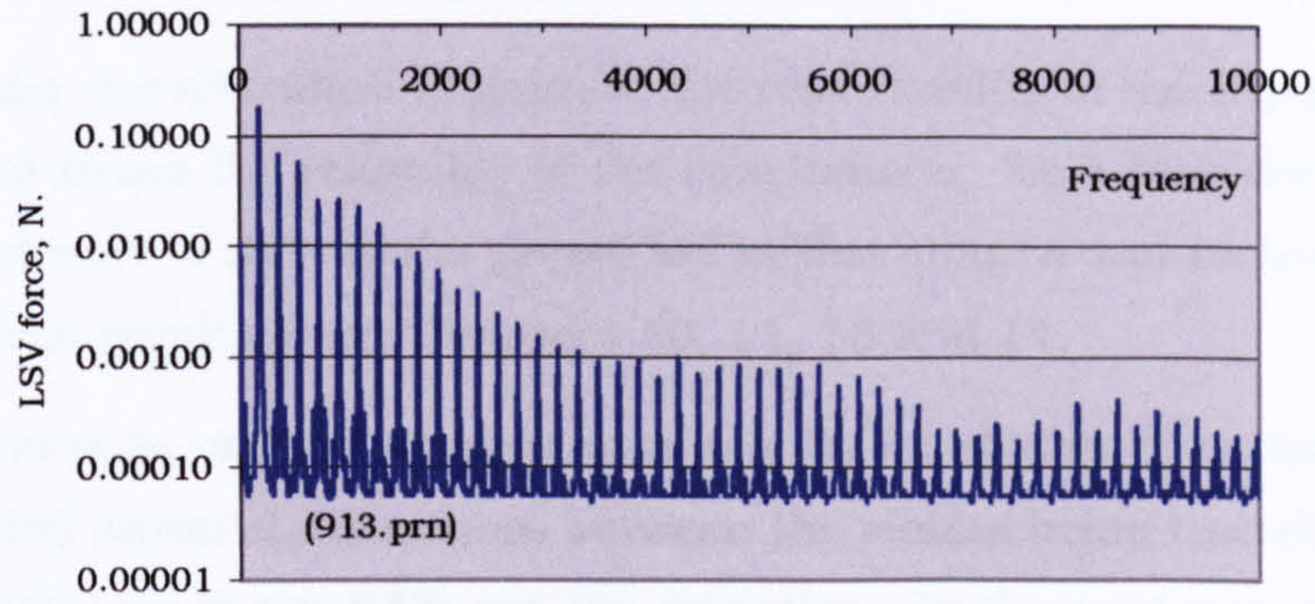

Fig. 11.27. LSV force, shaker driven G string, V157HD.

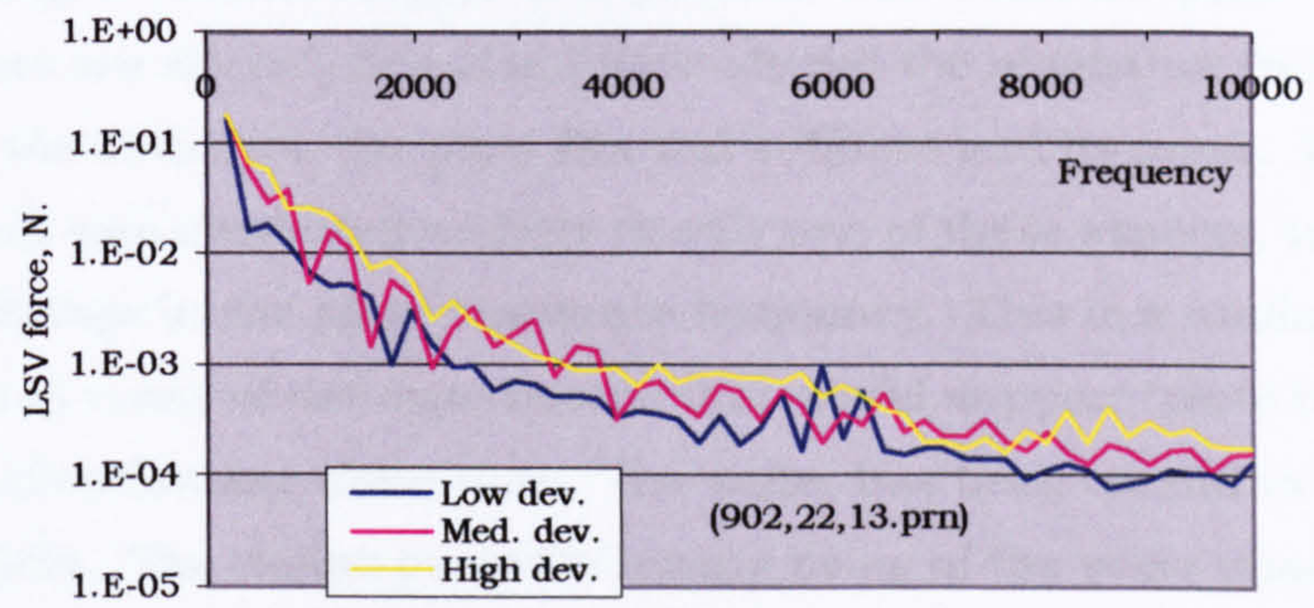

Fig. 11.28. Spectral envelope of LSV, shaker driven G string. Shown for 3 violins of differing deviation.

generally lies between the other two. The varnished violins do appear to have a smoother variation in the LSV force spectral envelope than the unvarnished violins.

11.4.3 Discussion

The qualitative analysis reasoned that the force on the EBX arches is proportional to the deviation. The spectrum for the high deviation violin is higher than that of the low deviation violin. If the LSV established in a violin string is a reflection of the dynamic activity of the violin it would appear that the dynamic activity of the violin is related to the EAR and the deviation and the force on the EBX arches. This is more fully analysed in section 12.1.4.

11.5 Repeatability of experimental results

At this point consideration is given to the repeatability of the experimental results and hence the reliability of the conclusions. This consideration applies not only to the results presented in this chapter but includes all the experimental results given Chapters 10, 11, 13 and 14.

The first issue is, can the experimental results be attributed exclusively to the intended physical differences between the violins being tested? That is, to the differences in the EAR and the deviation. In the past tests have been done where wood is removed to reduce the thickness of violin plates with tonal testing at various stages. It is possible that when the plate thicknesses are altered, this could have altered the resonance frequency, the EAR, the deviation, the plate flexural stiffness and its mass. But the tonal result was attributed entirely to only one of these aspects, usually the effect of change in the plate resonance frequency. This is a fundamental weakness in many of the experiments that would support "plate tuning" as a means of optimising violin tone. The writer has been careful to avoid these pitfalls. The violins made for testing being of the same wood, have close to the same mass and resonance frequencies. However there must inevitably be differences other than in the EAR and deviation. For example the belly end bouts cross arch height has to be different in these violins. The possibility has to be considered that experimental differences could arise from that cause alone and have nothing to do with the EAR and deviation. In fact, it will be shown later that some aspects of violin behaviour are attributed to that cause. Having reduced the violin

differences to only those differences that are being tested, one can only remain alert to the possibility of other factors.

The second issue is that of a small sample size. It would have been very nice to have five examples of every type of violin, low EAR, medium EAR, high EAR, and various deviations. That could have been achieved within a limited range of deviation, but at only one EAR, by testing violins made by the writer previously. However, a group of violins such as this would all have been of different wood with different thickness, mass and plate resonances. It was just not possible to build and test a large number of violins that only showed differences in EAR and deviation. The interchanging of body parts to make several violins for testing acts as extra insurance against the experimental result being affected by differences between the plates other than those intended. Generally, the differences in experimental result between violins of different EAR and deviation are sufficiently clear for them to be in little doubt.

The third issue is that of repeatability of experimental measurement. The actual ability of the measuring equipment to record highly repeatable readings in successive runs was not in doubt, having been constantly tested.

The fourth issue is that of setting up the same test with the same excitation for different violins. To test a violin involved establishing a sustainable and repeatable excitation. This is discussed in section 10.2.1. The contention that repeatability of this excitation was acceptable is supported by fig. 11.24. The variation that does exist between the curves in fig. 11.24 would be due in part to small differences between the violins being tested. The corresponding spectral envelope of LSV shown in fig. 11.28 also shows a high degree of repeatability the main difference being fully consistent with the expected effect of the difference in deviation. Severe failure of repeatability would not have allowed such close correspondence between these spectral envelopes.

Finally, in the processing of the results the conclusions are drawn from considering the results as ratios. For example, we do not just compare the sound radiated by three violins; we compare the sound per unit TSV or sound per unit LSV. This precaution compensates for differences there

may be, in the level of excitation or within the spectrum of the excitation. The validity of drawing conclusions from such ratios when the system is to some extent non-linear is justified in section 10.2.3.

11.6 Conclusions

- Compared with the high and low EAR violins, the medium EAR violin showed a lower LSV force in the first two harmonics, and a generally higher level of LSV force in the harmonics above 2kHz. This may be an indiction of a generally higher level of dynamic activity at all harmonics.
- The variation of LSV force with deviation showed that the LSV was monotonically linked to the deviation over most of the frequency range.

Chapter 12

FORCES, MODES, ADMITTANCE AND POWER

12.1 The forces on the body

12.1.1 Transverse force on bridge, TSV force

The velocity of the string at the location of the magnet was measured directly by analysing the EMF induced in the string. Fig 12.1 shows the rms velocity of the string at the magnet location for the open G string on violin 157, which has normal EAR and high deviation

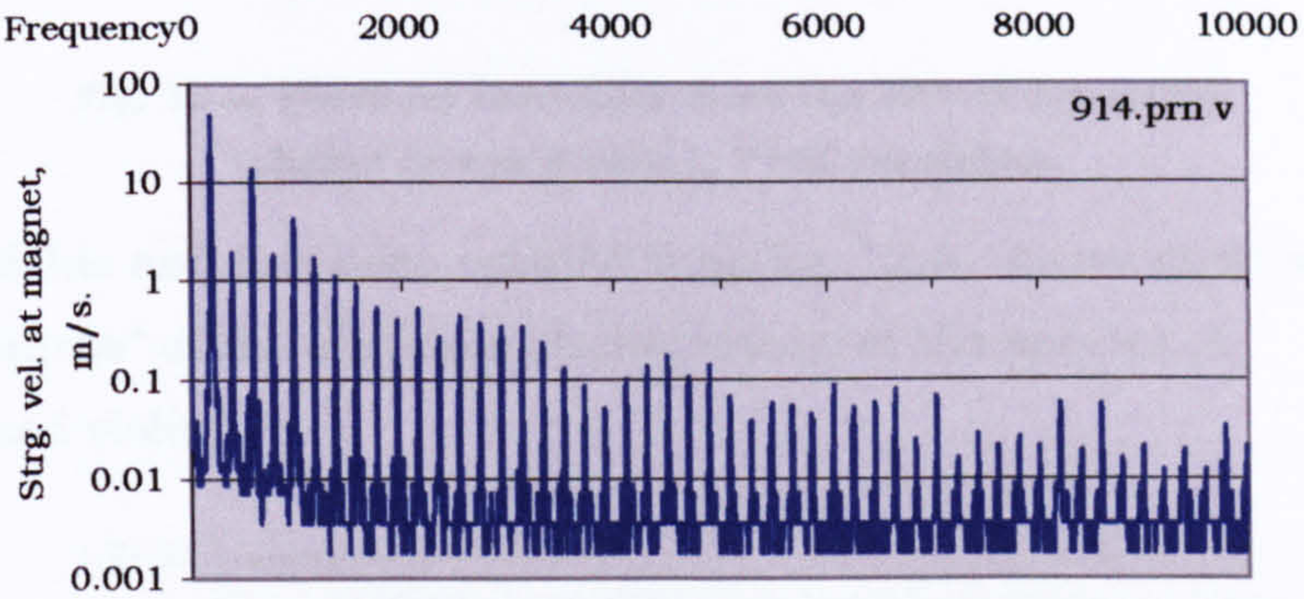

Fig. 12.1. Indicated rms string velocity at the point of location of the magnet, shaker driven G string, V157 varnished.

From the rms string velocity we can estimate the rms force on the bridge as follows;

$$F_{TSV} = -jr\bar{v}_m \qquad \text{where} \quad r = \frac{T\frac{n\pi}{L}\frac{n\pi a}{L}}{\omega \operatorname{Sin}\frac{n\pi x_0}{L}\operatorname{Sin}\frac{n\pi a}{L}}$$

$\bar{v}_m$ =indicated velocity in the magnet gap (space averaged)

2a =the effective width of the magnetic field at the magnet gap measured in the direction of the string length

x_0 = the distance from the centre of the magnetic field to the end of the string. T=40N, L=328mm., $n=f_n/196$

Fig. 12.2 shows the force on the bridge calculated from the transverse vibration of the fourth string for V157 varnished.

Fig. 12.3 shows the TSV force on the bridge for the three unvarnished violins of different EAR. The data collected above 6500Hz was intermittent

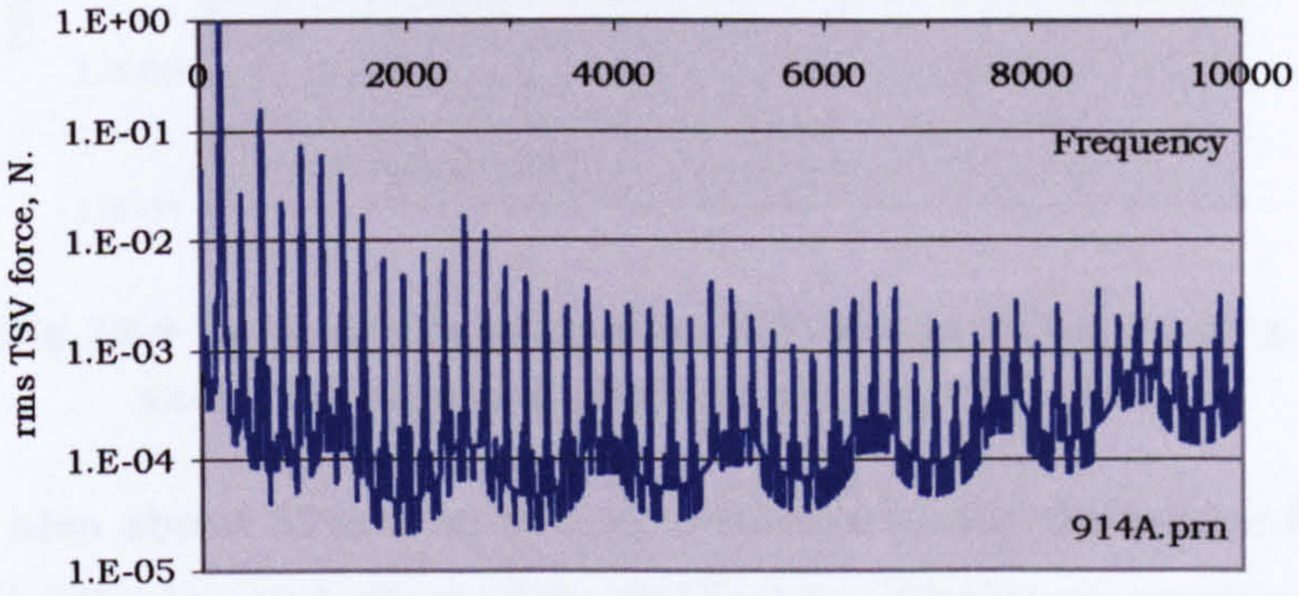

Fig. 12.2 Force on the bridge from the TSV of the string, shaker driven G string, V157 varnished.

and unreliable and has been omitted from fig. 12.3. As we shall see later, the "lumpiness" of the curves is characteristic of the spectra of unvarnished violins.

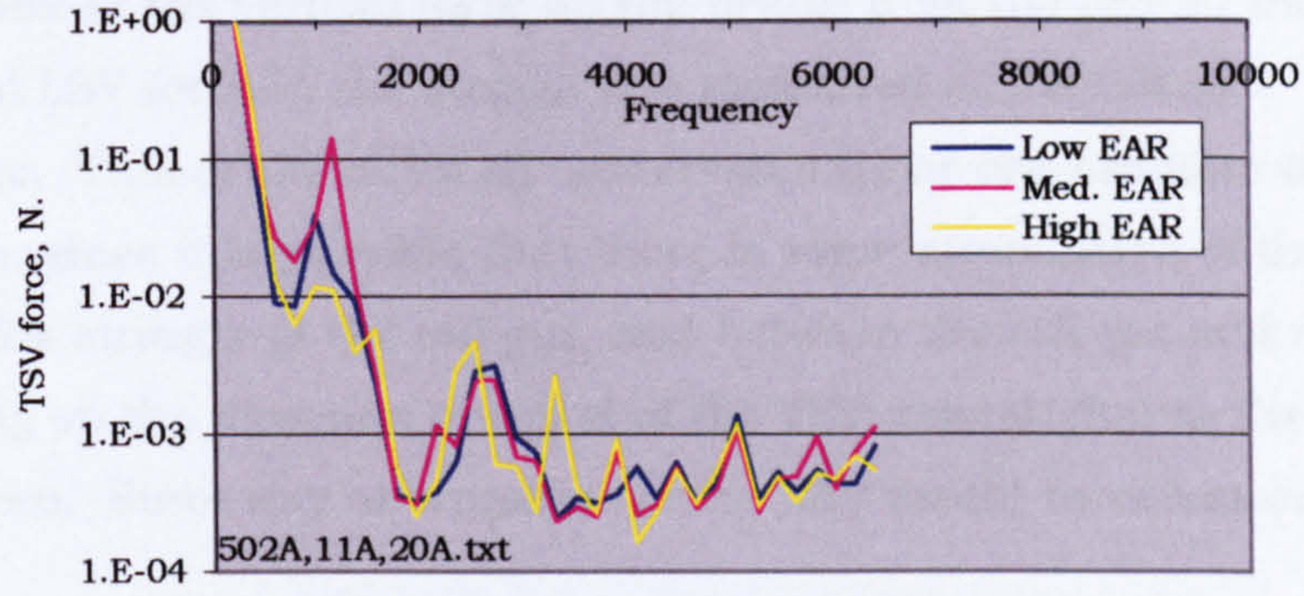

Fig. 12.3 Force on bridge from TSV, shaker driven G string. Shown for unvarnished violins of differing EAR.

Fig. 12.4 shows the force on the bridge for the three varnished violins of differing deviation. It is clear that the shape of the curves in fig. 12.4 is quite different from those in fig. 12.3. This comes from there being a different harmonic content in the transverse displacement of the string. (See Appendix A for discussion of the effect of varnish on string displacement.) This force is applied approximately horizontally at the top of the bridge. The bridge height is about 32mm and the distance between

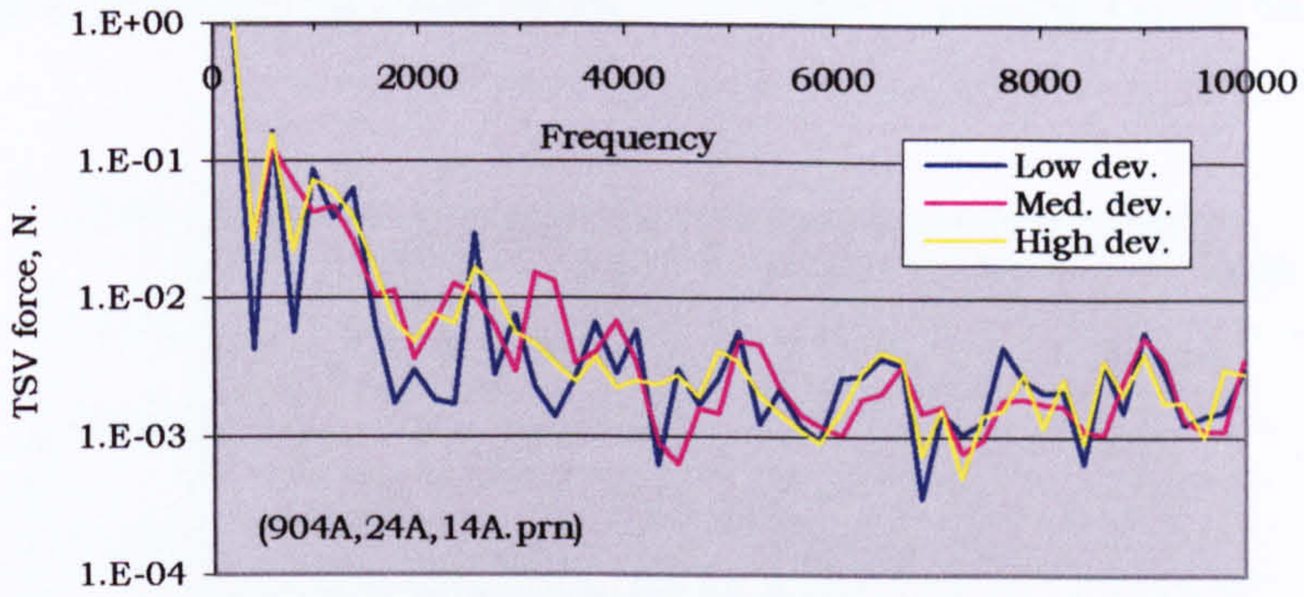

Fig. 12.4 Force on the bridge from TSV, shaker driven G string. Shown for varnished violins of differing deviation.

the feet is also about 32mm so taking moments about the bridge feet (and disregarding the inertial effect of the bridge) would give an upward or downward force at the bridge feet of about the same magnitude as the transverse force.

12.1.2 Vertical LSV force on the bridge

Shaker driven string

We now look at the vertical force on the bridge from the LSV in the string. The actual LSV force in the strings was measured at the tail gut transducer. This could variously underestimate or overestimate the LSV at the bridge, since it is possible that there is some attenuation of the LSV between the string and the tail gut, and between the tail gut and the string (depending on the direction of travel of the TSV waves), due to the mass of the tailpiece. Since any attenuation of the LSV would be common to all the

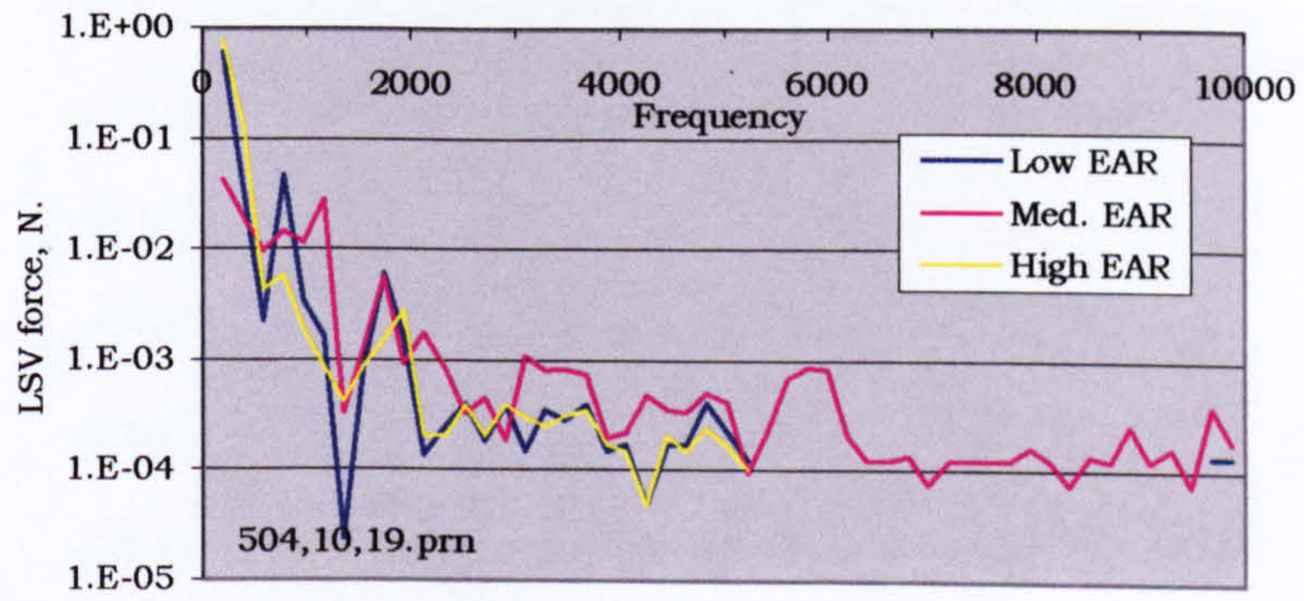

Fig. 11.7 (repeated) LSV force, shaker driven G string, shown for unvarnished violins of differing EAR.

violins tested, it would not invalidate conclusions reached on a comparative basis.

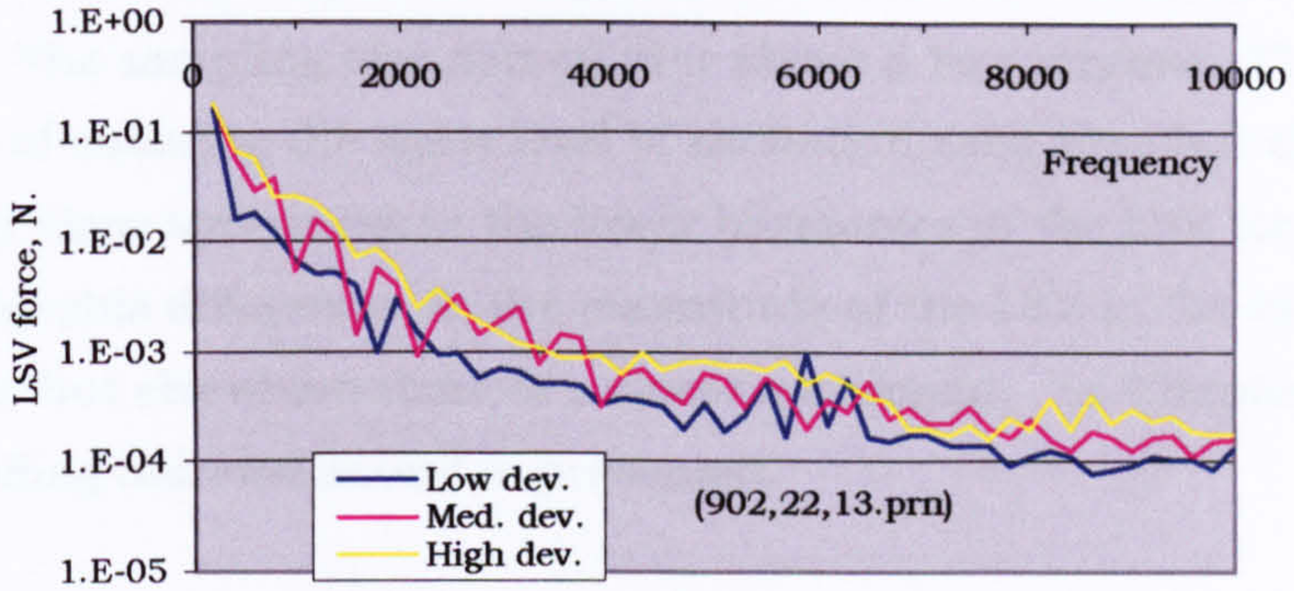

Fig. 11.24 (repeated) LSV force, shaker driven G string, shown for varnished violins of differing deviation.

Above 5500 Hz, the LSV for the high and low EAR violin was too low to be reliably recorded by the analyser and is therefore not shown.

The static analysis shows that the vertical force on the bridge is about 0.4 of the LSV force. This force will be split approximately equally between both bridge feet. This would give a vertical force at each bridge foot of about 0.2 of the LSV force. Figs. 11.7 and 11.24 show the LSV for various violins and are repeated again here. The variation of LSV with EAR and deviation has been discussed in Chapter 11.

Bowed string

The LSV produced by a shaker driven string at the TSV amplitudes employed, is much lower than that of a bowed string.

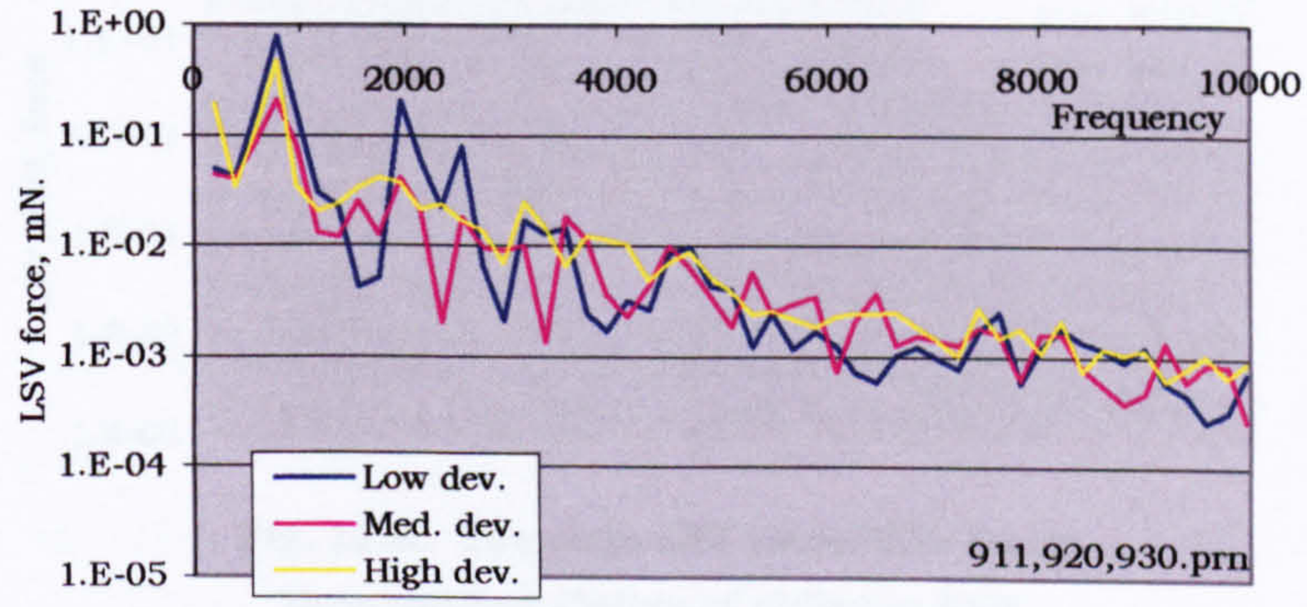

Fig 12.5. LSV, shown for violins of differing deviation, excited by hand bowing the G string.

The three violins of differing deviation were fitted with the tailpiece containing the tailgut transducer. The open G string was bowed strongly and as continuously as possible while the LSV and the radiated sound were recorded. The sampling was spread over about 5 bow strokes. There was no means of ensuring the same level of excitation each time but there is reasonably close agreement in the lower harmonics of the LSV force. There are considerable differences in the magnitude of the LSV in the range 1500 to 3500Hz, but elsewhere there is a closer agreement. In Chapter 13, the corresponding radiated sound is presented.

12.1.3 LSV per unit TSV, violins of different EAR

In order to compare the LSV developed in violins of different EAR and deviation with some precision, the LSV spectra should first be normalised on the input transverse displacement amplitude of the string. However, to do so would produce a curved line since the transverse displacement amplitude is proportional to the transverse force divided by the frequency. It was therefore decided to normalise the LSV force on the TSV force.

The LSV force spectrum for each violin (figs. 11.7 and 11.24) was divided by the TSV force spectrum (figs.12.3 and 12.4) and the results are shown in figs. 12.6 and 12.7. Fig. 12.6 shows that from 3000Hz to 5000Hz, the medium EAR violin produces somewhat more LSV force per unit TSV force than the violins of low and high EAR. Below 3000Hz there is little consistent difference with EAR.

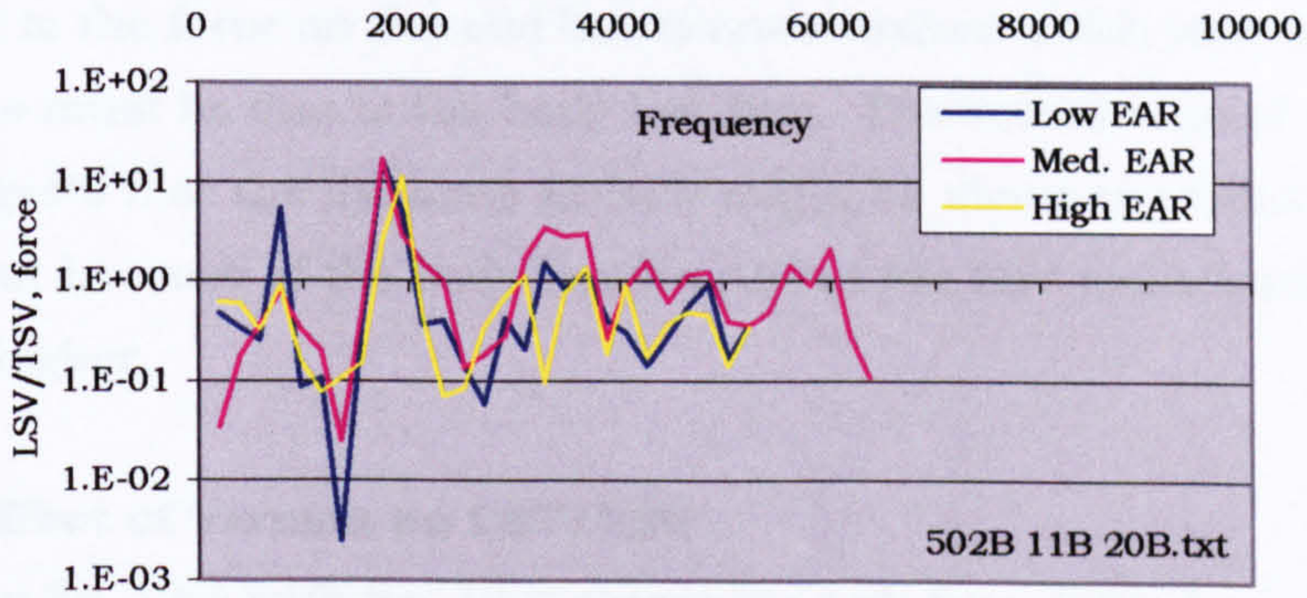

Fig. 12.6. The ratio LSV force/TSV force.
Unvarnished violins of differing EAR.

12.1.4 LSV per unit TSV, violins of different deviation

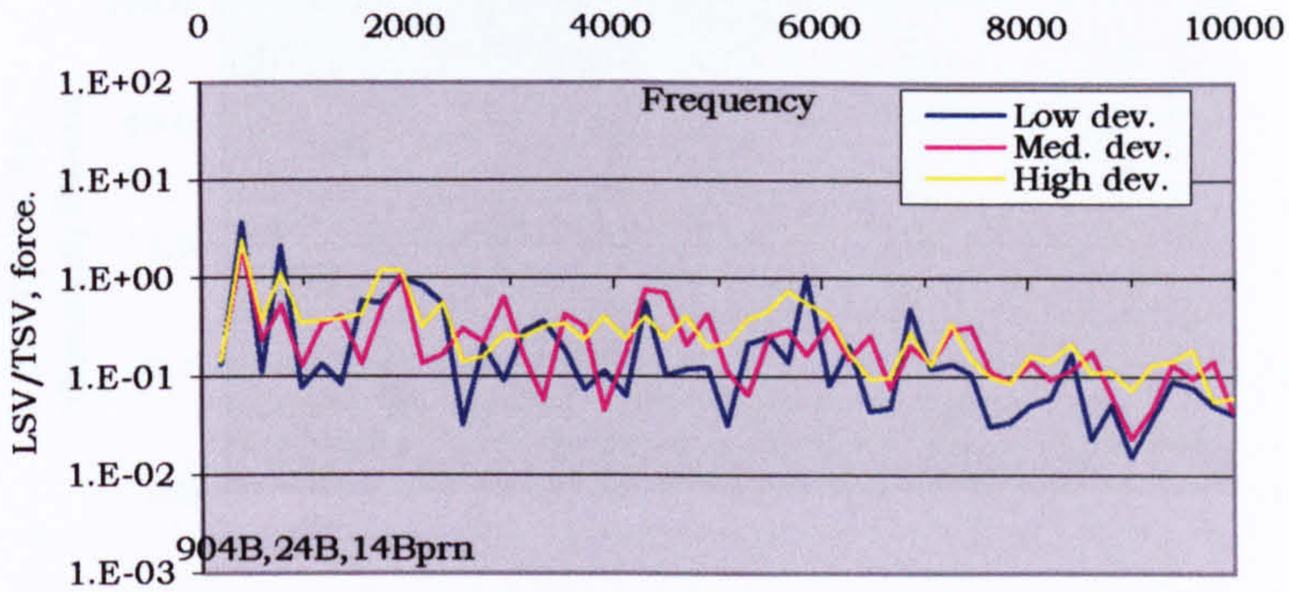

Fig. 12.7. The ratio LSV force/TSV force.
Varnished violins of differing deviation.

Fig. 12.7 shows that for a varnished violin the range of variation in LSV force/TSV force is rather less than it was for the unvarnished violins.

There is some evidence that the LSV per unit TSV increases with the deviation, which is to be expected since we have seen that it also shows dependence on the EAR. The average from 1500 to 10,000Hz is 0.22 for the low deviation violin, 0.245 for the medium deviation and 0.30 for the high deviation, the variation being in the ratio of 1 to 1.1 to 1.36. The difference in deviation between these violins is in the ratio 1 to 1.5 to 2. The deviation determines the force on the end bouts cross arch, this determines the amount of movement of the EBX arches that would be caused by LSV. If all the dynamic activity of the body had been caused by LSV, the LSV force/TSV force ratio should be 1 : 1.5 : 2, provided that it is all related to the force on the end bouts cross arches which may not be so since some must be due to the body bending. The actual ratio of 1 : 1.1 : 1.36, suggests that the dynamic activity might be about one third caused by LSV, but because of the body bending effect the LSV contribution is probably higher.

12.1.5 Effect of varnish on LSV/TSV

Comparing fig. 12.6 with fig. 12.7 shows the LSV force/TSV force has been lowered and made spectrally more uniform by applying varnish to the violin. The medium deviation violin in fig.12.7 is the same violin as the medium EAR violin of fig. 12.6 except that it has been varnished.

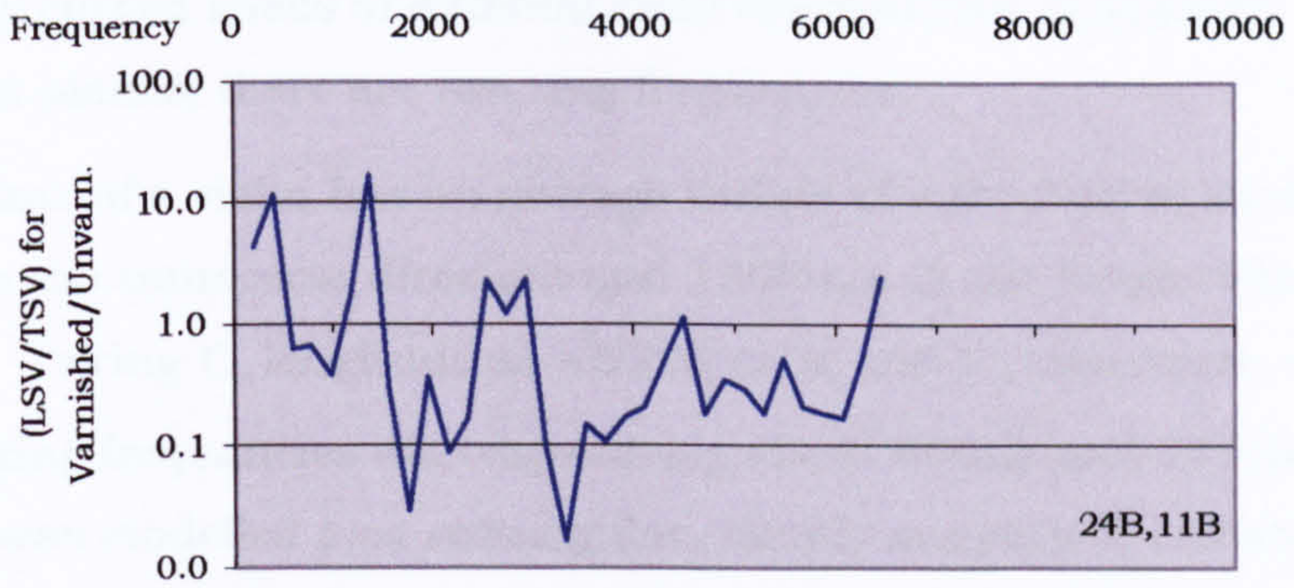

Fig. 12.8 Ratio LSV force/TSV force, for a varnished violin divided by that of an unvarnished violin.

Fig. 12.8 shows the LSV force/TSV force ratio for violin 156 varnished divided by that of the unvarnished violin. Above 1500Hz, there is mostly a lowering of the LSV force per unit of TSV. Below 1500Hz the LSV force/TSV force has increased.

The forces acting on the body excite modes. It is now time to consider the body modes.

12.2 The spectrum of body resonances

12.2.1 Theoretical assessment of modal density

The violin body can be considered approximately as comprising doubly curved, orthotropic plates. It is possible to make some theoretical prediction of the frequency distribution of the modal frequencies in curved plates.

In flat plates, the modal density of the flexural modes is independent of frequency. The effect of plate curvature is to introduce membrane stresses to the flexural waves. These in general increase wave speed and radiation efficiency, but lower the modal density below the ring frequency f_R. The modal density rises with frequency to a peak at f_R and above it the modal density is unchanged by the effects of curvature and is independent of frequency. The ring frequency of a singly curved shell of radius of curvature r is given by: $f_R = \frac{C_e}{2\pi r}$, where C_e = longitudinal wave speed in the material.

For doubly curved shells of different radii of curvature in opposite orthogonal planes, there are two ring frequencies.

The top plate of a violin has an average radius of curvature of about 250mm in the transverse direction and 1300mm in the longitudinal direction. Taking C_e longitudinal ≈ 6300 m/s; and C_e transverse ≈ 1400 m/s, the ring frequencies are respectively about 900Hz and 740Hz. The top plate was modelled as a rectangular, simply supported, orthotropic, doubly curved shell. Using Statistical Energy Analysis Software

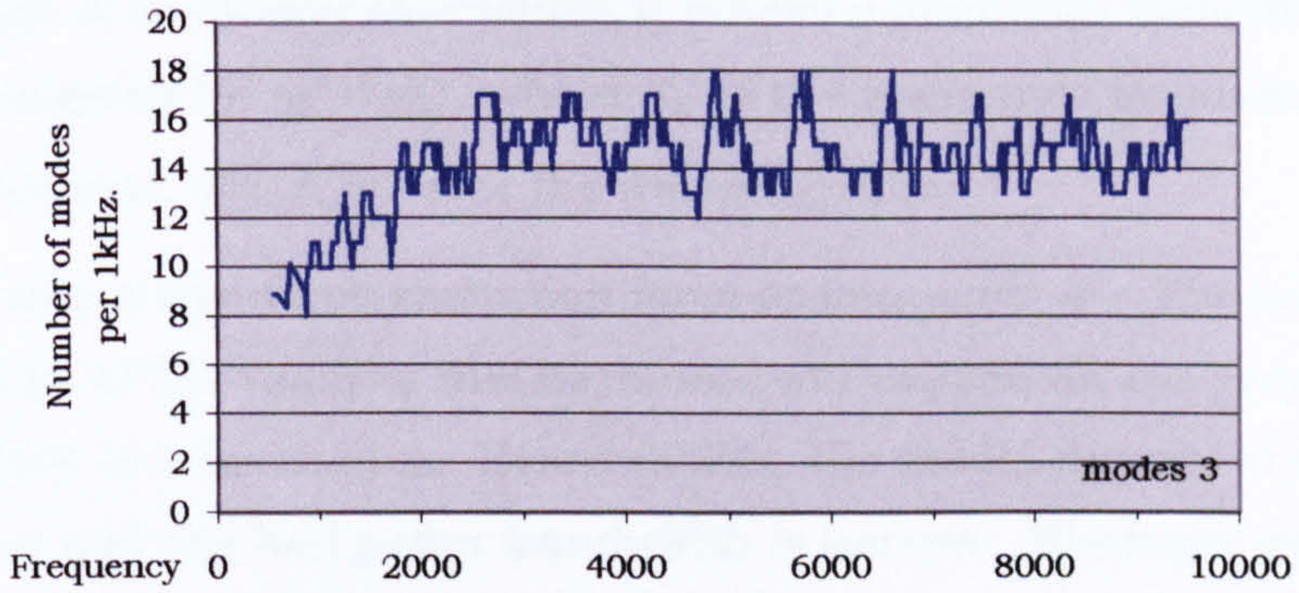

Fig. 12.9 Modal density, modes per 1kHz band.

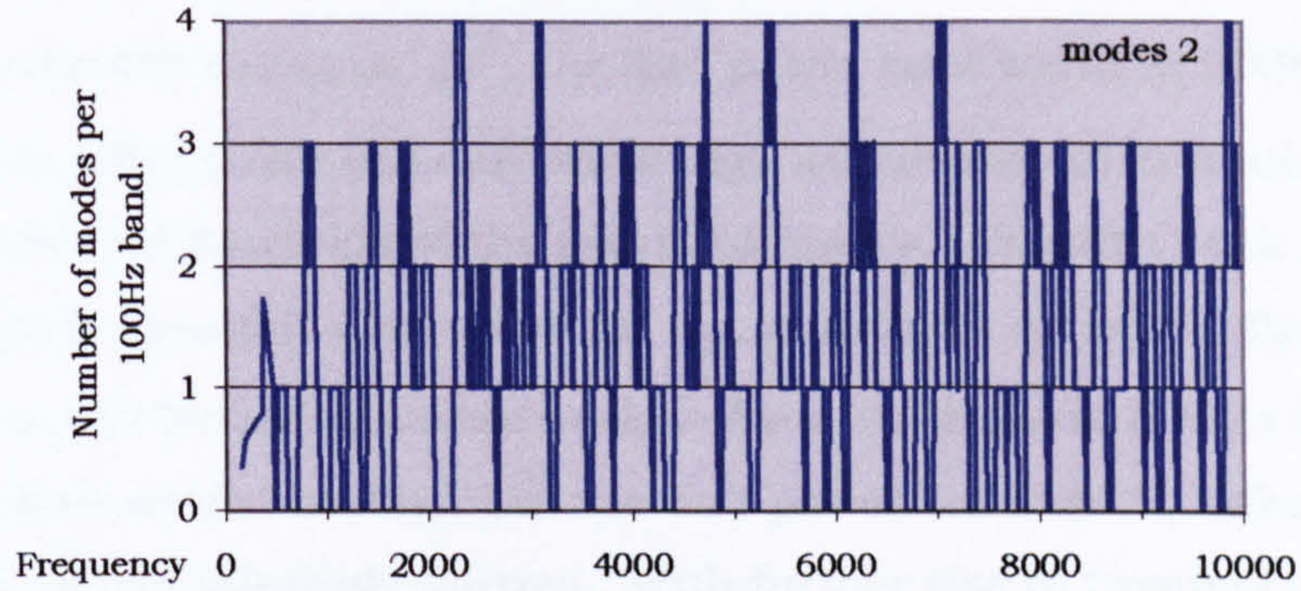

Fig. 12.10 Modal density, modes per 100Hz band.

"AUTOSEA2", a plot of the modal density was produced. This is shown in fig. 12.9. Every point on this graph shows the number of modes contained within a 1kHz wide band, centred on that point.

Generally, the modal density increases with rising frequency, becoming uniform above 2500Hz. Fig. 12.10 shows the number of modes within a 100Hz band, which is of course more variable. The modal density is very

low below 380Hz. There is small increase at 380Hz, bigger peaks at 870, 1480, 1800, and 2360Hz and above 2360Hz, the modal density becomes more uniformly high. This is not a spectrum of body resonances.

12.2.2 Theoretical assessment of the spectrum of body resonances

A plot of the admittance of the body to an external force, applied at any mobile point on the violin body, against the frequency for a single isolated violin mode would rise with increasing frequency reaching a maximum at resonance and then fall. The half power bandwidth of a mode Δ, which is in the range of frequency over which it makes a dominant contribution to response is given by $\Delta f = \eta f_0$, where f_0 is the resonance frequency, and η is the loss factor, which is twice the damping ratio.

Consider now a harmonic excitation force at frequency ω. The admittance at the bridge of the violin to this harmonic will depend on the proximity of its frequency to a resonance. Below 800Hz, the modal density of the top plate is low and the half power bandwidth is narrow. Bissinger gives a total loss factor of about 0.03 at 1000Hz. *(A personal communication, 2001, to F J Fahy, Southampton University, from G Bissinger, East Carolina University.)* This would give a half power bandwidth of 30Hz. In most structures the half power bandwidth varies as $\sqrt{f}$: the half power bandwidth at 800Hz is about 27Hz. The violin will only show high admittance to excitation very near the isolated locations of the resonant modes. Because peak modal admittance is inversely dependent on ω_0, and since ω_0 is low, the modal admittance will be high at these peaks. As ω rises above 800Hz it enters a zone of higher modal density, but the half power bandwidth, although increased, is still relatively narrow. With further rise in frequency, the half power bandwidth rises. An applied harmonic excitation is able to excite say a mode at resonance plus the tails of adjacent modes. This tendency to overlap more than one mode increases as ω moves further into the zone of higher modal density that began at about 800Hz. At 2500Hz, the half power bandwidth reaches 50Hz, and the modal separation is 60Hz. Once the modal overlap factor exceeds unity, individual admittance peaks will not be evident and the admittance will not vary as $1/\omega_0$ but will tend to become dependent on the modal density. This is approximately at 2500Hz.

With further increase in frequency beyond this point, the admittance would not increase. Moreover, with increasing modal overlap a multimode system tends to that of a modeless system. It is therefore reasonable to expect the admittance to rise with rising frequency above 800Hz and asymptote to a rather uniform value at higher frequencies.

12.2.3 Measured spectra of body resonances

If the body is excited by an external force at any one frequency, applied at any mobile point on the violin body, a number of modes will be excited. The admittance to an external force applied at the bridge is thought to be indicative of modal behaviour that will have significance in the bowed instrument. The admittance at the bridge is the transfer function of the transverse in-plane velocity at the top of the bridge divided by the external driving force. The admittance spectrum is commonly found by driving the bridge at all frequencies, with electromagnetic drivers, and recording the velocity of the bridge, or by impact excitation of the bridge. Fig. 12.11 shows the admittance at the bridge to a transverse force applied externally to a fine concert violin by Stradivari. The presence of the peaky zone below 1kHz, and a rise to a maximum at 2000Hz followed by a decline, was predicted by theoretical argument based on the theoretical distribution of modal density. In most literature, the broad hill is referred to as the bridge hill, because of earlier suggestions that it might be caused by bridge resonance. It was noted in Chapter 2 that later research showed that the bridge behaved as a semi-rigid lever at all frequencies. Our analysis shows that the hill coincides with a zone of high modal overlap. If it is true that the high frequency admittance reflects the average modal density and half power bandwidth of the body, then the shape of the high frequency admittance curve would be much the same regardless of where on the body the force was applied and the admittance measured.

The power transferred to the bridge per unit external force is proportional to the magnitude of the admittance multiplied by the cosine of the phase. It will be noticed that at the resonance peaks the phase passes through zero, enabling a maximum transfer of power. In the many areas where the phase moves towards +or- 90 degrees the power transfer per unit force is greatly reduced. At +or- 90 degrees, the power would go in at one part of

the cycle and out at the other. There are also anti-resonances where the phase is 0 degrees but the power transfer is small because the admittance is low. The value of curves showing the magnitude of the admittance is limited by the inconvenience of not embracing the phase and therefore telling us something about the power inflow to the body. The real part of the admittance does give a more direct indication of the power flow into a violin.

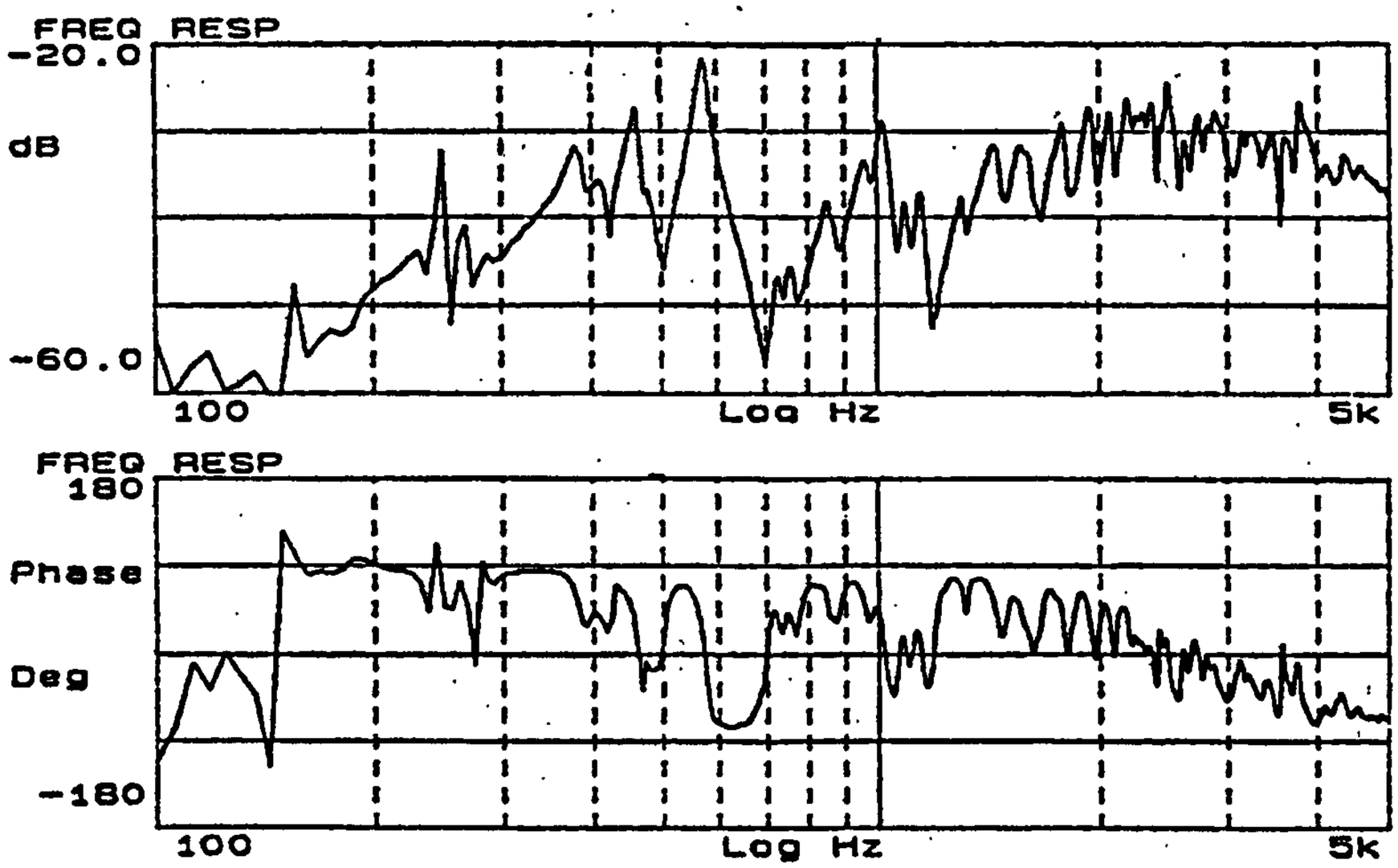

Fig 12.11 Frequency response (velocity/force) of a violin by Stradivari 1709. (0 db corresponds with 2 s/kg) (Jansson, 1994)

The admittance at the bridge is that resulting from the application of an external force. Because the admittance varies with the frequency, the power per unit force entering the body varies with the frequency. In a bowed violin, the string admits the external force. If an external force is applied directly to a string the admittance of the string would show very pronounced harmonic peaks but the envelope of harmonic peak heights would vary smoothly with the harmonic number. The string would accept a very different spectrum of input power from a unit external force than the bridge would. The power in the string then passes into the body, but not only through transverse excitation of the bridge. The admittance of the bridge to both transverse and vertically applied forces from the vibrating

string is examined in section 12.3. The transfer of power to the body is also considered.

12.3 The admittance and power transferred at the input ports.

12.3.1 The experimental method

If the transfer function of velocity and the force (admittance) at any input port is known, the power input per unit force can be derived. The TSV force can be calculated from the measured string velocity. The LSV force is measured at the tail gut transducer. In order to calculate the pseudo-admittance of the bridge to LSV the assumption is made that the LSV in the group of four strings is the same as that in a single combined string placed at the centroid (see concept of the combined string introduced in section 3.2.4), and that it is the same as that measured at the tail gut. This may be so up to the first string longitudinal resonance. The assumption is reasonable off longitudinal resonance. We have not discovered any evidence that longitudinal resonance in the string is significant. The acceleration in the direction of the string can be measured at both the saddle (over which the tailgut passes) and the nut (at the entrance to the peg box). This was done at the saddle but not (regrettably, with the benefit of hindsight) at the nut. By measuring the vertical acceleration at each foot of the bridge, it is possible to calculate the velocity in the both the transverse and vertical directions of the centre of the top of the bridge. This assumes that the bridge behaves as a semi-rigid lever [confirmed by, Runnemalm, Molin and Jansson, 1998] and that there is little horizontal movement of the bridge feet compared to the vertical movement.

An accelerometer was placed immediately in front of each bridge foot in turn (on the bow side) (see Chapter 6 for details of the accelerometer used). In addition to recording the output from the accelerometer, the LSV was measured, and the transfer function acceleration/LSV force was analysed. This enabled the phase difference between the two bridge feet to be determined. The bridge was assumed to have two degrees of freedom: rotation about the centre point of its base and vertical translation. The experimental results give information from which the displacement of the

bridge feet, the admittance of the bridge to TSV, LSV, and the power exchanged between the string and the body at the bridge and the saddle can be inferred.

The open G string was driven to a displacement amplitude of 3.25mm.
The measured data was as follows.

The rms spectrum of the LSV force at the tailgut.
The rms spectrum of the string velocity at the magnet location.
The following transfer functions,

(A+jB) where,

$A=R_e\left\{\frac{\alpha_1}{F_{LSV\,tail}}\right\}$, real part TF, accel/LSV force, at bass bar foot.

$B=I_m\left\{\frac{\alpha_1}{F_{LSV\,tail}}\right\}$, imaginary part TF, accel/LSV force, at bass bar foot.

(C+jD) where,

$C=R_e\left\{\frac{\alpha_2}{F_{LSV\,tail}}\right\}$, real part TF, accel/LSV force, at sound post foot.

$D=I_m\left\{\frac{\alpha_2}{F_{LSV\,tail}}\right\}$, imaginary part TF, accel/LSV force, at sound post foot.

(G+jH) where,

$H=I_m\left\{\frac{\alpha_1}{\bar{v}_m}\right\}$, imag. part, accel/vel. of string at the magnet, at bass bar foot.

$G=R_e\left\{\frac{\alpha_1}{\bar{v}_m}\right\}$, real part, accel/vel. of string at the magnet, at bass bar foot.

G was not measured.

(K+jL) where,

$L=I_m\left\{\frac{\alpha_2}{\bar{v}_m}\right\}$, imag. part, accel/vel. of string at the magnet, at sound post foot.

$K=R_e\left\{\frac{\alpha_2}{\bar{v}_m}\right\}$, real part, accel/vel. of string at the magnet, at sound post foot.

K was not measured.

$R = I_m\left\{\frac{\alpha}{F_{LSV\ tail}}\right\}$, imaginary part, accel/LSV force, at saddle.

The LSV force, $F_{LSV\ tail}$, is the LSV force in the string as measured at the tailgut. (The data was originally collected with another purpose in mind, which did not require G and K to be measured.) The following formulae were derived to convert the data to the information below. The derivation of the formulae is given in Appendix D. The formulae include the variables E,F,M, and N. These are parts of transfer functions as follows.

E+jF, the transfer function of the acceleration of the bass bar foot of the bridge over the TSV force on the bridge from the string.

M+jN, the transfer function of the acceleration of the soundpost foot of the bridge over the TSV force on the bridge from the string.

These variables are related to the measured transfer functions as follows; E=-H/r, F=G/r, M=-L/r, and N=K/r. (see Appendix D)

where $r = \dfrac{T\frac{n\pi}{L}\frac{n\pi a}{L}}{\omega\,\mathrm{Sin}\frac{n\pi x_0}{L}\mathrm{Sin}\frac{n\pi a}{L}}$

The rms vertical velocity of the centre top of the bridge,

$$V_v = \frac{F_{LSV\,tail}}{2\omega}\sqrt{(B+D)^2+(A+C)^2}$$

The rms horizontal velocity of the centre top of the bridge,

$$V_t = \frac{0.37\times F_{LSV\,tail}}{\omega}\frac{h}{w}\sqrt{(B-D)^2+(C-A)^2}$$

The magnitude of the bridge pseudo-admittance to LSV,

$$|Y_v| = \frac{1}{0.37\times 2\omega}\sqrt{(B+D)^2+(A+C)^2}$$

and the corresponding phase, $\phi_v = \mathrm{Cos}^{-1}\left(\dfrac{(B+D)}{\sqrt{(B+D)^2+(A+C)^2}}\right)$.

F and N are related to the unmeasured variables G and K. They can be estimated as; $F = S\,\mathrm{Sin}\left(\mathrm{Cos}^{-1}\frac{E}{S}\right)$, where $S=\sqrt{A^2+B^2}.\left|\frac{F_{LSV}}{F_{TSV}}\right|$

and $N = T\,\mathrm{Sin}\left(\mathrm{Cos}^{-1}\frac{M}{T}\right)$, where $T=\sqrt{C^2+D^2}.\left|\frac{F_{LSV}}{F_{TSV}}\right|$.

The magnitude of the bridge pseudo-admittance to TSV,

$$|Y_t| = \frac{h}{w}\frac{1}{\omega}\sqrt{(E-M)^2+(F-N)^2}$$

and the corresponding phase, $\varphi_t = \mathrm{Cos}^{-1}\left[\frac{(F-N)}{\sqrt{(E-M)^2+(F-N)^2}}\right]$.

The power to bridge from LSV, $W_{LSV} = \frac{0.37\,F_{LSV\,tail}^2}{2\omega}(B+D)$.

The power to bridge from TSV, $W_{TSV} = F_{TSV}^2\frac{h}{w}\frac{(F-N)}{\omega}$.

The power to saddle from LSV, $W_s = F_{LSV\,tail}^2\frac{R}{\omega}$.

The relative phase of LSV and TSV, $\frac{F_{TSV}}{F_{LSV}} = \mathrm{Tan}^{-1}\left[\frac{BE-AF}{AE+BF}\right]$

12.3.2 The displacement of the bridge feet

The vertical movement of the bridge feet was found. The results show no discernible consistent difference between the three violins of different deviation, and so the graph for one violin only (V158LD) is shown. The fig. 12.12 shows the displacement of the bass bar foot of the bridge, and fig. 12.13 that of the sound post foot. These very small displacements were not measured directly but were derived from the measured accelerations by dividing by the square of the frequency. It is not easy to compare figs. 12.12 and 12.13 to see the relative magnitude of the bridge foot movement. To facilitate the comparison, fig. 12.14 shows the peak displacement values of each bridge foot as a continuous line.

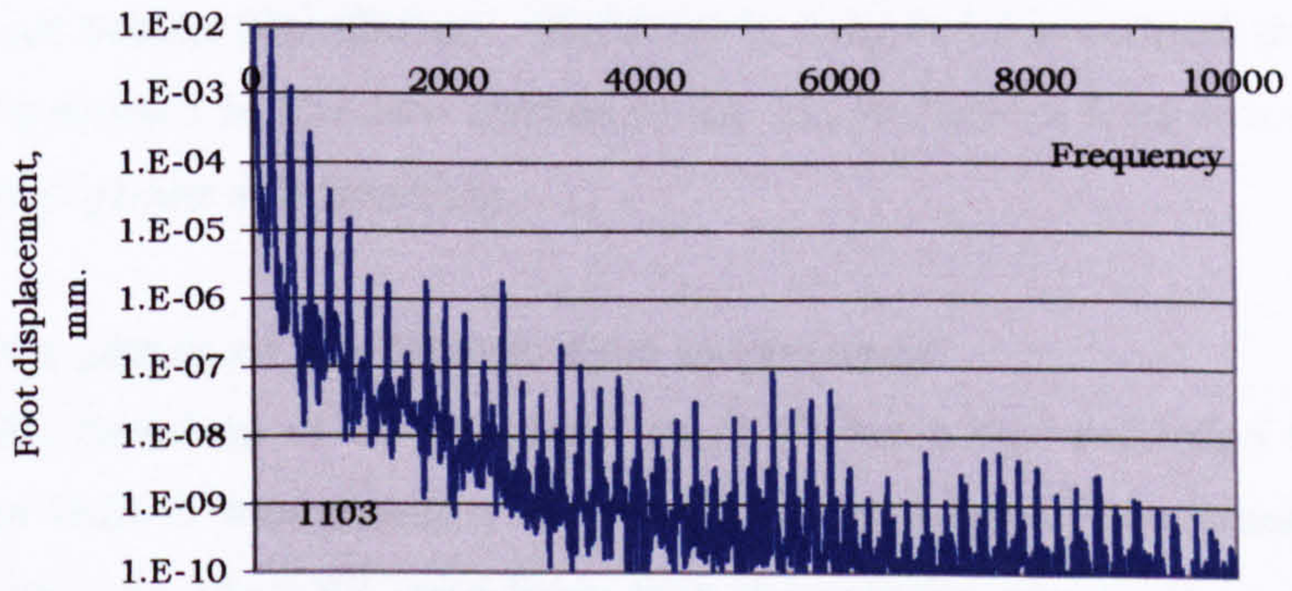

Fig. 12.12 Displacement of bass bar foot of bridge, shaker driven G string, V158.

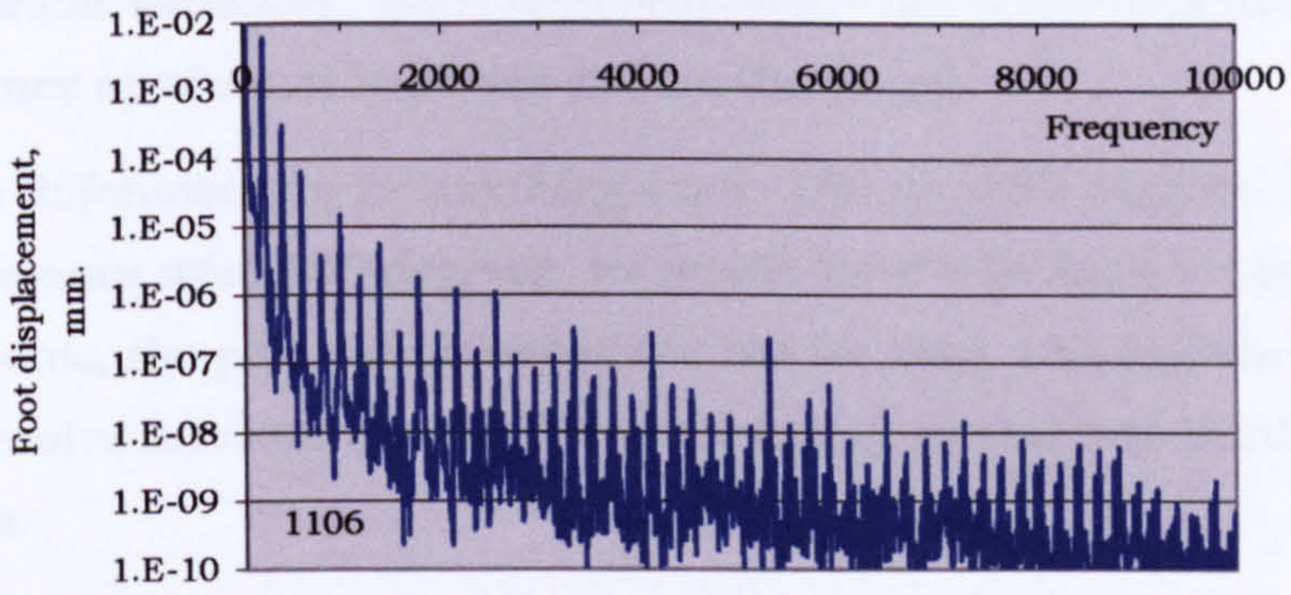

Fig. 12.13 Displacement of sound post foot of bridge, shaker driven G string, V158.

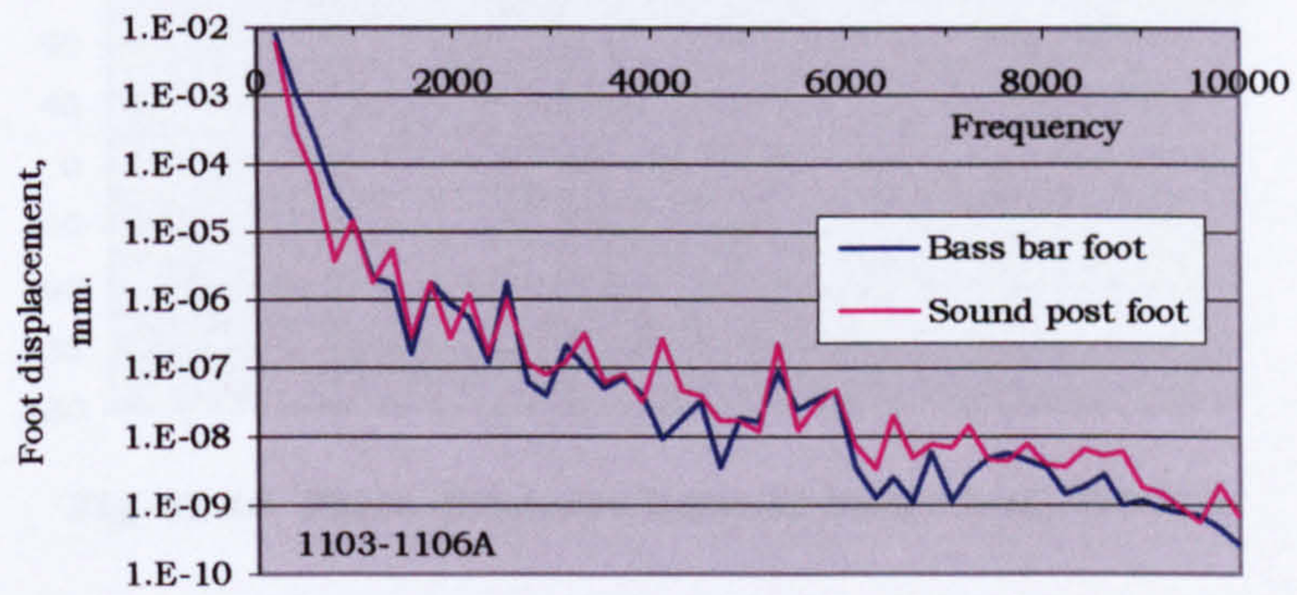

Fig. 12.14 Bridge foot displacement compared, V158.

At the first harmonic, the bass bar foot moves 25% more than the sound post foot. At the fourth harmonic, the bass bar foot moves ten times as much as the sound post foot. The bridge movement can be seen as a combination of two basic movements. These are a rotation about the centre of the base, and a vertical translation. It would be helpful to take the displacements shown in fig 12.14 and separate them into bridge rotation and bridge translation. However it cannot be assumed that the movements shown in the two curves of fig. 12.14 have a frequency-independent phase relationship.

12.3.3 The phase of the bridge foot movement

The transfer function of the acceleration/LSV force was recorded for each foot. From this, it was possible to calculate the phase of movement of each foot in relation to the LSV, and from this the relative phase of one foot to the other. This is shown in fig. 12.15 for V158. The other violins tested

showed similar variation. Each spot represents the phase of a harmonic at the frequency at which it is positioned on the graph.

The phase difference can be anything from -180 to +180 degrees. If the phase difference were 180 degrees, we would have a rocking bridge. In the first harmonic, the phase differences are not far from 180 degrees but there is a progressive movement away from this at the second and third harmonics.

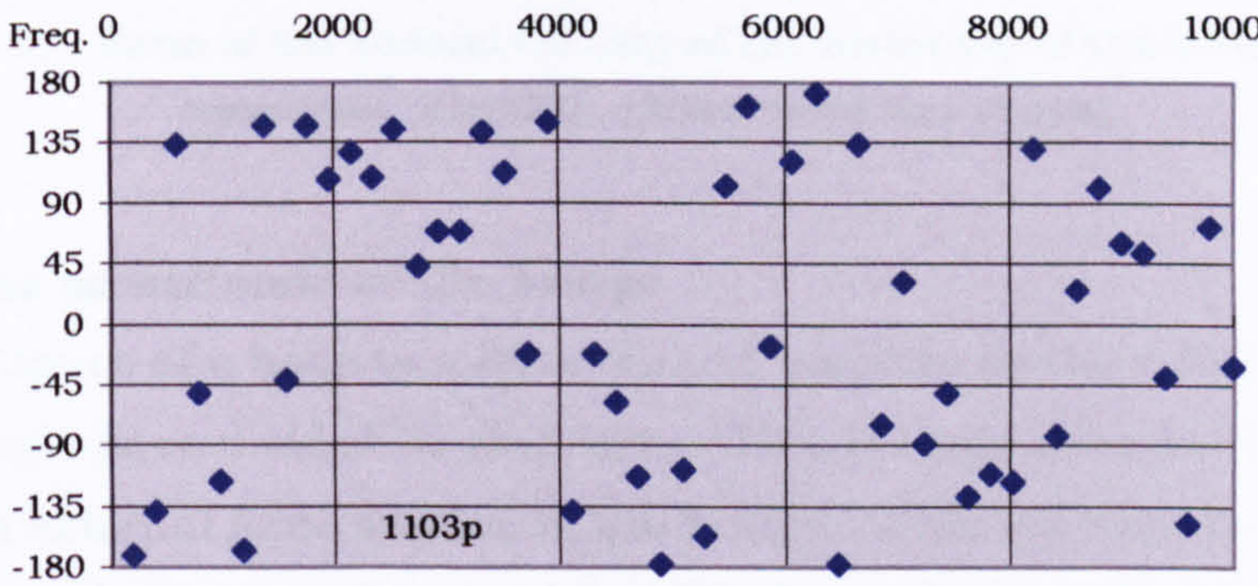

Fig. 12.15 Phase difference between bridge feet, V158LD.

12.3.4 Velocity of the top of the bridge

Using the formulae given in 12.3.1, the transverse and vertical velocity of the centre top of the bridge was found. Fig 12.17 shows that the trend of the ratio is to be less at the low frequencies and to increase with rising frequency.

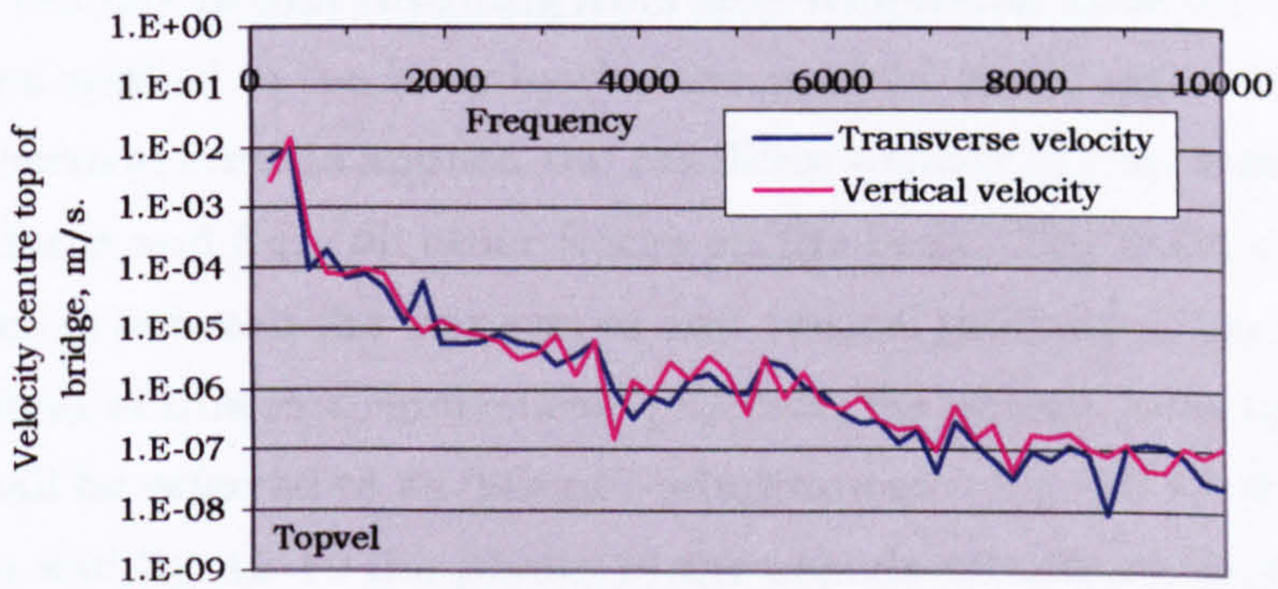

Fig 12.16. Transverse and vertical velocity magnitudes of the centre top of the bridge, shaker driven G string, V157 HD.

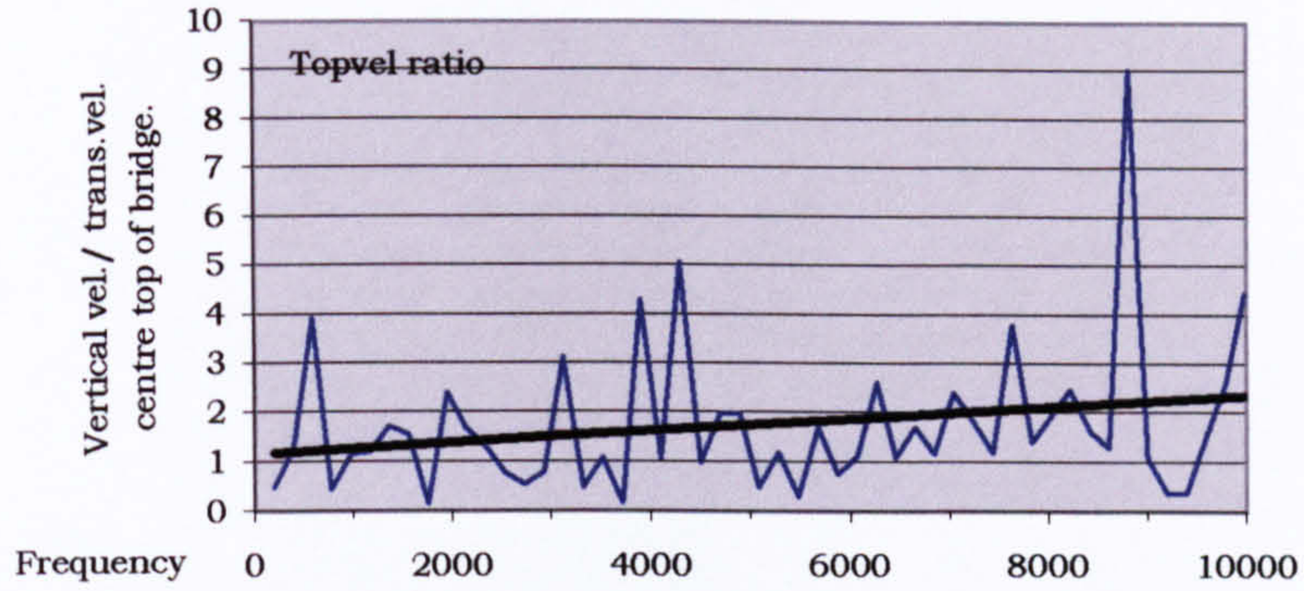

Fig 12.17. Ratio of the vertical velocity of the centre top of the bridge to the transverse, V157HD. (linear trend line shown)

12.3.5 The admittance of the bridge

The admittance of a body to a force should properly be the velocity arising from a single force divided by that force. This is easily measured in the case of an external force applied to the bridge. What we want to know is what is the admittance of the bridge to the forces from a vibrating string. These are internal forces because the string is part of the vibrating system. We can estimate the transverse force acting on the bridge from the string, together with the transverse motion of the bridge. We can also find the vertical LSV force acting on the bridge, together with the vertical motion of the bridge. We can therefore find the admittance of the bridge to these forces. However, the admittances found in this way are not fully independent of each other. When the transverse force is applied, the measured velocity is that resulting from that transverse force and from all other forces applied to the body by the string at the same time. Similarly, when the vertical force is applied the resulting velocity is that resulting from that force and from all other forces on the body. The main scope for interference is between the transverse and vertical motions of the bridge. In recognition of this insurmountable problem, the admittances found in this way will be referred to as 'pseudo-admittances'. Fig. 12.18 shows the magnitude and fig. 12.19 the phase, of the pseudo-admittances of the bridge to TSV and LSV forces. The admittance to vertical force is higher than that to the transverse force, and the difference increases with rising frequency.

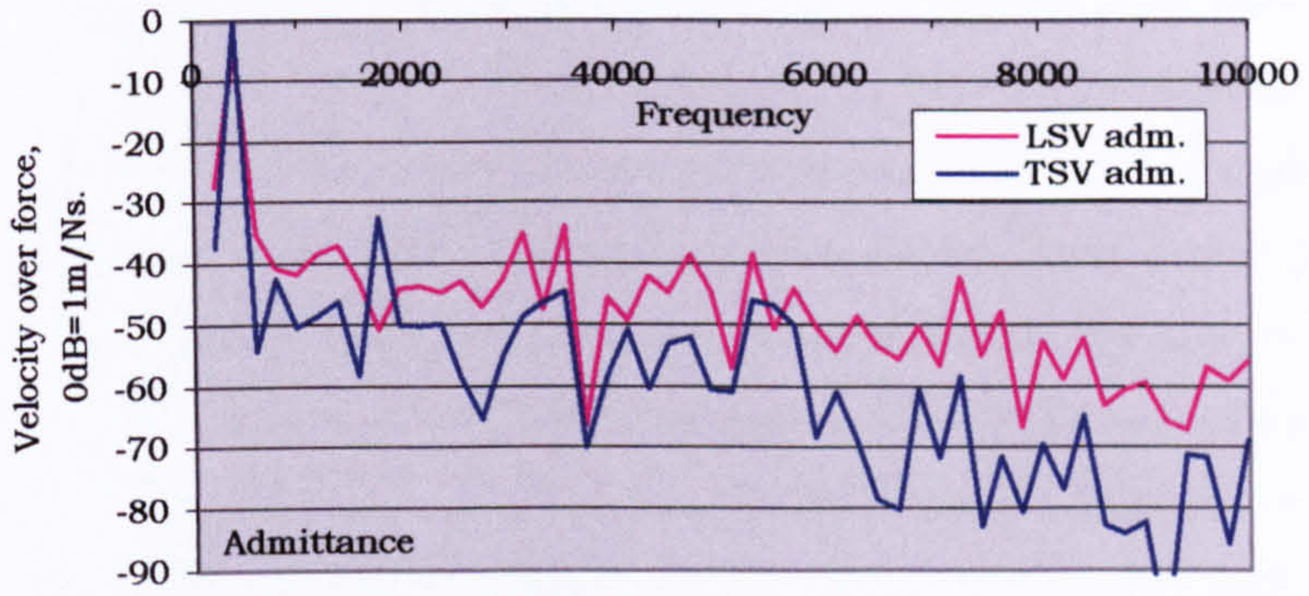

Fig 12.18 Magnitude of the pseudo-admittance of the bridge to TSV forces and LSV forces, V157HD.

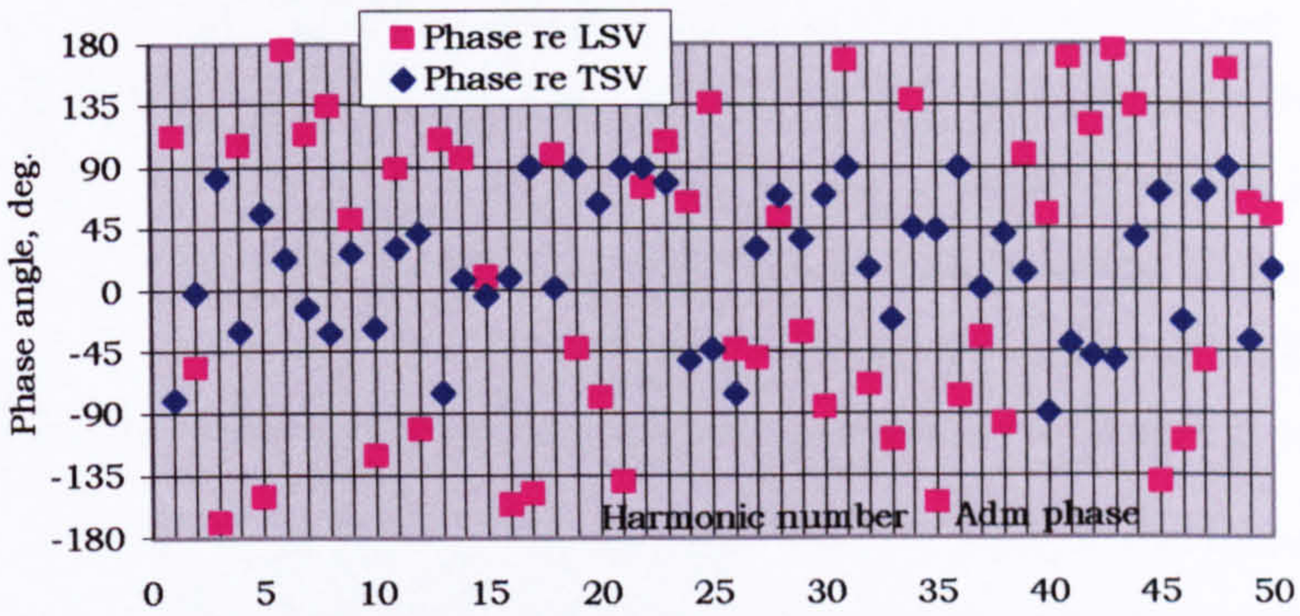

Fig 12.19. Phase of the pseudo admittance of the bridge to TSV forces and LSV forces, V157HD.

This difference reflects the difference in bridge top velocities shown in fig.12.17, together with the fact that the LSV force is lower than the TSV force. Interestingly, the TSV phase variation corresponds quite closely with that shown in fig. 12.11 but with an additional factor of π. The string swinging excitation must have produced lower bridge top translations than the external force.

Above 600Hz the magnitude of the pseudo-admittance of the bridge to a transverse force from the string as presented here is far smaller than that of the admittance to an external force found by others. It appears that there is some mechanism by which the free transverse vibration of the string that is not present in the direct measurements of admittance suppresses the transverse bridge velocity induced by TSV. The author has considered this matter carefully and cannot find a simple explanation. Inspection of the measured deformation of a violin body under string tension shown in Chapter 4 reveals that when the tension in the 'combined

string' is increased the bridge drops more on the sound post side than it does on the bass bar side. Thus it can cause a horizontal translation of the top of the bridge. The bellying component of the LSV takes its phase from a TSV harmonic of half the frequency and we do not have any information about the phase relationship. However, depending on the phase relationship, the TSV rotation of the bridge could either be reduced or increased by bellying LSV. If, as seems to be the case, the phase relationship caused the TSV rotation to be countered by the LSV rotation, then the bridge top translation would be reduced and the admittance reduced. The inter-harmonic phase relationships of a shaker driven string will not be the same as those of a bowed string where the harmonic content comes from the Helmholtz wave, in which case the pseudo-admittances found here would not apply to the bowed violin. However, there is some reason to doubt the assumption that the bridge admittance to an external force would be the same as to a transversely vibrating bowed string. Clearly more work should be done on this using a bowed string excitation.

If it were confirmed that the LSV-induced bridge movements were counter to those caused by the TSV, it would explain certain observations. All good violins feel to the player to be very firm in the string under the bow. As the LSV response increases, it reduces the bridge movement, and since the string firmness is sampled very near the bridge it would be influenced by the bridge movement.

The interdependence of the admittances must happen in a violin. If at a particular harmonic the TSV force is high and the LSV force low the velocity resulting from the TSV force will move the bridge a large amount and may increase its apparent admittance to the low LSV force. The reverse may also happen. The effect of this interdependence would be to even out the power exchange from TSV and LSV.

12.3.6 The real part of the admittance.

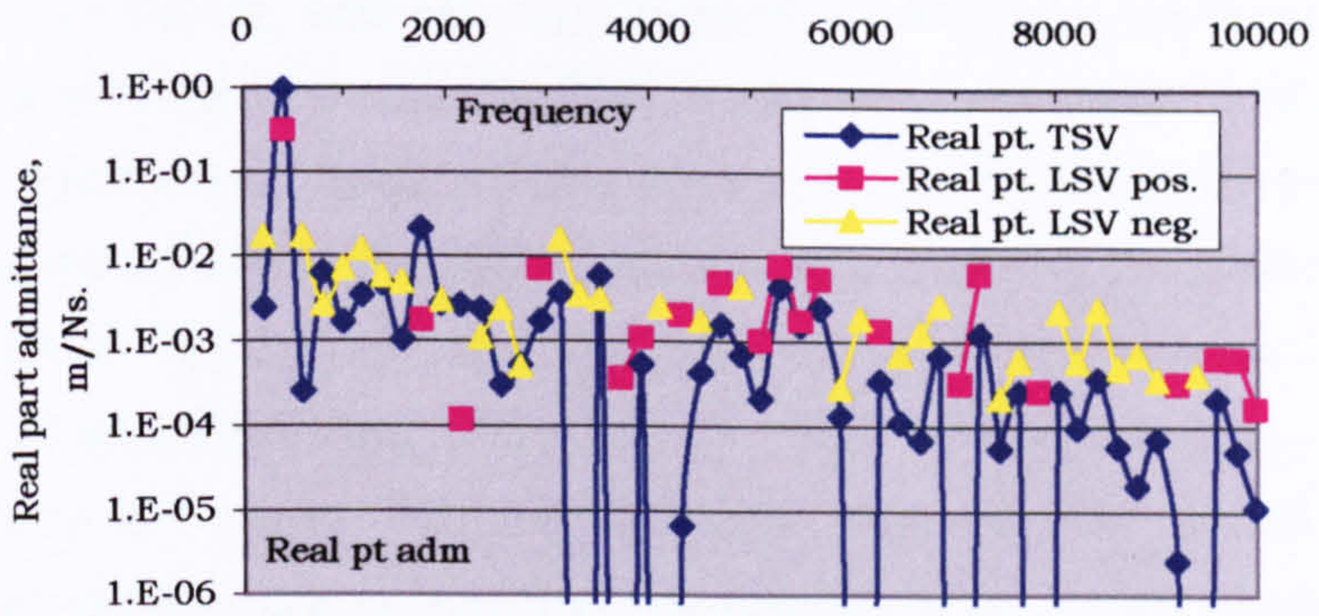

Fig. 12.20. Real part of the pseudo admittance of bridge to TSV and LSV, V157HD.

Fig. 12.20 shows the real part of the pseudo-admittances of a bridge to the forces applied by the strings. This represents the effectiveness of unit applied force as a means of transferring power. The TSV 'input' is always positive although it drops to very low values at some frequencies. The LSV 'input' can be positive or negative. The algebraic sum of the power input is shown later in fig. 12.24.

The second harmonic makes a very interesting study. At the second harmonic the transverse displacement of the string and the TSV are surprisingly low (see fig. 12.3). Fig. 12.18 shows that the magnitude of the bridge admittance to the TSV is very high at the second harmonic. At most harmonics the bridge is driven to rotate by the TSV force and this may be resisted by the bridge-rock LSV. Bellying LSV comes from the first harmonic and has a phase related to that. The very high admittance of the body to the second harmonic would suggest that the bellying LSV and the TSV are not far out of phase and combine to drive the bridge to a large transverse displacement. We have no means of confirming this since we only have phase information about the combined bridge-rock and bellying LSV, but the bellying LSV force was shown in fig. 10.2 to be of the same order as the TSV force and would have a considerable influence on the phase of the total LSV. Fig. 12.25 does show a total LSV phase to near that of the TSV. The pseudo-admittances shown in fig. 12.18, 12.19, are not independent of each other. Thus if a TSV force is applied to the bridge, and the resulting transverse movement is added to by that resulting from the bellying LSV, then the admittance will be high to that TSV force. This will

only happen at harmonics that have a strong bellying LSV contribution, i.e. the second and fourth, and can only happen if the phase relationship between the bellying LSV and the TSV is suitable. This may be the case at the second harmonic. These studies were made on a shaker driven string. If the string were bowed, the phase relationship between the harmonics could be different and so the very low even numbered harmonics in the transverse displacement spectrum and the high admittance at the second harmonic may not apply. The very high admittance to TSV is real enough, since it has resulted in a very low string displacement in the second harmonic. In the next Chapter, it will be shown that these phenomena have little effect on the radiated sound.

Fig 12.18 presents a very different picture to fig. 12.11. In making a quantitative comparison 6db should be added to the values in fig 12.11 to bring it to the same units as 12.18. Fig. 12.18 was drawn from data collected at 196Hz intervals. Despite the fact that this is only pseudo-admittance, it is apparent that an external force applied to a violin with damped strings excites a different array of internal forces.

12.3.7 Power per unit force

The time-average power exchanged at the input ports is the time-average product of force and velocity, or (for harmonic vibration) the real part of the admittance times half the square of the magnitude of the input force. The power exchanged was found for TSV driving the bridge transversely, LSV driving the bridge vertically, and for LSV driving the saddle in the direction of the string. The power exchanged at the nut (peg box end) in the direction of the line of the string was not measured. The power found in this way is not pseudo, but is the real power exchanged at the port. The three graphs presented in this section show the power divided by the square of the force. By dividing by the square of the force, the graphs represent the effectiveness with which unit force can transfer power at the port. The actual power is shown in section 12.3.8.

Fig. 12.20 shows the power divided by the square of the TSV force, entering the bridge from the string. Relative to the other inputs of power from the string the TSV contribution is high up to about 3500Hz. After that there are a number of frequencies where the power input (always positive) falls to

a very low figure. There is a general decline in the high harmonics. A TSV force applied at the second harmonic would take a large amount of power out of the string and input a large amount of power to the bridge. This reflects the high magnitude of the admittance and a phase of zero degrees. The TSV would also input quite effectively at the ninth harmonic.

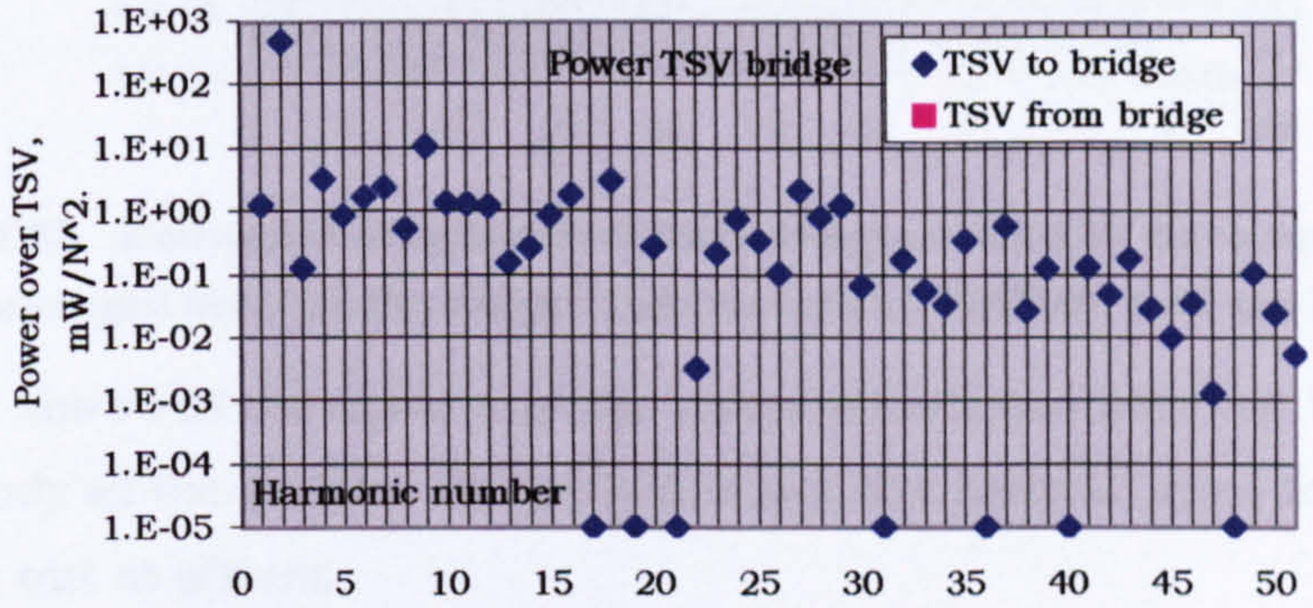

Fig 12.20. Power per unit TSV force squared, exchanged between the string and the bridge, V157HD. (mW per N²)

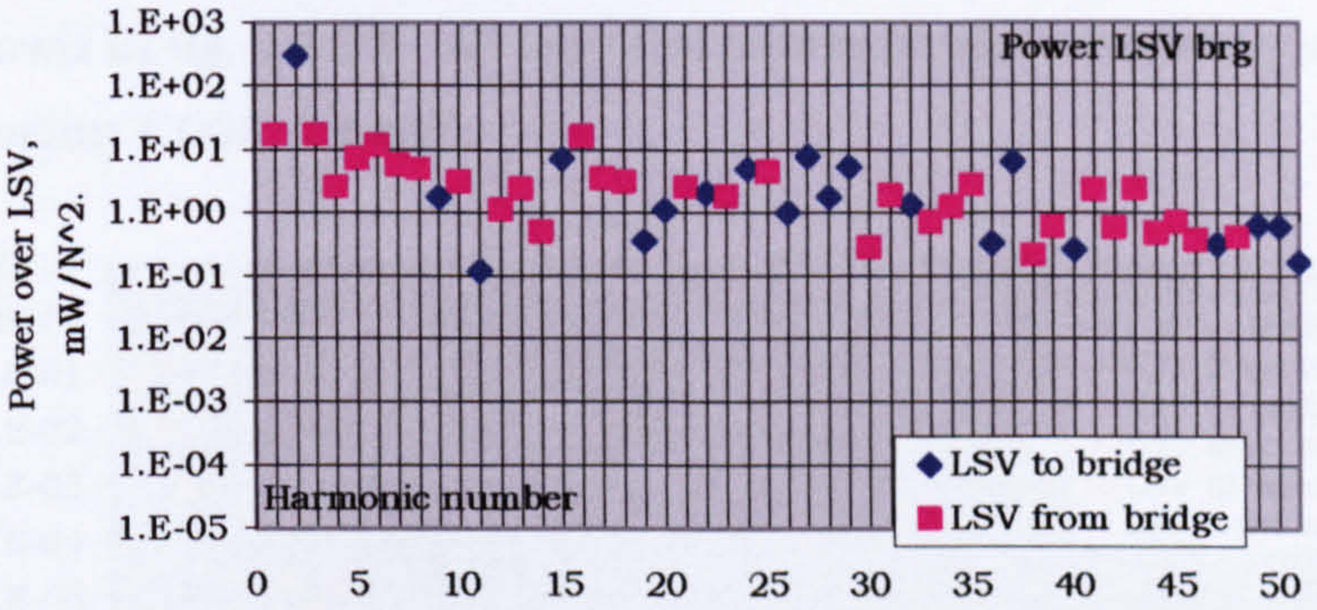

Fig 12.21. Power per unit of LSV force squared, exchanged between the string and the bridge, V157HD. (mW per N²)

Fig. 12.21 shows the power divided by the square of the LSV force, exchanged between the bridge and the string. Compared to the TSV the LSV power exchange is higher at the low frequencies and in general falls off less with rising frequency. Most obviously the power flow is more generally out of the bridge into the string. This is entirely consistent with the principle of bridge-rock LSV, where the rocking bridge does work on the string. At the second harmonic the LSV is predominantly developed from string bellying and this would explain why energy is put into the body from the string.

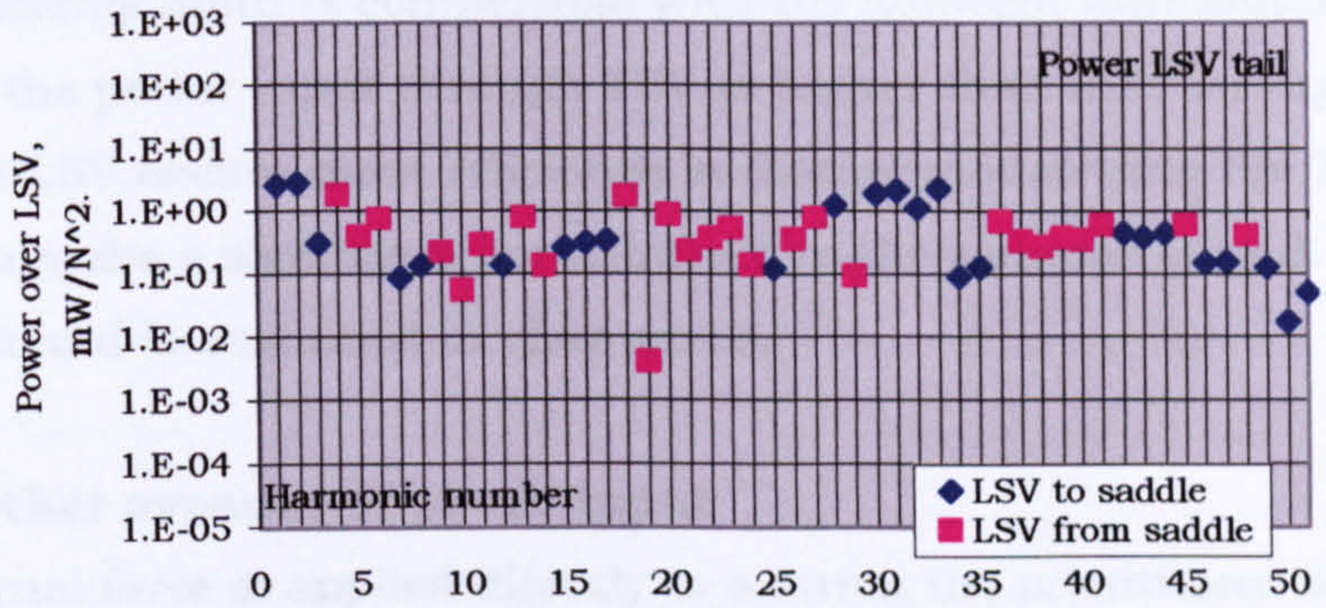

Fig 12.22. Horizontal component of the power per unit LSV force squared, exchanged between the tailgut and the saddle, V157HD. (mW per N²)

Fig. 12.22 shows in the same way the power exchanged between the tailgut and the body at the saddle. Power is put into the body at some frequencies and taken out at others.

12.3.8 Power exchanged at the ports

We now look at the absolute powers exchanged at the bridge and saddle. This is shown in fig. 12.23. All very low power levels are shown in the graph as being 1.00E-10 mW.

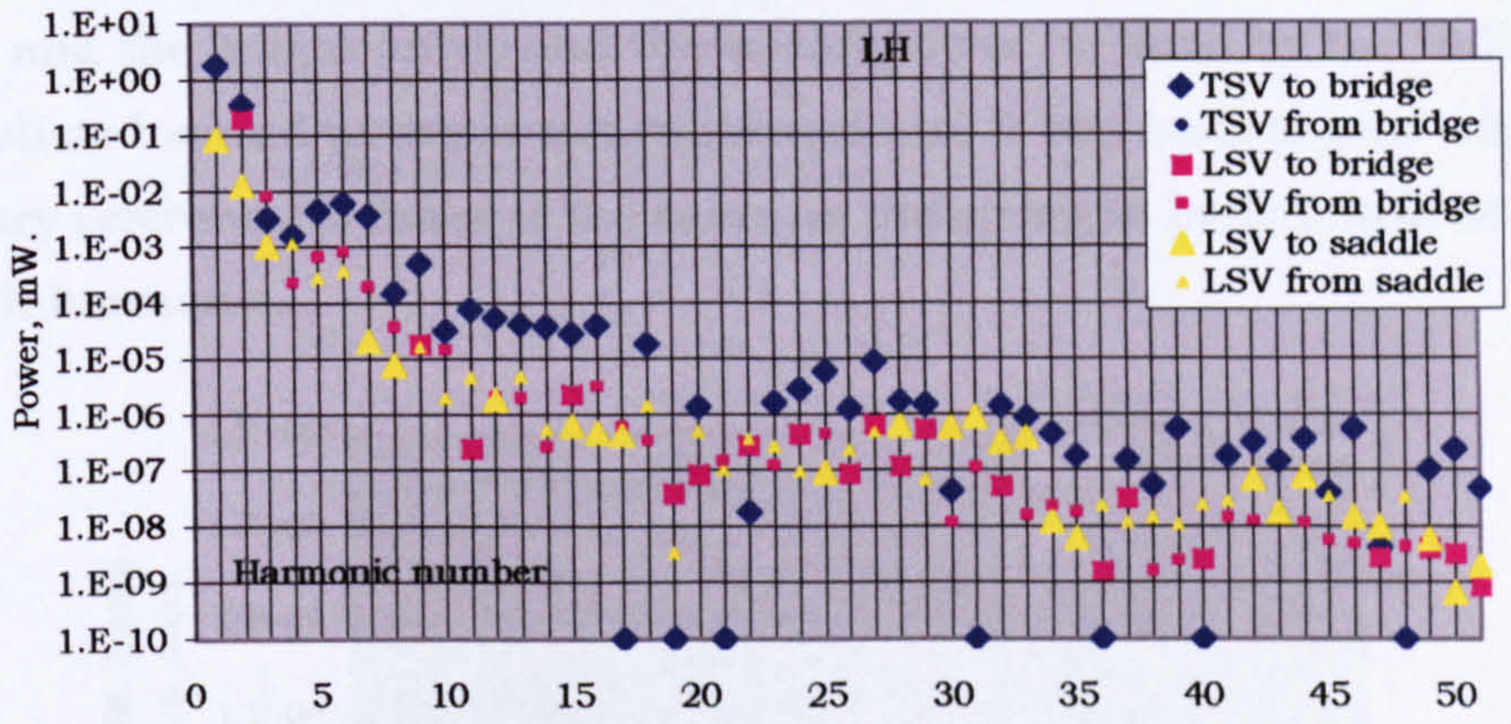

Fig. 12.23. Power exchanged at the bridge and saddle, V157HD. (mW)

Consider first the power exchanged at the bridge. At all harmonics, the TSV puts power into the bridge. At most harmonics, the LSV takes power out of the bridge. This is as one might expect it to be. The reason LSV puts power in at the second harmonic is that it is dominated by bellying LSV that has a different phase (see section 12.3.6). The very small TSV force at the second harmonic has met a very high admittance and the

resulting energy input is comparable with the adjacent harmonics. Generally the power input through TSV is higher than that through LSV, so unless the LSV excites more efficiently radiating modes than the TSV it is unlikely to make a significant contribution to the radiated sound. The radiated sound is examined in chapter 13.

12.3.9 Other avenues of power input

If an external force is applied directly to a string the admittance of the string would show very pronounced harmonic peaks but the envelope of harmonic peak heights would vary smoothly with the harmonic number. Thus the power supplied to a violin by a bow (or even by a shaker), at the string harmonics, must smoothly decline from low to high harmonic number. The envelopes of the sound spectra radiated by a violin are presented in the next chapter and these fairly smoothly decline with rising harmonic number. The power imparted to the string must pass through the violin to radiate. It follows that if the input to the violin is smooth and the output is smooth, then the power supplied to the body by the string must be fairly smooth and not show significant peaks. Fig. 12.24 shows the algebraic sum of the power supplied to the violin by the string (at the bridge and the tailgut only), and the sound power radiated by the violin. The radiated sound power is not calibrated and it has been shown with an arbitrary reference to make it the same as the string to body power at the seventh harmonic.

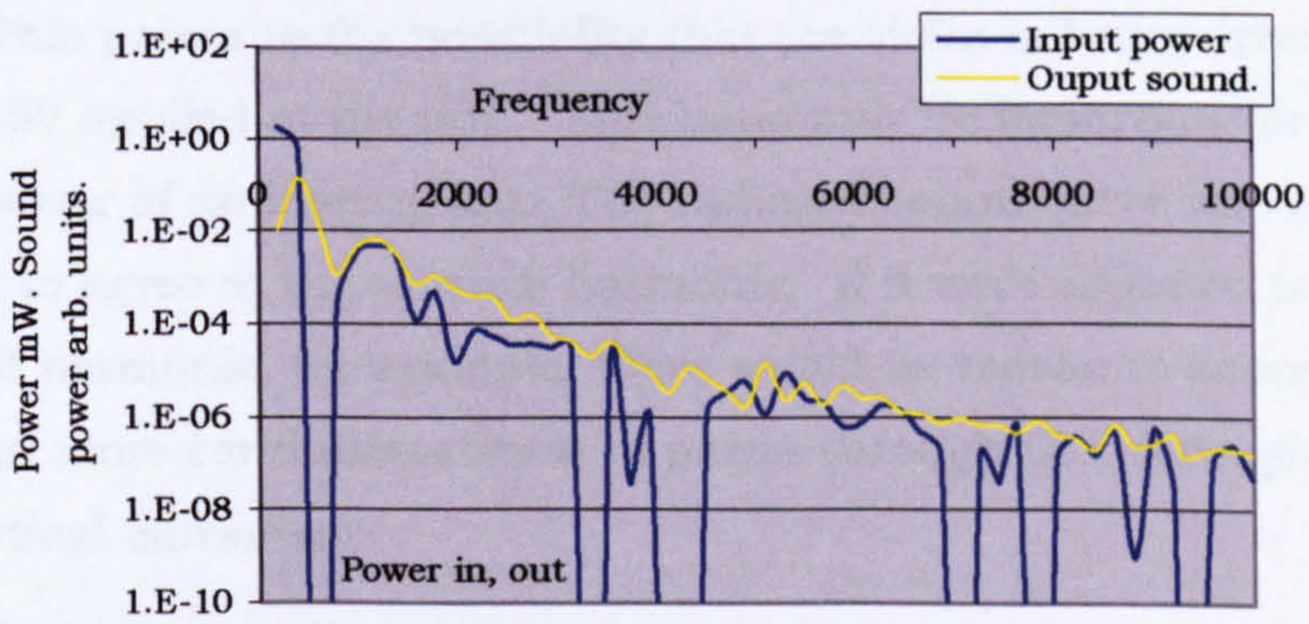

Fig 12.24. Algebraic sum of the power exchanged between the string and the body (mW), compared to the sound power radiated by the violin (arbitrary units), V157HD. Adjusted arbitrarily to agree at the seventh harmonic.

The purpose of this exercise is to see if the string is likely to be putting power into the body in a significant way at other ports. We have included in the algebraic sum the TSV and LSV power from the string to the bridge. We have included the power going in at the tailgut. What is not included or measured was the power going in at the nut from LSV in the direction of the string and the transverse force at the nut (or stopping finger) from the TSV. The transverse component caused by TSV at the nut is not thought to be significant because of poor admittance matching. However the pseudo-admittance may be larger than is generally supposed, since it is quite possible that some of the body modes might involve quite significant transverse displacements at the neck. This would give a TSV force applied at the neck a high admittance. Such displacements could result from the 'yawing' modes that have been identified [Marshall, 1985]. The component in the string direction at the nut could be as significant as the component in the string direction at the tailgut.

The algebraic sum of the power transferred to the body is low or negative at the third harmonic and between about 3000Hz and 4500Hz. There must be some other transfer of energy from the string to the body in these bands. At the third harmonic, it is possible that the string transfers energy to the body by vertical translation of the nut, caused by body bending modes. In Chapter 13 some evidence is given which would suggest that above 2000Hz the violin is largely LSV driven. Fig. 12.24 does not include any contribution there may be from driving power from TSV or LSV applied at the nut. This points to the possibility that the violin is being driven in this band by LSV applied at the nut. This band may be important for the carrying power of an instrument. The radiated sound curve was adjusted arbitrarily to agree at the seventh harmonic. If it were adjusted to agree at the second harmonic, for example, there would be reason to expect a greater and more continuous input of power through LSV through nut and saddle vertical movement.

It is significant to note that the good match between the power into the string and the sound power radiated enables us to estimate how the radiation efficiency varies with the frequency.

Now the radiation efficiency, $r = \frac{W_{rad.}}{W_{In}} = \frac{W_{rad.}}{W_{rad.} + W_{diss.}} = \frac{1}{1 + \frac{W_{diss.}}{W_{rad.}}} \approx$ a constant.

But $\frac{W_{diss.}}{W_{rad.}} = \frac{\eta_{mech.}}{\eta_{rad.}}$, and $\eta_{rad.} = \frac{\rho_0 c s \sigma}{\omega M}$, where

σ = radiation efficiency, s = radiating area,

M = mod al mass of radiating part of structure, which is approximately constant.

$\eta_{\text{mech.}}$ tends to vary as $f^{-1/2}$ (according to Bissinger)

$\therefore$ if $\frac{\eta_{\text{mech.}}}{\sigma/\omega}$ is a constant, then σ varies as $\omega^{1/2}$.

This is more or less what Bissinger finds (*a personal communication with F J Fahy*). The experimental finding that the radiation efficiency of a violin varies as the square root of the frequency is therefore consistent with the findings of Bissinger.

12.3.10 The relative phase of TSV and LSV

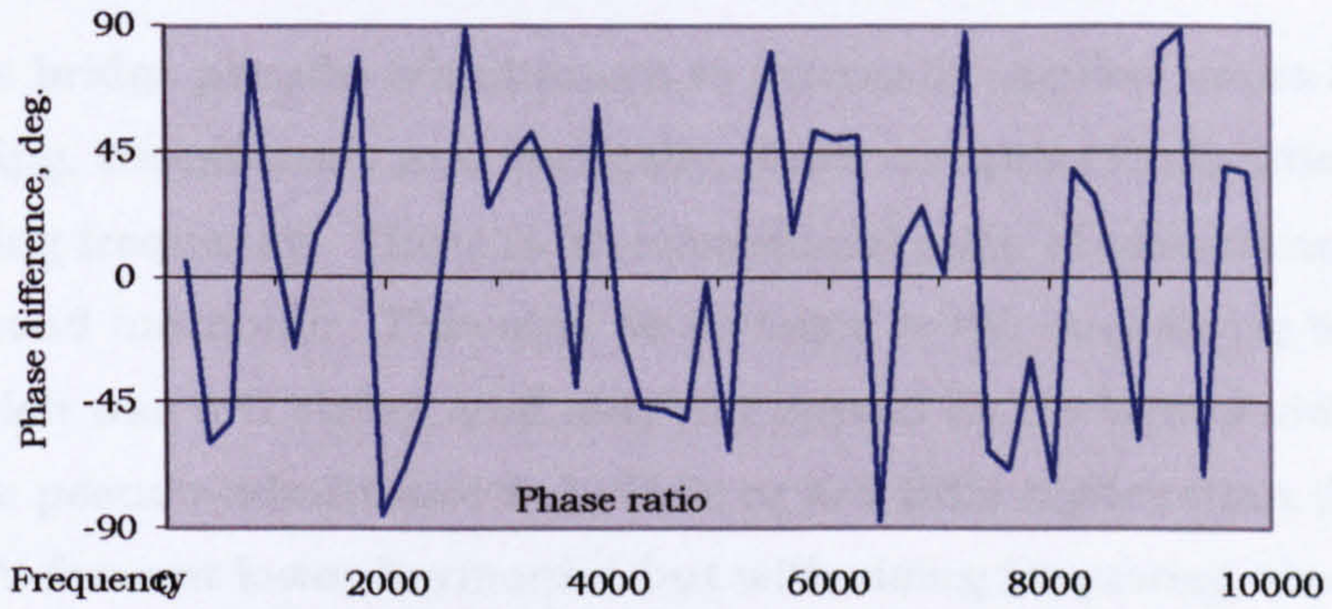

Fig. 12.25. Relative phase of TSV force and LSV force, (violin 157HD).

The difference in phase between the TSV force and the LSV force is shown in Fig. 12.26.

12.4 Conclusions

- In the bowed violin the total LSV varies from one harmonic to another, does not consistently strengthen the even numbered harmonics, and varies non-linearly with the TSV.

- The ratio of LSVforce/TSV force, from 3000Hz to 5000Hz, is higher for the medium EAR violin. Below 3000Hz there is little consistent difference with EAR.
- The LSV force per unit TSV force in a varnished violin throughout the spectrum generally shows a monotonic dependence on the deviation.
- The LSV force per unit TSV force for a varnished violin divided by that of an unvarnished violin shows that the effect of varnish was to lower the LSV/TSV ratio at harmonics above 1500Hz, and increase it below 1500Hz.
- The ratio of bridge vertical velocity to bridge transverse velocity shows a tendency to rise with rising frequency.
- The high frequency spectrum of the bridge admittance to an externally applied transverse force shows a relationship with the theoretical spectrum of the modal overlap of the body.
- The bridge pseudo-admittances to internally applied forces from the string, transversely and vertically, show a regular declination with rising frequency. There is an exceptional peak of admittance at the second harmonic. This may be peculiar to the only string tested, which was a G string, and may not appear in the bowed violin at all. The pseudo-admittance to LSV force is a little higher than that to TSV force at lower harmonics but with rising frequency, the gap widens to 15 or 20db.
- The validity of these admittances must be questioned until confirmed by tests on a bowed string, but they are supported by having a consistent relationship to the radiated sound power. The degree to which these results are typical of all violins can only be determined by doing more tests on other violins.
- The difference in the admittance of the bridge to internal and to external forces may be an indication that bellying LSV significantly affects which modes are excited. The modal difference may come from the super-resonance excitation of modes compatible with the force regime.

- The power transferred from the string to the bridge is dominated by TSV at low frequencies. In the range 3000 to 4500Hz, the TSV contribution is minor. It is possible there is another significant input of energy from the string to the body. This may be LSV-driven through movement at the nut, or TSV driven at the stopped end of the string.

Chapter 13

EFFECT OF BODY SHAPE ON RADIATED SOUND PRESSURE

13.1 Introduction

The radiated sound pressure was recorded together with the amplitude of transverse displacement of the string and the LSV. The amplitude of transverse displacement of the string and LSV have been presented and discussed in Chapter 12.

The violin was supported at the lower and upper extremities of the back on foam-lined blocks. See fig. 6.4. The violin was excited by driving the string with a shaker. The mid length transverse displacement of the string was 3.25 mm. The microphone was caused to swing while recording the sound as described in Chapter 6. For each set up the mean distance from the microphone to the violin was set at 2m. The sound radiated by the shaker mechanism was measured alone and subtracted from the sound recorded for the violin and shaker together. (See chapter 6 for details.) The magnitude of the sound pressure was uncalibrated. The tests were conducted in a room about 80 cubic metres in volume, with plasterboard walls and a timber floor. The room contained benches but no soft furnishings. The room may be considered moderately reverberant.

13.2 Unvarnished violins

13.2.1 Violins of differing EAR

The radiated sound pressure for three unvarnished violins of differing EAR is shown in figs. 13.1 to 13.3.

13.2.2 Discussion

To facilitate the comparison of the three graphs, the harmonic peak values have been joined in fig 13.4, to form continuous lines. The medium EAR violin generally radiates more strongly than the high and low EAR violins. The difference becomes more apparent above 1500Hz. The radiated sound

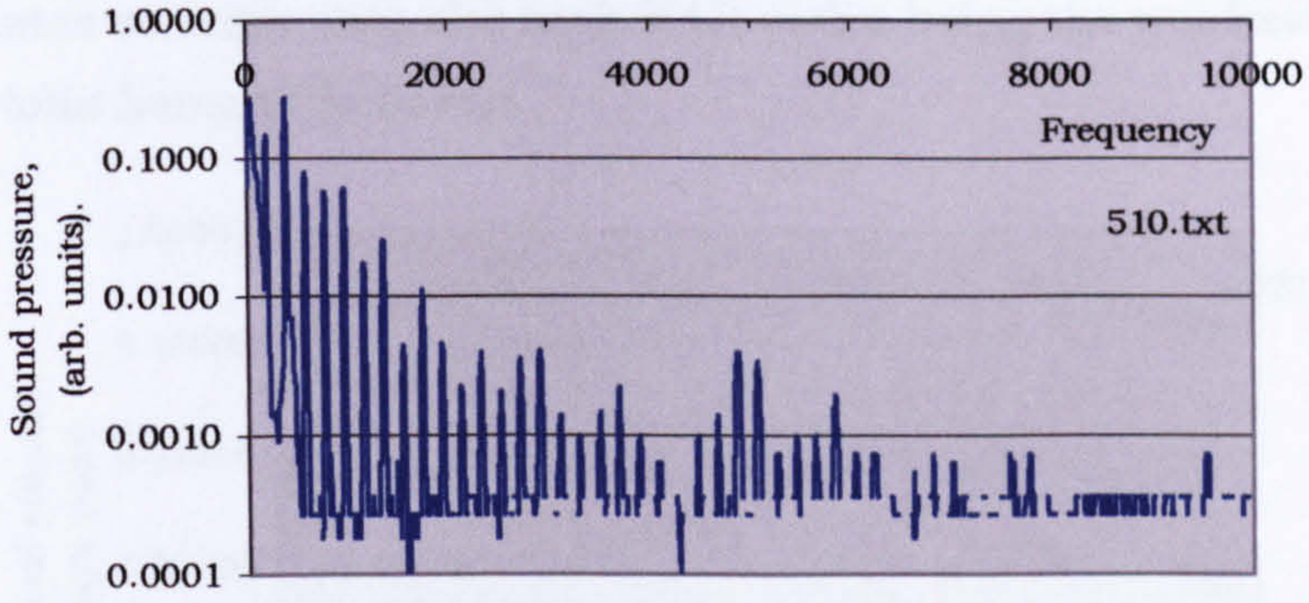

Fig. 13.1. Sound pressure radiated, low EAR violin. V157LE Shaker driven G string.

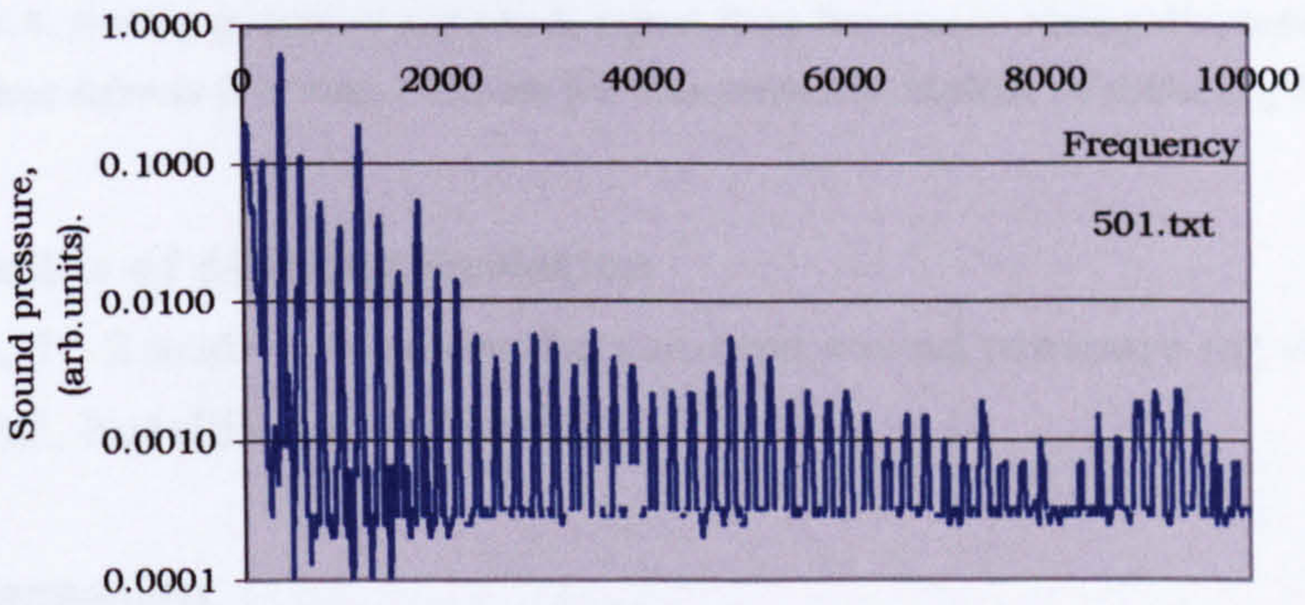

Fig. 13.2. Sound pressure radiated, medium EAR violin. V156. Shaker driven G string.

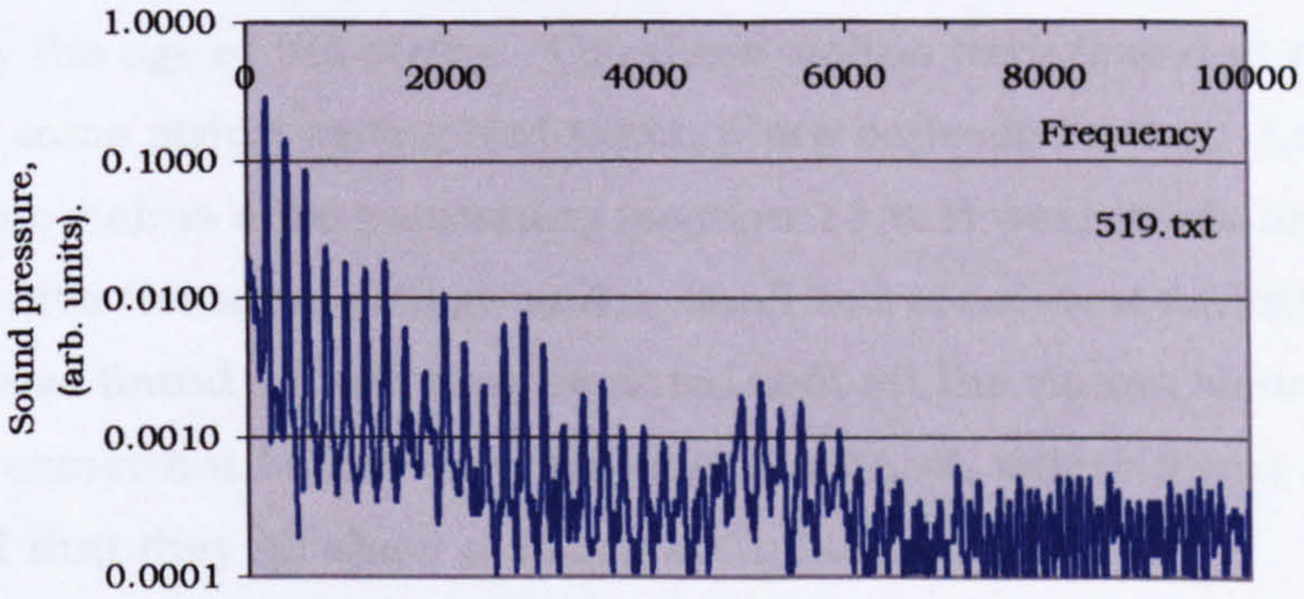

Fig. 13.3. Sound pressure radiated, high EAR violin. V158HE. Shaker driven G string.

pressure of the high EAR violin has a weak second harmonic, it falls off rapidly after the first harmonic and is weak around 4kHz. The radiated sound pressure of the low EAR violin is nearer that of the high EAR violin

throughout much of the range. At the second harmonic the medium EAR violin radiates strongly with the high EAR violin being the weakest and the low EAR violin being in between.

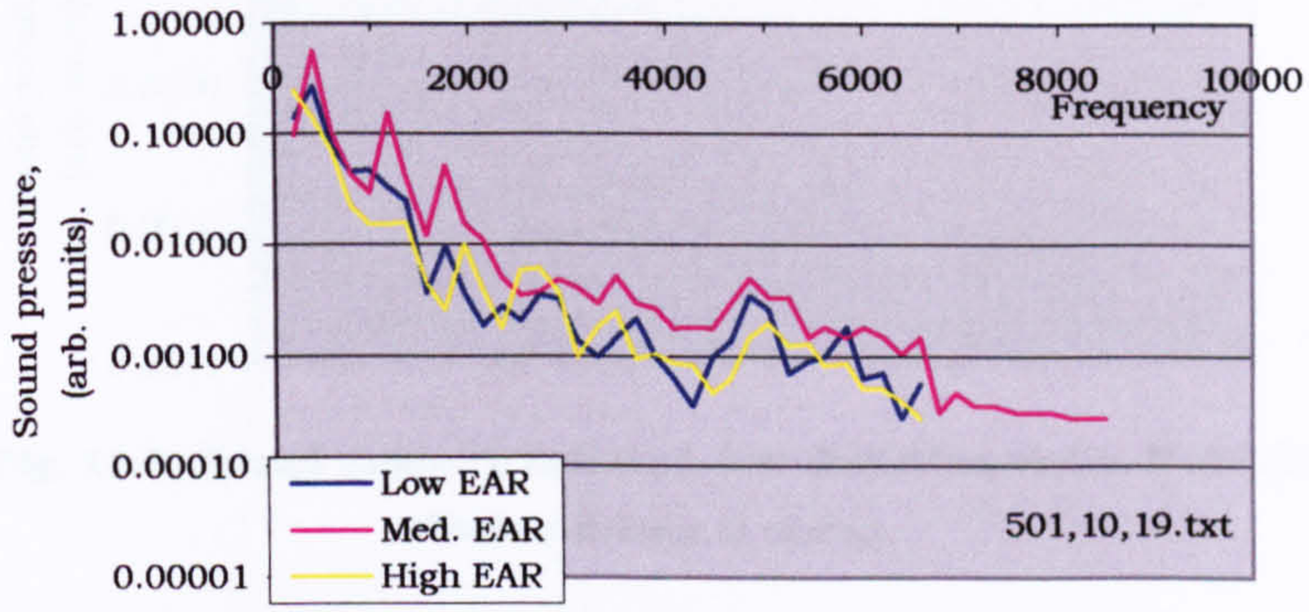

Fig. 13.4. Sound pressure radiated, equal first harmonic string displacement. Shaker driven G string. Shown for unvarnished violins of differing EAR.

13.2.3 Violins of differing deviation

Figs. 13.5, 13.2 and 13.6, show the radiated sound pressure for violins of normal EAR, but different deviation.

13.2.4 Discussion

These violins all have a normal EAR. There is too much minor variation in shape between these curves to conclude reliably that the sound radiated increases with the deviation. It was found later that the LSV developed is affected by the age of the string. The three violins were tested at different times and some string ageing had taken place between testing. Later tests on the same violins after varnishing (section 13.3.1) were made on the same day with the same strings and a small but consistent variation with deviation was found. It will also be noted that all the violins show a second harmonic somewhat higher than the first and third, where it was about the same, and that they all show a strong sixth harmonic.

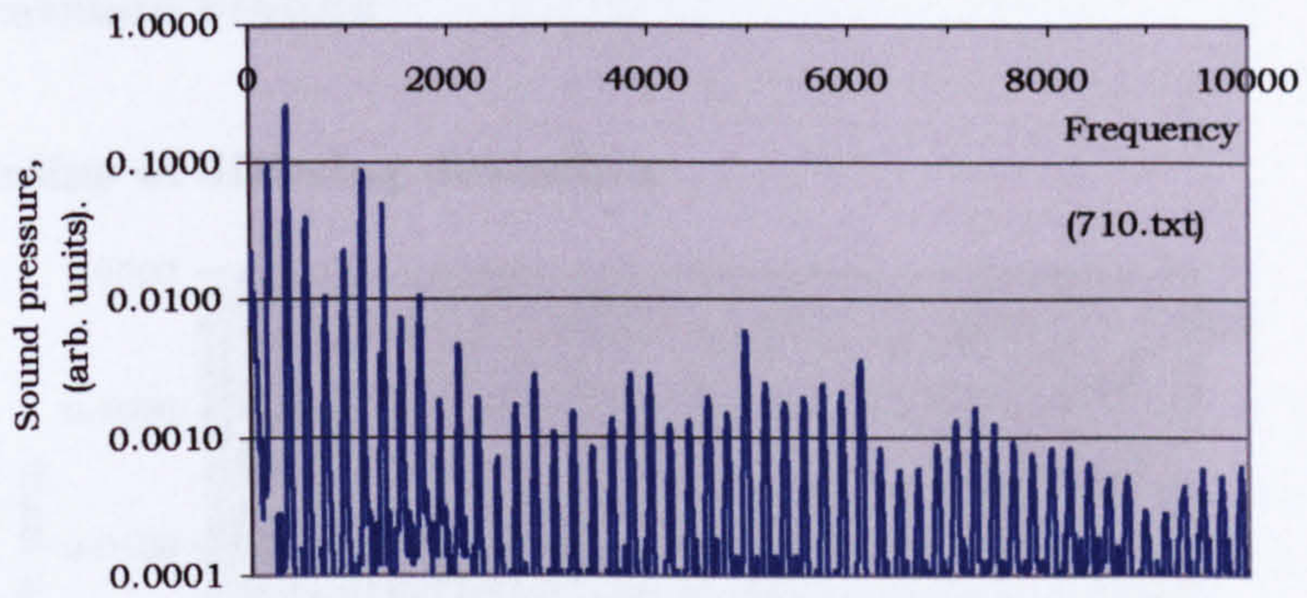

Fig. 13.5. Sound pressure radiated, low deviation violin. V158LD.
Shaker driven G string.

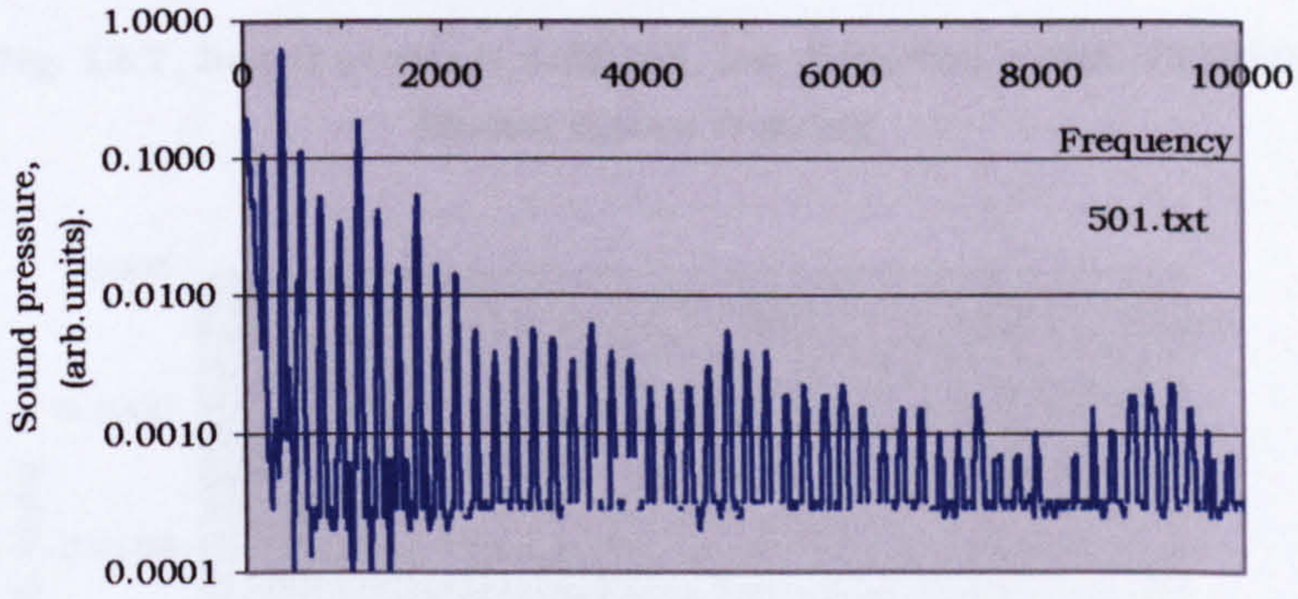

Fig. 13.2. (repeated) Sound pressure radiated, medium deviation violin. V156.
Shaker driven G string.

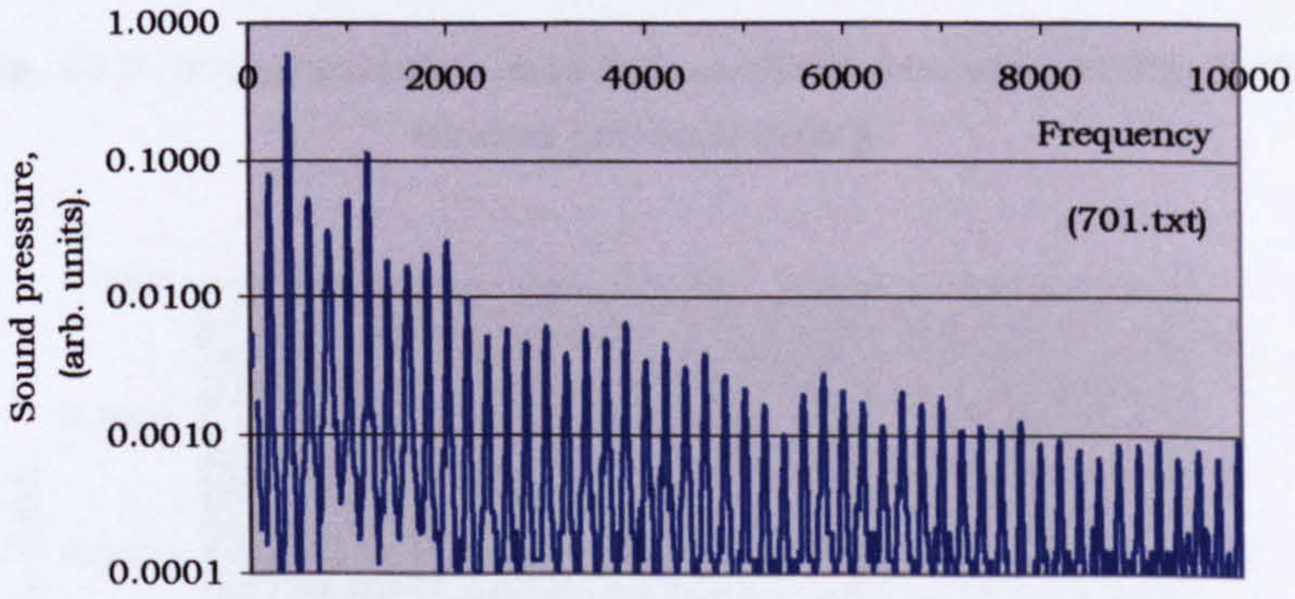

Fig. 13.6. Sound pressure radiated, high deviation violin. V157HD.
Shaker driven G string.

13.3 Varnished violins

13.3.1 Violins of differing deviation

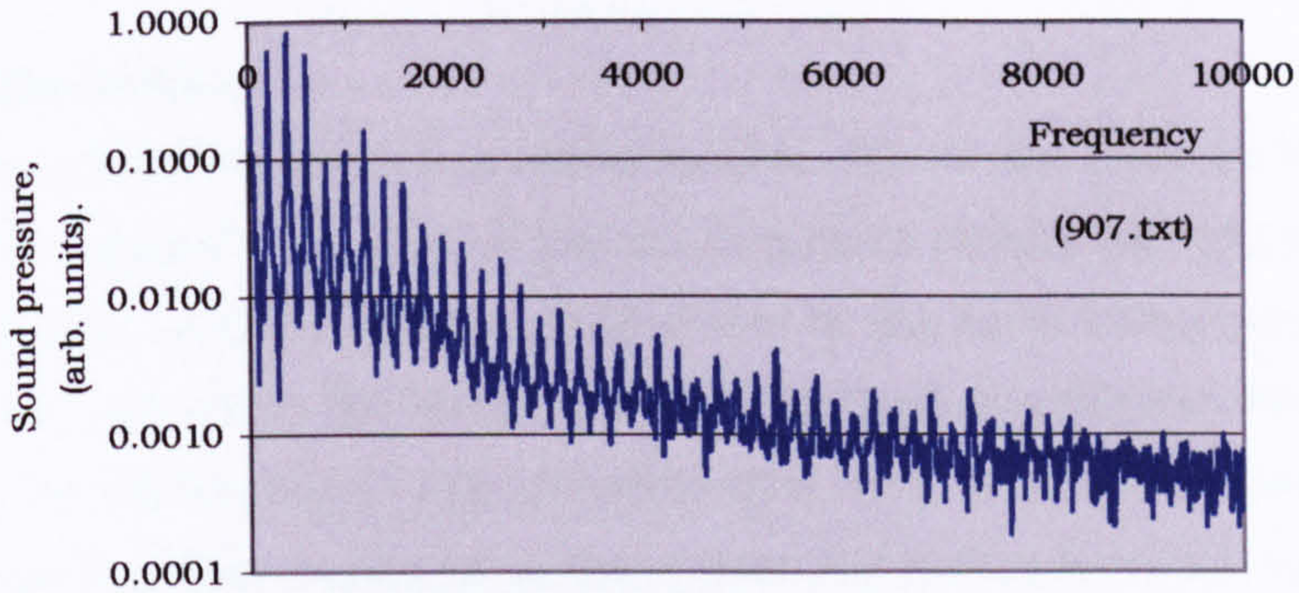

Fig. 13.7. Sound pressure radiated, low deviation violin. V158LD. Shaker driven G string.

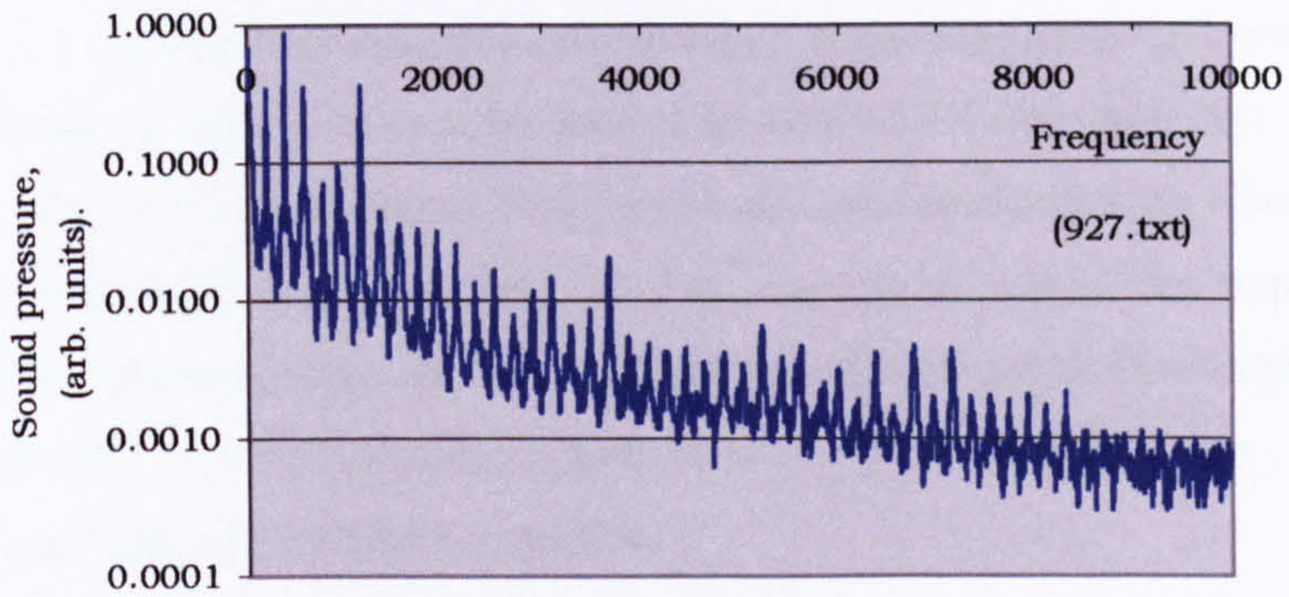

Fig. 13.8. Sound pressure radiated, medium deviation violin. V156. Shaker driven G string.

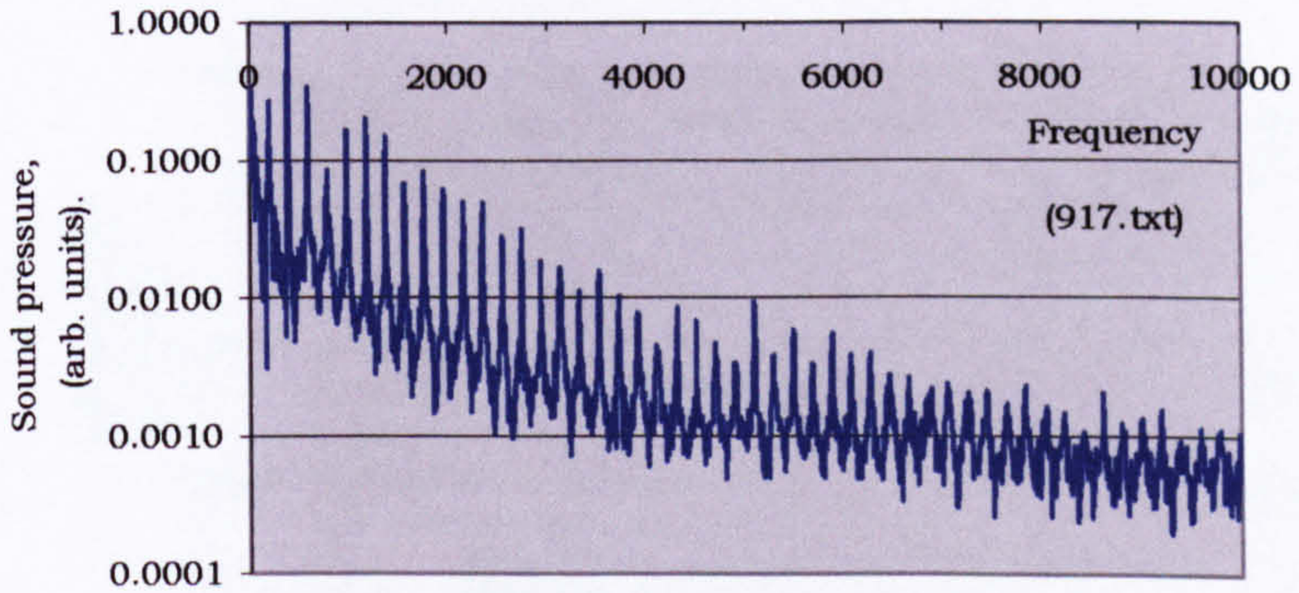

Fig. 13.9. Sound pressure radiated, high deviation violin. V157HD. Shaker driven G string.

After the three violins of normal EAR and differing deviation were varnished, they were again tested to compare their radiated sound. The results are shown in figs. 13.7 to 13.9.

13.3.2 Discussion

It is noticeable that there is a considerable rise in the 'floor' of the sound spectra compared with that of the unvarnished violins already presented. This could be certainly partly attributable to the tests being conducted at a time of the day when the background noise level was higher than it had been in the earlier tests. It is possible that this is the sole reason. There was however some reason to suspect that the violins were for some reason behaving differently. Experiments were also done on unvarnished violins of abnormal bass bar and bridge-heights. These also showed marked differences in spectral floor, which certainly could not be attributed to differences in ambient noise in the room. A corresponding level of background vibration was also found in the LSV force spectra. The reasons for the difference in spectral floor were not understood and since it was the peak heights that were germane to the main purpose of the experiments an exhaustive investigation of the reasons for the spectral floor variations was not pursued. Further research would be needed to gain more understanding of this phenomenon.

To facilitate comparison between these spectra and comparison with those of the unvarnished violins, fig. 13.10 shows the peak level of the three spectra.

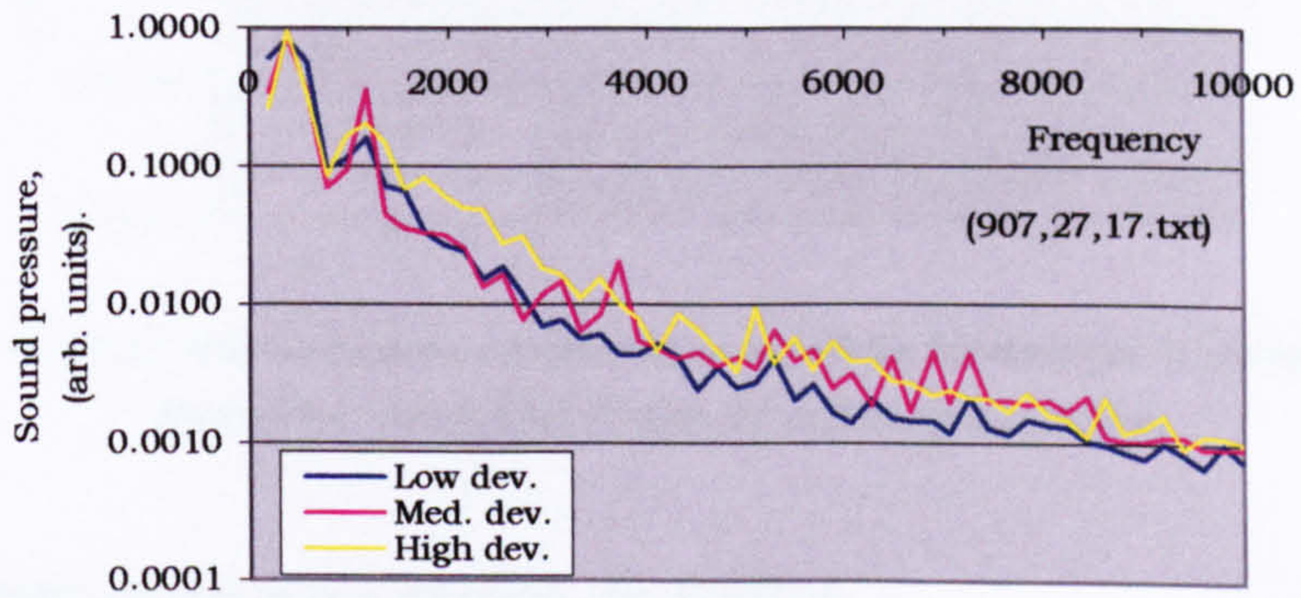

Fig. 13.10. Sound pressure radiated, equal first harmonic string displacement. Shaker driven G string. Shown for varnished violins of differing deviation.

In all the varnished violins, the peaks at the second and sixth harmonics project above those of the adjacent harmonics. Up to approximately 1000Hz, the difference in deviation has little effect on the radiated sound pressure. Above 1600Hz there is a clear difference between the low and high deviation violins, with the medium deviation violin for the most part being somewhere in between. It may be significant that in the first harmonic the low deviation violin radiates slightly more sound than other violins. We have shown that all the test violins have close to the same spectrum of transverse displacement of the string, yet the spectrum of radiated sound varies. There is on the other hand a compelling relationship between the spectrum of the LSV in the string and the radiated sound spectrum (see sections 13.6.1 and 13.6.2).

13.3.3 With bowed excitation

The three varnished violins of differing deviation were bowed as described in section 12.3.2 and the spectral peaks of the radiated sound spectra are shown in fig 13.11. This corresponds with the LSV shown in fig 12.4. The spectra are not significantly different and this accords with the report in Chapter 5 that violins of the same EAR but different deviation do not exhibit any consistent difference in radiated sound.

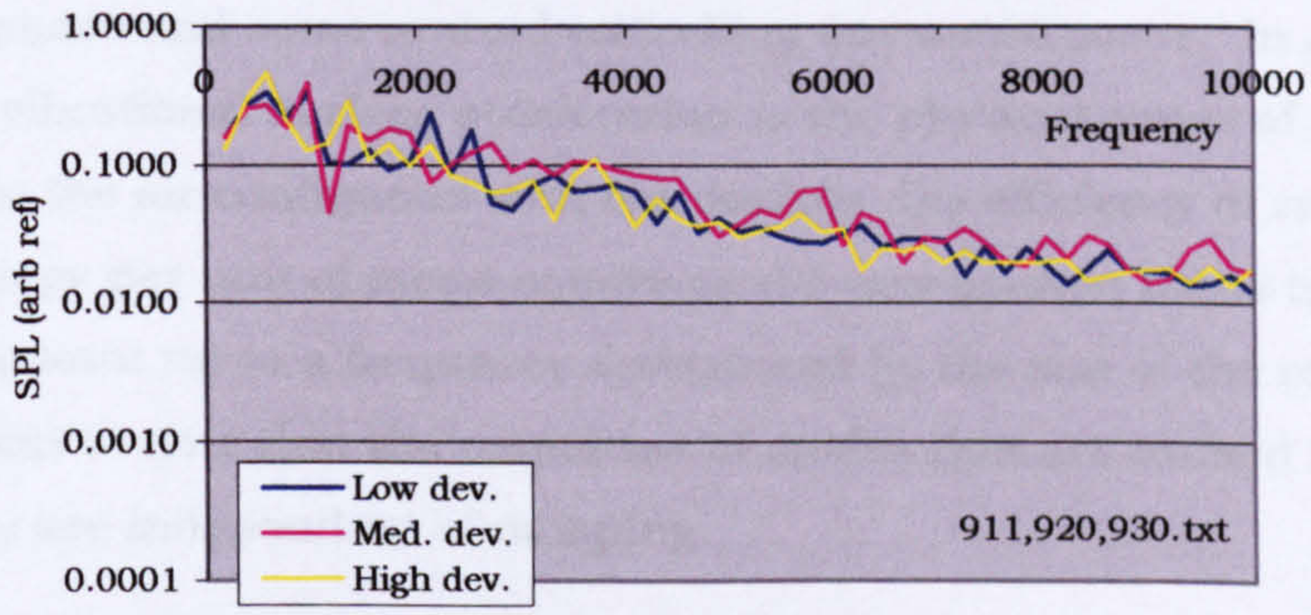

Fig 13.11 Sound pressure radiated, excited by bowing the G string. Shown for varnished violins of differing deviation.

13.4 Super-resonance modal excitation

The difference between the bridge admittance to an external force and an internal force suggests that there may be different modal combinations

excited in each case. The difference may lie in the excitation of modes at super-resonant frequencies.

13.4.1 Radiation of modes at super-resonance frequencies

The sound pressure radiated by a vibrating surface depends directly on the acceleration of the surface expressed by the Kirchhoff-Helmholtz Integral [Fahy, 2001]. Consider again our single frequency excitation. When ω considerably exceeds ω_m, the modal acceleration amplitude is given by; $\alpha_m \approx \frac{F_m}{M_m}$ where F_m is the amplitude of the modal excitation force and M_m is the modal mass. The modal acceleration is independent of the excitation frequency. The violin can radiate strongly by operating modes at frequencies well above resonance (super-resonance excitation). In fact, a mode that does not radiate well at resonance may be able to radiate comparatively well at frequencies well above resonance.

However, the total acceleration response at any point does not increase to infinity as the frequency increases because each mode has its response maxima and minima at different positions with nodal lines in between; and the phase of each modal response switches through 180 degrees as one moves across nodal lines. The excited modal accelerations may be of opposite phase and some mutual cancelling out would occur. In addition, although vibrational surface acceleration is the physical cause of density changes in the air contiguous with the surface, the efficiency of radiation of sound energy per unit of mean square modal acceleration tends to be more or less constant up to a frequency determined by the size of the radiator. It is important to note that the responses of modes that are excited super-resonantly are independent of damping.

13.4.2 The super-resonance excitation of modes in the violin

With rising driving frequency, there will be an increasing number of lower order modes that, given the right conditions, could be excited super-resonantly.

A crucial factor in determining which modes, if any, are excited, is the magnitude and spatial distribution of the applied forces. The driving forces will be most effective in exciting modes that have large displacements in the

regions of the application of the forces and in the direction of the forces. To excite a mode at resonance it would normally be sufficient to apply a periodic excitation force at the resonance frequency at any point other than a nodal point. The excitation of a mode super-resonantly would be favoured by the application of the periodic excitation forces at a number of points applied in the direction and relative phase consistent with that of the mode. Under these conditions, both strongly and weakly radiating modes may be excited both resonantly and super-resonantly.

The body of the violin is acted on by the TSV force on the bridge and the stopped end of the string, and forces arising from LSV, which are applied at the bridge, nut and saddle. It was shown in Chapters 3 and 4 that if these forces were applied statically the body would deform in a way that approximates to operating shapes that are likely to be strongly radiating. It does not follow in the dynamic situation that these forces would be applied in the required relative phases to encourage the super-resonance excitation of modes that would equate to these operating shapes, but it is possible that at some frequencies or frequency bands this happens.

13.5 The mix of modes excited at any harmonic

The resonant excitation of the body modes by an external transverse force applied to the bridge will best excite those modes that have the greatest displacement at that point and in that direction. When the swinging string excites the body, forces are applied directly at the ports from TSV at the bridge and the stopped end of the string, and from LSV at the bridge, nut and saddle. There is therefore a very different force regime on the body to that applied by a single external force to the bridge, which produces forces at the ports indirectly. It was shown in section 12.3.5 that the pseudo-admittance of the bridge to a single external force was significantly different to its admittance to the TSV force applied by a string vibrating at resonance. This supports the conclusion that the forces at ports applied directly by the vibrating string have excited different modes than those excited by an external force.

Our analysis of the deformation caused by static string tension showed that it was of a similar shape to the Nullstrahler. Is it conceivable that a

good violin will operate as a Nullstrahler throughout much of the frequency range and superimposed on top of this would be the shapes caused by the modes that are resonant at or near any frequency? Under these circumstances, the Nullstrahler shape would dominate the operating shape at frequencies where there is a resonance of the Nullstrahler mode, or at frequencies that are well away from those of other resonant modes. Could it be present and underlie other superimposed modes throughout much of the range? Saunders observed that the violin operated as a Nullstrahler at 685Hz, and Schelleng noted that this frequency was well away from a natural frequency. Weinreich considered the violin as an effective monopole source and found that its radiation efficiency would level off to unity at 1000Hz [Weinreich, G]. Bissinger (*in a personal communication to F J Fahy),* measured the radiation efficiency of a violin and found it was lower than one at 1000Hz and kept on climbing as the square root of the frequency above 1000Hz. This could be evidence that the violin is not radiating from the Nullstrahler. The question remains unanswered.

13.6 Radiated sound as a function of input force

13.6.1 Violins of differing EAR

Fig. 13.12 shows the radiated sound pressure divided by the TSV force, for the unvarnished violins of differing EAR. Above about 1500Hz the medium EAR violin radiates about 3 times more sound per unit TSV than the high and low EAR (about 9 times greater sound power per unit TSV, or an approximate doubling of the subjective loudness).

Fig. 13.13 shows the radiated sound pressure divided by the LSV force. The LSV force spectrum used to make this graph came from fig 11.7 which has no recorded LSV shown for the high and low EAR violins in the range above 5300Hz. Between 2000Hz and 5300Hz there is little consistent difference in the radiated sound pressure per unit LSV force with the EAR. Above 2000Hz the sound pressure per unit LSV force is much more constant than sound pressure per unit TSV force. These factors taken together could either be evidence that the radiated sound in this range is related more to the LSV force than to the TSV force, or that they are both products of a common cause.

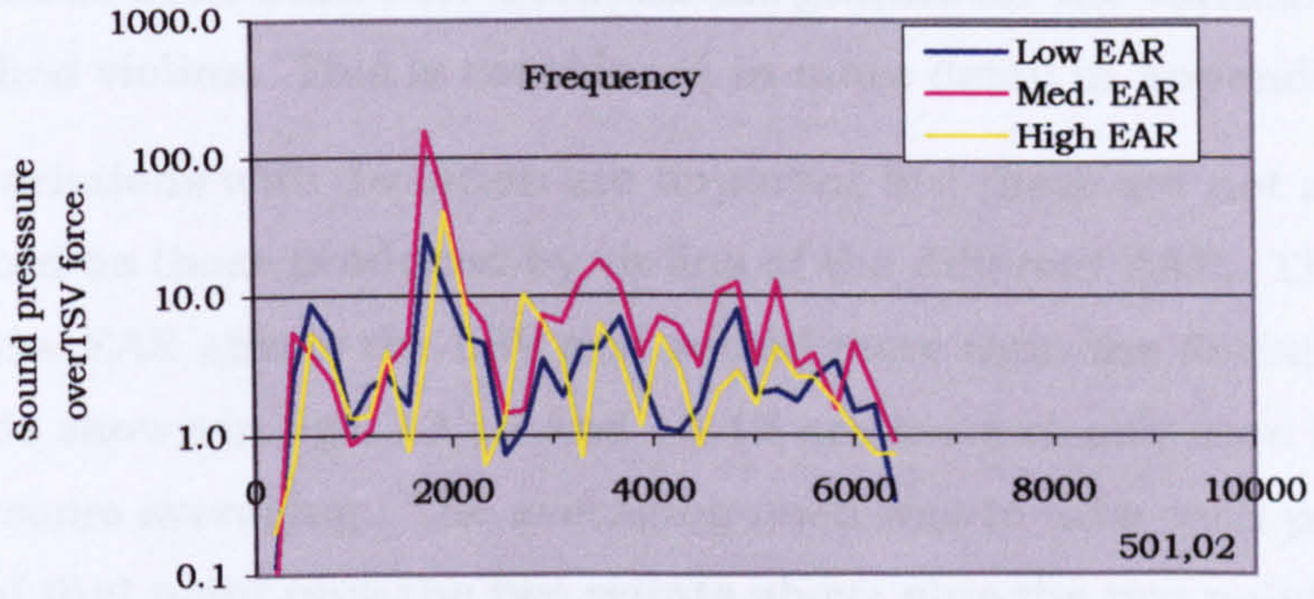

Fig. 13.12. Sound pressure per unit TSV force, unvarnished violins of differing EAR.

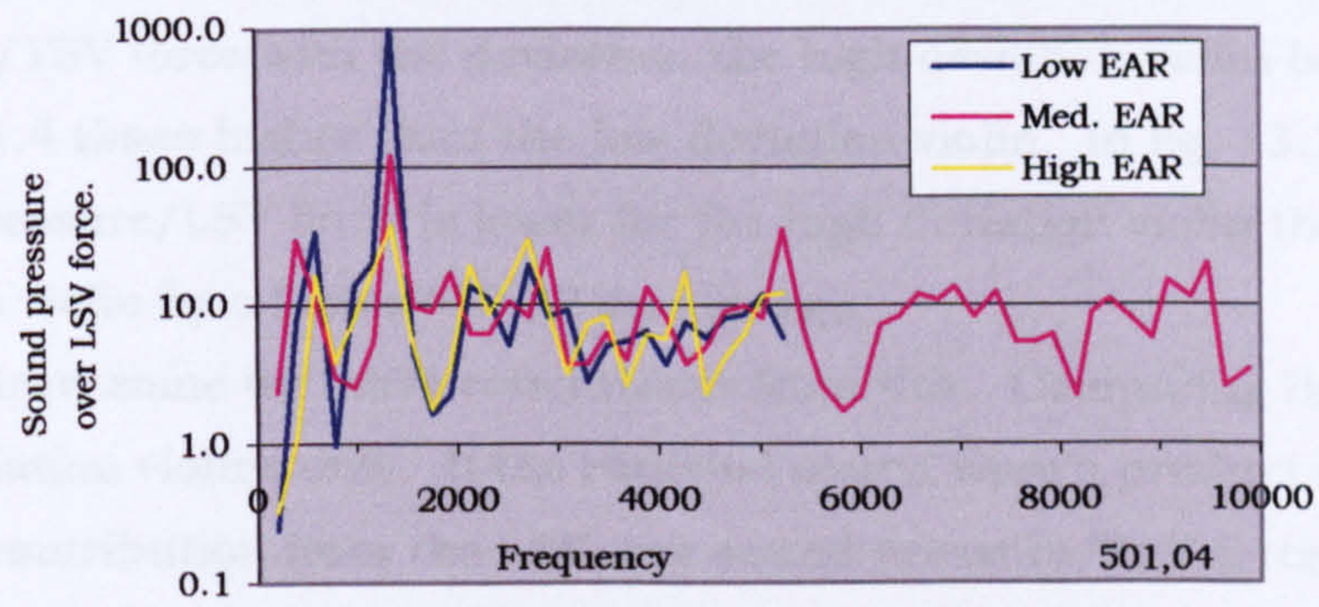

Fig. 13.13. Sound pressure per unit LSV force, unvarnished violins of differing EAR.

All the data on these graphs were sampled at harmonic intervals of 196Hz, therefore certain peaks and troughs could have been missed in the area below 1500Hz, where the values are changing rapidly. In the range 0 to 1500Hz the sound radiated per unit TSV force and per unit LSV force both vary considerably. There is no more variation with the TSV than with the LSV. This may be an indication that the violin relies on a combination of the TSV and LSV forces to drive the body to radiate in this band.

13.6.2 Violins of differing deviations

Fig. 13.14 shows the radiated sound pressure divided by the TSV force for the three violins of differing deviation. Fig. 13.15 shows the radiated sound pressure divided by the LSV force for the same violins. Again, the average sound pressure per unit TSV force curve declines with rising frequency but the sound pressure per unit LSV force is more constant. The variation from the average is less than in the unvarnished violins, indicating a more uniform radiative efficiency in varnished violins or more damping of modes.

There is an obvious difference between the graphs for the varnished and unvarnished violins. This is considered in more detail in Appendix A.

Certain variations with deviation are apparent but these are not as pronounced as those produced by violins of the different EAR. That is because the EAR affects the LSV and sound more than the deviation does. The trends shown in figs. 13.14 and 13.15 are more clearly seen by applying some averaging. The averaging used was to take each point as the average of that point plus the two points above plus the two points below. The graphs with the averaging applied are shown in figs. 13.16 and 13.17.

Fig 13.16 shows that above about 2000Hz, there is a variation in sound pressure/TSV force with the deviation, the high deviation violin being on average 1.4 times higher than the low deviation violin. In fig. 13.17 the sound pressure/LSV force is lower for the high deviation violin than the low deviation violin by a factor of 0.82 on average.

We can draw some tentative conclusions from this. Comparing the low and high deviation violins only. If the radiated sound were a product of the TSV with no contribution from the LSV, the sound pressure/TSV force would not vary with the deviation. Fig. 13.16 shows the high deviation violin generated 1.35 times more sound pressure in the range above 2000Hz. The sound pressure /LSV force should have decreased by a factor of 1/1.36, because the LSV force/TSV force was shown in section 12.1.4 to have increased by 1.36. Fig. 13.16 shows the sound pressure/LSV force did fall by a factor of 1/1.22 (above 2000Hz, on average). Taken together it would appear that the sound is not the product of the TSV alone.

If, on the other hand, the radiated sound were entirely a product of the LSV force, the sound pressure /TSV force for the high deviation violin, should be greater than that of the low deviation violin by a factor of 1.36 (because it was shown in section 12.1.4 that the ratio of LSV/TSV is 1.36 times greater for the high deviation violin). We have seen in fig. 13.16 that it was in fact 1.35 times greater. The sound pressure /LSV force should have been the same for all violins, but the high deviation violin was lower than the low deviation violin by a factor of 1/1.22. Taken together it would appear that TSV is contributing to the radiated sound to some extent, but there is a closer relationship to the LSV. The graphs for violins of different EAR shown above did give more compelling evidence that the radiated

evidence points to the LSV having made the greater contribution in the range above 2000Hz.

That the radiated sound is more closely related to the LSV than the TSV could be said to be only because they are both the result of some common cause, and that this common cause may be responsible for the sound radiation. That possibility cannot be ruled out entirely. But the variations in radiated sound with EAR and deviation, and the variations in the LSV force/TSV force ratio with EAR and deviation, can all be explained reasonably in terms of the mechanism of sound radiation proposed for LSV. No other mechanism has been found that explains the experimental evidence. The link between LSV and radiated sound stands as a hypothesis that is consistent with a considerable amount of experimental evidence.

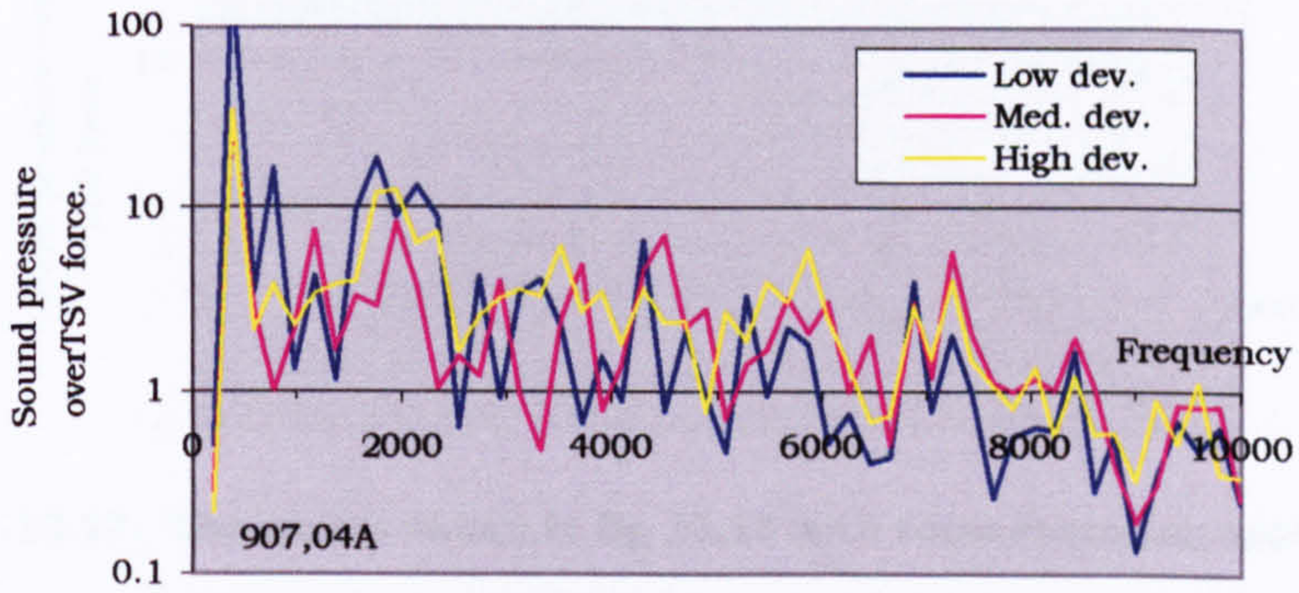

Fig. 13.14. Sound pressure per unit TSV force, varnished violins of differing deviation.

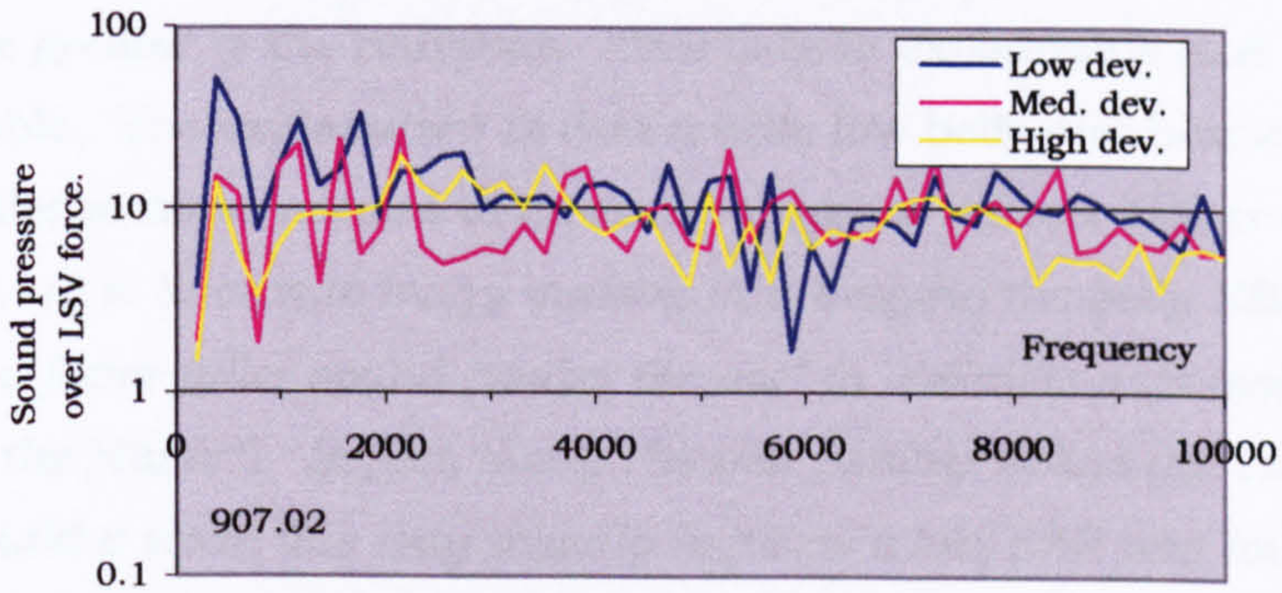

Fig. 13.15. Sound pressure per unit LSV force, varnished violins of differing deviation.

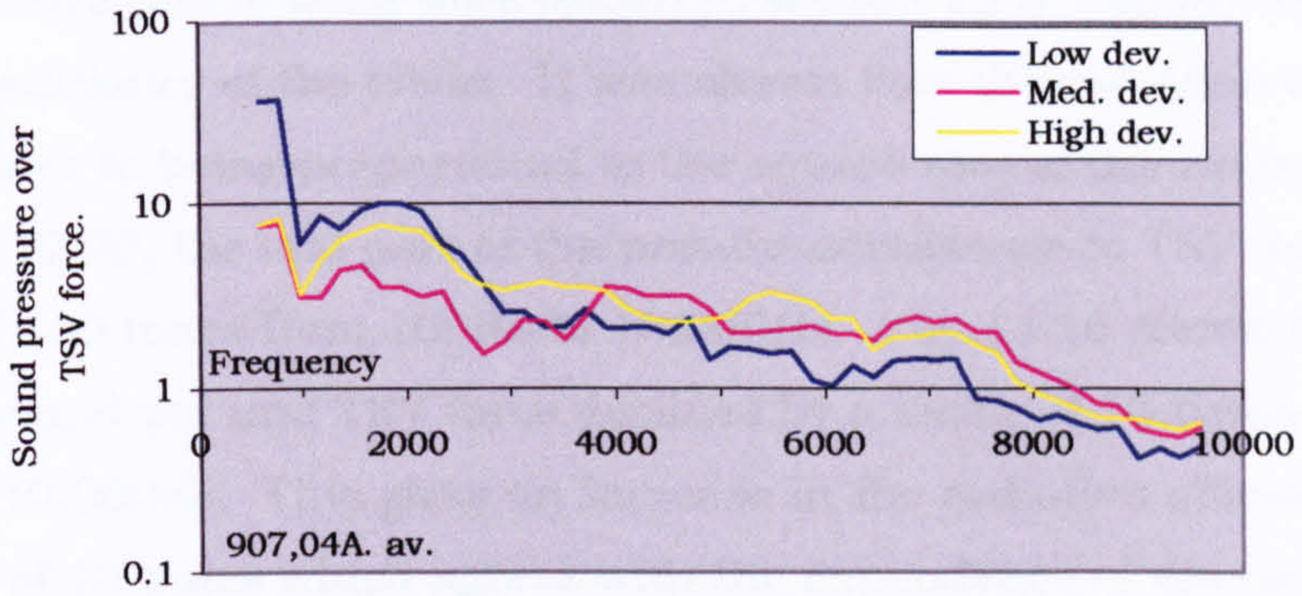

Fig. 13.16. The curves shown in fig 13.14 with some averaging applied.

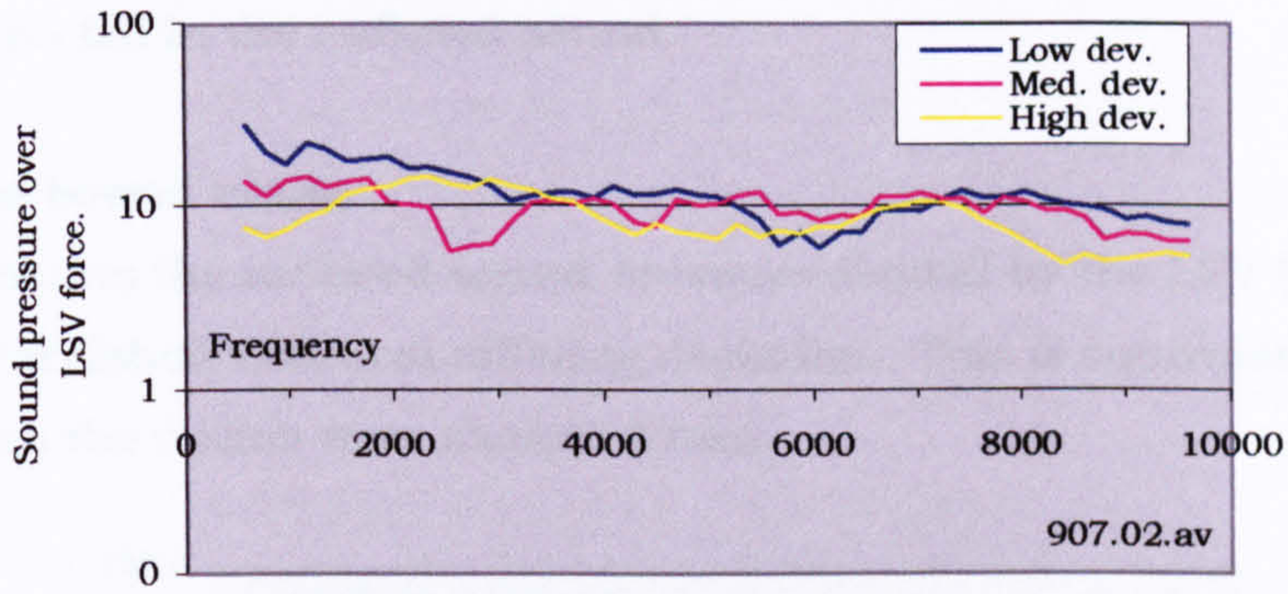

Fig. 13.17. The curves shown in fig 13.15 with some averaging applied.

However, in figs. 13.16 and 13.17, below 1500Hz there is a tendency for the radiated sound pressure per unit TSV force to vary inversely with the height of the belly end bouts cross arch. The lower the belly end bout cross arch is, the greater is the radiation. This is both explainable and demonstrable. The explanation is that a wide low belly end bouts cross arch is easier to move normal to its surface than a narrow higher end bouts cross arch. *(It is known to many makers that keeping the belly EBX arches low, gives a fatter fuller sound "under the ear" (a violinists expression which means "to the player"). In fact, many cheaper factory violins are built this way. To build a violin this way usually requires a low EAR and low deviation, and so a price is paid tonally in loss above 2000Hz, which probably would reduce the projection of the violin. However, even the great Guarneri Del Gesu flirted with this tendency in his later instruments. The result is that although they have a huge fat sound under the EAR, many players have found that they do not project as well in a big hall as a Stradivari, although the Strad may sound "thinner" under the ear.)*

Some tentative conclusions were drawn in section 12.3.9 about the radiation efficiency of the violin. It was shown that the radiation efficiency approximates to being proportional to the square root of the frequency. From Fig. 12.20, the real part of the pseudo-admittance to TSV declines by a factor of 100 times from 100Hz to 10,000Hz. Fig. 13.16 shows that the radiated sound per unit TSV force declines by a factor of 10 times from 100Hz to 10,000Hz. This gives an increase in the radiation efficiency over the range of 10 times which agrees with the dependence of the radiation efficiency on the square root of the frequency. Similarly there is a fall in the real part of the pseudo-admittance of the bridge to the LSV of about 10 times and no fall in the radiated sound.

13.6.3 The bowed violin

Fig 13.18 shows the radiated sound pressure divided by the LSV force for the three varnished violins of differing deviation. This is equivalent to fig 13.15, when the violins were shaker driven.

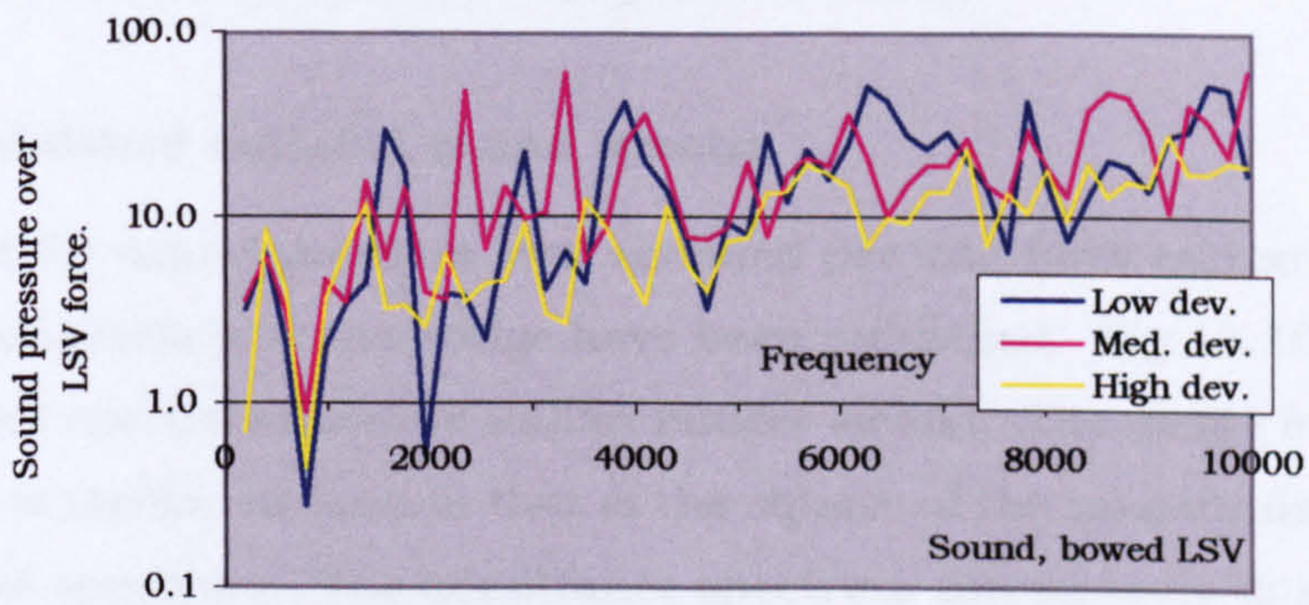

Fig 13.18 Sound pressure per unit LSV force, varnished violins of differing deviation. Excited by bowing the fourth string.

Because there was no way of ensuring equal excitation of these violins the result is of little interest as an indicator of the effect of deviation on the radiated sound per unit LSV. It does indicate that in a bowed violin the sound radiated per unit of LSV is lower in the lower frequencies and higher in the higher frequencies than that of the shaker driven violin. This could be explained by a non-linear variation of the radiated sound with the amplitude of transverse vibration of the string, in that a bowed string has a lower amplitude in the low harmonics and a higher amplitude in the high

harmonics than does a shaker driven string. The bowed string would therefore contribute less bellying LSV to the total LSV in the lower harmonics and more bellying LSV to the total LSV in the higher harmonics than the shaker driven violin. For this to have produced the difference between figs 13.15 and 13.18, the bellying LSV must be making a significant contribution to the radiated sound.

13.6.4 The contribution of LSV to the radiated sound

In Chapter 12 it was shown that the power input to the body from the string is contributed to by LSV. Except in the frequencies above 8500Hz and between 3000 and 4500Hz, LSV does not appear to make a greater contribution than TSV. In section 13.6, evidence was presented that the sound above 2000Hz is largely LSV driven. This suggests that the LSV operated modes have a relatively higher radiating efficiency. Such a finding would be consistent with the predictions made in Chapter 3.

13.7 Radiated sound on a comparative basis

13.7.1 Published radiated sound spectra

Spectra of the sound pressure level radiated per unit force excitation applied transversely at the bridge have been published. Fig 13.19 shows eleven such spectra all for old Italian master violins. The shape of this spectrum is similar in form to that of the square of the magnitude of the admittance spectrum. The admittance spectrum corresponds to a uniform force spectrum but a very irregular power input. The sound spectrum resulting is that due to a constant force but similarly uneven power excitation. Since the admittance curve and the radiated sound curve are of approximately the same form it suggests that if we had a constant force and constant power excitation the response would be much flatter. The force and power into a bowed or shaker driven violin string at resonance have a fairly constant relationship. The force and power from externally applying a force to the bridge do not. Fig. 13.19 is therefore of limited value, by itself but if it were divided by the spectrum of the square of the magnitude of the admittance it would give an indication of the radiative efficiency.

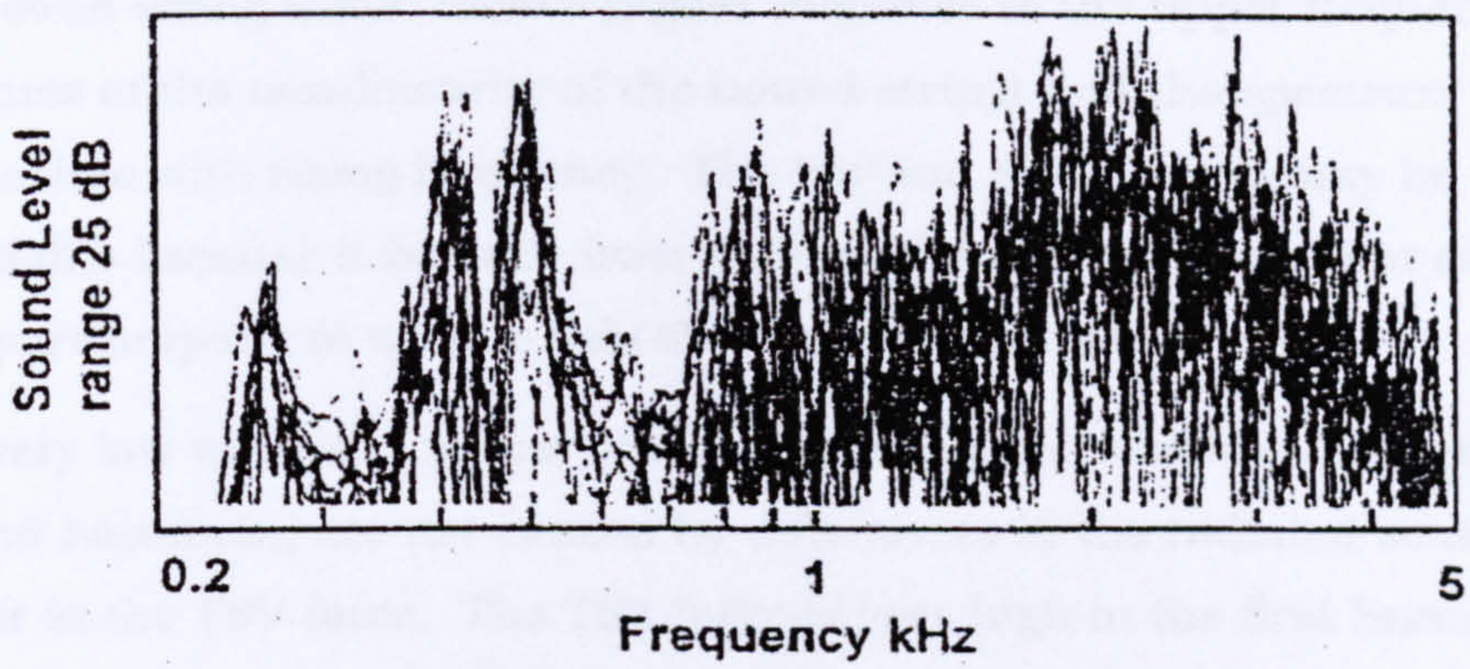

Fig 13.19 Sound radiated per unit of external transverse force at the bridge, by 11 master Italian violins. (from Dunwald, 1982)

13.7.2 Radiated sound spectrum as found in this research

Fig 13.20 is a radiated sound spectrum. This is fig 13.14 with the vertical scale changed to decibels (with an arbitrary reference) through a range of 60dB.

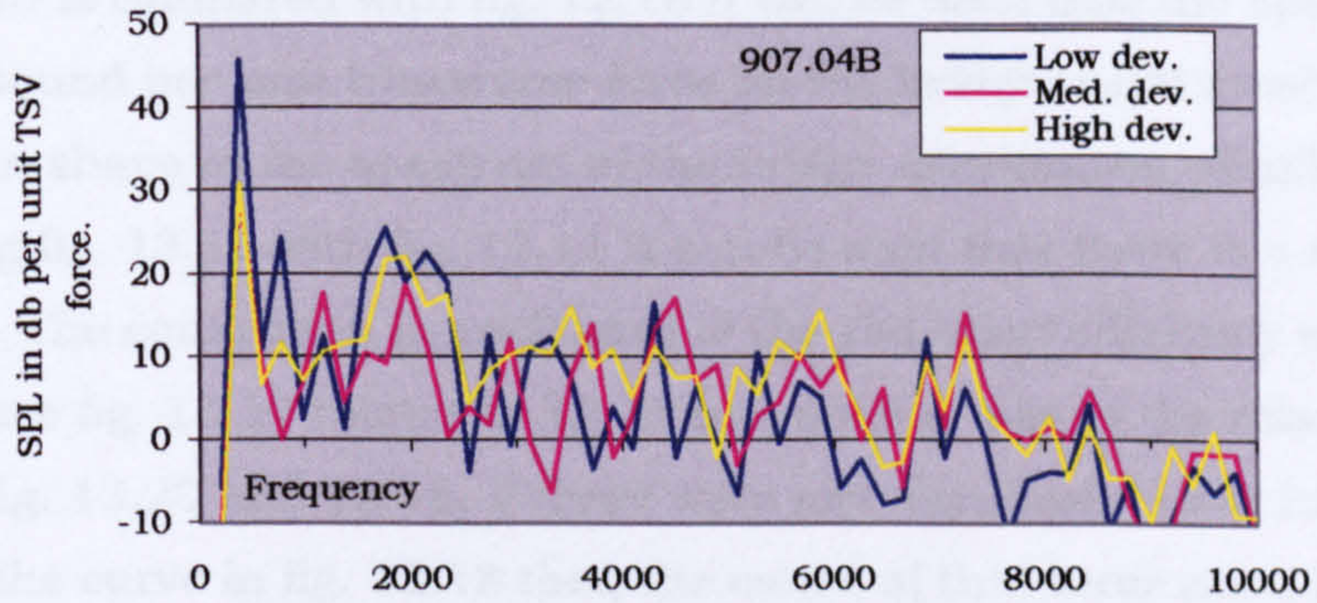

Fig. 13.20. Sound radiated per unit of transverse force on the bridge. The transverse force generated by vibrating the G string at resonance. Shown for 3 varnished violins, of differing deviation.

The traces are not uniform throughout the range, but above 1kHz they do show a steady decline with frequency. The main reason for the lack of uniformity is that the sound is not caused only by TSV but it shows a closer relationship to the LSV spectrum. This is for the note G (the open G string), which has 52 harmonics in the frequency range shown, and samples the response of the violin at intervals of 196Hz. The excitation was by driving the string with a shaker. From the evidence we have seen,

the bowed string would have a higher response in the upper frequencies (because of the non-linearity of the bowed string) and the spectrum would not decline with rising frequency. The low end of the range may be unreliable because it is made from data collected at intervals that are too far apart properly to sample this characteristically peaky area.

The very low value at the first harmonic and the very high value at the second harmonic, are not caused by differences in the radiated sound but rather in the TSV force. The TSV force is very high in the first harmonic and very low in the second. The admittance of the bridge to these forces is the reverse of this order. In fig.13.20 the low first harmonic and high second harmonic is due to a very uneven admittance to these forces. The only reason that spectra in fig. 13.20 are not a straight line from 20db to 0db (apart from minor fluctuations) is that we have normalised them on the TSV force on the bridge. This gives us a constant force excitation, but since the admittance of the bridge varies this is not a constant power excitation.

If fig. 13.20 is compared with fig. 12.18 it can be seen that the spectrum of radiated sound per unit transverse force on the bridge is not greatly different in shape to the spectrum of the bridge admittance. Similarly by comparing fig. 13.19 with fig. 12.11 it can be seen that there is a similarity in shape. The connection in each case is the radiation efficiency of the body. Since fig. 13.19 relates to 12.11 in a similar way to the relationship between fig. 13.20 and 12.18, if there were any significant error in the shape of the curve in fig. 12.18 then the cause of that error must have similarly affected fig. 13.20. The only common factor to both curves is the TSV force, which has been inferred from the transverse displacement of the string. It is hard to see that there can be a significant error in this simple calculation. This supports the validity of the pseudo-admittance spectra found in this research for a shaker driven string.

The close relationship between the shape of the admittance curves and the radiated sound per unit force curves indicates that the violin has smoothly varying radiation efficiency. The power input from the bow to the string at its resonance harmonics also varies smoothly. So if the input is smooth and the efficiency is smooth the output must be smooth. That is not the

impression given by fig 13.19, and indeed figures such as this are often misinterpreted. Several writers have, with recourse to spectra like that shown in fig 13.19, explained why the radiated sound spectrum must be that shape and have suggested that various features avoid shrillness, dullness and a nasal tone.

13.8 Conclusions

- Above 2000Hz, the medium EAR violin radiated more sound per unit TSV force than the violins of low and high EAR, and the spectra declined with rising frequency. There was no consistent variation with the EAR in the sound radiated per unit of LSV force. This indicated that the radiated sound is more closely related to the LSV than the TSV in this range. It is unlikely that the LSV force is simply reflecting the dynamic activity of the radiating modes, since this would not explain the dependence of the radiated sound on the EAR.

- Above 1500Hz, the sound radiated per unit TSV force varied with the deviation, and the spectra declined with rising frequency. There was a small contrary variation in the sound radiated per unit of LSV force, but the radiated sound was more closely related to the LSV force than the TSV force. Again it is unlikely that the LSV force is simply reflecting the dynamic activity of the radiating modes since this would not explain the variation of the radiated sound with the deviation.

- The sound radiated per unit TSV force below 1000Hz varies inversely with the height of the belly end bouts cross arch.

- The difference in spectral envelope of the radiated sound per unit LSV between bowed and shaker driven violins indicates that bellying LSV may be making a significant contribution to the radiated sound of the bowed violin.

- The relationship between the spectral envelope of the radiated sound per unit of TSV force at the bridge and the real part of the admittance of the bridge to TSV force is consistent with a radiation efficiency that varies as the square root of the frequency.

Chapter 14

RECIPROCAL EXCITATION

14.1 Introduction

Multi-mode vibroacoustic reciprocity for a structure in an enclosed sound field (which can be assumed to be diffuse) says that the harmonic response at any point on the structure, to a given harmonic sound pressure in an excitation field, is reciprocal with the space-average radiated sound pressure by the vibration of the structure when excited mechanically at that point. More generally, it says that good radiators are good responders. This is because the response of a structure to an incident diffuse sound field is proportional to its radiation efficiency, and the sound power radiated by a given structural vibration is proportional to the radiation efficiency. To employ this principle, a violin could be immersed in a sound field and the movement of the bridge or the LSV force could be measured. The measured result would be an indication of the radiative effect of a movement of the bridge or of the LSV.

However, a little thought leads one to conclude that there must be some limitations to the extent of the reciprocal action. If a violin were immersed in a sound field, the most efficient radiating modes would be excited most strongly. These modes of vibration would not necessarily be those of a violin driven by a bow at the same frequency. The bowed violin would best excite those body modes, not necessarily at resonance, which are compliant with the forces imposed on it. Reciprocity must also exclude the effects of the non-linear string vibration and so any LSV force that is measured must come from the linear response of the body to excited modes.

If the modes that are excited by the LSV system can be excited reciprocally, it is entirely possible that this would give an LSV as measured at the tail gut transducer. By reciprocal excitation then, it may be possible to check if the LSV system is closely coupled to the sound radiating body motions. It may be possible to find what effect the arching and bass bar stiffness, have on the involvement of LSV in sound producing modes.

14.2 Method

The violins were in turn placed 1.5m from a loudspeaker, which was fed with broadband random noise. The violin was supported on foam rubber mountings at the extreme ends of the back. The sound path from the speaker to the violin was made indirect by the violin being mounted on a table top above the level of the speaker. The violin would have been located within the reverberant sound field. The sound level in the room was of the order of 75 dB. The sound pressure in the room was measured by a microphone (B&K ½ inch free field) located 3 m from the source, in the manner described in section 6.3.6. In order to eliminate, as much as possible, the effect of variations in the uniformity of the radiated noise spectrum and acoustic variations in the room, the results were recorded as the transfer function of the LSV/field sound pressure. These were spectrally analysed for presentation.

14.3 Results

14.3.1 Method of presentation of results

Fig. 14.1 shows the spectrum of LSV/field sound pressure for violin 156 medium EAR, unvarnished. All the tests gave spectra that looked something like this and the "hairy" nature of the line made it difficult to compare them with each other. However, it was noted that all violins showed a deep trough at a frequency close to 1500Hz. Others have observed that a similar trough is present in the bridge admittance of the violin.

To facilitate comparison, the line was smoothed by making each point the average of all points in the range 125Hz below and 125Hz above. The results shown below have all been smoothed in this way. The smoothed version of fig. 14.1 is shown in fig. 14.3, as the medium EAR curve. The repeated recording of spectra produced results that were very close to each other.

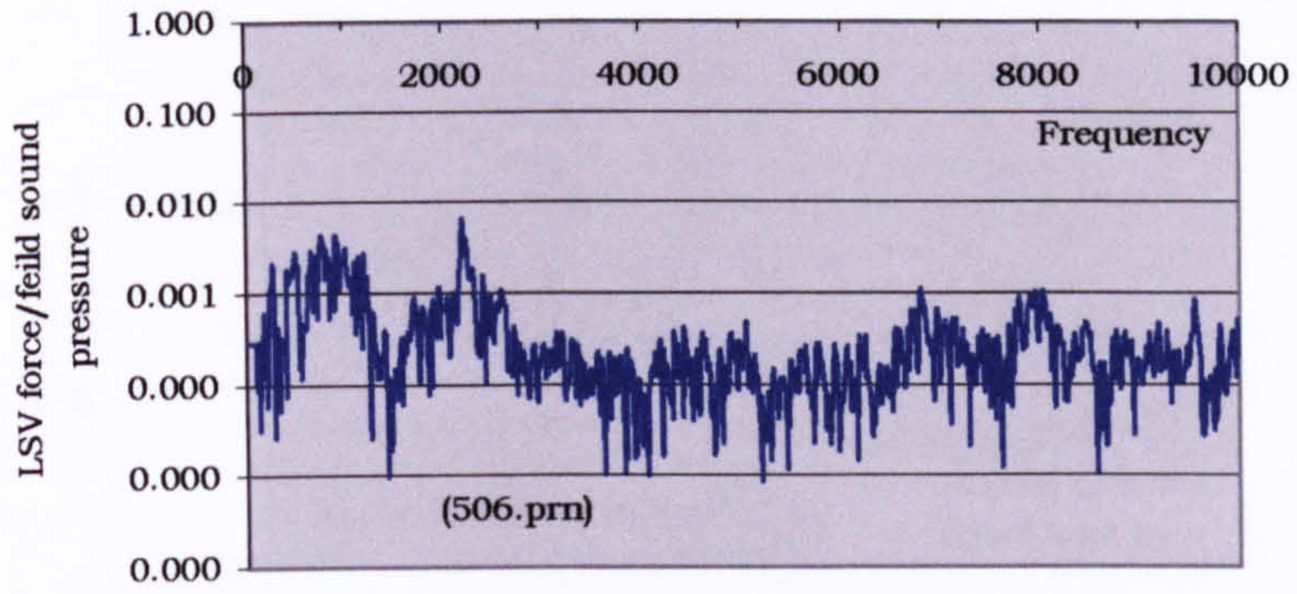

Fig. 14.1 Transfer function, LSV/field sound pressure, violin 156.

14.3.2 Violins of differing deviation

Fig. 14.2 shows our three varnished violins of normal EAR but differing deviation.

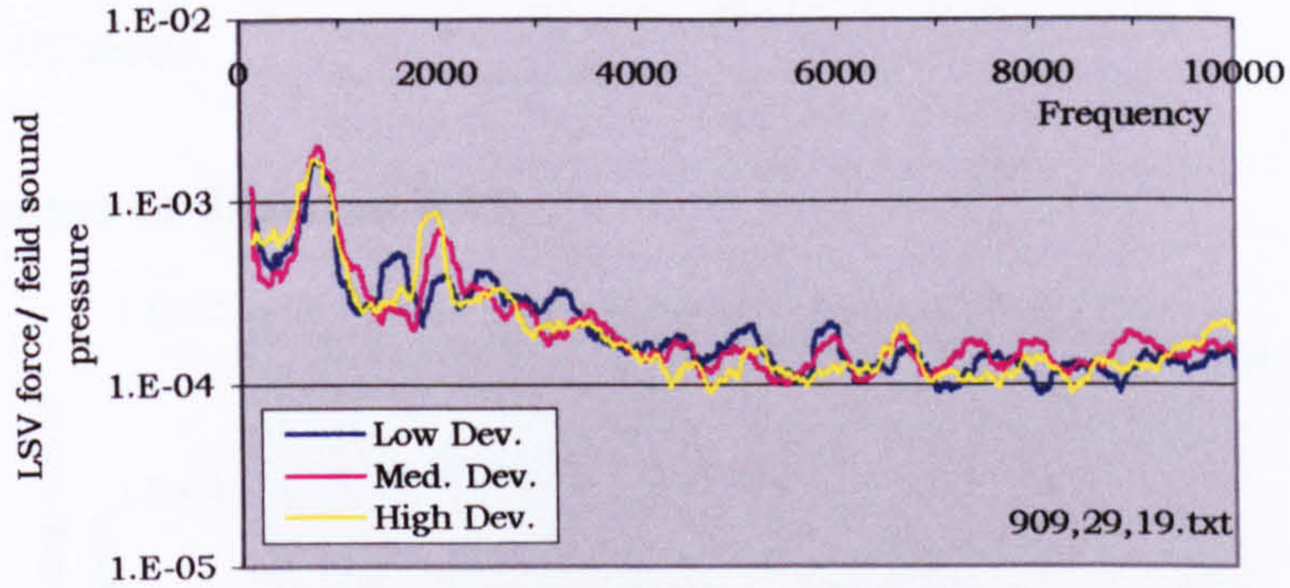

Fig. 14.2 Transfer function of LSV force/field sound pressure, varnished violins of same EAR and differing deviation.

This shows that LSV can be excited reciprocally. There is close agreement between these three violins and one would conclude that they are the same. There is no variation with deviation. In direct excitation, there is a small but discernable dependence of the radiated sound pressure on the deviation.

14.3.3 Violins of varying bass bar stiffness

Tests were conducted on violins V197Brq, and V198Mod. Both violins have the same EAR. There is a small difference in the deviation but it was shown in section 14.3.2 that this would not result in any difference in the LSV induced. Both violins are unvarnished. The essential difference

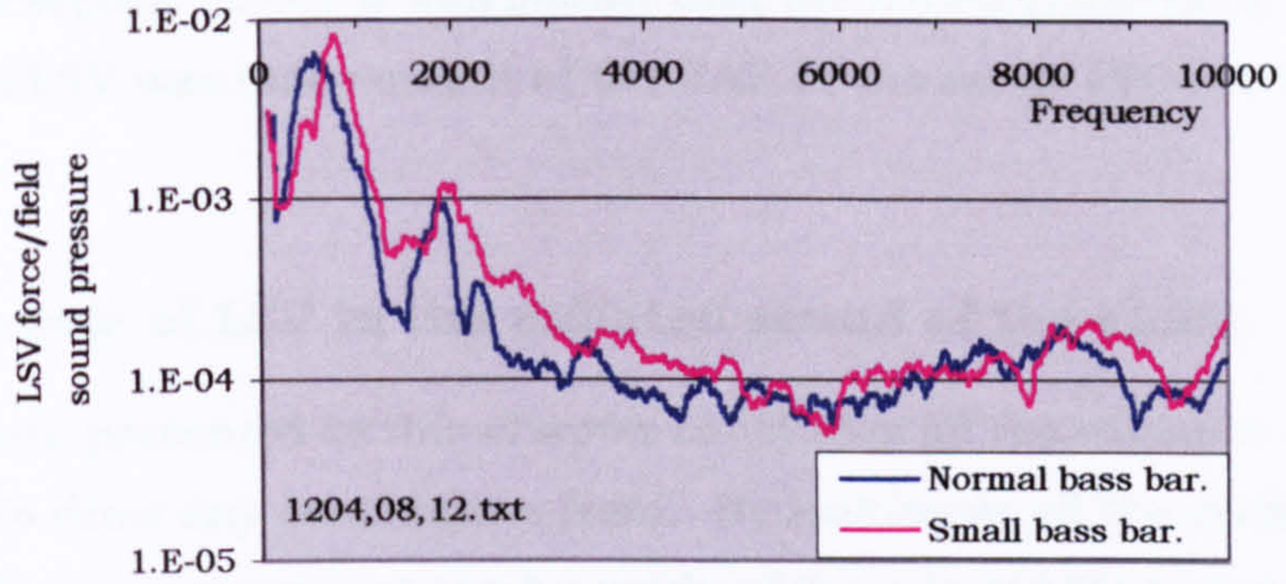

Fig. 14.3 Transfer function of LSV force/field sound pressure, violins of the same EAR and differing bass bar size.

between these violins is in the stiffness of the bass bar. Fig. 15.3 shows the transfer function LSV over field sound pressure for both violins.

From about 800Hz to 5000Hz, the violin with the small bass bar produces a higher LSV force.

14.3.4 Violins of differing EAR

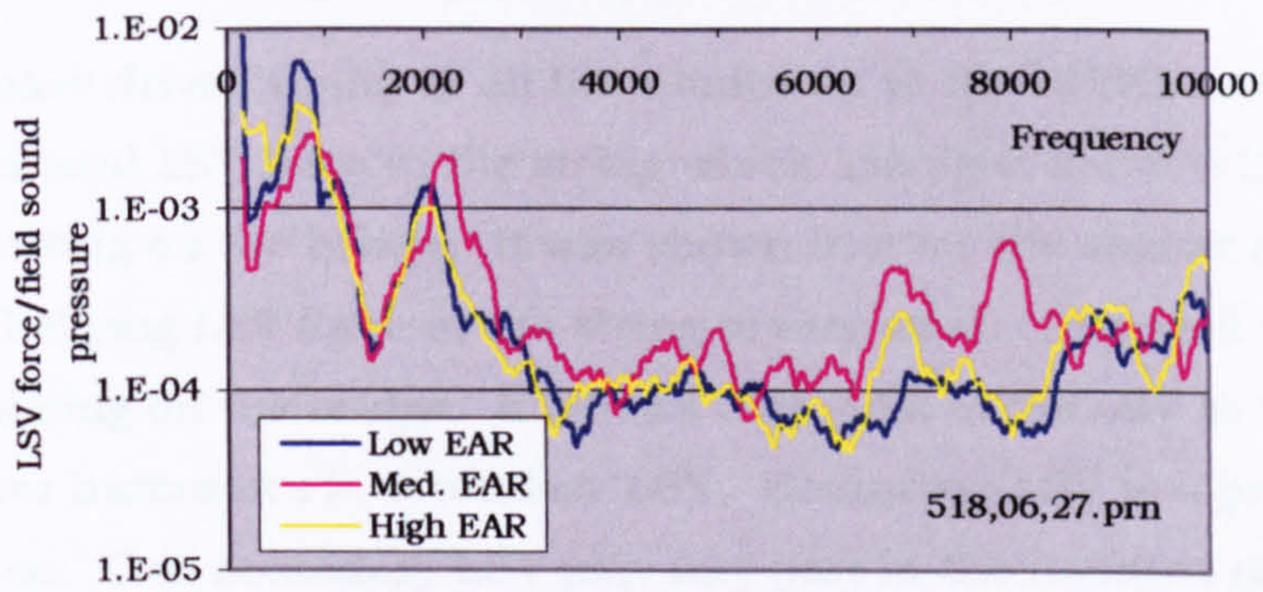

Fig. 14.4 Transfer function of LSV force/field sound pressure, unvarnished violins of differing EAR.

Fig. 14.4 compares three unvarnished violins of differing EAR. The three spectra in fig. 14.4 are all of the same form; the difference lies in the magnitude. It seems reasonable to conclude that the three violins all radiate from the same modes, the difference being due to the magnitude of the force driving the modes.

Below 1000Hz, the medium EAR violin produces less LSV than the others. From 1000Hz to 2000Hz, the three violins produce the same LSV and from 2000Hz to 8500Hz, the medium EAR violin produces more LSV than the

others. In section 13.6.1 it was shown that the sound radiated by a violin per unit of LSV was independent of the EAR in the range 2000Hz to 5000Hz.

14.4 The role of LSV in the radiated sound of the violin

The evidence presented in this chapter concludes all the evidence that is available to draw any conclusions from. By looking at all the evidence presented some assessment can be made of the role of LSV in the radiated sound of the violin.

Bellying LSV is capable of driving the violin rather efficiently. In the case of the bowed violin it was shown that the ratio of radiated sound per unit LSV was much lower than that of the shaker driven violin when the string displacement was less and much higher than that of the shaker driven violin when the string displacement was greater. This indicates that belling LSV is capable of making a significant contribution to the radiated sound. This seems an entirely reasonable conclusion given that bellying LSV is a primary source of driving energy for the violin.

For the shaker driven violin, at all harmonics up to the 10kHz investigated there was a total LSV force in the string which averaged about 0.25 of the TSV force acting on the bridge. It was shown that for the shaker driven violin, the bellying LSV force in the string is very small compared with the TSV force acting on the bridge. It follows that most of the LSV in the string in the higher harmonics is secondary LSV. Secondary LSV is a product of modal action. Can secondary LSV play any part in the radiated sound?

Above 1500Hz the envelope of the spectrum of the radiated sound in six different violins always shows a closer relationship to the envelope of the spectrum of the LSV than that of the TSV. Reciprocity indicated that the most efficient radiating modes involve LSV. The obvious conclusion from these observations is that the modal action that generates the radiated sound also generates the LSV.

However, it has been shown experimentally that the radiated sound (above 1500Hz) varies with the EAR and the deviation, in a way that is consistent with the body responding to an LSV force in the string as shown by the qualitative static analysis introduced in chapter 3. It was found that the

amount of LSV developed by reciprocal excitation was dependent on the EAR. These observations suggest that the LSV might 'drive' the body to radiate sound, rather than be a consequence of the modal actions that cause the sound.

But is that possible? It is important to understand in what way secondary LSV might 'drive' the body to radiate sound. Secondary LSV arises from the modal actions of the violin as whole. The TSV force and the primary bellying LSV force drive these modal actions. Almost all these motions could, to some degree, alter the string tension and put LSV in the string. However, we have seen that one such modal action can certainly give rise to LSV and we have called that bridge-rock LSV. It is worth looking again to see what contribution bridge-rock LSV might make to the radiated sound.

A TSV force applied transversely at the top of the bridge will cause the bridge to rotate about the sound post. The TSV driven action might do no more than to raise and lower the bass bar relative to the rest of the violin. But, we have seen that this action also effectively increases the distance from the centroid of the group of four strings to the top of the sound post. That increases the string tension while at the same time pushing down on the sound post and bending the violin in its length. Rather like an archer drawing the string on his bow. The qualitative static analysis and experimental measurements showed that the internal forces generated by this action would raise the end bouts cross arches in both the back and the belly. The static analysis suggested that any sound that might be radiated by this action would be dependent on the EAR and the deviation.

The first part of the action in twisting the belly at the bridge was a direct consequence of TSV action. The establishment of the LSV in the string was an additional effect of the TSV. The movements of the end bouts cross arches are the response to the LSV in the string but the energy driving the motion was from TSV. To summarise, secondary LSV does drive the violin to radiate sound but uses energy from TSV to do it. It can be seen as redirecting TSV energy to drive efficiently radiating modes.

Now, it could still be argued that the modal action that drives the body and puts LSV in the string, by some means puts in an amount of LSV that

varies with the EAR and the deviation. That the modal action moves the EBX arches and this movement induces the LSV in the string. But, can movement of the arches put LSV in the string? The reciprocity experiment shows that it can. But the LSV put into the string in this way was shown to be dependent on the EAR but not the deviation. Since the radiated sound is dependent on both it would appear that the LSV is not a by-product of the modal action that is causing the radiated sound.

14.5 Conclusions

- LSV can be excited reciprocally, by immersing the violin in a sound field. This implies that the most efficiently radiating modes of a violin involve LSV.
- The LSV excited reciprocally showed a higher response for the medium EAR violin but was independent of the deviation.
- Above 1500Hz the shaker driven violin radiates largely using TSV energy. Some of this energy is redirected as LSV, to which the body responds. The resulting motions are controlled by the EAR and deviation. We might say that the violin is driven by energy from TSV, but the radiated sound is contributed to significantly by modal responses to the LSV in the string.
- Below 1500Hz there is no clear evidence of the radiated sound being dominated by TSV or LSV, and the dependence on the arching is more a matter of the height of the belly end bouts cross arches.

Chapter 15
CONCLUSIONS

When a string on a violin is set in transverse vibration (TSV) by the bow, a longitudinal vibration (LSV), in part of the same frequency and in part of twice the frequency, is induced in the string. This is called bellying LSV and it has a non-linear relationship with the TSV. It is also called primary LSV and is capable of driving the body.

The primary bellying LSV force and the TSV force both act on the body and together they excite vibrational modes. The body including the strings takes part in these modes with the consequent generation of secondary LSV in the strings. Secondary LSV is a response to body motions. An example of secondary LSV generation is from bridge rock. The motions of the bridge in its own plane are very complex but that component of the motion that is a rotation about the sound post puts LSV in the strings. In this way some of the TSV driven motion transforms some of the TSV to LSV. This is one of many mechanisms where LSV functions as a channel for the redistribution of TSV energy. This transformation may be significant in that body modes may be excited by LSV that cannot be excited by TSV. The total LSV force (primary and secondary) acting vertically on the bridge is of the same order as the TSV force acting transversely on the bridge. That part of the total LSV force that arises from string bellying has a non-linear relationship with the TSV force.

The TSV force is applied to the body transversely at the bridge and transversely at the stopped end of the string. The LSV force is applied to the body vertically at the bridge and in the direction of the string at the nut and saddle.

A qualitative static analysis and experimental measurement suggested that an increase in the static tension in the string causes bending in the length of the body, an increase in the rise of all four end bouts cross arches and apart from an inwards movement of the belly edge in the area near the neck and tail saddle, it is probable that all other parts of the periphery of the belly and the back move outwards. If these movements are combined

with the static displacements caused by a bridge rotation, then the violin body enlarges by outward movement in every part, except a small area at the ends of the belly and an area of the belly centred on the sound post. The analysis indicated that the direction of static deformation would depend on two arching shape parameters called the 'EAR' and the 'deviation'.

The sensitivity of the tonal quality to variations in these parameters was informally tested and anecdotally reported. This report encouraged the idea that an experimental programme might be undertaken to investigate the role of LSV in the sound radiation of the violin, using violins purpose made to exhibit controlled variations in the arching parameters, EAR and deviation.

Most of the experiments were done with an open string driven transversely at resonance using a shaker. The driving was at single frequency but the large transverse displacement of the string introduced a non-linearity that generated an extended spectrum of harmonics in both the TSV and the LSV. Although the relationship between TSV and primary LSV is always non-linear, above the second harmonic of vibration of the shaker driven string the contribution from the non-linear source decreased significantly and there was some justification for assuming that the influence of the non-linearity was not significant in reaching conclusions from the experimental results. Further work would be needed to test this assumption thoroughly. Had the string been bowed the non-linearity would have been greater and may have been a concern. It is accepted that this is to some degree a non-linear system and that the results obtained at any one level of excitation cannot be assumed to be generic. Limitations on time and resources precluded experiments at varying levels of excitation.

Three violins of different EAR showed little difference in the TSV spectrum excited by the shaker. Above 1500Hz the medium EAR violin radiated more sound per unit TSV than the violins of high and low EAR. The radiated sound per unit TSV varied with the EAR but the radiated sound per unit LSV did not. The radiated sound and the LSV could both have been the result of the modal action that produced the sound. But, the dependence of the radiated sound on the EAR suggests that the LSV was

causing the radiated sound. Below 1500Hz the picture was less clear but there was some evidence that the radiated sound in this range varied as the inverse of the height of the end bouts cross arch.

Three violins of varying deviation again showed that above 1500Hz there was a closer relationship between the radiated sound and the LSV than between the radiated sound and the TSV, and the sound showed some dependency on the deviation. The radiated sound and the LSV could both result from a common cause, but the dependence on deviation suggests that the LSV was causing the radiated sound. Again, below 1500Hz the radiated sound varied inversely as the height of the belly end bouts cross arch.

By measuring the LSV induced in a violin when it was immersed in a broadband sound field it was shown that the most effectively radiating modes are associated with LSV forces in the string. The reciprocally excited LSV was dependent on the EAR but not the deviation. This indicated that when a violin is directly driven (by shaker or bow) the LSV is driving the end bouts cross arches rather than the reverse.

The pseudo-admittance of the violin bridge to a transverse force applied by a vibrating string was found to be very different to that found by others for an externally applied transverse force. The difference must be due to the added bellying LSV and possibly the TSV applied transversely at the stopped end of the string. This difference seriously questions the common assumption that the violin is predominantly driven by the transverse motions of the bridge, and that this can be modelled by applying an external force to the bridge. The pseudo-admittance of the bridge to the vertical force applied by the LSV force in the string was found to be higher than that due to the transverse force by about 10dB at 1kHz increasing to 20 dB at 10kHz.

The power exchanged at the bridge showed that the TSV force put power from the string into the bridge at most harmonics but there were a number of bands where the power input was small. The LSV force at the bridge put power into the violin from the string at some harmonics but took power from the bridge at others. The power exchanged at the saddle also showed that the flow was into the violin from the string at some harmonics and the

reverse at other harmonics. The envelope of the spectrum of the net power flowing into the violin from the string (to the extent that it was known) was shown to be very similar in shape to the envelope of the spectrum of the radiated sound power from the violin. This indicated a radiation efficiency that varied as the square root of the frequency.

The envelope of the spectrum of the radiated sound per unit TSV force on the bridge was similar in shape to that of the real part of the admittance of the bridge to the TSV force, except that it declines at a slower rate with rising frequency. A similar difference was noted between the radiated sound per unit LSV force and the real part of the admittance to the bridge to the vertical LSV force. In both cases the difference was consistent with a radiative efficiency that varied as the square root of the frequency.

The difference in spectral envelope of the radiated sound per unit LSV between bowed and shaker driven violins indicates that bellying LSV makes a significant contribution to the radiated sound of the bowed violin.

Above 1500Hz the shaker driven violin radiates using TSV energy. Much of this energy is transformed by modal action and is redistributed as LSV energy in the string. The motions of the body that respond to this LSV are dependent on the EAR and deviation. The radiated sound shows a closer relationship to the LSV than the TSV and shows dependence on the EAR and deviation. The conclusion is that the violin is driven by energy from TSV, but the radiated sound is contributed to significantly by modal responses to the LSV in the string.

Chapter 16

RECOMMENDATIONS FOR FURTHER RESEARCH

16.1 Repeating the experiments with bowed excitation

The use of a two-channel analyser is a source of limitation. In order to make a number of readings it is necessary to find a sustainable and repeatable excitation. For this reason the string was shaker driven. The results achieved from a shaker driven string will not necessarily be the same as those that would come from research using a bowed string (as indicated by the even number harmonic drop outs in the TSV spectrum). The answer is to use a multi channel analyser. This would enable excitation by bow strokes with a number of windows of data averaging during the stable or non-transient part of the stroke. Various levels of bowing could be used to make some assessment of the effects of non-linearity.

The same type of tail gut transducer could be used and a nut transducer should be designed and built to measure LSV within the vibrating length of the string, and enable power transfer calculations to be made with some accuracy at the nut. It should be possible to find a better way of recording the transverse amplitude of the string. More accelerometers (or optical methods) could be put on the violin, in addition to those at the bridge feet, the nut and saddle in two component directions.

16.2 Modal analysis

If repeating the experiments using a bowed excitation should confirm the conclusions reached in this thesis, the next step would be to do a modal analysis. Modal analysis has been done on a violin. The method of excitation has been that of striking the bridge with a pendulum. The body motion at a number of points on its surface has been recorded. From these data, the shape and resonance frequency of the important modes has been inferred. Since this method does not involve string swinging it may be subject to the errors that possibly exist in traditional methods of measuring bridge admittance by external excitation. The violin should be modally analysed when excited preferably by bowing the string.

If the violin were driven by bowing the open G-string by a shaker, there would be approximately 50 harmonic frequencies excited between zero and 10kHz. The gaps between these frequencies could be filled in by exciting other notes. The motion of the body at a number of points on its surface could be measured and from these data, the operating shape could be determined at each harmonic frequency. This would give a much more realistic impression of how the violin moves to radiate sound.

16.3 The effect of varnish on the radiated sound.

It was concluded in Appendix A that the only meaningful measure of the effect of varnish on the radiated sound of a violin is the sound radiated per unit bow stroke. A start has been made by the author to do this. Two violins were tested first unvarnished, and will be tested again when varnished. A professional player was asked to bow each violin (all four open strings) as strongly as possible, using a bow stroke of 4 seconds duration. The bowing is continued until 20 process averages of the radiated sound have been taken and analysed. This is repeated six times for each note. The standard deviation will be found and the repeatability assessed. After the instruments are varnished, the test will be repeated.

16.4 The timbre of violin sound

In this research, it was noted that the low EAR violin sounded hollow in tone and showed a different pattern in the first few harmonics. It should be possible to take a number of notes from existing commercial recordings of violins and spectrally analyse them to find the relative strengths of the first ten harmonics. This information could be related to the perceived tonal quality, as described by informed listeners.

16.5 Carrying power

There is some evidence that certain high frequency bands may determine the carrying power of the sound. To properly identify which bands are important would be very useful, but may also be difficult. It would be essential to listen to the violin against a background of competing sound. The ideal situation is that of a solo violin playing a concerto with an orchestra. It may be possible to record the orchestra alone (available on Music Minus One records) and play it to the soloist through earphones

while he plays and records the solo part. (It may be that a major recording company has such a separate recording of orchestra and soloist and would be prepared to make it available for this research and perhaps a financial grant also.) The solo tape could then be digitally modified to remove certain bands selectively and then recombined with the orchestra. The modified recordings could then be played to a panel of auditors who could rank them for the audibility of the soloist.

Alternatively, a solo violin could be listened to against a background of white noise. The effect on audibility of removing certain frequency bands could be investigated. This may make a useful preliminary study for the violin concerto test.

Appendix A

THE EFFECT OF VARNISH ON THE TSV, LSV AND THE RADIATED SOUND

Some interesting observations related to the effect of varnish on the TSV LSV and radiated sounds were made during the course of the research. Further research may be required to reach a conclusion in these matters but the interim results are presented in this Appendix.

A.1 Introduction

In the experimental results presented, we have discussed two groups of violins, those of differing EAR and those of the same EAR but differing deviation. It will be noticed that there are significant differences in the spectra of results between these groups. These differences are because the violins of differing EAR were unvarnished and those of differing deviation were varnished. Violin 156 (medium EAR and medium deviation), was common to both groups tested so we have results for this violin both varnished and unvarnished.

A.2 Effect on TSV

Fig. A1 shows the spectrum of transverse displacement set up in the string when both strings are driven to the same first harmonic displacement. Fig.

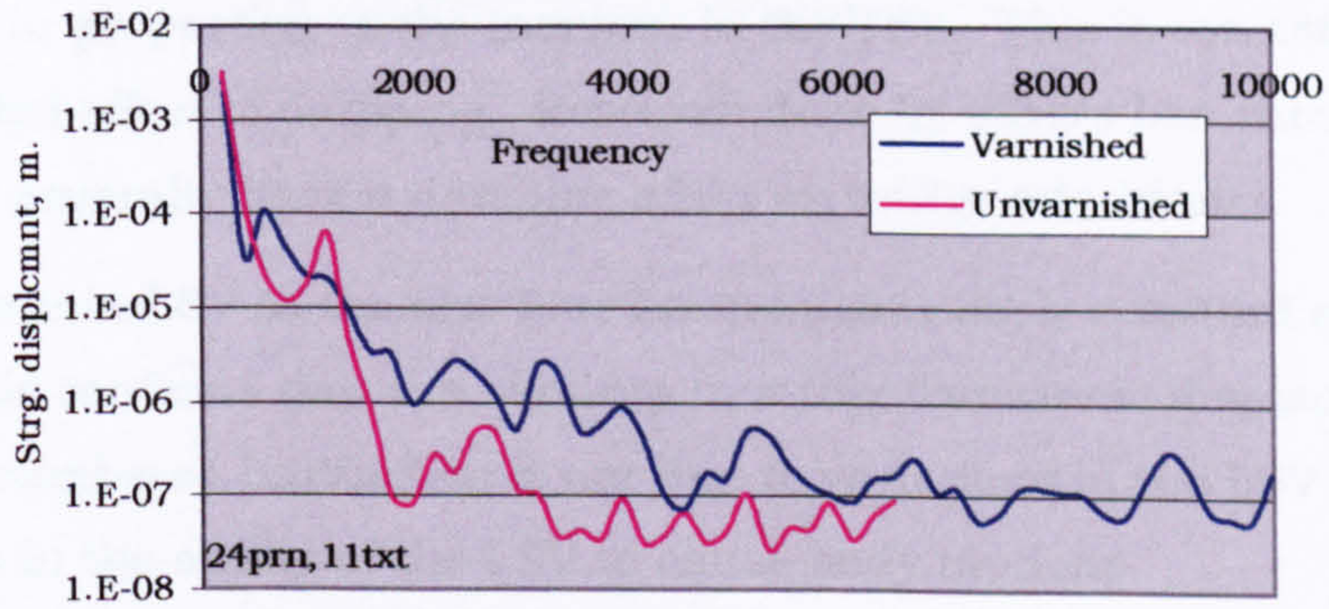

Fig. A1. Transverse string displacement for V156, varnished and unvarnished. Normalised on equal first harmonic displacement.

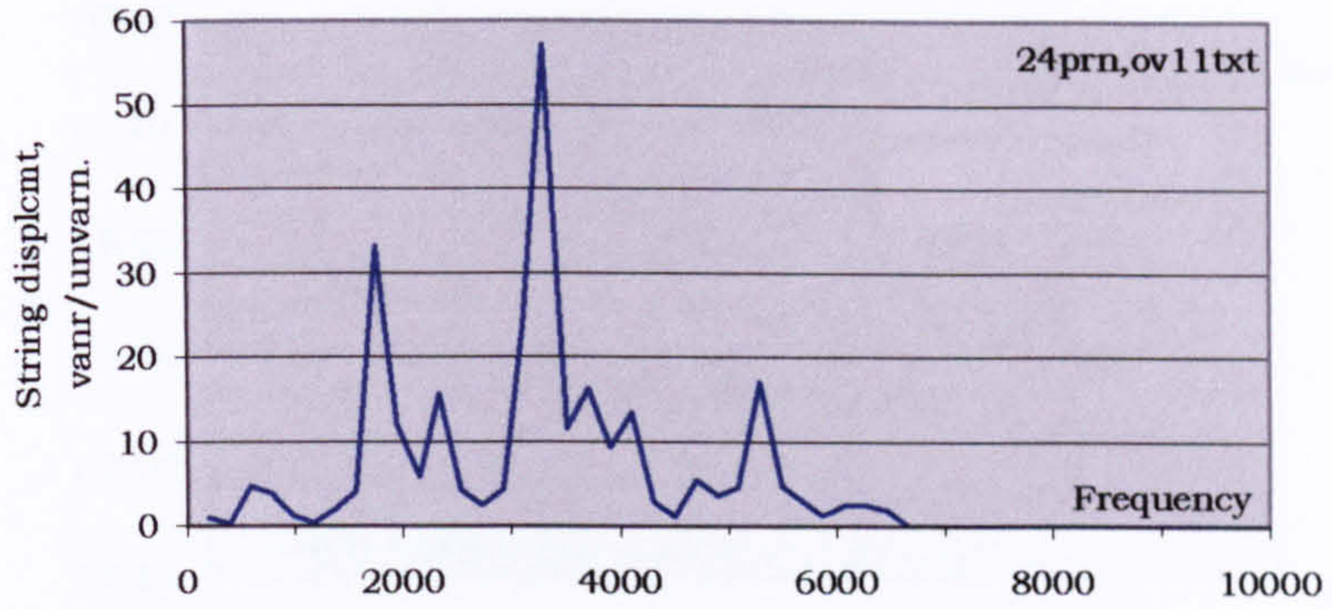

Fig. A2 Transverse string displacement for V156, varnished over unvarnished. Normalised on equal first harmonic string displacement.

A2 shows the spectrum for the varnished violin divided by that of the unvarnished violin. The difference is variable, it increases by an average of 10.2 times above 1500Hz and below 1500 Hz it reduces by 2.2 times.

It is interesting to note that the transverse string displacement is reduced in the second, fourth and sixth harmonics. This suggests that the reason for the difference in transverse displacement generally is related to LSV. If the varnished violin was able to respond more to LSV forces, then the pseudo-admittance of the second harmonic would increase and the string displacement would reduce. (see section 12.3.6)

A.3 Effect on LSV

Fig. A3 shows the spectrum of LSV set up in the string when both strings are driven to the same first harmonic displacement. Fig. A4 shows the spectrum for the varnished violin divided by that of the unvarnished violin. The ratio is very variable but averages two times. The LSV has not increased in proportion to the increase in the TSV. This is consistent with the expected effect of damping. Research done by others has shown that varnishes generally have a damping effect on bridge admittance.

The increase in LSV in the first four harmonics is fairly constant at about three. This confirms that the big drop in string transverse displacement in the even numbered harmonics is not due to variations in the LSV but to variations in the ability of the LSV to cause body motions.

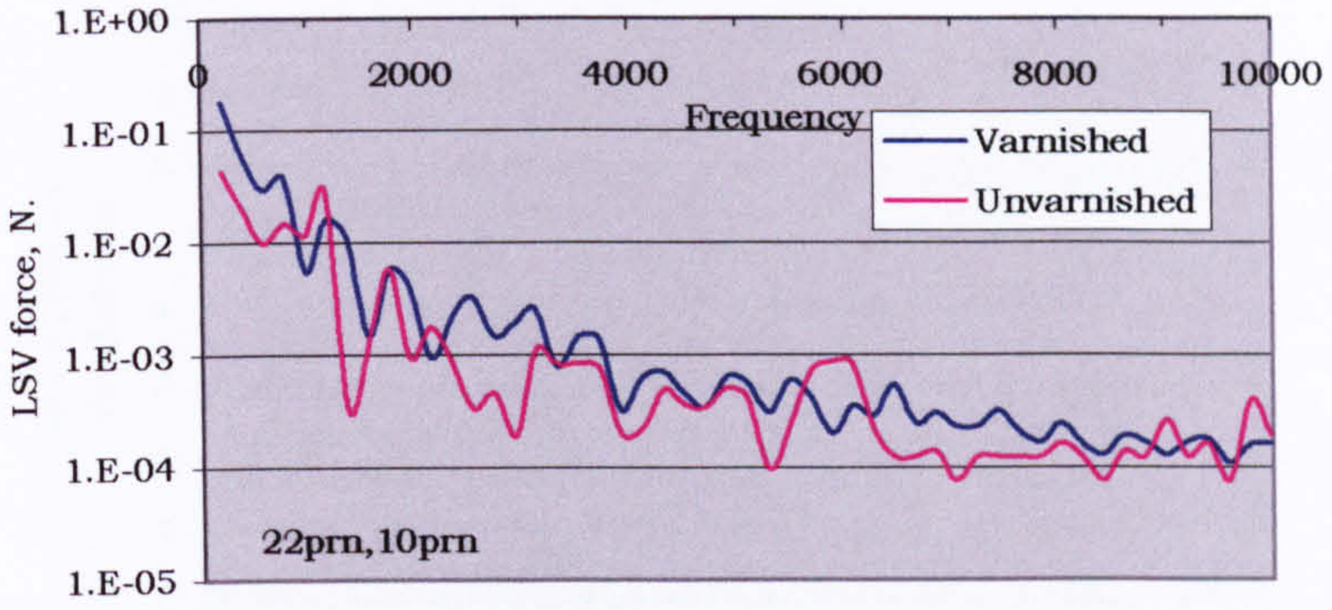

Fig. A3. LSV for V156, varnished and unvarnished.
Normalised on equal first harmonic string displacement.

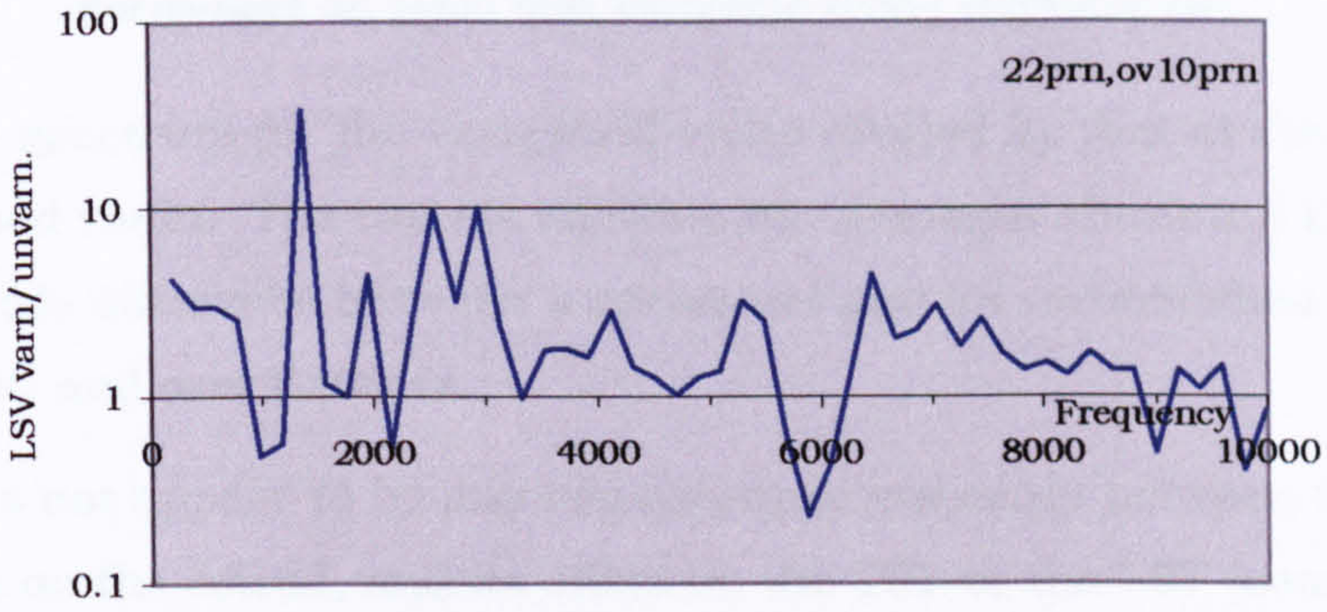

Fig. A4. LSV for V156, varnished over unvarnished.
Normalised on equal first harmonic string displacement.

A.4 Effect on radiated sound with the same first harmonic

Fig. A5 shows the spectrum of sound pressure radiated by the violin when both strings are driven to the same first harmonic displacement. Fig. A6

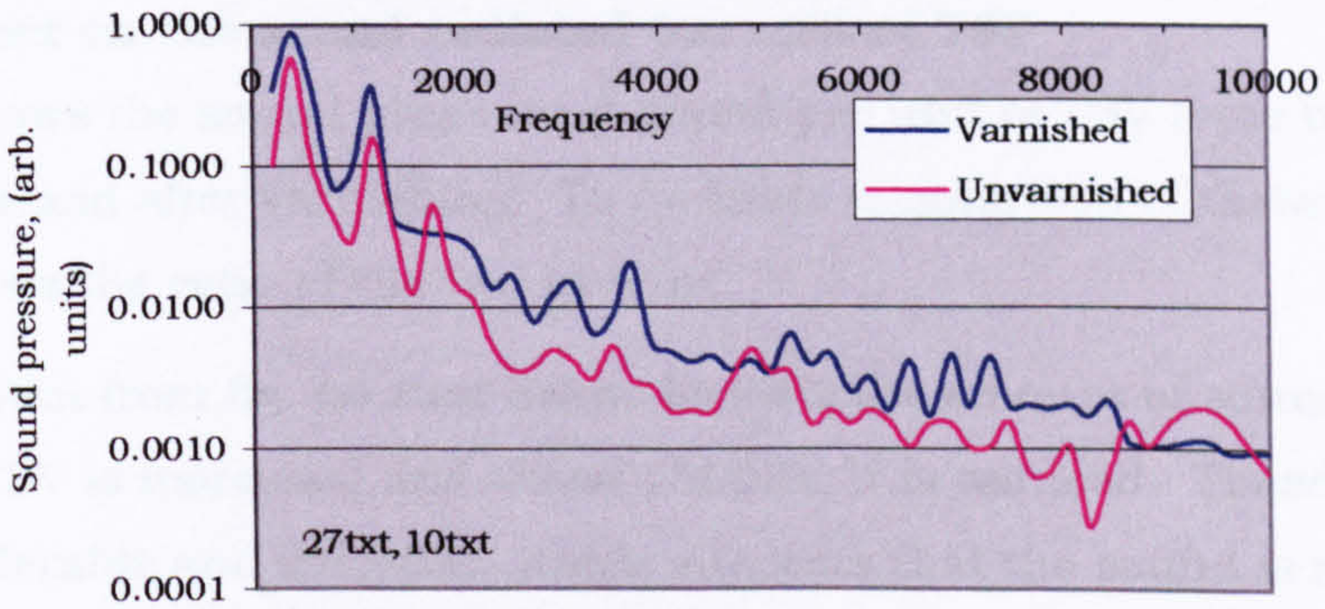

Fig. A5. Radiated sound pressure for V156, varnished and unvarnished.
Normalised on equal first harmonic string displacement.

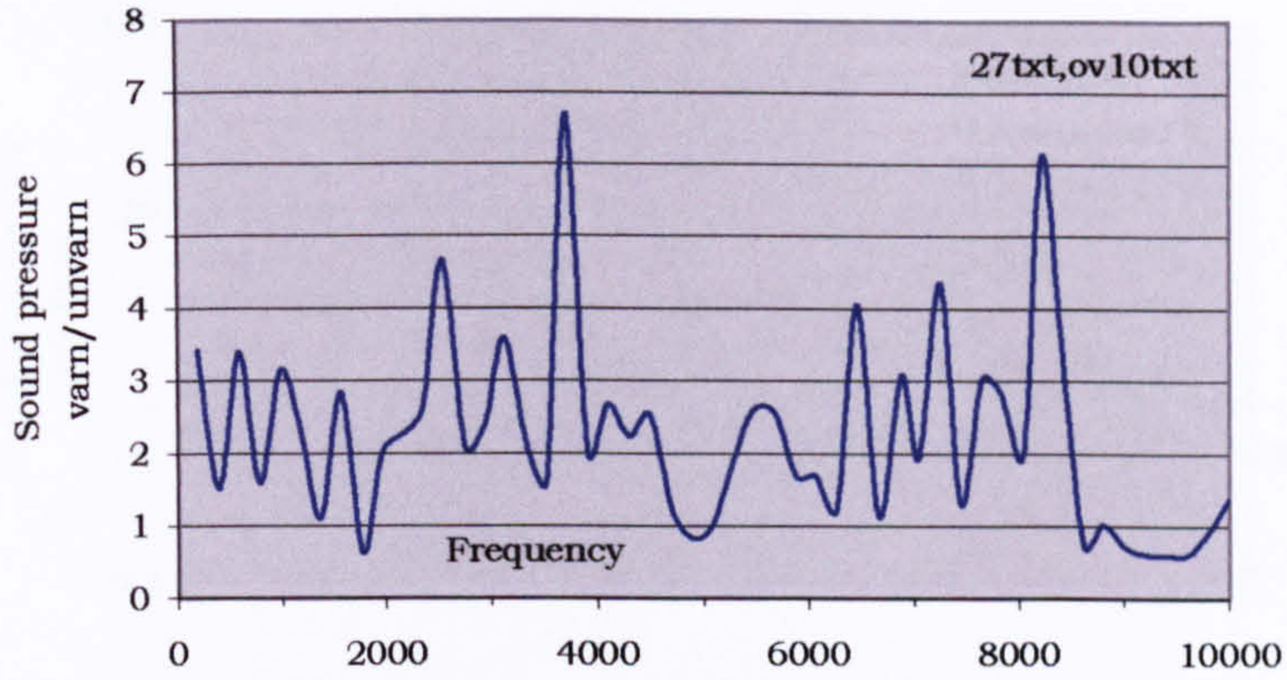

Fig. A6. V156. Radiated sound pressure, varnished violin over unvarnished. Normalised on equal first harmonic string displacement.

shows the spectrum for the varnished violin divided by that of the unvarnished violin. The ratio is variable but averages about 2.5 times. There is little difference between a varnished and an unvarnished violin at 1800, 5000 and over 8500Hz.

There does not appear to be any consistent relationship between the effect of varnish on the sound, and its effect on the TSV or the LSV (comparing figs. A6, A4 and A2.). Since the violin is a linear system, this is an indication that the change due to varnish must arise from a change in the functioning of the radiating system. That is, varnished and unvarnished violins assume different modes.

A.5 Radiated sound change related to driving forces

A.5.1 Effect on the sound radiated per unit of TSV

Fig. A7 shows the sound pressure radiated per unit of TSV force by violin 156 before and after varnishing. To facilitate comparison of these spectra, fig A8 shows the ratio of the two spectra.

It is apparent from fig. A8 that below 1500Hz the amount of sound radiated per unit TSV is increased and above 1500Hz, it is reduced. These changes are considerable and irregular, which suggests that the sound is not closely related to the TSV.

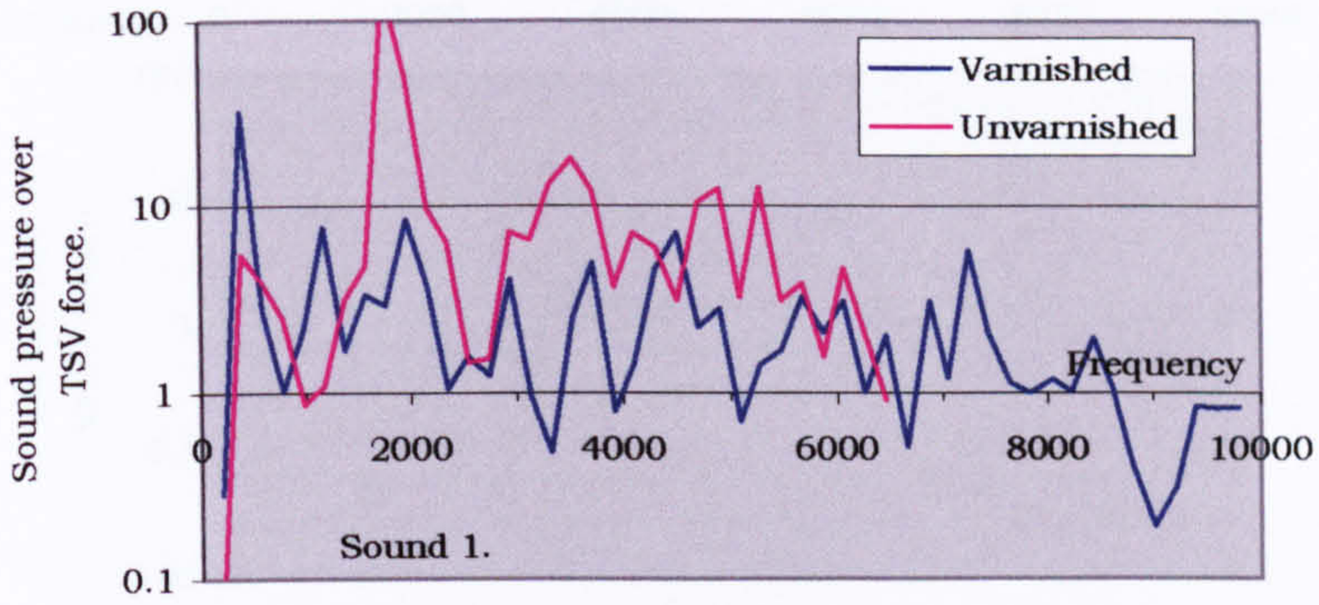

Fig. A7. Sound pressure radiated per unit TSV force in each harmonic, varnished and unvarnished.

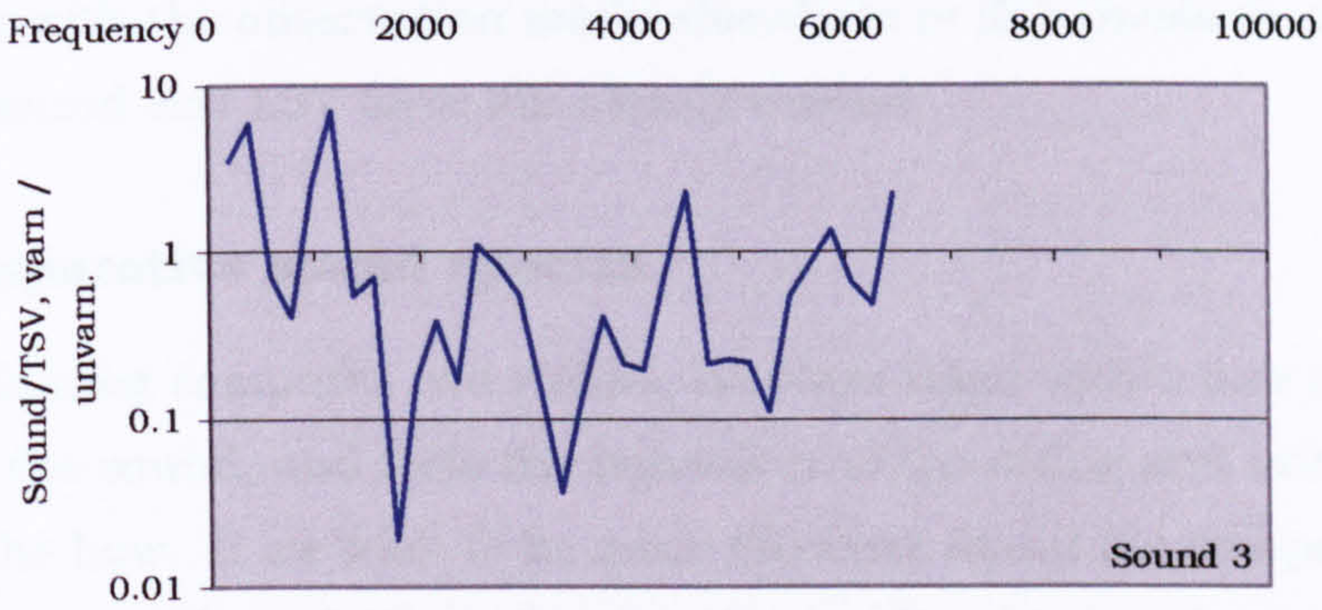

Fig. A.8 Sound pressure radiated per unit TSV force, varnished over unvarnished.

A.5.2 Effect on sound radiated per unit of LSV

Figs. A9 and A10 show that the sound radiated per unit of LSV force has been rather less affected by the varnish than was the sound radiated per unit TSV. Broadly speaking, the sound radiated per unit of LSV is little changed. This suggests again that the change in the LSV caused by the

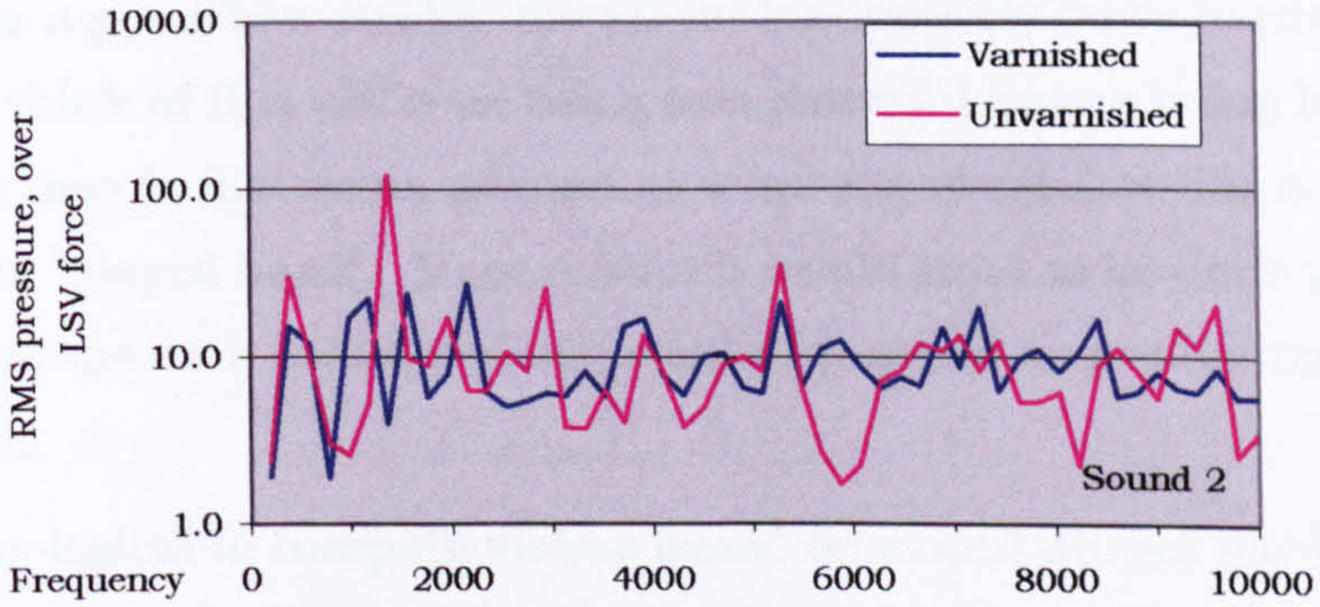

Fig. A9. Sound pressure radiated per unit LSV force, varnished and unvarnished.

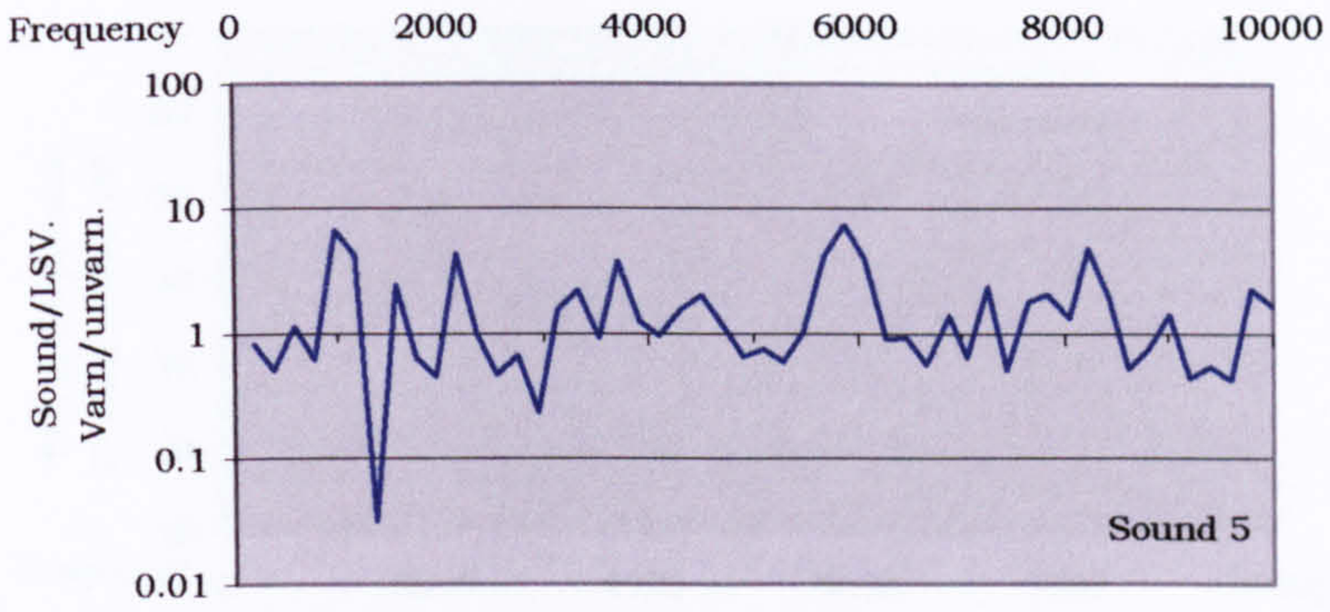

Fig. A10. Sound pressure radiated per unit LSV force, varnished over unvarnished.

varnish is matched by a similar change in the radiated sound. This is consistent with the observation made elsewhere in this thesis that the radiated sound and LSV force are closely related.

A.6 Comparative sound spectra

When a violinist compares two violins, he plays them with a bow and listens to the sound, and feels the behaviour of the string and bridge through the bow. If we wish to be more objective about the comparison we could Fourier analyse the sound and compare the spectra. Such accuracy of comparison of the sound calls for an equivalent accuracy of measurement of the bow stroke.

The input power from the bow depends on the bowing force and velocity. These are difficult to measure. A further complication is that there is no reason to believe that different violins extract the same energy from a given bow stroke. The input power due to a "standard bow stroke" could vary with the properties of the violin. It is possible that if a violin takes less power from a given bow stroke, the player instinctively bows harder. He might not think of this violin as being less powerful but as being harder to play. This may in fact be an advantage since many soloists like a violin that can be "played hard". More research would need to be done to find a basis for comparison that a violinist would recognise as producing valid indications.

It would be logical to compare violins based on sound output per unit of power input from the bow. However, that is too difficult. Published spectra of radiated sound usually present the sound radiated by a violin when the

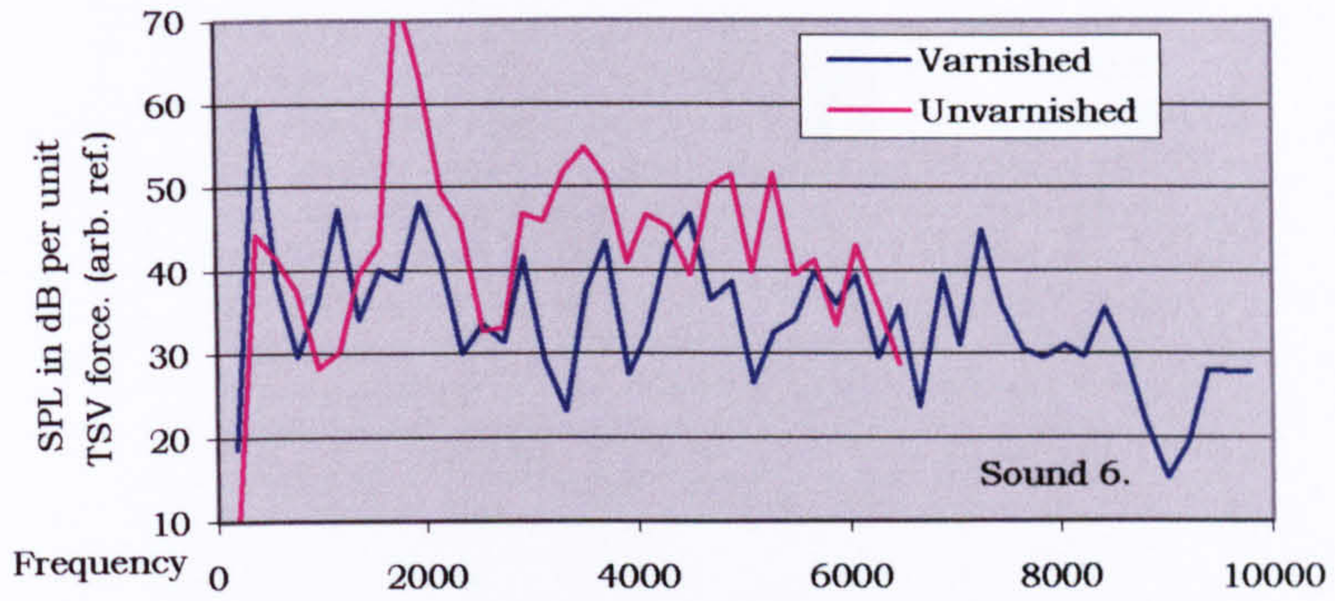

Fig. A11. Sound pressure level radiated per unit of TSV force. V 156 varnished and unvarnished. Shown on a decibel scale

bridge is driven by a constant force. Our equivalent of this is shown in fig. A11.

This is a misleading comparison because it fails to take into account that the transverse force on the bridge is less if the violin is unvarnished. By looking again at fig. A1 we know that the shaker established a very different transverse displacement spectrum in the string, depending on whether the violin was varnished or unvarnished. We clearly need to find a more realistic basis of comparison between violins.

Probably the best option is to compare radiated sound pressure based on equal first harmonic transverse displacement of the string. Fig. A5 shows such a comparison. A presentation such as this only has meaning on a comparative basis, since if there were only one curve on the graph it would tell us very little. If on the other hand we divided the curve by the TSV force, we would get something approaching a horizontal line. It is much easier to relate things to a horizontal line. Then of course we have come back to the traditional SPL/TSV curve, with the shortcomings mentioned. The problem seems to be insoluble.

A graph that gives a realistic picture of the effect of varnish on the SPL/TSV of a violin has been arrived at by the following means. If we take the graph in fig. A11 and divide the spectrum for the unvarnished violin by the increase in TSV caused by varnish (fig. A2), we get a truer comparison between the spectrum for a varnished violin and that for an unvarnished violin. The varnished violin spectrum is fairly uniformly higher than that of the unvarnished violin, the difference averaging 6.4dB.

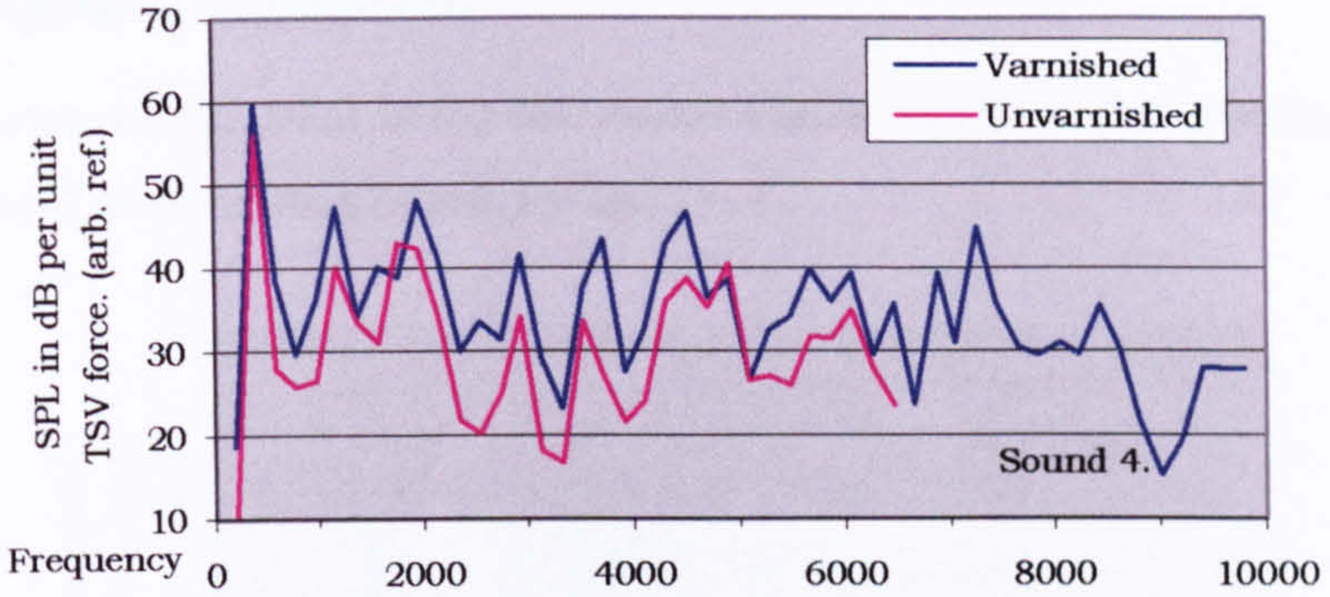

Fig. A12. Sound pressure level radiated by V156 varnished, per unit of TSV force on the bridge. Also shown is the same spectrum for the violin unvarnished, reduced by the ratio of the TSV force on the bridge for the unvarnished violin over that of the varnished violin. This is a device to give an effective comparison of spectra, varnished and unvarnished, of radiated sound per unit of string displacement.

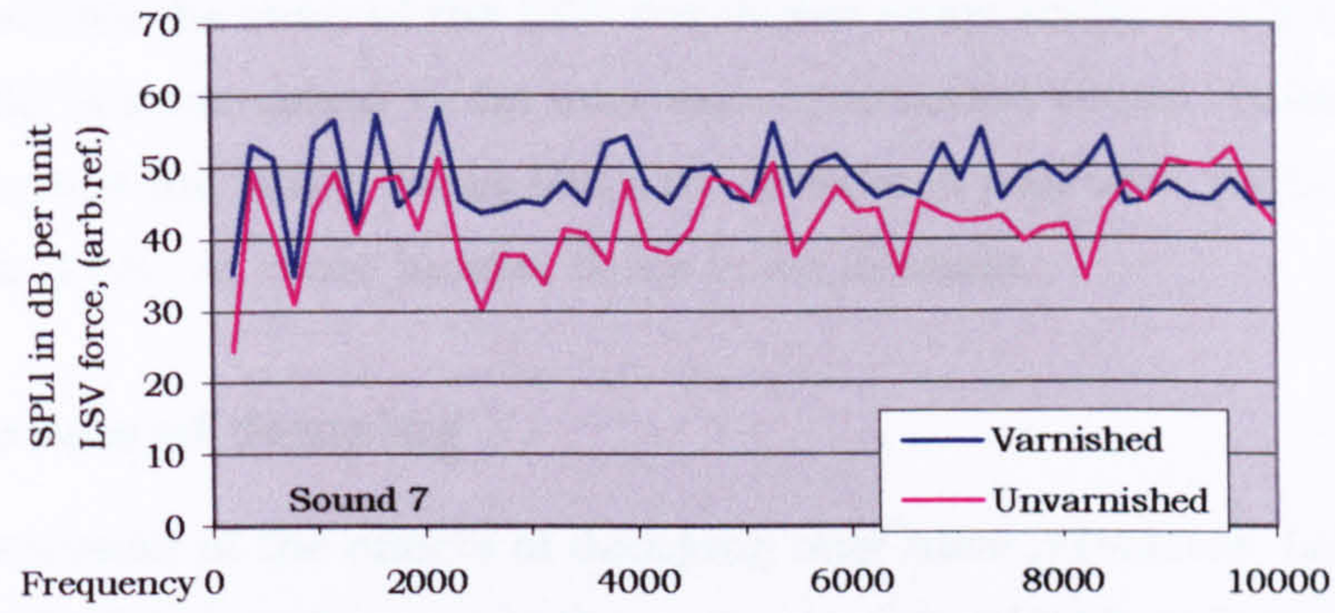

Fig. A13. Sound pressure level radiated by V156 varnished, per unit of LSV force in the string. Also shown is the same spectrum for the violin unvarnished, reduced by the ratio of the LSV force in the string for the unvarnished violin over that of the varnished violin. This is a device to give an effective comparison of spectra, varnished and unvarnished, of radiated sound per unit of LSV force.

Fig. A13 shows a similar presentation of the sound radiated per unit of LSV. The greater uniformity of the sound radiated per unit LSV does support the view that the change in radiated sound brought about by the varnish is more closely coupled to the LSV force than the TSV force. The difference averages 6.5dB, and is not due to more sound being radiated per unit LSV (see fig. A10), but more LSV radiating the same sound per unit of LSV.

The evidence presented up to this point suggests that the increase in the radiated sound caused by the varnish is LSV driven.

A.7 Reciprocal excitation

The red curve in fig. 14.2 is for the same violin as the red curve in fig. 14.4, except that it was unvarnished in fig. 14.4.

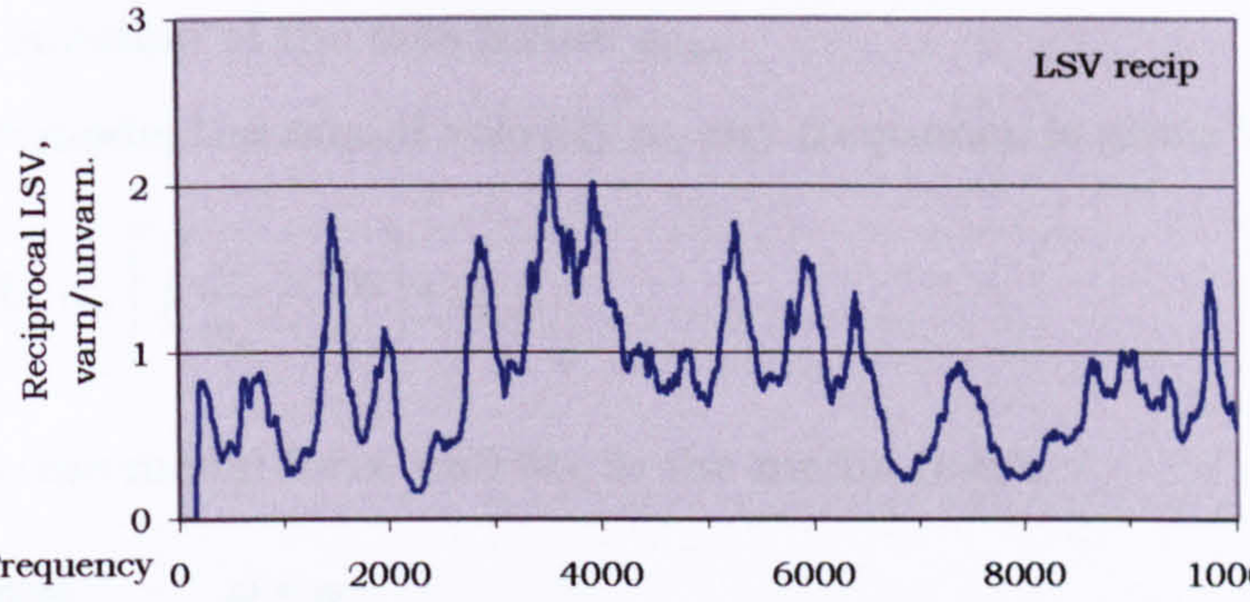

Fig. A13. LSV force developed by reciprocal excitation in a broad band sound field.

Fig. A13 shows the ratio of the LSV developed reciprocally in a broadband sound field of a varnished violin over an unvarnished violin. Taken on average across the whole range the LSV developed has been reduced by the varnish to 0.85. At some bands, there is an increase.

A.8 The role of damping

Some discussion of the effects of damping may have relevance. Let us define the body's loss factor η is the sum of mechanical loss factor and a radiation loss factor. The mechanical loss factor is $\eta_m = 1/Q_m$ which relates the stored vibration energy to that dissipated into heat, and the radiation loss factor is $\eta_r = 1/Q_r$ which the stored vibration energy to that radiated as sound (where Q_m and Q_r are the corresponding quality factors). If E is the time-averaged vibrational energy of the body, then the mechanical and radiated time averaged power losses are respectively: $\eta_m \omega_o E$ and $\eta_r \omega_0 E$.

Consider an excitation at an isolated structural resonance ω_0 by a given force F on the bridge. The input power = the power dissipated by mechanical loss + the radiated power.

Thus $\frac{1}{2}\left|\tilde{F}\right|^2 R_e\{Y_b\} = (\eta_m + \eta_r)\omega_0 E = \eta_{total}\,\omega_0 E$, where Y_b is the admittance of the bridge.

So, $E = \frac{1}{2}\left|\tilde{F}\right|^2 R_e\{Y_b\} / \omega_0(\eta_m + \eta_r)$

$\therefore$ Radiated power $W_r = \frac{1}{2}\left|\tilde{F}\right|^2 R_e\{Y_b\} . \frac{\eta_r}{\eta_m + \eta_r}$ ----------(A.1)

But Y_b is a function of the loss factor η_{total}.

For a single mode, the modal velocity at any frequency is given by:

$$\tilde{V}_m = \tilde{F}_m / M_m \omega_0 \left[j\left(\frac{\omega}{\omega_0} - \frac{\omega_0}{\omega}\right) + \eta_{total} \right]$$

where $\tilde{F}_m$ is the modal force and M_m is the modal mass.

At resonance $\omega = \omega_0$

So $\tilde{V}_m = \tilde{F}_m / M_m \omega_0 \eta_{total}$

Or $Y_m = \tilde{V}_m / \tilde{F}_m = 1/M_m \omega_0 \eta_{total} = R_e\{Y_m\}$

Substituting in equation 5.1 gives:

$$W_r = \frac{1}{2}\left|\tilde{F}\right|^2 . \frac{1}{M_m \omega_0 \eta_{total}} . \frac{\eta_r}{\eta_{total}}$$

or $W_r = \frac{1}{2}\left|\tilde{F}\right|^2 . \frac{1}{M_m \omega_0} . \frac{\eta_r}{(\eta_m + \eta_r)^2}$ ----------(A.2)

Broadband modal excitation As ω moves above 1000Hz, the excitation will include modes off resonance. Under these circumstances a broad band formula which allows for a mixture of excitation, close to resonance, and off resonance, would be required. Fahy *(in a personal communication)* proposes that an appropriate formula would be,

$$W_r = \frac{1}{2}\left|\tilde{F}\right|^2 . \frac{1}{M_m \omega_0} . \frac{\eta_r}{(\eta_m + \eta_r)}$$ ----------(A.3)

The radiation loss factor at any frequency ω_0 is given by;

$\eta_r = \frac{\rho_0 c \sigma}{\omega_0 m}$ where ρ_0 = the density of air = $1.2\,kg/m^3$

c = the speed of sound in air = $343\,m/sec.$

m = mass per unit area of top plate

$= 400kg/m^2 \times \frac{2.8}{1000} = 1.12\,kg/m^2$

σ = the radiation efficiency

$$\eta_r = \frac{1.2 \times 343 \times \sigma}{2\pi f \times 1.12} = 58.5 \times \frac{\sigma}{f}$$

A personal communication *(to F J Fahy, Southampton University, from G Bissenger, East Carolina University, 2001)* gives modal-average values of the radiation efficiency, of some of the resonant modes of a violin. From these figures, the value of the radiation loss factor η_r can be found. Bissenger also gives η_m as approximately 0.02 at 500Hz and 0.008 at 4000Hz. By interpolation η_m can be found for 1000 and 2000Hz.

F	σ	η_r	η_m	$\frac{\eta_r}{(\eta_r+\eta_m)^2}$	$\frac{\eta_r}{(\eta_r+\eta_m)}$
1000Hz	0.2	0.012	0.018	-9.7%	-5.8%
2000Hz	0.3	0.0088	0.014	-9.9%	-5.7%
4000Hz	1.0	0.015	0.008	-6.7%	-3.4%

The above tabulation shows for a particular frequency, the radiation efficiency, the radiation loss factor and the mechanical loss factor. The last two columns show the percent change in the radiated sound power arising from a 10% increase in the mechanical loss factor, as calculated using the factors shown at the head of the column. Where the radiation comes from modes at resonance, as may be the case below 1000Hz, a 10% increase in the damping would result in a similar loss in the radiated sound power. Using the broadband excitation formula that would apply increasingly above 1000Hz, the effect of damping on the radiated sound power is halved. The effect of damping on the power radiated by a super-resonant mode would be nil.

The violin does not appear to be sensitive to damping. This is demonstrated by the fact that one can touch the violin almost anywhere on its surface with little audible effect on the radiated sound. The violin's apparent low dependence on damping suggests that the modes that dominate the radiation are either super-resonantly excited or of high radiation efficiency. Touching may, and probably does, damp the non-radiating modes, but since they are non-radiating there is little audible effect on the sound.

A.9 Comparison with received wisdom

The writer has been unable to find any report of the effect of varnish on the radiated sound of a violin when it is excited by driving the string. There are reports of the effect of varnish on modal shapes, displacement and damping of a violin excited by direct excitation of the bridge. There are reports of the radiated sound resulting from swept sine wave excitation of the bridge. From these experiments, the presumption has been made by many that the effect of varnish on sound can only be to diminish it, Although the evidence produced here would show that the sound per unit of string displacement has increased, the production of that string displacement may have required a greater power input if the violin was varnished. It is therefore recognised that normalising on string displacement may not be relevant. The only fact that matters is the sound radiated per unit of bow stroke. To measure that would seem to be a logical next step.

The effect of varnish may be to slightly reduce modal displacements. A secondary effect may be to damp bridge rotation, thereby somehow transferring power from TSV driven modes to the more efficient LSV driven modes thereby increasing the radiated sound.

Appendix B

DETERMINATION OF THE SPRING CONSTANT OF THE STRINGS

B.1 Introduction

In order to make any comparison between theoretical prediction and experimental results, it is necessary to determine the spring stiffness of each string. The stiffness of the string may be influenced dynamically by visco-elastic effects. For this reason it was decided to that it should be determined dynamically, and at the static tension and frequency approximating to the range of application. The method employed had to involve vibrating a string in tension.

B.2 Method

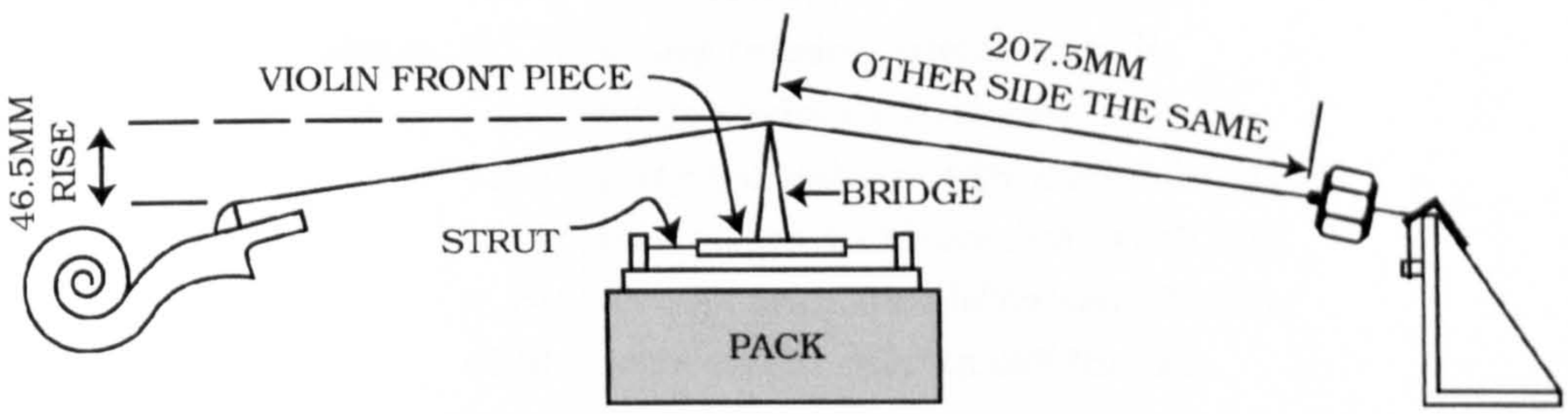

Fig B1. Apparatus for determining the spring constant of the strings.

The apparatus used is shown in fig. B1. The string passes from the peg box, over the bridge and is attached to a force transducer, which is in turn anchored by a thick but flexible nylon ligament to the anchor. The string was tensioned to normal playing tension. This was determined by plucking it and adjusting the tension to get a note appropriate to its free length. The bridge is mounted on a section of violin front (approx. 60mm by 70mm). This is supported by a rubber strip under the wood on the line of each bridge foot. The two rubber strips are of very different stiffness thus enabling the bridge to rotate about a point close to the first string foot, in a manner very similar to that on a real violin. The wood violin front piece is constrained by matchstick sized wood struts that extend to a rigid steel

surround, in such a manner as to eliminate horizontal movement while not restricting vertical movement. The bridge is driven by a shaker to rotate in its own plane, thus causing the crown of the bridge to rise and fall. All the strings being tested were located in what is normally the position of the third string. The length of string each side of the bridge was made equal in order to eliminate the complication of bridge flexure. The velocity of the vertical movement of the bridge at the point where the string contacts it was measured by an LDV.

B.3 Processing of results

The analyser recorded a transfer function of $\frac{\text{force}}{\text{velocity}}$.

$$\text{Analyser EMF} = \frac{\text{output from force gauge}}{\text{output from laser}}$$

$$= \frac{T_{LSV} \times 3.9 \times 10 \times 10}{v \times 6240} \text{ mV/mV}$$

where T_{LSV} = string tension vibration in N.

v = bridge velocity in m/sec.

3.9 = force transducer calibration in pC/N

10 = charge amp. calibration in mV/pC

10 = charge amp. amplification (20 dB).

6240 = laser calibration in mV/m/sec.

but $v = 2\pi Rf$

where $2R$ = bridge rise in m.

The force induced in the string per unit rise of the bridge is given by;

$$\frac{T_{LSV}}{R} = \text{analyser EMF} \times \pi f \times \frac{6240}{3.9 \times 10 \times 10}$$

$$= \text{analyser EMF} \times f \times 100.5$$

in N/m.

spring stiffness k_{st} = force required to stretch a 1m long string by 1m.

$$= T_{LSV} \times \frac{L}{A}$$

$$= \frac{T_{LSV}}{R} \times .2075 \times \frac{207.5}{46.5}$$

= Force per unit bridge rise × 0.9259 N/m/m, or simply N.

B.4 Results

The results probably show the influence of longitudinal string resonance. There was only a narrow frequency range from 0 to 500 or 700 Hz where there was a simple linear relationship between the displacement of the bridge and the resulting increase in string tension. To estimate the spring constant of the string the transfer function used was that found in the simple linear relationship. The experimental results and the calculation of the spring constant are shown in the following pages. The tolerance given with the result is such that there is a 90% probability that the error will be less than the tolerance. The figure of 90% has been used in both National and International Standards in acoustics and forms a recognised basis for comparing tolerances.

First string spring constant

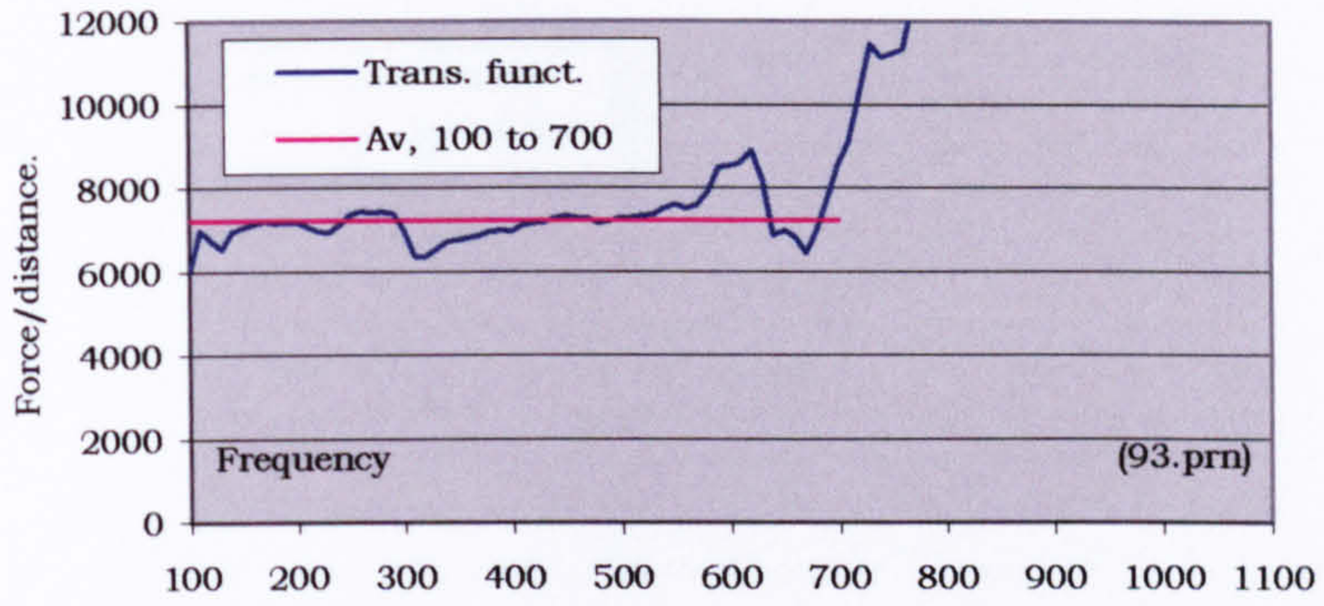

Fig B2. First string, transfer function of force/displacement.

Average transfer function 100 to 700Hz is 7224 stdev 560.

Spring constant =7224 x 0.9259 = 6688 N + or- 15.5% (90% probability).

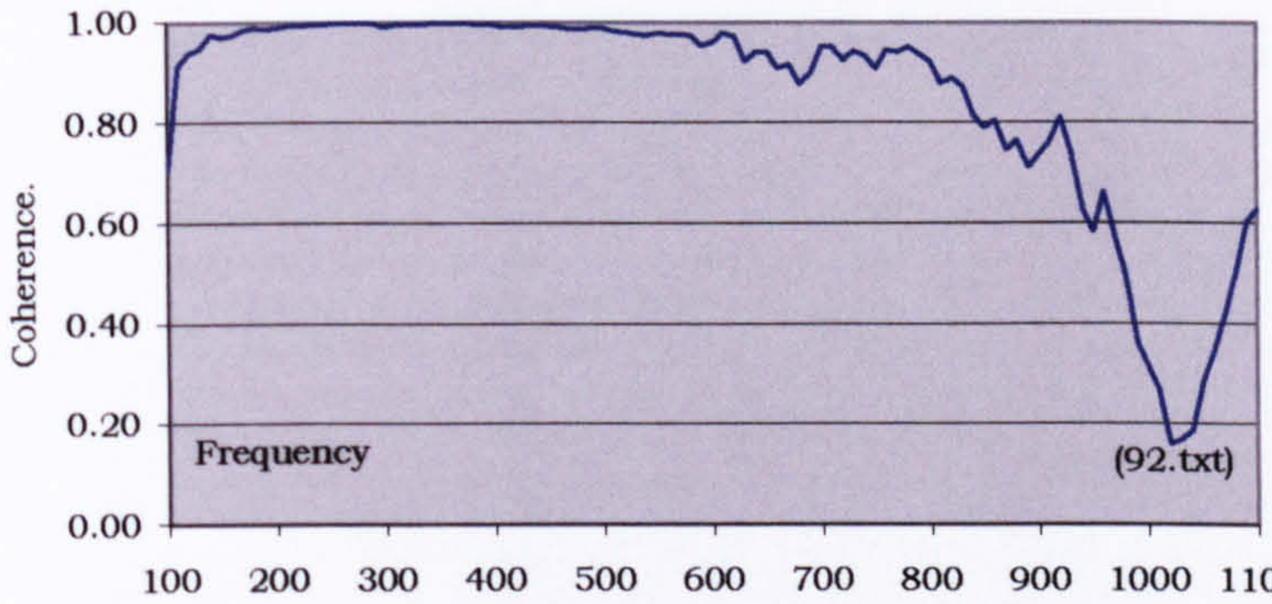

Fig B3. First string, coherence.

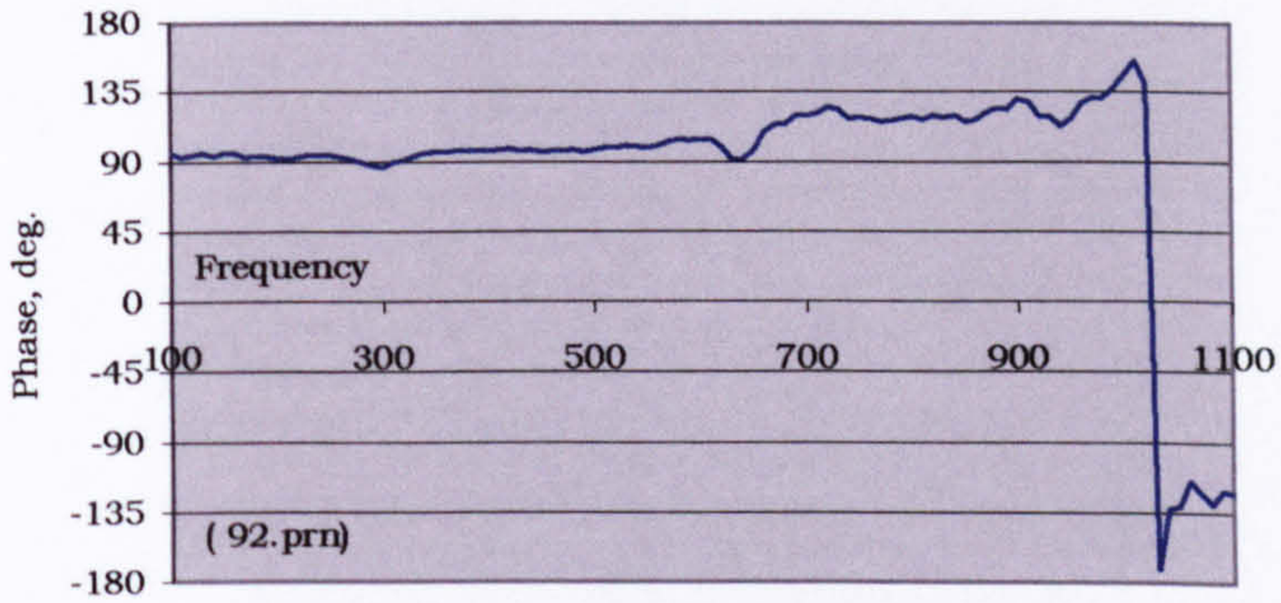

Fig B4. First string, phase.

Second string, spring constant

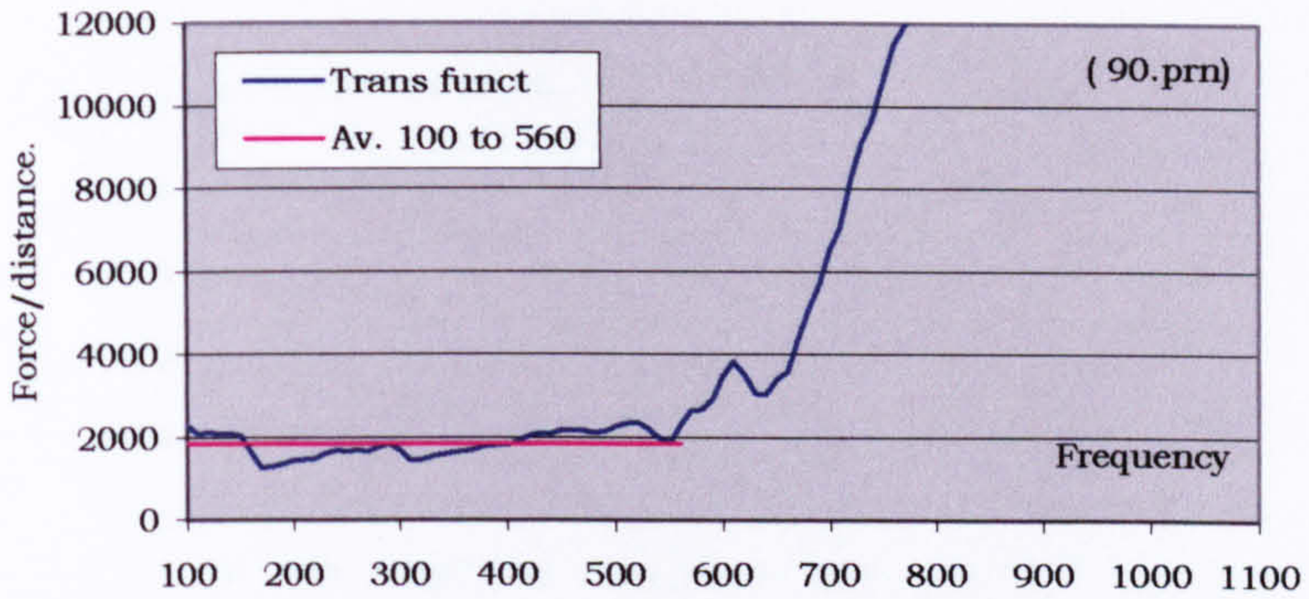

Fig B5. Second string, transfer function force/displacement.

Average transfer function 100 to 560 Hz is 1848 stdev 301.

Spring constant = 1848 x .9259 = 1711 N +or- 32% (90% probability).

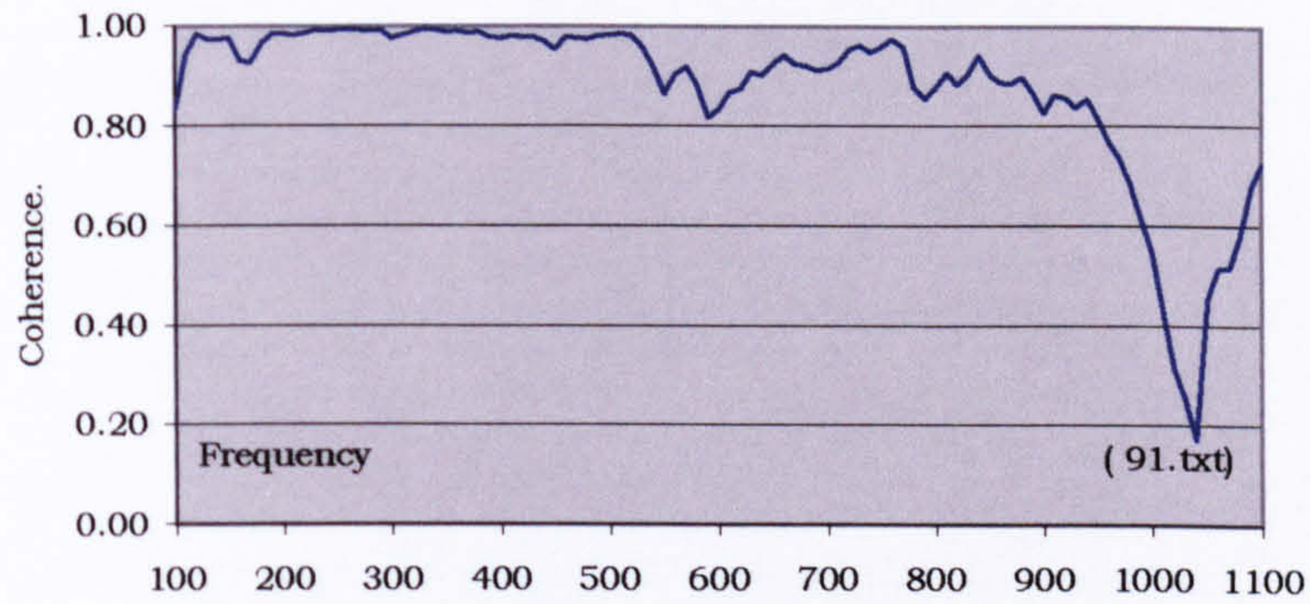

Fig B6. Second string, coherence.

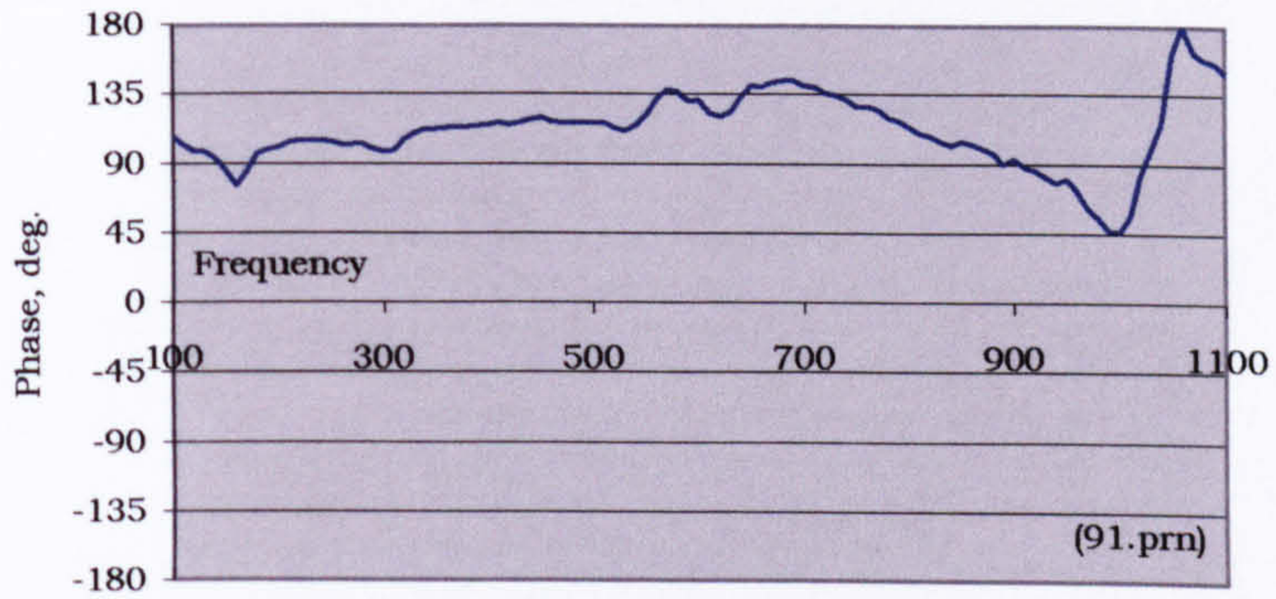

Fig B7. Second string, phase.

Third string, spring constant

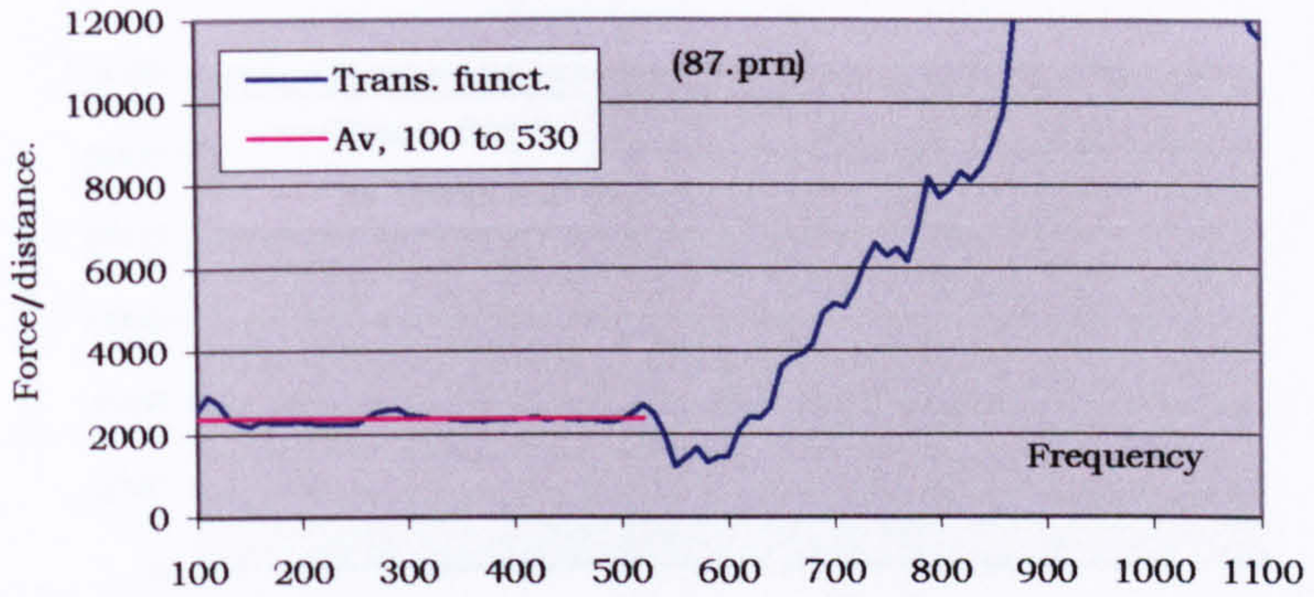

Fig B8. Third string, transfer function force/displacement.

Average transfer function 100 to 530Hz is 2390 st dev 148.

Spring constant = 2390 x 0.9259 = 2213 N +or- 12% (90% probability).

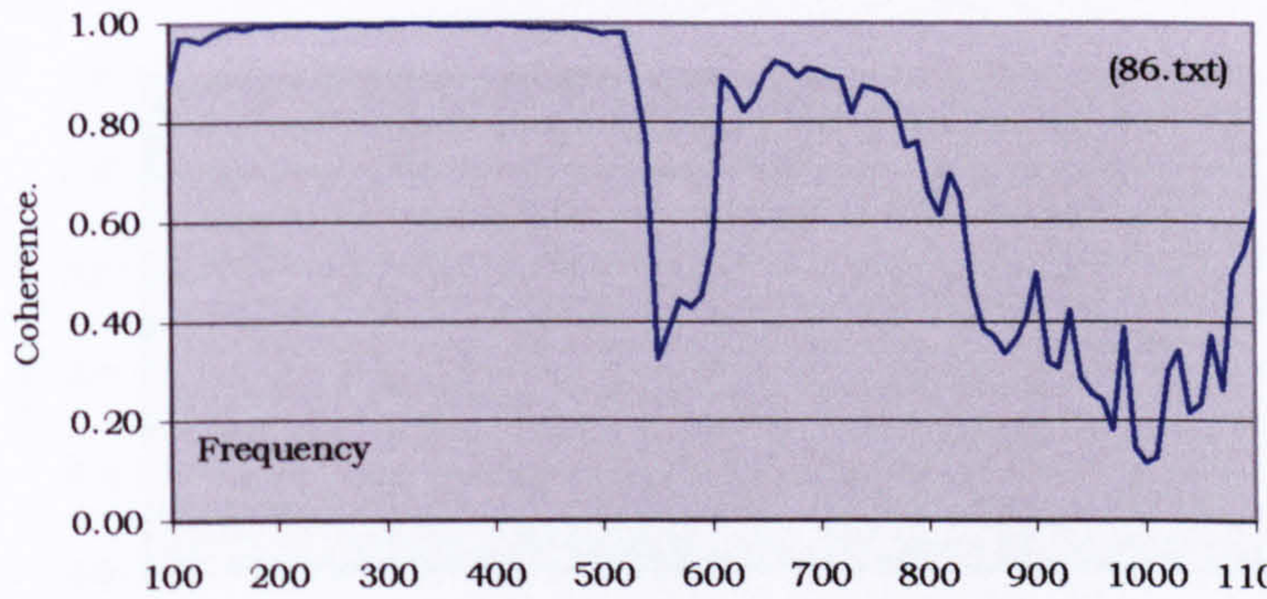

Fig B9. Third string, coherence.

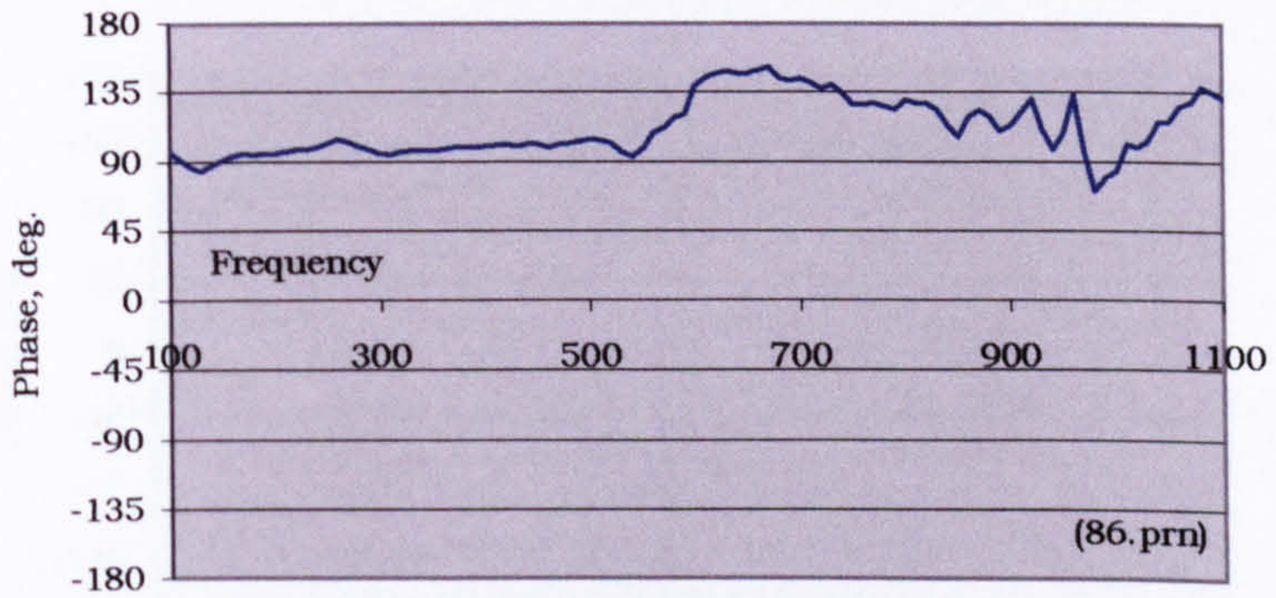

Fig B10. Third string, phase.

Fourth string, spring constant

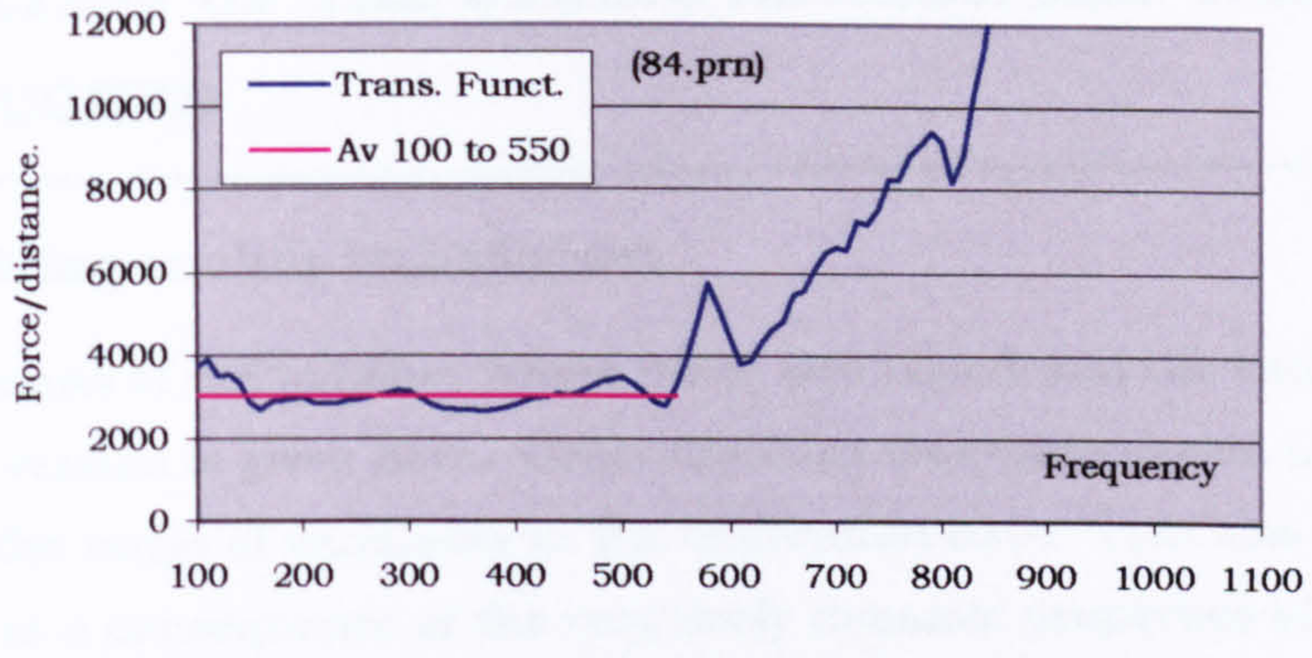

Fig B11. Fourth string, transfer function force/displacement.

Average transfer function 100 to 550 Hz is 3029 stdev 291.

Spring constant = 3029 x 0.9259 = 2804 N +or-19% (90% probability).

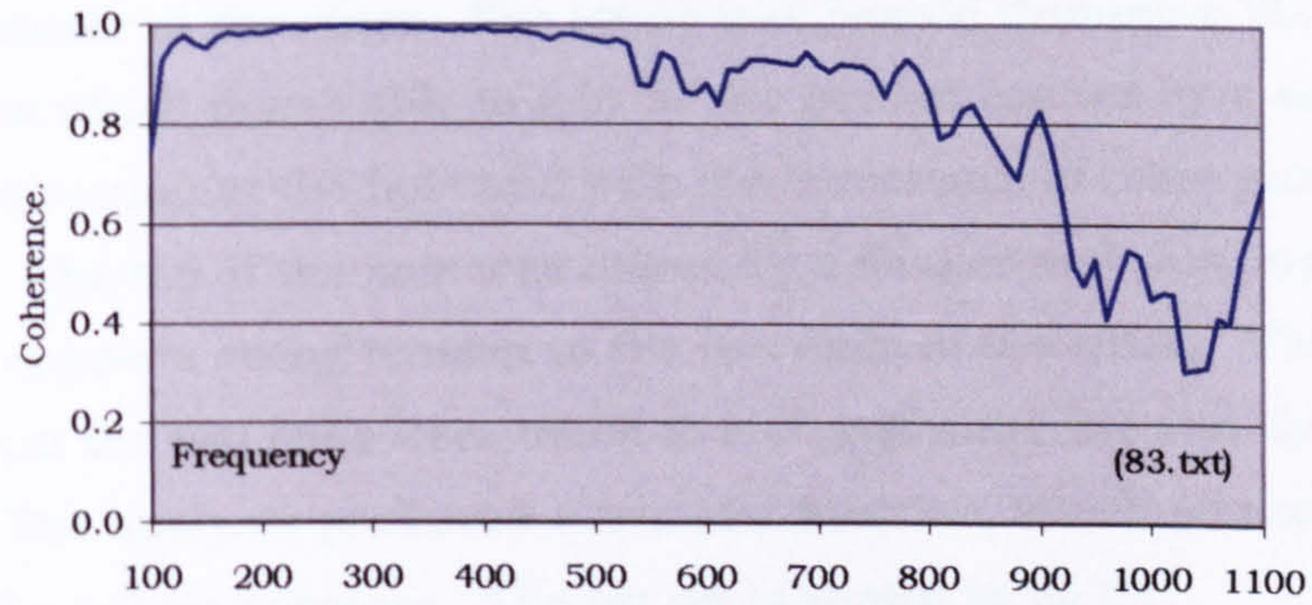

Fig B12. Fourth string, coherence.

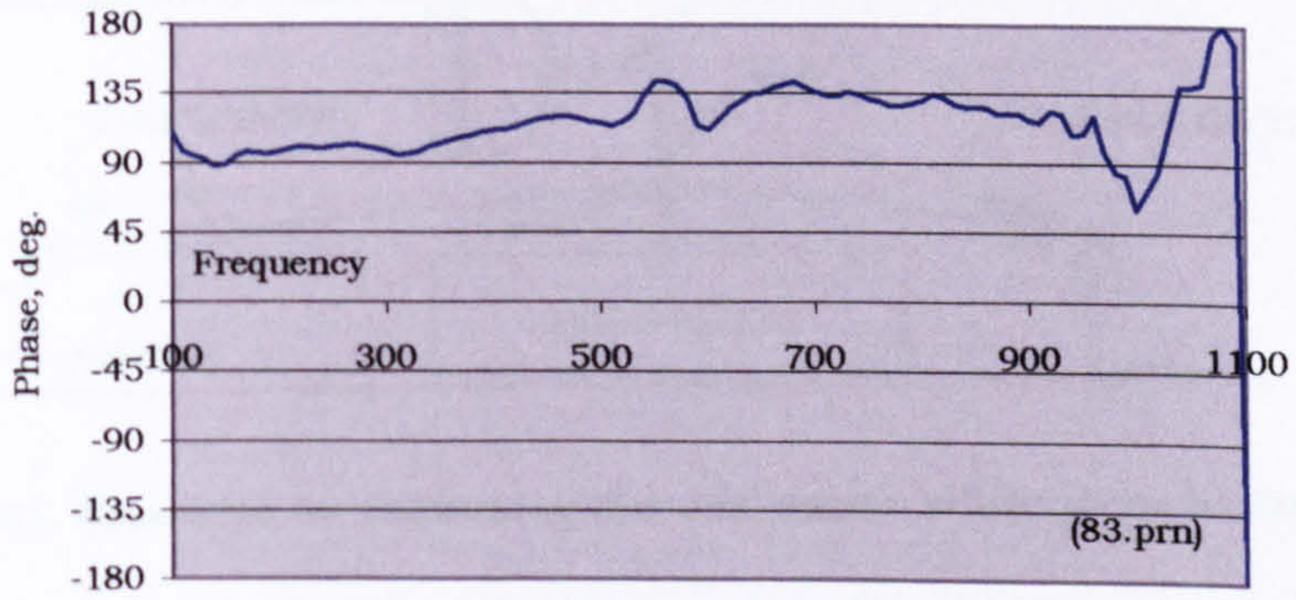

Fig B13. Fourth string, phase.

Appendix C

CALIBRATION OF THE STRING ANCHOR AND TAILGUT TRANSDUCERS

C.1 The string anchor transducers

Several versions of the tailpiece where made and tested and the calibration of the final version is given here. Great difficulty was experienced in narrowing the range of variability in the calibration data. This was later discovered to a consequence of the very lively dynamic properties of the tailpiece and string combination. The tolerance given with the result is such that there is a 90% probability that the error will be less than the tolerance. Several methods were used for its calibration. The final method used was to put the transducer tailpiece at one end of the string and put a force transducer at the other. The string was passed through a 50mm long pointed post which it was able to grip by the friction caused by a small change in direction at the hole and with the assistance of rosin powder on the string. The top of the post was driven by a shaker and this imparted an equal and opposite string tension to the two ends of the string. The outputs from the two ends were taken to a charge amplifier and then to an analyser. The analyser produced a transfer function, which was used to calibrate the tail transducers. The set up is shown in fig C1.

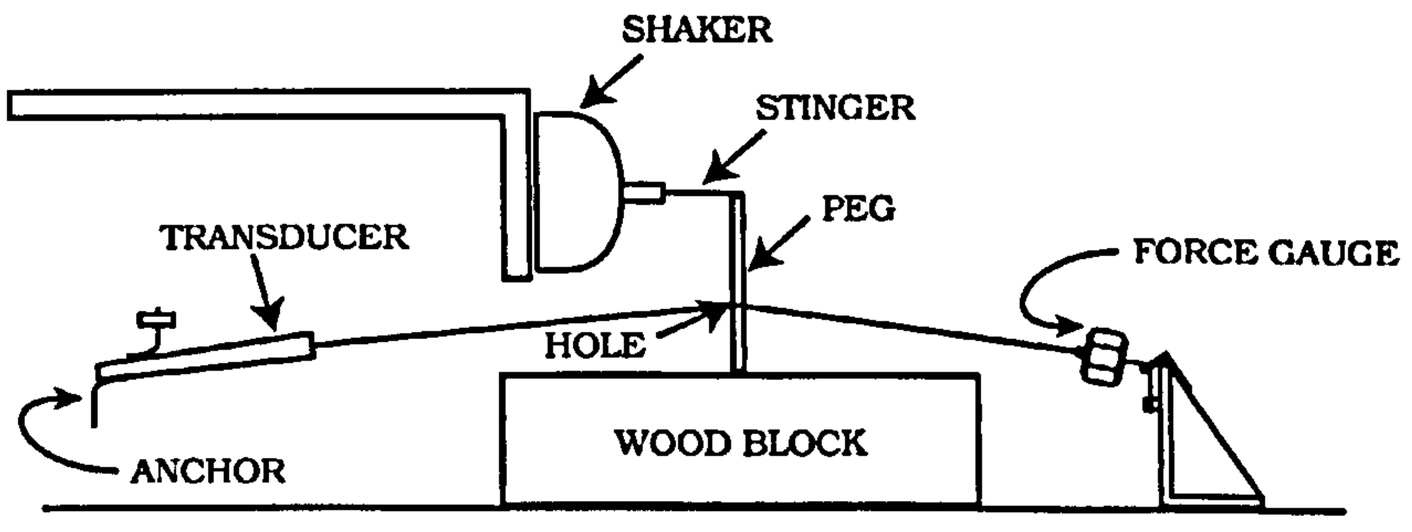

Fig C1. Apparatus for calibrating the transducers at the string anchors.

The output from the transducer and from the force gauge where both put through a charge amplifier with the same amplification and then to the analyser where the transfer function was recorded. The calibration of the force transducer (B&K No.803102) is -3.90pC/N. The minus sign denotes

that a tension on the force gauge produces a negative charge. Our convention is that tension is positive.

$$\text{Transfer function } TF_{An} = \frac{\text{Transducer output}}{\text{Force guage output}}$$

$$= \frac{\text{Force} \times \text{Calibration}}{\text{Force} \times (-3.9)}$$

$$\text{Calibration} = TF_{An} \times (-3.9)$$

C.2 Results

First string anchor transducer

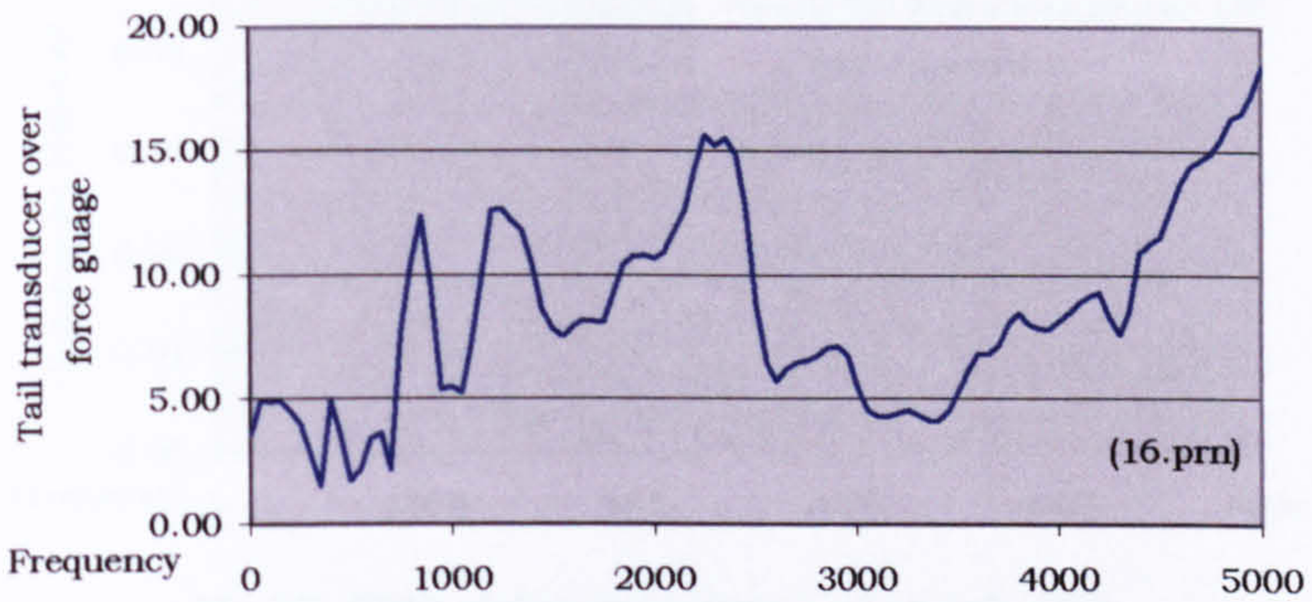

Fig C2. First string transducer, transfer function.

By averaging the transfer functions over the range of frequencies above 1000Hz (where the coherence is good), a transfer function of 9.38 is found. The method of excitation used should produce signals 180deg. out of phase. In this case, the signals are in phase therefore the transfer function is positive.

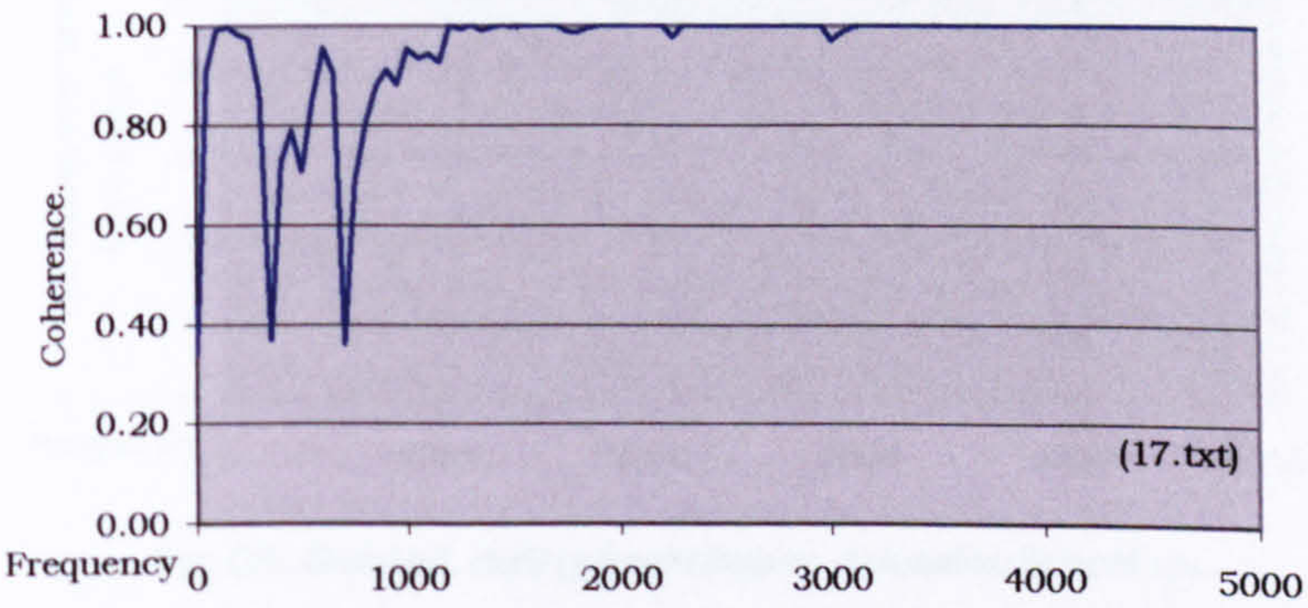

Fig C3. First string transducer, coherence.

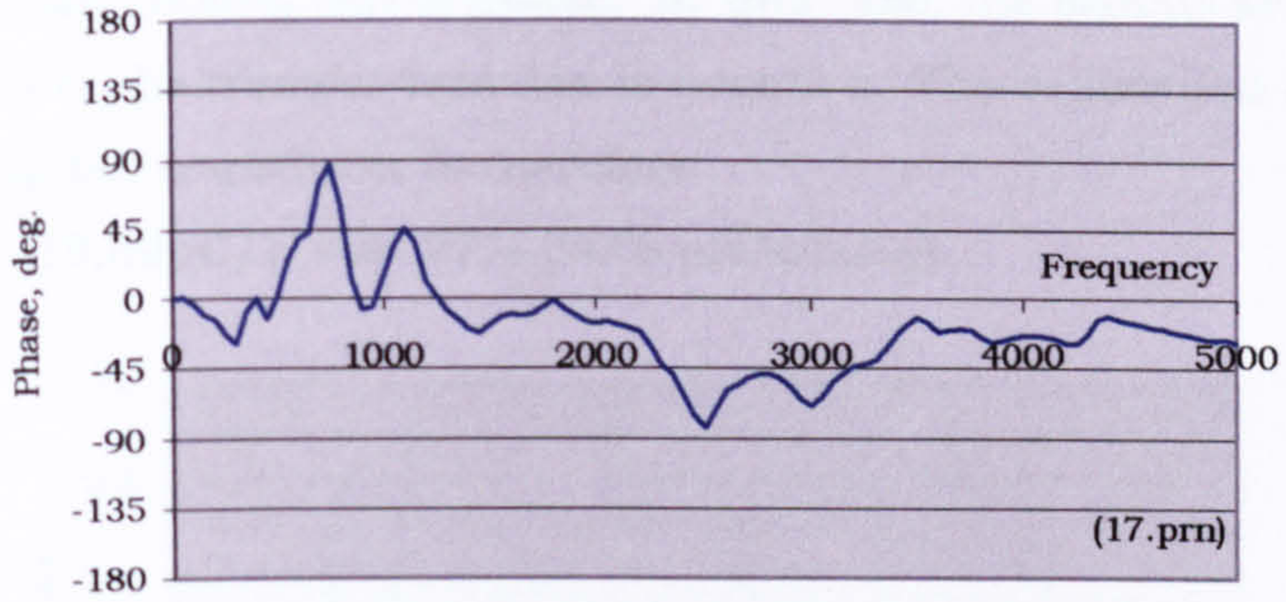

Fig C4. First string transducer, phase.

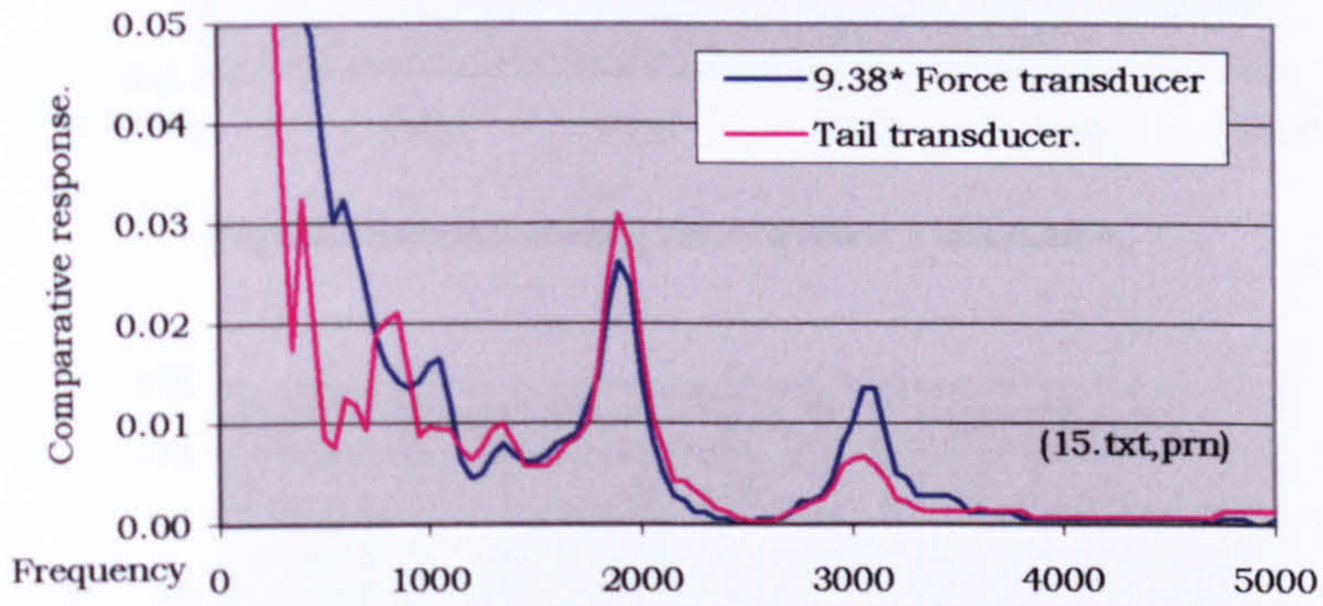

Fig C5. First string transducer, channels 1&2.

The calibration of the first string tail transducer is therefore 3.9× (-9.38)=+36pC/N +or- 77% (90% probability). Fig C5 shows trace for the tail transducer and that of the force transducer multiplied by 9.38.

Second string, anchor transducer

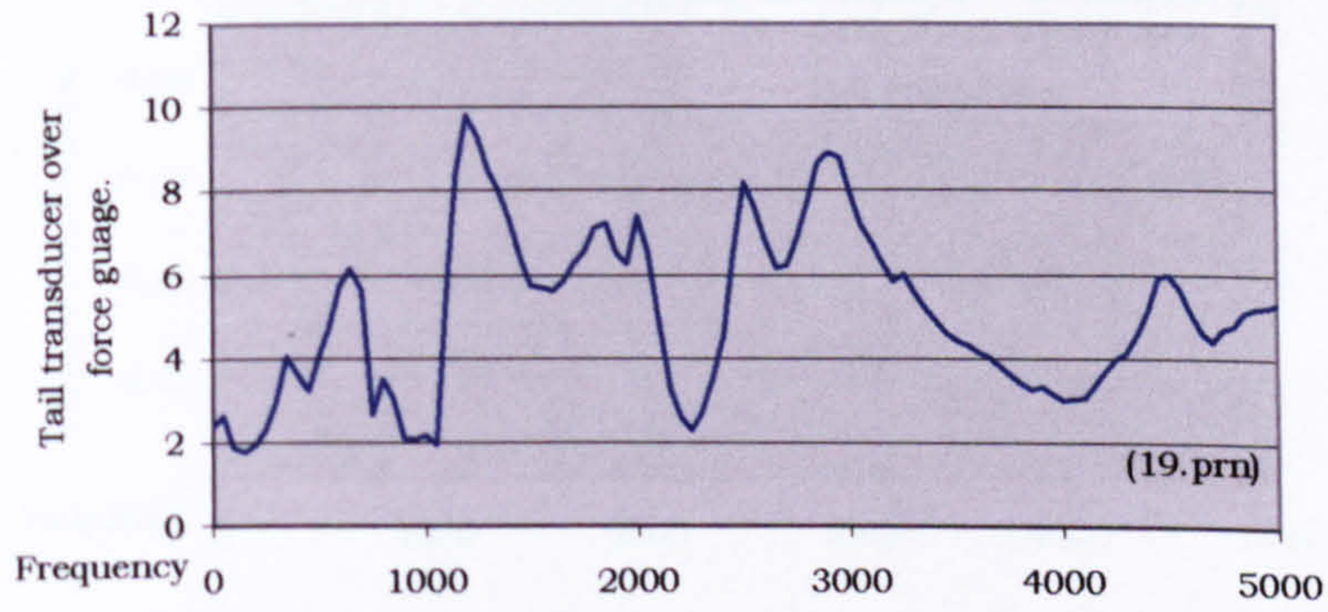

Fig C6. Second string transducer, transfer function.

By averaging the transfer functions at the whole range of frequencies, a transfer function of 5.05 is found. The method of excitation used should

produce signals 180deg. out of phase. In this case, the signals are in phase therefore the transfer function is negative. The calibration of the second string tail transducer is therefore

3.9×(5.05)=-19.69pC/N +or- 77% (90% probability).

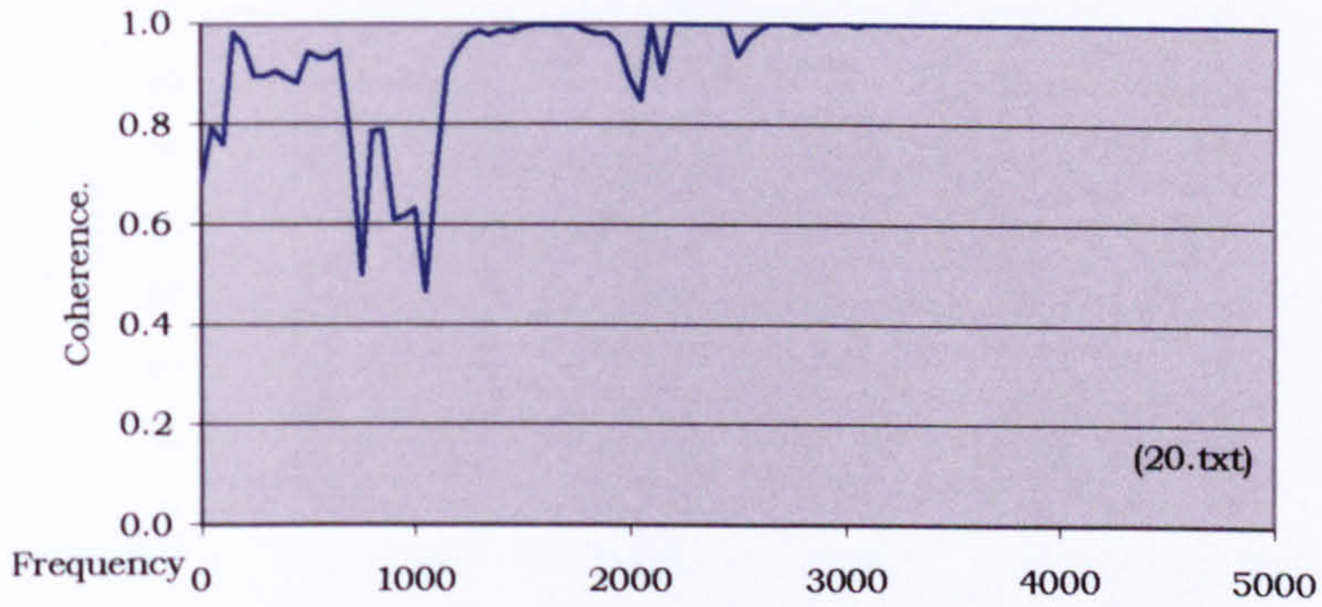

Fig C7. Second string transducer, coherence.

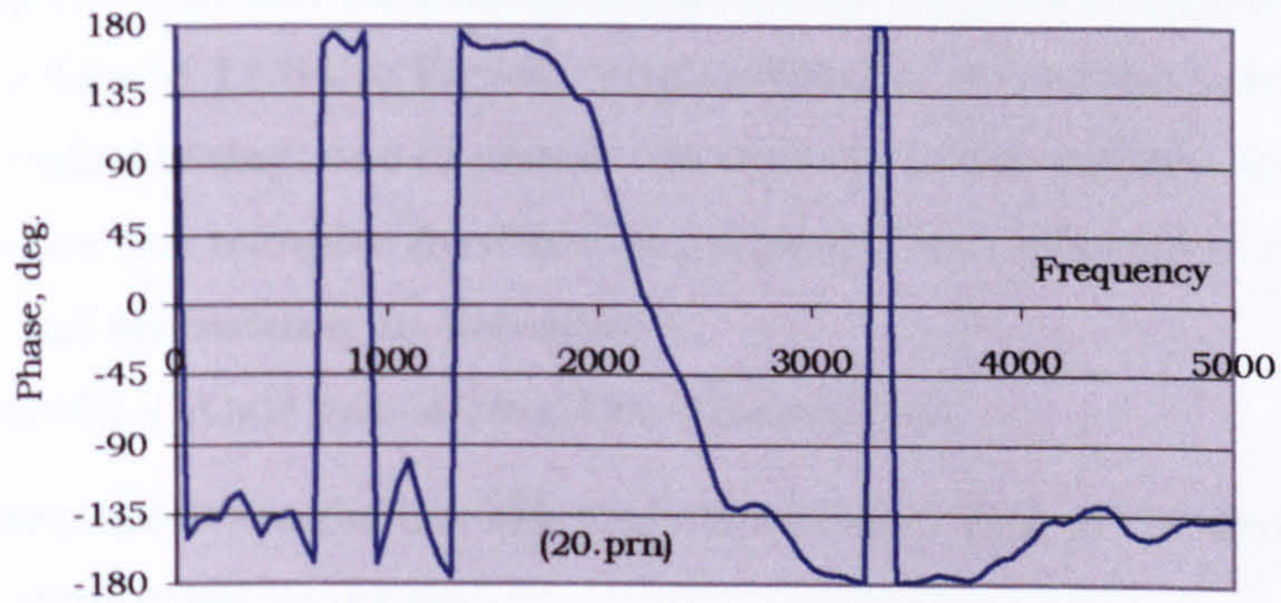

Fig C8. Second string transducer, phase.

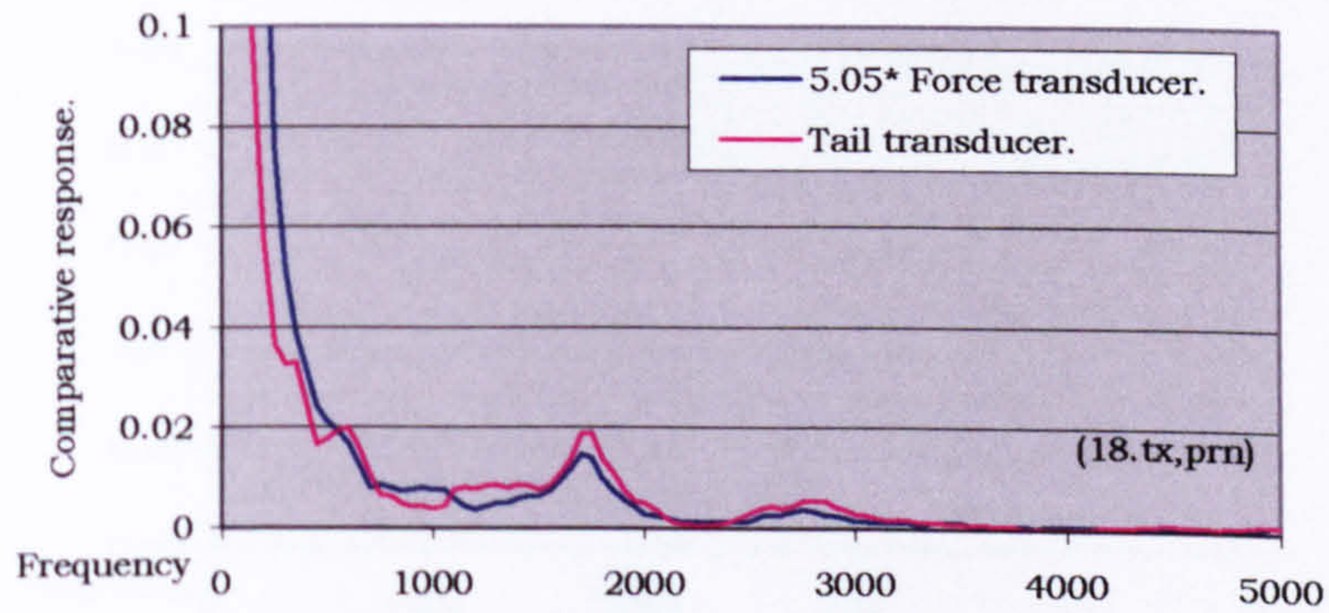

Fig C9. Second string transducer, channels 1&2.

Fig C9 shows the trace for the tail transducer and that of the force transducer multiplied by 5.05.

Third string, anchor transducer

For this string, the calibration was repeated at three different amplitudes in order to see if it was amplitude dependent. It was concluded that the results were not amplitude dependent.

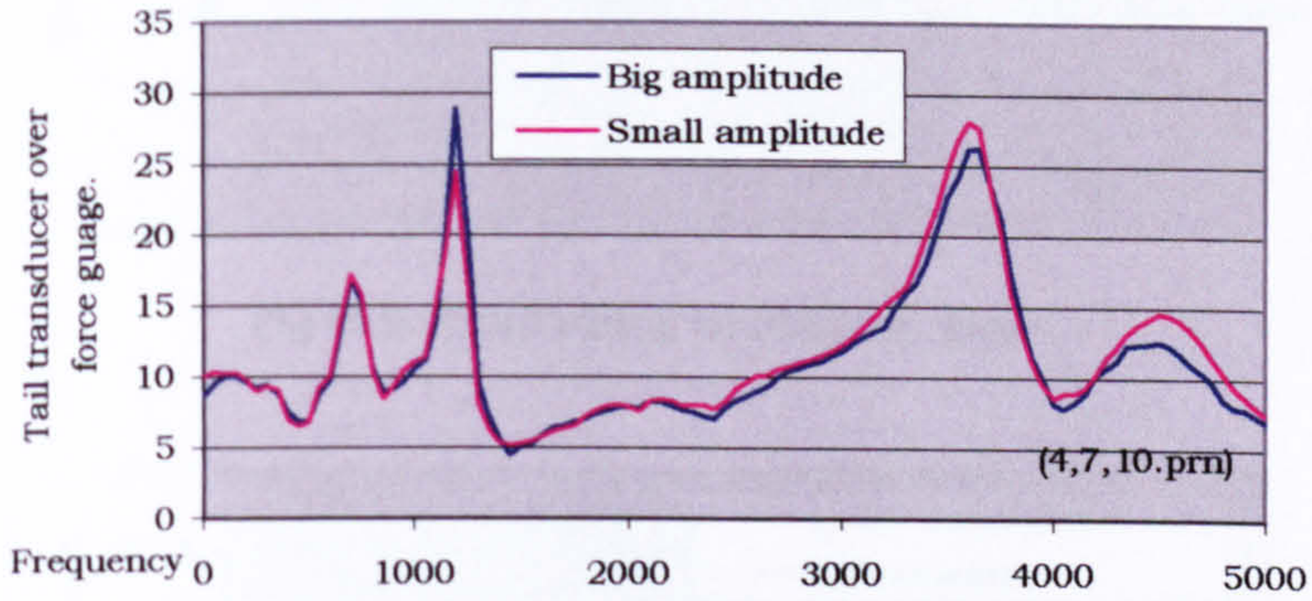

Fig C10. Third string transducer, transfer function.

By averaging the transfer functions at the whole range of frequencies, a transfer function of 11.64 is found. The method of excitation used should produce signals 180deg. out of phase. In this case, the signals are out of phase therefore the transfer function is positive. The calibration of the third string tail transducer is therefore

3.9×(-11.64)=45.4pC/N +or- 86% (90% probability).

Fig C13 shows the trace for the tail transducer and that of the force transducer multiplied by 11.64.

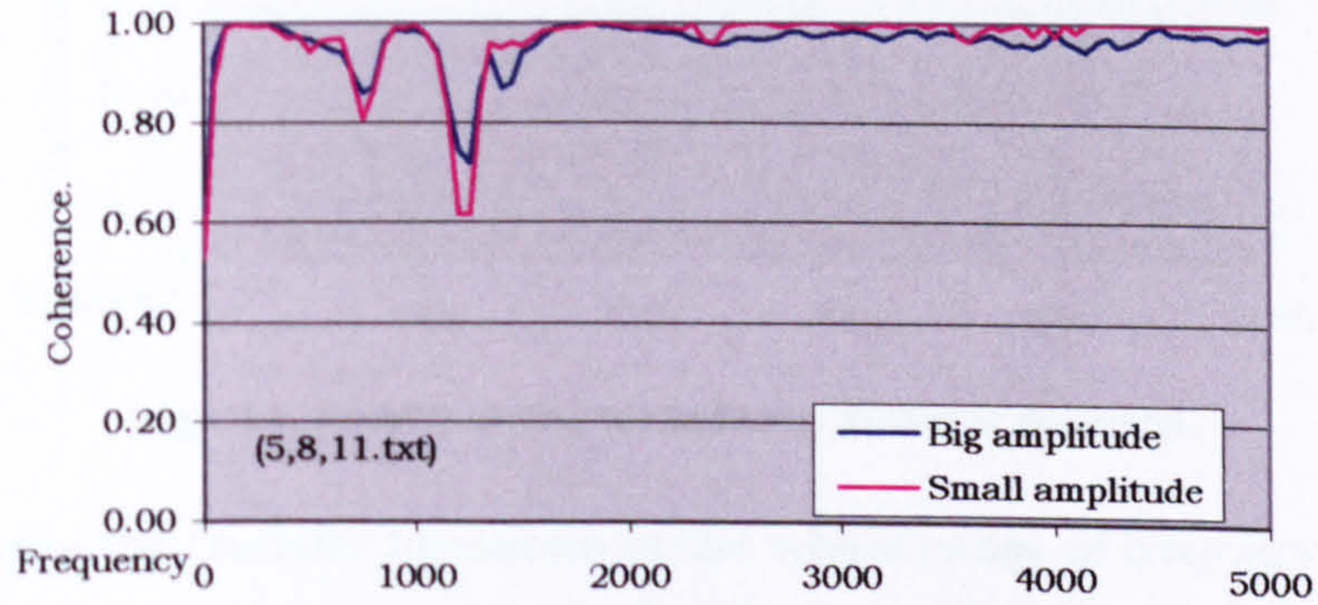

Fig C11. Third string transducer, coherence.

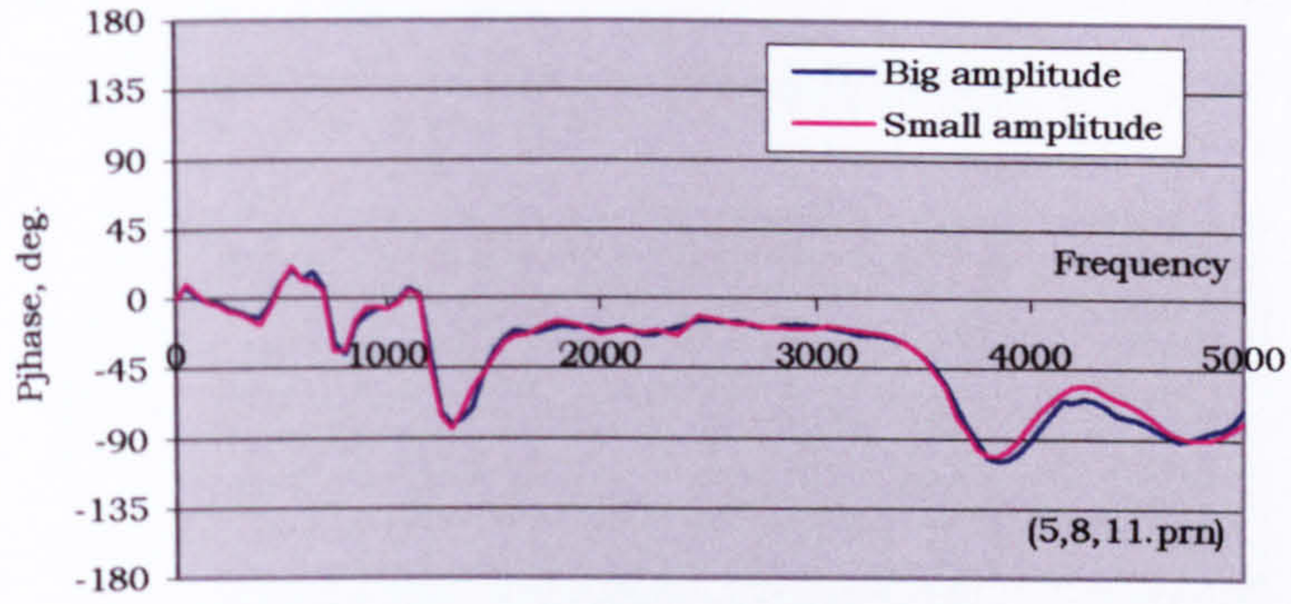

Fig C12. Third string transducer, phase.

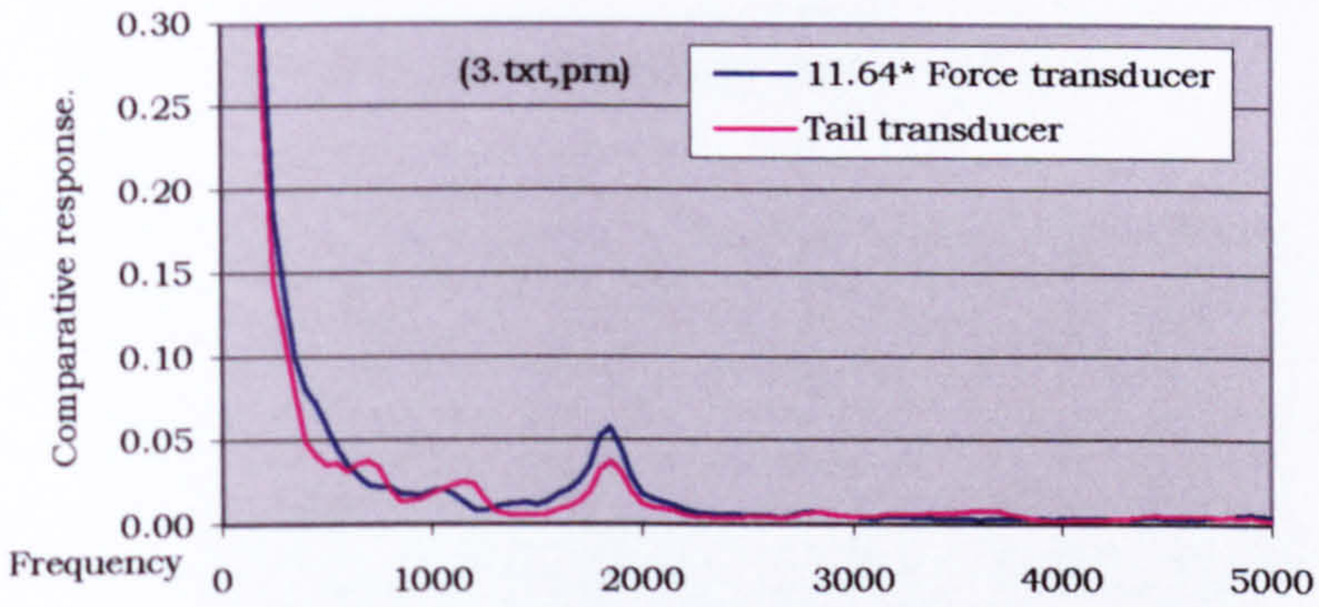

Fig C13. Third string transducer, channels 1&2.

Fourth string, anchor transducer

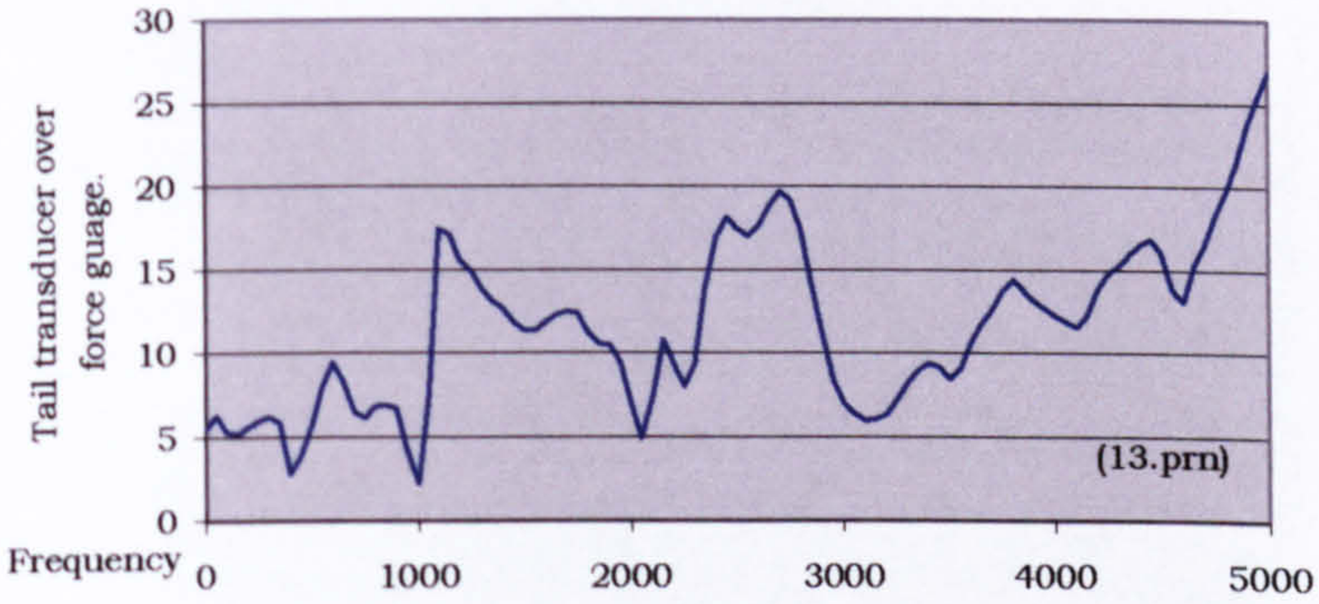

Fig C14. Fourth string transducer, transfer function.

By averaging the transfer functions at the whole range of frequencies, a transfer function of 12.03 is found. The method of excitation used should produce signals 180deg. out of phase. In this case the signals are in phase therefore the transfer function is negative. The calibration of the 4th string

tail transducer is therefore

3.9 × (12.03)=-46.92pC/N +or- 62% (90 % probability).

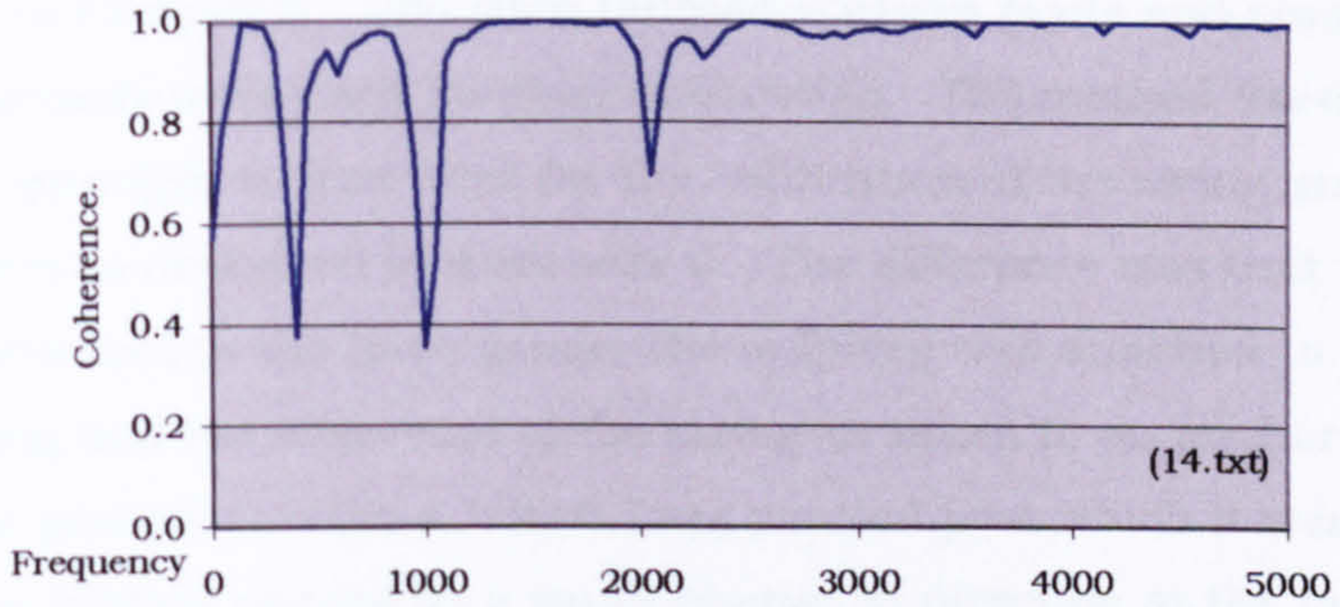

Fig C15. Fourth string transducer, coherence.

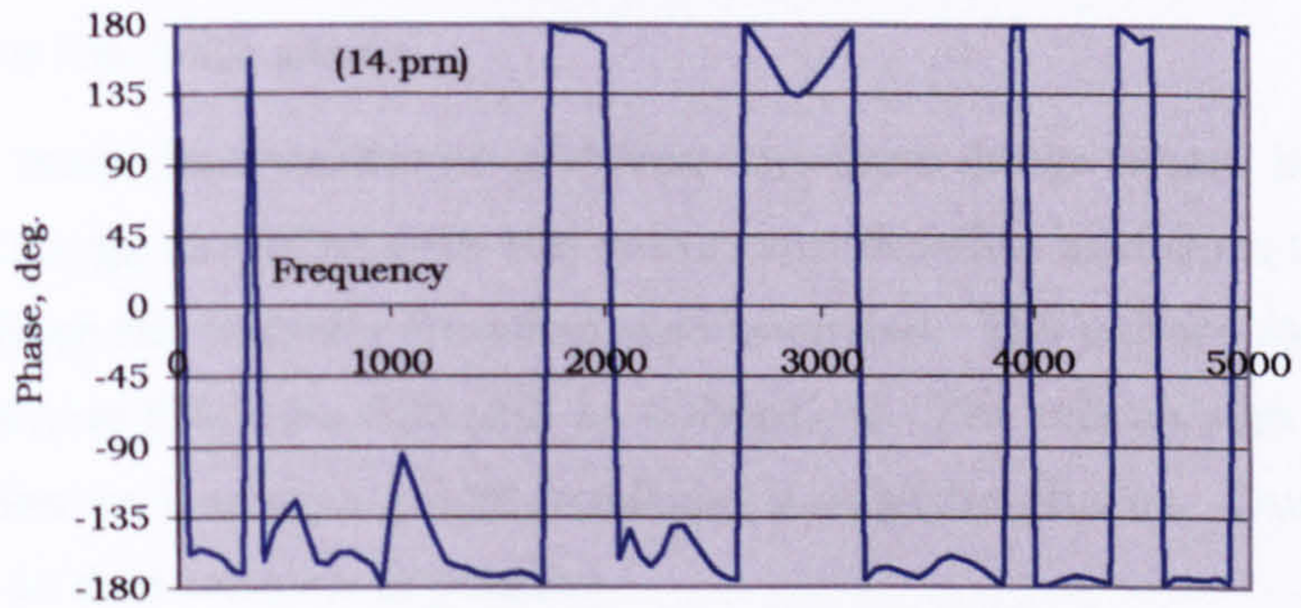

Fig C16. Fourth string transducer, phase.

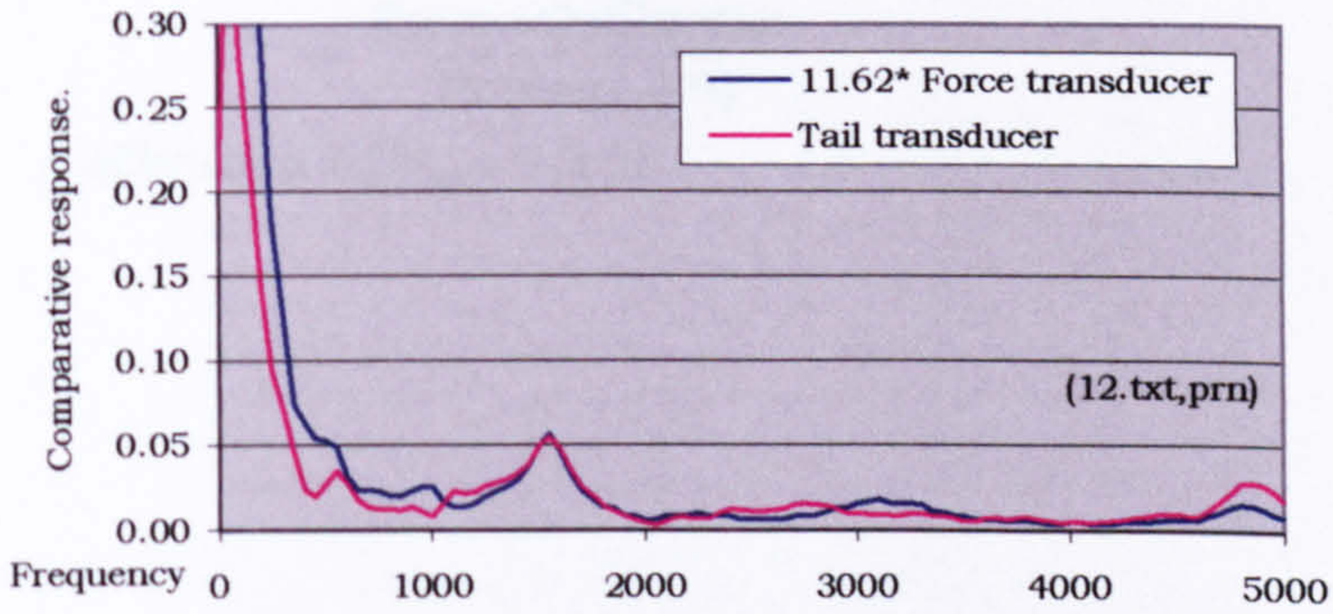

Fig C17. Fourth string transducer, channels 1&2.

Fig C17 shows the trace for the tail transducer and that of the force transducer multiplied by 11.62.

C.3 The tailgut transducers

The device for measuring the LSV vibration entering the tail gut is described in Chapter 6. Two such tailpieces where made and tested and several methods were used for their calibration. The method used was similar in principle to that used for the calibration of the string anchor transducers as described in Appendix C. The difference was that the tail gut was attached to the force gauge; the tailpiece was attached to one end of the string and the other end of the string as taken to an anchor. The string was passed through a 50mm long pointed post which it was able to grip by the friction caused by a small change in direction at the hole and with the assistance of rosin powder on the string. The top of the post was driven by a shaker and this imparted an LSV to the tailpiece and then through it to the force gauge.

The output from the transducer and from the force gauge where both put through a charge amplifier with the same amplification and then to the analyser where the transfer function was recorded. The calibration of the force transducer (B&K No.803102) is -3.90pC/N. The minus sign denotes that a tension on the force gauge produces a negative charge. Our convention is that tension is positive.

$$\text{Transfer function } TF_{An} = \frac{\text{Transducer output}}{\text{Force guage output}}$$

$$= \frac{\text{Force} \times \text{Calibration}}{\text{Force} \times (-3.9)}$$

$$\text{Calibration} = TF_{An} \times (-3.9)$$

C.4 Results

Calibration of tailgut transducer Mk1

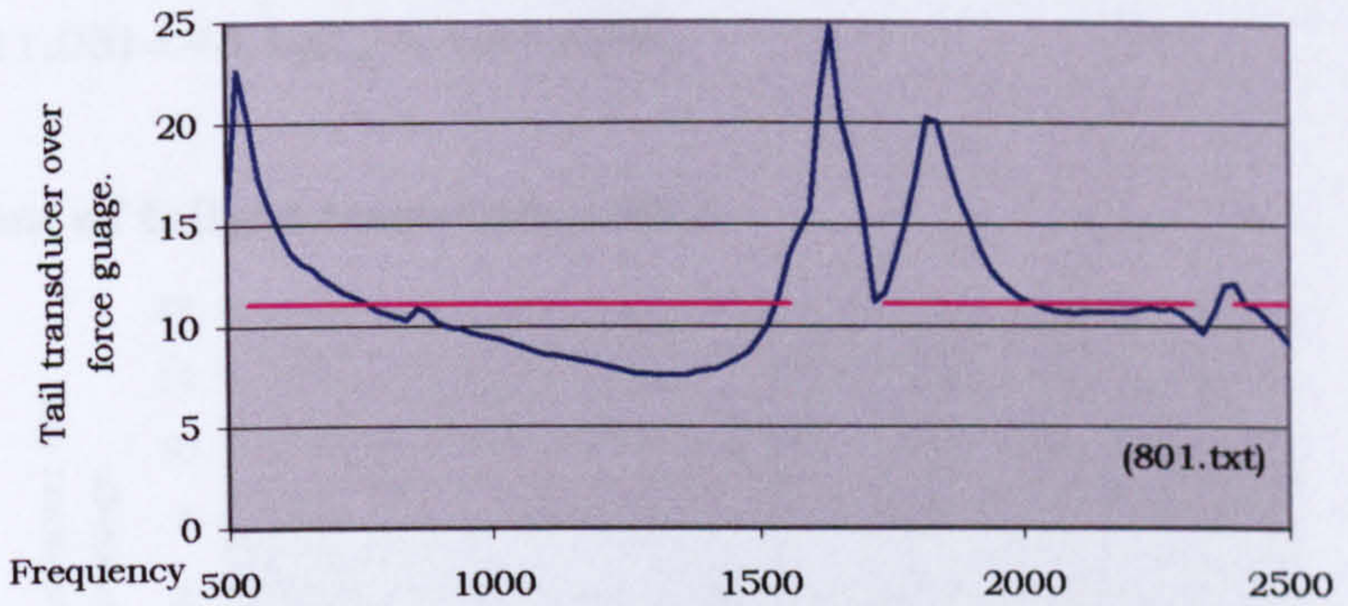

Fig C18. Tailgut transducer, transfer function.

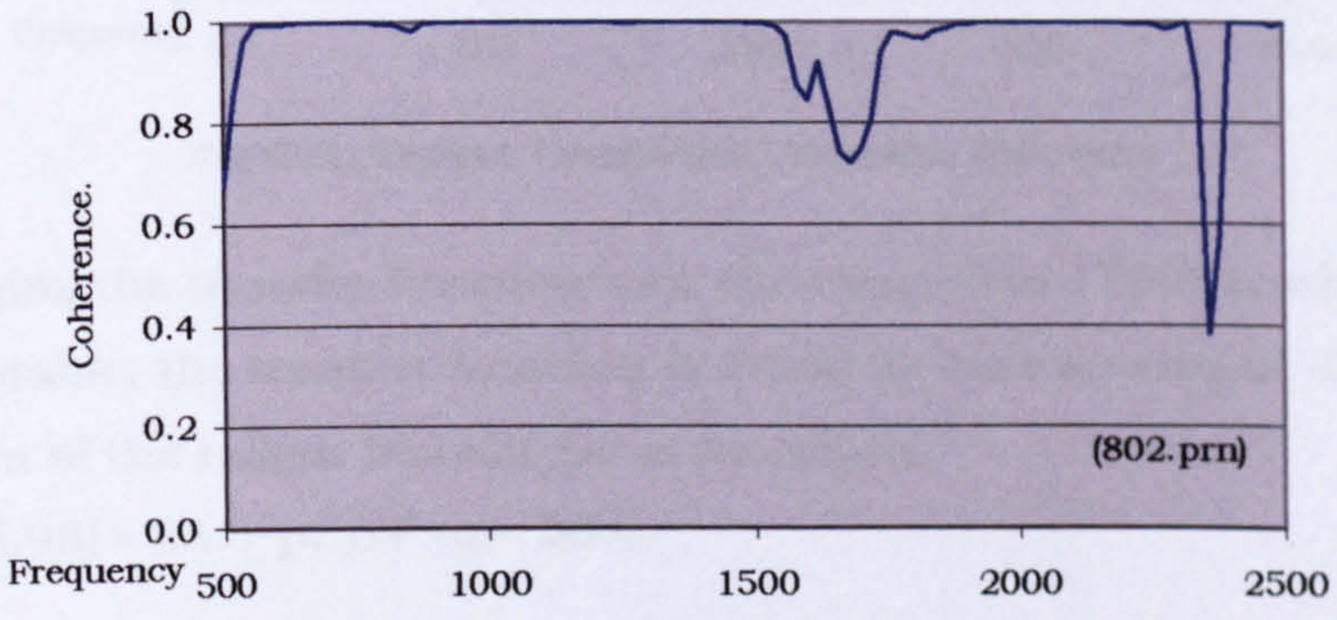

Fig C19. Tailgut transducer, coherence.

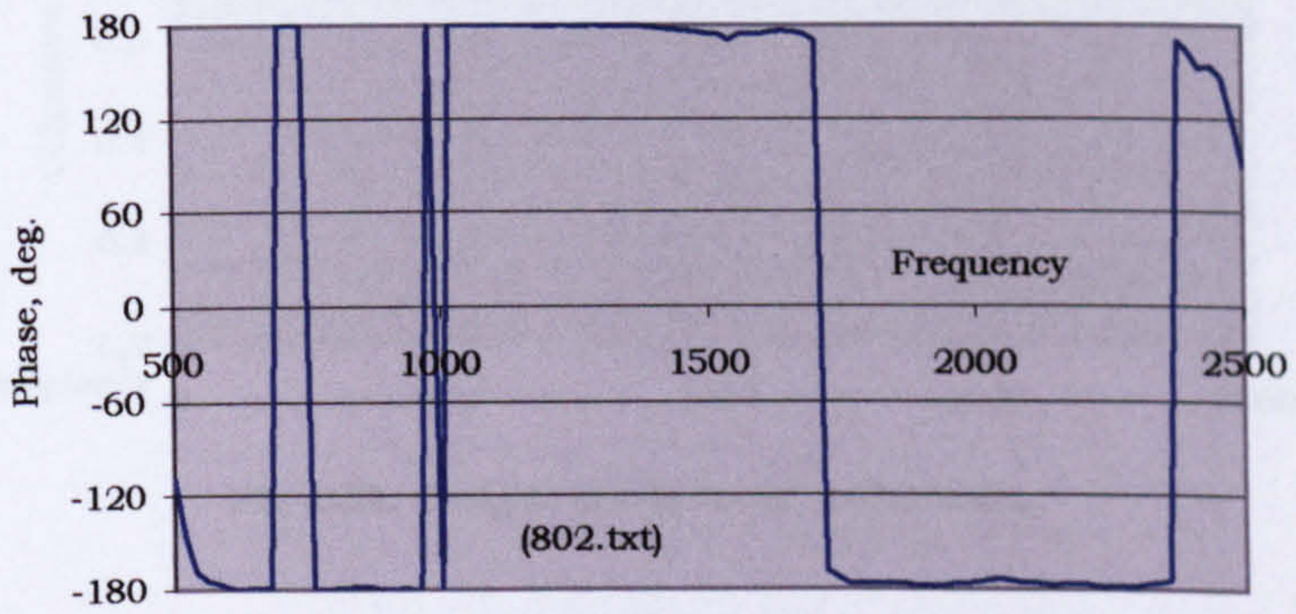

Fig C20. Tailgut transducer, phase.

The transfer function was taken as the average over the range that showed good coherence. This range is shown by the red line on the transfer function graph. The transfer function so found was 11.05. The method of

excitation should produce signals that are in phase. In this case, the signals are out of phase so the transfer function is negative. The calibration of the tailgut transducer is therefore,

$-3.9\times(-11.05)=43.1\,\text{pC/N}$ +or- 52%.

Calibration of tailgut transducer Mk2

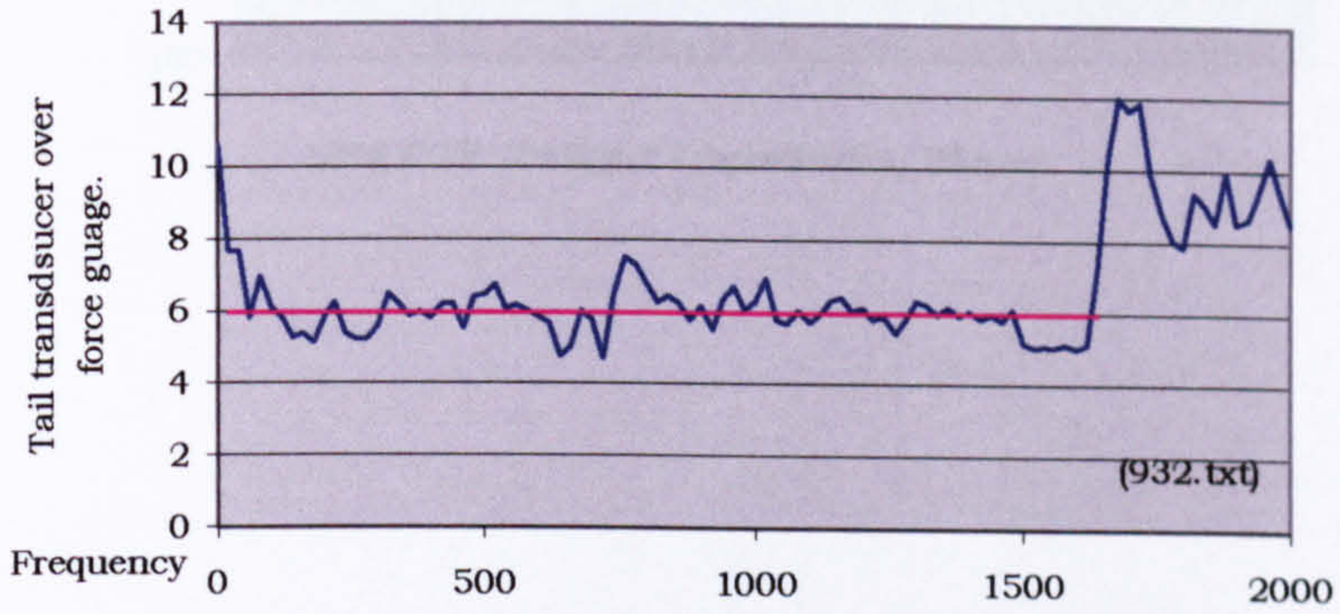

Fig C21. Tailgut transducer, Transfer function.

By averaging the transfer function over the range 0 to 1700Hz, which remains stable, the transfer function is found to have a value of -5.98. The calibration of the tailgut transducer is therefore,

$-3.9\times(-5.98)=23.3$ pC/N +or- 20%.

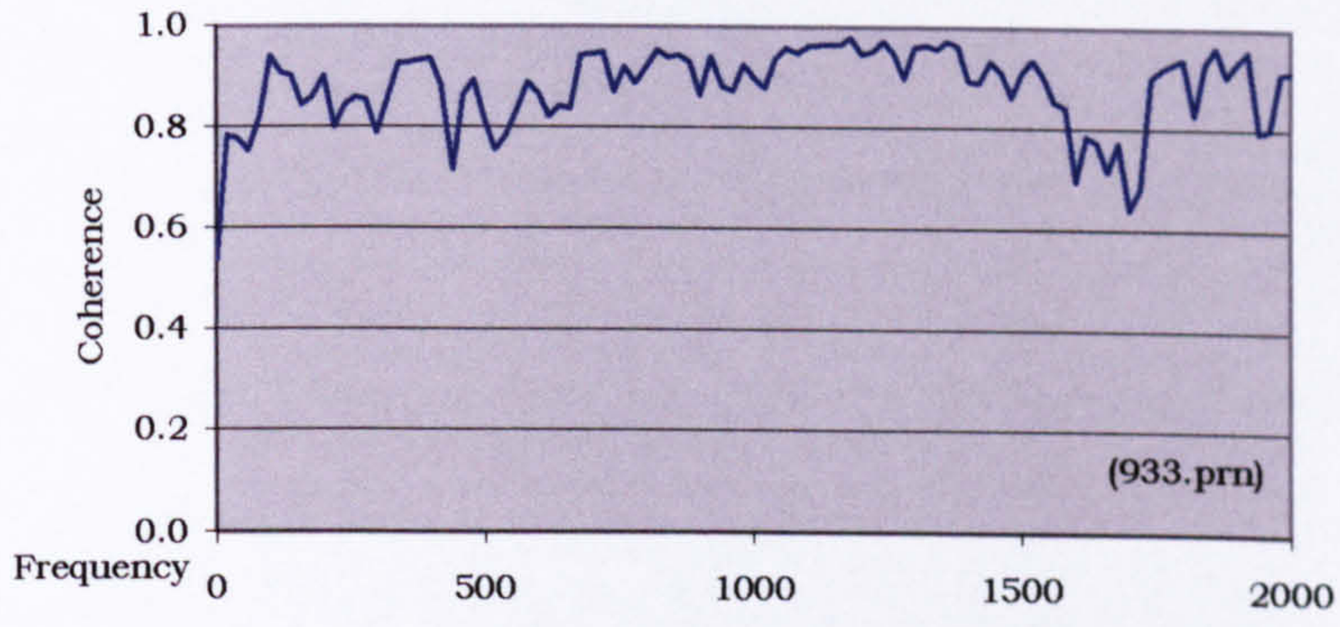

Fig C22. Tailgut transducer, coherence.

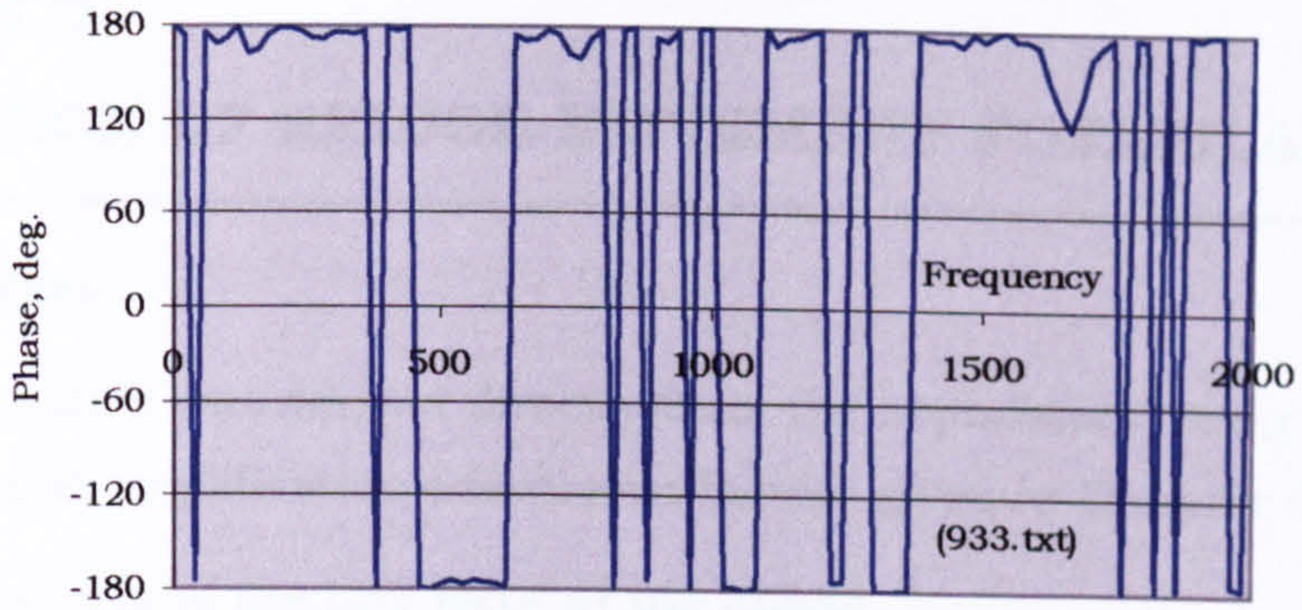

Fig C23. Tailgut transducer, Phase.

Appendix D

DERIVATION OF BRIDGE MOVEMENT FORMULAE

D.1 Given data

The following data was derived directly from the experiment using the calibration and amplification conversion factors given in Chapter 6.

The rms spectrum of the LSV force at the tailgut.
The rms spectrum of the string velocity at the magnet location.
The following transfer functions,

(A+jB) where,

$A = R_e\left\{\frac{\alpha_1}{F_{LSV\ tail}}\right\}$, real part TF, accel/LSV force, at bass bar foot of bridge.

$B = I_m\left\{\frac{\alpha_1}{F_{LSV\ tail}}\right\}$, imaginary part TF, accel/LSV force, at bass bar foot.

(C+jD) where,

$C = R_e\left\{\frac{\alpha_2}{F_{LSV\ tail}}\right\}$, real part TF, accel/LSV force, at sound post foot of bridge.

$D = I_m\left\{\frac{\alpha_2}{F_{LSV\ tail}}\right\}$, imaginary part TF, accel/LSV force, at sound post foot.

(G+jH) where,

$H = I_m\left\{\frac{\alpha_1}{\bar{v}_m}\right\}$, imag. part, accel/vel. of string at the magnet, at bass bar foot.

$G = R_e\left\{\frac{\alpha_1}{\bar{v}_m}\right\}$, real part, accel/vel. of string at the magnet, at bass bar foot.

G was not measured.

(K+jL) where,

$L = I_m\left\{\frac{\alpha_2}{\bar{v}_m}\right\}$, imag. part, accel/vel. of string at the magnet, at sound post foot.

$K = R_e\left\{\frac{\alpha_2}{\bar{v}_m}\right\}$, real part, accel/vel. of string at the magnet, at sound post foot.

K was not measured.

$R=I_m\left\{\frac{\alpha}{F_{LSV\ tail}}\right\}$, imaginary part, acceleration in the direction of the longitudinal axis of the violin/LSV force, at saddle.

D.2 Transformation of measured data

The transfer functions (G+jH) and (K+jL) are defined with respect to the EMF generated by the movement of the string in the magnetic field.

$$EMF \propto \frac{\text{number of lines cut}}{\text{time}} \propto \text{velocity of string at the magnet location.}$$

So the transfer functions relate to $\bar{v}_m$ the average string velocity over the width of the magnetic field. For convenience these transfer functions can be transformed to relate to the TSV force on the bridge, F_{TSV}.

The string displacement y_x in the nth string mode, at any point distance x from the end of a string of length L, is given by $y_x = A\sin\frac{n\pi x}{L}$, where A is the maximum displacement. The velocity at the same point would be $v_x = j\omega y_x$. The average velocity of the string over a magnet of width 2a, placed x_0 from the end of the string is given by,

$$\bar{v}_m = j\omega\frac{A}{2a}\int_{x_0-a}^{x_0+a}\text{Sin}\frac{n\pi x}{L}dx$$

$$=\frac{j\omega AL}{n\pi a}\text{Sin}\frac{n\pi a}{L}\text{Sin}\frac{n\pi x_0}{L}$$

$$F_{TSV} = TA\frac{n\pi}{L}\text{ (for small angles of string displacement)}$$

$$\frac{F_{TSV}}{\bar{v}_m}=TA\frac{n\pi}{L}\frac{n\pi a}{L}\frac{1}{j\omega A\,\text{Sin}\frac{n\pi a}{L}\text{Sin}\frac{n\pi x_0}{L}}$$

$$\frac{F_{TSV}}{\bar{v}_m}=-jr \quad \text{----------(1)}$$

where $$r=\frac{T\frac{n\pi}{L}\frac{n\pi a}{L}}{\omega\,\text{Sin}\frac{n\pi x_0}{L}\text{Sin}\frac{n\pi a}{L}}$$

The transfer function $\frac{\alpha_1}{F_{TSV}}=\frac{\alpha_1}{\bar{v}_m}.\frac{\bar{v}_m}{F_{TSV}}=\frac{(G+jH)(j)}{r}=\frac{jG-H}{r}$,

and the transfer function $\frac{\alpha_2}{F_{TSV}} = \frac{\alpha_2}{\bar{v}_m} \cdot \frac{\bar{v}_s}{F_{TSV}} = \frac{(K + jL)(j)}{r} = \frac{jK - L}{r}$.

So the transfer function of bass bar foot acceleration over F_{TSV}, can be written as **(E+jF)**, where E=-H/r, and F=G/r: and the transfer function of the soundpost foot acceleration over F_{TSV}, can be written as **(M+jN)**, where M=-L/r, and N=K/r.

D.3 Preliminary

Viewing the bridge from the tailpiece side, the TSV force and displacements are positive right to left. The vertical displacements are positive downwards. The vertical bass bar foot and soundpost foot displacements x_1 and x_2, are given by, $x_1 = x_c + \frac{w\theta}{2}$, and $x_2 = x_c - \frac{w\theta}{2}$, where θ (the angle of bridge rotation) is small, x_c is the vertical crown displacement, and w and h are the width and height of the bridge.

From this $x_c = (x_1 + x_2)/2$ ----------(2)

By similar argument $x_t = (x_1 - x_2)(h/w)$ ----------(3)

where x_t is the transverse crown displacement.

D.4 To find the vertical bridge admittance re LSV

The bass bar and soundpost foot transfer functions re LSV are;

$\left[\frac{\alpha_1}{F_{LSV\,tail}}\right] = A + jB$ and $\left[\frac{\alpha_2}{F_{LSV\,tail}}\right] = C + jD$

$$Y_v = \frac{v_v}{F_{LSV\,bridge}} = \frac{j\omega x_c}{0.37\,F_{LSV\,tail}} = \frac{j\omega(x_1 + x_2)}{0.37 \times 2\,F_{LSV\,tail}} = \frac{(\alpha_1 + \alpha_2)}{0.37 \times 2j\omega F_{LSV\,tail}}$$

$$Y_v = \frac{[(B + D) - j(A + C)]}{0.37 \times 2\omega} \quad \text{----------(4)}$$

The magnitude of the admittance, $|Y_v| = \frac{1}{0.37 \times 2\omega}\sqrt{(B + D)^2 + (A + C)^2}$ ------(5)

The phase of the admittance, $\varphi_{y_v} = \mathrm{Cos}^{-1}\left[\frac{(B + D)}{\sqrt{(B + D)^2 + (A + C)^2}}\right]$.--------(6)

The computer will only return a phase from 0 to π. This will be the correct phase unless (A+C) is positive, in which case the phase should be multiplied by –1. (By consideration of a phase diagram.)

D.5 To find the transverse bridge admittance re TSV

The admittance of the bridge can first be expressed in terms of the measured LSV transfer functions.

The admittance of the bridge $Y_t = \frac{v_t}{F_{TSV}} = \frac{v_t}{F_{LSV\ tail}} \frac{F_{LSV\ tail}}{F_{TSV}}$

$$Y_t = \frac{j\omega(x_1 - x_2)}{F_{LSV\ tail}} \frac{h}{w} \frac{F_{LSV\ tail}}{F_{TSV}} = \frac{(\alpha_1 - \alpha_2)}{j\omega . F_{LSV\ tail}} \frac{h}{w} \frac{F_{LSV\ tail}}{F_{TSV}}$$

$$Y_t = \frac{(A + jB - C - jD)}{j\omega} \frac{h}{w} \frac{F_{LSV\ tail}}{F_{TSV}}$$

$$Y_t = \frac{(B - D) + j(C - A)}{\omega} \frac{h}{w} \frac{F_{LSV\ tail}}{F_{TSV}} \quad \text{----------(7)}$$

The phase relationship between F_{LSV} and F_{TSV} is unknown so equation 6 can not be evaluated. However, the magnitude of the admittance can be evaluated.

The magnitude of the admittance, $|Y_t| = \frac{\sqrt{(B - D)^2 + (C - A)^2}}{\omega} \frac{h}{w} \frac{|F_{LSV\ tail}|}{|F_{TSV}|}$ ----(8)

From this we can find the unmeasured functions E and M.

D.6 Procedure to find the unmeasured terms F and N (or G and K)

By definition $\frac{\alpha_1}{F_{TSV}} = E + jF$

Now, $\left|\frac{\alpha_1}{F_{TSV}}\right| = \sqrt{A^2 + B^2} . \left|\frac{F_{LSV\ tail}}{F_{TSV}}\right| = \sqrt{E^2 + F^2}$

so $F = S \sin\left(\cos^{-1}\frac{E}{S}\right)$, where $S = \sqrt{A^2 + B^2} . \left|\frac{F_{LSV\ tail}}{F_{TSV}}\right|$.

Similarly $N = T \sin\left(\cos^{-1}\frac{M}{T}\right)$, where $T = \sqrt{C^2 + D^2} . \left|\frac{F_{LSV\ tail}}{F_{TSV}}\right|$.

However, the signs of F and N have been lost. The signs cannot be recovered by any mathematical process, but if one has regard to the physical outcome, sensible signs can be given to F and N.

Assuming the bridge is effectively rigid in its own plane and executes only one body mode. If E is of the opposite sign to M, the bridge must be rocking so F and N must be of opposite sign. Putting these requirements together, <u>if E and M are of opposite sign make F positive and N negative</u>.

If E and M are of the same sign, the bridge is bouncing, so F and N are of the same sign. The TSV must be putting power in so F-N must be positive (see equation (13)). To make (F-N) positive we must apply the following conditions. If E and M are of the same sign and F>N then both must be positive: and if F<N then both must be negative. These criteria for selecting the signs of F and N were followed in the graphs presented.

We can now find a direct expression for Y_t, in terms of the TSV transfer functions.

$$Y_t = \frac{v_t}{F_{TSV}} = \frac{(\alpha_1 - \alpha_2)}{j\omega F_{TSV}} \frac{h}{w} = \frac{(F-N)+j(M-E)}{\omega} \frac{h}{w} \qquad \text{----------(9)}$$

The magnitude of the admittance, $|Y_t| = \frac{h}{w}\frac{1}{\omega}\sqrt{(E-M)^2+(F-N)^2}$ ------(10)

and the corresponding phase, $\varphi_t = \mathrm{Cos}^{-1}\left[\frac{(F-N)}{\sqrt{(E-M)^2+(F-N)^2}}\right]$. ------(11)

This will be the correct phase unless, (E-M) is positive in which case the phase should be multiplied by -1.

D.7 The velocity of the top of the bridge

From equation (4), $v_v = |Y_v| F_{LSV\,bridge} = \frac{F_{LSV\,tail}}{2\omega}\sqrt{(B+D)^2+(A+C)^2}$

From equation (7), $v_t = |Y_t| F_{TSV} = \frac{0.37 \times F_{LSV\,tail}}{\omega}\frac{h}{w}\sqrt{(B-D)^2+(C-A)^2}$,

where all the velocities and forces are rms values.

D.8 To find power into bridge from LSV

$W_{LSV} = \frac{1}{2} R_e\{F_{LSV\,bridge} v_v^*\}$, where v_v^* is the complex conjugate of the velocity.

$$W_{LSV} = \frac{0.37}{2} R_e\{F_{LSV\,tail} v_v^*\}$$

We have shown that $v_v^* = F^*_{LSV\,tail} \frac{(B+D)+j(A+C)}{2\omega}$.

Therefore $$W_{LSV} = \frac{0.37}{2} R_e\left\{|F_{LSV\,tail}|^2 \frac{(B+D)+j(A+C)}{2\omega}\right\},$$

and so $$W_{LSV} = \frac{0.37\, F^2_{LSV\,tail}}{2\omega}(B+D). \qquad \text{----------(12)}$$

.

D.9 To find power into bridge from TSV

$W_{TSV} = \frac{1}{2} R_e \{F_{TSV} v_t^*\}$, where v_t^* is the complex conjugate of the velocity.

We have shown that $v_t^* = F^*_{TSV} \frac{(F-N) - j(M-E)}{\omega} \frac{h}{w}$

Therefore $W_{TSV} = \frac{1}{2} R_e \left\{ |F_{TSV}|^2 \frac{(F-N) - j(M-E)}{\omega} \frac{h}{w} \right\}$

and so $W_{TSV} = F_{TSV}^2 \frac{h}{w} \frac{(F-N)}{\omega}$. ----------(13)

D.10 The relative phase of TSV/LSV

$$\frac{\alpha_1}{F_{LSV}} = A + jB \qquad \frac{\alpha_1}{F_{TSV}} = E + jF$$

$$\therefore \frac{\alpha_1}{F_{LSV}} \frac{F_{TSV}}{\alpha_1} = \frac{A + jB}{E + jF} = \frac{(A + jB)(E - jF)}{F^2 + E^2}$$

Phase of $\frac{F_{TSV}}{F_{LSV}} = \mathrm{Tan}^{-1} \left[\frac{BE - AF}{AE + BF} \right]$ ----------(14)

Appendix E

PLATE FLEXURAL STIFFNESS AS A MEANS OF ACHIEVING CONSISTENCY IN VIOLIN PLAYABILITY

Violinmakers have to use some criterion for deciding how thick to make the front and back plates. Some simply make them to fixed dimensions for all instruments. Others have advocated weighing the plates and making all the fronts to a certain weight and the backs to another. Since the 1960s much work has been done in a quasi scientific way (Saunders and Hutchins) to define detached plate eigen modes which would produce a violin with a smooth continuous spectrum of response. Later Hutchins proposed that the appeal of an assembled violin varied with the frequency difference between the A1 (air mode) and the B1 (body mode). Chamber music players preferred instruments with a small difference, and soloists preferred a big difference, with the orchestral players in between. The frequency of the A1 mode of a violin does not move much being largely a function of the dimensions of the body. The B1 mode (and the difference between it and the A1) depends on the flexural stiffness and mass of the body.

In the past, the writer has made a number of violins with plates of fixed modal resonance frequencies. These violins were found to give inconsistent results from one to the other. Violins that achieved the resonant frequency with lightweight plates felt to the player very different to those with heavier plates. The actual thickness of the plates as a dimension made no discernible difference. It seemed that both the frequency and weight needed to be involved.

It has often been suggested that the old Cremonese makers may have tested their plates by bending and twisting them in the hands, and then thinning them until a certain flexibility had been achieved. A way had to be found of measuring the stiffness with greater control. Analysis shows that there is a simple solution to the problem.

If a plate is flexed by holding the edges in the fingers and pressing the thumbs into the middle, the deflection of any strip is given by:

Deflection $\delta \propto \frac{PL^3}{EI}$ where E is Young's modulus and I is the second moment of area of the cross section of the strip.

The stiffness K is the force P required to produce unit deflection δ.

$$\therefore K \propto \frac{EI}{L^3}$$

The resonance frequency f of the strip as a beam, is given by:

$f = \frac{1}{2\pi}\sqrt{\frac{g}{\Delta_{st}}}$ Where Δ_{st} = static deflection of the strip under its own weight.

But $\Delta_{st} = \frac{5}{384}.\frac{WL^3}{EI}$

$$\therefore f^2 \propto g.\frac{EI}{WL^3}$$

$$\therefore f^2 \propto \frac{1}{W}.\frac{EI}{L^3}$$

But $f^2 \propto \frac{K}{W}$

$$\therefore K \propto Wf^2$$

It will be seen that this formula is independent of length and therefore can be used for a violin, a viola or a cello. This simple formula can be used easily and precisely. The ring mode and the X mode of the plate taken together, involve bending over a large part of the plate. By holding the plates loosely with the fingers on a nodal line and tapping the plates with a knuckle at an antinode, each of these modes can separately be excited and their frequencies found. The plate is then weighed.

For the back, the ring mode frequency is kept one octave above the X mode frequency. This gives a constant relationship between the cross grain stiffness and the long grain stiffness in the plate. To lower the ring mode wood is removed in the end bout areas. To lower the X mode wood is removed in the centre bouts. For the belly, the wood thickness is made more or less uniform in thickness and the ring and X modes found.

The combining of the two modes into one formula makes it simpler. The average of the two modal stiffnesses is found.

$$K = W.\left(\frac{f_{\text{ring mode}} + f_{\text{X mode}}}{2}\right)^2$$

This is a weighted average because the X mode frequency is usually near half of the ring mode frequency. This is very satisfactory because it recognises what the writer has found from experience, that a violin is approximately twice as sensitive to the ring mode stiffness as the X mode stiffness.

It was found by many trials that a good stiffness K for the back is 7,250,000 g, and for the belly 4,250,000 g (the unit grams has been shown to indicate that these figures have been arrived at taking the weight of the plate in grams). The same figures apply to viola and cello plates. This was using a weight in grams and the frequency in Hz. The equation derived is an empirical equation and not an analytical one. The calculated result is not an absolute stiffness but a figure (in grams) that has proportionality to stiffness.

The result of using this method to achieve a constant flexural stiffness in the plates of the instruments was that a very desirable uniformity was found between one violin and another despite the wood varying widely.

Although all these violins had the same feel of response to the player, there were differences in the brightness of the sound. When the violin is new, plates that achieved their stiffness from a high resonant frequency and a low weight do sound brighter than those with plates that achieved the stiffness with more weight and low resonant frequency. After the violin had been played for a while this difference became much less noticeable. If the K of a violin is low, the violin is easily driven and would appeal to a lighter player (perhaps a chamber music player) and a violin with a high K would appeal to a heavier (soloist) player. Because the stiffness does not affect the mobility selectively but applies right across the frequency range, it does not in itself affect the quality. However because a stiff violin demands to be played harder it probably will be bowed closer to the bridge and a different string vibration spectrum will be produced, which will of course feed through to the radiated sound.

Determining the amount of wood in the body can be done using resonance criteria or stiffness criteria. This research shows that stiffness gives results that are much more consistent. This again would support the concept of a driven mode as the principal sound generator in the violin, rather than a dependence on resonance.

Appendix F

METHOD OF CALCULATING THE EAR

F.1 The shape factor of the arching

After making some violins using simple methods of calculating the EAR it became apparent that the violin is so sensitive to the EAR that more refined methods had to be used. It was necessary to take into account the arch shape and the wood thickness.

The way in which an arch behaves structurally depends not only on its crown height but also on its shape. In order to be able to take this into account a system of "arching shape factors" was developed. The standard for comparison for arches is the actual line taken by the forces in the arch. This is called the line of thrust.

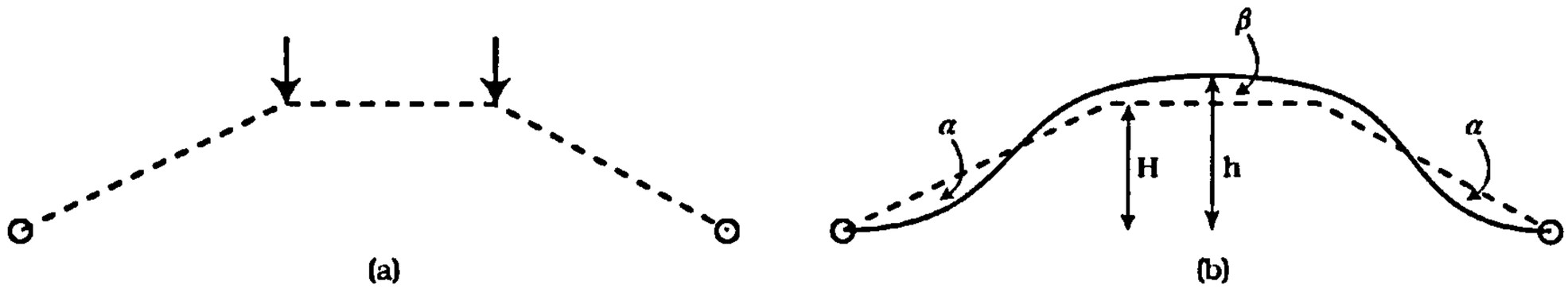

Fig F1. Centre belly arch shape compared to the line of thrust, to derive shape factors.

Fig. F1 (a), shows the line of thrust in a belly centre bouts cross arch, of a bridge load on the arch (the sound post contribution having been deducted). It will be seen then that the line of thrust is the simplest structure that can support the load in direct force without any bending. For the purposes of calculating the EAR the plate will behave as though the top of the CBX arch was the height of the line of thrust. But what is the height of the line of thrust? A useful approximation can be made as shown in (b). Draw the CBX arch, and over it draw the line of thrust such that the sum of the two areas "α" is equal to the area "β". The shape factor for the arch is the height of the line of thrust divided by the height of the arch. s = H/h or H = sh

In fig F2 (a), the line of thrust of a back centre bouts cross arch is shown, and for simplicity, shift the load to the centre to produce the symmetrical line of thrust shown in (d) (the resulting final error is surprisingly small). In (e) the actual arch is drawn, and the line of thrust superimposed on it such that the areas cut off above the line equal the areas cut off below the line. The back CBX arch will behave as though it were of height H and this we can find by multiplying the arch height h by the shape factor s.

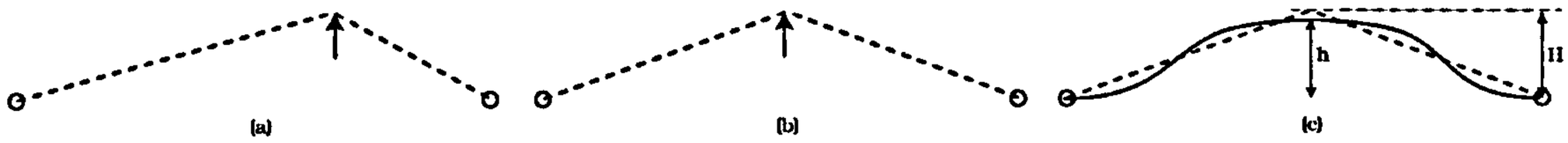

Fig F2. Centre back arch shape compared to line of thrust, to derive shape factors.

The EBX arches do not have simple point loads like the CBX arches, but have distributed loads. If the load were uniformly distributed the line of thrust would be of a parabolic form. It is not know exactly how the load is distributed but it must have a bias towards the centre of the span given that it arises from an interaction with the long arch. If the loading distribution is taken to be parabolic, the resulting line of thrust will be a third degree equation. By making a drawing of the shape of the end bouts cross arch and superimposing on this a line of thrust which is a third degree equation, such that the areas cut off above the line of thrust are equal to the areas cut off below the line of thrust, the shape factor as given by H/h can be found.

The shape of the arch is, from a structural point of view, the shape of its centre line. When a violin plate is made it is the outside surface of the plate that is shaped, but in calculating the effect of that arch the it must be regarded as being lower than it is built by half the wood thickness.

The method used for calculating the EAR is best demonstrated by a specimen calculation for a specific example. A calculation such as this was done for every instrument made. The example given here is violin number 132 and is taken from the record book.

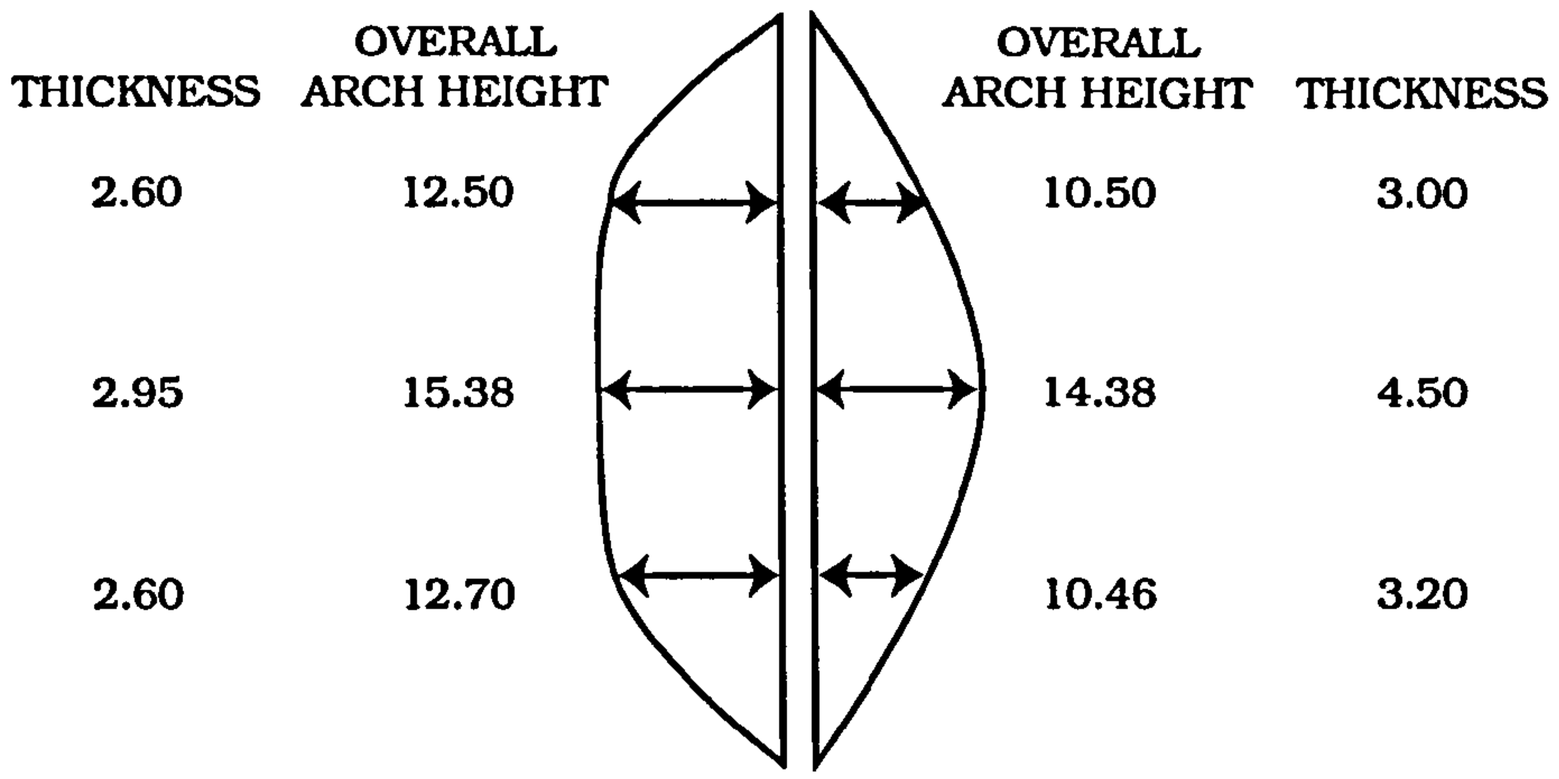

Fig F3. Arch heights and wood thickness used in specimen calculation of EAR.

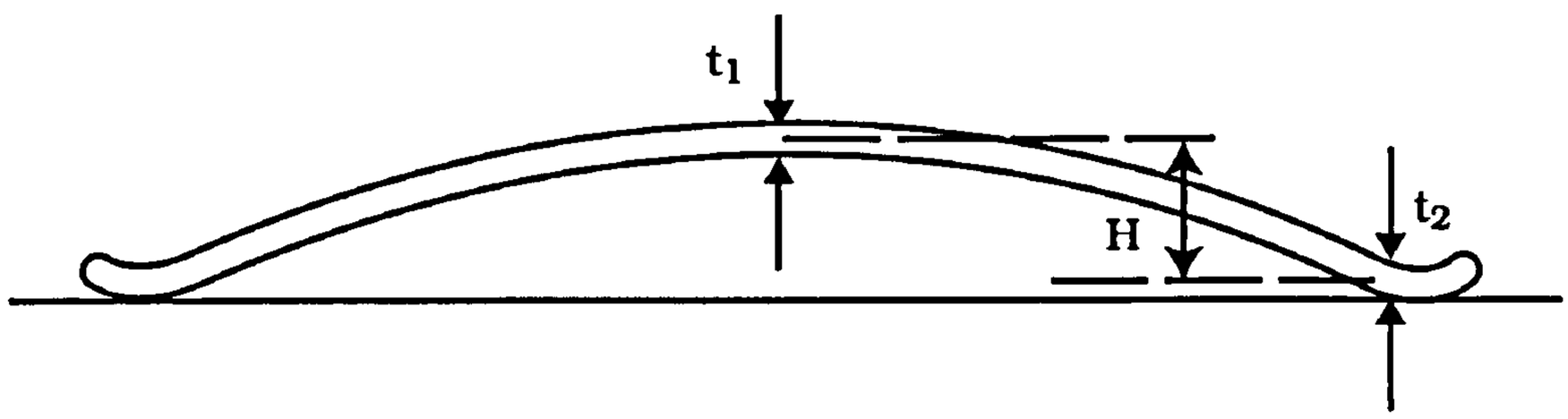

Fig F4. Effective arch height.

The effective arch height is the actual arch height minus half the thickness at the crown minus half the thickness at the edge multiplied by the shape factor.

Upper belly	Upper back
(12.50-1.3-1.625) 0.858 =8.22	(10.50-1.5-1.625) 0.803 =5.92
Centre belly	Centre back
(15.38-1.475-1.625) 0.960=11.79	(14.38-2.25-1.625) 1.099=11.54
Lower belly	Lower back
(12.70-1.3 -1.625) 0.878 =8.58	(10.46-1.6-1.625) 0.823 =5.95

Now divide the upper and lower bouts affective arch heights by the centre bouts effective height.

Upper belly, 0.6969 Upper back, 0.5130

Lower belly, 0.7280 Lower back, 0.5158

Now average the upper belly and upper back figures to find the upper bouts EAR and the deviation.

(0.6969+0.5130)/2 = 0.6049 +or- 0.0919 for the upper bouts

(0.7280+0.5158)/2 = 0.6219 +or- 0.1061 for the lower bouts

The deviations are usually near 0.1, being a little higher in the lower bouts than the upper, although as has been said before the amount of deviation does not seem to be particularly tonally significant. The arching shape factors used, all work out at less than 1, except for the centre back arch where the line of thrust projects outside the line of the arch. The EAR values given here, describe an arching of the tonal quality believed to be most acceptable to players. Virtually all the experimentation needed to find a good value for the EAR, was been done by making violins. When a viola, which may be proportionately wider than a violin, particularly across the centre, and may be proportionately lower in arching height, was made, the violin EAR values were modified by the factors given in section 6.2.

F.2 Getting the EAR right every time

The violins made in the writer's workshop use unvarying outline shapes, and arching templates, therefore the individual instrument calculation only needs to take into account variations in the wood thickness. It will be apparent that there is a problem here. The arching is formed before the plates are hollowed out and the final plate thickness is determined. To overcome this problem the following method is used.

The outside of the back is made to standard templates, and then the wood is given thickness appropriate to the wood, using criteria outside this thesis. Realistic estimates are made of the likely wood thickness for the front. The above data are fed into a simple computer program, which calculates the front arching heights at the centre and at the end bouts. The front is made and

during the graduation of its thickness, the thickness at the centre of the plate is adjusted to bring the EAR to the required figure, by again using the computer program.

LITERATURE CITED IN THE THESIS.

1. ARNOLD AND WEINREICH: Acoustical spectroscopy of violins: J. Acoust. Soc. Am. 72(6) Dec 1982.

2. BACKHAUS, H: Uber die schwingungsformen von geigenkorpern, I and II: Z Physik, 62, 142-166 (May-July 1930): 72, 218-255 (1931).

3. BEAMENT, J: The violin explained, components, mechanism, and sound: Clarendon Press, Oxford. 1997.

4. BELDIE, I P: Chladni figures and eigentones in violin plates: English translation in, Benchmark Papers in acoustics, Musical acoustics, Part 2: Edited by C M Hutchins. (1976).

5. BISSINGER, G: Some mechanical and acoustical consequences of the violin sound post: J. Acoust. Soc. Am.:May 1995.

6. BISSINGER, G: Modal analysis, radiation and the violin's sound post: Sound and Vibration: August 1995.

7. BISSINGER, G: Mode-ling the sound of the violin: Catgut acoust. Soc. J. Vol 3 No 5 May 1998.

8. BOUTILLON, X and WEINREICH, G: Three-dimensional mechanical admittance: Theory and new measurement method applied to the violin bridge: J Acoust. Soc. Am.: 105 (6), June 1999.

9. BOYDEN, D: Violin playing from its origins until 1761:London and New York:1965.

10. CRÈMER, L: The physics of the violin: The MIT Press; Cambridge Mass., London, England: 1983

11. DUNNWALD H: Zur messung von geigenfrequenzgangen: Acoustica Vol. 51, 1982.

12. DUNNWALD H: Ein Verfahren zu odjektiven bestimmung der klangqualitat von violinen: Acustica Vol.58, 1985.

13. FAHY F J: Foundations of Engineering Acoustics: Academic Press, London: 2001.

14. GIORDANO AND KORTY: Motion of a piano string, longitudinal vibrations and the role of the bridge: J. Acoust. Soc. Amer., Vol.100 Dec 1996.

15. GOUGH C: Science and the Stradivarius: Physics World: April 2000.

16. HACKLINGER M: Violin timbre and bridge frequency response: Acustica Vol.39 (1978).

17. HILL ALFRED, ARTHUR AND W. HENRY: Antonio Stradivari: His life and work: Dover 1901.

18. HUTCHINS, C M: The physics of violins: Scientific American: November, 1962.

19. HUTCHINS, C M: A study of the cavity resonances of a violin and their effects on its tone and playing qualities: J. Acoust. Soc. Am.: January 1990.

20. HUTCHINS, C M: The air and wood modes of the violin: J. Audio. Eng. Soc.: September 1998.

21. JANSSON, E V: On higher air modes in the violin: Catgut Acoust. Soc. Newsletter, No. 19, 13-15 (1973).

22. JANSSON, E V: Experiments with the violin string and bridge: Applied acoustics Vol.30, 1990.

23. JANSSON, MOLIN AND SALDNER: On eigenmodes of the violin- Electronic holography and admittance measurements: J. Acoust. Soc. Amer. 95 (2), February 1994.

24. JANSSON, E V: On the function of the violin- Vibration excitation and sound radiation: TMH-QPSR Vol.4, 1996.

25. JANSSON, E V: Admittance measurements of 25 high quality violins: Acustica: Vol.83, 1997.

26. JANSSON, BENEDYK AND NIEWCZYK: Admittance Measurements of Violins with High Arching: Acustica Vol. 83, (1997) 571-574.

27. JANSSON, MOLIN AND SALDNER: On eigenmodes of the violin- Electronic holography and admittance measurements: J. Acoust. Soc. Am.: February, (1994).

28. JANSSON E, MOLIN N E, AND SUNDIN H: Resonances of a violin body studied by hologram interferometry and acoustical methods: Phys. Scripta, 2, 243-256 (1970).

29. JANSSON AND NIEWCZYK: On the acoustics of the violin: P, T1, C3, B1, P1, P2, and the bridge or body hill.: TMH-QPSR Vol4, 1997.

30. JANSSON AND NIEWCZYK: Admittance measurements of violins with high arching: Acustica Vol.83, 1997.

31. JANSSON, NIEWCZYK AND FRYDEN: On the body resonance C3 and its relation to the top and back plate stiffness: TMH-QPSR 1/1996.

32. KINSLER, FREY, COPPENS AND SANDERS: Fundamentals of acoustics: John Wiley and Sons, New York, 1982.

33. LANGHOFF, A: Measurement of acoustic spectra and their interpretation using a 3D representation: Acustica Vol. 80, (1994).

34. LEE AND RAFFERTY: Longitudinal vibrations in violin strings: J. Acoust. Soc. Am. Vol.73, April 1983.

35. LEGGE, K A, AND FLETCHER, N H: Non-linear generation of missing modes on a vibrating string: J. Acoust. Soc. Am. Vol. 76, July 1984.

36. LEIPP, E: The violin, historic, aesthetic, construction and acoustics: University of Toronto Press, Toronto, 1969.

37. MARSHALL, K D: Modal analysis of a violin: J. Acoust. Soc. Am.: Vol.77, No 2, 1985.

38. MCINTYRE, M E, AND WOODHOUSE, J: The acoustics of stringed musical instruments: Interdisciplinary science reviews, Vol.3, No.2, 1978.

39. MEINEL H: Uber frequenzkurven von geigen: Akust. Zeits. Vol.2, p22 (1937).

40. MEINEL H: Regarding the sound quality of violins and a scientific basis for violin construction: J. Acoust. Soc. Amer. 29(7), 817-822, 1957.

41. MINAERT M AND VLAM C C: The Vibrations of the violin bridge: Physica Vol.4, No.5, 1937.

42. MORAL AND JANSSON: Eigenmodes, input admittance, and the function of the violin: Acustica: Vol.50, 1982.

43. PASQUALINI, G: L'acoustica applicata alla liuteria: Ann. R. Accad. S.,Cecelia. P.405, (1938-39).

44. PICKERING, N C: The bowed string: Amereon Ltd: 1991.

45. RAMAN, C V: Experiments with mechanically played violins: Proc. Indian Assos. For cultivation of science, Pg.37, 1920.

46. REINICKE, W AND CREMER, L: Application of holographic interferometry to vibrations of the bodies of string instruments: J. Acoust. Soc. Amer. 48(4), Pt 2, 988-992 (1970).

47. REINICKE, W: Ubertragungseigenschaften des streichinstrumenttenstegs: Catgut Acoust. Soc. Newsletter No.19, 26-34 (1973).

48. ROHLOFF, E: Uber die innere reibung und die strahlungdamfung von geigen: Ann. d. Phys. Vol.38, No.3, (1940).

49. ROHLHOFF, E: Der Klangcharacter altitalienischer Meistergeigen, Zeitschrift fur angewandte Physik, 4/1950.

50. RUNNEMALM, MOLIN AND JANSSON: Operating deflection shapes and the function of the violin: TMH-QPSR Vol.3, 1998.

51. SACCONI S F: The secrets of Stradivari: Libreria del Convegno, Cremona, 1972.

52. SALDNER, MOLIN AND JANSSON: Vibration modes of the violin forced via the bridge and action of the sound post:J. Acoust. Soc. Am.: August, 1996.

53. SAUNDERS F A: The mechanical action of violins: J Acoust. Soc. Amer. 9, 81-98 (Oct. 1937).

54. SAUNDERS F A: The mechanical action of instruments of the violin family: J. Acoust. Soc. Amer., 17 (3), 169-186 (1946).

55. SAUNDERS F A: Recent work on violins: J. Acoust. Soc. Amer. 25 (3), 491-498 (1953).

56. SAVART F: Memoire sur la construction des instruments a cordes et a archet: Determille, Paris:1819.

57. SAVART, F: The violin: L'Institut, 8 54-56 (1840).

58. SCHELLENG, J C: Acoustical effects of violin varnish: J. Acoust. Soc. Amer. 44 (5), 1175-1183 (1968).

59. SCHELLENG, J C: On the polarity of resonance: Catgut Acoust. Soc. Newletter, No.10, 14-18 (1968).

60. SCHELLENG, J C: The action of the soundpost: Catgut Acoust. Soc Newsletter. No.16, 11-15 (1971).

61. SCHLESKE, M: On the acoustical properties of violin varnish: Catgut Acoust. Soc Journal, Vol.3 No. 6, Nov. 1998.

62. SEGERMAN, E: Deep Tensions: The Strad: April 1988.

63. SHAW, E A G: Cavity resonance in the violin: J. Acoust. Soc. Am.:January 1990.

64. WEINREICH, G: Violin radiativity: Concepts and measurements: Research papers in violin acoustics 1975-1993. Vol.2. Ed. C M Hutchins and V Benade. Acoust. Soc. Amer.

65. WOODHOUSE, J: On the acoustics and mechanics of stringed musical instruments: PhD thesis, University of Cambridge: July 1977.

66. WOODHOUSE, J: On the playability of violins; Part1 and Part 2: Acustica Vol.78 (1993).